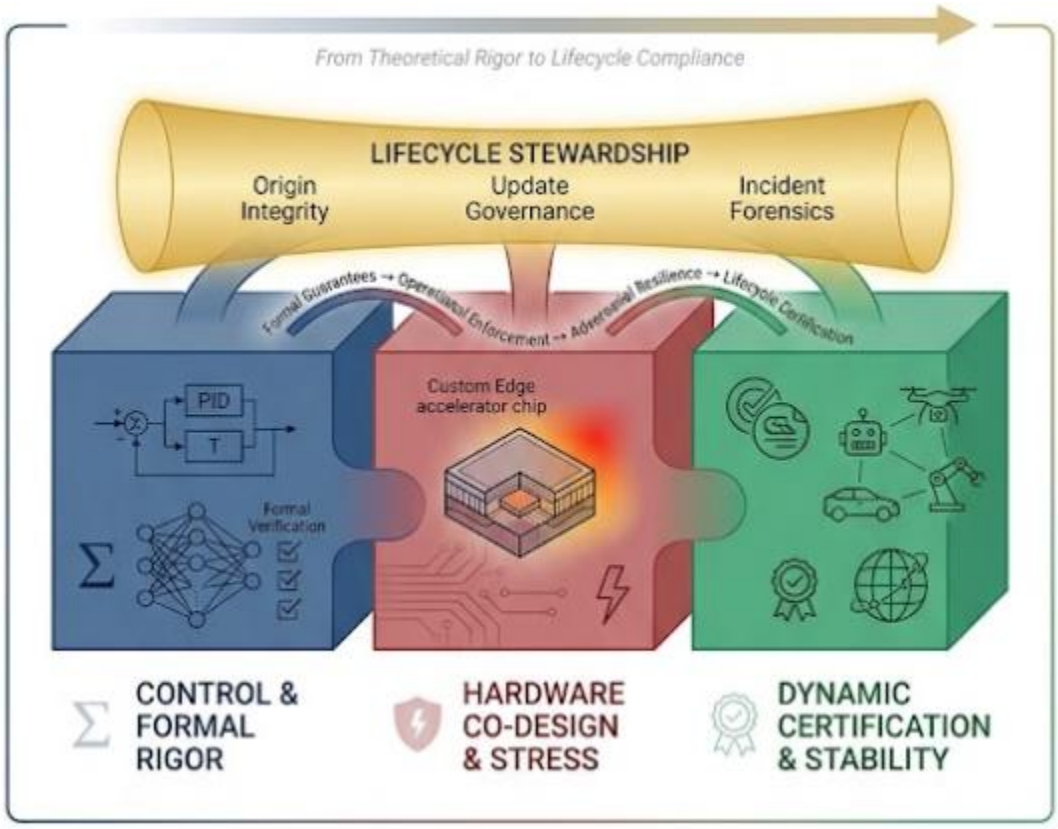
FRONTIER AI ENGINEERING:

AGENTIC AI AUTONOMY, MULTIMODAL ARTIFICIAL INTELLIGENCE, AND DETERMINISTIC EDGE AI INTELLIGENCE



THAO MONG LE

Copyright © 2026 Thao M. Le

All rights reserved.

No part of this book may be reproduced, stored in a retrieval system, or transmitted in any form or by any means — electronic, mechanical, photocopying, recording, or otherwise — without prior written permission from the author.

This book is a work of nonfiction. All facts, historical references, and technical descriptions are presented to the best of the author's knowledge at the time of publication.

ISBN: [To be assigned]

Cover and Interior Design: Thao M. Le

Printed in the United States of America

Frontier AI Engineering:

Agentic AI Autonomy, Multimodal Artificial Intelligence, and Deterministic Edge AI Intelligence

Frontier AI Engineering:

Agentic AI Autonomy, Multimodal Artificial Intelligence, and Deterministic Edge AI Intelligence

Volume IV

Edge AI Hardware, Silicon Accelerators and Systems Co-Design

Part III

Hardware–Software Co-Design and System Optimization

Thao Mong Le

CONTENTS

PREFACE TO VOLUME IV v

PREFACE TO PART III xii

EXECUTIVE SUMMARY xviii

ABOUT THIS VOLUME xxvii

LIST OF FIGURES & TABLES xxxiii

8. EDGE AI ACCELERATORS, REAL-TIME SYSTEMS, AND HARDWARE–SOFTWARE CO-DESIGN 1

8.4 Hardware–Software Co-Design: AI Accelerators, Sensor Pipelines, and Cross-Layer Optimization 3

APPENDIX A: TECHNICAL SUPPORTING MATERIAL / REFERENCE SPECIFICATIONS 667

APPENDIX B: GLOSSARY 731

APPENDIX C: ACRONYMS 747

PREFACE

Volume IV: Edge AI Hardware, Silicon Accelerators, and Systems Co-Design

The modern evolution of artificial intelligence is defined by its transition from centralized cloud datacenters into embodied, real-world physical systems. While hyperscale computing infrastructures provide immense computational throughput for training foundation models and large-scale neural networks, the next generation of intelligent systems must increasingly operate beyond the boundaries of the datacenter. Autonomous vehicles navigate dynamically changing environments in real time, aerial platforms execute mission-critical maneuvers under stringent timing constraints, industrial robots manipulate physical objects with precision, and distributed sensor networks continuously interpret multimodal streams of information at the edge. In these environments, intelligence must be executed where data are generated and decisions are required.

For physical AI systems, latency, energy consumption, thermal behavior, memory bandwidth, and deterministic execution are not merely performance metrics. They are hard physical constraints that directly influence safety, stability, operational endurance, reliability, and mission success. A delayed perception update, a missed control deadline, an overheated processor, or a saturated memory subsystem can have consequences that extend far beyond reduced computational efficiency. Unlike cloud environments, where computational resources can often be scaled elastically, edge AI systems must operate within fixed hardware budgets while maintaining predictable and reliable behavior under continuously changing real-world conditions.

Volume IV, **Edge AI Hardware, Silicon Accelerators, and Systems Co-Design**, explores the computational substrate that makes physical artificial intelligence possible. It bridges high-level perception, reasoning, learning, and control algorithms with the silicon architectures, memory hierarchies, communication fabrics, real-time operating environments, and co-design methodologies required to deploy intelligence at the physical edge. The volume is founded on a simple but increasingly important principle: modern AI capability emerges not only from algorithms, but from the coordinated interaction among hardware, software, memory, communication, and control systems.

As artificial intelligence continues to expand in scale and sophistication, hardware architecture has evolved from a supporting implementation detail into a primary determinant of capability. Processing performance, memory locality, thermal constraints, communication overhead, energy efficiency, and execution determinism now influence the practical limits of AI deployment as profoundly as neural-network design itself. This transformation has given rise to

a new engineering discipline at the intersection of machine learning, semiconductor design, embedded systems, computer architecture, systems engineering, and cyber-physical systems: **hardware–software co-design**.

The central objective of this volume is to provide a rigorous foundation for understanding how intelligent systems are designed, implemented, optimized, and deployed across the entire computing stack. The discussion begins at the silicon layer, advances through the physical constraints that govern system behavior, and culminates in system-level optimization frameworks that unify models, compilers, accelerators, communication infrastructures, memory architectures, and runtime orchestration mechanisms. Throughout the volume, emphasis is placed on engineering integration rather than isolated technologies, reflecting the reality that contemporary AI systems derive their capabilities from interactions among multiple layers of the computational ecosystem.

Organization and Scope Across the Tri-Part Structure

To provide comprehensive technical coverage while maintaining structural clarity across an approximately **2,150-page body of material**, Volume IV is published as **three interconnected yet independently accessible physical volumes**. Each part addresses a distinct layer of the edge AI computing stack, progressing from computational substrate, through physical constraints, to holistic hardware–software optimization.

Together, these three parts form a complete systems-engineering framework for understanding how contemporary artificial intelligence is translated from mathematical models into deployable, real-time, physical systems.

Figure V4 provides a high-level architectural overview of Volume IV and illustrates the relationships among silicon accelerators, physical limitations, and hardware–software co-design methodologies.

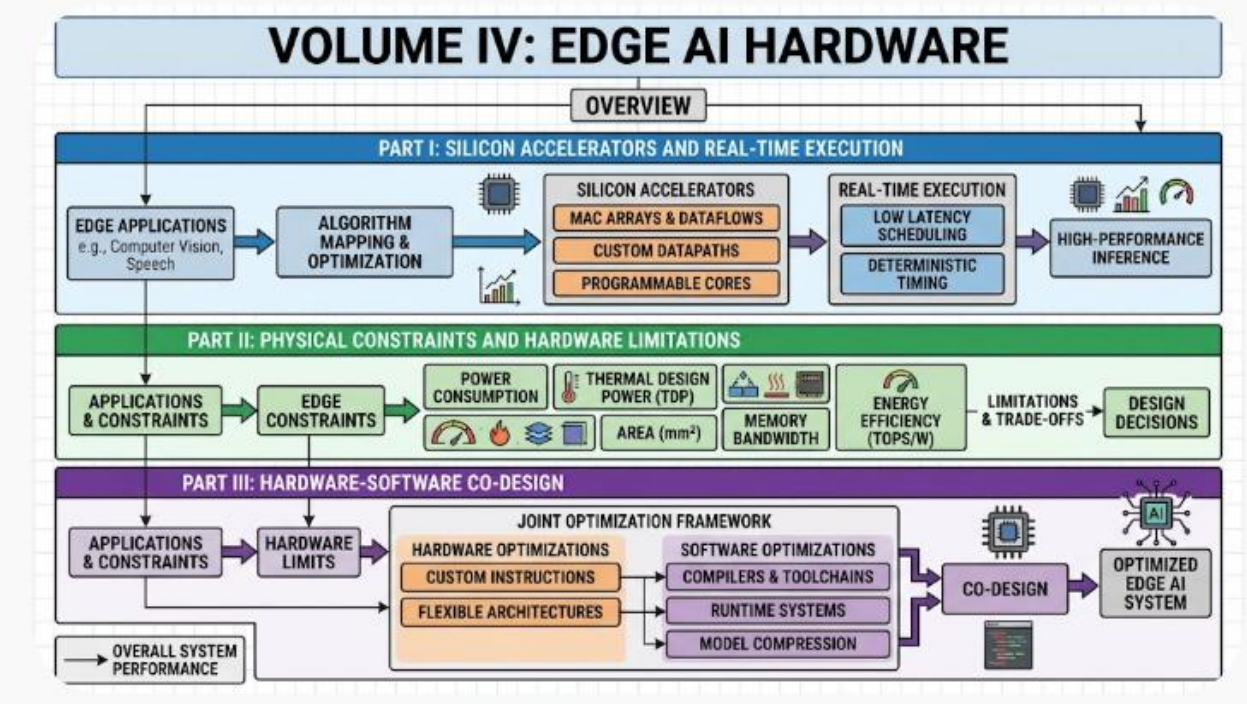


Figure V4 — Architectural Overview of Volume IV: Edge AI Hardware, Silicon Accelerators, and Systems Co-Design

The figure illustrates the layered progression followed throughout Volume IV. Part I introduces the computational substrates and deterministic execution mechanisms that support AI workloads. Part II examines the physical limitations and engineering constraints that bound system behavior. Part III then integrates these foundations into a unified optimization framework, demonstrating how hardware and software can be designed cooperatively to maximize performance, efficiency, scalability, and deployment readiness.

Part I: Silicon Accelerators and Deterministic Real-Time Execution

(Sections 8.1–8.2)

Part I establishes the computational foundation of modern edge AI systems by examining the specialized silicon architectures that execute machine-learning workloads under real-world deployment constraints.

The discussion explores a broad spectrum of domain-specific accelerators, including low-power **System-on-Chip (SoC)** platforms, **Neural Processing Units (NPUs)**, **Tensor Processing Units (TPUs)**, **Field-Programmable Gate Arrays (FPGAs)**, and custom **Artificial Intelligence Application-Specific Integrated Circuits (AI ASICs)**. Particular attention is devoted to how these architectures balance throughput, energy efficiency, memory locality, and deterministic execution.

Part I also investigates the sensor-ingestion and communication infrastructures that connect physical environments to computational systems, including CAN-FD, PCI Express (PCIe), Ethernet Time-Sensitive Networking (TSN), and MIPI CSI-2. The discussion concludes with Real-Time Operating Systems (RTOSs), interrupt-management frameworks, scheduling policies, and bounded-latency execution models required to support closed-loop autonomous control systems.

Part II: Physical Constraints and Hardware Limitations

(Section 8.3)

Part II focuses on the fundamental physical realities that govern the operation of edge AI platforms.

Regardless of architectural sophistication, all intelligent systems are ultimately constrained by limits imposed by energy, heat, timing, memory, communication bandwidth, and information transfer. Understanding these constraints is essential because they frequently determine system performance more directly than theoretical computational capability.

This part presents rigorous mathematical and architectural analyses of static and dynamic power dissipation, thermal-management principles, **Thermal Design Power (TDP)** boundaries, latency budgets, timing jitter, memory bandwidth limitations, cache hierarchies, and memory-footprint optimization strategies. Engineering models and quantitative methodologies are used throughout to demonstrate how physical limitations influence system-level design decisions.

Part II therefore serves as the bridge between computational capability and deployment feasibility.

Part III: Hardware–Software Co-Design and System Optimization

(Section 8.4)

Part III synthesizes the architectural foundations of Part I and the physical realities of Part II into a unified framework for AI-system optimization.

The central theme of this section is that modern AI performance emerges not from isolated hardware improvements or software innovations, but from coordinated optimization across the entire computational stack. Topics include hardware-aware programming frameworks, customized instruction set architectures (ISAs), domain-specific compiler toolchains, tensor-graph optimization, distributed orchestration systems, memory-efficient attention mechanisms, state-space architectures, structured sparsity, conditional computation, low-precision execution, quantization, pruning, and hardware-aware neural architecture search (HW-NAS).

Part III further explores emerging accelerator paradigms, including processing-in-memory architectures, reconfigurable spatial fabrics, hybrid AI co-processors, optical interconnect technologies, and advanced runtime execution frameworks. Collectively, these topics demonstrate how future AI systems increasingly derive efficiency from cross-layer co-design rather than isolated improvements within individual system components.

As the culminating section of Volume IV, Part III integrates silicon architectures, physical constraints, and software intelligence into a unified methodology for designing efficient, scalable, and deployment-ready AI systems.

Position Within the Multi-Volume Series

Volume IV occupies a unique position within the broader AI Engineering series by serving as the primary bridge between intelligent algorithms and physical computing infrastructure.

Preceding Foundation: Volumes I–III

The preceding volumes establish the theoretical foundations of modern artificial intelligence, including mathematical frameworks, machine-learning methodologies, deep-learning architectures, embodied cognition models, autonomous-control systems, and physical AI reasoning frameworks.

Collectively, these volumes answer the question:

How should intelligent systems perceive, learn, reason, and act?

Hardware Realization: Volume IV

Volume IV translates those theoretical capabilities into deployable computational systems.

It addresses the practical engineering challenge:

How can intelligence be implemented efficiently, reliably, and deterministically on physical hardware?

To answer this question, the volume examines silicon architectures, accelerator fabrics, memory systems, communication infrastructures, real-time execution environments, physical resource constraints, and hardware–software co-design methodologies.

Subsequent Expansion: Volume V

Volume V builds upon the hardware and systems foundations established in Volume IV and extends the discussion to the macro-level architecture of distributed AI ecosystems. It examines how intelligent devices, sensing networks, edge platforms, and cloud infrastructure are

interconnected and coordinated to support large-scale AI deployment.

Topics include:

- Distributed Edge AI Networks
- AI-Driven Internet of Things (AIoT) Sensing Networks
- Swarm Intelligence Architectures
- Multi-Agent Coordination
- Hybrid Edge–Cloud Topologies and Computing Continua
- Collaborative AI Infrastructure
- Enterprise-Wide AI Architectural Synthesis
- Large-Scale Autonomous System Deployment

Volume IV focuses on the computational foundations of AI systems, including silicon accelerators, deterministic execution, physical hardware constraints, and hardware–software co-design within individual platforms and integrated computing systems. **Volume V: Distributed Edge AI Architectures & Cloud-Edge Topologies** extends this foundation to the macro-architectural scale, examining how AI capabilities are distributed, coordinated, and integrated across interconnected computational environments. Its scope encompasses AIoT sensing networks, distributed edge intelligence, hybrid edge–cloud architectures, multi-agent coordination, and enterprise-wide architectural synthesis.

Together, the two volumes address complementary levels of AI systems engineering. Volume IV examines how AI workloads execute efficiently and reliably within computational platforms, while Volume V examines how those platforms, intelligent devices, sensing networks, edge resources, and cloud services are architecturally integrated and coordinated to form larger, distributed AI ecosystems.

Concluding Perspective

Volume IV represents the hardware foundation of the AI Engineering series. It is the point at which intelligent algorithms encounter physical reality and must adapt to the constraints and opportunities of silicon, memory, communication, power, thermodynamics, and real-time execution.

By unifying accelerator architectures, deterministic computing principles, physical resource limitations, and hardware–software co-design methodologies, this volume provides a

comprehensive engineering framework for the implementation of real-world artificial intelligence. It is intended to serve not only as a technical reference for researchers, architects, compiler developers, embedded-systems engineers, and AI practitioners, but also as a systems-engineering guide for understanding how modern intelligent systems are built, optimized, and deployed.

As artificial intelligence becomes increasingly embedded within physical environments, the distinction between algorithm design and system design continues to diminish. The future of AI will be shaped not solely by advances in machine learning, but by the ability to integrate intelligence with efficient hardware, deterministic execution, scalable architectures, and robust engineering practices. Volume IV provides the foundation for understanding that convergence and for participating in the design of the next generation of intelligent systems operating at the physical edge.

PREFACE

Volume IV – Part III: Hardware–Software Co-Design and System Optimization

Section 8.4

The history of computing is often presented as a progression of increasingly powerful processors, larger memory systems, and more sophisticated software. In practice, however, the greatest advances in computational capability have frequently emerged not from improvements in any single component, but from the coordinated evolution of hardware and software together. Nowhere is this principle more evident than in modern artificial intelligence systems.

The preceding parts of Volume IV established the foundations required to understand this relationship. Part I examined the silicon substrates that execute AI workloads, including domain-specific accelerators, memory architectures, sensor-ingestion pathways, and deterministic runtime environments. Part II then explored the physical realities that ultimately govern system behavior, including power dissipation, thermal management, latency budgets, timing jitter, memory bandwidth limitations, and resource constraints. Together, these discussions demonstrated a fundamental truth of physical AI systems: computational capability is meaningful only when aligned with the underlying realities of hardware execution.

Part III builds directly upon these foundations and addresses the next critical question:

How can intelligent systems be optimized when hardware capabilities and physical constraints are treated as inseparable components of the same engineering problem?

The answer lies in **hardware–software co-design**.

Traditional computing methodologies often separate hardware development from software development. Processors are designed first, and software is later adapted to execute efficiently on available hardware. Modern AI systems increasingly challenge this model. The computational structure of transformer architectures, state-space models, mixture-of-experts networks, sparse execution graphs, and long-context reasoning workloads exhibits characteristics that directly influence hardware behavior. At the same time, hardware constraints such as memory locality, communication bandwidth, execution latency, energy consumption, and thermal limits increasingly shape the design of AI models themselves.

As a result, optimization can no longer occur within a single layer of the computational stack. Neural architectures, compilers, runtimes, memory hierarchies, communication fabrics, and accelerator microarchitectures must instead be developed as interconnected components of a unified system. Hardware–software co-design represents the methodology through which these

interactions are analyzed, optimized, and ultimately transformed into deployable intelligent systems.

Part III therefore serves as the culmination of Volume IV. It synthesizes silicon capability, physical constraint awareness, and systems-level optimization into an integrated framework for designing efficient, scalable, and deployment-ready AI infrastructures.

Scope and Organization of Part III

Part III explores the synergistic integration of hardware architectures and software execution frameworks that collectively determine the performance, efficiency, and scalability of modern AI systems.

Unlike conventional optimization approaches that focus on isolated system components, this section adopts a cross-layer perspective in which models, compilers, memory systems, execution fabrics, communication infrastructures, and accelerators are optimized as a cohesive whole. The objective is not merely to improve individual performance metrics, but to create systems in which hardware and software cooperate to maximize overall computational effectiveness.

The discussion is organized around a comprehensive exploration of **Section 8.4: Hardware–Software Co-Design: AI Accelerators, Sensor Pipelines, and Cross-Layer Optimization**, which examines the architectural principles, optimization methodologies, and execution frameworks that define contemporary AI deployment environments.

Joint Optimization Frameworks

The section begins by examining methodologies that integrate hardware architecture, software frameworks, compiler technologies, and neural-network design within a unified optimization process. Topics include **Hardware-Aware Neural Architecture Search (HW-NAS)**, automated **Design Space Exploration (DSE)**, accelerator-aware model generation, and multi-objective optimization techniques that simultaneously consider accuracy, latency, energy consumption, memory utilization, thermal behavior, and deployment constraints.

Custom Instruction Sets and Extensible Processors

The discussion then investigates domain-specific **Instruction Set Architectures (ISAs)**, specialized tensor instructions, vector-processing extensions, matrix-execution engines, and reconfigurable datapaths developed specifically for AI workloads. Particular attention is given to how customized hardware execution pathways improve computational density, increase throughput, and reduce energy consumption.

Compilers, Toolchains, and Runtime Systems

Modern AI performance increasingly depends on compiler intelligence rather than hardware capability alone. Accordingly, this section explores hardware-aware compilation frameworks, graph-level optimization, kernel generation, memory scheduling, tensor fusion, runtime orchestration, and Just-In-Time (JIT) execution strategies designed to maximize utilization across heterogeneous accelerator fabrics.

Model Compression and Hardware Mapping

A substantial portion of Part III is devoted to understanding how model structures can be transformed to match hardware constraints. Topics include quantization, pruning, structured sparsity, low-precision execution, conditional computation, and memory-aware execution strategies. These techniques demonstrate how software-level transformations can map directly onto physical processing elements, yielding significant improvements in performance-per-watt, memory efficiency, and deployment scalability.

Distributed Orchestration and Cross-Layer Optimization

Part III extends co-design methodologies beyond individual devices into distributed execution environments. Tensor parallelism, context parallelism, pipeline optimization, communication scheduling, latency masking, collective communication frameworks, and multi-accelerator orchestration illustrate how system-level optimization complements device-level optimization.

Emerging Hardware–Software Co-Designed Architectures

The final sections investigate advanced computational paradigms that blur traditional distinctions between hardware and software. These include processing-in-memory architectures, reconfigurable spatial fabrics, hybrid AI co-processors, optical interconnect technologies, hardware-aware execution frameworks, and next-generation accelerator ecosystems that are increasingly shaped through integrated co-design methodologies.

The Tri-Part Structural Context

Part III represents the culmination of the architectural progression established throughout Volume IV.

Figure V4.3-1 - Volume IV – Part III Architectural Overview highlights Part III: Hardware–Software Co-Design and System Optimization (Section 8.4)

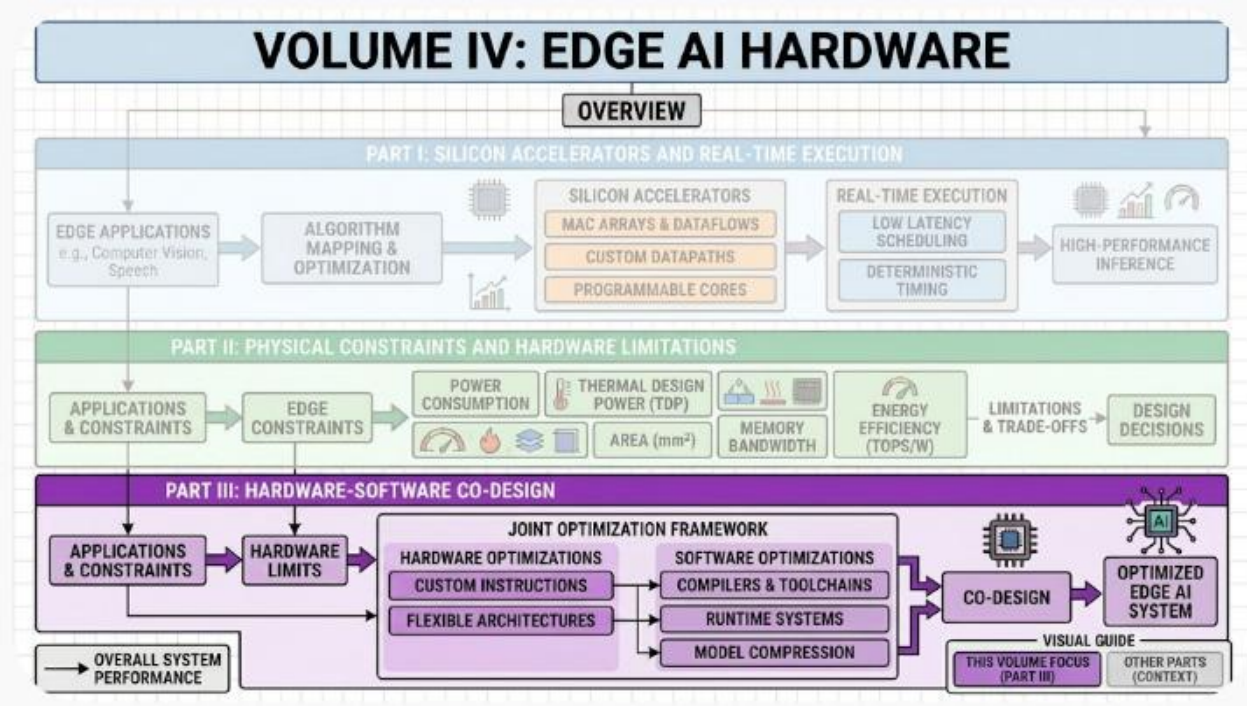


Figure V4.3A — *Volume IV – Part III Architectural Overview*

The figure illustrates how Part III synthesizes the computational foundations established throughout the earlier sections of Volume IV. Rather than viewing hardware architectures and software frameworks as independent domains, Part III focuses on the optimization methodologies that emerge when these domains are treated as components of a unified engineering ecosystem.

Part I: Silicon Accelerators and Deterministic Real-Time Execution

(Sections 8.1–8.2)

Part I established the computational substrate upon which AI systems operate. It introduced domain-specific accelerators, execution fabrics, memory pathways, communication infrastructures, and deterministic runtime environments. Through the study of NPUs, TPUs, FPGAs, AI ASICs, RTOS environments, interrupt systems, and bounded-latency scheduling frameworks, it provided the silicon foundations upon which modern AI execution depends.

Part II: Physical Constraints and Hardware Limitations

(Section 8.3)

Part II examined the physical realities that ultimately govern all computational systems. Through quantitative analyses of power consumption, thermal behavior, Thermal Design Power (TDP), timing jitter, latency constraints, memory bandwidth limitations, and storage requirements, it established the engineering boundaries within which intelligent systems must operate.

Part III: Hardware–Software Co-Design and System Optimization

(Section 8.4)

Part III synthesizes these foundations through cross-layer optimization methodologies that jointly consider hardware architecture, compiler infrastructure, runtime systems, memory organization, communication networks, and neural-network execution patterns. It demonstrates how silicon capabilities and physical constraints can be transformed into efficient, scalable, and deployment-ready AI systems through systematic co-design.

By unifying computational capability, physical constraint awareness, and optimized execution frameworks, Part III completes the architectural framework established throughout Volume IV. It provides the methodological bridge between individual edge AI platforms and the distributed intelligent infrastructures explored in subsequent volumes of the series.

Position Within the Broader Series

Part III occupies a unique position within the AI Engineering series because it serves as the transition point between hardware implementation and large-scale intelligent-system deployment.

The preceding volumes established the mathematical, algorithmic, and control-theoretic foundations of artificial intelligence. Parts I and II of Volume IV translated those abstractions into physical computational systems and quantified the limits within which they must operate. Part III now demonstrates how those systems can be systematically optimized and integrated.

The resulting hardware–software co-design framework provides the foundation for the topics explored in subsequent volumes, including distributed edge intelligence, multi-agent systems, cloud–edge orchestration, collaborative AI infrastructures, swarm-intelligence architectures, and large-scale autonomous deployments.

Concluding Perspective

Part III represents the convergence of all major themes introduced throughout Volume IV. It is the point at which silicon architectures, physical resource constraints, compiler technologies, runtime systems, memory hierarchies, communication fabrics, and AI workloads are unified into a single systems-engineering framework.

The central message of this section is straightforward yet profound: **modern AI performance is no longer determined solely by better algorithms or more powerful hardware. It emerges from the coordinated optimization of both.**

As intelligent systems continue to grow in complexity, scale, autonomy, and capability, the importance of hardware–software co-design will only increase. Future advances in artificial intelligence will depend not merely on what models can compute, but on how effectively computation can be mapped onto physical hardware while respecting the realities of energy, latency, memory, communication, and deployment.

Part III provides the conceptual foundation for understanding that transformation and the engineering methodologies required to realize it. In doing so, it completes the journey begun in Volume IV: from silicon, through physics, to optimized intelligence operating in the physical world.

EXECUTIVE SUMMARY

Volume IV: Edge AI Hardware, Silicon Accelerators, and Systems Co-Design

Part III: Hardware–Software Co-Design and System Optimization

Section 8.4: Hardware–Software Co-Design: AI Accelerators, Sensor Pipelines, and Cross-Layer Optimization

1. Overview and Engineering Context

The increasing computational demands of artificial intelligence, combined with the physical limitations of embedded computing platforms, have made hardware–software co-design an essential discipline in modern AI engineering. As AI applications expand from centralized computing environments into autonomous vehicles, robotics, industrial automation, intelligent sensing, and other physically embodied systems, their performance can no longer be evaluated solely through model accuracy or theoretical computational throughput.

Practical deployment requires coordinated consideration of computational architecture, accelerator capabilities, memory organization, software execution, sensor-data processing, communication, power consumption, thermal behavior, and real-time requirements. Optimizing one component independently may improve its local performance while introducing bottlenecks elsewhere in the system.

Part III of Volume IV addresses this challenge through a cross-layer engineering approach. It examines how AI models, specialized hardware, compiler toolchains, runtime systems, sensor pipelines, and real-time execution frameworks can be designed and optimized as an integrated architecture.

Building on the silicon architectures and execution mechanisms introduced in Part I and the physical constraints examined in Part II, Part III brings these foundations together to establish a systematic methodology for developing efficient, predictable, and resource-aware edge AI systems.

Figure V4.3B presents the architectural relationship among the three parts of Volume IV, highlighting the progression from silicon accelerators and real-time execution, through physical constraints and hardware limitations, to integrated hardware–software co-design. Particular emphasis is placed on Part III, which brings together hardware optimization, software optimization, and joint system-level design to develop efficient and deployment-ready edge AI architectures.

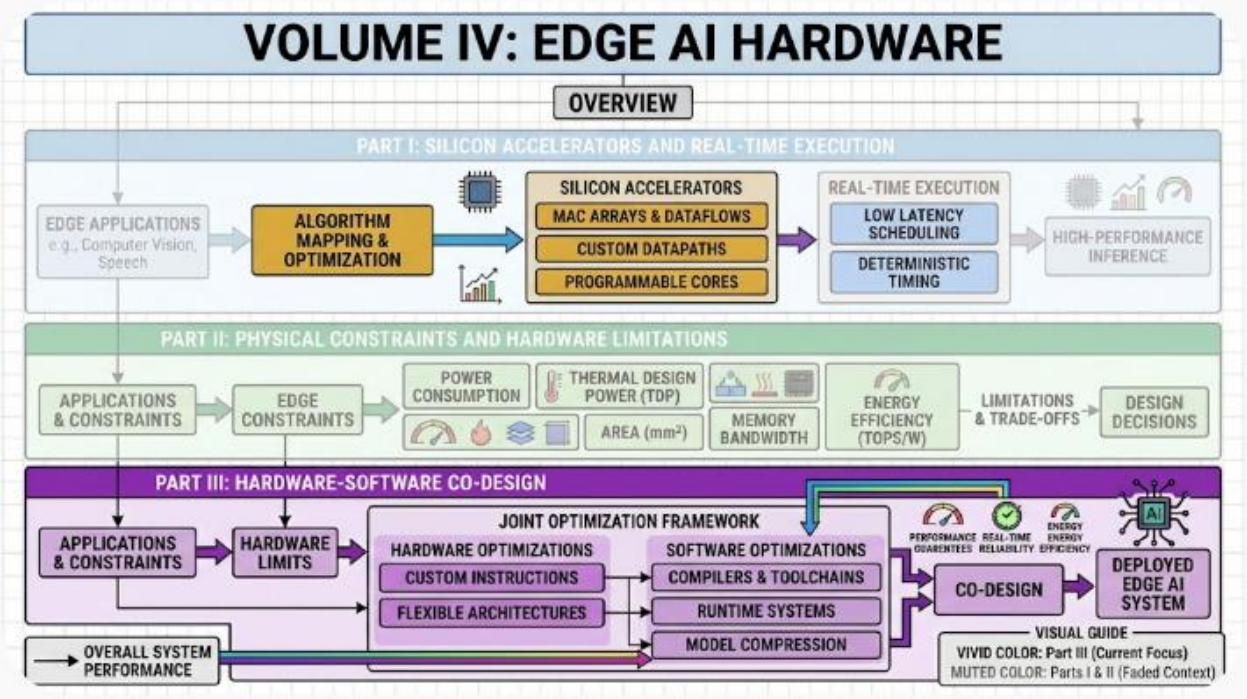


Figure V4.3B — Architectural Overview of Volume IV: Edge AI Hardware, Silicon Accelerators, and Systems Co-Design — Part III: Hardware–Software Co-Design and System Optimization.
Highlighting Section 8.4: Joint Optimization Frameworks, Domain-Specific Instruction Set Architectures (ISAs), Tensor Graph Compilers, and Hardware-Mapped Quantization and Pruning.

2. Six Foundational Areas of Hardware–Software Co-Design

Section 8.4 organizes the engineering discussion around six interdependent areas.

2.1 Model Architectures in AI Systems

Model architecture determines how computational workloads are structured and executed. Its design influences operation counts, memory footprint, data dependencies, parallelism, inference latency, and the ability to operate within constrained hardware environments.

This area examines architectural approaches relevant to efficient AI deployment, including structured sparsity, memory-efficient attention mechanisms, linear-attention and state-space architectures, and conditional computation.

These approaches address different sources of computational and memory overhead. Structured sparsity can reduce selected operations when supported by the execution hardware; memory-efficient attention seeks to reduce intermediate data movement and storage requirements; linear-attention and state-space approaches provide alternative mechanisms for

processing long sequences; and conditional computation activates selected portions of a model according to the input or execution requirements.

The central engineering principle is that model architecture should be evaluated in relation to its target hardware, memory capacity, numerical requirements, and application workload. A model with fewer theoretical operations does not necessarily execute faster unless its structure maps efficiently to the available processing resources.

2.2 Hardware Accelerators in AI Systems

Specialized accelerators provide the computational resources required to execute increasingly demanding AI workloads within constrained power and thermal budgets.

This area examines accelerator architectures and execution mechanisms, including low-precision numerical formats, on-chip scheduling, asynchronous vector execution, processing-in-memory approaches, static weight streaming, reconfigurable spatial architectures, and coarse-grained reconfigurable arrays.

It also considers emerging and hybrid accelerator concepts that combine different computational and memory technologies.

The discussion emphasizes several important design considerations:

- Matching numerical precision and computational operations to available hardware capabilities.
- Improving data reuse and reducing unnecessary transfers between memory and processing elements.
- Coordinating compute execution with memory bandwidth and data availability.
- Exploiting parallelism without exceeding power, thermal, or resource constraints.
- Evaluating sustained application performance rather than relying exclusively on peak theoretical throughput.

Accelerator effectiveness therefore depends on the interaction between computational architecture, memory hierarchy, software support, and the characteristics of the target AI workload.

2.3 Software Paradigms, Compilers, and Runtime Systems

Hardware capabilities become useful only when software can map workloads onto them effectively. Compiler infrastructure and runtime systems provide the mechanisms for translating

AI models into executable operations, allocating resources, coordinating computation, and managing heterogeneous processing devices.

This area examines hardware-aware kernel compilation, operator and tensor optimization, multi-accelerator orchestration, overlapping computation with data transfers, dynamic memory management, and decentralized execution strategies.

Compiler transformations can improve execution efficiency through operator fusion, memory-aware scheduling, optimized kernel selection, and the elimination of unnecessary intermediate operations. Runtime systems coordinate the resulting workloads across available processors and accelerators, taking account of resource availability, data dependencies, and execution priorities.

The discussion also considers how parallel execution and multi-accelerator coordination can improve throughput while introducing additional challenges involving communication overhead, synchronization, memory allocation, and workload balancing.

The principal lesson is that software compilation and runtime management must be treated as architectural components of an AI system rather than as final implementation steps performed after hardware selection.

2.4 Sensor Pipelines and Multimodal Data Processing

Edge AI systems depend on continuous information from their physical environments. Sensor pipelines transform raw observations into data representations that AI models can process for perception, prediction, decision-making, and control.

This area examines high-throughput and low-latency sensor-processing mechanisms, including zero-copy data ingestion, on-chip preprocessing, multimodal synchronization, high-bandwidth frame decoding, and event-driven neuromorphic processing.

Particular attention is given to the movement of data from sensor acquisition through preprocessing and synchronization to model execution. Avoiding unnecessary memory copies, coordinating data transfers, and reducing processing overhead can improve throughput and lower end-to-end latency.

Multimodal systems introduce additional requirements because cameras, radar, LiDAR, inertial sensors, and other sources may operate at different sampling rates and produce data with different temporal and spatial characteristics. Timestamping, synchronization, calibration, buffering, and sensor-fusion mechanisms are therefore essential to maintaining the consistency and usefulness of combined observations.

The key engineering principle is that sensor-pipeline performance must be evaluated as part of the complete AI execution path. Faster inference alone cannot compensate for delayed, misaligned, or inadequately processed sensor information.

2.5 Real-Time Frameworks and Predictable AI Execution

Real-time AI systems must coordinate computation according to explicit temporal requirements. A correct result may have limited operational value if it becomes available after the deadline for the intended decision or control action.

This area examines deterministic runtime mechanisms, telemetry-driven adaptation, inter-process communication, virtualized execution environments, and edge-to-cloud execution strategies.

The technical discussion addresses mechanisms for controlling execution variability, managing communication between critical tasks, isolating workloads, monitoring system conditions, and adapting resource allocation in response to changing computational demand.

Telemetry can provide information about processor utilization, memory pressure, accelerator availability, and thermal conditions. Runtime systems can use such information to guide workload placement and resource management, provided that adaptation itself is bounded and does not compromise critical timing requirements.

Virtualization and multi-tenant isolation introduce additional considerations involving resource partitioning, execution interference, and communication overhead. Edge-to-cloud execution introduces network latency and variability, making it necessary to distinguish workloads that can tolerate remote processing from those that require local execution.

An important qualification is that deterministic behavior and hard real-time guarantees cannot be established by a runtime framework or scheduling mechanism alone. They depend on the complete hardware–software configuration, explicit workload assumptions, bounded resource behavior, timing analysis, and system-level verification and validation.

2.6 Cross-Layer Optimization and System Integration

Cross-layer optimization integrates the preceding areas into a coordinated engineering methodology. Rather than optimizing models, processors, compilers, memory systems, sensor pipelines, and runtime environments independently, it evaluates how decisions at one layer affect the behavior and performance of the complete system.

This area examines AI intermediate representations and compilation foundations, graph simplification, hardware-aware neural architecture search, silicon-to-software observability,

and secure enclave architectures.

Important mechanisms include:

- **Intermediate representations and compiler integration:** Providing structured representations through which models and computational graphs can be transformed, analyzed, and mapped to different hardware targets.
- **Graph-level simplification:** Reducing unnecessary operations and improving computational structure while preserving the intended model behavior.
- **Hardware-aware neural architecture search:** Exploring model architectures in relation to target hardware characteristics and measurable deployment objectives.
- **Silicon-to-software observability:** Connecting hardware telemetry, compiler information, runtime measurements, and application-level performance to identify bottlenecks and guide optimization.
- **Secure execution environments:** Using hardware-supported isolation and protected execution mechanisms to strengthen the confidentiality and integrity of sensitive AI workloads.

These methods support a more systematic approach to design-space exploration and performance optimization. They also make it possible to evaluate trade-offs among accuracy, latency, throughput, energy consumption, memory requirements, security, reliability, and implementation complexity.

The objective is not to maximize every metric simultaneously, but to identify a configuration that satisfies the application's requirements while balancing competing system constraints.

3. Integrated Engineering Principles

The six areas establish several principles that guide the design and evaluation of practical edge AI systems.

First, model and hardware design must be coordinated. Computational structures, numerical formats, memory requirements, and accelerator capabilities should be considered together from the early stages of development.

Second, data movement must be optimized alongside computation. Memory transfers, sensor ingestion, synchronization, and communication can dominate end-to-end latency even when accelerator throughput is high.

Third, compilation and runtime systems are part of the hardware architecture. Their ability to map, schedule, and manage workloads directly influences hardware utilization and system responsiveness.

Fourth, real-time requirements must be evaluated end to end. Sensor acquisition, preprocessing, inference, communication, and downstream processing collectively determine whether an application can meet its timing objectives.

Fifth, optimization must account for physical operating conditions. Power limits, thermal behavior, memory capacity, and resource contention affect sustained performance and may change the feasibility of a design.

Finally, security, observability, and validation must be integrated into the engineering process. A high-performance system must also provide appropriate mechanisms for monitoring its behavior, protecting critical workloads, identifying failures, and demonstrating that its requirements are satisfied.

4. Engineering Value and Practical Applications

The methodologies developed in Part III provide a foundation for engineering teams responsible for deploying AI on heterogeneous and resource-constrained computing platforms.

For AI researchers and model developers, the material explains how model topology, numerical precision, sparsity, and computational complexity influence deployment feasibility.

For hardware and accelerator architects, it provides a framework for evaluating processing structures, memory organization, data movement, and hardware capabilities in relation to representative AI workloads.

For compiler and runtime engineers, it highlights the importance of hardware-aware compilation, optimized execution graphs, memory scheduling, workload orchestration, and heterogeneous resource management.

For embedded-system and robotics engineers, it connects sensor processing, multimodal synchronization, inference execution, and real-time behavior within complete system architectures.

For technical leaders and system architects, it provides a basis for evaluating alternative designs across performance, energy consumption, latency, accuracy, thermal limits, security, and integration complexity.

These principles are relevant to autonomous vehicles, industrial robotics, intelligent

manufacturing, distributed sensing, aerial platforms, and other applications in which AI computation must operate within defined physical and operational constraints.

5. Relationship to Parts I and II of Volume IV

Part III completes the technical progression established throughout Volume IV.

Part I: Silicon Accelerators and Deterministic Real-Time Execution (Sections 8.1–8.2) introduced the computational hardware, specialized accelerators, communication interfaces, and real-time execution mechanisms that support edge AI workloads.

Part II: Physical Constraints and Hardware Limitations (Section 8.3) examined the physical boundaries that govern these systems, including power consumption, thermal dissipation, memory capacity, bandwidth limitations, and latency budgets.

Part III: Hardware–Software Co-Design and System Optimization (Section 8.4) integrates these foundations through coordinated optimization across model architectures, hardware accelerators, software toolchains, sensor pipelines, real-time frameworks, and system-level execution.

Together, the three parts establish a unified engineering perspective:

- Part I explains the computational and execution foundations.
- Part II identifies the physical constraints governing their operation.
- Part III develops the cross-layer methodologies for optimizing the complete system.

This progression moves from understanding individual technologies to engineering their interactions within an integrated edge AI platform.

6. Overall Contribution

The principal contribution of Part III is its treatment of hardware–software co-design as a system-level engineering discipline. It demonstrates why practical AI deployment requires more than selecting a capable accelerator or optimizing an individual neural network. The model, silicon architecture, compiler, runtime, memory system, sensor pipeline, and execution framework must be considered together.

There is no universally optimal hardware–software configuration. Different applications impose different requirements, and improvements in one dimension may introduce costs in another. Reducing numerical precision, for example, may improve computational efficiency but requires appropriate accuracy evaluation. Increasing parallelism may improve throughput while increasing memory contention or power demand. Moving computation to a remote resource

may expand available processing capacity while introducing communication latency and dependence on network conditions.

Effective co-design therefore requires measurable objectives, informed architectural choices, representative workload testing, and systematic validation. It also requires an understanding of how local optimizations influence system-level behavior.

Ultimately, Part III establishes the engineering framework for translating AI models and specialized silicon into integrated computing systems that can operate efficiently within real-world constraints. By connecting model architecture, hardware capabilities, software execution, sensing, timing, observability, and security, it completes the hardware and systems foundation developed throughout Volume IV.

The broader objective is to advance edge AI engineering from isolated component optimization toward **coordinated, measurable, and validated system-level design**—a foundation for intelligent platforms that are efficient, responsive, adaptable, and suitable for deployment in increasingly demanding physical environments.

ABOUT THIS VOLUME

A Practical Guide to Hardware–Software Co-Design, AI Accelerators, and Edge AI System Optimization

Volume IV, Part III of *Frontier AI Engineering: Agentic AI Autonomy, Multimodal Artificial Intelligence, and Deterministic Edge AI Intelligence* examines how AI models, computing hardware, software execution environments, and sensor-processing pipelines can be designed and optimized as an integrated system.

As artificial intelligence moves beyond centralized computing environments into embedded devices, robots, industrial platforms, autonomous machines, and other edge applications, system designers must address constraints that extend beyond model accuracy or computational throughput. Memory capacity, data movement, power consumption, thermal behavior, sensor timing, execution latency, and resource contention can all influence whether an AI application performs effectively in its intended environment.

Hardware–software co-design provides a systematic approach to these challenges. Rather than optimizing an AI model, compiler, processor, or sensor pipeline in isolation, it considers how decisions at one layer affect the performance and behavior of the complete system. A model architecture influences computational demand; the selected accelerator determines which operations can be executed efficiently; compiler and runtime decisions affect memory traffic and scheduling; and sensor acquisition and synchronization influence the quality and timeliness of the information supplied to the model.

This part focuses on the engineering principles and design methods needed to understand these relationships. It brings together model architecture, hardware acceleration, software execution, sensor pipelines, real-time frameworks, and cross-layer optimization to establish a system-level perspective on edge AI engineering.

Target Audience

This part is intended for readers who design, implement, evaluate, or study AI systems operating under practical hardware and software constraints.

AI Researchers and Machine Learning Engineers

Researchers and engineers developing neural networks and other AI models will find material relevant to understanding how model architecture, numerical precision, memory requirements, and computational complexity affect deployment on resource-constrained hardware. The discussion also provides context for evaluating model optimization techniques in relation to

actual execution platforms rather than theoretical operation counts alone.

Hardware Engineers and Accelerator Architects

Hardware engineers, embedded-system designers, and processor architects can use this material to examine how accelerator capabilities interact with model workloads, memory hierarchies, data movement, software toolchains, and system-level requirements. Topics include hardware-aware design decisions, computational efficiency, power and thermal constraints, and the importance of evaluating accelerators with representative workloads.

Software, Compiler, and Runtime Engineers

Software engineers working on AI deployment, compiler toolchains, runtime environments, and embedded computing systems will find guidance on the interactions among model graphs, operator execution, memory allocation, workload scheduling, and heterogeneous processing resources. The material emphasizes that efficient execution depends not only on the capabilities of the hardware but also on how software maps and manages workloads on that hardware.

Embedded-System Architects and Robotics Engineers

System architects and robotics engineers can use this part to understand the relationships among sensing, computation, timing, and control. Particular attention is given to sensor-data processing, synchronization, resource allocation, end-to-end latency, and the challenges of maintaining system performance under power, thermal, and computational constraints.

Technical Leaders and Engineering Decision-Makers

Technical leaders responsible for selecting AI platforms or defining system architectures will find a framework for comparing design alternatives across multiple criteria. These include latency, energy consumption, memory capacity, model accuracy, programmability, thermal behavior, software support, and integration complexity. The objective is to support informed engineering trade-offs rather than relying on a single performance metric.

Graduate Students and Advanced Practitioners

Graduate students, advanced undergraduates, and self-directed learners with a foundation in computing or artificial intelligence can use this part to develop a system-level understanding of edge AI implementation. The material connects AI model concepts with hardware architecture, software execution, sensor processing, and practical system optimization.

Prerequisites

Readers will benefit most from this part if they have a basic understanding of artificial

intelligence, computer architecture, and software engineering. Extensive prior experience designing custom processors or developing production AI compilers is not required, although familiarity with embedded computing will be helpful.

Conceptual and Technical Background

Recommended background includes:

- Fundamental concepts in machine learning and neural network architectures.
- A general understanding of AI training and inference.
- Basic computer architecture, including processors, memory, and data movement.
- Familiarity with software execution, operating systems, and concurrent workloads.
- General knowledge of sensors and embedded computing systems.

Mathematical and Engineering Background

Readers should be comfortable with basic algebra, performance calculations, graphs, and quantitative comparisons. Familiarity with latency, throughput, memory capacity, bandwidth, power, and energy will help readers follow the engineering analyses.

More advanced topics may involve numerical precision, computational complexity, scheduling, and resource utilization. These concepts should be interpreted in the context of the system being analyzed; not every discussion requires detailed mathematical derivations.

Readers without a specialized hardware background can focus initially on the architectural explanations and engineering examples, then revisit the more quantitative material as needed.

Scope of Volume IV – Part III

This part concentrates on **Section 8.4: Hardware–Software Co-Design: AI Accelerators, Sensor Pipelines, and Cross-Layer Optimization**. Its scope is organized around six closely related areas.

1. Model Architectures in AI Systems

This area examines how the structure of an AI model affects computational demand, memory footprint, data flow, and deployment feasibility. It considers why model architecture should be evaluated in relation to the target hardware and application requirements.

2. Hardware Accelerators in AI Systems

This area examines specialized processing resources for AI workloads, including the capabilities and limitations that influence computational throughput, memory access, power consumption,

and sustained performance. It emphasizes evaluating hardware using representative application workloads rather than relying exclusively on peak theoretical specifications.

3. Software Paradigms in AI Systems

This area considers how software architecture, compiler transformations, runtime systems, concurrency, and resource management influence AI execution. It explores how software decisions affect hardware utilization, memory traffic, responsiveness, and the coordination of multiple workloads.

4. Sensor Pipelines in AI Systems

This area examines the processing path from sensor acquisition to model-ready data and downstream system outputs. Relevant concerns include preprocessing, timestamping, synchronization, data transfer, buffering, sensor quality, and the effects of pipeline design on end-to-end latency and system behavior.

5. Real-Time Frameworks in AI Systems

This area addresses the timing requirements of AI-enabled systems. It considers scheduling, deadlines, execution variability, resource contention, and the distinction between average performance and demonstrated timing guarantees. Real-time behavior must be assessed against the actual system requirements and supported by appropriate analysis and validation.

6. Cross-Layer Optimization in AI Systems

This area brings the preceding topics together. It examines how coordinated decisions across model design, hardware selection, compilation, memory management, sensor processing, scheduling, and system integration can improve overall performance. It also considers the trade-offs among latency, energy consumption, accuracy, reliability, security, and implementation complexity.

These six areas are interdependent. A model that is computationally efficient may still perform poorly if its operations map inefficiently to the accelerator. A fast accelerator may not improve system responsiveness if sensor synchronization or data movement dominates latency. Similarly, an optimized inference kernel does not by itself establish that the complete application will meet its timing, energy, or reliability requirements.

The central objective of this part is therefore to develop an integrated engineering perspective in which component-level decisions are evaluated according to their effects on the complete AI system.

Relationship to the Broader Series

Volume IV addresses the hardware and system-engineering considerations involved in implementing AI capabilities on physical computing platforms. Part III builds on the broader hardware and physical-constraint topics developed elsewhere in Volume IV by focusing on how those considerations can be coordinated through hardware–software co-design.

Readers who have studied the preceding parts of Volume IV may approach Section 8.4 as a synthesis of earlier material. Readers who are primarily interested in system integration may also use this part as a focused reference, consulting earlier discussions of hardware architectures, memory, power, thermal behavior, and real-time execution when additional background is needed.

The broader series provides context for the AI models and autonomous applications that may run on these platforms. However, the principal concern of this part is not the general theory of agentic AI or multi-agent coordination. Its emphasis is the engineering of the computing systems that execute AI workloads and the interactions among hardware, software, sensing, and timing.

How to Use This Part

Readers can approach the material according to their objectives.

Sequential Study. Readers seeking a systematic understanding should follow Section 8.4 from model architecture through hardware acceleration, software execution, sensor pipelines, real-time frameworks, and cross-layer optimization. This progression moves from individual design elements toward their integration into a complete system.

Focused Technical Reference. Readers addressing a particular engineering problem can begin with the relevant topic. For example, accelerator selection may require attention to model architecture and software mapping, while a latency problem may require examining sensor acquisition, memory transfers, inference execution, and scheduling together.

Engineering Analysis and Design. Readers applying the material to a project should identify the application's requirements before selecting an optimization strategy. Relevant requirements may include latency targets, energy or power budgets, memory limits, accuracy thresholds, thermal conditions, security needs, and failure-handling behavior. Design alternatives should then be evaluated against these requirements using appropriate measurements and analysis.

Assessments and Exercises. The assessment material associated with Section 8.4 can be used to reinforce conceptual understanding, practice quantitative reasoning, and evaluate system-level

trade-offs. Applied exercises encourage readers to distinguish theoretical specifications from measured performance and to identify assumptions that require verification.

Primary Objective

The primary objective of Volume IV, Part III is to help readers understand and apply the principles of hardware–software co-design to AI systems operating under real-world constraints.

By examining model architectures, accelerators, software execution, sensor pipelines, real-time frameworks, and cross-layer optimization as connected engineering concerns, this part provides a foundation for reasoning about the performance and behavior of complete edge AI systems.

The intended outcome is not a single universally optimal architecture. Different applications impose different requirements, and improvements in one dimension may introduce costs in another. Instead, this part develops the ability to identify relevant constraints, compare alternative designs, understand interactions across system layers, and validate engineering decisions against measurable objectives.

The guiding principle is that effective edge AI engineering depends not only on the capability of an individual model or processor, but also on how the complete system is designed, integrated, measured, and validated.

LIST OF FIGURES & TABLES

List of Tables

Table 8.4 — Core Components of Hardware–Software Co-Design in Autonomous AI Systems 6

Table 8.4-A — Core Architectural Dimensions in Model Architectures for Autonomous AI Systems 19

Table 8.4-A1 — Operational Efficiency vs Architectural Limits 28

Table 8.4-A2— Structured AI Sparsity Mechanisms and Hardware Alignment 48

Table 8.4-A3 — Memory Optimized AI Attention Mechanisms for Bandwidth Constrained Models 68

Table 8.4-A4 — Core Mechanisms in Linear Attention and State Space AI Architectures 88

Table 8.4-A5 — Core Mechanisms in Conditional Computation AI Micro Architectures 107

Table 8.4-B — Core Accelerator Dimensions in AI Hardware 125

Table 8.4-B1 — Core Mechanisms in AI Low Precision Data Types 132

Table 8.4-B2 — Core Mechanisms in On Chip AI Schedulers and Asynchronous Vector Execution Pipelines 150

Table 8.4-B3 — Core Mechanisms in AI Processing in Memory and On Die Static Weight Streaming 172

Table 8.4-B4 — Core Mechanisms in Reconfigurable AI Spatial Architectures and Coarse Grained Arrays 187

Table 8.4-B5 — Architectural Components of Hybrid AI Co Processors Integrating Non Volatile Memory Lattices and Optical Interconnects 206

Table 8.4-C — Core Software Paradigms in AI Systems 230

Table 8.4-C1 — Core Mechanisms in Hardware Aware AI Kernel Compilation 238

Table 8.4-C2 — Distributed AI Orchestration Mechanisms Across Multi Accelerator Systems 260

Table 8.4-C3 — AI Latency Masking Mechanisms for Overlapped Compute and Fabric-Level Transfers 283

Table 8.4-C4 — Memory-Elastic Mechanisms for Dynamic AI Defragmentation and PagedAttention Retention 296

Table 8.4-C5 — Mechanisms Enabling Decentralized AI Execution and Federated Asymmetric Coordination 309

Table 8.4-D — Mechanisms Enabling High Fidelity, Low Latency Sensor Pipelines in AI Systems 324

Table 8.4-D1 — Zero-Copy Ingestion Mechanisms for Autonomous AI Systems 329

Table 8.4-D2 — On Chip AI Preprocessing Engines and Their Operational Roles 348

Table 8.4-D3 — Multi-Modal AI Sensor Synchronization Mechanisms and Their Operational Roles 367

Table 8.4-D4 — High-Bandwidth AI Frame Decoding Mechanisms and Their Operational Roles 387

Table 8.4-D5 — Neuromorphic AI Event Processing Mechanisms and Their Operational Roles 406

Table 8.4-E — Real Time AI Framework Mechanisms and Their Operational Roles 424

Table 8.4-E1 — Deterministic AI Runtime Mechanisms and Their Execution Guarantees 430

Table 8.4-E2 — Telemetry-Driven AI Adaptation Mechanisms and Their Stability Guarantees 442

Table 8.4-E3 — Deterministic AI IPC Mechanisms and Their Real Time Guarantees 454

Table 8.4-E4 — Virtual AI Prototyping Mechanisms and Their Isolation Guarantees 465

Table 8.4-E5 — Edge-to-Cloud Continuum Mechanisms and Their Deterministic Guarantees 477

Table 8.4-F — Cross Layer Optimization in AI Systems 495

Table 8.4-F1 — AI Intermediate Representation and Compilation Foundations 507

Table 8.4-F2 — AI Graph Simplification Foundations 527

Table 8.4-F3 — Hardware Aware NAS Optimization Dimensions 554

Table 8.4-F4 — Silicon to Software AI Observability Dimensions 584

Table 8.4-F5 — Full Stack AI Secure Enclave Defense Dimensions 608

List of Figures

Figure V4 — Architectural Overview of Volume IV: Edge AI Hardware, Silicon Accelerators, and Systems Co-Design

vii

Figure V4.3A — Volume IV – Part III Architectural Overview xv

Figure V4.3B — Architectural Overview of Volume IV: Edge AI Hardware, Silicon Accelerators, and Systems Co-Design — Part III: Hardware–Software Co-Design and System Optimization xix

Figure 8.4 — Hardware–Software Co Design Stack for Autonomous AI Systems 11

Figure 8.4-A1 - Architectural Limits vs Operational Efficiency in the Roofline Model 31

Figure 8.4-A2 — Tensor Core Aligned Structured Sparsity Pipeline 52

Figure 8.4-A3 — Memory Optimized Attention Pipeline for Bandwidth Constrained AI Models 73

Figure 8.4-A4 — AI Systems Dataflow Architecture of Linear Attention and State Space Models 93

Figure 8.4-A5 — Conditional Computation Dataflow Architecture in AI Systems 111

Figure 8.4-B1 — AI Low Precision Execution Pipeline 136

Figure 8.4-B2 — On Chip AI Scheduler and Asynchronous Vector Execution Pipeline Overview 155

Figure 8.4-B3 — AI Processing in Memory and On Die Static Weight Streaming Overview 177

Figure 8.4-B4 — Reconfigurable AI Spatial Architecture and CGRA Topology Overview 192

Figure 8.4-B5 — Hybrid AI Co Processor Architecture Integrating Non Volatile Memory Lattices and Optical Interconnects 212

Figure 8.4-C1 — Software–Hardware Alignment in Tile Optimized Kernel Compilation 243

Figure 8.4-C2 — Distributed AI Parallelism Modes Across Multi Accelerator Execution Fabric 265

Figure 8.4-C3 — Overlapped Compute and Fabric-Level Transfers in Distributed AI Execution 285

Figure 8.4-C4 — Dynamic Memory Defragmentation and PagedAttention Retention in Distributed AI Execution 298

Figure 8.4-C5 — Decentralized AI Execution, Local Cache Eviction, and Federated Asymmetric Protocols 311

Figure 8.4-D — Sensor Pipelines in AI Systems 326

Figure 8.4-D1 — Zero-Copy AI Ingestion Architecture 332

Figure 8.4-D2 — On-Chip AI Preprocessing Architecture 350

Figure 8.4-D3 — Multi-Modal AI Sensor Synchronization Architecture 368

Figure 8.4-D4 — High-Bandwidth AI Frame Decoding and Starvation-Control Architecture 389

Figure 8.4-D5 — Neuromorphic AI Event Slicing and Asynchronous Embedding Architecture 408

Figure 8.4-E — Real Time AI Execution and Distributed Determinism Architecture 426

Figure 8.4-E1 — Deterministic AI Runtime and Predictable Execution Architecture 432

Figure 8.4-E2 — Telemetry-Driven AI Adaptation and Thermal-Safe Execution Architecture 444

Figure 8.4-E3— Deterministic AI IPC Fabric with Hard Real Time Messaging and Fail Safe Interrupts 455

Figure 8.4-E4 — Virtual AI Prototyping Architecture with Multi Tenant Isolation and Hardware Sliced Context Domains 467

Figure 8.4-E5 — Edge-to-Cloud AI Continuum Splitting with Dynamic Layer Offload and Jitter-Buffered Networking 479

Figure 8.4-F — Cross Layer Optimization Continuum 498

Figure 8.4-F1 — AI Intermediate Representation Compilation Flow 509

Figure 8.4-F2 — AI Graph Simplification Flow 530

Figure 8.4 F3 — Hardware Aware NAS Optimization Flow 559

Figure 8.4-F4 — Silicon-to-Software AI Observability Flow 587

Figure 8.4 F5 — Full Stack AI Secure Enclave Defense Flow 610

Figure A3 — End-to-End Edge AI Model Optimization, Compression, and Compiler Deployment Pipeline 713

Volume IV:

Edge AI Hardware, Silicon Accelerators & Systems Co-Design

PART III

Hardware–Software Co-Design and System Optimization

Chapter 8: Edge AI Accelerators, Real-Time Systems, and Hardware–Software Co-Design

Chapter Overview & Part III Scope

Chapter 8 examines the hardware foundations, physical constraints, and system-level co-design principles that enable artificial intelligence to operate efficiently, reliably, and safely on real-time edge platforms. As AI increasingly migrates from centralized cloud environments to autonomous vehicles, intelligent robotics, industrial automation systems, aerospace platforms, and distributed sensing infrastructures, successful deployment requires the integration of specialized hardware, deterministic execution frameworks, and optimization strategies that span the entire computing stack.

Part I (Sections 8.1–8.2) established the computational and runtime foundations of Edge AI through specialized accelerator architectures, sensor-ingestion infrastructures, and deterministic real-time operating environments. **Part II (Section 8.3)** then quantified the physical boundaries that constrain these systems, including power dissipation, thermal-management requirements, memory-bandwidth limitations, latency budgets, and timing variability. Together, these sections demonstrated that AI performance at the edge is governed not only by algorithms and computational resources but also by the physical realities of energy, heat, memory movement, and real-time execution.

Building upon those foundations, **Part III (Section 8.4)** focuses on the integration and optimization of the complete hardware-software ecosystem. While Parts I and II examined the computational architecture and physical constraints of Edge AI platforms, Part III explores how those elements can be jointly optimized to achieve higher performance, greater efficiency, improved reliability, and stronger system-level resilience.

Section 8.4 — Hardware–Software Co-Design and System Optimization

Section 8.4 examines the principles and methodologies of **hardware-software co-design**, in which algorithms, compiler infrastructures, runtime systems, and silicon architectures are developed and optimized as a unified system rather than as independent components.

Key topics include:

- Cross-layer optimization frameworks spanning hardware, runtime, compiler, and application levels.
- Domain-specific compiler toolchains for AI accelerators and heterogeneous computing platforms.

- Tensor-graph transformations and execution-graph optimization techniques.
- Hardware-aware quantization, pruning, sparsity exploitation, and model-compression strategies.
- Memory-aware and bandwidth-aware workload optimization.
- Runtime adaptation and workload-placement mechanisms.
- Security hardening for Edge AI accelerators and embedded systems.
- Fault-tolerant architectures and resilience mechanisms for autonomous operation.
- Silicon-level reliability, verification, and protection techniques.

These topics demonstrate how system performance emerges from the coordinated interaction of hardware resources, compiler transformations, runtime scheduling, memory-management strategies, and AI model architectures. In modern Edge AI platforms, significant performance gains often arise not from improvements in any single subsystem but from the optimization of interactions among multiple layers of the computing stack.

Part III therefore serves as the architectural synthesis of Chapter 8. It connects the specialized silicon capabilities introduced in Part I with the physical limits analyzed in Part II and demonstrates how co-design methodologies can maximize performance while respecting the constraints imposed by power, thermal behavior, memory capacity, communication bandwidth, and real-time execution requirements.

Taken together, Section 8.4 establishes the **unified hardware-software co-design substrate** that underlies contemporary Edge AI systems. It illustrates how computational architectures, compiler technologies, runtime environments, security mechanisms, and resilience frameworks can be optimized collectively to create intelligent systems capable of operating efficiently and predictably within the demanding conditions of real-world physical environments.

Section 8.4: Hardware–Software Co-Design: AI Accelerators, Sensor Pipelines, and Cross-Layer Optimization

The rapid expansion of artificial intelligence (AI) workloads has pushed computing architectures to a structural inflection point. For decades, the industry relied on strict abstraction boundaries: algorithm designers optimized mathematical formulations and convergence behavior while hardware architects delivered increasingly capable silicon through predictable scaling trends. This separation is no longer viable. The slowdown of Dennard scaling, the emergence of dark silicon, and the extreme computational demands of modern deep learning have collapsed the traditional divide between software and hardware. Treating these domains as independent entities now produces severe inefficiencies, unpredictable performance, and unsustainable energy costs.

Earlier material examined the specialized hardware that underpins contemporary AI systems—Graphics Processing Units (GPUs), Tensor Processing Units (TPUs), neuromorphic processors, and Application-Specific Integrated Circuits (ASICs)—and the immutable physical constraints that govern their operation, including thermal envelopes, power budgets, memory bandwidth ceilings, and latency limits. These constraints define the outer boundaries of feasible computation. Part III advances from understanding these limits to engineering systems that operate within them through deliberate, integrated co-design.

Hardware–software co-design replaces the legacy model of optimizing software atop fixed hardware or manufacturing hardware for static computational graphs. Instead, it establishes a concurrent, bidirectional design process in which algorithmic structure, execution runtimes, compiler toolchains, memory hierarchies, and hardware data paths are shaped together. This approach ensures that intelligence is not merely computed but delivered efficiently, predictably, and safely under real-world constraints.

High-performance embedded autonomy depends on tight integration across six foundational pillars:

- **Model Architectures in AI Systems** – Model architectures define the structure of intelligence, determining how perception, prediction, and control are organized and how inference pathways adapt under stress. Their topology influences computational load, memory footprint, and the system's ability to degrade gracefully under resource constraints.
- **Hardware Accelerators in AI Systems** – Hardware accelerators provide the computational substrate for real-time autonomy. Their parallelism, thermal characteristics, and power efficiency determine which models can execute, how quickly

they respond, and how long they can sustain operation under demanding conditions.

- **Software Paradigms in AI Systems** – Software paradigms govern how autonomy is expressed and executed across heterogeneous hardware. They define concurrency models, scheduling policies, memory isolation, and safety boundaries, ensuring predictable behavior even when workloads spike or hardware becomes partially degraded.
- **Sensor Pipelines in AI Systems** – Sensor pipelines transform raw environmental data into actionable state representations. Their fidelity, latency, and robustness determine how effectively the system can perceive hazards, track agents, and maintain situational awareness under noise, occlusion, or sensor degradation.
- **Real-Time Frameworks in AI Systems** – Real-time frameworks enforce deterministic timing across perception, prediction, and control loops. Their guarantees prevent latency-induced hazards, ensuring that critical operations execute within strict deadlines even during stress or rapid environmental change.
- **Cross-Layer Optimization in AI Systems –** Cross-layer optimization aligns all layers of the autonomy stack, enabling dynamic adaptation to hardware limits, environmental stressors, and mission demands. It integrates model behavior, accelerator performance, software scheduling, sensor fidelity, and timing guarantees into a cohesive, resilient system.

Through these dimensions, Section 8.4 provides a comprehensive methodology for overcoming contemporary compute plateaus. By requiring software and hardware to interact deliberately at every layer of the execution stack, co-design unlocks the efficiency thresholds necessary for scalable, resilient, and ubiquitous artificial intelligence. This philosophy forms the foundation of modern autonomous systems, enabling reliable, efficient, and safe AI deployment across industrial, commercial, and mission-critical environments.

The six pillars of hardware–software co-design form an integrated framework for engineering autonomous AI systems that can operate reliably under real-world constraints. Each pillar contributes a distinct dimension of resilience, efficiency, and predictability, yet none can function in isolation. Their interactions determine how intelligence is structured, how computation is delivered, how data is interpreted, and how timing guarantees are enforced. To clarify these relationships, the following table organizes the core components of co-design into a unified view, highlighting their roles, constraints, and contributions to system safety.

The preceding sections in Volume IV – Part I and Volume IV – Part II examined the physical

constraints, robustness challenges, fail-safe mechanisms, coordination strategies, and communication fallback protocols that influence the reliability of autonomous AI systems. Collectively, these discussions reveal a common theme: system behavior cannot be understood by analyzing hardware, software, sensing, communication, or AI models in isolation. Decisions made at one layer often create constraints or opportunities at another. A perception model affects processor utilization, processor limitations influence scheduling decisions, scheduling behavior alters latency characteristics, and latency directly impacts safety-critical control functions. As a result, modern autonomous systems increasingly rely on **hardware–software co-design**, an engineering approach in which computational architectures, AI models, sensing pipelines, runtime frameworks, and safety mechanisms are designed as an integrated system. Table 8.4 introduces the core components of this co-design philosophy and illustrates how coordinated optimization across multiple system layers contributes to resilient and safe autonomous operation.

Table 8.4 presents the principal elements that comprise hardware–software co-design within autonomous AI systems. Hardware–software co-design is an engineering methodology that treats computational infrastructure, AI algorithms, operating frameworks, sensing architectures, and control systems as interdependent components of a single integrated platform.

Traditional computing systems often separate hardware and software development into largely independent activities. Autonomous AI systems, however, operate under strict constraints involving power consumption, thermal budgets, memory capacity, communication latency, safety requirements, and real-time responsiveness. Optimizing one subsystem without considering the others can create bottlenecks that compromise overall system performance.

The table identifies six foundational co-design components: model architectures, hardware accelerators, software paradigms, sensor pipelines, real-time frameworks, and cross-layer optimization mechanisms. Together, these components define the structure through which sensing, computation, decision-making, and control interact within an autonomous platform.

For each component, the table highlights its role within the broader co-design ecosystem, the primary constraints influencing implementation, and the corresponding safety benefits obtained through effective integration. This perspective emphasizes that autonomous-system reliability emerges from coordinated design across all computational layers rather than from isolated optimization efforts.

Table 8.4 — Core Components of Hardware–Software Co-Design in Autonomous AI Systems

Component	Role in Co-Design	Key Constraints	Safety Contribution
Model Architectures	Structure intelligence and inference pathways	Compute load, memory footprint, latency	Enables graceful degradation and predictable decision-making
Hardware Accelerators	Provide specialized compute for autonomy	Thermal limits, power budget, parallelism	Maintains real-time perception and control under stress
Software Paradigms	Govern scheduling, concurrency, and execution	Determinism, resource contention, isolation	Prevents timing failures and unsafe interactions
Sensor Pipelines	Convert raw data into actionable state	Noise, occlusion, bandwidth, calibration	Preserves situational awareness during degradation
Real-Time Frameworks	Enforce timing guarantees across loops	Deadline enforcement, jitter, priority	Prevents latency-induced hazards and instability
Cross-Layer Optimization	Aligns behavior across all layers	Heterogeneous constraints, dynamic load	Ensures adaptive, resilient autonomy under stress

Table 8.4 demonstrates that reliable autonomous operation depends upon coordinated interaction among hardware, software, sensing, and control subsystems. Each component contributes unique capabilities and constraints, yet no component independently determines system performance or safety.

The table illustrates that hardware–software co-design is fundamentally concerned with balancing competing requirements, including computational capability, timing guarantees, resource efficiency, and operational reliability. Successful autonomous systems therefore emerge from system-level optimization rather than component-level excellence alone.

The first component identified in the table is **model architectures**, which define the structure of perception, prediction, planning, and inference pipelines. Model architectures determine how information flows through the AI system and influence computational complexity, memory

requirements, latency characteristics, and decision quality.

The table highlights compute load, memory footprint, and latency as key design constraints. These factors directly affect the feasibility of deployment on embedded platforms and real-time systems. From a safety perspective, well-designed model architectures support graceful degradation and predictable behavior by ensuring that computational demands remain aligned with available resources. Consequently, the model architecture often serves as the starting point for broader co-design decisions.

Closely related are **hardware accelerators**, which provide specialized computational resources capable of executing AI workloads efficiently. Graphics processing units (GPUs), tensor processing units (TPUs), field-programmable gate arrays (FPGAs), and dedicated AI accelerators exist specifically to handle the computational intensity of machine-learning algorithms.

The table identifies thermal constraints, power budgets, and parallel-processing limitations as primary concerns. These constraints become particularly important in autonomous platforms operating under strict energy and cooling limits. The safety contribution of hardware accelerators stems from their ability to maintain real-time perception and control performance even under demanding operational conditions. Without sufficient computational resources, latency increases and decision-making may become unstable.

The third component, **software paradigms**, governs how computational resources are managed. Scheduling policies, concurrency strategies, process isolation mechanisms, and execution models determine how workloads compete for hardware resources.

The table draws attention to determinism, resource contention, and isolation as major challenges. Autonomous systems frequently execute multiple sensing, planning, control, and communication processes simultaneously. If execution priorities are poorly managed, timing failures can occur. Effective software architectures reduce these risks by ensuring predictable resource allocation and preventing unsafe interactions among competing system functions.

Another critical component is the **sensor pipeline**, which transforms raw environmental observations into information that can be used for decision-making. Sensor pipelines encompass acquisition, filtering, calibration, synchronization, feature extraction, and sensor-fusion processes.

The constraints identified in the table include noise, occlusion, bandwidth limitations, and calibration requirements. Because perception serves as the foundation for subsequent autonomy functions, sensor-pipeline reliability directly affects situational awareness. Effective pipeline design therefore contributes significantly to resilience by preserving environmental

understanding during degraded operating conditions.

The table next identifies **real-time frameworks** as a central element of autonomous-system design. Unlike conventional computing applications, autonomous systems must satisfy strict timing requirements. Sensor updates, planning cycles, and control commands must occur within well-defined deadlines.

The primary constraints governing real-time frameworks include deadline enforcement, jitter management, and priority scheduling. These frameworks contribute to safety by preventing latency-induced instability and ensuring that critical control loops remain synchronized with environmental conditions. In many cases, timely responses are as important as correct responses.

The final component is **cross-layer optimization**, which serves as the integrating mechanism connecting all other elements. Rather than optimizing perception, computation, communication, and control independently, cross-layer optimization seeks to align behavior across the entire stack.

The table correctly identifies heterogeneous constraints and dynamic workloads as important challenges. Autonomous systems frequently encounter changing environmental conditions, varying computational demands, and fluctuating resource availability. Cross-layer optimization enables adaptive responses that maintain acceptable performance despite these changes. As a result, the system remains resilient even when individual subsystems experience stress or degradation.

A broader insight emerging from the table is that each component contributes both capabilities and constraints. Model architectures provide intelligence but consume resources. Hardware accelerators provide performance but generate heat and require power. Sensor pipelines provide environmental awareness but introduce uncertainty and bandwidth requirements. Real-time frameworks improve responsiveness but impose strict scheduling requirements. Effective co-design therefore requires balancing benefits and limitations simultaneously.

The table also highlights the close relationship between efficiency and safety. Resource limitations are often viewed as performance problems, yet many resource constraints directly influence safety-critical behavior. Excessive latency, inadequate memory capacity, poor scheduling decisions, and sensing bottlenecks can all compromise reliable operation. Consequently, hardware–software co-design should be viewed as a safety engineering discipline as much as a performance engineering discipline.

From a systems-engineering perspective, the framework presented in the table encourages

holistic thinking. Individual subsystem optimization may improve local performance while degrading overall system behavior. By contrast, co-design emphasizes coordinated decision-making that accounts for interactions among all layers of the autonomy stack.

Another important observation is that co-design becomes increasingly important as system complexity grows. Advanced autonomous systems must integrate increasingly sophisticated AI models, diverse sensor suites, heterogeneous processors, real-time communication frameworks, and multi-agent coordination mechanisms. Managing these interactions requires deliberate architectural planning rather than independent subsystem development.

Ultimately, Table 8.4 demonstrates that hardware–software co-design is a foundational principle of modern autonomous-system engineering. Through the coordinated integration of model architectures, hardware accelerators, software paradigms, sensor pipelines, real-time frameworks, and cross-layer optimization strategies, autonomous AI systems can balance computational performance, resource constraints, timing requirements, and safety objectives. This integrated approach enables reliable operation under the demanding conditions that characterize real-world autonomous environments.

Table 8.4 identified the primary components that contribute to hardware–software co-design in autonomous AI systems, including model architectures, hardware accelerators, software paradigms, sensor pipelines, real-time frameworks, and cross-layer optimization mechanisms. While the table examined these elements individually, autonomous-system behavior emerges from their continuous interaction rather than from their isolated operation. Resource constraints encountered in one layer frequently propagate into other layers, creating complex dependencies among sensing, computation, scheduling, memory management, and control processes. Understanding these dependencies requires a structural view of the autonomy stack that highlights both vertical interactions and shared constraints. Figure 8.4 provides this perspective by illustrating the layered architecture of hardware–software co-design and showing how optimization decisions propagate across the entire autonomous-computing ecosystem.

Figure 8.4 presents a layered representation of the hardware–software co-design stack used in modern autonomous AI systems. The diagram illustrates how sensing, computation, scheduling, model execution, and optimization interact as parts of a unified architecture rather than as independent engineering domains.

Autonomous systems operate under multiple constraints simultaneously. AI models require computational resources, software frameworks must manage execution timing, sensor systems produce large volumes of data, and hardware platforms impose limits on power consumption,

memory capacity, thermal dissipation, and communication bandwidth. These constraints interact continuously, making system-level optimization essential for reliable operation.

The figure organizes the autonomy stack into five primary operational layers: hardware accelerators, sensor pipelines, real-time frameworks, software paradigms, and model architectures. Above these layers sits a cross-layer optimization function that coordinates behavior across the overall architecture. The diagram also highlights several major constraints, including thermal limits, bandwidth scarcity, latency budgets, resource contention, and memory footprint limitations.

By depicting the autonomy stack as an interconnected hierarchy rather than a collection of isolated technologies, the figure emphasizes the importance of coordinated design in achieving safe, efficient, and resilient autonomous behavior.

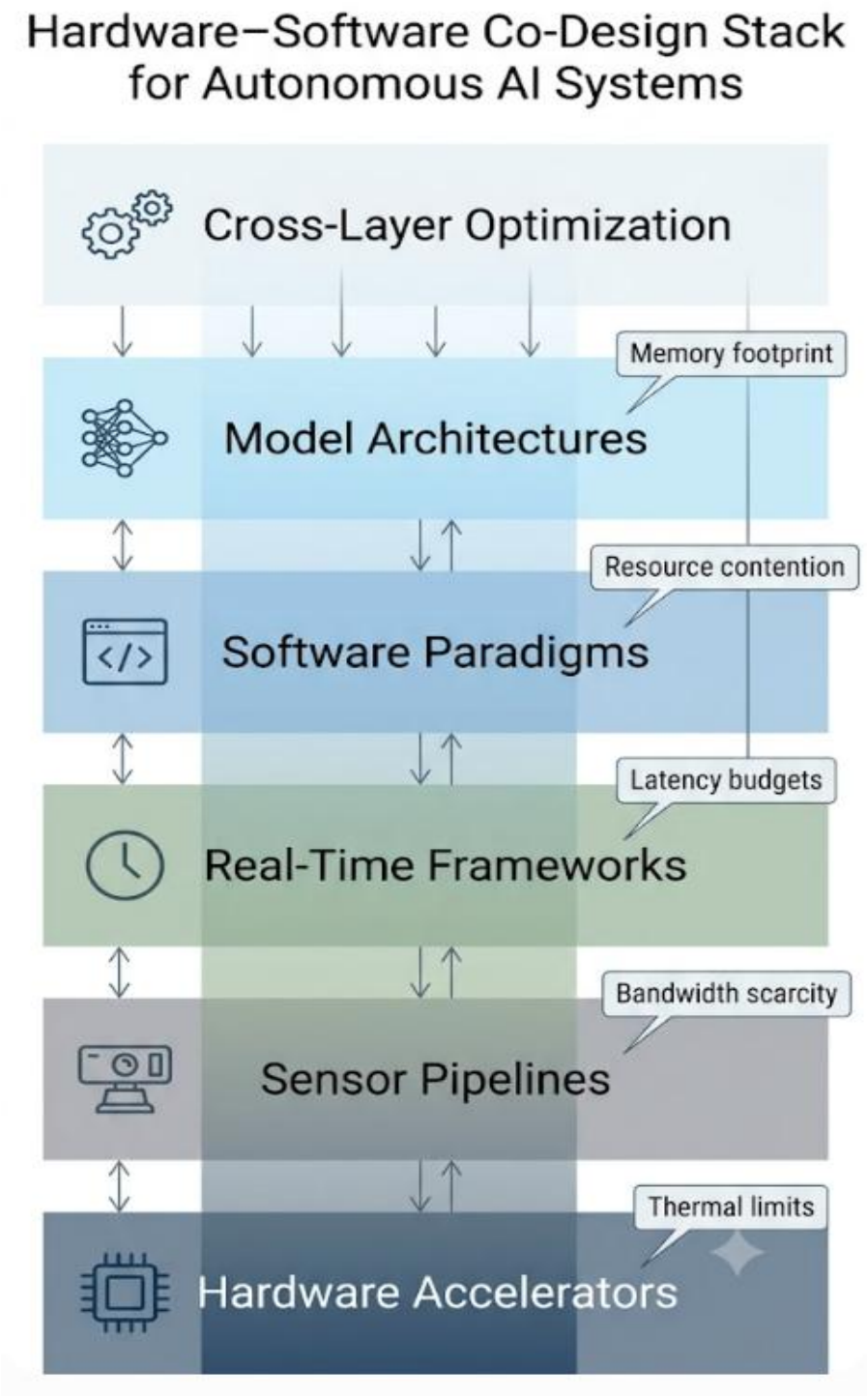


Figure 8.4 — Hardware–Software Co-Design Stack for Autonomous AI Systems

Layered conceptual model illustrating the interactions among hardware accelerators, sensor pipelines, real-time frameworks, software paradigms, and AI model architectures within autonomous systems. The figure highlights major cross-layer constraints, including thermal limits, bandwidth scarcity, latency

budgets, resource contention, and memory footprints, while demonstrating how cross-layer optimization coordinates behavior across the autonomy stack to maintain safety, efficiency, and real-time performance.

Legend

Component	***Description***
Cross-Layer Optimization	*System-wide coordination mechanism that aligns performance, resource allocation, timing, and safety objectives across all layers.*
Model Architectures	*AI perception, prediction, planning, and inference models responsible for autonomous decision-making.*
Memory Footprint	*Memory requirements associated with model execution, parameters, activations, and runtime state.*
Software Paradigms	*Scheduling, concurrency, execution management, isolation, and orchestration mechanisms governing software behavior.*
Resource Contention	*Competition among workloads for shared computational resources.*
Real-Time Frameworks	*Timing and scheduling infrastructure enforcing execution deadlines and deterministic behavior.*
Latency Budgets	*Maximum allowable delays across sensing, processing, decision-making, and control loops.*
Sensor Pipelines	*Data-acquisition, filtering, synchronization, calibration, and fusion processes.*
Bandwidth Scarcity	*Limitations affecting movement of sensor data and computational outputs.*
Hardware Accelerators	*GPUs, TPUs, AI accelerators, FPGAs, and other specialized processing devices.*
Thermal Limits	*Physical constraints imposed by heat generation and cooling capacity.*

Bidirectional Arrows Between Layers	*Continuous interaction and dependency among architecture layers.*
Vertical Constraint Pathways	*Flow of limitations and optimization effects throughout the autonomy stack.*

Figure 8.4 illustrates that autonomous-system performance cannot be attributed to a single layer of the computational architecture. Instead, performance, safety, and reliability emerge from interactions among sensing, processing, scheduling, model execution, and optimization processes.

The figure highlights a central principle of hardware–software co-design: constraints introduced at one layer inevitably influence behavior throughout the rest of the stack. Effective autonomy therefore requires coordinated optimization rather than isolated subsystem improvements.

The figure presents a vertically organized autonomy stack composed of interconnected layers. Each layer performs a specialized function while simultaneously influencing the performance and limitations of adjacent layers.

At the foundation of the stack are **hardware accelerators**. These devices provide the computational resources required for AI inference, sensor processing, planning, and control. Graphics processing units, tensor processors, specialized AI accelerators, and related hardware execute the workloads that make autonomy possible.

The figure identifies **thermal limits** as a primary constraint affecting this layer. Every computational operation consumes power and generates heat. When heat production approaches cooling-system capacity, processor performance may be reduced through throttling mechanisms. This relationship highlights the fact that computational performance is ultimately bounded by physical constraints rather than software alone.

Above the hardware layer reside the **sensor pipelines**. These pipelines collect, filter, synchronize, calibrate, and process environmental observations before information becomes available to higher-level autonomy functions.

The figure associates this layer with **bandwidth scarcity**, reflecting the large volumes of information produced by cameras, LiDAR systems, radar sensors, and other perception devices. If data movement cannot keep pace with sensor output, bottlenecks emerge that affect perception quality and responsiveness. Consequently, sensing performance depends not only on sensor quality but also on the system's ability to transport and process information

efficiently.

The next layer consists of **real-time frameworks**, which manage timing relationships across the autonomy stack. Autonomous systems must often satisfy strict deadlines governing perception updates, planning cycles, and control outputs.

The figure illustrates **latency budgets** as a defining constraint at this level. Excessive delays in any part of the system can compromise responsiveness and destabilize control behavior. Real-time frameworks therefore enforce execution priorities and scheduling policies that help maintain deterministic operation despite changing workloads.

Above the real-time layer are the **software paradigms** responsible for execution management, concurrency control, workload scheduling, and resource allocation.

The figure identifies **resource contention** as a major challenge within this layer. Multiple processes frequently compete for processing resources, memory bandwidth, communication pathways, and scheduling opportunities. Without effective coordination, resource contention can produce timing failures, degraded performance, and unpredictable behavior. Software architectures therefore play a critical role in maintaining system stability.

The highest operational layer consists of **model architectures**, which provide perception, prediction, planning, and decision-making capabilities.

The figure highlights **memory footprint** as a major constraint affecting model execution. Larger models generally provide more sophisticated reasoning and environmental understanding, but they also require greater memory capacity and computational resources. Memory requirements propagate downward through the stack, impacting software scheduling, real-time performance, sensor throughput, and hardware utilization.

A particularly important feature of the figure is the presence of **bidirectional arrows** connecting adjacent layers. These arrows emphasize that influence flows in both directions.

For example, model architectures influence computational workload requirements, yet available hardware resources constrain feasible model complexity. Similarly, sensing requirements affect scheduling demands, while scheduling limitations may constrain sensor-processing rates. This reciprocal relationship demonstrates why autonomous-system engineering cannot be performed effectively through isolated optimization efforts.

Overseeing all layers is the **cross-layer optimization** component. Rather than functioning as another layer within the stack, it serves as a coordinating mechanism that continuously balances competing objectives throughout the architecture.

Cross-layer optimization manages trade-offs among performance, timing, memory usage, thermal behavior, communication requirements, and safety objectives. For example, increasing model complexity may improve perception accuracy but increase latency and memory consumption. Cross-layer optimization evaluates these competing effects and identifies operating points that preserve overall system objectives.

A broader insight emerging from the figure is that many performance limitations originate from interactions among constraints rather than from individual constraints alone. Thermal limits influence processing throughput. Processing throughput affects latency. Latency influences control-loop stability. Memory requirements affect scheduling flexibility. Consequently, addressing a single constraint in isolation may not improve overall system performance.

The diagram also illustrates the layered nature of resource management. Constraints become increasingly abstract when moving upward through the stack. Thermal limits originate in physical hardware. Bandwidth limitations affect information movement. Latency budgets govern timing. Resource contention influences software behavior. Memory footprint affects model capability. Together, these factors form an interconnected chain that determines system performance.

From a systems-engineering perspective, the figure reinforces the principle that autonomy should be viewed as a cyber-physical system. Computational decisions influence physical behavior, while physical constraints shape computational possibilities. Hardware–software co-design provides a framework for managing these relationships systematically.

Another important observation is that safety emerges from coordination across layers rather than from excellence within any individual layer. Highly accurate models provide limited value if latency budgets are violated. Powerful hardware contributes little if thermal limits force frequent throttling. High-bandwidth sensors may be ineffective if software architectures cannot process incoming data efficiently.

Ultimately, Figure 8.4 demonstrates that autonomous AI systems operate as integrated computational ecosystems rather than collections of independent technologies. Hardware accelerators, sensor pipelines, real-time frameworks, software paradigms, and model architectures interact continuously while sharing responsibility for perception, decision-making, and control. Through cross-layer optimization, these components collectively manage thermal limits, bandwidth constraints, latency budgets, resource contention, and memory footprints, enabling autonomous systems to achieve reliable, efficient, and safe operation under demanding real-world conditions.

Because every tensor operation, attention computation, sparsity optimization, and routing

decision ultimately translates into physical activity within processors, memory hierarchies, cache systems, and interconnect fabrics, **model architectures represent the most critical convergence point between algorithmic intelligence and hardware reality**. Architectural choices determine not only how information is represented and processed, but also how effectively computational workloads align with constraints imposed by memory capacity, bandwidth availability, thermal budgets, latency requirements, and energy consumption. The following discussion examines this relationship in greater depth, exploring how modern AI architectures leverage arithmetic intensity, structured sparsity, memory-conscious attention mechanisms, cache-aware computation, and adaptive micro-architectural designs to achieve efficient, resilient, and real-time performance within the resource constraints illustrated throughout the hardware–software co-design stack.

A. Model Architectures in AI Systems

Model architectures define the computational structure of intelligence in autonomous AI systems. They determine how perception, prediction, and control are expressed as executable graphs, how these graphs map onto hardware substrates, and how inference pathways behave when resources tighten or environmental stressors emerge. In hardware–software co-design, model architectures are not abstract algorithmic constructs; they are physical workloads whose tensor shapes, memory footprints, and parallelism patterns directly influence accelerator utilization, cache behavior, and real-time feasibility. Every architectural choice—attention formulation, sparsity pattern, routing topology, or tiling strategy—propagates through the autonomy stack and shapes the system's ability to operate safely and efficiently under real-world constraints.

Modern AI workloads have reached a scale where naïve dense computation is no longer viable. Autonomous systems must execute large models within strict latency budgets, limited thermal envelopes, and constrained memory hierarchies. As a result, model architectures increasingly incorporate hardware-aware design principles that optimize arithmetic intensity, reduce memory traffic, exploit structured sparsity, and align computation with accelerator data paths. These principles ensure that intelligence is not only expressive but also executable within the physical limits of silicon.

- **AI Compute-Bound Graphs and High-Intensity Arithmetic Workloads** - Arithmetic intensity, roofline profiles, and compute-bound graph topologies form the foundation of hardware-efficient model design. These properties determine whether a model saturates available compute or stalls on memory bandwidth. Architectures with high arithmetic intensity and compute-bound structures operate closer to accelerator peak

performance, enabling real-time inference even when thermal or power constraints restrict sustained throughput.

- **Structured AI Sparsity with Tensor-Core-Aligned Execution Patterns** - Structured sparsity and tensor core alignment transform dense neural operations into hardware-efficient compute patterns. By pruning weights in regular, accelerator-friendly formats and aligning matrix shapes with tensor core tile geometry, architectures reduce memory movement and increase parallel execution efficiency. These techniques allow models to exploit specialized hardware datapaths without sacrificing functional accuracy, enabling larger architectures to run within constrained thermal envelopes, power budgets, and memory hierarchies. Structured sparsity ensures that computation scales intelligently with available resources, making high-capacity models deployable on embedded and real-time autonomous platforms.
- **Memory-Optimized AI Attention Mechanisms for Bandwidth-Constrained Models** - Memory-optimized attention mechanisms—such as FlashAttention, FlashDecoding, and SRAM-aware tiling—address the bandwidth bottlenecks inherent in transformer-based architectures. These reformulations restructure attention computation to minimize off-chip memory access, reduce activation footprint, and maximize locality within SRAM and cache. By keeping critical data on-chip and reducing redundant reads, these mechanisms maintain stable latency even as sequence lengths grow or sensor pipelines generate high-volume inputs. This memory-aware design enables high-fidelity perception and reasoning within strict bandwidth and memory constraints, making transformer-class models viable for real-time autonomous systems.
- **Linear-Attention AI Architectures and State-Space Sequence Models**— Linear attention mechanisms, state space models, and cache-optimized formulations provide scalable alternatives to quadratic attention for long-context reasoning. These architectures exploit locality, recurrence, or convolutional structure to reduce memory pressure and improve cache utilization, enabling efficient execution on accelerators with limited bandwidth or small on-chip memory. By replacing global attention with hardware-friendly formulations, they support long-horizon prediction, temporal modeling, and continuous-time reasoning without overwhelming compute or memory resources. This scalability is essential for autonomous systems that must process extended sensor histories while maintaining deterministic timing.
- **Conditional-Computation AI Micro-Architectures with Dynamic Execution Paths** - Conditional computation micro-architectures—such as Mixture-of-Experts routing and dynamic token slicing—introduce adaptive execution pathways that scale compute with

workload complexity. These mechanisms activate only the necessary experts or token subsets, reducing unnecessary computation and aligning workload distribution with accelerator topology. Conditional execution allows models to expand representational capacity without proportionally increasing compute cost, enabling high-resolution reasoning within strict real-time constraints. By adapting dynamically to sensor load, environmental complexity, or mission demands, these micro-architectures enhance both efficiency and resilience in autonomous AI systems.

Together, these dimensions illustrate how model architectures have evolved into a central pillar of hardware–software co-design. Intelligence in autonomous systems is shaped not only by algorithmic innovation but by how effectively those algorithms conform to the contours of silicon, memory hierarchies, and execution frameworks. These architectural principles enable modern AI systems to achieve resilience, efficiency, and scalability through deliberate co-design across the entire autonomy stack.

Model architectures sit at the top of the hardware–software co-design stack because they define the computational expression of intelligence and determine how every downstream layer—accelerators, memory hierarchies, software paradigms, and real-time frameworks—must behave to support autonomous operation. The architectural choices embedded in these models shape arithmetic intensity, memory traffic, sparsity patterns, cache locality, and conditional execution pathways. To clarify how these choices interact with hardware constraints and real-time requirements, the following table organizes the core architectural dimensions that govern modern AI model design. This table provides a structured view of the mechanisms that allow large-scale models to operate efficiently and predictably within the physical limits of autonomous systems.

Figure 8.4 illustrated how model architectures occupy a pivotal position within the hardware–software co-design stack, linking sensing, scheduling, memory systems, real-time execution frameworks, and hardware accelerators. However, not all AI model architectures interact with computational resources in the same manner. Architectural design choices determine how efficiently models utilize memory, exploit parallelism, manage attention computation, distribute workload across accelerators, and operate within strict latency and power constraints. As AI systems increasingly transition from cloud-scale environments into autonomous vehicles, robots, industrial platforms, and edge devices, model architectures must be designed with explicit awareness of hardware realities. Table 8.4-A examines the principal architectural dimensions that shape this relationship and illustrates how modern AI architectures are engineered to balance computational performance, resource utilization, scalability, and real-time safety requirements.

Table 8.4-A presents the key architectural dimensions that define how modern AI models interact with computational hardware within autonomous systems. These dimensions represent specialized design strategies that address the growing challenges associated with compute scalability, memory efficiency, latency management, and resource-constrained deployment.

Historically, AI model development focused primarily on improving predictive performance through larger parameter counts and deeper network structures. As models expanded in complexity, however, computational bottlenecks increasingly shifted from algorithmic accuracy to hardware feasibility. Limitations in memory bandwidth, accelerator utilization, power consumption, thermal capacity, and real-time responsiveness began to constrain practical deployment.

To address these challenges, contemporary model architectures incorporate design principles specifically intended to improve alignment with hardware characteristics. These include maximizing arithmetic intensity, exploiting structured sparsity, reducing memory-access costs, improving cache utilization, and dynamically allocating computational resources according to workload requirements.

The table identifies five particularly significant architectural dimensions: compute-bound graphs and arithmetic intensity, structured sparsity and tensor-core alignment, memory-optimized attention mechanisms, linear attention and state-space models, and conditional-computation micro-architectures. Each dimension addresses a distinct set of hardware constraints while contributing to the broader goals of efficiency, scalability, and operational safety.

By examining these architectural strategies through the lens of hardware–software co-design, the table illustrates how AI models have evolved from purely algorithmic constructs into hardware-aware computational systems.

Table 8.4-A — Core Architectural Dimensions in Model Architectures for Autonomous AI Systems

Architectural Dimension	Description	Hardware–Software Co-Design Implications	Primary Constraints Addressed	Safety & Real-Time Contribution
Compute-Bound Graphs and Arithmetic Intensity	Maximizes FLOPs per byte and aligns model graphs	Enables models to saturate compute units, reduce memory stalls, and	Memory bandwidth ceilings, compute	Supports stable real-time inference by minimizing latency spikes caused by

Architectural Dimension	Description	Hardware–Software Co-Design Implications	Primary Constraints Addressed	Safety & Real-Time Contribution
	with accelerator roofline behavior.	operate near peak throughput.	saturation, thermal envelopes.	bandwidth bottlenecks.
Structured Sparsity and Tensor Core Alignment	Converts dense operations into structured sparse patterns aligned with accelerator tile geometry.	Improves parallelism, reduces memory traffic, and increases energy efficiency through hardware-aligned sparsity.	Tensor core tile alignment, cache locality, power budgets.	Preserves accuracy while reducing compute cost, enabling large models on embedded or resource-constrained platforms.
Memory-Optimized Attention Mechanisms	Reformulates attention to minimize off-chip memory access and reduce activation footprint.	Aligns attention computation with SRAM capacity, tiling strategies, and accelerator memory hierarchies.	Off-chip bandwidth limits, activation footprint, SRAM size.	Ensures predictable latency for perception and prediction even with long sequences or high sensor throughput.
Linear Attention and State Space Models	Provides scalable long-context reasoning through locality, recurrence, or convolutional structure.	Enhances cache utilization, reduces memory pressure, and enables efficient execution on constrained accelerators.	Cache size, memory bandwidth, sequence length scalability.	Supports long-horizon reasoning without overwhelming hardware resources, improving temporal safety.

Architectural Dimension	Description	Hardware–Software Co-Design Implications	Primary Constraints Addressed	Safety & Real-Time Contribution
Conditional Computation Micro-Architectures	Introduces adaptive execution pathways such as MoE routing and dynamic token slicing.	Scales compute with workload complexity, reduces unnecessary activation, and aligns routing with accelerator topology.	Compute budget variability, routing overhead, token-level parallelism.	Maintains high-fidelity reasoning while respecting strict real-time deadlines through adaptive compute allocation.

Table 8.4-A demonstrates that modern AI architectures are increasingly shaped by the physical realities of computational systems. Rather than viewing model design solely as a machine-learning problem, contemporary architectures incorporate explicit strategies for managing memory traffic, computational throughput, energy efficiency, and timing behavior.

The architectural dimensions presented in the table reveal that many of the most important advances in AI scalability stem not from increasing model size alone, but from improving the efficiency with which models interact with underlying hardware resources.

The first architectural dimension identified in the table is **compute-bound graphs and arithmetic intensity**. This approach seeks to maximize the amount of useful computation performed for each unit of data movement within the system. Modern accelerators frequently possess more computational capability than memory systems can efficiently supply. As a result, throughput often becomes limited by memory bandwidth rather than processor performance.

Architectures designed for high arithmetic intensity reduce memory stalls by ensuring that data retrieved from memory undergoes substantial computation before additional transfers occur. This strategy allows accelerators to operate closer to peak utilization and reduces performance losses associated with memory bottlenecks. From a safety perspective, improved arithmetic intensity contributes to predictable real-time inference because latency becomes less sensitive to fluctuations in memory traffic.

The table next identifies **structured sparsity and tensor-core alignment**, which represent a hardware-aware approach to reducing computational cost. Instead of processing all parameters equally, structured sparsity removes or bypasses selected computations according to predefined

patterns aligned with accelerator hardware.

Unlike unstructured sparsity, which can introduce irregular memory-access behavior, structured sparsity is designed to match the execution characteristics of specialized processing units such as tensor cores. This alignment increases parallelism, improves energy efficiency, and reduces memory traffic. By decreasing computational requirements without significantly compromising accuracy, structured sparsity enables large and sophisticated models to operate on platforms possessing limited power and thermal budgets.

Another major architectural dimension is **memory-optimized attention mechanisms**. Traditional attention mechanisms often require substantial memory movement because large quantities of intermediate activations must be stored and retrieved during computation. This behavior becomes especially problematic as context lengths and sensor throughput increase.

Memory-optimized attention reformulates attention computation to reduce off-chip memory accesses and activation-storage requirements. By aligning attention calculations with accelerator memory hierarchies and local SRAM resources, these approaches lower bandwidth demands while maintaining effective context processing. The resulting predictability in memory utilization is particularly important for perception and prediction systems operating under strict latency constraints.

The table further highlights **linear attention and state-space models**, which have emerged as important alternatives to conventional transformer architectures. Traditional attention mechanisms scale poorly as sequence lengths increase because memory and computation often grow rapidly with context size.

Linear-attention techniques and state-space formulations address this challenge by exploiting locality, recurrence, or structured temporal representations. Rather than requiring global attention across all tokens simultaneously, these methods process information more efficiently, reducing memory pressure and computational demand. Their ability to support long-context reasoning without overwhelming available resources makes them particularly valuable in autonomous systems that must continuously process sensor streams over extended time horizons.

The final architectural dimension identified is **conditional-computation micro-architectures**, including mechanisms such as mixture-of-experts routing and dynamic token selection. These architectures depart from the traditional assumption that every input must activate the same computational pathway.

Instead, computation is allocated adaptively according to the complexity and informational

content of incoming data. More demanding inputs may activate additional resources, while simpler inputs receive only the computation necessary for accurate processing. This adaptive behavior improves overall efficiency by reducing unnecessary activation and aligning workload distribution with available hardware resources. From a real-time perspective, conditional computation helps maintain performance within strict latency and power budgets while preserving reasoning quality.

A broader insight emerging from the table is that architectural innovation increasingly focuses on reducing data movement rather than simply accelerating computation. Memory transfers often consume more energy and generate greater latency than arithmetic operations themselves. Consequently, many contemporary architectural strategies emphasize improving locality, reducing bandwidth requirements, and maximizing cache utilization.

The table also illustrates the close relationship between efficiency and scalability. Architectural dimensions that reduce memory traffic, exploit sparsity, or allocate computation adaptively not only improve performance but also permit larger models and more sophisticated capabilities within fixed resource envelopes. This capability becomes increasingly important as autonomous systems seek to deploy advanced AI functionality on embedded and edge-computing platforms.

From a systems-engineering perspective, the architectural dimensions summarized in the table can be viewed as mechanisms for balancing competing objectives. High reasoning capability must coexist with finite compute budgets. Rich contextual awareness must operate within memory constraints. Advanced perception must satisfy real-time timing requirements. The architectural innovations described in the table address these tensions directly.

Another important observation is that these dimensions are often complementary rather than competing. A single model may simultaneously employ structured sparsity, memory-optimized attention, hardware-aware tensor operations, and adaptive routing mechanisms. Together, these optimizations create architectures that are significantly more efficient than would be possible through any single technique alone.

Ultimately, Table 8.4-A demonstrates that modern AI architectures are increasingly defined by their interaction with hardware resources. Through arithmetic-intensity optimization, structured sparsity, memory-aware attention mechanisms, scalable temporal models, and adaptive computational pathways, contemporary architectures align algorithmic intelligence with physical computing constraints. These dimensions not only improve efficiency and scalability but also contribute directly to the real-time predictability, resilience, and safety required for autonomous AI systems operating in complex real-world environments.

The architectural dimensions summarized in Table 8.4-A further illustrate that effective

hardware-aware model design begins with a fundamental understanding of how computational workloads interact with the physical characteristics of modern accelerators. Before techniques such as structured sparsity, memory-optimized attention, cache-efficient execution, or conditional computation can deliver meaningful gains, the underlying computational graph must be aligned with the throughput, memory, and parallel-processing capabilities of the target hardware. This alignment is governed by concepts such as arithmetic intensity, roofline performance behavior, and the extent to which a model operates as a compute-bound rather than memory-bound workload. Collectively, these properties determine whether an architecture can fully utilize available computational resources, minimize bandwidth-induced stalls, and sustain predictable latency under real-time operating constraints. The following discussion examines these foundational principles in greater depth, establishing the performance framework upon which subsequent hardware-aware architectural optimizations are built.

a. AI Compute-Bound Graphs and High-Intensity Arithmetic Workloads

AI models increasingly operate in regimes where arithmetic throughput, rather than memory bandwidth, dictates the dominant performance ceiling. These compute-bound graphs exhibit exceptionally high FLOP-to-byte ratios, dense tensor contractions, and sustained utilization of specialized accelerator units like Tensor Cores, SIMD lanes, and matrix engines. In these workloads, the governing challenge shifts from fetching data quickly to feeding compute units with sufficiently large, structurally sound operations to maintain peak throughput.

Compute-bound AI graphs typically arise in:

- Large-batch transformer inference
- Dense MLP blocks with high-aspect-ratio matrices
- Fused multi-tensor kernels
- High-order attention mechanisms
- State-space models with long-sequence convolutional expansions

Sustaining efficiency across these workloads demands careful orchestration of arithmetic intensity, tensor core alignment, vector-lane mapping, and balanced graph partitioning.

These graphs do not exist in isolation; they emerge from the tight interplay between software operational efficiency and hardware architectural limits. Operational efficiency refers to how effectively software organizes computation—via kernel fusion, tiling strategies, operand reuse, vector alignment, and partitioning. Architectural limits represent the physical constraints of the

accelerator—including Tensor Core throughput, memory bandwidth, register file size, warp scheduling, and on-chip SRAM capacity. Together, these forces determine whether a deep learning workload reaches its theoretical performance ceiling or suffers from graph inefficiencies.

This relationship is foundational to performance engineering. When optimizing accelerator workloads, the software stack must shape the compute graph to align with peak arithmetic capabilities. If a graph's arithmetic intensity drops too low, Tensor Cores stall waiting for data. If its structure is irregular, vector lanes sit idle. If memory access patterns are poorly organized, the workload becomes bandwidth-bound even when the hardware is capable of far more. Operational efficiency is therefore the definitive mechanism by which software maps a workload into the architectural envelope defined by the hardware.

These ideas naturally lead into the concept of **tensor-core intensity thresholds**, which represent the minimum arithmetic density required for software to fully exploit the hardware's compute potential. The threshold is expressed mathematically as

$$I_{\text{threshold}} = \frac{P_{\text{TC}}}{B},$$

where P_{TC} is peak tensor-core throughput and B is memory bandwidth. Software performance becomes compute-bound only when the workload's intensity I exceeds this threshold. Below it, architectural limits dominate; above it, operational efficiency determines how close the workload gets to peak FLOPs. This threshold is the gateway into understanding how AI compute graphs behave under high-intensity conditions and sets the stage for deeper exploration of tensor-core alignment, roofline saturation, vector-lane mapping, and balanced graph partitioning.

Once the threshold is crossed, the workload enters the compute-bound region of the roofline model, where performance is governed by

$$\text{Perf} = \min(P_{\text{peak}},\, I \cdot B).$$

Here, architectural limits define the upper bound P_{peak}, while operational efficiency determines how close the workload gets to that bound. Techniques such as kernel fusion, operand reuse, and SRAM residency mitigate memory stalls and push the workload toward the plateau. FlashAttention, fused MLP blocks, and tiled GEMMs exemplify how software can reshape computation to exploit architectural strengths.

Non-linear layers introduce additional complexity. Operations like GELU, SiLU, softmax, rotary embeddings, and state-space convolutions must be mapped onto vectorized accelerator lanes. Lane utilization

$$U_{\text{lane}} = \frac{\text{Active Lanes}}{\text{Total Lanes}}$$

captures how effectively software fills the hardware's parallel execution units. Architectural limits define the number and width of lanes; operational efficiency determines how well the workload fits into them. Fusing non-linear ops with surrounding linear algebra is often necessary to maintain compute-bound behavior.

Even with optimal tensor-core usage and vector-lane mapping, compute-bound performance collapses if arithmetic load is unevenly distributed across the graph. Balanced graph partitioning ensures that each region maintains sufficient intensity:

$$I_{\text{subgraph}} = \frac{\sum \text{FLOPs}}{\sum \text{Bytes}}.$$

Architectural limits dictate tile sizes, register capacities, and memory-hierarchy constraints; operational efficiency determines how the graph is partitioned to respect those limits. Transformer blocks, MoE routing, and fused attention kernels all rely on this balance to sustain high throughput.

The interplay between operational efficiency and architectural limits becomes increasingly important once an AI workload enters the compute-bound regime. At that point, software performance is no longer governed by how quickly data can be fetched from memory but by how effectively the compute graph is shaped to exploit the accelerator's peak arithmetic capabilities. Kernel fusion, tiling strategies, operand reuse, vector-lane alignment, and balanced graph partitioning all serve the same purpose: to mold the workload so that it fits within the physical envelope defined by tensor-core throughput, memory bandwidth, register file size, warp scheduling behavior, and on-chip SRAM constraints. This relationship is the foundation of performance engineering in deep learning systems. It explains why two models with identical mathematical definitions can exhibit radically different runtime characteristics depending on how well their compute graphs align with the underlying GPU architecture. These ideas naturally lead into the following table, which contrasts the software-driven mechanisms that enhance operational efficiency with the hardware-imposed ceilings that ultimately bound performance.

The architectural dimensions presented in Table 8.4-A demonstrated that modern AI models are designed not only to improve predictive performance but also to operate efficiently within the physical constraints imposed by computing hardware. Achieving this objective requires more than selecting an appropriate architecture; it requires understanding the interaction between software-level optimization techniques and the underlying hardware resources upon which those techniques depend. Concepts such as arithmetic intensity, tensor-core utilization, vector-lane efficiency, memory reuse, and graph partitioning determine whether computational workloads can fully exploit available processing capacity or become limited by bandwidth, scheduling inefficiencies, and resource contention. Table 8.4-A1 examines this relationship in greater detail by comparing operational-efficiency mechanisms implemented in software with the architectural constraints imposed by hardware and demonstrating how their interaction defines achievable system performance.

Table 8.4-A1 explores the relationship between software-level optimization techniques and the hardware constraints that ultimately govern computational efficiency in autonomous AI systems. While algorithmic advances often receive significant attention, practical performance depends on how effectively software execution strategies align with the capabilities and limitations of the underlying hardware architecture.

Modern AI accelerators possess enormous computational throughput, frequently capable of executing trillions of operations per second. However, achieving this theoretical performance requires overcoming numerous bottlenecks associated with memory bandwidth, data movement, register availability, vector-lane utilization, and scheduling efficiency. Consequently, operational efficiency emerges not only from raw computational power but also from the ability to organize workloads in a manner that matches hardware execution characteristics.

The table identifies four foundational concepts that influence this relationship: tensor-core thresholds, roofline saturation, vector-lane mapping, and graph partitioning. Each concept illustrates a different aspect of the interaction between software design and hardware capabilities. Together, these factors determine how effectively AI workloads translate theoretical accelerator performance into real-world execution efficiency.

By examining both the software and hardware perspectives simultaneously, the table reinforces the central principle of hardware–software co-design: optimal performance is achieved through alignment rather than through isolated optimization.

Table 8.4-A1 — Operational Efficiency vs Architectural Limits

Concept	Operational Efficiency (Software)	Architectural Limits (Hardware)	Combined Impact
Tensor-Core Thresholds	Kernel fusion, tiling, operand reuse	Tensor-core peak FLOPs, memory bandwidth	Determines compute-bound transition
Roofline Saturation	Reducing stalls, maximizing reuse	Peak FLOPs, bandwidth ceiling	Defines achievable performance
Vector-Lane Mapping	Non-linear fusion, tile reshaping	SIMD/SIMT width, warp scheduling	Controls lane utilization
Graph Partitioning	Balanced subgraph shaping	Tile size, register file limits	Maintains uniform arithmetic intensity

Table 8.4-A1 demonstrates that computational efficiency is fundamentally a collaborative property emerging from both software execution strategies and hardware architecture. Software may be designed to maximize throughput and minimize stalls, but performance remains bounded by physical limitations such as bandwidth availability, vector-execution width, tensor-core utilization, and memory hierarchy behavior.

The concepts summarized in the table reveal that many performance bottlenecks arise not because hardware lacks computational capability, but because software workloads fail to align fully with the structure through which that capability is delivered.

The first concept identified in the table is **tensor-core thresholds**, which represent the conditions under which specialized accelerator units can operate at maximum efficiency. Modern AI processors include tensor cores or equivalent matrix-processing hardware designed to accelerate dense linear-algebra operations.

From the software perspective, techniques such as kernel fusion, tiling strategies, and operand reuse increase the likelihood that workloads will satisfy the conditions necessary for efficient tensor-core execution. From the hardware perspective, throughput remains constrained by maximum computational capacity and memory-bandwidth limits. The interaction between these factors determines the transition point at which a workload becomes compute-bound rather than memory-bound. Consequently, tensor-core thresholds serve as a critical indicator of overall hardware-utilization efficiency.

The second concept is **roofline saturation**, one of the most important frameworks for understanding AI-computing performance. The roofline model describes the relationship between arithmetic intensity and achievable computational throughput.

Software techniques attempt to reduce stalls, increase data reuse, and maximize useful work performed per unit of memory traffic. Hardware, however, imposes upper limits determined by peak floating-point performance and available memory bandwidth. As shown in the table, roofline saturation defines the maximum achievable performance under given resource conditions. AI workloads approach optimal efficiency when they move closer to the roofline boundary defined by the architecture.

Another significant concept is **vector-lane mapping**, which refers to how computations are distributed across the parallel execution units within modern processors. Contemporary accelerators rely heavily on SIMD (Single Instruction, Multiple Data) and SIMT (Single Instruction, Multiple Threads) execution models.

Software optimization techniques such as nonlinear fusion and tile reshaping attempt to organize workloads so that execution lanes remain fully utilized. Hardware constraints including SIMD width, warp scheduling behavior, and execution-lane availability determine how effectively this can be achieved. The interaction between these factors controls overall lane utilization and directly influences throughput efficiency. Poor vector-lane mapping often leaves portions of the hardware idle despite apparent computational demand.

The final concept identified in the table is **graph partitioning**, which involves dividing computational graphs into smaller execution units that align with hardware resources. Large AI workloads often contain complex dependency structures, making efficient partitioning essential for maintaining balanced execution.

From the software perspective, balanced subgraph decomposition helps distribute workload evenly and sustain arithmetic intensity. Hardware constraints such as tile size and register-file capacity impose limits on how these partitions can be structured. When graph partitioning is performed effectively, computation remains evenly distributed and hardware resources are utilized consistently. Poor partitioning, by contrast, introduces load imbalance and reduces effective throughput.

A broader insight emerging from the table is that performance optimization increasingly depends on minimizing data movement rather than maximizing arithmetic operations alone. Many AI accelerators possess sufficient computational capability to process workloads rapidly, yet practical performance frequently becomes constrained by the cost of moving data between memory hierarchies and execution units.

The table also illustrates that operational efficiency exists at the intersection of software and hardware design. Software optimization determines how workloads are organized, while hardware architecture determines the efficiency with which those workloads can be executed. Neither domain can achieve optimum performance independently.

From a systems-engineering perspective, the concepts summarized in the table form the foundation for many higher-level architectural optimizations discussed elsewhere in hardware-aware AI design. Structured sparsity, memory-efficient attention, adaptive routing, and cache-aware execution all depend on the principles of tensor-core utilization, roofline behavior, vector efficiency, and graph organization.

Another important observation is that these concepts directly influence real-time performance. Inefficient hardware utilization increases execution variability, introduces latency fluctuations, and reduces computational predictability. Efficient alignment between software and hardware therefore contributes not only to computational throughput but also to system determinism and safety.

The table further demonstrates that performance tuning is ultimately an exercise in balancing competing constraints. Maximizing arithmetic intensity, increasing hardware utilization, reducing memory stalls, and preserving execution predictability must occur simultaneously. Effective hardware–software co-design addresses these objectives collectively rather than independently.

Ultimately, Table 8.4-A1 demonstrates that operational efficiency emerges from the interaction between software optimization strategies and hardware architectural limits. Tensor-core thresholds, roofline saturation, vector-lane mapping, and graph partitioning each illustrate how computational workloads must be structured to align with the realities of modern accelerators. Understanding these relationships provides a foundation for developing AI architectures capable of achieving high throughput, predictable latency, and efficient resource utilization in autonomous systems operating under real-world constraints.

Table 8.4-A1 introduced the central concepts governing the relationship between software-level optimization and hardware-level performance limits, including tensor-core utilization, roofline saturation, vector-lane mapping, and graph partitioning. While these factors can be examined independently, their collective influence is best understood through a unifying performance model that relates computational throughput to data movement. The roofline model provides such a framework by illustrating how achievable performance evolves as arithmetic intensity increases and by identifying the transition between memory-bound and compute-bound execution. Figure 8.4-A1 visualizes this relationship, demonstrating how architectural limits

establish an upper performance boundary while software optimizations progressively move workloads toward more efficient regions of execution.

Figure 8.4-A1 presents a conceptual representation of the roofline model, one of the most widely used frameworks for analyzing performance in high-performance computing and AI accelerators. The roofline model relates achieved computational performance to arithmetic intensity, providing insight into whether a workload is constrained primarily by memory bandwidth or by available computational throughput.

As AI architectures continue to grow in complexity, performance limitations increasingly emerge from data movement rather than arithmetic operations alone. Even accelerators capable of trillions of operations per second may fail to achieve peak throughput if computational units spend significant time waiting for data to arrive from memory. Consequently, understanding the balance between computation and data movement has become a central aspect of hardware-aware AI design.

The figure illustrates how workloads progress from memory-bound execution, where performance is limited by bandwidth, toward compute-bound execution, where throughput approaches the architectural limits imposed by peak floating-point performance. It also highlights the role of software optimizations in increasing arithmetic intensity and improving accelerator utilization.

By connecting software-level efficiency strategies with physical hardware constraints, the figure provides a performance-oriented perspective on hardware–software co-design.

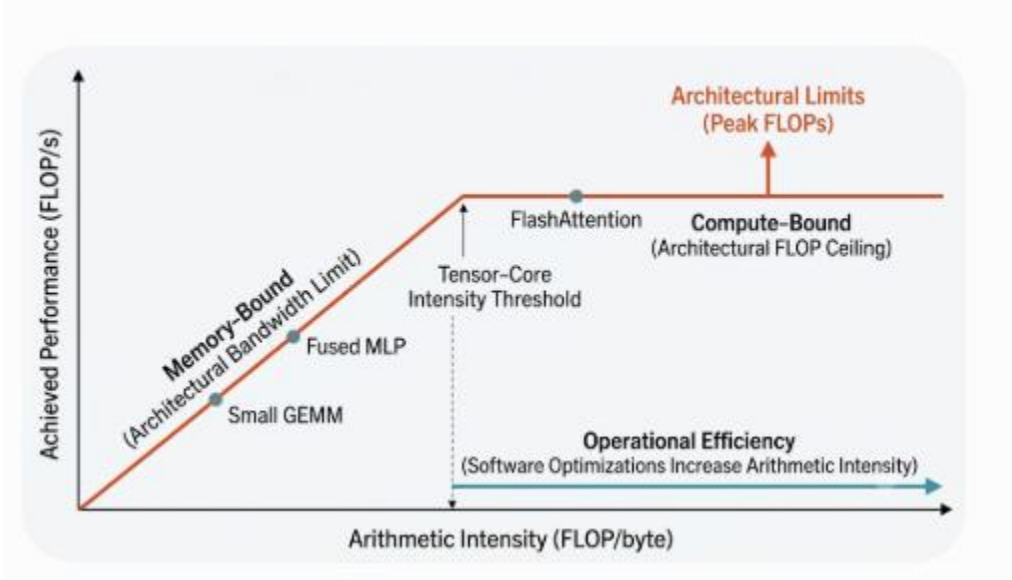


Figure 8.4-A1 - Architectural Limits vs Operational Efficiency in the Roofline Model

Conceptual roofline-performance model illustrating the relationship between arithmetic intensity and achieved computational throughput. The figure shows how workloads evolve from memory-bound execution toward compute-bound execution as software optimizations increase data reuse and computational density. The diagram highlights tensor-core utilization thresholds, bandwidth limitations, and architectural FLOP ceilings that collectively define the upper limits of AI accelerator performance.

Legend

Component	***Description***
Arithmetic Intensity (FLOP/byte)	*Ratio of useful computation performed per unit of data movement.*
Achieved Performance (FLOP/s)	*Effective computational throughput obtained during execution.*
Memory-Bound Region	*Performance domain limited primarily by memory bandwidth rather than computational capability.*
Architectural Bandwidth Limit	*Maximum throughput achievable when execution is constrained by memory transfer rates.*
Roofline Slope	*Linear performance increase associated with increasing arithmetic intensity in the memory-bound region.*
Tensor-Core Intensity Threshold	*Point at which workloads begin utilizing specialized matrix-processing hardware efficiently.*
Fused MLP	*Example workload benefiting from increased arithmetic intensity through operation fusion.*
Small GEMM	*Example workload exhibiting lower arithmetic intensity and stronger bandwidth dependence.*
FlashAttention	*Example architecture engineered to improve memory efficiency and increase arithmetic intensity.*
Compute-Bound Region	*Performance domain limited by available computational throughput rather than memory bandwidth.*
Architectural FLOP Ceiling	*Maximum performance achievable based on peak accelerator computational capability.*
Peak FLOPs	*Upper hardware limit imposed by accelerator arithmetic resources.*
Operational Efficiency Direction	*Path through which software optimizations increase arithmetic intensity and approach hardware limits.*

Figure 8.4-A1 illustrates that AI-system performance is governed by two competing factors: the ability to perform computation and the ability to supply data for that computation. The roofline model demonstrates that many workloads underutilize available hardware not because insufficient computational resources exist, but because data movement remains the dominant bottleneck.

The figure highlights how software optimizations increase arithmetic intensity, enabling workloads to transition from bandwidth-constrained execution toward full utilization of available computational throughput.

The figure presents the classical roofline-performance relationship between **arithmetic intensity** and **achieved computational performance**. Arithmetic intensity appears along the horizontal axis and represents the amount of computation performed for every byte of data moved through the system. The vertical axis measures achieved throughput, expressed as floating-point operations per second.

A central feature of the figure is the roofline itself, which consists of two distinct regions. The first region is the ascending diagonal segment representing the **memory-bound regime**. In this domain, performance scales approximately with arithmetic intensity because computational units spend a substantial portion of time waiting for data transfers rather than executing calculations.

The figure identifies this boundary as the **architectural bandwidth limit**. Any workload operating in this region is constrained primarily by memory-transfer capacity. Even if additional computational resources are available, performance cannot increase significantly unless data movement becomes more efficient.

The examples labeled **Small GEMM** and **Fused MLP** illustrate workloads positioned at different locations along this memory-bound region. Small matrix operations frequently exhibit relatively low arithmetic intensity because memory transfers represent a substantial fraction of total execution cost. Larger fused operations increase data reuse and therefore move toward higher efficiency.

An important characteristic of the memory-bound region is that improving performance often requires optimizing memory-access behavior rather than increasing computational capability. Techniques such as data tiling, cache reuse, kernel fusion, and activation locality are specifically designed to move workloads rightward along the arithmetic-intensity axis.

The figure next highlights the **tensor-core intensity threshold**, representing a transition point at

which workloads become sufficiently compute-dense to utilize specialized accelerator hardware effectively. Modern tensor-processing engines achieve maximum efficiency only when data structures and computational patterns provide enough arithmetic work to justify their use.

Crossing this threshold produces a fundamental change in performance behavior. The workload begins shifting away from bandwidth-dominated execution and toward utilization of available arithmetic resources.

The architecture labeled **FlashAttention** appears near this transition region. FlashAttention is frequently cited as an example of hardware-aware algorithm design because it reduces off-chip memory traffic and increases arithmetic intensity through efficient use of on-chip memory resources. As a result, the workload approaches the upper performance boundary more closely than conventional attention implementations.

Beyond the tensor-core threshold lies the **compute-bound region**, represented by the horizontal portion of the roofline. In this domain, memory bandwidth ceases to be the dominant limitation. Instead, performance becomes constrained by the total arithmetic capability of the hardware.

The horizontal boundary represents the **architectural FLOP ceiling**, which corresponds to the maximum throughput the accelerator can theoretically deliver. Once a workload reaches this region, additional increases in arithmetic intensity yield diminishing performance gains because computational resources are already near saturation.

The figure labels this upper boundary as **Peak FLOPs**, emphasizing that hardware imposes an absolute ceiling on achievable throughput. Regardless of software sophistication, performance cannot exceed the physical limits established by processor architecture.

A particularly important element of the figure is the arrow labeled **Operational Efficiency**. This arrow illustrates the role of software optimization in moving workloads from lower-efficiency regions toward higher-efficiency regions of execution.

Software techniques such as operation fusion, tensor-core alignment, graph restructuring, data tiling, memory-efficient attention mechanisms, and cache-aware execution all serve the same fundamental purpose: increasing arithmetic intensity. By doing so, they reduce the proportion of execution time spent waiting for memory transfers and increase the proportion spent performing useful computation.

A broader insight emerging from the figure is that AI-performance optimization frequently involves improving data locality rather than increasing computational complexity. Modern accelerators already possess enormous arithmetic capacity. The primary challenge is supplying

those resources with data efficiently enough to sustain continuous execution.

The roofline model also illustrates why architectural innovations such as structured sparsity, memory-optimized attention, and hardware-aware micro-architectures have become increasingly important. These techniques alter the balance between computation and data movement, allowing workloads to approach architectural limits more closely.

From a systems-engineering perspective, the figure demonstrates that performance optimization must account for both software and hardware simultaneously. Software determines arithmetic intensity, while hardware establishes the performance boundaries within which optimization occurs. Neither perspective alone can fully explain observed system behavior.

Another important observation is that different AI workloads occupy different regions of the roofline. Small matrix operations may remain bandwidth-bound, while well-optimized transformer kernels may become compute-bound. Consequently, optimization strategies must be tailored to the dominant bottleneck associated with the specific workload under consideration.

Ultimately, Figure 8.4-A1 demonstrates that operational efficiency emerges from the interaction between software optimization and hardware constraints. Arithmetic intensity determines how effectively workloads convert memory transfers into useful computation, while architectural bandwidth limits and computational ceilings define the upper bounds of achievable performance. By increasing data reuse, reducing memory traffic, and aligning execution with hardware capabilities, AI architectures can move closer to the roofline and more fully exploit available computational resources. This relationship forms one of the foundational principles of hardware-aware AI design and hardware–software co-optimization.

The roofline model presented in Figure 8.4-A1 demonstrates that the transition from memory-bound execution to compute-bound execution is governed by a workload's arithmetic intensity. The diagonal bandwidth-limited region and the horizontal computational ceiling illustrate two fundamentally different performance regimes: one constrained by data movement and the other constrained by the maximum computational throughput of the accelerator. As arithmetic intensity increases through software optimizations such as kernel fusion, tiling, operand reuse, and memory-efficient execution strategies, workloads move progressively closer to the point where available compute resources become fully utilized. This transition does not occur arbitrarily. Rather, it is defined by a hardware-specific arithmetic-intensity threshold that determines when tensor cores and related matrix-processing units can operate near peak efficiency. Below this threshold, performance remains dominated by memory bandwidth

limitations; above it, throughput increasingly approaches the architectural FLOP ceiling. Understanding this boundary is essential because it establishes the conditions under which AI compute graphs can fully exploit accelerator capabilities while maintaining predictable performance characteristics. The following discussion examines **Tensor Core Intensity Thresholds for AI Compute Graphs**, formalizing the mathematical and architectural conditions that govern the transition into the compute-bound regime and enable near-peak utilization of modern AI accelerators.

i. Tensor Core Intensity Thresholds for AI Compute Graphs

Tensor core intensity thresholds define the precise arithmetic-density boundary at which an AI workload transitions from bandwidth-limited execution into full tensor-core saturation. In modern accelerators, tensor cores are engineered to deliver extraordinary matrix-multiply throughput, but they can only do so when the workload supplies enough computation per byte of data moved. Tensor cores achieve peak throughput only when the **arithmetic intensity** exceeds a hardware-specific threshold:

$$I = \frac{\text{FLOPs}}{\text{Bytes Moved}}$$

This requirement is captured by the arithmetic intensity ***I***, the ratio of total floating-point operations to total memory traffic. When ***I*** is too low, the hardware spends more time waiting for operands than performing computation, leaving tensor cores under-utilized. When ***I*** exceeds a hardware-defined minimum, the workload enters the compute-bound plateau illustrated in Figure 10.4-94, where performance is capped only by the accelerator's peak FLOP rate.

The threshold itself is determined by the relationship between the tensor core's peak compute capability P_{TC} and the memory subsystem's bandwidth B. The ratio

$$I_{\text{threshold}} = \frac{P_{\text{TC}}}{B}$$

defines the minimum arithmetic intensity required for the workload to saturate the compute units.

If $I > I_{threshold}$, the workload is compute-bound.

For example, NVIDIA H100 tensor cores:

$$P_{\text{TC}} \approx 4 \times 10^{14}\ \text{FLOP/s}$$

$$B \approx 3.35 \times 10^{12} \text{ bytes/s}$$

$$I_{\text{threshold}} \approx 119 \text{ FLOP/byte}$$

Dense GEMMs, fused attention kernels, and large-batch MLPs easily exceed this threshold.

This expression is not merely theoretical; it reflects the physical reality that tensor cores can consume operands far faster than memory can supply them. For example, a modern GPU may deliver hundreds of TFLOP/s of tensor-core throughput while offering only a few terabytes per second of memory bandwidth. The resulting threshold often exceeds one hundred FLOP per byte, meaning that only dense, well-structured operations—large GEMMs, fused attention kernels, high-batch MLP expansions—can reach the compute-bound plateau.

AI compute graphs must therefore be shaped to exceed this threshold. Kernel fusion increases operand reuse by combining multiple operations into a single pass, raising intensity by reducing memory round-trips. Tiling strategies ensure that submatrices remain resident in on-chip SRAM, allowing tensor cores to repeatedly operate on the same data without reloading it from DRAM. Fused attention mechanisms such as FlashAttention dramatically increase intensity by restructuring the algorithm to minimize memory traffic while maximizing arithmetic density. Even the layout of tensors—row-major vs column-major, block-sparse vs dense—can determine whether the workload crosses the threshold.

The threshold also explains why small or fragmented operations struggle to achieve peak performance. A small GEMM may have high theoretical FLOP density, but if its tile size is too small to fully occupy tensor-core pipelines, its effective intensity falls below the threshold. This is why AI frameworks aggressively batch operations, fuse kernels, and reshape graphs: the goal is not merely correctness but ensuring that every operation is large enough and dense enough to saturate the hardware.

In deep learning workloads, the tensor-core intensity threshold becomes a practical design constraint. Transformer blocks, MLP expansions, and attention mechanisms must be arranged so that their arithmetic intensity remains above the threshold across varying sequence lengths, batch sizes, and hidden dimensions. When intensity dips—due to small batches, short sequences, or irregular graph structures—the workload falls back into the memory-bound region, losing the performance benefits of tensor-core acceleration. This is why high-performance AI systems often enforce minimum batch sizes, fuse non-linear operations into GEMM pipelines, and restructure compute graphs to maintain intensity even under dynamic workloads.

Ultimately, tensor-core intensity thresholds serve as the mathematical boundary between software-driven operational efficiency and hardware-defined architectural limits. They quantify the exact point at which the accelerator transitions from bandwidth-limited behavior to full compute saturation. Crossing this threshold is the prerequisite for achieving the performance plateau shown in Figure 8.4-A1, and it is the reason deep learning performance engineering revolves around increasing arithmetic intensity through fusion, tiling, batching, and graph restructuring. In AI systems, the threshold is not just a metric—it is the gateway to unlocking the full computational potential of modern tensor-core architectures.

Once a compute graph exceeds the tensor-core intensity threshold, its execution behavior shifts fundamentally. Arithmetic density becomes sufficient for the accelerator to operate on the compute-bound plateau, where performance is limited not by memory bandwidth but by the hardware's peak FLOP capability. In this region, the dominant challenge is no longer achieving saturation but maintaining it. Even workloads that surpass the intensity threshold can fall off the plateau if memory stalls, cache-miss patterns, or suboptimal operand reuse reintroduce bandwidth pressure. Sustaining compute-bound execution therefore requires careful mitigation of memory-stall pathways and deliberate structuring of data movement to preserve high effective intensity. This transition sets the stage for examining **Roofline Saturation and Memory-Stall Mitigation in AI Workloads**, where the focus shifts from crossing the threshold to stabilizing performance within the architectural limits defined by the roofline model.

ii. Roofline Saturation and Memory-Stall Mitigation in AI Workloads

Roofline saturation describes the execution regime in which an AI workload has surpassed the tensor-core intensity threshold and now operates at the accelerator's peak FLOP capability. In this region, arithmetic intensity is sufficiently high that compute units remain fully engaged, and performance becomes constrained only by the architectural FLOP ceiling rather than memory bandwidth. The roofline model captures this behavior through a horizontal plateau that represents the maximum achievable performance for a given hardware configuration. Once a compute graph reaches this plateau, further increases in arithmetic intensity do not yield higher throughput; the workload is already operating at the architectural limit. This regime is where dense GEMMs, fused MLP blocks, and optimized attention mechanisms such as FlashAttention typically reside, as their high operand reuse and large tile sizes naturally sustain the intensity required for saturation.

Even within the compute-bound plateau, maintaining roofline saturation is not guaranteed. Memory stalls can erode effective performance by interrupting the steady flow of operands required to keep tensor cores fully utilized. These stalls arise from cache-miss patterns, irregular memory access sequences, insufficient tiling, or suboptimal data locality. In AI workloads, the

most common sources of stalls include KV-cache lookups in attention mechanisms, fragmented tensor layouts, and non-fused sequences of small operations that repeatedly access DRAM. When these stalls occur, the workload temporarily drops below the plateau, reintroducing bandwidth pressure and reducing effective FLOP throughput. The roofline model makes this behavior visible: the workload oscillates between the diagonal memory-bound region and the horizontal compute-bound region depending on how efficiently memory traffic is managed.

Mitigating memory stalls requires deliberate structuring of data movement to preserve high effective intensity. Kernel fusion reduces the number of memory round-trips by combining multiple operations into a single pass, allowing intermediate results to remain in registers or on-chip SRAM. Tiling strategies ensure that submatrices fit within the accelerator's local memory hierarchy, enabling repeated reuse without reloading from DRAM. Techniques such as paged attention and FlashAttention restructure algorithms to minimize global memory traffic, replacing bandwidth-heavy operations with compute-dense alternatives. Even tensor layout choices—such as block-sparse formats or contiguous row-major storage—can determine whether memory accesses remain predictable enough to avoid stalls.

Roofline saturation also depends on how well the compute graph maintains operand locality across layers. Transformer blocks, for example, benefit from fusing layer-norm, linear projections, and activation functions into larger composite kernels that reduce memory fragmentation. State-space models achieve similar benefits by restructuring convolutional expansions to maximize reuse of intermediate states. In both cases, the goal is to keep the workload on the compute-bound plateau by ensuring that memory traffic remains subordinate to arithmetic throughput.

The **roofline model** provides a geometric interpretation of compute-bound vs memory-bound behavior:

$$\text{Performance} = \min\left(P_{\text{peak}},\ I \cdot B\right)$$

Compute-bound workloads operate on the **horizontal plateau** of the roofline.

Memory-stall mitigation strategies include:

- Operand reuse via tiling
- KV-cache compression
- Fused kernels to reduce memory round-trips
- On-chip SRAM residency for intermediate tensors

These techniques push workloads rightward (higher intensity) and upward (closer to peak FLOPs).

Ultimately, roofline saturation represents the ideal execution state for AI workloads: a regime where operational efficiency has elevated arithmetic intensity beyond the tensor-core threshold and architectural limits define the maximum achievable performance. Memory-stall mitigation is the mechanism that stabilizes this state, preventing regressions into bandwidth-bound behavior and ensuring that the compute graph continues to exploit the full capabilities of the accelerator. In deep learning systems, sustaining roofline saturation is not merely an optimization—it is a prerequisite for unlocking the performance promised by modern tensor-core architectures.

Sustaining roofline saturation depends not only on mitigating memory stalls but also on ensuring that every stage of the compute graph can fully exploit the accelerator's parallel execution fabric. Even when arithmetic intensity is high enough to remain on the compute-bound plateau, performance can degrade if downstream operations fail to map efficiently onto Single Instruction, Multiple Data (SIMD) or Single Instruction, Multiple Threads (SIMT) lanes. This challenge becomes most apparent in non-linear layers, where activation functions, normalization steps, rotary embeddings, and state-space updates introduce irregular computation patterns that differ from the dense, tile-friendly structure of General Matrix–Matrix Multiplications (GEMMs). These operations often exhibit shapes or dependencies that under-utilize vector lanes unless they are fused, reshaped, or reorganized to align with the accelerator's vectorization model. The transition from roofline saturation to vector-lane efficiency therefore marks the next critical dimension of performance engineering, leading directly into the exploration of **Non-Linear AI Layer Mapping onto Vectorized Accelerator Lanes**, where the focus shifts to how non-linear components of AI workloads can be structured to maintain full hardware utilization.

iii. Non-Linear AI Layer Mapping onto Vectorized Accelerator Lanes

Non-linear layers in modern AI models introduce computation patterns that differ fundamentally from the dense, regular structure of matrix multiplications. While GEMMs naturally align with the wide vector lanes and matrix-multiply tiles of contemporary accelerators, non-linear operations such as Gaussian Error Linear Unit (GELU), Sigmoid Linear Unit (SiLU), softmax, layer normalization, rotary embeddings, and state-space updates often exhibit irregular shapes, branching behavior, or elementwise dependencies that do not map cleanly onto SIMD or SIMT execution units. This mismatch creates a performance challenge: even when the surrounding linear layers operate on the compute-bound plateau, non-linear

components can under-utilize vector lanes, reducing effective throughput and interrupting the steady execution flow required to maintain roofline saturation.

Vectorized accelerator lanes are designed to process multiple data elements in parallel, relying on uniform control flow and predictable memory access patterns. Non-linear AI layers frequently violate these assumptions. Activation functions apply elementwise transformations that may require transcendental operations, normalization layers depend on reductions that introduce synchronization points, and attention mechanisms incorporate exponentiation and division steps that disrupt the regularity of tile-based computation. When these operations are executed as standalone kernels, they often leave a portion of the vector lanes idle, reducing lane utilization and lowering the effective FLOP rate. This inefficiency becomes especially visible in large transformer models, where non-linear layers appear repeatedly between GEMM-heavy projections.

Mapping non-linear layers efficiently onto vectorized hardware requires restructuring these operations so they align with the accelerator's parallel execution model. One approach is kernel fusion, where non-linear functions are combined with adjacent linear operations to form a single composite kernel. By embedding GELU or SiLU directly into the epilogue of a GEMM, the activation can be applied while the data remains in registers or on-chip SRAM, eliminating separate memory accesses and ensuring that vector lanes remain fully occupied. Fused softmax implementations in attention mechanisms achieve similar benefits by combining exponentiation, scaling, and normalization into a single pass that preserves operand locality and minimizes control-flow divergence.

Another strategy involves reshaping non-linear operations into tile-friendly forms. Layer normalization, for example, can be reorganized to operate on blocks that match the accelerator's tile dimensions, allowing reductions and scaling operations to proceed in parallel across vector lanes. Rotary embeddings can be expressed as fused multiply-add sequences that align with the hardware's vector width, reducing the overhead associated with trigonometric operations. State-space models benefit from restructuring convolutional expansions so that intermediate states are reused across tiles, increasing arithmetic density and reducing memory fragmentation.

Modern accelerators expose **vector lanes** or **matrix-multiply tiles** that require careful mapping of non-linear AI layers:

- GELU
- SiLU

- Softmax
- Rotary embeddings
- State-space convolution expansions

Lane utilization (U_{lane}) provides a quantitative measure of how effectively non-linear layers exploit vectorized hardware. It can be expressed as

$$U_{\text{lane}} = \frac{\text{Active Lanes}}{\text{Total Lanes}},$$

where active lanes represent the subset of execution units performing useful work at any given moment. High utilization indicates that the non-linear operation has been successfully reshaped or fused to match the accelerator's parallel structure. Low utilization signals that the operation is too small, too irregular, or too fragmented to fully occupy the hardware. Maintaining high lane utilization across non-linear layers is essential for preserving the performance gains achieved in the compute-bound plateau of the roofline model.

Non-linear ops often under-utilize lanes unless fused with surrounding linear ops (e.g., GEMM + activation fusion). In large-scale AI workloads, non-linear layer mapping becomes a critical component of performance engineering. Even when arithmetic intensity is sufficient to saturate tensor cores, inefficient mapping of non-linear operations can introduce stalls, reduce effective throughput, and disrupt the steady execution required to maintain roofline saturation. By fusing, reshaping, or reorganizing these operations to align with vectorized accelerator lanes, compute graphs can sustain high utilization across all stages of execution. This alignment ensures that non-linear layers do not become bottlenecks and that the full computational potential of modern AI accelerators is realized.

The efficiency of non-linear layer mapping highlights a broader structural requirement within AI compute graphs: every region of the graph must sustain sufficient arithmetic density to keep accelerator resources uniformly engaged. Even when non-linear operations are successfully fused or reshaped to maintain high vector-lane utilization, overall throughput can still degrade if the surrounding graph exhibits uneven computational load. Imbalances between dense GEMM regions, activation-heavy segments, attention blocks, and memory-centric components create fluctuations in arithmetic intensity that disrupt steady compute-bound execution. These fluctuations cause certain subgraphs to fall below tensor-core thresholds or reintroduce bandwidth pressure, fragmenting performance across the model. Ensuring that arithmetic work is distributed evenly across the compute graph becomes essential for maintaining consistent

saturation of tensor cores, vector lanes, and memory hierarchies. This need for uniform scaling leads directly into **Graph Partitioning for Balanced Arithmetic Scaling in AI Models**, where the focus shifts to structuring the compute graph so that every partition sustains the intensity required for stable, high-throughput execution across the entire model.

iv. Graph Partitioning for Balanced Arithmetic Scaling in AI Models

Graph partitioning for balanced arithmetic scaling addresses a structural challenge that emerges once AI workloads begin operating near the compute-bound plateau. Even when tensor-core thresholds are exceeded, roofline saturation is achieved, and non-linear layers are efficiently mapped onto vectorized accelerator lanes, overall throughput can still fluctuate if the compute graph exhibits uneven arithmetic distribution. Modern AI models—particularly transformers, diffusion architectures, and state-space models—contain heterogeneous regions with vastly different computational characteristics. Dense GEMM blocks deliver extremely high arithmetic intensity, while attention score computations, normalization layers, residual pathways, and embedding transformations may introduce lower-intensity segments. These disparities create oscillations in effective throughput, causing certain subgraphs to fall below the intensity required for sustained tensor-core saturation.

Balanced graph partitioning aims to eliminate these oscillations by distributing arithmetic work uniformly across the compute graph. The goal is to ensure that each partition maintains a sufficiently high ratio of FLOPs to memory traffic so that tensor cores, vector lanes, and memory hierarchies remain consistently engaged. To maintain compute-bound behavior across the entire model, graphs must be partitioned so each subgraph maintains sufficient arithmetic intensity. This requirement can be expressed through the subgraph-level intensity metric

$$I_{\text{subgraph}} = \frac{\sum \text{FLOPs}}{\sum \text{Bytes}},$$

which quantifies how well each region of the model aligns with the hardware's compute-bound regime. When a subgraph's intensity falls below the threshold defined by the accelerator's compute-to-bandwidth ratio, that region becomes bandwidth-limited, reducing overall throughput even if surrounding partitions remain compute-bound.

Balanced partitioning ensures:

- No subgraph falls below tensor-core thresholds
- Arithmetic load is evenly distributed across accelerator tiles
- Fused kernels maintain high operand reuse

- Vector lanes remain saturated

Partitioning strategies include:

- Layer-wise tiling
- Attention-block fusion
- MLP-block consolidation
- KV-cache locality grouping

Balanced partitioning ensures that no region becomes a performance sink that drags the entire model off the roofline plateau.

Achieving balanced scaling often requires restructuring the compute graph. In transformer architectures, attention blocks may be fused with adjacent linear projections to increase operand reuse and raise intensity. Residual pathways can be reorganized to minimize memory fragmentation and reduce the number of low-intensity elementwise operations executed in isolation. In diffusion models, convolutional expansions and cross-attention layers can be tiled or fused to maintain uniform arithmetic density across timesteps. State-space models benefit from partitioning recurrent updates into tile-aligned segments that preserve locality and reduce memory-stall pathways. In each case, the objective is to ensure that every partition contributes meaningfully to sustained compute-bound execution.

Graph partitioning also plays a critical role in large-scale distributed AI training and inference. When compute graphs are sharded across multiple GPUs or nodes, imbalanced partitions lead to synchronization delays, idle tensor cores, and uneven memory pressure. Balanced arithmetic scaling ensures that each shard receives a workload with comparable intensity, preventing stragglers and maintaining high utilization across the entire cluster. Techniques such as pipeline parallelism, tensor parallelism, and expert routing in mixture-of-experts models rely on carefully balanced partitions to avoid bottlenecks that arise from uneven computational load.

Ultimately, graph partitioning for balanced arithmetic scaling ensures that the entire AI model—not just isolated high-intensity regions—operates within the compute-bound plateau defined by the roofline model. By distributing arithmetic work evenly across partitions, the compute graph maintains stable tensor-core saturation, high vector-lane utilization, and minimal bandwidth regressions. This alignment transforms the model from a collection of heterogeneous operations into a uniformly optimized pipeline capable of exploiting the full computational potential of modern AI accelerators.

AI compute-bound graphs represent the execution regime in which arithmetic intensity is

sufficiently high for tensor cores and vectorized execution units to operate at their architectural limits. In this state, dense linear algebra, fused attention mechanisms, and high-reuse compute patterns sustain the throughput required to remain on the roofline plateau. Achieving this regime depends on surpassing tensor-core intensity thresholds, mitigating memory stalls, and ensuring that non-linear layers map efficiently onto vector lanes. When these conditions are met, the compute graph transitions from bandwidth-limited behavior to stable, high-throughput execution where performance is governed solely by the accelerator's peak FLOP capability. This alignment between workload structure and hardware topology defines the essence of high-intensity AI computation: a pipeline in which every stage contributes to maintaining full utilization of the accelerator's arithmetic resources.

The behavior of compute-bound graphs highlights the importance of dense, high-reuse arithmetic patterns for sustaining peak throughput, yet many modern AI architectures increasingly rely on structured sparsity to reduce computational cost and improve scalability. Sparsity introduces irregularity into the compute graph, potentially lowering arithmetic intensity and disrupting the uniform execution patterns required for stable tensor-core saturation. However, when sparsity is organized into hardware-aligned structures—block-sparse matrices, tile-sparse attention, or expert-routing patterns that preserve locality—it can reduce workload size without sacrificing the dense arithmetic characteristics needed for compute-bound execution. This transition from dense high-intensity workloads to sparsity-driven efficiency leads directly into **Structured AI Sparsity with Tensor-Core-Aligned Execution Patterns**, where the focus shifts to how sparsity can be engineered to maintain tensor-core compatibility, preserve arithmetic density, and sustain high-throughput execution across increasingly large and complex AI models.

b. Structured AI Sparsity with Tensor-Core-Aligned Execution Patterns

Structured sparsity reduces computational cost in AI workloads while preserving the dense arithmetic characteristics required for tensor-core acceleration. Unlike unstructured sparsity, which scatters zeros unpredictably and disrupts tile-aligned execution, structured sparsity organizes zero patterns into regular, hardware-aligned forms that maintain high arithmetic intensity, predictable memory access, and full vector-lane utilization. This alignment allows sparse workloads to remain near the compute-bound plateau even as the number of FLOPs is reduced.

One foundational mechanism is matrix block segmentation, exemplified by the 2:4 sparsity pattern. In this format, every group of four weights contains exactly two non-zero values. The weight matrix is segmented into contiguous 4-element blocks along the innermost dimension, ensuring that tensor cores can deterministically skip zero operands. The accelerator loads only

the two non-zero values and their indices, compressing the matrix into a dense half-sized representation while preserving tile-aligned execution. This pattern is widely used in MLP expansions, attention projections, and convolutional kernels, where the regularity of 2:4 segmentation aligns naturally with the hardware's vector width.

Structured sparsity also requires alignment with vector registers to avoid under-utilization of SIMD or SIMT lanes. Strided pruning enforces sparsity patterns that match the accelerator's vector width, ensuring that pruning occurs in blocks whose size equals the number of elements processed per cycle. If a vector lane processes k elements per cycle, sparsity must be applied in multiples of k:

$$\text{Stride} = k \quad \Rightarrow \quad \text{Prune groups of } k \text{ elements.}$$

This alignment prevents the hardware from loading zeros or performing masked operations that reduce effective throughput. Transformer architectures benefit significantly from strided pruning because their hidden dimensions often align with vector widths such as 64, 128, or 256. When sparsity respects these widths, sparse kernels maintain full vector-lane occupancy and avoid regressions into bandwidth-bound behavior.

Zero-skip scheduling further enhances structured sparsity by eliminating unnecessary accumulation of zero values. Dense GEMMs compute

$$C_{ij} = \sum_{k} A_{ik} B_{kj},$$

but structured sparsity guarantees that many terms in this sum are zero. Zero-skip scheduling rewrites the accumulation loop to iterate only over non-zero indices:

$$C_{ij} = \sum_{k \in NZ} A_{ik} B_{kj},$$

where NZ is the set of non-zero positions defined by the sparsity pattern. Because the pattern is structured, the scheduler can precompute index maps that align with tile boundaries, enabling efficient traversal of sparse blocks. This approach preserves arithmetic intensity by ensuring that tensor cores operate only on meaningful data, preventing sparse workloads from collapsing into memory-bound execution.

Dynamic sparsity introduces masks that change during training or inference, requiring efficient

mask generation to avoid overhead that negates the benefits of sparsity. Mask generation typically involves scoring weights or activations,

$$s_i = f(w_i) \quad \text{or} \quad s_i = f(a_i),$$

selecting top-k or thresholded values,

$$NZ = \{i \mid s_i \geq \tau\},$$

and constructing masks that conform to block, tile, or stride constraints. Hardware-friendly mask formats—such as block-sparse masks—allow dynamic sparsity to coexist with high-throughput execution. This capability is essential for mixture-of-experts routing, activation sparsity, and adaptive pruning, where mask patterns evolve but must remain compatible with tensor-core execution.

Together, these mechanisms transform sparsity from an irregular, bandwidth-limited phenomenon into a structured, compute-efficient strategy that scales across modern AI architectures. By enforcing block-aligned patterns, aligning sparsity with vector registers, skipping zero operations, and generating hardware-friendly dynamic masks, sparse workloads maintain high arithmetic intensity and remain compatible with tensor-core acceleration. Structured sparsity thus becomes a means of reducing computational cost without sacrificing the dense arithmetic characteristics required for high-throughput AI execution.

The mechanisms that enable tensor-core-aligned sparsity—block segmentation, vector-aligned pruning, zero-skip scheduling, and dynamic mask generation—form a coherent pipeline that transforms sparsity from an irregular pattern into a structured, hardware-efficient execution strategy. Each mechanism contributes a distinct form of alignment between the compute graph and the accelerator's architectural constraints, ensuring that sparse workloads maintain high arithmetic intensity and predictable memory behavior. The following table consolidates these mechanisms into a unified view, highlighting how each contributes to sustained throughput and stable execution on modern AI accelerators.

The roofline analysis presented in Figure 8.4-A1 demonstrated that achieving compute-bound execution depends on maximizing arithmetic intensity and minimizing unnecessary data movement. However, as AI models continue to increase in size, simply increasing computational workload is not a sustainable path toward higher efficiency. Modern accelerators frequently execute large numbers of arithmetic operations that contribute little to final model outputs, creating inefficiencies in both energy consumption and resource utilization. Structured sparsity

addresses this challenge by deliberately eliminating selected computations while preserving hardware-friendly execution patterns. Unlike arbitrary sparsity, which can introduce irregular memory accesses and underutilized compute units, structured sparsity is designed to align closely with accelerator architectures, tensor-core organizations, and vector-processing hardware. Table 8.4-A2 examines the principal sparsity mechanisms employed in modern AI systems and illustrates how carefully structured reductions in computation improve efficiency while maintaining hardware utilization and real-time performance.

Table 8.4-A2 presents several structured sparsity techniques that have emerged as important components of hardware-aware AI architecture design. Structured sparsity refers to the deliberate removal, masking, or bypassing of selected computations according to predictable patterns that can be exploited efficiently by modern hardware accelerators.

Traditional neural-network optimization often emphasizes reducing parameter counts or computational operations. However, unstructured reductions frequently create irregular execution behavior that is difficult for hardware to accelerate effectively. Modern AI systems therefore increasingly employ sparsity mechanisms that preserve predictable computational structures while reducing overall workload.

The table identifies four representative approaches: matrix block segmentation, vector-aligned strided pruning, zero-skip scheduling, and dynamic mask generation. Each technique addresses a specific aspect of computational efficiency while maintaining alignment with tensor-core designs, vector-processing architectures, memory subsystems, and sparse-computation hardware.

By examining these mechanisms through the lens of hardware alignment, the table demonstrates how sparsity is no longer viewed merely as a model-compression strategy but as a central element of hardware–software co-design.

Table 8.4-A2— Structured AI Sparsity Mechanisms and Hardware Alignment

Mechanism	Purpose	Hardware Alignment	Mathematical Structure	AI Workload Impact
Matrix Block Segmentation (2:4)	Reduce compute by 50% with predictable patterns	Aligns with tensor-core tile width	2 non-zeros per 4-element block	Efficient sparse GEMMs and MLPs

Mechanism	Purpose	Hardware Alignment	Mathematical Structure	AI Workload Impact
Vector-Aligned Strided Pruning	Maintain vector-lane utilization	Aligns sparsity with SIMD/SIMT width	Stride = vector width	Stable throughput in transformers
Zero-Skip Scheduling	Avoid zero multiplications	Aligns accumulation loops with sparse indices	Sum over non-zero set NZ	High intensity in sparse GEMMs
Dynamic Mask Generation	Adaptive sparsity with hardware-friendly masks	Aligns masks with block/tile formats	Thresholded selection $s_i \geq \tau$	Efficient MoE routing and activation sparsity

Table 8.4-A2 demonstrates that the effectiveness of sparsity depends not only on reducing computation but also on preserving architectural regularity. Sparse models achieve meaningful performance improvements only when sparsity patterns align with the execution capabilities of the underlying hardware.

The mechanisms summarized in the table reveal that modern AI accelerators derive the greatest benefit from sparsity when computation is removed in structured, predictable ways that maintain efficient scheduling, memory access, and parallel execution behavior.

The first sparsity mechanism identified in the table is **matrix block segmentation (2:4)**, one of the most widely adopted structured-sparsity approaches in contemporary AI accelerators. Under this strategy, computations are organized so that a fixed number of nonzero values are retained within predefined blocks. The example shown in the table retains two nonzero values within each four-element block.

This approach offers a significant advantage over arbitrary sparsity because the hardware can anticipate the location and pattern of retained values. By aligning sparsity with tensor-core tile structures, matrix block segmentation allows accelerators to eliminate approximately half of the computation while maintaining highly regular execution behavior. The result is improved efficiency for sparse matrix multiplications and multilayer perceptron (MLP) workloads without introducing substantial scheduling complexity.

The table next identifies **vector-aligned strided pruning**, which focuses on preserving efficient

vector-lane utilization. Modern processors perform computations using SIMD and SIMT execution models, where multiple operations are executed simultaneously across groups of vector lanes.

Random sparsity can leave some execution lanes underutilized, reducing throughput despite fewer arithmetic operations. Vector-aligned pruning avoids this problem by organizing sparsity according to the width of the vector-processing architecture. Because sparsity patterns align with execution lanes, hardware utilization remains high and throughput remains stable. This characteristic is particularly important for transformer workloads, where sustained throughput often determines real-time performance.

Another key mechanism is **zero-skip scheduling**, which targets one of the most common inefficiencies in neural-network execution: performing multiplications involving zero-valued operands. Traditional dense execution treats zero-valued and nonzero-valued elements identically, consuming computational resources even when arithmetic results contribute nothing meaningful.

Zero-skip scheduling addresses this issue by identifying sparse indices and directing computation only toward nonzero elements. Accumulation loops and execution pipelines are structured around useful work rather than dense storage representations. This approach increases effective arithmetic intensity and allows sparse GEMM operations to achieve substantially higher utilization of available hardware resources. The resulting improvements are particularly valuable in applications involving high-dimensional sparse representations.

The final sparsity mechanism presented in the table is **dynamic mask generation**, which represents a more adaptive approach to workload reduction. Rather than imposing static sparsity patterns, dynamic masking generates hardware-friendly sparsity structures in response to the characteristics of the current workload.

The table highlights threshold-based selection mechanisms that identify computations likely to provide the greatest contribution to output quality. Importantly, these masks remain aligned with block and tile structures supported by the hardware. This capability allows the system to reduce computation dynamically without sacrificing execution efficiency. Dynamic masking is especially valuable in architectures such as mixture-of-experts (MoE) networks, where only a subset of model components may need to be activated for a given input.

A broader insight emerging from the table is that modern sparsity design focuses on preserving execution regularity rather than maximizing sparsity alone. Historically, sparsity research often emphasized the percentage of computations removed from a model. Contemporary hardware-aware approaches place equal emphasis on preserving alignment with memory hierarchies,

execution units, and scheduling mechanisms.

The table also illustrates the close relationship between sparsity and arithmetic intensity. By reducing the amount of unnecessary computation and memory traffic, structured sparsity allows a larger fraction of available resources to be devoted to useful work. This contributes directly to the roofline optimization objectives discussed previously.

From a systems-engineering perspective, the sparsity mechanisms summarized in the table represent different methods of balancing efficiency and predictability. Matrix segmentation optimizes tensor-core utilization. Vector-aligned pruning maintains SIMD efficiency. Zero-skip scheduling improves sparse execution throughput. Dynamic masking provides workload adaptability. Together, these techniques improve performance without disrupting hardware utilization patterns.

Another important observation is that structured sparsity contributes not only to efficiency but also to deployability. Large AI models often exceed power, thermal, and memory constraints when deployed on embedded platforms. By reducing unnecessary computation while preserving predictable execution behavior, structured sparsity expands the range of hardware environments capable of supporting advanced AI workloads.

The table further demonstrates the evolution of AI architecture from purely algorithmic optimization toward integrated hardware–software design. Sparsity patterns are increasingly selected not only because they improve model efficiency but also because they correspond directly to architectural features present within modern accelerators.

Ultimately, Table 8.4-A2 demonstrates that structured sparsity is a fundamental mechanism for improving AI efficiency under real-world hardware constraints. Through matrix block segmentation, vector-aligned pruning, zero-skip scheduling, and dynamic mask generation, modern AI systems reduce computational workload while maintaining compatibility with tensor cores, vector processors, and memory hierarchies. These techniques allow AI workloads to achieve higher performance, lower energy consumption, and improved scalability while remaining aligned with the physical realities of modern computing hardware.

Table 8.4-A2 examined several structured sparsity mechanisms that improve computational efficiency while maintaining alignment with modern accelerator architectures. Although each mechanism offers distinct benefits, their greatest value emerges when they are applied as parts of an integrated sparsity pipeline rather than as isolated optimization techniques. Effective sparse execution requires more than removing computations; it requires transforming dense model representations into hardware-friendly formats that preserve vector-lane utilization, tensor-core occupancy, memory locality, and scheduling efficiency. Figure 8.4-A2 illustrates this

transformation process, tracing the progression from structured sparsity constraints through pruning, scheduling, adaptive masking, and final tensor-core-aligned execution. The figure demonstrates how software-defined sparsity patterns are systematically converted into forms that modern AI accelerators can exploit efficiently.

Figure 8.4-A2 presents a step-by-step view of a hardware-aware structured sparsity pipeline designed for modern AI accelerators. The figure demonstrates how sparsity evolves from a mathematical abstraction into a hardware-efficient execution format capable of improving throughput, reducing energy consumption, and lowering memory-traffic requirements.

Traditional dense neural-network execution treats every parameter equally, regardless of its contribution to inference. Structured sparsity introduces constraints that selectively preserve high-value computations while eliminating lower-value operations. However, the practical benefits of sparsity depend heavily on whether the resulting computational patterns remain compatible with accelerator execution units.

The figure illustrates a pipeline consisting of five major stages: matrix block segmentation, vector-aligned strided pruning, zero-skip scheduling, dynamic mask generation, and tensor-core-aligned sparse representation. Each stage progressively transforms the workload into a form that increases execution efficiency while preserving regularity and hardware compatibility.

By visualizing these transformations as a continuous process, the figure highlights the close relationship between algorithmic sparsity and hardware-aware execution.

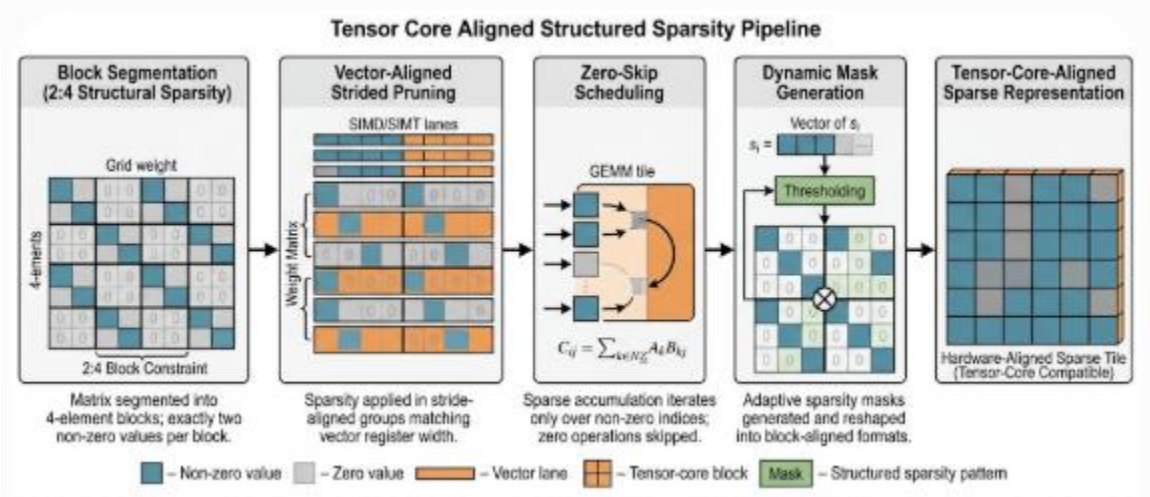


Figure 8.4-A2 — Tensor-Core-Aligned Structured Sparsity Pipeline
Multi-stage workflow illustrating the transformation of dense neural-network representations into hardware-efficient sparse formats. The figure traces the progression from 2:4 structural sparsity through vector-aligned pruning, zero-skip scheduling, adaptive mask generation, and tensor-core-aligned sparse

representations. The pipeline demonstrates how structured sparsity preserves computational efficiency, accelerator utilization, and memory locality while reducing arithmetic workload.

Legend

Component	***Description***
Block Segmentation (2:4 Structural Sparsity)	*Initial sparsity constraint retaining two nonzero values within each four-element block.*
Matrix Segment	*Representative weight matrix divided into structured sparsity blocks.*
Non-Zero Value (Blue)	*Parameter retained for execution.*
Zero Value (White)	*Parameter removed through sparsity.*
2:4 Block Constraint	*Hardware-friendly sparsity rule governing value retention.*
Vector-Aligned Strided Pruning	*Alignment of sparsity with SIMD/SIMT execution lanes.*
SIMD/SIMT Lanes	*Parallel execution units within modern accelerators.*
Vector Lane (Orange)	*Hardware execution pathway mapped to sparse computation.*
Weight Matrix with Strided Sparsity	*Matrix reorganized to match vector-processing structures.*
Zero-Skip Scheduling	*Scheduling stage that bypasses zero-valued operations.*
GEMM Tile	*Matrix multiplication unit used in tensor-core execution.*
Sparse Accumulation Loop	*Computation restricted to nonzero elements.*
Skipped Zero Operations	*Eliminated arithmetic contributing no useful output.*
Dynamic Mask Generation	*Adaptive creation of hardware-friendly sparsity masks.*
Thresholding Function	*Selection mechanism identifying retained values.*
Structured Sparsity Mask (Green)	*Binary mask governing computation retention and removal.*
Tensor-Core-Aligned Sparse Representation	*Final accelerator-friendly sparse format.*
Sparse Tile Layout	*Structured representation aligned with tensor-core geometry.*
Hardware-Aligned Sparse Tile	*Sparse execution format optimized for tensor-core processing.*

Tensor-Core Block	*Specialized matrix-processing hardware unit.*

Figure 8.4-A2 illustrates that the effectiveness of structured sparsity depends not only on removing computations but also on preserving execution regularity throughout the optimization process. The figure demonstrates how sparsity patterns are progressively refined until they align with the execution characteristics of tensor cores and vector-processing hardware.

Rather than treating sparsity as a single operation, the pipeline highlights a sequence of transformations that convert mathematical sparsity into practical computational efficiency.

The figure begins with **block segmentation using 2:4 structural sparsity**, which serves as the foundation for the entire optimization pipeline. In this stage, weights are organized into groups of four elements, with exactly two elements retained and two removed.

This structure differs significantly from random pruning approaches. By enforcing a predictable sparsity pattern, the accelerator can recognize the organization of the data and optimize execution accordingly. The blue cells in the matrix represent retained parameters, while the white cells represent eliminated values. Importantly, the retained values preserve the structure required for efficient tensor-core execution.

The next stage introduces **vector-aligned strided pruning**. Modern processors achieve high throughput through SIMD and SIMT execution models that process multiple values simultaneously.

Random sparsity can disrupt these execution lanes, leaving portions of the hardware underutilized. The figure illustrates how sparse values are reorganized so that retained parameters align with vector widths and execution-lane structures. This alignment ensures that sparse computations continue to exploit hardware parallelism effectively.

A key consequence of this alignment is sustained lane utilization. Rather than reducing workload at the cost of execution efficiency, strided pruning preserves both sparsity and throughput.

The third stage is **zero-skip scheduling**, which converts structured sparsity into execution-level savings. In conventional dense execution, all matrix elements are processed regardless of value. Sparse matrices contain large numbers of zeros, many of which contribute no useful information.

The figure shows a GEMM tile entering a scheduling stage where computation loops iterate only across retained nonzero values. Zero-valued operations are skipped entirely rather than

executed and discarded. As a result, arithmetic resources become concentrated on meaningful computations.

This stage is particularly important because it transforms sparsity from a storage property into a runtime-performance advantage. Eliminating unnecessary arithmetic directly increases computational efficiency and reduces energy consumption.

The fourth stage introduces **dynamic mask generation**, adding an adaptive element to the sparsity pipeline. Instead of relying exclusively on fixed sparsity structures, the system generates masks in response to workload characteristics.

The figure illustrates a thresholding process applied to a vector of values. Elements falling below the threshold are removed from execution, while higher-value elements remain active. The resulting binary mask controls which computations proceed through the pipeline.

Importantly, the generated masks remain aligned with block structures compatible with hardware execution requirements. This preserves regularity while providing flexibility to adapt sparsity according to workload demands.

Such mechanisms are particularly valuable in adaptive AI architectures, including mixture-of-experts systems and conditional-computation networks, where activations vary dynamically across inputs.

The final stage produces the **tensor-core-aligned sparse representation**, which serves as the execution-ready format consumed by the accelerator.

The resulting sparse tile retains all structural constraints introduced in previous stages while maximizing compatibility with tensor-core execution units. The visualization highlights how sparse values are organized into regular block structures that correspond closely to accelerator tile geometries.

This alignment allows tensor cores to process sparse workloads efficiently without sacrificing the high throughput for which they were designed. In effect, the pipeline converts sparse neural-network representations into hardware-native computational structures.

A broader insight emerging from the figure is that successful sparsity optimization requires cooperation between algorithm design and hardware architecture. Removing parameters alone does not guarantee performance gains. Performance improvements occur only when sparsity patterns respect the execution characteristics of the underlying hardware.

The figure also illustrates the importance of regularity in modern AI computing. Structured sparsity succeeds because it preserves predictable memory-access patterns, scheduling

behavior, and execution geometry. These properties allow hardware accelerators to exploit sparsity efficiently without introducing significant management overhead.

From a systems-engineering perspective, the pipeline demonstrates how optimization occurs across multiple abstraction layers. Mathematical sparsity constraints are transformed into scheduling decisions, execution patterns, and hardware representations. This progression exemplifies the principles of hardware–software co-design discussed throughout Section 8.4.

Another important observation is that each pipeline stage addresses a different performance challenge. Block segmentation reduces arithmetic workload. Vector alignment preserves parallelism. Zero-skip scheduling improves execution efficiency. Dynamic masking introduces adaptability. Tensor-core alignment maximizes hardware utilization. Together, these stages create a cohesive optimization framework.

Ultimately, Figure 8.4-A2 demonstrates that structured sparsity is most effective when implemented as a coordinated pipeline rather than as a simple pruning technique. Through block segmentation, vector-aware organization, zero-skipping, adaptive masking, and tensor-core alignment, AI models reduce computational workload while preserving efficient accelerator execution. This integrated process enables substantial improvements in throughput, energy efficiency, and scalability while maintaining compatibility with the execution characteristics of modern AI hardware.

Figure 8.4-A2 illustrates that structured sparsity is not implemented as a single optimization technique but rather as a coordinated pipeline that progressively transforms dense computations into hardware-efficient execution patterns. At the foundation of this pipeline lies **block segmentation**, which establishes the regular sparsity structure required for all subsequent optimization stages. Before vector-aligned pruning can preserve SIMD and SIMT utilization, before zero-skip scheduling can eliminate redundant multiply–accumulate operations, and before dynamic masking can adapt computation to workload demands, the model must first organize parameters into predictable, hardware-compatible blocks. This initial structuring step defines the granularity of sparsity, determines metadata organization, and creates the regular execution patterns that modern accelerators require for efficient sparse computation. Consequently, **AI Matrix Block Segmentation for 2:4 Structural Sparsity** serves as the fundamental building block of hardware-aligned sparsity, providing the architectural framework upon which tensor-core utilization, scheduling efficiency, and sparse execution performance ultimately depend.

i. AI Matrix Block Segmentation for 2:4 Structural Sparsity

AI Matrix Block Segmentation for 2:4 Structural Sparsity represents a foundational co-design

strategy that tightly couples neural network pruning with accelerator-native sparse execution. The 2:4 constraint enforces that, within every contiguous 4-element window of a weight matrix, exactly two elements remain non-zero while the other two are pruned. This pattern is not arbitrary; it is engineered to match the operand-fetch granularity of Sparse Tensor Cores, which rely on fixed-width blocks to maintain predictable memory access and deterministic zero-skipping behavior. By constraining sparsity at this granularity, the accelerator can bypass half of the multiplications while still operating on tile-aligned data structures that preserve high arithmetic intensity.

The segmentation process begins by partitioning each row of the weight matrix into non-overlapping 4-element windows:

$$W = \{w_1, w_2, w_3, w_4\} \rightarrow \text{select two non-zero elements}$$

This selection is typically magnitude-based, choosing the two largest-magnitude weights to retain. The remaining two weights are pruned and replaced with zeros. The positions of the retained weights are encoded using a compact **2-bit metadata map**, which specifies which two of the four positions contain non-zero values. Sparse Tensor Cores use this metadata to reconstruct the compressed representation during execution, allowing the hardware to load only the non-zero values and skip the zero positions entirely.

The mathematical structure of 2:4 sparsity introduces both benefits and constraints. The enforced 50% sparsity doubles theoretical compute throughput because the accelerator performs half the multiplications. However, the segmentation window is strictly local: pruning decisions are made within each 4-element block rather than across the entire row or layer. This locality can limit pruning flexibility and introduce accuracy degradation if applied naively. Sparse-aware fine-tuning mitigates this issue by retraining the model after segmentation, allowing weights to adapt to the imposed sparsity pattern. Empirically, fine-tuned 2:4 sparse models often recover most of the accuracy lost during initial pruning, demonstrating that the structured constraint can coexist with high-quality inference.

The hardware-software co-design aspect becomes especially clear when examining how 2:4 sparsity interacts with accelerator execution. Sparse Tensor Cores expect compressed blocks that align with their internal tile dimensions, ensuring that each tile contains a predictable number of non-zero values. This alignment preserves the dense arithmetic behavior required for compute-bound execution, preventing sparse workloads from collapsing into bandwidth-bound regimes. The metadata map allows the hardware to reconstruct the sparse pattern on the fly, enabling efficient zero-skip scheduling and maintaining high utilization of

vector lanes.

In practical AI development ecosystems, mastering 2:4 segmentation requires navigating post-training pipelines and leveraging specialized toolkits. Frameworks such as **NVIDIA cuSPARSELt**, **TensorRT**, and **PyTorch Semi-Structured Sparsity APIs** provide end-to-end support for pruning, metadata generation, compressed matrix formats, and sparse GEMM execution. These tools automate the segmentation process, enforce hardware-compatible patterns, and integrate sparse-aware fine-tuning routines. As a result, developers can incorporate 2:4 sparsity into large-scale transformer models, MLP expansions, and convolutional layers without manually managing metadata or tile alignment.

Ultimately, AI Matrix Block Segmentation for 2:4 Structural Sparsity is more than a pruning technique—it is a disciplined engineering method that balances physical hardware constraints, mathematical pruning rules, and model-level accuracy requirements. By enforcing predictable block-level sparsity and pairing it with sparse-aware fine-tuning, AI workloads can achieve substantial compute savings while maintaining compatibility with tensor-core acceleration. This alignment transforms sparsity from a theoretical optimization into a practical, high-throughput strategy for modern deep learning systems.

The 2:4 segmentation pattern establishes the foundational granularity that allows sparse weights to be compressed, indexed, and interpreted by accelerator hardware without losing tile-level regularity. Yet segmentation alone does not guarantee efficient execution across the full hierarchy of compute units. Once weights have been pruned into predictable 4-element blocks, the next challenge is ensuring that these surviving values align with the physical width of vector registers and warp-level execution lanes. Sparse Tensor Cores operate on tile-aligned fragments, but SIMD and SIMT pipelines require stride-aligned operand layouts to avoid masked operations, misaligned loads, and lane divergence. This makes **Vector Register Alignment and Strided Pruning** the natural continuation of the sparsity pipeline: it extends the structural regularity introduced by 2:4 segmentation into the broader vectorization fabric of CPUs, GPUs, and AI accelerators, ensuring that sparse parameters map cleanly onto register boundaries and maintain full instruction-level parallelism.

ii. Vector Register Alignment and Strided Pruning in AI Models

Vector Register Alignment and Strided Pruning represent a critical hardware-software co-design paradigm that enforces periodic, stride-based sparsity patterns on neural network weights to maximize Single Instruction, Multiple Data (SIMD) efficiency. This optimization is rooted in the physical structure of vector registers—such as AVX-512, ARM Neon, SVE, and GPU warp-level vector lanes—which operate on fixed-width chunks of data per instruction. When sparsity is

applied without regard for these widths, the hardware must load misaligned memory segments, introduce masked operations, or execute divergent control paths, all of which reduce effective throughput. Strided pruning solves this by ensuring that surviving weights align perfectly with the byte-boundaries and lane widths of the underlying vector architecture.

The core idea is that sparsity must be applied in **stride-aligned windows** whose size matches the number of elements processed per SIMD instruction. If a vector lane processes k elements per cycle, pruning must operate on blocks of size k:

$$\text{Stride} = k \quad \Rightarrow \quad \text{Prune groups of } k \text{ elements.}$$

This ensures that each SIMD lane receives a consistent number of non-zero operands, eliminating the need for conditional masking or lane-level divergence. For example, AVX-512 processes 16 FP32 values per instruction, while many GPU tensor-core pipelines operate on 32-wide or 64-wide fragments. Strided pruning enforces sparsity patterns that respect these widths, guaranteeing that each vector register contains a predictable distribution of non-zero values.

The hardware implications are significant. Vector registers are designed to fetch contiguous memory segments, and misaligned sparsity forces the hardware to perform additional loads, shuffle operations, or masked multiplications. These operations break cache coalescing, reduce memory bandwidth efficiency, and introduce control-flow divergence across lanes. By contrast, stride-aligned sparsity preserves contiguous memory access, enabling multi-vector multiplications to proceed without interruption. This alignment ensures that sparse workloads maintain high arithmetic intensity and remain compatible with compute-bound execution regimes.

The mathematical rigidity of strided pruning introduces constraints similar to those seen in 2:4 block sparsity. Pruning decisions must be made within fixed-width windows rather than across entire layers, limiting flexibility but enabling hardware determinism. Magnitude-based selection within each stride window is commonly used, retaining the most influential weights while pruning the rest. Sparse-aware fine-tuning then compensates for the imposed structure, allowing the model to adapt to the periodic sparsity pattern and recover accuracy lost during initial pruning.

The software stack plays an equally important role. Low-level compilers—LLVM, GCC, NVCC, and MLIR-based toolchains—must map sparse parameters directly onto native register boundaries. This requires careful coordination between pruning algorithms, memory layout transformations, and code generation passes. Compiler backends must ensure that surviving weights are packed

into register-aligned buffers, that load/store operations remain coalesced, and that vector instructions operate without masked divergence. When these conditions are met, instruction-level parallelism is maximized, and sparse kernels achieve throughput comparable to dense execution.

In practical AI development ecosystems, vector-aligned sparsity is supported through specialized libraries and frameworks. GPU-oriented toolchains leverage warp-aligned pruning to maintain SIMT efficiency, while CPU-oriented frameworks use AVX-512-aligned pruning to optimize inference on x86 servers. PyTorch, TensorFlow, and JAX integrate strided pruning through custom pruning hooks and graph-level transformations, ensuring that sparsity patterns remain compatible with backend vectorization strategies.

Ultimately, Vector Register Alignment and Strided Pruning transform sparsity from a purely algorithmic optimization into a hardware-aware execution strategy. By aligning pruning windows with physical vector lane widths, AI workloads eliminate control divergence, preserve cache coalescing, and maintain high SIMD/SIMT utilization. This alignment ensures that sparse models retain the dense arithmetic characteristics required for high-throughput execution, making strided pruning a cornerstone of modern accelerator-optimized sparsity pipelines.

Vector-aligned strided pruning ensures that sparse parameters map cleanly onto SIMD and SIMT register boundaries, eliminating lane divergence and preserving the uniform operand layout required for high-throughput vector execution. Yet even with perfectly aligned sparsity, the accelerator still faces a second challenge: sparse operands must be consumed efficiently during accumulation. Register alignment determines *where* non-zero values reside, but it does not determine *how* they flow through the arithmetic pipeline. Sparse workloads contain irregular distributions of non-zero elements across tiles, rows, and layers, and executing MAC operations on zero operands would negate the benefits of strided pruning. This transition leads directly into **Zero-Skip Scheduling for Sparse AI Accumulation**, where the focus shifts from structural alignment to runtime execution. Here, hardware schedulers dynamically traverse only the valid non-zero indices, bypassing redundant operations and ensuring that sparse data streams enter the MAC pipeline without stalls, hazards, or wasted cycles.

iii. Zero-Skip Scheduling for Sparse AI Accumulation

Zero-Skip Scheduling for Sparse AI Accumulation represents a critical hardware-software co-design paradigm that restructures the execution of multiply-accumulate (MAC) operations so that only meaningful, non-zero contributions enter the arithmetic pipeline. In dense linear algebra, accumulation proceeds uniformly across all indices, regardless of whether operands contain useful values. Sparse AI workloads, however, contain large regions of guaranteed

zeros—introduced through structured pruning, activation sparsity, or block-sparse attention—and executing MAC operations on these zeros wastes compute cycles, memory bandwidth, and energy. Zero-skip scheduling eliminates this waste by enforcing real-time computational gating: the hardware executes accumulation only when operands are non-zero, bypassing redundant operations entirely.

The mathematical foundation of zero-skip scheduling begins with the standard dense accumulation:

$$C_{ij} = \sum_{k} A_{ik} B_{kj}.$$

Under sparsity, many terms in this summation are guaranteed to be zero. Zero-skip scheduling rewrites the accumulation loop to iterate only over the set of non-zero indices:

$$C_{ij} = \sum_{k \in NZ} A_{ik} B_{kj},$$

where NZ is the sparsity-defined index set. This transformation appears simple, but its hardware implications are profound. Instead of executing a fixed-length loop, the accelerator dynamically traverses only the coordinates that contain valid operands. This requires compressed metadata—coordinate lists, bitmasks, or block-sparse index maps—to guide the scheduler. Sparse Tensor Cores and dataflow accelerators use this metadata to route non-zero values directly into MAC units while skipping over null entries without triggering pipeline stalls.

The hardware-software co-design challenge lies in managing the **non-uniformity** of sparse data. Dense workloads have predictable memory access patterns and uniform loop bounds, enabling straightforward pipelining. Sparse workloads, by contrast, introduce irregularity: the number of non-zero elements varies across tiles, rows, and layers. Zero-skip scheduling must track these variations in real time without incurring excessive microarchitectural overhead. Hardware schedulers accomplish this by using compressed index maps that encode sparsity in formats aligned with tile boundaries. These maps allow the scheduler to fetch only the relevant operands, preserving cache locality and minimizing memory bus traffic.

Energy efficiency is a central motivation for zero-skip scheduling. MAC operations dominate the power budget of AI accelerators, and skipping half or more of these operations yields substantial reductions in dynamic power consumption. Because memory accesses also consume significant energy, bypassing loads associated with zero operands further reduces the total energy footprint. This makes zero-skip scheduling particularly valuable in large-scale inference

deployments, where billions of MAC operations are executed per second.

Zero-skip scheduling also interacts closely with dataflow accelerator architectures. In systolic arrays, for example, data flows through fixed pipelines, and skipping operations must be carefully coordinated to avoid hazards. Compressed metadata ensures that valid operands enter the array at the correct cycle, preventing bubbles or stalls. In GPU tensor-core pipelines, zero-skip scheduling is integrated with warp-level execution, ensuring that only active lanes participate in accumulation while inactive lanes remain masked without causing divergence. In CPU vector pipelines, zero-skip scheduling aligns with vector-register packing, ensuring that non-zero values are grouped contiguously to maximize SIMD efficiency.

Mastering zero-skip scheduling requires understanding how runtime execution constraints interact with sparse data structures. Coordinate lists, compressed sparse row (CSR) formats, block-sparse masks, and 2-bit metadata maps must be laid out so that hardware can traverse them without unpredictable branching. Compiler passes must generate sparse-aware loops that map non-zero indices directly into arithmetic pipelines. Runtime systems must ensure that metadata is prefetched and cached efficiently to avoid latency spikes. When these conditions are met, sparse workloads achieve throughput comparable to dense execution while consuming significantly less energy.

Ultimately, Zero-Skip Scheduling for Sparse AI Accumulation transforms sparsity from a static pruning strategy into a dynamic execution optimization. By ensuring that only meaningful operands enter the MAC pipeline, AI accelerators maintain high utilization, reduce energy consumption, and avoid the performance penalties typically associated with irregular sparsity. This alignment between sparse data structures and physical arithmetic pipelines makes zero-skip scheduling a cornerstone of modern accelerator-optimized AI sparsity frameworks.

Zero-skip scheduling establishes the runtime discipline required for sparse workloads to maintain high arithmetic intensity by ensuring that only meaningful, non-zero operands enter the MAC pipeline. However, zero-skip scheduling assumes that the sparsity pattern is already known and encoded before execution begins. In many modern AI architectures—particularly mixture-of-experts models, activation-sparse transformers, and conditional-compute systems—the sparsity pattern is not static but evolves dynamically based on input-dependent activation behavior. This introduces a new challenge: the accelerator must generate masks in real time, encode them into hardware-friendly formats, and route valid operands into execution lanes without stalling pipelines or saturating memory bandwidth. This transition leads directly into **Dynamic Mask Generation for AI Sparsity Pipelines**, where sparsity becomes an adaptive, data-driven mechanism that reshapes the compute graph on the fly. Here, the focus shifts from skipping zeros to *deciding which values should exist at all*, enabling AI models to prune

computation paths dynamically while preserving alignment with underlying hardware execution structures.

iv. Dynamic Mask Generation for AI Sparsity Pipelines

Dynamic Mask Generation for AI Sparsity Pipelines represents a critical hardware-software co-design paradigm that enables real-time, data-dependent pruning decisions during model execution. Unlike static sparsity, which fixes zero patterns at training time, dynamic sparsity adapts to fluctuating activation distributions, routing computation only through the most informative pathways at each forward pass. This adaptivity allows AI workloads to reduce computational cost while preserving responsiveness to input-dependent structure, making dynamic mask generation essential for mixture-of-experts models, activation-sparse transformers, and conditional computation architectures.

The mathematical foundation of dynamic mask generation begins with computing a relevance score for each weight or activation:

$$s_i = f(w_i) \quad \text{or} \quad s_i = f(a_i),$$

where f(·) may represent magnitude, gradient sensitivity, gating logits, or attention-derived importance. A threshold or top-k selection rule then determines which elements remain active:

$$NZ = \{i \mid s_i \geq \tau\},$$

producing a mask that identifies the non-zero set NZ. This mask is not merely a logical structure—it must be encoded in hardware-friendly formats such as block-sparse masks, tile-aligned bitmaps, or compressed coordinate lists. These formats ensure that dynamically generated sparsity patterns remain compatible with accelerator execution pipelines.

The hardware implications are substantial. Dynamic masks must be generated quickly enough to avoid stalling the forward pass, yet structured enough to align with physical execution lanes. Dataflow accelerators, systolic arrays, and Sparse Tensor Cores require masks that map directly onto tile boundaries, ensuring that valid operands enter arithmetic pipelines without causing hazards or bubbles. If masks are misaligned, the hardware must perform masked loads, divergent branching, or irregular memory fetches—operations that degrade throughput and saturate memory bandwidth.

Dynamic mask generation bypasses static architectural limitations by allowing computation blocks to activate or deactivate based on real-time activation patterns. For example, in

activation-sparse transformers, only tokens with high activation magnitudes propagate through expensive MLP expansions, while low-magnitude tokens are dropped early. In mixture-of-experts routing, masks determine which experts receive input, dynamically shaping the compute graph based on gating logits. These mechanisms reduce parameter usage and computational load across highly conditional layers, enabling large models to scale efficiently without uniformly activating all components.

The microarchitectural challenge lies in computing sparse metadata masks during the forward pass without introducing latency spikes. Mask generation must be pipelined, cached, and aligned with vector register widths. Hardware schedulers must interpret masks in real time, routing valid operands into MAC units while skipping inactive lanes. Memory systems must fetch mask metadata efficiently to avoid bandwidth saturation. When these constraints are met, dynamic sparsity achieves near-dense throughput while drastically reducing compute and energy consumption.

Software frameworks play an equally important role. Adaptive sparsity requires integration with runtime systems capable of generating masks on the fly, updating compressed metadata, and coordinating mask-aware kernel launches. Frameworks such as PyTorch's dynamic sparsity APIs, TensorFlow's conditional computation primitives, and JAX's XLA-based mask fusion pipelines provide the necessary infrastructure. Specialized silicon—such as Sparse Tensor Cores, adaptive systolic arrays, and mask-aware vector units—further accelerates dynamic sparsity by embedding mask interpretation directly into hardware.

Ultimately, Dynamic Mask Generation for AI Sparsity Pipelines transforms sparsity from a static pruning strategy into a real-time adaptive execution mechanism. By generating masks that reflect instantaneous activation patterns and mapping them onto hardware-aligned formats, AI workloads achieve substantial computational savings without sacrificing responsiveness or accuracy. This alignment between dynamic metadata generation and physical execution lanes makes dynamic mask generation a cornerstone of modern conditional-compute architectures and accelerator-optimized sparsity pipelines.

Structured AI sparsity transforms the traditional notion of pruning from a static compression technique into a hardware-aligned execution strategy capable of sustaining high throughput on modern accelerators. By enforcing predictable block structures, aligning surviving weights with vector register widths, skipping zero operations during accumulation, and generating dynamic masks that adapt to real-time activation patterns, sparsity becomes a coordinated pipeline rather than an isolated optimization. Each mechanism contributes a distinct form of alignment—spatial, temporal, or architectural—that ensures sparse workloads retain the dense arithmetic characteristics required for compute-bound execution. The result is a sparsity

framework that reduces computational cost, lowers energy consumption, and preserves model accuracy while remaining fully compatible with tensor-core acceleration. In effect, structured sparsity allows AI models to scale more efficiently without sacrificing the performance guarantees traditionally associated with dense computation.

The structured sparsity pipeline demonstrates how computation can be reduced without undermining accelerator utilization, but sparsity alone cannot address the growing imbalance between compute capability and memory bandwidth in large-scale AI models. As model sizes increase and sequence lengths expand, attention mechanisms—not matrix multiplications—become the dominant source of memory pressure. Even perfectly structured sparsity cannot prevent attention layers from saturating memory channels, fragmenting cache locality, or exceeding on-chip buffer capacity. This transition shifts the optimization focus from arithmetic reduction to bandwidth conservation. **Memory-Optimized AI Attention Mechanisms for Bandwidth-Constrained Models** therefore emerges as the next critical frontier, exploring how attention can be reorganized, tiled, compressed, or approximated to operate within the strict memory budgets of modern accelerators while preserving the expressive power that makes attention indispensable in contemporary AI architectures.

c. Memory-Optimized AI Attention Mechanisms for Bandwidth-Constrained Models

Memory-Optimized AI Attention Mechanisms for Bandwidth-Constrained Models represent a critical shift in modern accelerator design, where the limiting factor is no longer raw compute throughput but the ability to feed attention layers with sufficient data at the right time. As sequence lengths grow and model sizes expand, attention becomes the dominant consumer of memory bandwidth, outpacing even large GEMM operations. Optimizing attention therefore requires a coordinated hardware-software strategy that reduces off-chip traffic, improves on-chip data reuse, and restructures the attention pipeline to operate within strict bandwidth budgets.

One foundational technique is **on-chip SRAM tiling for softmax attention**, which reorganizes the Q, K, and V matrices into tile-aligned fragments that fit entirely within the accelerator's SRAM or shared memory. Instead of repeatedly streaming large matrices from HBM, the attention kernel loads tiles once, performs all required dot-products and softmax operations locally, and writes back only the final results. This tiling strategy dramatically reduces HBM traffic and ensures that the most bandwidth-intensive operations—QK^T multiplication and softmax normalization—occur entirely on-chip. The mathematical structure of attention,

$$\text{Attention}(Q, K, V) = \text{softmax}\left(\frac{QK^T}{\sqrt{d}}\right)V,$$

is preserved, but the dataflow is reorganized so that each tile of Q and K is reused multiple times before eviction. This transforms attention from a bandwidth-bound operation into a compute-bound one, allowing accelerators to sustain high throughput even for long-context workloads.

Complementing SRAM tiling is **HBM traffic reduction for high-throughput attention**, which focuses on minimizing redundant reads and writes across the memory hierarchy. Techniques such as fused QKV loading, prefetch-aware scheduling, and compressed KV representations reduce the number of bytes transferred per token. Hardware-aware attention kernels exploit burst-aligned memory accesses and coalesced loads to maximize effective bandwidth. In multi-head attention, shared K and V tensors are streamed once and reused across heads, eliminating redundant memory fetches. These optimizations ensure that HBM bandwidth is reserved for essential data movement rather than wasted on repeated transfers of identical tensors.

The next challenge arises in decoder-only architectures, where autoregressive generation requires maintaining a growing KV-cache. **KV-cache slicing and parallel query execution** address this by partitioning the KV-cache into smaller slices that align with on-chip buffer boundaries. Instead of loading the entire cache for each new token, the decoder loads only the relevant slices, dramatically reducing memory pressure. Parallel query execution pipelines multiple Q vectors through the attention mechanism simultaneously, amortizing cache loads across multiple tokens. This approach transforms KV-cache access from a monolithic bandwidth bottleneck into a parallelizable, slice-aware dataflow that scales efficiently with sequence length.

Finally, long-context inference introduces a unique challenge: attention cost grows quadratically with sequence length, and even optimized tiling cannot prevent memory saturation. **Asymmetric attention barriers** solve this by imposing structural constraints on how far each token can attend. Instead of full-sequence attention, models use sliding windows, dilated attention, or hierarchical memory blocks that restrict attention to a subset of the context. These barriers reduce the size of QK^T operations and limit the amount of KV data that must be fetched from memory. The result is a bandwidth-controlled attention mechanism that preserves long-range reasoning while avoiding the quadratic explosion in memory traffic.

Together, these techniques form a cohesive pipeline for memory-optimized attention. SRAM

tiling improves on-chip reuse, HBM reduction minimizes off-chip traffic, KV-cache slicing restructures decoder dataflow, and asymmetric barriers constrain long-context memory growth. Each mechanism addresses a different layer of the memory hierarchy, ensuring that attention remains feasible even as models scale to millions of tokens and trillions of parameters. In effect, memory-optimized attention transforms bandwidth from a limiting factor into a manageable resource, enabling next-generation AI models to operate efficiently under real-world hardware constraints.

The mechanisms introduced in this discussion collectively reframe attention not as a purely algorithmic construct but as a memory-hierarchy optimization problem. Each technique—SRAM tiling, HBM traffic reduction, KV-cache slicing, and asymmetric attention barriers—targets a different layer of the memory stack, ensuring that attention can operate efficiently even when bandwidth becomes the dominant bottleneck. To consolidate these ideas and highlight their complementary roles, the following table organizes the four mechanisms into a unified framework that maps their purpose, memory alignment strategy, mathematical structure, and practical impact on real-world AI workloads. This table serves as the conceptual anchor for understanding how attention can be systematically redesigned to fit within the constraints of modern accelerator architectures.

Table 8.4-A2 demonstrated how structured sparsity reduces computational workload by eliminating unnecessary arithmetic operations while maintaining alignment with accelerator execution units. However, even highly optimized sparse workloads often encounter a second and equally significant constraint: memory movement. In contemporary transformer architectures, attention computation frequently consumes more bandwidth and memory resources than the arithmetic operations themselves. As context lengths increase and sequence-processing requirements expand, the cost of moving query, key, value, and activation data through memory hierarchies can dominate overall execution time. Consequently, hardware-aware AI design must address not only computational efficiency but also memory efficiency. Table 8.4-A3 examines the principal memory-optimized attention mechanisms used in modern AI systems and illustrates how architectural innovations reduce off-chip memory traffic, improve data locality, and sustain high-performance inference under bandwidth-constrained conditions.

Table 8.4-A3 presents several architectural techniques designed to reduce the memory and bandwidth burden associated with attention-based AI models. While attention mechanisms have become a foundational component of modern transformers, their computational efficiency is often limited less by arithmetic throughput than by memory-access behavior.

In large-scale AI systems, queries (Q), keys (K), values (V), intermediate activations, and cached

context states must be repeatedly transferred among memory hierarchies. These transfers consume bandwidth, increase latency, and place significant pressure on accelerator memory resources. Consequently, memory movement frequently becomes the primary bottleneck even when substantial computational capacity remains available.

The table identifies four representative optimization strategies: on-chip SRAM tiling for softmax attention, high-bandwidth-memory (HBM) traffic reduction techniques, KV-cache slicing with parallel query execution, and asymmetric attention barriers for long-context inference. Each technique addresses a different component of the memory-access problem while preserving or improving model performance.

By examining attention optimization through the lens of memory hierarchy design, the table illustrates a central principle of modern AI architecture: performance gains increasingly originate from reducing data movement rather than from increasing computational capability alone.

Table 8.4-A3 — Memory-Optimized AI Attention Mechanisms for Bandwidth-Constrained Models

Mechanism	Purpose	Memory-Hierarchy Alignment	Mathematical / Dataflow Structure	AI Workload Impact
On-Chip SRAM Tiling for Softmax Attention	Increase data reuse and reduce off-chip memory traffic	Aligns Q/K/V tiles with SRAM/shared memory capacity	Tile-wise evaluation of $QK^{T,}$ softmax, and V multiplication	Converts attention from bandwidth-bound to compute-bound; improves throughput for long sequences
HBM Traffic Reduction for High-Throughput Attention	Minimize redundant reads/writes across memory channels	Aligns fused QKV loads and burst-coalesced transfers with HBM bandwidth	Fused QKV fetch, compressed KV formats, coalesced multi-head reuse	Sustains high attention throughput under strict HBM limits

Mechanism	Purpose	Memory-Hierarchy Alignment	Mathematical / Dataflow Structure	AI Workload Impact
KV-Cache Slicing & Parallel Query Execution	Reduce KV-cache load footprint during autoregressive decoding	Aligns KV slices with on-chip buffer boundaries and parallel pipelines	Slice-aware KV access; multi-query pipelining	Enables scalable decoding for long contexts; reduces per-token latency
Asymmetric Attention Barriers for Long-Context Inference	Constrain quadratic memory growth in long-context attention	Aligns windowed/dilated attention with memory budget	Sliding windows, dilated patterns, hierarchical blocks	Supports million-token contexts without saturating memory bandwidth

Table 8.4-A3 demonstrates that many attention-related performance limitations originate from memory bandwidth constraints rather than insufficient arithmetic resources. The optimization mechanisms summarized in the table seek to reduce memory traffic, improve locality, and maximize reuse of data already resident within accelerator memory.

These techniques reveal a broader architectural trend: modern AI systems increasingly achieve performance gains by aligning model execution with memory hierarchies rather than solely by increasing computational throughput.

The first mechanism identified in the table is **on-chip SRAM tiling for softmax attention**, which addresses one of the most significant sources of memory traffic in transformer architectures. Traditional attention computation frequently transfers large query, key, and value tensors between on-chip and off-chip memory resources. These transfers introduce latency and consume valuable bandwidth.

SRAM tiling mitigates this challenge by partitioning attention computation into smaller regions that fit within accelerator-local memory. Query, key, and value data remain resident on-chip for longer periods, reducing repeated memory transfers. The table highlights tile-wise evaluation of attention operations, including softmax computation and value aggregation. By increasing data reuse and limiting off-chip access, this approach effectively shifts attention workloads from bandwidth-constrained execution toward compute-bound execution, improving throughput for long-context processing.

The second optimization strategy is **HBM traffic reduction for high-throughput attention**. High-bandwidth memory provides substantially greater throughput than conventional memory systems, but even HBM becomes a bottleneck when attention workloads repeatedly access large data structures.

To address this issue, modern architectures employ fused QKV loading, compressed KV representations, and coalesced memory-access strategies. Rather than transferring redundant information across memory channels, these techniques maximize data reuse during execution. As the table indicates, the result is sustained attention throughput even when HBM capacity and bandwidth remain limited. This optimization is particularly important in large-scale language models where attention layers dominate memory consumption.

Another critical mechanism is **KV-cache slicing and parallel query execution**, which targets autoregressive generation workloads. During token generation, transformer architectures maintain key-value caches that grow continuously as context length increases.

Without optimization, these caches place significant pressure on memory systems and increase access latency. KV-cache slicing addresses this issue by partitioning cached information into segments aligned with on-chip memory boundaries and parallel-processing structures. Combined with parallel query execution, this approach reduces the time required to access context information while maintaining scalability. The resulting reduction in per-token latency is especially valuable for conversational AI systems and long-context reasoning applications.

The final optimization technique identified in the table is **asymmetric attention barriers for long-context inference**. Traditional attention implementations often exhibit quadratic memory growth as context length increases, making very long sequences difficult to process efficiently.

Asymmetric attention mechanisms impose architectural constraints that limit the need for unrestricted attention across the entire sequence. Techniques such as sliding-window attention, dilated attention, and hierarchical memory structures reduce the volume of context that must be accessed simultaneously. By constraining memory growth while preserving useful contextual information, these methods enable processing of extremely long sequences without saturating available bandwidth. The table highlights support for million-token contexts as a particularly important benefit of this approach.

A broader insight emerging from the table is that memory access has become a dominant factor in attention-system performance. In many modern accelerators, arithmetic resources are abundant, but memory bandwidth remains constrained. Consequently, reducing unnecessary data movement often provides larger performance gains than increasing floating-point throughput.

The table also illustrates the importance of memory-hierarchy awareness in AI architecture design. Local SRAM, cache structures, HBM resources, and context-storage systems each possess different performance characteristics. Effective attention mechanisms exploit these hierarchies strategically, placing frequently reused information in faster memory layers and minimizing expensive off-chip transfers.

From a systems-engineering perspective, the optimization strategies summarized in the table represent complementary approaches to the same challenge. SRAM tiling improves locality. HBM optimization reduces transfer redundancy. KV-cache slicing improves context-access efficiency. Asymmetric barriers limit memory growth itself. Together, these techniques create a comprehensive framework for managing memory-intensive attention workloads.

Another important observation is that these mechanisms contribute directly to real-time performance and system reliability. Excessive memory traffic introduces latency variability and resource contention, both of which complicate real-time scheduling and safety-critical operation. By reducing memory bottlenecks, the techniques presented in the table help maintain predictable execution characteristics.

The table further demonstrates a significant shift in AI-system optimization philosophy. Earlier generations of AI hardware focused primarily on increasing computational throughput. Contemporary architectures increasingly focus on reducing memory-access costs because data movement has become one of the dominant contributors to energy consumption, latency, and performance limitations.

Ultimately, Table 8.4-A3 demonstrates that memory optimization has become a foundational component of modern attention architectures. Through SRAM tiling, HBM-aware dataflow strategies, KV-cache partitioning, and long-context attention barriers, AI systems reduce bandwidth pressure, improve data locality, and sustain high-performance execution under realistic hardware constraints. These techniques enable scalable attention computation while preserving the throughput, responsiveness, and efficiency required for advanced autonomous AI applications.

Table 8.4-A3 introduced several architectural techniques that reduce memory traffic and improve data locality within attention-based AI systems, including SRAM tiling, HBM traffic optimization, KV-cache partitioning, and long-context attention constraints. While each mechanism addresses a specific source of bandwidth pressure, practical attention acceleration emerges from their coordinated application within a unified execution pipeline. Modern attention systems achieve high throughput not through a single optimization but through a sequence of memory-aware transformations that progressively reduce off-chip accesses,

increase data reuse, and align dataflow with accelerator memory hierarchies. Figure 8.4-A3 visualizes this progression by illustrating how attention computation moves through multiple stages of memory optimization before producing a bandwidth-efficient output representation suitable for large-scale and long-context AI workloads.

Figure 8.4-A3 presents a conceptual architecture for memory-optimized attention execution in modern AI systems. The figure traces the transformation of attention computation from a memory-intensive operation into a hardware-efficient pipeline that minimizes bandwidth consumption and maximizes accelerator utilization.

Attention mechanisms have become a fundamental component of transformer-based models because they enable context-aware reasoning across large sequences. However, attention operations also impose significant memory demands. Query (Q), key (K), and value (V) tensors must be repeatedly loaded, stored, and reused, creating substantial traffic across memory hierarchies. As sequence lengths increase, this memory activity often becomes a greater performance limitation than the arithmetic computation itself.

The figure illustrates four major optimization stages: on-chip SRAM tiling, high-bandwidth-memory traffic reduction, KV-cache slicing with parallel query execution, and asymmetric attention barriers for long-context inference. Together, these stages form a pipeline that incrementally reduces memory pressure while preserving the contextual reasoning capabilities of attention architectures.

By visualizing attention computation as a memory-aware workflow, the figure highlights one of the defining trends in contemporary AI-system design: performance increasingly depends on optimizing data movement rather than increasing computational throughput alone.

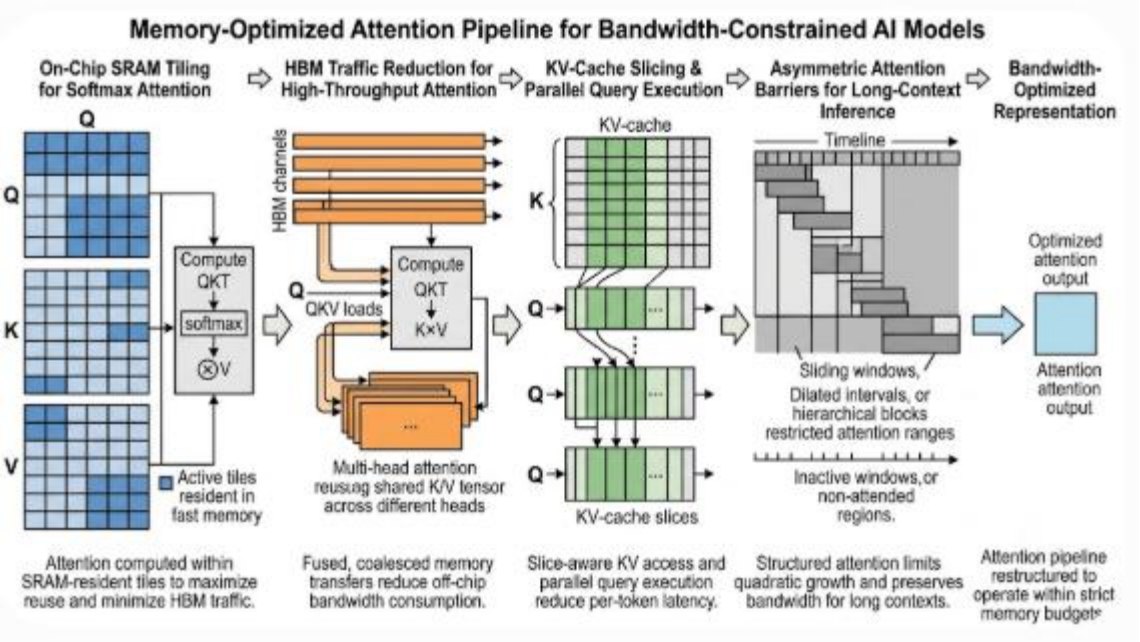


Figure 8.4-A3 — Memory-Optimized Attention Pipeline for Bandwidth-Constrained AI Models
Multi-stage attention-processing workflow illustrating how modern transformer architectures reduce memory traffic and improve accelerator utilization. The figure traces the progression from SRAM-resident attention tiling through HBM-traffic reduction, KV-cache slicing, and long-context attention barriers to produce a bandwidth-optimized attention representation. The pipeline demonstrates how memory-aware execution transforms attention from a bandwidth-bound workload into a more computationally efficient process capable of supporting large-context AI systems.

Legend

Component	***Description***
Q (Query Matrix)	*Query representations used during attention computation.*
K (Key Matrix)	*Key representations against which queries are compared.*
V (Value Matrix)	*Contextual information aggregated by the attention mechanism.*
On-Chip SRAM Tiling for Softmax Attention	*Stage that partitions attention computation into SRAM-resident tiles to increase data reuse.*
Active Tiles Resident in Fast Memory	*Working data blocks retained within local accelerator memory.*

Compute QK^T	*Matrix multiplication step producing attention scores.*
Softmax	*Normalization stage applied to attention scores.*
QKV Attention Output	*Contextual representation generated by the attention mechanism.*
HBM Traffic Reduction for High-Throughput Attention	*Dataflow optimization stage reducing redundant memory transfers.*
HBM Channels	*High-bandwidth memory pathways supplying data to accelerators.*
Fused QKV Loads	*Combined memory-access operations minimizing transfer overhead.*
Multi-Head Attention Reuse	*Reuse of shared KV tensors across attention heads.*
KV-Cache Slicing and Parallel Query Execution	*Stage partitioning cached context into multiple execution slices.*
KV Cache	*Cached key and value representations used during autoregressive inference.*
Parallel Query Streams	*Multiple query-execution pathways accessing cache partitions simultaneously.*
KV-Cache Slices	*Segmented cache regions supporting parallel processing.*
Asymmetric Attention Barriers for Long-Context Inference	*Mechanism limiting unrestricted global attention growth.*
Sliding Windows	*Localized attention regions restricting memory growth.*
Dilated Intervals	*Attention connections spaced at regular intervals.*
Restricted Attention Ranges	*Controlled context access preventing quadratic expansion.*
Bandwidth-Optimized Representation	*Final attention format optimized for efficient memory usage.*
Attention Output	*Resulting contextual representation after memory-aware optimization.*

Figure 8.4-A3 illustrates that attention optimization is fundamentally a problem of managing memory movement rather than solely accelerating computation. The figure demonstrates how

successive optimization stages reduce bandwidth consumption while preserving the contextual reasoning capabilities that make attention mechanisms effective.

The pipeline highlights a recurring principle of hardware-aware AI design: maximizing data reuse and minimizing memory transfers often contributes more to performance than increasing raw computational resources.

The figure begins with **on-chip SRAM tiling for softmax attention**, the first stage in the memory-optimization pipeline.

Traditional attention mechanisms repeatedly move large query, key, and value matrices between off-chip memory and accelerator compute units. These transfers consume substantial bandwidth and frequently become the dominant performance bottleneck. To address this issue, the pipeline partitions attention computation into smaller tiles that fit within on-chip SRAM resources.

The diagram shows the query, key, and value matrices being divided into active tiles that remain resident within fast memory while the attention operation is executed. Computation of QK^T, softmax normalization, and value aggregation occur locally rather than requiring repeated access to external memory. This arrangement significantly increases data reuse and reduces off-chip bandwidth consumption.

The second stage introduces **HBM traffic reduction for high-throughput attention**.

Although high-bandwidth memory provides substantial throughput, attention workloads often generate redundant reads and writes that consume valuable memory resources. The figure illustrates fused QKV loading and shared KV reuse across attention heads. Rather than repeatedly transferring the same information through multiple memory channels, data movement is consolidated and reused whenever possible.

This stage is particularly important because it reduces pressure on HBM subsystems without requiring changes to the underlying attention formulation. Through more efficient dataflow organization, throughput improves while memory-access costs decline.

The pipeline then proceeds to **KV-cache slicing and parallel query execution**, a critical optimization for autoregressive inference systems.

In transformer-based generation, KV caches grow continuously as sequence length increases. Over time, accessing these caches can become a major source of latency. The figure shows the cache being segmented into slices that align with accelerator memory boundaries.

These cache slices support parallel query streams, allowing multiple sections of contextual

memory to be accessed simultaneously. Rather than treating the cache as a single monolithic structure, the architecture distributes access across several execution pathways. This improves scalability and reduces the per-token latency associated with long-context generation.

The fourth stage introduces **asymmetric attention barriers for long-context inference**.

One of the most challenging problems in transformer architectures is the rapid growth of attention-related memory requirements as sequence length expands. Without constraints, attention complexity can increase dramatically as models attempt to consider every token simultaneously.

The figure illustrates several mechanisms for restricting this growth. Sliding windows focus attention on nearby context. Dilated intervals preserve access to distant information while reducing connection density. Restricted attention ranges limit unnecessary interactions among tokens.

These techniques effectively impose structure on the attention pattern. Rather than attending globally at all times, the model allocates attention selectively according to architectural rules designed to preserve useful context while limiting memory growth.

The final stage produces a **bandwidth-optimized representation**, shown at the right side of the figure.

This representation embodies the cumulative effect of all preceding optimizations. SRAM tiling has increased locality. HBM optimization has reduced redundant transfers. KV-cache slicing has improved cache-access efficiency. Long-context barriers have constrained memory growth. Together, these transformations produce an attention pipeline that operates within practical memory budgets while maintaining high throughput.

A broader insight emerging from the figure is that every stage addresses a different component of the memory hierarchy. On-chip SRAM optimization targets local memory efficiency. HBM optimization addresses accelerator-wide bandwidth constraints. KV-cache slicing focuses on inference-time context management. Attention barriers target long-sequence scalability. The resulting pipeline represents a coordinated approach to memory optimization rather than a single isolated technique.

The figure also illustrates why data movement has become one of the dominant factors in AI-system performance. Modern accelerators possess enormous arithmetic capability, yet transferring data to those compute units often remains more expensive than performing the computations themselves. Consequently, reducing memory traffic frequently produces larger performance gains than increasing computational throughput.

From a systems-engineering perspective, the attention pipeline demonstrates the importance of co-design across architectural layers. Mathematical formulations, memory hierarchies, scheduling strategies, and accelerator capabilities must all be considered simultaneously to achieve efficient execution.

Another important observation is that these mechanisms contribute directly to scalability. Without memory optimization, long-context transformers would rapidly exceed available bandwidth and memory resources. The techniques illustrated in the figure therefore serve not only as performance enhancements but also as enabling technologies for large-context reasoning.

Ultimately, Figure 8.4-A3 demonstrates how modern AI systems transform attention computation from a bandwidth-limited workload into a more efficient and scalable process. Through SRAM tiling, HBM-traffic optimization, KV-cache partitioning, and structured long-context attention mechanisms, memory-aware execution substantially reduces data movement while preserving model capability. This pipeline exemplifies how hardware–software co-design enables advanced attention architectures to operate efficiently within the practical constraints of contemporary AI accelerators.

Viewed holistically, Figure 8.4-A3 demonstrates that memory-efficient attention is not the result of a single optimization, but rather the product of a carefully orchestrated sequence of hardware-aware transformations applied across the entire attention dataflow. Each stage reduces a different source of memory overhead while aligning computation more closely with the hierarchical organization of modern accelerators. SRAM tiling increases locality and data reuse, HBM optimization minimizes redundant transfers, KV-cache partitioning reduces context-access latency, and structured attention constraints bound memory growth during long-context processing. Together, these mechanisms transform attention from a bandwidth-limited operation into a scalable, high-throughput computational primitive capable of supporting increasingly large models and context windows. At the foundation of this optimization hierarchy lies **On-Chip SRAM Tiling for AI Softmax Attention**, which serves as the first and most fundamental control point for reducing memory traffic. By retaining active query, key, and value tiles within fast local memory, SRAM tiling establishes the locality and data-reuse patterns upon which all subsequent attention optimizations depend. The following discussion examines this mechanism in detail as a foundational hardware–software co-design strategy for modern attention architectures.

i. On-Chip SRAM Tiling for AI Softmax Attention

On-Chip SRAM Tiling for AI Softmax Attention represents a foundational hardware-software

co-design strategy that restructures attention computation around the physical limits of the accelerator's fastest memory tier. In modern AI systems—particularly large-scale transformers—the dominant bottleneck is no longer arithmetic throughput but the bandwidth required to repeatedly stream massive Q, K, and V matrices from high-bandwidth memory (HBM). SRAM tiling directly addresses this constraint by decomposing attention into small, spatially localized tiles that fit entirely within on-chip SRAM or shared memory, enabling the most bandwidth-intensive operations to occur without touching off-chip memory.

The core idea is simple but transformative: instead of computing attention over full matrices, the compiler partitions Q, K, and V into tiles sized to match the accelerator's SRAM capacity. Each tile is loaded once, reused extensively, and evicted only after all relevant dot-products, softmax operations, and value-weighted aggregations have been completed. This tile-local execution dramatically reduces HBM traffic, converting attention from a bandwidth-bound operation into a compute-bound one. The mathematical structure of attention remains unchanged:

$$\text{Attention}(Q, K, V) = \text{softmax}\left(\frac{QK^T}{\sqrt{d}}\right)V,$$

but the dataflow is reorganized so that each tile of Q and K participates in multiple dot-products before leaving SRAM. This reuse is the key to sustaining high throughput during massive transformer context windows.

Achieving this tiling behavior requires sophisticated compiler support. Deep learning compilers—such as Triton, XLA, and custom FlashAttention kernels—generate schedules that fuse QK^T multiplication, softmax normalization, and V-weighted aggregation into a single on-chip pipeline. These fused kernels bypass the heavy cost of reading and writing intermediate attention matrices to HBM, instead keeping all intermediate results in registers or SRAM. The compiler must also track the non-linear softmax operation in real time, maintaining running statistics (max logits, normalization factors) within each tile. Although this introduces microarchitectural overhead, the bandwidth savings far outweigh the cost, enabling accelerators to operate near peak FLOP utilization even for extremely long sequences.

From a hardware perspective, SRAM tiling aligns perfectly with spatial accelerators and tensor-core-based architectures. These units thrive when data movement is predictable, localized, and aligned with physical compute limits. By mapping Q/K/V tiles directly to SRAM banks and register files, the accelerator avoids pipeline stalls caused by HBM latency and ensures that compute units remain fully fed. This alignment is especially critical for large-context transformers, where attention windows can span tens of thousands of tokens.

Without tiling, such workloads would saturate memory bandwidth and collapse throughput; with tiling, they remain compute-bound and scalable.

Ultimately, mastering On-Chip SRAM Tiling for AI Softmax Attention requires understanding how tile configurations interact with compiler fusion, spatial dataflow, and hardware memory hierarchies. When these elements are co-designed, attention becomes a high-throughput operation capable of sustaining peak performance even under extreme sequence lengths. This technique forms the backbone of modern memory-optimized attention kernels and is a cornerstone of next-generation transformer acceleration.

On-chip SRAM tiling establishes the foundation for memory-optimized attention by ensuring that the most bandwidth-intensive components of the softmax operation—QK^T multiplication, normalization, and V-weighted aggregation—occur entirely within fast, local memory. However, even with perfect tile-local reuse, attention kernels must still interact with High-Bandwidth Memory to fetch key-value tensors, update KV-caches, and sustain multi-head execution across long sequences. As sequence lengths grow and model sizes scale, these off-chip transfers become the next dominant bottleneck, threatening to stall compute units despite efficient SRAM utilization. This transition naturally leads into **HBM Traffic Reduction for High-Throughput AI Attention**, where the optimization focus shifts from maximizing on-chip reuse to minimizing off-chip communication. Here, fused QKV loads, coalesced memory bursts, and shared multi-head KV reuse work together to reduce HBM pressure, ensuring that accelerators remain fully fed even under extreme attention workloads.

ii. HBM Traffic Reduction for High-Throughput AI Attention

HBM Traffic Reduction for High-Throughput AI Attention represents a critical hardware-software co-design paradigm that directly targets the dominant bottleneck in modern transformer workloads: the overwhelming volume of off-chip memory traffic required to repeatedly stream key-value tensors during attention computation. As transformer sequence lengths grow and model sizes scale into the billions of parameters, the limiting factor is no longer arithmetic throughput but the ability of High-Bandwidth Memory (HBM) to supply data fast enough to keep compute units saturated. Reducing HBM traffic is therefore essential for sustaining high-throughput attention on contemporary accelerators.

The central strategy is to enforce strict spatial data-reuse protocols within the fastest cache hierarchies—SRAM, shared memory, and register files—so that key-value segments are fetched from HBM as infrequently as possible. Instead of repeatedly loading full K and V matrices for each attention head or each query token, custom memory virtualization patterns map localized K/V segments directly into on-chip SRAM registers. These segments are then reused across

multiple heads, multiple tiles, or multiple queries before being evicted. This approach transforms attention from a memory-bound operation into a compute-bound one by dramatically reducing the number of bytes transferred across the HBM bus.

The mathematical structure of attention remains unchanged:

$$\text{Attention}(Q,K,V) = \text{softmax}\left(\frac{QK^T}{\sqrt{d}}\right)V,$$

but the dataflow is reorganized so that K and V tensors are streamed once and reused many times. Multi-head attention benefits especially from this optimization: instead of each head independently loading K and V from HBM, the accelerator loads them once into SRAM and shares them across all heads. This eliminates redundant read-write cycles and reduces communication power, which is a major contributor to energy consumption in large-scale inference.

Implementing this optimization requires sophisticated compiler support. Deep learning kernel compilers—such as Triton, XLA, and custom FlashAttention variants—generate fused memory schedules that combine QKV loading, scaling, softmax normalization, and V-weighted aggregation into a single pipeline. These schedules ensure that intermediate activations remain on-chip, preventing unnecessary round-trips to HBM. The compiler must also track online scaling statistics for transcendental operations like softmax, maintaining running maxima and normalization factors within registers. Although this introduces microarchitectural overhead, the bandwidth savings are enormous, enabling accelerators to sustain near-peak utilization even for extremely long sequences.

From a hardware perspective, HBM traffic reduction aligns perfectly with the physical constraints of modern AI accelerators. HBM offers high bandwidth but relatively high latency and high energy cost per bit transferred. SRAM, by contrast, offers low latency and low energy consumption but limited capacity. By virtualizing K/V segments into SRAM and orchestrating their reuse, the accelerator avoids saturating HBM channels and prevents thread idling caused by memory stalls. This alignment is crucial for large-context transformers, where attention windows can span tens of thousands of tokens and naive implementations would overwhelm HBM bandwidth.

Ultimately, mastering HBM Traffic Reduction for High-Throughput AI Attention requires understanding how memory virtualization, compiler fusion, and spatial dataflow interact to minimize off-chip communication. When these elements are co-designed, attention becomes a high-throughput operation capable of scaling to massive sequence lengths without collapsing

under memory pressure. This technique is a cornerstone of modern transformer acceleration and a prerequisite for efficient long-context inference.

Reducing HBM traffic ensures that attention kernels can sustain high throughput by minimizing redundant off-chip transfers of key-value tensors, but even perfectly optimized memory scheduling cannot overcome the inherent growth of the KV-cache during autoregressive decoding. As each new token extends the sequence, the KV-cache expands and must be repeatedly accessed for every subsequent query, creating a new bandwidth bottleneck that SRAM tiling and fused HBM loads cannot fully mitigate. This shift in workload dynamics moves the optimization challenge from *how* K and V tensors are fetched to *how* the KV-cache itself is organized, partitioned, and consumed during decoding. This transition leads directly into **KV-Cache Slicing and Parallel Query Execution in AI Decoders**, where the focus becomes restructuring the KV-cache into slice-aligned segments and distributing query processing across synchronized execution lanes. By slicing the cache and pipelining multiple queries, decoders bypass sequential token dependencies and eliminate memory-bus starvation, enabling large-scale generative models to achieve massive throughput across multi-GPU inference pipelines.

iii. KV-Cache Slicing and Parallel Query Execution in AI Decoders

KV-Cache Slicing and Parallel Query Execution in AI Decoders represents a critical hardware-software co-design paradigm that redefines how generative AI systems manage memory and parallelism during autoregressive decoding. In large-scale transformer decoders, the KV-cache grows with every generated token, and naïve implementations repeatedly load the entire cache for each new query. This creates severe bandwidth pressure, induces memory bus starvation, and forces compute units to idle while waiting for data. KV-cache slicing solves this bottleneck by partitioning the cache into spatially localized segments that align with on-chip buffer boundaries, enabling accelerators to fetch only the relevant slices needed for each query. Parallel query execution then pipelines multiple queries through the attention mechanism simultaneously, amortizing cache loads and dramatically increasing throughput.

The mathematical structure of decoder attention remains unchanged:

$$\text{Attention}(q_t, K_{1:t}, V_{1:t}) = \text{softmax}\left(\frac{q_t K_{1:t}^T}{\sqrt{d}}\right) V_{1:t},$$

but the dataflow is reorganized so that $K_{1:t}$ and $V_{1:t}$ are no longer treated as monolithic tensors. Instead, the KV-cache is divided into slices—aligned with tile boundaries, head partitions, or sequence segments—that can be independently loaded into SRAM or shared memory. Each

slice is reused across multiple queries before eviction, reducing the number of bytes transferred from HBM and preventing memory stalls that would otherwise throttle decoding throughput.

Parallel query execution builds on this foundation by distributing queries across synchronized hardware execution lanes. Instead of processing one token at a time, tensor-parallel engines pipeline multiple queries, allowing each lane to operate on different KV-cache slices concurrently. This multi-headed compute partitioning bypasses the sequential nature of autoregressive generation and unlocks massive concurrency across attention blocks. The result is a decoder that scales linearly with available compute resources rather than being constrained by sequential token dependencies.

Implementing KV-cache slicing and parallel query execution requires advanced compiler and runtime support. Distributed inference frameworks such as **vLLM**, **NVIDIA TensorRT-LLM**, and **DeepSpeed-Inference** generate memory-aware schedules that map KV slices to specific GPUs, NUMA domains, or tensor-parallel partitions. These frameworks must manage low-latency cross-node communication, synchronize partial attention results, and ensure that slice boundaries align with hardware interconnect topologies (NVLink, NVSwitch, PCIe, or InfiniBand). Although this introduces microarchitectural overhead—such as coordinating slice ownership, merging partial results, and tracking per-query metadata—the concurrency gains far outweigh the cost.

From a hardware perspective, KV-cache slicing aligns perfectly with multi-GPU and multi-node architectures. By distributing KV segments across devices and enabling parallel access, the accelerator avoids saturating any single memory bus and prevents thread idling caused by cache fetch delays. This alignment is essential for high-throughput decoding workloads, where thousands of tokens may be generated per second and any memory stall can cascade into large latency spikes.

Ultimately, mastering KV-Cache Slicing and Parallel Query Execution in AI Decoders requires understanding how distributed memory scheduling, tensor-parallel execution, and interconnect-aware partitioning interact to eliminate structural bottlenecks. When these elements are co-designed, generative AI systems achieve near-linear scaling across GPUs, enabling massive throughput improvements for large-context, multi-head transformer decoders. This technique is a cornerstone of modern high-performance inference and a prerequisite for efficient deployment of trillion-parameter models.

KV-cache slicing and parallel query execution resolve the throughput bottlenecks of autoregressive decoding by distributing cache segments across execution lanes and pipelining multiple queries in parallel. This redesign transforms decoding from a strictly sequential process

into a highly concurrent one, allowing large-scale generative models to maintain high token-generation rates even as context windows expand. Yet, as sequence lengths stretch into the hundreds of thousands or millions of tokens, a deeper structural challenge emerges: the quadratic growth of full-sequence attention itself. Even perfectly sliced KV-caches and fully parallelized query pipelines cannot prevent the attention map from ballooning beyond the limits of memory bandwidth, cache capacity, and numerical stability. This shift in scaling pressure leads directly into **Asymmetric Attention Barriers in Long-Context AI Inference**, where the optimization focus moves from parallelizing access to *constraining* access. By imposing directional, context-aware boundaries on how queries interact with keys and values, asymmetric barriers reshape long-context attention into a bandwidth-controlled, stability-preserving mechanism capable of supporting million-token inference without overwhelming hardware resources.

iv. Asymmetric Attention Barriers in Long-Context AI Inference

Asymmetric Attention Barriers in Long-Context AI Inference represent a critical hardware-software co-design paradigm that restructures how transformer models process extremely long sequences by imposing directional, context-aware boundaries on attention flow. Traditional full-sequence attention scales quadratically with context length, saturating memory bandwidth, overwhelming KV-cache capacity, and destabilizing token recall. Asymmetric barriers solve this by enforcing non-uniform, selectively constrained attention windows that allow queries to attend only to the most relevant portions of the context while preventing unnecessary or harmful cross-sequence interactions. This transforms long-context inference from an unbounded memory problem into a structured, bandwidth-controlled execution pattern.

The mathematical structure of attention remains intact:

$$\text{Attention}(Q, K, V) = \text{softmax}\left(\frac{QK^T}{\sqrt{d}}\right)V,$$

but the domain over which the softmax is computed is no longer symmetric. Instead of allowing each query to attend to all keys, asymmetric barriers restrict the attention domain to a context-aware subset:

$$A(t) = \{\, i \mid i \in \text{Window}(t) \cup \text{Dilated}(t) \cup \text{Hierarchical}(t) \,\},$$

where each region—sliding window, dilated interval, or hierarchical block—represents a different form of structured constraint. These constraints are asymmetric because the

boundaries applied to queries differ from those applied to keys and values. For example, a query token may attend only backward within a sliding window, while key-value vectors may be partitioned into hierarchical blocks that preserve long-range recall without requiring full attention.

The hardware implications are profound. Asymmetric barriers reduce the size of QK^T operations, lower the number of KV-cache slices that must be fetched, and prevent memory saturation during million-token inference. Custom inference engines bypass symmetric scaling bottlenecks by mapping distinct partitioning indexes separately onto Q and KV tensors. This allows accelerators to fetch only the relevant KV segments for each query, eliminating the need to stream the entire context from HBM. The result is a dramatic reduction in memory traffic and communication power, enabling long-context inference to operate within realistic hardware limits.

Implementing asymmetric barriers requires sophisticated runtime support. Optimized attention kernels—such as those used in FlashAttention-Long, Mistral's sliding-window attention, and hierarchical memory transformers—must dynamically compute partition boundaries, track non-uniform sparsity patterns, and fuse barrier logic into the attention pipeline. These kernels must also predict data-adaptive sparsity patterns online, determining which regions of the context are relevant for each query without introducing latency spikes or pipeline stalls. Although this introduces microarchitectural overhead, the computational savings across million-token windows are enormous.

From a hardware perspective, asymmetric barriers stabilize token recall by preventing catastrophic information dilution—where mid-sequence tokens lose influence due to uniform softmax scaling across massive contexts. By restricting attention to structured regions, the accelerator avoids stalling memory lanes and maintains predictable dataflow patterns. This alignment is essential for long-context inference, where naïve full-sequence attention would collapse under bandwidth pressure and degrade model accuracy.

Ultimately, mastering Asymmetric Attention Barriers in Long-Context AI Inference requires understanding how directional constraints, context-aware partitioning, and hardware-aligned sparsity interact to preserve model fidelity at extreme sequence lengths. When these elements are co-designed, transformers achieve stable, high-throughput long-context reasoning without overwhelming memory systems. This technique is a cornerstone of next-generation long-context architectures and a prerequisite for scaling inference to million-token windows and beyond.

Memory-optimized attention mechanisms redefine how modern AI systems handle the rapidly

expanding computational and memory demands of long-context transformers. By restructuring attention around the physical constraints of the memory hierarchy—SRAM, cache, HBM, and distributed KV-stores—these techniques transform attention from a bandwidth-bound operation into a scalable, high-throughput dataflow. On-chip SRAM tiling maximizes local reuse of Q/K/V tiles, fused HBM scheduling eliminates redundant off-chip transfers, KV-cache slicing enables parallel decoding across multi-GPU systems, and asymmetric attention barriers constrain quadratic growth during million-token inference. Together, these mechanisms form a cohesive optimization pipeline that preserves the expressive power of attention while ensuring that memory bandwidth, not arithmetic throughput, becomes the controllable variable. This discussion demonstrates that attention can be engineered to operate efficiently even under extreme sequence lengths, provided that its dataflow is carefully aligned with the underlying hardware architecture.

While memory-optimized attention mechanisms significantly reduce bandwidth pressure, they still inherit the fundamental quadratic scaling of traditional softmax attention. Even with SRAM tiling, HBM reduction, KV-cache slicing, and asymmetric barriers, the underlying computation remains tied to pairwise token interactions. As models push toward million-token contexts, this quadratic structure becomes increasingly difficult to sustain, even with aggressive hardware-software co-design. This limitation motivates the transition to **Linear-Attention AI Architectures and State-Space Sequence Models**, which abandon the quadratic formulation entirely. These architectures replace full attention maps with kernelized projections, recurrent state updates, or continuous-time dynamical systems that scale linearly with sequence length. In doing so, they offer a fundamentally different pathway for long-context reasoning—one that is not merely optimized for bandwidth, but architecturally liberated from the constraints of traditional attention.

d. Linear-Attention AI Architectures and State-Space Sequence Models

Linear-Attention AI Architectures and State-Space Sequence Models represent a decisive architectural pivot away from the quadratic scaling laws that constrain traditional softmax attention. Rather than optimizing around the memory hierarchy to make quadratic attention *less expensive*, these models eliminate the quadratic formulation entirely. They replace pairwise token interactions with recurrent state updates, kernelized projections, and continuous-time dynamical systems that scale linearly with sequence length. This shift transforms long-context reasoning from a bandwidth-dominated challenge into a mathematically structured, hardware-aligned computation pipeline capable of sustaining million-token inference without saturating HBM channels, KV-cache capacity, or on-chip memory.

A central mechanism in these architectures is the use of **recurrent state representations** that

evolve with each token, capturing contextual information through learned dynamical updates rather than explicit attention maps. Instead of storing full key-value histories, the model maintains a compact hidden state that is updated in constant time. Hardware-optimized ring-buffer memory maps store these states in fixed-size circular buffers, ensuring predictable memory access patterns and eliminating the unbounded KV-cache growth that limits transformer decoders. This streaming formulation aligns perfectly with accelerators: recurrent updates fit within SRAM or register files, enabling sustained throughput even under extreme sequence lengths.

Linear-attention models also exploit **parallel scan execution** to break free from the sequential bottlenecks of autoregressive decoding. Many linear-attention kernels—such as prefix-sum transforms, kernelized projections, and state-space convolution operators—are associative, allowing them to be executed using parallel scan algorithms across vectorized processor arrays. Hardware units such as tensor-core matrices, systolic arrays, and SIMD engines thrive under these workloads, processing thousands of tokens simultaneously and amortizing memory access costs across wide compute lanes. This parallelism enables linear-attention architectures to achieve near-linear speedups for long-context inference, a feat unattainable for traditional attention mechanisms.

State-space sequence models extend this paradigm by grounding long-range reasoning in **matrix exponential approximations** that describe continuous-time dynamical systems. These models rely on structured operators whose evolution is governed by matrix exponentials, but exact computation is prohibitively expensive. Hardware-aware approximations—low-rank factorizations, polynomial expansions, kernelized transforms—allow accelerators to evaluate these operators efficiently. Crucially, approximate state updates are stored in **low-bit register caches**, enabling compact representations that fit entirely within on-chip memory. This reduces bandwidth pressure and ensures that state updates can be computed without touching HBM, making state-space models exceptionally well-suited for long-context workloads.

Finally, linear-attention and state-space architectures require **cache-aware eviction policies** to manage dynamic hidden states without overwhelming memory systems. Unlike transformers, which store explicit KV-caches, these models maintain evolving hidden states that must be retained, compressed, or evicted based on relevance. Eviction decisions are guided by learned relevance scores, temporal decay functions, or structural constraints derived from the underlying dynamical system. By aligning hidden-state management with hardware cache behavior, these policies prevent memory stalls, avoid bandwidth saturation, and ensure stable performance across dynamic, evolving contexts.

Together, these mechanisms form a cohesive architectural strategy that liberates long-context AI

from the constraints of quadratic attention. Linear-attention and state-space models do not merely optimize memory usage—they fundamentally restructure the computation itself, enabling scalable, hardware-aligned sequence processing that remains efficient even at million-token scales. This discussion demonstrates that the future of long-context AI lies not in making attention cheaper, but in replacing it with architectures designed from the ground up for linear scalability.

As linear-attention and state-space architectures replace quadratic attention with hardware-aligned recurrence, parallel scan execution, lightweight dynamical approximations, and bounded hidden-state management, the underlying design space becomes both broader and more structured. Each mechanism contributes a distinct optimization pathway—some mathematical, some architectural, some memory-centric—but all converge toward the same goal: enabling long-context AI systems to operate at scale without saturating bandwidth or collapsing under sequential bottlenecks. To clarify how these components interact and to highlight their complementary roles within the overall dataflow, the following table organizes the four foundational mechanisms into a unified comparative framework that exposes their functional purpose, hardware alignment, and long-context performance benefits.

Table 8.4-A3 demonstrated that substantial performance gains can be achieved by optimizing the memory behavior of attention mechanisms through SRAM tiling, bandwidth-aware dataflows, KV-cache partitioning, and long-context attention constraints. These techniques improve the efficiency of conventional attention architectures, but they do not eliminate the fundamental challenge that attention-based systems must continually manage growing context representations and increasingly complex memory-access patterns as sequence lengths expand. As a result, researchers have explored alternative architectural paradigms that move beyond traditional attention altogether. Linear-attention and state-space architectures address long-context processing by replacing explicit pairwise attention computations with compressed state representations, recurrence mechanisms, and hardware-friendly sequence-processing models. Table 8.4-A4 examines the core mechanisms underlying these architectures and illustrates how they achieve scalable long-range reasoning while operating within practical memory, bandwidth, and latency constraints.

Table 8.4-A4 presents the principal computational mechanisms used in modern linear-attention and state-space architectures. These architectures have emerged as important alternatives to conventional transformer models because they address many of the memory-scaling and bandwidth challenges associated with long-context processing.

Traditional attention mechanisms derive much of their effectiveness from the ability to establish dynamic relationships among tokens. However, maintaining these relationships often requires

large memory footprints, extensive KV-cache growth, and substantial bandwidth consumption. As sequence lengths increase, these requirements can become dominant system bottlenecks, limiting scalability and increasing deployment costs.

Linear-attention and state-space models address these challenges by reorganizing how historical information is represented, updated, and retrieved. Rather than maintaining increasingly large context caches, these architectures compress information into evolving state representations that can be updated efficiently over time. This approach shifts the computational emphasis from explicit attention matrices toward continuous state evolution, recurrence, and memory-efficient sequence processing.

The table identifies four foundational mechanisms supporting this paradigm: recurrent state representations with ring-buffer memory maps, parallel scan execution on vectorized processor arrays, matrix exponential approximations with low-bit register caching, and cache-aware eviction policies for dynamic hidden states. Together, these mechanisms provide a framework for processing long sequences while maintaining predictable memory usage and efficient hardware utilization.

By examining the interaction between these architectural techniques and modern hardware resources, the table highlights how long-context AI systems increasingly depend on memory-efficient state modeling rather than unrestricted attention expansion.

Table 8.4-A4 — Core Mechanisms in Linear-Attention and State-Space AI Architectures

Mechanism	Primary Function	Hardware Alignment	Key Benefits for Long-Context AI
Recurrent State Representations with Ring-Buffer Memory Maps	Compress historic context into fixed-dimension hidden states updated per token	Circular SRAM/register-file buffers with constant-time access	Eliminates KV-cache growth; predictable memory footprint; streaming throughput
Parallel Scan Execution on Vectorized Processor Arrays	Execute associative recurrence operations across many tokens simultaneously	SIMD lanes, systolic matrices, Tensor Core arrays	Near-linear scaling; removes sequential bottlenecks; high compute saturation

Mechanism	Primary Function	Hardware Alignment	Key Benefits for Long-Context AI
Matrix Exponential Approximations with Low-Bit Register Caching	Replace exact dynamical system exponentials with polynomial/low-rank approximations	Quantized operators stored in registers/SRAM tiles	Constant-time updates; avoids HBM traffic; stable long-range dynamics
Cache-Aware Eviction Policies for Dynamic Hidden States	Retain, compress, or evict hidden states based on learned relevance and decay	Tiered SRAM/HBM staging with compiler-fused eviction routines	Prevents bandwidth saturation; maintains deterministic throughput; bounded memory usage

Table 8.4-A4 demonstrates a significant shift in architectural philosophy. Rather than scaling performance through increasingly large attention structures and context caches, linear-attention and state-space models achieve scalability by compressing contextual information into compact, continuously updated state representations.

The mechanisms presented in the table reveal how modern architectures transform sequence processing into a state-management problem, allowing long-context reasoning to occur with more predictable memory consumption, lower bandwidth requirements, and improved hardware efficiency.

The first mechanism identified in the table is **recurrent state representations with ring-buffer memory maps**. This approach replaces explicit storage of extensive context histories with compressed state variables that summarize relevant information from previous inputs.

Rather than maintaining continuously growing KV caches, the architecture updates a hidden state after each token or input event. Ring-buffer memory structures provide constant-time access to recently updated information while preserving efficient use of local memory resources. The hardware alignment described in the table reflects the suitability of such structures for SRAM and register-file storage systems.

One of the most important benefits of this approach is its predictable memory footprint. Because memory usage remains largely independent of sequence length, very long sequences can be processed without the rapid memory growth characteristic of traditional attention models. This property is particularly valuable in autonomous systems that must process continuous data streams over extended durations.

The second mechanism is **parallel scan execution on vectorized processor arrays**. State-space and recurrence-based models traditionally face challenges associated with sequential dependencies. If updates must occur one token at a time, throughput may become constrained by limited parallelism.

Parallel scan methods address this issue by exploiting associative recurrence structures that can be evaluated across multiple tokens simultaneously. As shown in the table, these computations align effectively with SIMD units, systolic arrays, tensor cores, and related vector-processing hardware. The result is near-linear scalability combined with high hardware utilization.

This mechanism is particularly significant because it demonstrates that recurrence-based architectures need not sacrifice accelerator efficiency. Through appropriate mathematical restructuring, sequential dependency can be transformed into highly parallel computation.

The table next identifies **matrix exponential approximations with low-bit register caching**. State-space models often rely on matrix dynamics to govern how hidden representations evolve over time. Direct computation of these dynamics may be expensive if high-precision calculations are required at every step.

To improve efficiency, low-order approximations and quantized operators are used to represent state-transition dynamics. These representations fit naturally within registers and small SRAM regions, reducing dependence on external memory systems. The resulting constant-time updates avoid the extensive memory traffic associated with large context caches.

An additional advantage of this mechanism is stability. Well-designed state-transition approximations can maintain meaningful long-range information while avoiding excessive computational complexity, allowing state evolution to remain efficient even for extremely long sequences.

The final mechanism identified in the table is **cache-aware eviction policies for dynamic hidden states**. Although state-space architectures reduce memory growth, not all hidden information remains equally relevant over time. Intelligent state-management strategies therefore determine which information should be retained, compressed, or discarded.

The table highlights learned relevance scoring and temporal decay mechanisms as methods for identifying information that continues to contribute meaningfully to future predictions. Hardware alignment occurs through tiered SRAM and HBM staging systems that allocate resources according to the importance of stored states.

This capability helps maintain deterministic memory utilization while preventing bandwidth saturation during long-context processing. By ensuring that memory resources are devoted

primarily to high-value information, cache-aware management improves both efficiency and scalability.

A broader insight emerging from the table is that these mechanisms collectively replace context expansion with state evolution. Traditional attention systems often scale by storing more information. Linear-attention and state-space systems instead scale by representing information more efficiently.

The table also highlights the strong relationship between architecture and memory hierarchy. Ring buffers, register caching, parallel scan execution, and intelligent state eviction are all designed to align with hardware structures that provide low-latency access and efficient data reuse. This alignment reflects a broader trend toward architectures explicitly optimized for accelerator characteristics.

From a systems-engineering perspective, these mechanisms address multiple objectives simultaneously. Memory consumption becomes more predictable. Bandwidth requirements decrease. Throughput improves. Latency variability is reduced. As a result, long-context processing becomes increasingly compatible with real-time autonomous systems operating under strict resource constraints.

Another important observation is that the benefits extend beyond efficiency alone. Predictable memory behavior contributes directly to reliability and system stability. Autonomous systems frequently require deterministic execution properties that are difficult to guarantee when memory usage grows rapidly with context length. State-space architectures help mitigate this challenge through controlled resource utilization.

The table further illustrates the evolution of AI architectures from static attention-centric designs toward dynamic state-oriented computational frameworks. As model deployment increasingly moves toward edge computing, robotics, autonomous vehicles, and long-horizon reasoning applications, this shift may become increasingly important.

Ultimately, Table 8.4-A4 demonstrates how linear-attention and state-space architectures achieve scalable long-context processing through efficient state management rather than unrestricted attention growth. Through recurrent state representations, parallel scan execution, matrix-exponential approximations, and cache-aware hidden-state management, these systems maintain high performance while reducing memory pressure and bandwidth consumption. Together, these mechanisms provide a hardware-aligned foundation for the next generation of long-context AI architectures.

Table 8.4-A4 identified the core computational mechanisms that enable linear-attention and

state-space architectures to process long sequences efficiently through recurrent state compression, parallel scan execution, quantized state transitions, and cache-aware hidden-state management. While the table examined these mechanisms individually, practical deployment requires them to operate as an integrated dataflow architecture spanning multiple levels of the hardware hierarchy. The effectiveness of state-space models depends not only on the underlying mathematical formulation but also on how state updates, recurrence propagation, memory management, and numerical approximations interact throughout the execution pipeline. Figure 8.4-A4 visualizes this end-to-end architecture, illustrating how streaming input data moves through successive layers of state evolution, parallel computation, quantized updates, and memory management before producing high-throughput long-context outputs.

Figure 8.4-A4 presents a hardware-aware dataflow architecture for linear-attention and state-space AI systems. The figure illustrates how these architectures transform continuous input streams into compact state representations that evolve efficiently over time while avoiding the memory-growth characteristics associated with conventional attention mechanisms.

Unlike transformer architectures that often rely on expanding context caches and repeated attention computations, state-space and linear-attention models maintain a compact internal representation of historical information. This representation evolves continuously as new inputs arrive, allowing the model to process long sequences using bounded memory resources and predictable computational workloads.

The architecture depicted in the figure is organized into four major processing modules layered across different hardware resources. These modules include recurrent state updates, parallel recurrence propagation, matrix-exponential approximation layers, and cache-aware hidden-state management mechanisms. Together, they form a pipeline that converts long-range sequence processing into a sequence of efficient state transformations.

By emphasizing the interaction between algorithmic operations and hardware structures such as SRAM, register files, vectorized processor arrays, and memory-control systems, the figure demonstrates how state-space architectures achieve scalability through hardware–software co-design.

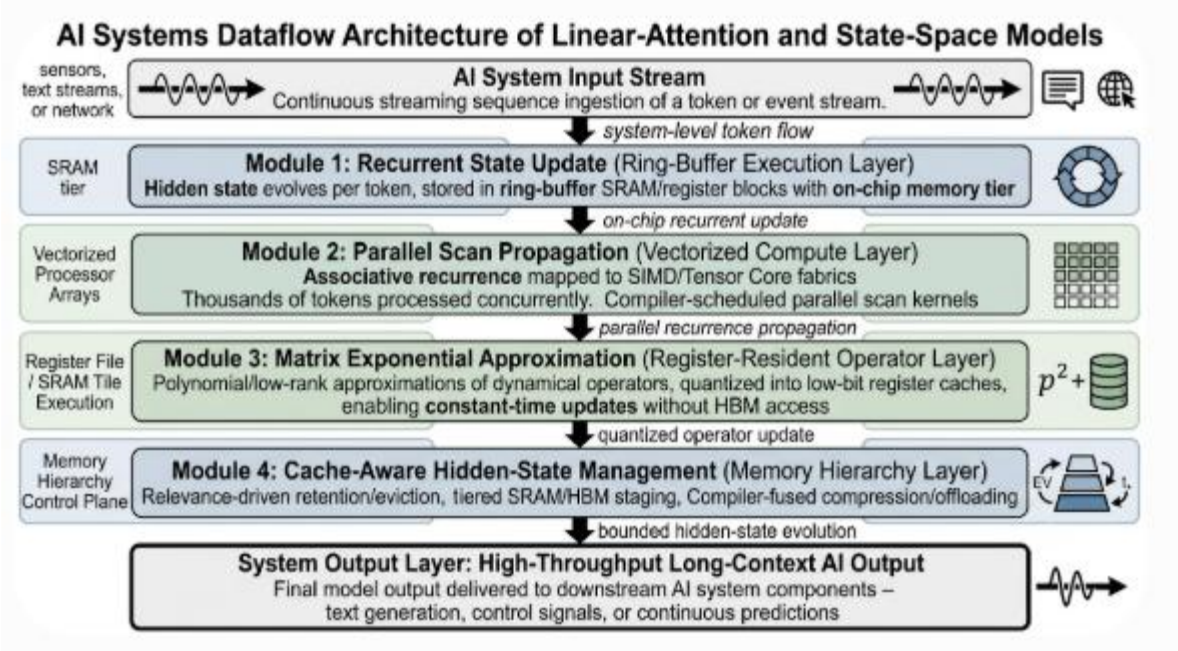


Figure 8.4-A4 — AI Systems Dataflow Architecture of Linear-Attention and State-Space Models
Multi-layer dataflow architecture illustrating how linear-attention and state-space models process continuous input streams through recurrent state updates, parallel recurrence propagation, quantized state-transition operators, and cache-aware hidden-state management. The figure demonstrates how long-context reasoning is achieved through evolving state representations rather than growing attention caches, enabling scalable throughput, bounded memory consumption, and efficient alignment with modern hardware

Legend

Component	***Description***
AI System Input Stream	*Continuous sequence of tokens, sensor updates, events, or data observations entering the model.*
System-Level Token Flow	*Streaming data path connecting input processing and output generation.*
Module 1: Recurrent State Update (Ring-Buffer Execution Layer)	*Layer responsible for updating hidden-state representations after each token or event.*

Ring-Buffer SRAM/Register Blocks	*Fast local storage structures holding compressed state information.*
On-Chip Recurrent Update	*State-update computation performed using local memory resources.*
SRAM Tier	*Hardware layer providing low-latency memory access for recurrent states.*
Module 2: Parallel Scan Propagation (Vectorized Compute Layer)	*Layer executing associative recurrence operations across multiple tokens simultaneously.*
Associative Recurrence Mapping	*Transformation enabling parallel evaluation of recurrent computations.*
SIMD/Tensor-Core Fabrics	*Parallel execution resources supporting high-throughput recurrence propagation.*
Compiler-Scheduled Parallel Scan Kernels	*Optimized execution routines coordinating parallel recurrence evaluation.*
Vectorized Processor Arrays	*Hardware units providing broad parallelism for sequence processing.*
Module 3: Matrix Exponential Approximation (Register-Resident Operator Layer)	*Layer responsible for efficient state-transition computations.*
Polynomial/Low-Rank Approximations	*Computational simplifications replacing expensive exact operators.*
Quantized Operators	*Low-precision state-transition representations stored in fast memory.*
Register File / SRAM Tile Execution	*Hardware resources supporting low-latency operator access.*
Module 4: Cache-Aware Hidden-State Management (Memory Hierarchy Layer)	*Layer managing retention and eviction of hidden states.*

Relevance-Driven Retention/Eviction	*Mechanism determining which states remain active.*
Tiered SRAM/HBM Staging	*Multi-level memory hierarchy used to manage hidden-state storage.*
Compiler-Fused Compression/Offloading	*Automated techniques reducing memory pressure.*
Bounded Hidden-State Evolution	*Controlled growth of stored state information.*
System Output Layer	*Final output stage generating predictions, actions, or textual responses.*
High-Throughput Long-Context AI Output	*Efficient output generation supported by compressed state representations.*

Figure 8.4-A4 illustrates a fundamentally different approach to sequence modeling than that employed by traditional attention-based architectures. Rather than maintaining increasingly large context windows and KV caches, the architecture relies on continuously evolving state representations that summarize historical information efficiently.

The figure demonstrates how state-space models distribute sequence processing across multiple hardware-aware layers, enabling scalable long-context reasoning while maintaining bounded memory usage and predictable computational cost.

The figure begins with the **AI System Input Stream**, representing a continuous flow of tokens, sensor observations, network events, or other sequential data entering the model.

A key characteristic of this architecture is that the input arrives as a stream rather than as a fixed block of context. This distinction is important because state-space systems are designed to process information incrementally, updating internal representations as new observations arrive without reconstructing the entire context at each step.

The first processing stage, **Module 1: Recurrent State Update**, serves as the foundation of the architecture.

This module maintains a compressed hidden-state representation stored within ring-buffer SRAM and register structures. Rather than preserving all previous observations explicitly, the model updates a compact state that summarizes relevant historical information.

The use of on-chip memory is particularly significant. By storing recurrent state locally, the architecture avoids repeated accesses to slower external memory resources. This design reduces latency and enables constant-time state access regardless of sequence length.

The second stage, **Module 2: Parallel Scan Propagation**, addresses one of the traditional limitations of recurrent architectures: limited parallelism.

Conventional recurrence often requires sequential token processing. The parallel-scan framework shown in the figure transforms recurrence into an associative operation that can be evaluated concurrently across many tokens. This restructuring allows state-space models to exploit SIMD processors, tensor cores, and other parallel-acceleration resources.

The diagram highlights compiler-scheduled parallel scan kernels that coordinate this execution process. Through these mechanisms, recurrence becomes compatible with high-throughput accelerator architectures rather than being confined to strictly sequential execution.

The architecture then proceeds to **Module 3: Matrix Exponential Approximation**, which governs the evolution of state-transition dynamics.

State-space models frequently rely on continuous or discrete state-transition operators that would otherwise require expensive matrix computations. The figure shows these operators being approximated through polynomial and low-rank formulations.

These approximations are stored within registers and SRAM tiles using quantized representations. As a result, state transitions can be computed efficiently without frequent access to external memory. This characteristic contributes directly to the constant-time update behavior emphasized in the table accompanying this figure.

The next stage is **Module 4: Cache-Aware Hidden-State Management**, which controls long-term memory behavior.

Although state-space architectures avoid the explosive growth of attention caches, hidden-state management remains important because not all information retains equal relevance over time. The figure illustrates a memory-control layer that evaluates hidden-state significance and determines whether information should be retained, compressed, or evicted.

The use of tiered SRAM and HBM staging reflects a broader memory-hierarchy strategy. Frequently used state information remains in fast local memory, while less critical information may be compressed or transferred to slower storage layers.

This mechanism ensures that memory usage remains bounded even during extended operation. As a result, long-context processing becomes predictable from both a performance and

resource-management perspective.

The architecture concludes with the **System Output Layer**, which generates predictions, control actions, text, or other task-specific outputs.

A notable aspect of the figure is that output generation occurs without maintaining a continually expanding context cache. Instead, all relevant historical information has already been integrated into the evolving hidden-state representation. This approach enables efficient long-range reasoning while avoiding many of the memory bottlenecks associated with attention-based systems.

A broader insight emerging from the figure is that state-space architectures shift the computational focus from context storage to state evolution. Traditional transformers preserve extensive contextual information explicitly, whereas state-space systems encode historical information within dynamic state updates.

The figure also illustrates the close relationship between algorithm design and hardware structure. Each module aligns naturally with a specific portion of the memory hierarchy or execution architecture. Ring buffers align with SRAM storage, recurrence propagation aligns with vectorized processors, state-transition approximations align with register-resident computation, and hidden-state management aligns with memory-control systems.

From a systems-engineering perspective, this layered architecture supports predictable resource utilization. Memory consumption remains bounded, bandwidth demands remain controlled, and computational complexity grows more slowly than in conventional attention systems. These characteristics are particularly valuable in autonomous platforms operating under strict power, latency, and memory constraints.

Another important observation is that the architecture addresses both scalability and determinism. Long-context reasoning becomes feasible without introducing the large memory growth often associated with transformer-based approaches. As a result, execution behavior remains more predictable across varying sequence lengths.

Ultimately, Figure 8.4-A4 demonstrates how linear-attention and state-space architectures achieve efficient long-context processing through hardware-aligned state evolution rather than explicit context expansion. Through recurrent state updates, parallel recurrence propagation, quantized transition operators, and cache-aware hidden-state management, these systems provide a scalable framework for sequence modeling that aligns naturally with modern compute and memory hierarchies. This architecture represents an important step toward AI systems capable of processing increasingly long and complex information streams while

remaining computationally efficient and hardware aware.

Figure 8.4-A4 places linear-attention and state-space architectures within a complete hardware-aware execution pipeline, illustrating how long-context processing emerges from the coordinated interaction of streaming inputs, on-chip memory resources, vectorized compute fabrics, and hierarchical storage systems. At the foundation of this pipeline lies the **recurrent state-update layer**, positioned immediately beneath the input stream and serving as the primary mechanism through which temporal information is accumulated and preserved. This placement reflects its fundamental role within the architecture. Before parallel scan operations can accelerate recurrence, before matrix-exponential approximations can compress state-transition dynamics, and before cache-aware policies can regulate hidden-state retention, the system must first establish a compact and continuously evolving representation of past information. Recurrent state representations provide precisely this capability by transforming unbounded input streams into fixed-size internal states that can be updated efficiently with constant-time access and predictable memory requirements. Consequently, **Recurrent State Representations with AI Ring-Buffer Memory Maps** serve as the foundational building block of linear-attention and state-space architectures, providing the bounded-memory substrate upon which scalable sequence modeling, high-throughput execution, and long-context reasoning ultimately depend.

i. Recurrent State Representations with AI Ring-Buffer Memory Maps

Recurrent State Representations with AI Ring-Buffer Memory Maps establish a foundational hardware-software co-design strategy for linear-attention and state-space sequence models. Instead of storing unbounded key-value histories—as required by traditional attention—these architectures compress all historic context into a fixed-dimension hidden state that evolves continuously with each new token. This transformation replaces quadratic memory growth with constant-time updates, enabling long-context reasoning to scale gracefully across millions of tokens without overwhelming memory bandwidth or cache capacity.

At the core of this approach is the **ring-buffer memory map**, a hardware-aligned circular buffer that stores recurrent state vectors in a fixed-size, wrap-around structure. Each new token triggers a learned dynamical update that modifies the hidden state, and the buffer advances by one position, overwriting the oldest entry. Because the buffer size is constant, memory usage remains bounded regardless of sequence length. This design eliminates the need for KV-cache expansion, dramatically reducing memory traffic and preventing the bandwidth saturation that plagues transformer-based attention.

Linear-attention and state-space architectures leverage this structure by mapping continuous

state updates directly onto localized SRAM or register-file blocks. These updates typically involve lightweight matrix multiplications, gating functions, or structured state-space operators that fit entirely within on-chip memory. By keeping recurrent state evolution inside the fastest memory tiers, the model avoids costly HBM round-trips and maintains high compute intensity throughout the sequence. The result is a streaming computation pipeline where each token is processed in constant time, independent of the total context length.

This design introduces microarchitectural overhead: historic context must be compressed into a unified hidden state vector, and the model must learn to preserve long-range dependencies without explicit attention maps. However, the overhead is small compared to the massive reductions in memory traffic and the elimination of quadratic scaling. The ring-buffer ensures predictable memory access patterns, allowing accelerators to prefetch state updates, avoid cache thrashing, and maintain stable throughput even under extreme sequence lengths.

Ultimately, mastering Recurrent State Representations with AI Ring-Buffer Memory Maps requires aligning the mathematical structure of linear-attention and state-space models with the physical constraints of modern hardware. When recurrent state updates are grounded in optimized SRAM or register-file layouts, streaming token access patterns align perfectly with memory boundaries, compute units remain fully utilized, and the communication bottlenecks inherent in traditional attention matrices disappear. This technique forms the backbone of scalable long-context architectures and is a key enabler of next-generation AI systems capable of processing continuous, unbounded sequences efficiently.

ii. Parallel Scan Execution on Vectorized AI Processor Arrays

Parallel Scan Execution on Vectorized AI Processor Arrays represents a foundational hardware-software co-design strategy that allows linear-attention and state-space sequence models to break free from the sequential bottlenecks inherent in autoregressive processing. Instead of advancing token by token—each step waiting for the previous one to complete—these architectures restructure long-context recurrence equations into associative operations that can be executed using parallel scan algorithms. This transformation enables thousands of tokens to be processed concurrently across wide compute lanes, dramatically increasing throughput and eliminating the latency penalties that dominate traditional transformer inference.

The key insight is that many linear-attention and state-space formulations can be expressed as associative prefix-sum or cumulative-update operations. Once expressed in this form, they can be mapped directly onto **vectorized Single Instruction, Multiple Data (SIMD) processor arrays**, systolic matrices, or Tensor Core blocks. These hardware units excel at performing identical

operations across large batches of data, making them ideal for executing parallel scans over long sequences. Instead of computing recurrence updates sequentially, the model distributes them across vector lanes, allowing each lane to process a different segment of the sequence simultaneously.

This design introduces microarchitectural overhead: parallel scans require log-step communication passes to merge partial results, synchronize intermediate states, and ensure consistency across vector lanes. Intermediate pooling operations must be carefully orchestrated to avoid pipeline stalls or register pressure. However, these costs are small compared to the massive speedups achieved when thousands of tokens are processed in parallel. The result is near-linear scaling across long-context blocks, enabling models to sustain high throughput even under extreme sequence lengths.

To fully realize these gains, parallel scan routines must be grounded in hardware-aligned data layouts. Systolic matrices and Tensor Core arrays impose strict constraints on register lane widths, tile boundaries, and memory-access patterns. Linear-attention kernels must therefore transform their internal representations—hidden states, kernel projections, or state-space operators—so that they align perfectly with these physical boundaries. When data is laid out to match the underlying hardware, instruction-level parallelism is maximized, memory stalls are minimized, and compute units remain fully saturated throughout the entire sequence.

Ultimately, mastering Parallel Scan Execution on Vectorized AI Processor Arrays requires understanding how associative recurrence equations, vectorized compute fabrics, and memory-aligned data transformations interact to eliminate sequential dependencies. When these elements are co-designed, linear-attention and state-space models achieve unprecedented throughput, transforming long-context inference from a sequential bottleneck into a fully parallelized, hardware-accelerated pipeline capable of scaling to million-token contexts with ease.

Recurrent state representations grounded in ring-buffer memory maps establish the foundation for linear-time sequence processing by ensuring that hidden-state updates remain constant-time and fully contained within on-chip memory. But once the model compresses historic context into a fixed-dimension recurrent state, the next challenge is accelerating how these states propagate across long sequences. Even with efficient ring-buffer storage, naïve recurrence still advances token by token, limiting throughput under extreme context lengths. This is where **parallel scan execution on vectorized AI processor arrays** becomes essential. By reformulating recurrent updates as associative operations, linear-attention and state-space models can distribute state evolution across wide SIMD lanes, systolic matrices, and Tensor Core arrays, transforming what was once a strictly sequential recurrence into a massively parallel

computation pipeline. In this way, parallel scan execution becomes the natural continuation of ring-buffer-based recurrence—scaling hidden-state updates from constant-time per token to constant-time per thousand-token block.

Parallel scan execution on vectorized processor arrays transforms long-sequence recurrence from a strictly sequential operation into a massively parallel computation pipeline, allowing linear-attention and state-space models to propagate hidden states across thousands of tokens at once. But once recurrence is parallelized, the next challenge becomes the *quality* and *efficiency* of the underlying state-update operators themselves. State-space architectures rely on continuous-time dynamical systems whose evolution is governed by matrix exponentials—operators far too expensive to compute exactly at scale. To sustain the throughput unlocked by parallel scans, these exponentials must be approximated in a form that fits entirely within on-chip memory and can be evaluated with high arithmetic intensity. This leads directly into **matrix exponential approximations with low-bit AI register caching**, where structured polynomial expansions, low-rank factorizations, and kernelized operators are quantized and stored in fast registers, enabling constant-time updates without touching HBM. In this way, matrix exponential approximation becomes the natural continuation of parallel scan execution—ensuring that the operators driving parallel recurrence are lightweight, hardware-aligned, and capable of sustaining peak compute intensity across extreme context lengths.

iii. Matrix Exponential Approximations with Low-Bit AI Register Caching

Matrix Exponential Approximations with Low-Bit AI Register Caching represent a pivotal hardware-software co-design strategy that enables state-space sequence models to perform long-range reasoning without incurring the prohibitive computational and memory costs of exact continuous-time dynamical system evaluations. In architectures such as S4, Mamba, and other structured state-space models, the evolution of hidden states is governed by matrix exponentials—operators that, if computed directly, would require large matrix multiplications, high-precision arithmetic, and repeated access to high-bandwidth memory (HBM). Approximating these exponentials with hardware-aligned techniques transforms this process into a lightweight, streaming computation that fits entirely within on-chip memory.

The core idea is to replace exact exponentials with **truncated polynomial expansions, low-rank factorizations, or kernelized operator approximations** that preserve the essential dynamics of the underlying system while dramatically reducing computational complexity. These approximations are then stored and updated using **low-bit register caching**, where quantized representations of intermediate states fit neatly into SRAM tiles or register files. By keeping

these approximated operators and state updates on-chip, the model avoids costly HBM round-trips and maintains constant-time latency regardless of sequence length.

This approach introduces a delicate balance: the model must tolerate small approximation errors introduced by low-precision arithmetic while ensuring that long-range dependencies remain stable and expressive. Structured state-space models are uniquely suited to this tradeoff because their dynamics are governed by well-behaved operators—banded matrices, diagonal-plus-low-rank structures, or kernelized convolutional forms—that remain stable under quantization. As a result, low-bit caching does not merely reduce memory usage; it becomes an integral part of the model's computational identity, enabling high arithmetic intensity within localized memory blocks.

To fully exploit these approximations, the computation must be grounded in **specialized compiler kernels** that fuse polynomial evaluation, state updates, and quantization steps into a single, hardware-aligned pipeline. These kernels orchestrate data layout transformations so that approximated operators align perfectly with vector processing lanes, systolic array boundaries, and Tensor Core tile dimensions. When the quantized matrices and intermediate states match the physical register widths, instruction-level parallelism is maximized, register spills are avoided, and compute units remain fully saturated throughout long-context inference.

Ultimately, mastering Matrix Exponential Approximations with Low-Bit AI Register Caching requires understanding how mathematical structure, quantization strategy, and hardware execution pipelines interact to eliminate HBM dependency. When these elements are co-designed, state-space models achieve constant-time updates, massive reductions in memory traffic, and stable long-range reasoning—all within the confines of on-chip memory. This technique is a cornerstone of modern linear-attention and state-space architectures, enabling them to scale to million-token contexts with efficiency that traditional attention mechanisms cannot match.

Matrix exponential approximations stored in low-bit register caches allow state-space models to update their hidden dynamics with constant-time, on-chip operations, eliminating the bandwidth-heavy dependence on HBM and stabilizing long-range reasoning under extreme sequence lengths. But once these lightweight, quantized operators are in place, a new challenge emerges: how to manage the evolving hidden states themselves as they accumulate over continuous streams of input. Even with efficient approximations, hidden states must be selectively retained, compressed, or discarded to prevent memory pressure from escalating as context windows expand. This transition leads directly into **cache-aware eviction policies for dynamic AI hidden states**, where learned relevance metrics, temporal decay functions, and hardware-tiered memory boundaries determine which states remain in fast SRAM and which

are offloaded to lower-tier storage. In this way, eviction logic becomes the natural continuation of low-bit matrix exponential caching—ensuring that hidden-state evolution remains both computationally efficient and memory-bounded, even as models process unbounded, real-time sequences.

iv. Cache-Aware Eviction Policies for Dynamic AI Hidden States

Cache-Aware Eviction Policies for Dynamic AI Hidden States represent a crucial hardware-software co-design strategy that enables linear-attention and state-space sequence models to maintain stable long-context performance without overwhelming memory systems. Unlike transformer architectures, which accumulate ever-growing key-value caches, linear-attention and state-space models maintain evolving hidden states whose relevance changes over time. These hidden states must be retained, compressed, or evicted based on their contribution to ongoing inference. Cache-aware eviction policies orchestrate this process by enforcing tiered memory staging and importance-driven retention metrics that keep memory footprints bounded and prevent bandwidth saturation during continuous stream processing.

The core idea is to map **learned relevance scores, temporal decay functions, and structural state-space constraints** directly onto the physical boundaries of the on-chip SRAM hierarchy. Recent hidden states—those most critical for maintaining short-range coherence—are stored in the fastest memory tiers, while older or lower-value states are compressed or offloaded to lower-tier memory. This ensures that the model accesses the most relevant information with minimal latency, bypassing the performance penalties associated with lower-bandwidth storage layers. By aligning eviction decisions with hardware memory tiers, the model maintains predictable dataflow patterns even as context windows expand into the hundreds of thousands or millions of tokens.

This design introduces microarchitectural overhead: the system must compute dynamic, data-dependent eviction priority scores in real time. These scores may incorporate learned gating signals, decay kernels, or structural invariants from the underlying dynamical system. However, the overhead is small compared to the benefits. Cache-aware eviction policies eliminate memory stalls, prevent register pressure from escalating, and ensure that hidden-state updates remain bounded and stable across long-range inference. The result is a memory system that behaves deterministically, even under highly variable sequence workloads.

To fully realize these gains, eviction schedules must be grounded in **spatial accelerator compilers** that fuse state compression, offloading, and retrieval operations directly into the compute pipeline. These compilers coordinate eviction routines with active computation, ensuring that compression kernels, DMA transfers, and state-update operations interleave

seamlessly without introducing execution stalls. When eviction logic is fused into the same pipeline as recurrent updates or linear-attention kernels, accelerators maintain peak compute intensity while avoiding the catastrophic bandwidth spikes that occur when hidden states are misaligned with memory hierarchies.

Ultimately, mastering Cache-Aware Eviction Policies for Dynamic AI Hidden States requires understanding how learned relevance metrics, temporal decay functions, and hardware memory tiers interact to maintain bounded, stable hidden-state representations. When these elements are co-designed, linear-attention and state-space models achieve deterministic throughput, predictable memory behavior, and robust long-context reasoning—all without relying on the massive KV-cache structures that limit traditional attention. This technique is essential for scaling AI systems to continuous, unbounded sequence processing while preserving both computational efficiency and model fidelity.

e. Conditional-Computation AI Micro-Architectures with Dynamic Execution Paths

Conditional-computation micro-architectures represent a major evolution in how modern AI systems allocate compute. Instead of applying the same dense sequence of operations to every token, these architectures activate computation selectively, routing tokens to specialized units only when needed and reducing unnecessary work for predictable or low-value inputs. This shift mirrors the behavior of large distributed systems, where tasks are dispatched to specialized workers, workloads are balanced dynamically, and execution paths adapt continuously to avoid bottlenecks. In AI models, conditional computation enables architectures to scale to billions of parameters without proportional increases in compute cost, latency, or memory pressure.

A central mechanism in this paradigm is sparse expert routing. Large models often contain many expert modules, each specializing in different patterns or semantic domains. Sparse routing allows the system to activate only a small subset of these experts for each token, guided by learned gating functions that determine relevance. This reduces dense compute while increasing specialization, but it also introduces new system-level challenges: dispatch queues must be balanced, routing decisions must be hardware-aligned, and interconnect bandwidth must be managed carefully to avoid contention. When implemented effectively, sparse routing becomes the backbone of conditional-computation architectures, enabling massive models to operate efficiently at scale.

Once tokens are routed to experts, the system must ensure that workloads are evenly distributed across compute clusters. Dynamic token load-balancing prevents hotspots and idle compute units, maintaining high throughput even under highly variable input streams. This mechanism treats tokens as distributed tasks that must be scheduled across heterogeneous

compute fabrics. The system monitors queue depths, token complexity, and cluster utilization, redistributing workloads in real time to maintain balanced execution. Effective load-balancing ensures that sparse routing remains efficient and that compute units remain fully saturated.

Conditional execution also introduces divergence: different tokens may follow different paths, activate different experts, or require different levels of computation. SIMD architectures, however, rely on uniform execution across lanes. Conditional AI execution pipelines and divergence-control mechanisms reconcile these opposing constraints by grouping tokens with similar execution paths, masking divergent operations, and reconfiguring pipelines to maintain high SIMD efficiency. These mechanisms preserve throughput while enabling dynamic, token-dependent compute paths, ensuring that conditional computation remains compatible with vectorized hardware.

As models grow larger and more specialized, not all layers need to be fully active for every token. Asymmetric layer slicing divides layers into independently activatable segments, while weight paging moves inactive segments out of fast memory tiers. This allows the system to scale model size without scaling memory footprint or compute cost. By activating only the necessary portions of each layer, the system reduces memory pressure, avoids unnecessary compute, and enables models to grow in parameter count without overwhelming hardware resources. When combined with sparse routing, load-balancing, and divergence control, asymmetric slicing and weight paging create a fully dynamic execution environment where compute, memory, and routing adapt continuously to the structure and difficulty of the input stream.

Together, these mechanisms form a cohesive micro-architectural strategy for conditional computation. Sparse routing determines where computation should occur, load-balancing ensures that workloads are evenly distributed, divergence control maintains SIMD efficiency, and asymmetric slicing with weight paging keeps memory usage bounded. This integrated approach allows modern AI systems to deliver high throughput, low latency, and scalable specialization—transforming conditional computation from a theoretical optimization into a practical, hardware-aligned execution model capable of supporting the next generation of large-scale AI architectures.

Table 8.4-A4 demonstrated how linear-attention and state-space architectures achieve scalability by compressing historical information into compact state representations, thereby avoiding the memory-growth characteristics associated with conventional attention mechanisms. Although these architectures significantly improve long-context efficiency, they typically apply a largely uniform computational pathway to all inputs. In many real-world AI workloads, however, informational complexity varies substantially across tokens, events, sensor observations, and contextual states. Processing every input with the same computational

intensity can lead to unnecessary resource consumption and reduced hardware efficiency. This challenge has motivated the development of **conditional-computation architectures**, which dynamically allocate computational resources according to input relevance and workload complexity. Rather than executing an identical computational pathway for every token, these architectures selectively activate model components, route workloads adaptively, and manage resources in real time. Table 8.4-A5 examines the foundational mechanisms that enable conditional computation and illustrates how dynamic execution strategies improve efficiency, scalability, and hardware utilization.

Table 8.4-A5 presents the principal mechanisms used in conditional-computation AI architectures, a class of systems designed to activate computational resources selectively rather than uniformly. These architectures represent an important evolution in hardware-aware AI design because they seek to align computational effort with informational value.

Traditional neural networks generally execute all layers, parameters, and operations regardless of input complexity. While this approach simplifies execution, it often results in substantial computational redundancy. Simple inputs may receive the same level of processing as highly complex inputs, even when significantly less computation would be sufficient.

Conditional-computation architectures address this inefficiency by introducing routing, gating, load-balancing, dynamic scheduling, and adaptive-memory techniques. These mechanisms allow portions of a model to remain inactive unless required, reducing unnecessary computation while preserving predictive capability.

The table identifies four core mechanisms supporting dynamic execution: sparse expert routing, dynamic token load balancing across compute clusters, conditional execution pipelines with SIMD divergence control, and asymmetric layer slicing with weight paging. Together, these mechanisms enable AI systems to scale capacity while maintaining efficient hardware utilization and predictable execution behavior.

By examining the interaction between adaptive computation and hardware architecture, the table illustrates how modern AI systems increasingly emphasize selective activation rather than universal execution.

Table 8.4-A5 — Core Mechanisms in Conditional-Computation AI Micro-Architectures

Mechanism	Primary Function	Hardware / System Alignment	Key Benefits for Dynamic Execution
Sparse Expert Routing	Selectively activate expert modules based on token relevance	Gating networks fused with dispatch queues and interconnect schedulers	Reduces dense compute; increases specialization; avoids dispatch bottlenecks
Dynamic Token Load-Balancing Across Core Clusters	Redistribute tokens across compute clusters to prevent hotspots	Runtime schedulers, cluster-level utilization monitors, adaptive queueing	Maintains throughput; prevents idle cores; stabilizes conditional execution
Conditional Execution Pipelines with SIMD Divergence Control	Align divergent token paths with vectorized hardware execution	Token grouping, masked execution, pipeline reconfiguration	Preserves SIMD efficiency; avoids lane underutilization; supports dynamic paths
Asymmetric Layer Slicing and Weight Paging	Activate only relevant layer segments; offload inactive weights	Tiered memory paging, compiler-driven layer segmentation	Reduces memory footprint; avoids unnecessary compute; enables larger models

Table 8.4-A5 demonstrates a fundamental shift in AI architecture design from static computation toward adaptive computation. Rather than assuming that every input demands the same level of processing, conditional-computation systems dynamically determine where and how resources should be allocated.

The mechanisms presented in the table reveal that scalability is no longer achieved solely through larger models or faster hardware. Increasingly, efficiency emerges from the ability to activate computational resources selectively while maintaining high utilization of underlying hardware systems.

The first mechanism identified in the table is **sparse expert routing**, a foundational component of many contemporary mixture-of-experts (MoE) architectures. Rather than forwarding each token through every available computational pathway, sparse expert routing evaluates token characteristics and activates only the most relevant expert modules.

The table highlights gating networks, dispatch queues, and interconnect schedulers as essential

hardware-alignment mechanisms supporting this process. These systems ensure that tokens are distributed efficiently among available experts while minimizing routing overhead. The resulting execution pattern reduces dense computation, improves specialization, and allows model capacity to increase without requiring proportional growth in active computation. Consequently, sparse expert routing has become an important strategy for scaling modern AI systems efficiently.

The second mechanism is **dynamic token load balancing across compute clusters**, which addresses a common challenge associated with conditional execution. Because routing decisions concentrate computation in selected pathways, some processing resources may become overloaded while others remain underutilized.

Load-balancing systems continuously monitor cluster utilization and redistribute workloads to maintain efficient use of available hardware resources. Runtime schedulers, adaptive queues, and utilization monitors help prevent computational hotspots that would otherwise reduce throughput. As shown in the table, the primary benefit is stable and predictable conditional execution, even when workload distribution varies substantially across inputs.

The table next identifies **conditional execution pipelines with SIMD divergence control**. Conditional-computation architectures often introduce execution diversity because different tokens may follow different computational pathways. While beneficial algorithmically, such divergence can reduce efficiency on vectorized hardware platforms designed for synchronized execution.

To address this issue, token grouping, masked execution, and pipeline reconfiguration techniques are employed to preserve SIMD and SIMT efficiency. By reorganizing execution according to shared routing behavior, the architecture minimizes lane underutilization and maintains high levels of hardware occupancy. This mechanism is particularly important because it reconciles the flexibility of conditional computation with the structural requirements of parallel processors.

Another significant mechanism is **asymmetric layer slicing and weight paging**, which extends conditional computation into memory-management strategies. Rather than loading all model parameters into active computation simultaneously, the system activates only the portions required for the current workload.

Layer segmentation and compiler-assisted paging permit inactive weights to remain in secondary storage while critical model components remain readily accessible. This strategy reduces memory footprints and avoids unnecessary computation. The table highlights an additional advantage: large models can be deployed on hardware platforms that would

otherwise be incapable of storing all parameters simultaneously in active memory.

A broader insight emerging from the table is that conditional-computation architectures transform AI execution from a static process into a dynamic resource-allocation problem. Computational effort becomes a function of input complexity rather than a fixed property of the model.

The table also illustrates the close relationship between routing decisions and hardware utilization. Selective activation improves efficiency only when routing, scheduling, and memory-management systems remain aligned with hardware execution patterns. Without careful coordination, computational savings achieved through conditional execution could be offset by dispatch overhead and resource fragmentation.

From a systems-engineering perspective, the mechanisms summarized in the table represent complementary layers of a unified adaptive-computing framework. Sparse routing controls which experts are activated. Load balancing distributes work efficiently. Divergence control preserves vector-processor efficiency. Weight paging manages memory consumption. Together, these mechanisms create a scalable architecture capable of responding dynamically to workload characteristics.

Another important observation is that conditional computation addresses both performance and resource constraints simultaneously. By activating only relevant pathways, these architectures reduce power consumption, memory bandwidth usage, thermal load, and unnecessary arithmetic operations. Such benefits are particularly valuable in autonomous systems operating within strict energy and latency budgets.

The table further highlights an emerging trend in AI-system design: increasing model capability does not necessarily require increasing active computation. Conditional-computation architectures enable systems to expand total model capacity while maintaining manageable execution costs through selective activation.

Ultimately, Table 8.4-A5 demonstrates that conditional-computation micro-architectures provide a powerful framework for aligning computational resources with input complexity and informational relevance. Through sparse expert routing, dynamic load balancing, SIMD-aware execution control, and adaptive memory management, these systems reduce unnecessary computation while preserving throughput and scalability. As AI models continue to grow in size and complexity, conditional computation is likely to play an increasingly important role in achieving efficient, hardware-aligned execution across a wide range of autonomous and intelligent systems.

Table 8.4-A5 introduced the fundamental mechanisms that enable conditional-computation architectures to allocate resources dynamically, including sparse expert routing, workload balancing, SIMD-aware execution control, and adaptive memory management. While each mechanism contributes independently to computational efficiency, their full benefit emerges only when integrated into a coordinated execution pipeline. Conditional computation is not merely a collection of optimization techniques; it is a dataflow architecture in which routing decisions, scheduling policies, execution pathways, and memory hierarchies interact continuously to determine how computational resources are allocated. Figure 8.4-A5 visualizes this architecture by tracing the flow of tokens through successive decision and execution stages, demonstrating how dynamic inference systems transform input-dependent workload variation into efficient, hardware-aligned computation.

Figure 8.4-A5 presents a hardware-aware dataflow architecture for conditional-computation AI systems. The figure illustrates how modern adaptive models selectively activate computational resources in response to input characteristics rather than processing all data through a uniform execution pathway.

Traditional neural-network architectures treat every input similarly, executing the same layers and computational operations regardless of informational complexity. While this approach simplifies implementation, it often results in substantial computational redundancy and inefficient utilization of hardware resources. Conditional-computation architectures address this limitation by introducing mechanisms that dynamically determine which portions of a model should be activated for a given input.

The architecture depicted in the figure consists of four coordinated processing modules: sparse expert routing, dynamic token load balancing, SIMD-aware conditional execution control, and asymmetric layer slicing with weight paging. Together, these modules create a pipeline that adapts computation according to workload requirements while preserving high hardware utilization and predictable execution behavior.

By illustrating the interaction between routing logic, processor scheduling, vectorized execution, and memory management, the figure highlights how conditional computation serves as a key component of modern hardware–software co-design.

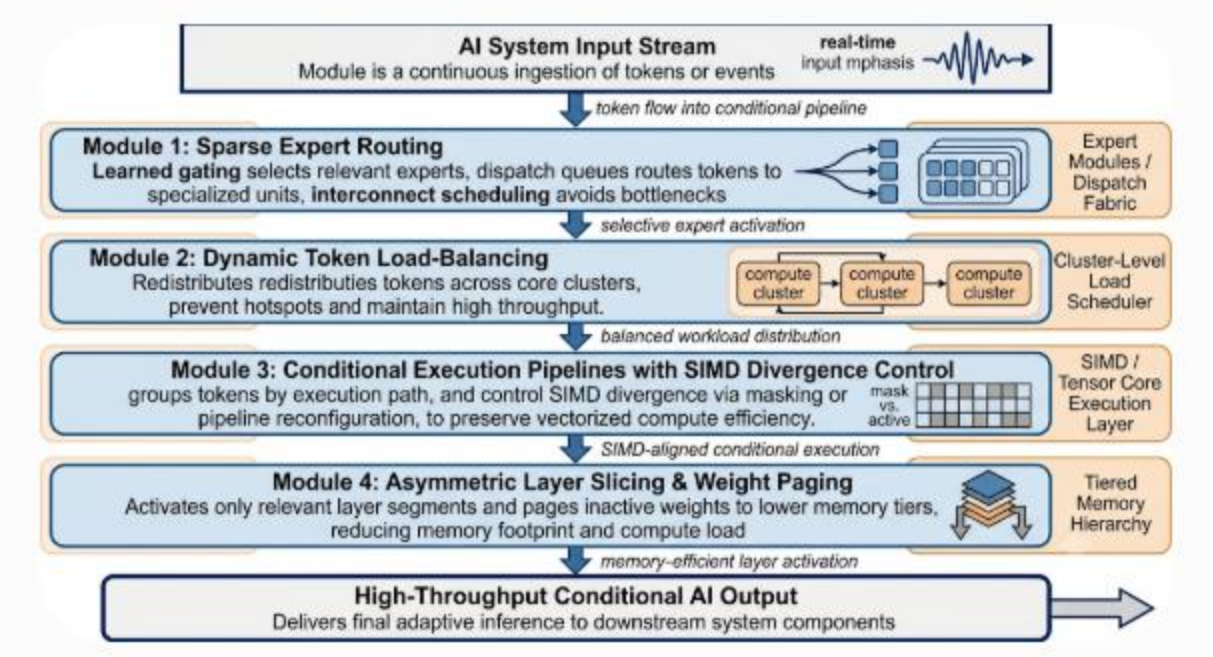


Figure 8.4-A5 — Conditional-Computation Dataflow Architecture in AI Systems

Multi-stage adaptive execution architecture illustrating how AI systems dynamically allocate computational resources according to input complexity and token relevance. The figure traces the flow of data through sparse expert routing, dynamic workload balancing, SIMD-aware conditional execution, and memory-efficient layer activation. The architecture demonstrates how conditional computation reduces unnecessary workload while maintaining throughput, hardware utilization, and scalable model capacity.

Legend

Component	***Description***
AI System Input Stream	*Continuous flow of tokens, events, sensor data, or observations entering the conditional-computation pipeline.*
Token Flow into Conditional Pipeline	*Input pathway directing workloads into adaptive execution mechanisms.*
Module 1: Sparse Expert Routing	*Routing layer that selects specialized computational experts based on token relevance.*
Learned Gating Network	*Decision mechanism determining which experts are activated.*

Expert Modules	*Specialized processing units optimized for particular task characteristics.*
Dispatch Fabric	*Communication infrastructure responsible for routing tokens to selected experts.*
Selective Expert Activation	*Dynamic activation of only the experts required for a specific input.*
Module 2: Dynamic Token Load-Balancing	*System for distributing workload across compute resources.*
Compute Clusters	*Groups of processors executing routed workloads.*
Cluster-Level Load Scheduler	*Component balancing token assignments among compute clusters.*
Balanced Workload Distribution	*Even allocation of processing demand across available resources.*
Module 3: Conditional Execution Pipelines with SIMD Divergence Control	*Execution layer preserving vectorized processing efficiency during conditional routing.*
Execution Mask	*Control structure governing active computation paths.*
SIMD/Tensor-Core Execution Layer	*Parallel processing hardware executing grouped workloads.*
SIMD-Aligned Conditional Execution	*Mechanism minimizing vector-lane underutilization.*
Module 4: Asymmetric Layer Slicing and Weight Paging	*Memory-management layer controlling parameter activation.*
Tiered Memory Hierarchy	*Multi-level storage system managing active and inactive model weights.*
Memory-Efficient Layer Activation	*Activation of relevant model segments while paging inactive weights.*
High-Throughput Conditional AI Output	*Final adaptive inference output delivered to downstream systems.*

Figure 8.4-A5 illustrates a fundamental transition in AI-architecture design from uniform computation to adaptive computation. Rather than applying identical processing pathways to every input, the architecture selectively activates computational resources based on token content, workload distribution, and execution requirements.

The figure demonstrates how conditional computation combines routing, scheduling, execution control, and memory management into a unified framework for improving efficiency without sacrificing model capability.

The figure begins with the **AI System Input Stream**, representing a continuous flow of tokens, sensor observations, events, or other forms of incoming data. Unlike traditional dense neural networks, which process all incoming information using a fixed computational pathway, the conditional-computation architecture immediately evaluates how computational resources should be allocated.

The first stage, **Module 1: Sparse Expert Routing**, serves as the entry point for adaptive decision-making.

A learned gating mechanism analyzes incoming tokens and determines which expert modules are most appropriate for processing them. Rather than activating the entire model, the routing system selectively engages only a subset of available experts.

The figure illustrates tokens being directed through a dispatch fabric toward specialized expert modules. This selective activation reduces unnecessary computation and allows different experts to develop specialized capabilities while maintaining efficient execution. Because only a fraction of the total model becomes active for a given input, computational costs remain significantly lower than would be required in a fully dense architecture.

Following routing, workloads enter **Module 2: Dynamic Token Load-Balancing**.

A challenge inherent to sparse routing is the possibility that some experts or compute resources may become overloaded while others remain underutilized. The load-balancing system addresses this problem by continuously distributing tokens across available compute clusters.

The cluster-level scheduler shown in the figure monitors resource utilization and directs workloads toward underutilized processing resources when necessary. This mechanism prevents computational hotspots and maintains high throughput despite varying workload patterns.

A key contribution of this stage is operational stability. Efficient expert selection alone is insufficient if processing resources become unevenly loaded. Load balancing ensures that adaptive routing does not create new bottlenecks elsewhere in the system.

The third stage, **Conditional Execution Pipelines with SIMD Divergence Control**, addresses one of the most significant hardware challenges associated with conditional computation.

Modern accelerators rely heavily on SIMD and SIMT execution models in which groups of

operations execute simultaneously. Divergent token paths can reduce utilization by causing different execution lanes to follow different instruction paths.

To address this issue, the architecture groups similar workloads together and applies execution masks that align conditional computations with vectorized hardware structures. The figure shows workload masks interacting with a SIMD/tensor-core execution layer to preserve efficient parallel processing.

This stage is particularly important because it reconciles the flexibility of conditional computation with the performance requirements of modern accelerators. Without divergence control, computational savings achieved through expert routing could be partially offset by reduced hardware utilization.

The next stage, **Module 4: Asymmetric Layer Slicing and Weight Paging**, introduces adaptive memory management.

Not all model layers or parameters must remain active simultaneously. The architecture therefore partitions model parameters into segments and activates only those required for current computations. Inactive portions are moved into lower-priority memory tiers.

The figure depicts a tiered memory hierarchy supporting this process. Frequently used parameters remain readily accessible, while less relevant weights are paged to lower storage levels. This approach reduces active memory footprints and allows substantially larger models to operate within finite memory resources.

An important consequence of this strategy is improved scalability. By controlling parameter residency dynamically, the system supports larger model capacities without requiring proportional increases in active memory consumption.

The final stage produces the **High-Throughput Conditional AI Output**.

The output reflects the cumulative effect of all previous optimization stages. Sparse routing has reduced unnecessary computation. Load balancing has maintained throughput. Divergence control has preserved hardware efficiency. Weight paging has minimized memory consumption. Together, these mechanisms produce an adaptive inference system that delivers strong performance while utilizing substantially fewer resources than traditional dense architectures.

A broader insight emerging from the figure is that conditional computation transforms AI inference into a resource-allocation problem. Rather than assuming that every input deserves equal computational treatment, the architecture continuously evaluates where computation should be applied and where it can be avoided.

The figure also demonstrates that efficient conditional computation requires coordination across multiple system layers. Routing decisions, scheduling policies, execution management, and memory allocation must operate in concert. Optimizing one layer in isolation is insufficient because inefficiencies can migrate elsewhere in the system.

From a systems-engineering perspective, the architecture exemplifies hardware–software co-design. Gating networks align with dispatch fabrics, load balancing aligns with cluster scheduling, divergence control aligns with vectorized execution hardware, and weight paging aligns with memory hierarchies. Each optimization is explicitly matched to a corresponding hardware capability.

Another important observation is that conditional computation improves both efficiency and scalability simultaneously. Computational workload, memory consumption, and energy usage are reduced, while total model capacity can continue increasing through selective activation rather than dense execution.

Ultimately, Figure 8.4-A5 demonstrates that conditional-computation architectures achieve efficiency through adaptive resource allocation rather than uniform execution. By integrating sparse expert routing, dynamic load balancing, SIMD-aware execution control, and memory-efficient layer activation into a unified pipeline, these systems align model behavior with hardware characteristics and enable scalable, high-performance AI inference under real-world resource constraints.

Figure 8.4-A5 demonstrates that conditional-computation architectures achieve efficiency by decomposing inference into a sequence of adaptive routing, scheduling, execution, and memory-management stages. At the front of this pipeline lies **sparse expert routing**, the mechanism responsible for determining where computation should occur before any workload-balancing, SIMD-alignment, or memory-optimization decisions can be made. This positioning reflects its foundational role within conditional-computation systems. Before tokens can be distributed efficiently across compute clusters, before divergence-control mechanisms can preserve vectorized execution efficiency, and before inactive model segments can be paged from memory, the architecture must first identify which computational experts are relevant to a given input. Consequently, sparse expert routing serves as the primary decision layer governing resource allocation throughout the system. By selectively activating specialized expert modules while avoiding unnecessary computation, it establishes the adaptive execution patterns upon which all subsequent stages of the conditional-computation pipeline depend. The following discussion therefore examines **Sparse Expert Routing for AI Dispatch Bottleneck Reduction** as the initial and most influential mechanism in dynamic AI execution architectures, providing the routing foundation that enables scalable, high-throughput conditional inference.

i. Sparse Expert Routing for AI Dispatch Bottleneck Reduction

Sparse expert routing is a foundational optimization in conditional-computation architectures, enabling large Mixture-of-Experts (MoE) models to scale without collapsing under dispatch bottlenecks or interconnect congestion. As models grow, traditional gating mechanisms introduce severe communication overhead: tokens are routed indiscriminately across nodes, triggering all-to-all traffic patterns, uneven expert utilization, and synchronization stalls that throttle throughput. Sparse routing resolves these issues by tightly coupling the gating network with the physical topology of the underlying hardware. Instead of treating experts as abstract functions, topology-aware gating incorporates the structure of NVLink domains, InfiniBand rails, and cluster-local interconnects, preferentially steering tokens toward experts reachable through low-latency paths.

To prevent execution divergence—where a single GPU warp stalls waiting for an overloaded expert—routing pipelines enforce strict expert-capacity limits and dynamic tensor packing. Token embeddings are compacted into dense, contiguous memory blocks, ensuring that each expert receives uniformly sized tensors and that excess tokens are either rerouted or dropped according to predefined capacity rules. This maintains warp-level uniformity and eliminates the thread serialization that typically arises from non-uniform expert loads.

Evaluating sparse expert routing requires analyzing how custom communication kernels bypass fragmented memory packets by mapping token-to-expert indices directly onto non-blocking all-to-all primitives. These kernels overlap network transfers with active Tensor Core execution, reducing synchronization barriers and enabling the system to sustain high throughput even under highly non-uniform routing patterns. Ultimately, mastering sparse expert routing means grounding dispatch schedules within distributed inference frameworks that balance routing accuracy against strict hardware alignment—ensuring that token allocation remains both mathematically optimal and microarchitecturally efficient across massively parallel clusters.

Sparse expert routing determines *which* experts should process each token, but it does not guarantee that the resulting workloads are evenly distributed across the system. Even with topology-aware gating and strict expert-capacity limits, token streams can exhibit bursty, highly skewed patterns that overload certain experts while leaving others underutilized. To sustain peak throughput, the system must complement routing with a second mechanism: dynamic token load-balancing across AI core clusters. This next stage redistributes tokens in real time, smoothing out routing-induced imbalances, preventing cluster hotspots, and ensuring that conditional-computation pipelines remain fully saturated even under unpredictable or adversarial input distributions.

ii. Dynamic Token Load-Balancing Across AI Core Clusters

Dynamic token load-balancing across AI core clusters is a central hardware-software co-design strategy that ensures real-time redistribution of workloads across parallel processing units, preventing execution stalls and maintaining uniform accelerator utilization. In large-scale distributed inference systems, token streams exhibit natural variability—sentence complexity, branching semantic structures, and fluctuating sequence lengths all contribute to uneven computational demand. Without corrective mechanisms, some GPU clusters become overloaded while others sit idle, creating localized bottlenecks that propagate backward through the pipeline and degrade system-wide throughput.

Load-balancing resolves these imbalances by introducing high-speed runtime schedulers that continuously monitor token-level compute pressure across clusters. These schedulers dynamically shift token batches away from congested nodes and toward underutilized ones, transforming rigid, static allocation schemes into elastic distribution protocols. By smoothing queue depths and eliminating hotspots, the system prevents warp-level stalls and ensures that all arithmetic pipelines—matrix-multiplication units, Tensor Cores, and vector engines—operate at peak saturation.

A complete technical evaluation of load-balancing must consider how distributed schedulers bypass traditional synchronization barriers. Instead of waiting for global coordination signals, they map live routing states directly onto low-latency interconnect fabrics such as NVLink or InfiniBand. This approach overlaps token-shuffling kernels with active compute loops, allowing the system to rebalance workloads without interrupting ongoing execution. The microarchitectural cost of computing and transmitting load-distribution maps is offset by dramatic reductions in end-to-end latency and the elimination of cluster-wide execution skew. Ultimately, mastering dynamic load-balancing requires integrating these runtime schedulers into distributed deep learning frameworks so that token redistribution occurs seamlessly alongside matrix-multiplication pipelines, sustaining high throughput even under volatile, real-world deployment workloads.

Dynamic load-balancing ensures that tokens are evenly distributed across clusters, but balanced workloads alone do not guarantee efficient execution on vectorized hardware. Once tokens reach their assigned compute units, they may still follow different conditional paths—activating different experts, invoking different layer segments, or requiring different levels of computation. This divergence poses a direct challenge to SIMD and Tensor Core architectures, which rely on uniform execution across lanes. To maintain high utilization after load-balancing has redistributed tokens, the system must introduce mechanisms that align conditional execution with vectorized compute fabrics. This leads naturally into the next concept: **Conditional AI**

Execution Pipelines and SIMD Divergence Control, where token grouping, masked execution, and pipeline reconfiguration preserve SIMD efficiency even as execution paths become increasingly dynamic.

iii. Conditional AI Execution Pipelines and SIMD Divergence Control

Conditional AI execution pipelines and SIMD divergence control form a crucial hardware-software co-design strategy that preserves uniform instruction sequencing across parallel processing threads, ensuring that Single Instruction, Multiple Data (SIMD) hardware remains fully saturated even when models exhibit highly dynamic behavior. Modern deep learning workloads frequently introduce conditional operations—dynamic token pruning, sparse expert activation, variable-length sequences, and data-dependent branching—that naturally fragment execution paths. When threads within a GPU warp or vector register diverge, the hardware is forced to serialize execution, leaving inactive lanes idle and collapsing arithmetic intensity.

This optimization paradigm addresses divergence by introducing hardware-aligned prediction masks, instruction predication, and data-repacking algorithms that reorganize tokens and thread groups according to shared execution states. Instead of allowing uncoordinated branching to scatter threads across incompatible paths, the pipeline clusters tokens with similar conditional requirements, transforming irregular, data-dependent flows into dense, synchronized parallel operations. Divergence control ensures that vector lanes remain uniformly active, eliminating the structural serialization that arises when conditional logic forces the hardware to execute multiple paths sequentially.

A complete technical evaluation of this mechanism requires analyzing how vectorized compiler architectures and custom kernels map localized bitmask predicates directly onto hardware register lanes. These compilers track divergence in real time, reordering thread groups and applying predication masks that allow inactive lanes to skip work without breaking lock-step execution. The microarchitectural overhead of maintaining these masks and reorganizing thread paths is outweighed by the substantial throughput gains achieved when SIMD units avoid branch serialization. Ultimately, mastering conditional execution pipelines requires integrating divergence-control mechanisms deeply into the low-level compilation stack, ensuring that dynamically predicated data flows align perfectly with physical vector lane widths. This alignment prevents execution stalls, maximizes arithmetic intensity, and enables highly conditional neural network layers to run at full hardware efficiency.

Even with divergence-controlled execution pipelines, conditional computation still faces a fundamental challenge: not all parts of a model need to be active for every token. SIMD

alignment ensures that conditional paths execute efficiently, but it does not address the memory and compute overhead of activating entire layers when only a subset of their parameters is relevant. To fully capitalize on dynamic execution, the system must introduce mechanisms that selectively activate portions of each layer while paging inactive weights out of fast memory tiers. This leads directly into the next concept—**Asymmetric Layer Slicing and Weight Paging in AI Models**—where conditional computation extends beyond routing and divergence control to reshape the internal structure of layers themselves, reducing memory pressure, eliminating unnecessary compute, and enabling models to scale in size without overwhelming hardware resources.

iv. Asymmetric Layer Slicing and Weight Paging in AI Models

Asymmetric layer slicing and weight paging represent a critical hardware-software co-design paradigm that enables non-uniform neural layer partitioning and demand-driven parameter streaming, allowing large models to operate efficiently even when their parameter footprint exceeds on-chip memory capacity. In highly scaled or memory-constrained environments, modern deep learning architectures routinely surpass the physical limits of accelerator memory, triggering allocation failures, excessive off-chip traffic, and severe throughput degradation. This optimization technique addresses these constraints by decomposing layers according to their compute-to-memory characteristics—slicing dense attention matrices differently from feed-forward blocks, for example—and streaming these heterogeneous layer segments into high-speed local memory precisely when needed.

By replacing rigid, uniform model-parallel configurations with heterogeneous data partitioning and speculative prefetching protocols, the execution pipeline becomes fluid and memory-efficient. Upcoming layer segments are pre-cached before execution begins, while inactive weights are paged out to lower-tier memory, ensuring that only the parameters required for the next compute step occupy scarce on-chip resources. This transforms model execution into a dynamic, demand-driven process where memory footprint scales elastically with the active portion of the network rather than with the full parameter set.

A complete technical evaluation of this mechanism requires analyzing how deep learning compilers and virtual memory managers bypass the latency of synchronous host-to-device transfers. Instead of relying on blocking copies, they map non-uniform layer slices directly onto asynchronous Unified Memory (UM) pathways or NVLink/PCIe streaming rings. This approach balances the overhead of predicting layer execution timelines and tracking non-sequential page tables against the substantial reductions in physical memory pressure and hardware idle states achieved across large-model deployments. Ultimately, mastering asymmetric slicing and weight paging requires integrating these scheduling layers into runtime execution frameworks so that

paging kernels overlap seamlessly with active matrix-multiplication loops, maximizing arithmetic intensity and sustaining high token throughput even when model parameters far exceed native accelerator memory capacity.

Conditional-computation micro-architectures demonstrate how modern AI systems can transform dense, uniform execution into a fluid, adaptive pipeline that responds intelligently to the structure and complexity of incoming tokens. Sparse expert routing selectively activates specialized modules, reducing unnecessary computation while increasing the model's expressive capacity. Dynamic token load-balancing ensures that these routed workloads remain evenly distributed across heterogeneous compute clusters, preventing hotspots and maintaining full accelerator saturation. Conditional execution pipelines and SIMD divergence control preserve vectorized efficiency even when tokens follow divergent paths, aligning dynamic behavior with the rigid constraints of hardware execution fabrics. Asymmetric layer slicing and weight paging extend this adaptability into the memory hierarchy itself, activating only the necessary portions of each layer and streaming weights on demand to avoid overwhelming limited on-chip memory.

Together, these mechanisms form a coherent strategy for scaling AI systems under real-world conditions where token complexity fluctuates, workloads shift unpredictably, and hardware resources must be used with surgical precision. Conditional-computation architectures reveal that efficiency at scale is not achieved through brute force, but through dynamic specialization, intelligent routing, and continuous alignment between algorithmic behavior and physical execution pathways.

Model architectures define the computational grammar through which AI systems interpret, transform, and generate information. Across the architectural landscape, the most significant breakthroughs arise from designs that blend mathematical elegance with hardware awareness. Linear-attention and state-space models show how long-context reasoning can be achieved through compressed recurrence, parallel scan propagation, and memory-aligned hidden-state management. Conditional-computation micro-architectures demonstrate how dynamic routing, load-balancing, divergence control, and demand-driven parameter streaming allow models to scale efficiently without overwhelming compute or memory resources.

Taken together, these architectural innovations reveal a clear trajectory: modern AI systems increasingly rely on models that are not only more expressive, but also more efficient, more adaptive, and more tightly integrated with the physical constraints of the machines that execute them. The future of AI architecture lies in designs that treat computation as a dynamic resource, allocating it precisely where it is needed and eliminating waste wherever it appears.

The architectural strategies described above achieve their full potential only when paired with hardware capable of executing them efficiently. Linear-time recurrence, parallel scan propagation, sparse expert routing, divergence-controlled pipelines, and demand-driven weight paging all depend on accelerators with high-bandwidth memory systems, low-latency interconnects, vectorized compute fabrics, and sophisticated runtime schedulers. To understand how these models translate into real-world performance, the next step is to examine the physical systems that power them. This transition shifts the focus from how AI models are designed to how they are executed, revealing the deep co-design relationship between algorithm and machine that ultimately determines the scalability, efficiency, and responsiveness of modern AI systems.

B. Hardware Accelerators in AI Systems

Hardware accelerators define the physical substrate on which intelligence is executed in autonomous AI systems. They determine how tensor programs are scheduled, how memory moves through silicon, how parallelism is expressed at the circuit level, and how inference behaves when thermal, bandwidth, or latency constraints tighten. In hardware–software co-design, accelerators are not passive devices; they are active computational environments whose data types, execution pipelines, memory hierarchies, and interconnect fabrics directly shape the feasibility of real-time autonomy. Every accelerator choice—precision format, scheduler topology, memory architecture, spatial array configuration, or co-processor integration—propagates through the autonomy stack and governs how efficiently models can operate under real-world constraints.

Modern AI workloads have reached a scale where naïve high-precision computation and uniform memory access are no longer viable. Autonomous systems must execute large models within strict latency budgets, constrained thermal envelopes, and limited on-chip memory. As a result, hardware accelerators increasingly incorporate model-aware design principles that optimize data movement, exploit low-precision arithmetic, fuse scheduling with vector execution, and integrate memory directly into compute fabrics. These principles ensure that intelligence is not only architecturally expressive but also physically executable within the limits of silicon, interconnect bandwidth, and power delivery.

- **AI Low-Precision Data Types: FP4, INT4, and MX-Format Execution** - Low-precision data types such as FP4, INT4, and mixed-format MX encodings redefine the arithmetic landscape of AI accelerators. By compressing numerical representations into ultra-compact formats aligned with tensor-core tile geometry, accelerators dramatically increase compute density, reduce memory traffic, and expand effective on-chip capacity. These formats allow large models to run within tight thermal and power budgets while

maintaining functional accuracy through quantization-aware training and hardware-aligned rounding schemes. Low-precision execution is now a cornerstone of real-time AI deployment, enabling high-throughput inference on embedded and resource-constrained platforms.

- **On-Chip AI Schedulers and Asynchronous Vector Execution Pipelines** - On-chip schedulers and asynchronous vector pipelines transform accelerators from static compute engines into dynamic execution environments. These schedulers orchestrate tensor movement, fuse kernels, and overlap compute with memory operations to eliminate idle cycles. Asynchronous vector pipelines allow independent execution streams to progress without global synchronization, maximizing utilization of SIMD lanes, tensor cores, and matrix engines. This scheduling intelligence ensures that accelerators maintain deterministic latency even when workloads fluctuate or conditional-computation pathways activate irregular execution patterns.
- **AI Processing-in-Memory and On-Die Static Weight Streaming** — Processing-in-memory (PIM) and static weight streaming collapse the traditional boundary between compute and memory. By embedding arithmetic units directly within memory arrays or streaming weights from on-die storage, accelerators minimize off-chip traffic and eliminate bandwidth bottlenecks that dominate transformer-class workloads. These techniques keep critical parameters physically close to compute units, reducing latency and enabling high-fidelity reasoning even when external memory bandwidth is limited. PIM and weight streaming are essential for long-context models, sensor-dense autonomy stacks, and deployments where memory access patterns dominate runtime behavior.
- **Reconfigurable AI Spatial Architectures and Coarse-Grained Arrays** - Spatial architectures and coarse-grained reconfigurable arrays (CGRAs) provide hardware that adapts to the structure of the model itself. Instead of fixed datapaths, these accelerators dynamically reconfigure compute tiles, routing networks, and memory banks to match the parallelism and locality patterns of each layer. This spatial flexibility allows accelerators to optimize execution for convolutional blocks, attention heads, state-space operators, or sparse expert modules without requiring separate hardware designs. Reconfigurable arrays enable high utilization across diverse workloads, making them ideal for autonomous systems with heterogeneous compute demands.
- **Hybrid AI Co-Processors with Non-Volatile Memory Lattices and Optical Interconnects** — Hybrid co-processors integrate non-volatile memory lattices, photonic links, and emerging device technologies to push beyond the limits of electrical interconnects and volatile SRAM. Non-volatile lattices provide persistent, low-leakage storage for massive

parameter sets, while optical interconnects offer ultra-low-latency, high-bandwidth communication across chiplets and distributed nodes. These hybrid architectures reduce energy consumption, expand memory capacity, and enable accelerators to sustain high throughput even under extreme model sizes or distributed inference conditions. They represent the frontier of AI hardware design, where new physical media redefine the boundaries of compute and communication.

Together, these dimensions illustrate how hardware accelerators have evolved into a central pillar of hardware–software co-design. Intelligence in autonomous systems is shaped not only by model architecture but by how effectively those architectures conform to the contours of silicon, memory hierarchies, interconnect fabrics, and execution pipelines. These accelerator principles enable modern AI systems to achieve resilience, efficiency, and scalability through deliberate co-design across the entire autonomy stack.

Hardware accelerators sit directly beneath model architectures in the co-design hierarchy because they determine how every downstream layer—memory systems, runtime frameworks, compiler stacks, and real-time control loops—must behave to support autonomous operation. The physical constraints embedded in these accelerators shape arithmetic precision, memory traffic, scheduling behavior, spatial parallelism, and interconnect topology. To clarify how these constraints interact with model requirements and real-time demands, the next step is to organize the core accelerator dimensions that govern modern AI hardware design. This structured view reveals the mechanisms that allow large-scale models to operate efficiently and predictably within the physical limits of autonomous systems.

The accelerator mechanisms described above reveal how modern AI hardware has evolved from fixed-function compute engines into adaptive, memory-aware, precision-optimized execution platforms. But understanding these mechanisms individually is only the first step. To appreciate how they interact within real systems—how low-precision arithmetic reshapes memory traffic, how asynchronous schedulers sustain vector utilization, how processing-in-memory collapses bandwidth bottlenecks, how spatial arrays adapt to heterogeneous workloads, and how hybrid co-processors extend compute beyond electrical limits—it is necessary to view them as a unified hardware design framework. The following table organizes these dimensions into a structured reference model, clarifying the foundational hardware strategies that enable large-scale AI workloads to operate efficiently, predictably, and within the physical constraints of silicon, interconnects, and power delivery.

The preceding discussions examined how hardware-aware AI architectures improve efficiency through structured sparsity, memory-optimized attention mechanisms, state-space computation, and conditional-execution pipelines. Although these innovations originate at the

model and software levels, their success ultimately depends on the capabilities provided by the underlying hardware. Architectural techniques can only deliver meaningful performance gains when supported by accelerators specifically designed to execute AI workloads efficiently. As model complexity, context length, and parameter scale continue to increase, conventional processor architectures increasingly struggle to satisfy the requirements of modern AI systems. This challenge has driven the development of specialized accelerator technologies that optimize numerical precision, scheduling behavior, memory organization, data movement, and interconnect performance. Table 8.4-B introduces the core dimensions of contemporary AI accelerators and illustrates how hardware innovations complement software-level optimization strategies within the broader hardware–software co-design framework.

Table 8.4-B presents several foundational accelerator dimensions that define contemporary AI hardware architectures. These dimensions represent specialized hardware innovations designed to address the computational, memory, bandwidth, and energy challenges posed by modern AI workloads.

The rapid growth of AI models has transformed performance bottlenecks across the computing stack. While earlier generations of AI systems were primarily constrained by arithmetic throughput, modern workloads often encounter limitations associated with data movement, memory hierarchy efficiency, scheduling overhead, and interconnect scalability. As a result, AI accelerators have evolved beyond simple matrix-multiplication engines into highly integrated systems optimized for the unique characteristics of neural-network execution.

The table identifies five major accelerator dimensions: low-precision numerical formats, on-chip schedulers with asynchronous vector-execution pipelines, processing-in-memory architectures, reconfigurable spatial computing fabrics, and hybrid co-processors integrating advanced memory and optical-interconnect technologies. Each dimension addresses a distinct challenge associated with scaling AI systems while improving efficiency and maintaining predictable execution behavior.

By examining these accelerator technologies alongside their hardware alignment strategies and execution benefits, the table demonstrates how modern AI hardware increasingly serves as an active participant in computational optimization rather than merely a platform for executing software instructions.

Table 8.4-B — Core Accelerator Dimensions in AI Hardware

Accelerator Dimension	Primary Function	Hardware / System Alignment	Key Benefits for AI Execution
AI Low-Precision Data Types (FP4, INT4, MX-Formats)	Compress numerical representations for high-density compute	Tensor-core tile geometry, quantization-aware rounding, mixed-precision datapaths	Increased compute throughput, reduced memory traffic, expanded effective on-chip capacity
On-Chip AI Schedulers & Asynchronous Vector Execution Pipelines	Orchestrate tensor movement and fuse execution streams	SIMD lane controllers, kernel fusion engines, dependency-aware schedulers	Eliminates idle cycles, overlaps compute with memory ops, maintains deterministic latency
AI Processing-in-Memory & On-Die Static Weight Streaming	Embed compute within memory arrays and stream weights locally	SRAM-embedded ALUs, stacked memory dies, on-die parameter stores	Minimizes off-chip bandwidth, reduces latency, supports long-context workloads
Reconfigurable AI Spatial Architectures & Coarse-Grained Arrays	Adapt compute topology to model structure	Dynamic tile routing, CGRA fabrics, spatially programmable datapaths	High utilization across heterogeneous workloads, optimized locality and parallelism
Hybrid AI Co-Processors with Non-Volatile Memory & Optical Interconnects	Extend compute and memory beyond electrical limits	Photonic links, persistent memory lattices, chiplet-scale optical fabrics	Ultra-low-latency communication, massive parameter capacity, reduced energy consumption

Table 8.4-B demonstrates that modern AI accelerators are no longer general-purpose computational devices adapted for machine learning workloads. Instead, they are purpose-built architectures that incorporate hardware mechanisms specifically designed to support AI

execution patterns.

The accelerator dimensions summarized in the table reveal a common objective: reducing the cost of data movement while maximizing computational density, resource utilization, and execution efficiency. These goals align closely with the architectural principles discussed throughout the preceding discussions on hardware-aware model design.

The first accelerator dimension identified in the table is **AI low-precision data types**, including formats such as FP4, INT4, and emerging MX-based numerical representations. These formats reduce the number of bits required to represent weights, activations, and intermediate computations.

The primary purpose of low-precision arithmetic is to increase computational density while reducing memory traffic. Smaller numerical representations require fewer storage resources and allow greater numbers of values to be processed simultaneously. The table highlights tensor-core geometry and mixed-precision datapaths as key alignment mechanisms supporting this capability.

The benefits are substantial. Reduced memory requirements increase the effective capacity of on-chip storage resources, allowing larger portions of the model to remain close to compute units. In addition, lower-precision operands reduce bandwidth demands and enable higher arithmetic throughput, making low-precision computation one of the most influential developments in contemporary AI acceleration.

The second dimension is **on-chip AI schedulers and asynchronous vector-execution pipelines**, which address the increasingly complex task of coordinating large numbers of concurrent neural-network operations.

Modern AI workloads contain extensive opportunities for parallel execution. However, maintaining high utilization requires careful orchestration of tensor movement, kernel scheduling, and dependency management. The table identifies SIMD-lane controllers, kernel-fusion engines, and dependency-aware scheduling systems as key mechanisms supporting this process.

These components eliminate idle cycles and allow computation to overlap with memory operations, improving overall efficiency. Perhaps more importantly for autonomous and real-time systems, sophisticated scheduling mechanisms contribute to deterministic latency behavior by reducing unpredictable execution delays.

The third accelerator dimension is **AI processing-in-memory and on-die static weight streaming**, which addresses one of the most persistent challenges in AI computing: the cost of

moving data between memory and compute units.

Traditional architectures separate storage and computation, requiring continuous data transfers that consume energy and bandwidth. Processing-in-memory systems partially overcome this limitation by embedding arithmetic capabilities directly within memory structures. The table references SRAM-embedded arithmetic units, stacked memory dies, and local parameter stores as examples of this approach.

By reducing off-chip communication, processing-in-memory architectures lower latency, improve energy efficiency, and enable sustained execution of memory-intensive workloads. These characteristics make them particularly attractive for long-context inference and edge-deployment scenarios where bandwidth is a critical resource.

Another important dimension is **reconfigurable AI spatial architectures and coarse-grained arrays**. Unlike fixed-function accelerators optimized for a narrow class of workloads, reconfigurable architectures adapt computational topology to match model requirements dynamically.

The table highlights dynamic tile routing, coarse-grained reconfigurable-array (CGRA) fabrics, and spatially programmable dataflow structures as representative technologies. These systems allocate hardware resources according to workload characteristics, increasing utilization across diverse model architectures.

This flexibility is especially important as AI systems evolve rapidly. New architectures often exhibit execution patterns that differ significantly from those envisioned by earlier hardware generations. Reconfigurable spatial architectures provide adaptability while preserving high efficiency and locality.

The final accelerator dimension identified in the table is **hybrid AI co-processors with non-volatile memory and optical interconnects**, representing one of the most forward-looking directions in accelerator development.

As model sizes continue expanding, traditional electrical interconnects increasingly become bottlenecks. The integration of persistent memory technologies, advanced photonic communication links, and chiplet-scale optical fabrics seeks to overcome these limitations. Such systems support ultra-low-latency communication while enabling access to significantly larger parameter spaces.

The hardware alignment mechanisms listed in the table illustrate how these technologies extend computational systems beyond conventional electrical scaling limits. Their benefits include reduced energy consumption, improved communication efficiency, and support for

extremely large AI models.

A broader insight emerging from the table is that modern accelerator innovation increasingly focuses on reducing data movement rather than increasing arithmetic capability alone. Although computational throughput continues to improve, memory transfers and communication overhead often dominate execution cost. Many of the accelerator technologies summarized here directly target these challenges.

The table also highlights a strong correspondence between accelerator design and model architecture. Low-precision formats align with quantized neural networks. Asynchronous schedulers support conditional-computation systems. Processing-in-memory techniques complement memory-optimized attention architectures. Reconfigurable fabrics adapt to evolving computational graphs. This alignment demonstrates the deep interdependence between hardware and software design.

From a systems-engineering perspective, the dimensions summarized in the table represent complementary mechanisms rather than competing alternatives. Low-precision arithmetic improves compute density. Advanced scheduling increases utilization. Embedded memory reduces movement costs. Spatial fabrics improve adaptability. Optical interconnects improve scalability. Together, they create a holistic accelerator ecosystem capable of supporting increasingly sophisticated AI workloads.

Another important observation is that many of these technologies contribute directly to energy efficiency. As AI deployment expands across cloud infrastructure, edge computing, robotics, and autonomous systems, energy consumption increasingly becomes a central design constraint. Accelerator innovations therefore aim to improve performance while simultaneously reducing power requirements.

Ultimately, Table 8.4-B demonstrates that AI accelerators have evolved into highly specialized computing platforms optimized around the unique demands of machine-learning workloads. Through innovations in numerical precision, scheduling, memory integration, spatial computation, and communication infrastructure, these accelerators provide the hardware foundation necessary to support modern AI architectures. In doing so, they extend the principles of hardware–software co-design from the model level into the physical computing substrate itself, enabling higher performance, greater efficiency, and improved scalability across the next generation of AI systems.

The accelerator dimensions summarized in Table 8.4-B reveal that many of the most significant gains in modern AI hardware arise not from increasing transistor counts alone, but from rethinking how numerical information is represented and processed. Among these innovations,

low-precision computation occupies a foundational position because it directly influences memory capacity, bandwidth consumption, energy efficiency, and computational throughput across the entire accelerator stack. Before advanced scheduling systems can maximize utilization, before processing-in-memory architectures can reduce data movement, and before reconfigurable fabrics can adapt to diverse workloads, the underlying numerical representation must be optimized for efficient execution. Low-precision formats such as FP4, INT4, and emerging MX-family representations reduce the cost of arithmetic operations while increasing the volume of data that can be stored, transferred, and processed within fixed hardware resources. Consequently, these numerical formats serve as one of the primary enablers of modern AI acceleration, establishing the computational density and memory efficiency upon which many subsequent hardware optimizations depend. The following discussion therefore examines **AI Low-Precision Data Types: FP4, INT4, and MX-Format Execution** as a foundational accelerator technology that reshapes the balance among precision, performance, memory utilization, and energy consumption in contemporary AI systems.

a. AI Low-Precision Data Types: FP4, INT4, and MX-Format Execution

AI low-precision data types—FP4, INT4, and MX-format encodings—represent one of the most consequential hardware–software co-design paradigms in modern accelerator engineering. They enforce extreme numerical compression and specialized bit-level register mapping to maximize arithmetic intensity, reduce memory traffic, and eliminate bandwidth bottlenecks in next-generation AI systems. As deep learning architectures scale into the hundreds -of-billions-parameter regime, traditional FP16 or INT8 formats impose unsustainable energy costs and communication latency during large-scale matrix multiplication. Low-precision execution resolves these physical scaling limits by deploying ultra-dense sub-byte quantization alongside Microscaling (MX) specifications that share exponent registers across small parameter blocks.

Traditional FP16, INT8, FP4, INT4, and MX-format encodings represent the spectrum of numerical precision strategies used in modern AI accelerators, each balancing dynamic range, memory footprint, and execution efficiency in different ways. **FP16** provides a 5-bit exponent and 10-bit mantissa, offering wide dynamic range at half the storage cost of FP32, making it suitable for training and stable inference. **INT8** reduces values to 8-bit integers with per-tensor or per-channel scaling factors, dramatically lowering bandwidth and energy consumption while maintaining acceptable accuracy for most inference workloads. Ultra-low-precision formats push this compression further: **FP4** uses a 2-bit exponent and 2-bit mantissa to encode floating-point values in only four bits, while **INT4** represents activations or weights as 4-bit integers with minimal scaling metadata. These formats enable extreme compute density and

drastically reduce memory traffic, but require careful quantization and compiler support to avoid numerical instability. **Microscaling (MX) formats** extend low-precision arithmetic by sharing a single exponent across a small block of 4-bit mantissas, preserving dynamic range while achieving sub-byte compression. MX encodings operate as hybrid floating-point structures: they retain the expressive scaling behavior of FP formats but apply it across tightly packed mantissa groups, allowing accelerators to execute large models with high throughput, low power, and minimal memory footprint.

By systematically replacing wide data lanes with narrow bit-width formats, accelerators pack multiple parameters into single registers, dramatically increasing data streaming throughput while reducing silicon area and power consumption. This compression is not merely a numerical trick—it is a structural transformation of the execution pipeline. Sub-byte mantissas, shared-exponent blocks, and fixed-point accumulation arrays allow hardware to operate at higher parallelism levels without overwhelming memory hierarchies or thermal envelopes.

A complete technical evaluation of low-precision execution requires understanding how Arithmetic Logic Units (ALUs) bypass precision loss and format incompatibilities by mapping 4-bit mantissas and shared-exponent groups directly onto fixed-point accumulation paths. This microarchitectural strategy relies on four integrated pillars:

- **Sub-Byte AI Quantization and ALU Bit-Width Mapping** — Aligns 4-bit structures with physical lane widths to maximize instruction-level parallelism and reduce register pressure.
- **MX-Format Block Scaling with Shared AI Exponent Registers** — Shares a single exponent across multiple 4-bit mantissas, preserving dynamic range while drastically reducing memory overhead.
- **Mantissa-Free AI Integer Units and Fixed-Point Accumulation** — Eliminates floating-point logic for integer paths, enabling ultra-fast bit-shifted accumulation with minimal power draw.
- **Mixed-Precision AI Execution and Dynamic Format Emulation** — Uses compiler-driven emulation to run ultra-low-precision formats on legacy hardware while dynamically casting intermediate activations to FP16/BF16 for numerical stability.

Mastering low-precision execution requires integrating these physical data layouts into modern compiler ecosystems so that multi-format pipelines balance extreme compression against model convergence. When properly aligned, these techniques deliver up to a 4× throughput increase without catastrophic accuracy degradation—making low-precision arithmetic a

cornerstone of scalable AI deployment.

Low-precision arithmetic introduces a radically different numerical environment for AI accelerators—one where parameters are compressed into sub-byte formats, exponents are shared across mantissa blocks, integer units replace floating-point logic, and mixed-precision stabilization ensures accuracy under aggressive quantization. These mechanisms operate together, not in isolation. To understand how they collectively reshape compute density, memory traffic, and execution throughput, it is useful to view them as a unified design framework. The following table organizes these mechanisms into their core functional dimensions, clarifying how each contributes to the broader goal of sustaining high-performance AI inference under extreme numerical compression.

Table 8.4-B introduced low-precision numerical formats as one of the most influential dimensions of modern AI accelerator design. The discussion highlighted how formats such as FP4, INT4, and MX-based representations improve computational density, reduce memory traffic, and enable higher throughput across contemporary AI systems. However, these benefits do not arise solely from reducing numerical precision. Achieving efficient low-precision execution requires coordinated hardware mechanisms that manage quantization, arithmetic operations, data representation, accumulation accuracy, and compatibility with existing computational pipelines. Understanding how these formats function therefore requires examining the architectural techniques that allow low-bit representations to maintain useful computational accuracy while delivering substantial performance gains. Table 8.4-B1 explores these foundational mechanisms and illustrates how low-precision execution is translated into practical accelerator efficiency.

Core Mechanisms in AI Low-Precision Data Types

Table 8.4-B1 presents the principal architectural mechanisms that enable modern AI accelerators to execute low-precision workloads efficiently. These mechanisms form the foundation of contemporary numerical-computing strategies that prioritize computational density, memory efficiency, and energy-aware execution.

Historically, AI systems relied predominantly on full-precision floating-point arithmetic, using formats such as FP32 to perform neural-network computation. While these representations provided numerical flexibility and stability, they also required substantial memory resources, data movement bandwidth, and computational energy. As AI models continued to grow in size and complexity, full-precision computation increasingly became a limiting factor in system scalability.

The industry response has been the development of increasingly compact numerical formats,

including FP16, BF16, INT8, INT4, FP4, and emerging MX-family representations. These formats reduce storage requirements and enable more operations to be executed in parallel. However, low-precision computation introduces new challenges related to scaling, accumulation accuracy, numerical stability, and hardware compatibility.

The table identifies four key mechanisms that address these challenges: sub-byte quantization with ALU bit-width mapping, MX-format block scaling with shared exponent registers, mantissa-free integer execution with fixed-point accumulation, and mixed-precision execution with dynamic format emulation. Together, these mechanisms provide the infrastructure required to support efficient low-precision AI computation while preserving acceptable model performance.

By examining the relationship between numerical representation and hardware execution, the table demonstrates how low-precision computing has evolved into a sophisticated accelerator design strategy rather than a simple reduction in data precision.

Table 8.4-B1 — Core Mechanisms in AI Low-Precision Data Types

Mechanism	Primary Function	Hardware Alignment	Key Benefits
Sub-Byte Quantization & ALU Bit-Width Mapping	Compress parameters into 4-bit lanes	Maps 4-bit values directly onto SIMD/Tensor Core lanes	Higher parallelism, reduced register pressure
MX-Format Block Scaling with Shared Exponent Registers	Preserve dynamic range with minimal overhead	Shared exponent per block of mantissas	Lower memory footprint, stable scaling
Mantissa-Free Integer Units & Fixed-Point Accumulation	Execute integer paths without floating-point logic	Bit-shift accumulation arrays, integer ALUs	Ultra-low power, high-speed accumulation
Mixed-Precision Execution & Dynamic Format Emulation	Maintain accuracy while using low-precision formats	Compiler-driven casting to FP16/BF16	Numerical stability, compatibility with legacy hardware

Table 8.4-B1 demonstrates that low-precision AI execution depends upon far more than reducing the number of bits used to represent data. Effective low-precision systems require specialized hardware mechanisms that preserve accuracy, manage numerical range, and align computation with accelerator execution structures.

The mechanisms presented in the table reveal a common objective: increasing the amount of useful computation that can be performed within fixed memory, power, and bandwidth constraints without introducing unacceptable levels of numerical error.

The first mechanism identified in the table is **sub-byte quantization and ALU bit-width mapping**, which represents one of the most direct approaches to improving computational density.

Traditional processor architectures were designed around standard numerical widths such as 32-bit or 64-bit values. Modern AI accelerators increasingly support sub-byte formats, including 4-bit representations, allowing significantly larger numbers of parameters and activations to be stored within the same memory footprint.

The table highlights the direct mapping of 4-bit values onto SIMD and tensor-core execution lanes. This mapping enables many more arithmetic operations to be executed simultaneously than would be possible using higher-precision formats. The resulting increase in parallelism reduces pressure on register files, improves throughput, and allows accelerators to process larger workloads within fixed hardware resources.

An important consequence of this mechanism is that memory bandwidth requirements decline proportionally with representation size. Smaller numerical formats require fewer data transfers, helping alleviate one of the primary bottlenecks discussed throughout earlier discussions.

The second mechanism is **MX-format block scaling with shared exponent registers**, an emerging strategy for balancing low precision with numerical dynamic range.

One of the principal challenges associated with very small numerical formats is maintaining adequate representation across values that differ widely in magnitude. MX-style representations address this issue by assigning a shared exponent to a block of mantissas rather than storing an exponent for each individual value.

As indicated in the table, this approach reduces memory requirements while preserving useful dynamic-range properties. From a hardware perspective, shared exponents simplify data movement and storage while maintaining scalable numerical behavior. The result is a format that combines the efficiency of low-bit arithmetic with greater numerical flexibility than purely integer-based approaches.

The table next identifies **mantissa-free integer units and fixed-point accumulation**, which illustrate an alternative path toward low-precision acceleration.

Rather than relying on floating-point arithmetic, these architectures execute computations using integer representations and fixed-point accumulation structures. Integer arithmetic

generally requires fewer hardware resources, consumes less power, and supports highly efficient execution pipelines.

The alignment described in the table includes bit-shift accumulation arrays and specialized integer arithmetic units. Together, these structures support extremely fast execution while avoiding the complexity of floating-point logic. As a result, ultra-low-power inference becomes feasible even in constrained deployment environments such as embedded systems and edge AI platforms.

However, integer-only execution requires careful management of scaling factors and accumulation precision to prevent excessive numerical error, emphasizing the importance of hardware-assisted numerical control mechanisms.

The final mechanism presented in the table is **mixed-precision execution and dynamic format emulation**, which addresses the trade-off between efficiency and accuracy.

While low-precision formats provide substantial performance benefits, certain operations remain sensitive to numerical precision. Mixed-precision systems therefore execute different portions of a workload using different numerical representations.

The table identifies compiler-driven conversion mechanisms that dynamically cast values into formats such as FP16 or BF16 when higher precision is needed. This capability enables low-precision hardware to retain numerical stability while minimizing unnecessary computational expense.

An important benefit of mixed-precision execution is compatibility. Existing software ecosystems and model architectures can often be adapted to low-precision hardware without complete redesign. As a result, mixed-precision execution serves as a practical bridge between legacy computing paradigms and next-generation accelerator architectures.

A broader insight emerging from the table is that low-precision execution is fundamentally a systems-level optimization strategy. Reducing precision affects memory usage, bandwidth requirements, arithmetic throughput, energy consumption, and accelerator occupancy simultaneously. Consequently, low-precision formats influence nearly every aspect of AI-system performance.

The table also highlights the close relationship between numerical representation and hardware architecture. Quantization formats are increasingly designed alongside accelerator datapaths, tensor-core organizations, and memory hierarchies rather than being treated as purely mathematical abstractions.

From a systems-engineering perspective, the mechanisms summarized in the table address

complementary aspects of the same challenge. Sub-byte quantization increases density. Shared exponent structures preserve dynamic range. Integer execution improves efficiency. Mixed precision maintains accuracy. Together, these mechanisms create a balanced framework for efficient AI computation.

Another important observation is that many contemporary AI accelerators derive a substantial portion of their performance gains from low-precision computation rather than solely from increases in transistor count or operating frequency. Numerical optimization has therefore become a major driver of accelerator innovation.

Ultimately, Table 8.4-B1 demonstrates that low-precision AI execution is enabled by a collection of carefully coordinated hardware mechanisms. Through sub-byte quantization, shared exponent scaling, integer arithmetic, and mixed-precision execution strategies, modern accelerators dramatically increase computational density while reducing memory traffic, power consumption, and execution latency. These mechanisms provide a critical foundation for scaling future AI systems within realistic hardware and energy constraints.

Table 8.4-B1 introduced the core mechanisms that enable low-precision AI computation, including sub-byte quantization, MX-format scaling, integer-based accumulation, and mixed-precision execution. While each mechanism contributes independently to computational efficiency, modern AI accelerators derive their greatest benefits when these techniques operate as an integrated execution pipeline. Low-precision inference is not achieved merely by reducing numerical precision at a single stage of computation. Instead, data representations, scaling strategies, arithmetic units, accumulation structures, and precision-management policies work together to ensure that compressed numerical formats maintain sufficient accuracy while maximizing throughput. Figure 8.4-B1 illustrates this progression, tracing the flow of data from low-bit quantized representations through scaling, accumulation, and mixed-precision correction stages to produce high-throughput AI outputs.

Figure 8.4-B1 presents a conceptual execution pipeline for low-precision AI computation. The figure illustrates how modern accelerators transform compressed numerical representations into efficient inference operations while preserving sufficient numerical fidelity for practical AI workloads.

Contemporary AI systems increasingly rely on numerical formats significantly smaller than traditional floating-point representations. Formats such as FP4, INT4, and MX-family encodings reduce storage requirements and memory traffic, allowing hardware accelerators to process more data within fixed resource constraints. However, these benefits can be realized only through architectural mechanisms that compensate for the limitations of reduced precision.

The figure organizes low-precision execution into four major stages: sub-byte quantization and bit-width mapping, MX-format block scaling with shared exponents, mantissa-free integer execution with fixed-point accumulation, and mixed-precision execution with dynamic format emulation. Together, these stages form a coordinated computational pathway that balances efficiency and numerical stability.

By visualizing these mechanisms as an integrated pipeline, the figure demonstrates how modern AI hardware converts aggressive numerical compression into practical high-performance execution.

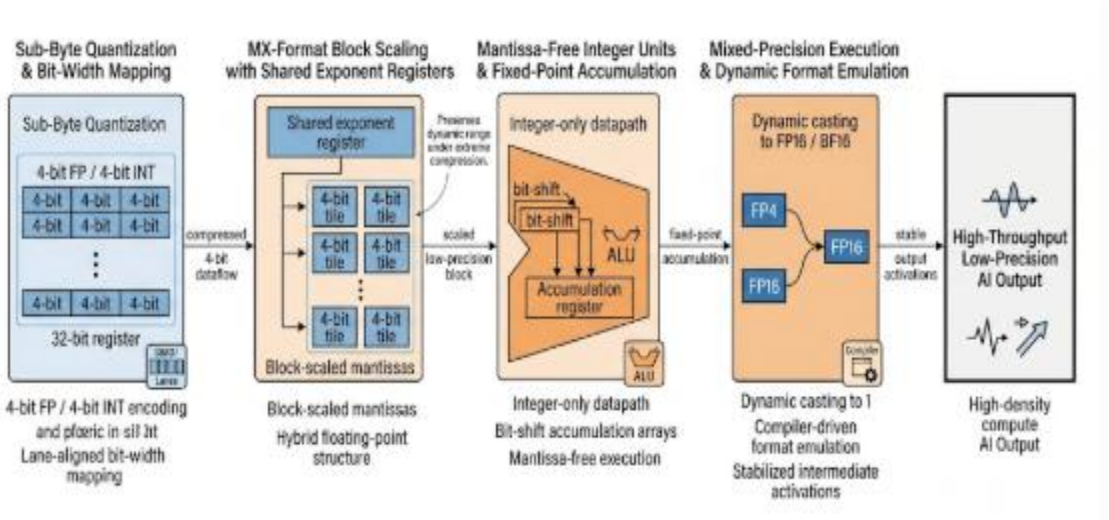


Figure 8.4-B1 — AI Low-Precision Execution Pipeline
Multi-stage computational workflow illustrating how low-precision numerical formats are transformed into efficient AI inference operations. The figure traces the progression from sub-byte quantization through MX-format scaling, integer-based accumulation, and mixed-precision stabilization. The pipeline demonstrates how AI accelerators balance computational density, memory efficiency, throughput, and numerical reliability while executing low-bit workloads.

Legend

Component	Description
Sub-Byte Quantization & Bit-Width Mapping	Initial stage converting model parameters and activations into low-bit numerical formats.
4-Bit FP4 / 4-Bit INT Encoding	Compact numerical representations used to reduce storage and bandwidth requirements.

Lane-Aligned Bit-Width Mapping	Direct mapping of low-bit values onto SIMD and tensor-core execution lanes.
Compressed Dataflow	Reduced-bandwidth representation transferred between pipeline stages.
MX-Format Block Scaling with Shared Exponent Registers	Mechanism preserving dynamic range in low-precision computations.
Shared Exponent Register	Common exponent applied across blocks of mantissas.
4-Bit Tiles	Block-organized low-precision numerical groups.
Block-Scaled Mantissas	Mantissa values sharing a common scaling factor.
Hybrid Floating-Point Structure	Low-precision numerical representation combining compression and dynamic range.
Mantissa-Free Integer Units & Fixed-Point Accumulation	Arithmetic stage executing integer operations efficiently.
Integer-Only Datapath	Computation path avoiding floating-point arithmetic.
Bit-Shift Accumulation Arrays	Hardware structures supporting fixed-point accumulation.
Accumulator Register	Register storing partial and final accumulation results.
Quantized ALU	Integer arithmetic unit performing low-bit operations.
Mixed-Precision Execution & Dynamic Format Emulation	Numerical-stabilization layer introducing higher precision where required.
Dynamic Casting to FP16/BF16	Conversion mechanism supporting selective precision enhancement.
FP4 / FP16 / BF16 Formats	Numerical representations participating in mixed-precision execution.

Compiler-Controlled Format Selection	Adaptive precision-management strategy.
Stable Activations	Accuracy-preserving output of the mixed-precision stage.
High-Throughput Low-Precision AI Output	Final AI output generated through efficient low-bit computation.
High-Density Compute Output	Optimized result balancing throughput and accuracy.

Figure 8.4-B1 illustrates that low-precision AI execution is not simply a matter of reducing numerical precision. Rather, it is a carefully coordinated process in which quantization, scaling, arithmetic execution, accumulation, and precision correction operate together to maximize computational efficiency while controlling numerical error.

The figure demonstrates how modern accelerators treat numerical representation as an active design variable, allowing hardware resources to be used more efficiently without sacrificing practical model performance.

The pipeline begins with **sub-byte quantization and bit-width mapping**, the stage responsible for compressing numerical representations into highly compact formats.

Traditionally, AI models relied on FP32 arithmetic, which stores each value using thirty-two bits. The figure illustrates a substantially more compact approach in which values are represented using FP4 or INT4 encodings. Multiple low-bit values can therefore occupy the space previously required for a single full-precision value.

A key feature of this stage is lane-aligned mapping. Rather than treating low-bit values as software abstractions, the architecture maps them directly onto tensor-core and SIMD execution lanes. This alignment allows processors to execute a larger number of operations in parallel while simultaneously reducing register pressure and memory-transfer requirements.

After quantization, the compressed numerical representation enters the **MX-format block-scaling stage**.

One of the primary challenges of low-precision arithmetic is maintaining numerical range. Very small representations often struggle to represent values that vary significantly in magnitude. The figure addresses this issue through the use of shared exponent registers applied to groups

of low-precision values.

Block-scaled mantissas preserve much of the dynamic range associated with floating-point arithmetic while reducing storage costs substantially. By sharing a single exponent among multiple values, numerical efficiency increases without completely sacrificing representational flexibility.

This stage highlights an important principle of low-precision design: reducing bit width alone is insufficient. Effective low-precision systems must also address scaling behavior and dynamic-range preservation.

The next stage is **mantissa-free integer execution and fixed-point accumulation**.

Here, arithmetic operations are performed using integer-only datapaths rather than conventional floating-point units. Integer computation requires fewer hardware resources and generally consumes less energy than floating-point computation.

The figure depicts bit-shift accumulation arrays and accumulator registers supporting this process. Rather than relying on floating-point normalization and mantissa handling, fixed-point accumulation structures maintain numerical values using highly efficient integer operations.

This design produces exceptionally high throughput because arithmetic units remain simple and densely packed. At the same time, careful accumulation management prevents excessive precision loss during repeated operations.

The pipeline then transitions into **mixed-precision execution and dynamic format emulation**, which serves as a numerical-stability layer.

Although low-bit arithmetic provides significant efficiency benefits, certain operations remain sensitive to precision limitations. The figure illustrates dynamic casting between FP4, FP16, and BF16 representations, allowing selected computations to execute at higher precision when necessary.

Compiler-controlled format management determines when precision enhancement should occur. Rather than executing all operations at a higher precision level, the system selectively increases numerical resolution only for sensitive calculations.

The result is the generation of stable activations that retain much of the accuracy associated with larger numerical formats while preserving the efficiency benefits of low-precision execution.

The pipeline concludes with the production of **high-throughput low-precision AI outputs**.

By this stage, numerical representations have passed through compression, scaling, accumulation, and stabilization phases. The resulting outputs maintain sufficient numerical quality for AI inference while benefiting from dramatically reduced bandwidth, memory consumption, and arithmetic cost.

A broader insight emerging from the figure is that low-precision execution represents a sequence of compensating mechanisms rather than a single optimization. Quantization introduces efficiency. Block scaling preserves dynamic range. Integer execution improves throughput. Mixed precision restores stability. Each stage addresses limitations introduced by preceding stages.

The figure also highlights the relationship between hardware design and numerical representation. Every stage is explicitly aligned with accelerator structures such as tensor-core lanes, register files, integer arithmetic units, and compiler-controlled execution pathways. This alignment demonstrates how numerical formats and hardware architectures increasingly evolve together.

From a systems-engineering perspective, the pipeline provides a framework for understanding why low-precision computing has become central to modern AI acceleration. Reducing numerical precision affects memory capacity, bandwidth utilization, arithmetic throughput, energy consumption, and accelerator occupancy simultaneously. Consequently, low-precision execution produces benefits across the entire computing stack.

Another important observation is that low-precision execution does not eliminate the need for numerical accuracy. Instead, it manages precision strategically by allocating higher-precision resources only where they provide meaningful value. This selective approach enables substantial efficiency improvements without requiring universal precision reduction.

Ultimately, Figure 8.4-B1 demonstrates how modern AI accelerators transform compressed numerical formats into reliable computational results through a carefully staged execution pipeline. Through sub-byte quantization, shared-exponent scaling, integer-based arithmetic, and mixed-precision stabilization, low-precision systems achieve high throughput, reduced memory traffic, lower energy consumption, and scalable AI execution while maintaining the numerical reliability required for advanced machine-learning workloads.

Figure 8.4-B1 presents low-precision execution as a coordinated computational pipeline in which numerical compression, scaling, accumulation, and precision management operate together to maximize hardware efficiency. At the foundation of this pipeline lies **sub-byte quantization and ALU bit-width mapping**, the stage responsible for transforming high-precision model parameters and activations into compact numerical representations aligned with

accelerator execution hardware. This step serves as the entry point for all subsequent low-precision processing. Before MX-format scaling can preserve dynamic range, before integer-only datapaths can accelerate arithmetic execution, and before mixed-precision mechanisms can selectively restore numerical stability, data must first be encoded into formats that match the physical organization of SIMD lanes, tensor-core tiles, and register structures. The efficiency achieved throughout the remainder of the pipeline therefore depends directly on how effectively these compressed representations are packed, scheduled, and mapped onto available hardware resources. The following discussion examines **Sub-Byte AI Quantization and ALU Bit-Width Mapping** in detail, exploring how FP4, INT4, and related low-bit formats are encoded and aligned with accelerator datapaths to increase parallelism, reduce memory traffic, and establish the computational density that underpins modern low-precision AI execution.

i. Sub-Byte AI Quantization and ALU Bit-Width Mapping

Sub-Byte AI Quantization and ALU Bit-Width Mapping represents a foundational hardware–software co-design paradigm that enables modern accelerators to execute large-scale neural workloads under extreme memory, bandwidth, and power constraints. In contemporary AI systems—where transformer blocks, attention heads, and feed-forward layers routinely exceed billions of parameters—the numerical width of each value directly determines how much computation, memory traffic, and energy the accelerator must expend per inference step. Traditional FP16 and INT8 formats, while efficient relative to FP32, still impose substantial pressure on memory buses, register files, and execution pipelines when scaled across massive tensor graphs.

Sub-byte quantization resolves these bottlenecks by compressing neural weights, activations, and intermediate tensors into ultra-dense 2-bit and 4-bit encodings that align directly with the physical geometry of SIMD lanes and tensor-core datapaths. Instead of treating arithmetic lanes as fixed-width structures, the accelerator splits and repurposes them into multiple low-precision fragments, allowing several independent multiply-accumulate operations to execute concurrently within the silicon footprint of a single traditional lane. This transforms the processor into a highly concentrated, ultra-high-throughput vector engine capable of sustaining the arithmetic intensity required by modern AI workloads.

From an AI-centric perspective, sub-byte quantization is not merely a numerical compression technique—it is a structural redefinition of how neural computation is expressed at the hardware level. By packing multiple FP4 or INT4 values into standard register widths, the accelerator increases operand density, reduces memory traffic, and enables more tokens, heads, or channels to be processed per cycle. This is especially critical for attention mechanisms, expert routing layers, and large feed-forward blocks, where compute demand

scales superlinearly with model width and sequence length.

A complete technical analysis must examine how compilers and hardware jointly enforce alignment between these compressed formats and the ALU's physical bit boundaries. Sub-byte values must be unpacked, sign-extended, shifted, and routed through custom logic networks that preserve numerical correctness while maintaining deterministic timing. This introduces microarchitectural overhead—bit-shifting fabrics, localized unpacking units, and precision-aware lane schedulers—but the resulting gains in compute density and memory efficiency far outweigh these costs.

Ultimately, mastering sub-byte quantization requires integrating these physical mapping primitives into AI-specific tensor compilation frameworks. Neural graph compilers must schedule quantization, packing, and ALU mapping in a way that aligns perfectly with vector lane widths, prevents register-shuffling hazards, and avoids execution stalls. When executed correctly, sub-byte quantization delivers massive throughput improvements without catastrophic accuracy degradation, enabling next-generation AI accelerators to sustain real-time inference even under extreme model scales.

Once sub-byte quantization has compacted neural parameters into tightly packed 2-bit and 4-bit encodings aligned with ALU bit-widths, the next challenge is preserving dynamic range without reintroducing the overhead of full floating-point formats. Ultra-low-precision mantissas alone cannot represent the wide activation and weight distributions found in large transformer blocks, attention heads, and feed-forward layers. To maintain numerical expressiveness under extreme compression, accelerators employ MX-format block scaling—a technique that shares a single exponent across a small group of low-precision mantissas. This shared-exponent structure acts as a lightweight floating-point scaffold around sub-byte values, enabling them to span broader ranges while retaining their compact physical footprint. The next discussion explores how MX-format scaling integrates with quantized data layouts, how shared exponents are stored and updated, and how this hybrid representation allows low-precision AI workloads to remain both memory-efficient and numerically stable at scale.

ii. MX-Format Block Scaling with Shared AI Exponent Registers

MX-Format Block Scaling with Shared AI Exponent Registers represents a pivotal hardware–software co-design strategy that allows ultra-low-precision AI workloads to retain wide dynamic range while operating within aggressively compressed numerical formats. As modern deep learning systems adopt FP4, INT4, and other narrow mantissa encodings to reduce memory footprint and increase compute density, the absence of per-value exponents becomes a critical limitation. Without a mechanism to scale these compact mantissas, neural activations and

weights would frequently underflow or overflow—especially in transformer attention layers, feed-forward expansions, and high-variance expert routing paths.

MX-format scaling resolves this challenge by grouping a small vector segment of low-precision mantissas into a shared floating-point block and assigning them to a single, higher-precision exponent register. Instead of dedicating exponent bits to every individual value—a practice that wastes memory and undermines the benefits of sub-byte quantization—the MX specification treats the exponent as a structural property of a local tile. This shared-exponent architecture preserves the expressive mathematical range of floating-point arithmetic while maintaining the compact storage footprint of 4-bit and 6-bit mantissas. It is a hybrid numerical structure designed explicitly for AI workloads, where dynamic range must be preserved even when precision is aggressively compressed.

From an AI-centric perspective, MX-format scaling is essential for stabilizing large transformer workloads. Attention score distributions, softmax outputs, and residual pathways often span several orders of magnitude; without block-level scaling, low-precision mantissas would collapse these distributions and degrade model fidelity. By computing block-level maximums and dynamically adjusting the shared exponent, the accelerator ensures that each mantissa operates within an appropriate numerical window, preventing saturation and preserving gradient-like behavior during inference.

Technically, MX-format scaling requires specialized microarchitectural units capable of performing real-time exponent selection, mantissa normalization, and fused scaling operations. These units must integrate seamlessly with vector lanes, tensor-core tiles, and register banks to avoid execution hazards. The microarchitectural overhead—dynamic exponent computation, block-level reduction operations, and fused scaling logic—is offset by massive reductions in memory traffic and silicon area compared to traditional floating-point formats.

Mastering MX-format scaling requires deep integration with AI-specific compiler kernels. Neural graph compilers must align block boundaries with vector processing lanes, schedule exponent updates deterministically, and ensure that shared-exponent registers synchronize with quantized data layouts. When executed correctly, MX-format scaling enables ultra-low-precision AI workloads to maintain numerical stability, avoid catastrophic precision loss, and operate efficiently across large-scale transformer and MoE architectures.

Once MX-format scaling has established a stable numerical window for ultra-low-precision mantissas, the accelerator can transition from floating-point scaffolding to pure integer arithmetic. At this stage, the shared exponent has already normalized the mantissas, allowing the hardware to discard floating-point logic entirely and route the values through lightweight

integer datapaths optimized for bit-shifted accumulation. This shift marks a fundamental transformation in how AI workloads are executed: instead of relying on expensive floating-point units, the accelerator performs dense matrix multiplications using mantissa-free integer units that deliver higher throughput, lower latency, and dramatically reduced power consumption. The next topic explores how these integer units operate, how fixed-point accumulation arrays maintain deterministic timing under extreme compression, and how this stage integrates seamlessly into the broader low-precision execution pipeline.

iii. Mantissa-Free AI Integer Units and Fixed-Point Accumulation

Mantissa-Free AI Integer Units and Fixed-Point Accumulation represent a critical hardware–software co-design paradigm that replaces floating-point arithmetic with uniform integer-only representations to maximize silicon throughput and eliminate the area, latency, and power overhead associated with mantissa alignment and exponent normalization. In large-scale AI accelerators—especially those deployed in edge environments or thermally constrained inference systems—floating-point MAC loops impose significant microarchitectural complexity. Aligning mantissas, matching exponents, and normalizing intermediate results all require wide datapaths, deep pipeline stages, and high-power arithmetic units. These operations become a dominant bottleneck when executing massive matrix multiplications across transformer blocks, attention heads, and feed-forward expansions.

This optimization technique resolves these constraints by stripping away floating-point mantissa processing entirely and converting neural activations and weights into clean, scale-adjusted integer representations. Once MX-format scaling has established a stable shared exponent for a block of low-precision mantissas, the accelerator can discard floating-point logic and route the scaled values through lightweight integer datapaths. These datapaths rely on bit-shifted arithmetic rather than mantissa normalization, enabling rapid fixed-point accumulation using compact, low-latency hardware units. Packed integers flow directly into fixed-point accumulation arrays—often 32-bit or 48-bit registers—where raw summations are performed at high speed without the overhead of floating-point pipelines.

A complete technical evaluation of this technique requires understanding how compiler frameworks and digital logic circuits jointly prevent precision loss and overflow during integer-only execution. Neural graph compilers must track static or dynamic quantization scale factors, propagate them through tensor graphs, and ensure that integer operations map cleanly onto high-precision accumulation registers. Hardware designers must implement bit-shift networks, saturation logic, and overflow guards that preserve numerical correctness while maintaining deterministic timing. The microarchitectural overhead of managing scale factors offline is far outweighed by the reductions in silicon area, gate count, and energy per instruction

achieved inside the execution core.

Mastering mantissa-free integer execution requires aligning integer layout configurations with vector lane geometry, ensuring that packed integer values flow through the accelerator without pipeline hazards or register-shuffling penalties. When properly integrated into deep learning compilers and spatial architectures, integer-only execution delivers massive throughput improvements while maintaining accuracy under extreme precision compression. It transforms the accelerator into a high-density, low-power math engine capable of sustaining real-time inference across large transformer and MoE workloads.

With integer-only datapaths providing high-speed fixed-point accumulation, the final challenge in the low-precision pipeline is ensuring that aggressively compressed values do not destabilize the broader neural computation. Even with MX-format scaling and fixed-point accumulation, certain operations—such as attention softmax, residual additions, and normalization layers—require higher precision to maintain numerical fidelity. Mixed-precision execution and dynamic format emulation address this need by selectively casting intermediate values to FP16 or BF16 and emulating low-precision formats on hardware that lacks native FP4 or INT4 support. This final stage closes the loop between extreme compression and numerical stability, enabling ultra-low-precision accelerators to execute large-scale AI models without sacrificing accuracy or convergence behavior.

iv. Mixed-Precision AI Execution and Dynamic Format Emulation

Mixed-Precision AI Execution and Dynamic Format Emulation represent a critical hardware–software co-design paradigm that enables accelerators to adapt numerical precision in real time, preserving model accuracy while exploiting the throughput advantages of ultra-low-precision arithmetic. Enforcing a uniform 4-bit or 6-bit precision across an entire neural network is rarely viable; sensitive layers such as attention softmax, normalization, and residual pathways require wider numerical formats to maintain stability. At the same time, much of the deployed hardware ecosystem lacks native support for emerging sub-byte formats like FP4, INT4, or MX-encoded mantissas. Mixed-precision execution resolves these constraints by dynamically casting selected tensors to FP16 or BF16 when higher precision is needed, while executing less sensitive layers in aggressively compressed formats. This adaptive precision strategy allows large transformer and MoE workloads to retain convergence behavior even when most of the computation is performed at ultra-low precision.

Dynamic format emulation extends this capability to legacy hardware by synthesizing low-precision operations through compiler-driven instruction sequences. When an accelerator lacks native FP4 or MX-format datapaths, the compiler constructs these formats using register

masks, bitwise manipulation loops, and synthetic arithmetic patterns that mimic the behavior of sub-byte instructions. This transforms rigid, fixed-format hardware into a flexible multi-precision execution engine capable of running next-generation quantization schemes on existing enterprise systems. The result is a unified execution environment where precision becomes a software-defined attribute rather than a fixed hardware constraint.

A complete technical evaluation of mixed-precision execution requires understanding how low-level drivers and optimizing compilers bypass hardware format limitations by mapping un-native sub-byte tensor structures onto native vector ALUs. This involves injecting dynamic unpacking routines, format-casting instructions, and real-time scaling operations into the execution pipeline. Although these transformations introduce microarchitectural overhead, the benefits—reduced memory bandwidth, improved compute density, and immediate deployability across diverse hardware generations—far outweigh the costs. Runtime frameworks must synchronize these conversion boundaries with active compute threads, ensuring that casting operations do not trigger register spills, pipeline stalls, or accuracy degradation. When properly integrated, mixed-precision execution enables ultra-low-precision inference to operate reliably across heterogeneous hardware environments while preserving the numerical fidelity required by large-scale AI models.

Low-precision formats such as FP4, INT4, and MX-encoded blocks dramatically increase compute density, but their full performance potential is unlocked only when the accelerator can schedule, route, and retire these compressed values without stalls or synchronization barriers. After parameters have been quantized, block-scaled, accumulated, and stabilized—as shown in Table 4.10-115 and Figure 4.10-99—the next challenge is ensuring that these ultra-compact data streams move through SIMD lanes, tensor cores, and memory hierarchies with cycle-level precision. This requires on-chip schedulers capable of fusing kernels, reordering tensor flows, issuing asynchronous vector operations, and overlapping compute with memory transfers to prevent idle cycles. The next topic, **On-Chip AI Schedulers and Asynchronous Vector Execution Pipelines**, examines how modern accelerators orchestrate this flow, transforming low-precision arithmetic from a numerical optimization into a fully synchronized, high-throughput execution environment that sustains large-scale AI workloads.

b. On-Chip AI Schedulers and Asynchronous Vector Execution Pipelines

On-Chip AI Schedulers and Asynchronous Vector Execution Pipelines represent one of the most strategically important hardware–software co-design paradigms in modern accelerator architecture. They enforce dynamic workload orchestration, fine-grained thread control, and cycle-accurate vector dispatching to maximize compute utilization, reduce pipeline stalls, and eliminate synchronization bottlenecks in large-scale AI systems. As transformer models expand

to thousands of layers and sequence lengths stretch into the tens of thousands, traditional synchronous scheduling approaches impose prohibitive latency, underutilize vector lanes, and create memory-hierarchy choke points. Asynchronous scheduling resolves these physical scaling limits by enabling independent workgroups, speculative token dispatch, and out-of-order vector execution that keeps the accelerator saturated even under irregular or conditional graph workloads.

Modern AI workloads introduce highly variable compute patterns—dynamic attention windows, conditional MoE routing, ragged sequence boundaries, and token-dependent branching—that cannot be efficiently executed using rigid, lock-step scheduling. On-chip schedulers address this challenge by continuously analyzing tensor dependencies, issuing vector operations opportunistically, and overlapping memory transfers with compute at cycle-level granularity. They transform the accelerator from a static SIMD engine into a fluid, latency-tolerant execution fabric capable of sustaining high throughput even when the underlying neural graph exhibits unpredictable structure.

This scheduling paradigm spans a spectrum of execution strategies. Variable-length input dispatching ensures that ragged batches and uneven token counts do not stall vector lanes. Asynchronous workgroup scheduling allows independent compute groups to progress without waiting for global synchronization barriers. Speculative token scheduling predicts future execution paths and pre-loads register states to avoid starvation during conditional graph traversal. Warp-level thread optimization restructures execution at the granularity of individual vector lanes, ensuring that divergent control flow does not collapse parallelism. Together, these mechanisms form a unified orchestration layer that keeps the accelerator fully utilized, minimizes idle cycles, and maintains deterministic timing across massive AI workloads.

A complete technical evaluation of on-chip scheduling requires understanding how hardware schedulers, compiler runtimes, and vector pipelines cooperate to bypass dependency hazards and memory-latency bottlenecks. Schedulers must track tensor readiness, reorder instruction streams, and manage register allocation dynamically while avoiding deadlocks and race conditions. Compiler frameworks must generate dependency graphs, annotate asynchronous boundaries, and fuse kernels to maximize locality. Vector pipelines must support out-of-order execution, rollback mechanisms, and warp-level divergence handling without compromising correctness. When properly integrated, these scheduling techniques deliver substantial improvements in throughput, latency, and energy efficiency—making asynchronous vector execution a cornerstone of scalable AI deployment.

On-chip scheduling introduces a radically different execution environment for AI accelerators—one where workgroups progress independently, vector lanes operate out of order, speculative

dispatch hides latency, and warp-level optimization ensures parallelism even under irregular control flow. These mechanisms operate together, not in isolation. To understand how they collectively reshape compute utilization, memory-hierarchy behavior, and execution throughput, it is useful to view them as a unified orchestration framework. Table 4.10-116 organizes these mechanisms into their core functional dimensions, clarifying how each contributes to the broader goal of sustaining high-performance AI inference under dynamic and irregular workloads.

- **Variable-Length AI Input Dispatching and Pipeline Stall Control** — Dynamically routes ragged batches, uneven token counts, and irregular sequence lengths into vector lanes without triggering stall cycles, ensuring that SIMD and tensor-core pipelines remain saturated even under non-uniform AI workloads.
- **Asynchronous AI Workgroup Scheduling and Out-of-Order Vector Execution** — Allows independent compute groups to progress without global synchronization barriers, issuing vector operations opportunistically and reordering tensor flows to maximize utilization and hide memory latency.
- **Speculative AI Token Scheduling and Register Rollback Mechanisms** — Predicts future execution paths in conditional or branching neural graphs, pre-loads register states, and uses rollback logic to recover from mis-speculation, preventing starvation and maintaining throughput during dynamic token-dependent execution.
- **Warp-Level AI Thread Optimization for Conditional Graph Execution** — Restructures execution at the granularity of individual vector lanes, mitigating warp divergence caused by attention masks, MoE routing, or conditional branches, and preserving parallelism even when control flow becomes irregular.

AI accelerators increasingly rely on asynchronous scheduling to meet the demands of large-scale inference. These techniques transform execution pipelines into adaptive, latency-tolerant systems that align directly with the irregular structure of modern neural graphs. The mechanisms summarized here capture the foundational strategies that make this orchestration viable: variable-length dispatching that prevents ragged-batch stalls, asynchronous workgroup scheduling that eliminates global barriers, speculative token scheduling that hides latency, and warp-level thread optimization that preserves parallelism under divergence. Together, these mechanisms define the hardware blueprint for executing massive models within strict latency, bandwidth, and power envelopes.

Once the architectural foundations of on-chip scheduling have been established—variable-length dispatching, asynchronous workgroup progression, speculative token execution,

and warp-level divergence control—it becomes essential to organize these mechanisms into a coherent framework that clarifies their functional roles within the accelerator. Each mechanism addresses a different bottleneck in modern AI workloads, from ragged sequence boundaries to conditional graph traversal, and together they form the orchestration layer that keeps vector lanes saturated under dynamic execution conditions. The following table summarizes these core mechanisms, mapping each to its optimization target and architectural benefit, and providing a structured reference for understanding how asynchronous scheduling transforms irregular neural graphs into high-throughput execution pipelines.

Table 8.4-B1 examined how low-precision numerical formats increase computational density by reducing memory requirements, bandwidth consumption, and arithmetic complexity. However, numerical compression alone cannot guarantee high accelerator utilization. Even highly optimized low-precision workloads may fail to achieve peak throughput if execution pipelines experience stalls, synchronization delays, resource contention, or inefficient scheduling behavior. As modern AI architectures increasingly incorporate dynamic sequence lengths, sparse routing decisions, conditional execution pathways, and irregular computational graphs, efficient execution depends not only on how data are represented but also on how computation is orchestrated across processing resources. This challenge has elevated on-chip scheduling and asynchronous execution mechanisms into central components of contemporary AI accelerator design. Table 8.4-B2 examines the core mechanisms that enable modern accelerators to maintain throughput under irregular workloads by dynamically coordinating tensor movement, vector execution, pipeline utilization, and control-flow management.

Table 8.4-B2 presents the principal hardware mechanisms that govern scheduling, dispatch, synchronization, and execution management within modern AI accelerators. These mechanisms form the control infrastructure responsible for ensuring that computational resources remain active and productive despite the increasingly dynamic behavior of contemporary AI workloads.

Traditional processor scheduling models were developed primarily for predictable computational tasks with relatively stable execution patterns. By contrast, modern AI systems frequently operate on irregular workloads characterized by variable sequence lengths, sparse expert routing decisions, conditional execution paths, attention masks, and dynamically changing tensor dimensions. These characteristics introduce execution variability that can reduce hardware utilization if not managed carefully.

To address these challenges, advanced accelerators incorporate specialized scheduling architectures capable of adapting execution behavior in real time. The table identifies four representative mechanisms: variable-length input dispatching with pipeline stall control, asynchronous workgroup scheduling with out-of-order vector execution, speculative token

scheduling with register rollback mechanisms, and warp-level thread optimization for conditional graph execution.

Together, these mechanisms enable accelerators to maintain high throughput, minimize idle cycles, hide memory latency, and preserve efficient vector utilization even when confronted with complex and highly irregular AI workloads.

By examining the interaction between scheduling intelligence and hardware execution resources, the table highlights the increasingly important role of accelerator control architectures in sustaining performance at scale.

Table 8.4-B2 — Core Mechanisms in On-Chip AI Schedulers and Asynchronous Vector Execution Pipelines

Mechanism	Functional Role	Primary Optimization Target	Key Architectural Benefit
Variable-Length AI Input Dispatching and Pipeline Stall Control	Dynamically routes ragged batches, uneven token counts, and irregular sequence lengths into vector lanes without stalling pipelines.	Eliminates stall cycles caused by non-uniform tensor shapes and irregular sequence boundaries.	Maintains full SIMD/tensor-core saturation under variable-length workloads.
Asynchronous AI Workgroup Scheduling and Out-of-Order Vector Execution	Allows independent compute groups to progress without global synchronization barriers; issues vector operations opportunistically.	Hides memory latency and bypasses dependency bottlenecks.	Maximizes utilization by enabling continuous, out-of-order vector execution.
Speculative AI Token Scheduling and Register Rollback Mechanisms	Predicts future execution paths in conditional or branching neural graphs; pre-loads register states and rolls back on mis-speculation.	Prevents starvation and latency stalls during dynamic token-dependent execution.	Preserves throughput under conditional graph traversal and irregular control flow.
Warp-Level AI Thread	Restructures execution at the granularity of	Reduces performance collapse caused by	Maintains parallelism and deterministic

Mechanism	Functional Role	Primary Optimization Target	Key Architectural Benefit
Optimization for Conditional Graph Execution	individual vector lanes to mitigate warp divergence.	divergent control flow (MoE routing, attention masks).	timing even when execution paths diverge.

Table 8.4-B2 demonstrates that modern AI accelerator performance depends not only on arithmetic capability but also on the ability to coordinate computation efficiently across thousands of concurrent execution units. As AI models become more dynamic, hardware utilization increasingly depends on scheduling intelligence rather than raw computational throughput alone.

The mechanisms summarized in the table reveal a common objective: eliminating execution inefficiencies caused by irregular control flow, nonuniform tensor structures, synchronization bottlenecks, and workload imbalance. Through adaptive scheduling and asynchronous execution, accelerators preserve high utilization even under highly variable computational conditions.

The first mechanism identified in the table is **variable-length AI input dispatching and pipeline stall control**. This capability addresses one of the most common challenges in modern AI workloads: the presence of nonuniform tensor dimensions and variable-length sequences.

In many AI systems, particularly large language models and event-driven architectures, input sequences vary significantly in length. If hardware pipelines process these sequences naively, shorter sequences may complete early while longer sequences continue executing, creating idle execution lanes and reducing overall throughput.

The dispatching mechanisms described in the table dynamically route irregular workloads into vectorized execution pipelines in ways that minimize idle resources. By controlling how tensors enter execution units and managing boundary conditions intelligently, these mechanisms reduce pipeline stalls and maintain accelerator saturation even when input dimensions vary substantially.

The second mechanism is **asynchronous AI workgroup scheduling and out-of-order vector execution**.

Traditional synchronous scheduling often forces computational resources to wait for slower operations to complete before additional work can proceed. This approach simplifies control logic but can significantly reduce utilization when workloads exhibit uneven execution times.

Asynchronous scheduling addresses this limitation by allowing independent computational groups to advance without global synchronization barriers. The table highlights opportunistic execution and out-of-order scheduling as key strategies for exploiting available computational resources. By hiding memory latency and bypassing dependency bottlenecks where possible, these mechanisms ensure continuous hardware activity even when portions of the workload become temporarily stalled.

This capability is particularly important for bandwidth-intensive AI workloads where data availability often fluctuates across execution units.

The third mechanism identified is **speculative AI token scheduling and register rollback mechanisms**.

Conditional-computation architectures and dynamically routed neural networks frequently create uncertainty regarding future execution paths. Waiting until all routing decisions become known may introduce substantial latency and leave hardware resources underutilized.

Speculative scheduling addresses this challenge by predicting likely execution paths and preloading relevant data into registers before final execution decisions are confirmed. The table emphasizes rollback mechanisms that restore correct system state when predictions prove inaccurate.

Although speculative execution introduces additional control complexity, it allows accelerators to avoid latency stalls associated with conditional execution. As a result, throughput remains high even for workloads exhibiting unpredictable branching behavior.

The fourth mechanism is **warp-level AI thread optimization for conditional graph execution**.

Modern AI accelerators often rely on SIMD and SIMT execution models in which groups of threads execute instructions simultaneously. Conditional-computation models, sparse routing architectures, and masked attention mechanisms can cause different execution lanes to follow different control paths, creating divergence.

The table identifies thread-level restructuring strategies that reorganize execution groups to mitigate this problem. By maintaining alignment among execution lanes and reducing divergence-related inefficiencies, warp-level optimization preserves parallelism and prevents throughput degradation.

This capability is particularly valuable in mixture-of-experts architectures and dynamically routed models where execution patterns may differ significantly across tokens.

A broader insight emerging from the table is that scheduling intelligence has become

increasingly important as AI architectures grow more adaptive. Earlier neural networks generally followed static execution pathways. Contemporary models frequently make runtime decisions regarding routing, attention allocation, memory access, and computational activation. Scheduling systems must therefore adapt continuously to changing execution conditions.

The table also highlights a fundamental shift in accelerator design philosophy. Historically, performance improvements were driven primarily by larger arithmetic units and higher clock frequencies. Modern accelerators increasingly derive performance from sophisticated execution orchestration mechanisms that maximize utilization of existing computational resources.

From a systems-engineering perspective, the mechanisms described in the table operate at different levels of execution management but pursue a shared objective. Variable-length dispatching addresses workload irregularity. Asynchronous scheduling mitigates synchronization delays. Speculative execution reduces conditional latency. Warp-level optimization controls divergence. Together, these techniques maintain steady throughput despite highly dynamic computational behavior.

Another important observation is that these mechanisms directly support many of the model architectures discussed earlier in Section 8.4. Conditional-computation networks, sparse-expert systems, long-context processing architectures, and state-space models all generate irregular execution patterns that benefit from intelligent scheduling.

The table further demonstrates that efficient execution increasingly depends on the ability to predict, reorganize, and adapt computational workflows proactively rather than merely executing instructions reactively.

Ultimately, Table 8.4-B2 illustrates that on-chip scheduling and asynchronous vector execution represent essential components of modern AI accelerators. Through intelligent dispatching, out-of-order execution, speculative scheduling, and divergence-aware thread management, these architectures minimize idle cycles, hide latency, and preserve high hardware utilization under complex real-world workloads. As AI systems continue to adopt increasingly dynamic execution models, such scheduling mechanisms will play an increasingly important role in sustaining efficient and scalable accelerator performance.

Table 8.4-B2 identified the primary scheduling and execution-control mechanisms that enable modern AI accelerators to maintain utilization under irregular workloads, including variable-length dispatching, asynchronous workgroup progression, speculative token scheduling, and warp-level divergence management. While the table examined these mechanisms individually, practical accelerator performance emerges from their coordinated operation within a unified execution pipeline. Modern AI hardware must continuously manage irregular tensor shapes,

conditional execution paths, dynamic routing decisions, and memory-latency variations without allowing computational resources to remain idle. Figure 8.4-B2 illustrates how these scheduling mechanisms interact sequentially to transform an irregular neural-graph workload into a fully utilized stream of vectorized operations, ultimately delivering deterministic, high-throughput execution across SIMD and tensor-core resources.

Figure 8.4-B2 presents a systems-level view of the scheduling infrastructure that governs execution within modern AI accelerators. The figure traces the progression of a workload from arrival at the neural-graph input stage through multiple layers of scheduling, prediction, optimization, and execution management before reaching hardware compute units.

As AI models become increasingly dynamic, execution pipelines must accommodate variable-length sequences, sparse expert routing, conditional-computation graphs, attention masks, and other forms of runtime variability. These characteristics create challenges that cannot be addressed through arithmetic throughput alone. High-performance accelerators therefore incorporate sophisticated scheduling architectures designed to maintain hardware utilization even when workloads exhibit irregular structure and unpredictable behavior.

The figure organizes this process into four scheduling layers: variable-length input dispatching and pipeline stall control, asynchronous workgroup scheduling, speculative token scheduling, and warp-level thread optimization. Each stage removes a specific class of execution inefficiency before computation reaches SIMD lanes and tensor-core arrays.

By visualizing scheduling as a layered optimization framework, the figure demonstrates that modern AI accelerator performance depends as much on execution orchestration as on computational capability.

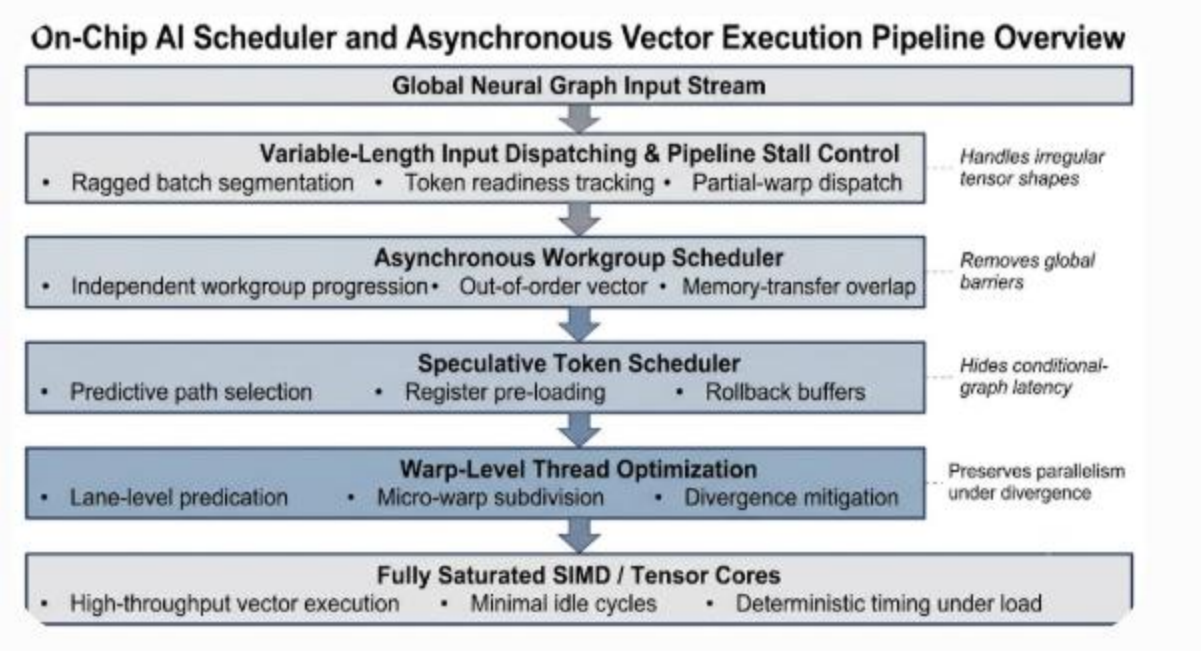


Figure 8.4-B2 — On-Chip AI Scheduler and Asynchronous Vector Execution Pipeline Overview
Multi-stage execution-management architecture illustrating how modern AI accelerators transform irregular neural-network workloads into efficiently scheduled vectorized computation. The figure traces the flow of data through variable-length input dispatching, asynchronous workgroup scheduling, speculative token execution, and warp-level optimization. Together, these mechanisms eliminate pipeline stalls, hide memory latency, mitigate execution divergence, and maintain high utilization of SIMD and tensor-core resources.

Legend

Component	***Description***
Global Neural Graph Input Stream	***Incoming stream of tokens, tensors, activations, or workload requests entering the execution pipeline.***
Variable-Length Input Dispatching & Pipeline Stall Control	***Initial scheduling layer responsible for handling irregular tensor shapes and sequence lengths.***
Ragged Batch Segmentation	***Partitioning of uneven workloads into scheduler-friendly execution units.***
Token Readiness Tracking	***Monitoring mechanism determining when individual work items can proceed.***

Partial-Warp Dispatch	***Execution strategy allowing incomplete workgroups to advance without stalling pipelines.***
Handles Irregular Tensor Shapes	***Primary optimization objective of the dispatch layer.***
Asynchronous Workgroup Scheduler	***Layer managing independent progression of workgroups without global synchronization barriers.***
Independent Workgroup Progression	***Execution model enabling concurrent advancement of workloads.***
Out-of-Order Vector Execution	***Scheduling mechanism allowing ready operations to execute before blocked operations.***
Memory-Transfer Overlap	***Simultaneous execution of computation and memory movement.***
Removes Global Barriers	***Principal benefit of asynchronous scheduling.***
Speculative Token Scheduler	***Prediction-based scheduler that anticipates future execution paths.***
Predictive Path Selection	***Forecasting mechanism used to reduce conditional execution latency.***
Register Pre-Loading	***Early loading of likely execution data into register resources.***
Rollback Buffers	***Recovery structures used when speculative execution predictions prove incorrect.***
Hides Conditional-Graph Latency	***Optimization objective of the speculative scheduling stage.***
Warp-Level Thread Optimization	***Execution-alignment layer mitigating divergence across execution lanes.***
Lane-Level Prediction	***Control mechanism coordinating SIMD/SIMT execution behavior.***

Micro-Warp Subdivision	***Reorganization of execution groups to improve utilization.***
Divergence Mitigation	***Reduction of inefficiencies caused by conditional execution paths.***
Preserves Parallelism Under Divergence	***Primary benefit of warp-level optimization.***
Fully Saturated SIMD / Tensor Cores	***Final execution stage achieving maximum hardware utilization.***
High-Throughput Vector Execution	***Sustained accelerator throughput under dynamic workloads.***
Minimal Idle Cycles	***Reduction of execution inefficiencies and resource waste.***
Deterministic Timing Under Load	***Consistent execution behavior despite workload variability.***

Figure 8.4-B2 illustrates that modern AI accelerators achieve high performance not simply through powerful compute units but through sophisticated scheduling systems that continuously reorganize workloads before execution. The figure demonstrates how multiple layers of scheduling intelligence progressively remove inefficiencies associated with variable-length inputs, synchronization barriers, conditional execution paths, and thread divergence.

The architecture highlights a central principle of accelerator design: maximizing throughput often requires optimizing workload flow before optimization of arithmetic execution itself.

The figure begins with the **Global Neural Graph Input Stream**, representing the incoming flow of tensors, tokens, activations, and computational tasks generated by modern AI models.

Unlike traditional scientific-computing workloads, these inputs frequently exhibit substantial variability. Sequence lengths differ across requests, sparse-routing decisions activate different computational paths, and conditional-execution mechanisms introduce irregular control-flow structures. The scheduling pipeline therefore begins with mechanisms designed to normalize and organize this diversity before execution occurs.

The first stage, **Variable-Length Input Dispatching and Pipeline Stall Control**, addresses irregular workload structure directly.

The figure illustrates three principal mechanisms: ragged-batch segmentation, token-readiness tracking, and partial-warp dispatch. Together, these mechanisms ensure that workloads of differing sizes can enter the execution pipeline without forcing uniform synchronization.

Ragged-batch segmentation reorganizes variable-length inputs into scheduler-friendly units. Token-readiness tracking determines when individual computations are eligible for execution. Partial-warp dispatch allows subsets of execution groups to proceed even when some lanes remain inactive.

The overall objective of this stage is to prevent idle hardware resources caused by nonuniform input structure. By handling irregular tensor shapes early in the pipeline, the scheduler preserves downstream execution efficiency.

The next stage introduces the **Asynchronous Workgroup Scheduler**, one of the most important innovations in modern accelerator architectures.

Traditional scheduling systems often rely on global synchronization barriers that require groups of computations to progress together. Such barriers can dramatically reduce utilization when some tasks complete earlier than others.

The asynchronous scheduler eliminates this constraint by allowing workgroups to advance independently. The figure highlights independent progression, out-of-order vector execution, and memory-transfer overlap as key components of this mechanism.

Through asynchronous scheduling, hardware resources remain active even when portions of the workload experience latency or dependency delays. This capability is especially valuable in AI systems where memory access times and computational complexity vary substantially across different parts of the model.

Following asynchronous scheduling, workloads enter the **Speculative Token Scheduler**.

Conditional-computation architectures and sparse-routing models frequently create uncertainty regarding future execution paths. Waiting until every routing decision is finalized would introduce significant latency into the execution pipeline.

Speculative scheduling reduces this cost by predicting likely future execution states. The figure illustrates predictive path selection, register pre-loading, and rollback buffers as the principal tools supporting this approach.

When predictions prove correct, computational resources begin executing without delay because necessary data have already been loaded. When predictions are incorrect, rollback mechanisms restore architectural state and redirect execution appropriately.

This stage effectively hides conditional-graph latency, allowing hardware resources to remain productive despite uncertainty regarding future execution paths.

Workloads then proceed to the **Warp-Level Thread Optimization** stage.

Modern AI accelerators rely heavily on SIMD and SIMT execution models in which groups of threads execute instructions in parallel. Conditional execution can cause different lanes to follow different branches, reducing utilization due to divergence.

The figure illustrates lane-level prediction, micro-warp subdivision, and explicit divergence-mitigation mechanisms designed to reduce this problem. By reorganizing execution groups dynamically, the scheduler aligns similar workloads and minimizes idle execution lanes.

This stage plays a particularly important role in architectures employing mixture-of-experts routing, sparse attention mechanisms, and adaptive execution pipelines, all of which generate varying execution paths across tokens.

The final result appears at the bottom of the figure as **Fully Saturated SIMD / Tensor Cores**.

By the time workloads reach this stage, major sources of inefficiency have already been addressed. Irregular tensor shapes have been normalized, synchronization bottlenecks minimized, conditional-latency effects reduced, and execution divergence mitigated.

The compute units therefore operate under near-ideal conditions, delivering high-throughput vector execution with minimal idle cycles and predictable timing behavior.

A broader insight emerging from the figure is that scheduling layers progressively remove bottlenecks as workloads move toward execution hardware. Each layer targets a different category of inefficiency: irregular workloads, synchronization delays, prediction uncertainty, and divergence. Together, these mechanisms create a cascade of optimizations that maximizes accelerator utilization.

The figure also highlights the evolution of AI hardware from passive execution devices into active workload-management systems. Modern accelerators no longer simply execute instructions; they continuously analyze, predict, reorder, and optimize computational workflows before arithmetic operations occur.

From a systems-engineering perspective, the layered architecture demonstrates how execution efficiency emerges from cooperation among multiple scheduling mechanisms. No single technique is sufficient to maintain utilization across complex AI workloads. Instead, performance depends on a hierarchy of complementary scheduling strategies operating simultaneously.

Another important observation is that the scheduling pipeline directly supports many of the advanced AI architectures discussed earlier in Section 8.4. Sparse-expert models, conditional-computation networks, state-space systems, and memory-optimized attention architectures all benefit from the scheduling intelligence illustrated here.

Ultimately, Figure 8.4-B2 demonstrates that modern AI accelerator performance is as much a scheduling problem as it is a computational problem. Through intelligent dispatching, asynchronous workgroup management, speculative execution, and warp-level optimization, accelerators transform highly irregular AI workloads into efficiently organized streams of parallel computation. This layered scheduling architecture enables high utilization, low latency, and deterministic execution behavior, forming a critical foundation for scalable AI acceleration.

Collectively, the stages shown in Figure 8.4-B2 illustrate how modern accelerators transform irregular neural-network workloads into smooth, high-throughput execution streams through multiple layers of scheduling intelligence. The figure extends the concepts introduced in Table 8.4-B2 by revealing not only the individual functions of each scheduling mechanism, but also their interdependence within a unified execution pipeline. Each layer progressively removes a different source of inefficiency, allowing the workload to approach the ideal state of continuously saturated SIMD and tensor-core execution. Within this hierarchy, **Variable-Length AI Input Dispatching and Pipeline Stall Control** occupies a foundational position because it serves as the entry point for all subsequent scheduling operations. Before workgroups can advance asynchronously, before speculative scheduling can anticipate future execution paths, and before warp-level optimizations can mitigate control-flow divergence, incoming tensors and token streams must first be organized into execution-ready workloads. This front-end dispatch layer is responsible for handling ragged batch structures, variable sequence lengths, and irregular tensor geometries while preventing the stall conditions that would otherwise propagate throughout the pipeline. By converting nonuniform input streams into efficiently scheduled execution units, it establishes the operational conditions required for all downstream scheduling and optimization mechanisms to function effectively. The following discussion examines **Variable-Length AI Input Dispatching and Pipeline Stall Control** in detail, exploring how modern accelerators maintain continuous hardware utilization despite the increasingly irregular data structures characteristic of contemporary AI workloads.

i. Variable-Length AI Input Dispatching and Pipeline Stall Control

Variable-Length AI Input Dispatching and Pipeline Stall Control represent a foundational hardware–software co-design paradigm that enables accelerators to maintain full vector-lane utilization even when processing ragged batches, uneven token counts, or dynamically sized attention windows. Modern AI workloads rarely present uniform tensor shapes; transformer

inference frequently involves variable sequence lengths, truncated contexts, conditional MoE routing, and token-dependent branching that disrupt traditional SIMD execution. Without specialized dispatch logic, these irregularities cause pipeline bubbles, warp divergence, and underutilization of compute units, ultimately collapsing throughput in the earliest stages of the execution pipeline.

This mechanism addresses these inefficiencies by transforming irregular input tensors into dispatchable micro-fragments that align with the physical geometry of vector lanes and tensor-core tiles. Instead of waiting for full batches or uniform sequence lengths, the dispatch engine continuously segments incoming data into minimal executable units—micro-batches, token slices, or partial-warp fragments—that can be issued immediately. Hardware schedulers track token readiness, dependency resolution, and lane availability at cycle-level granularity, ensuring that no vector lane remains idle simply because the input tensor is uneven or incomplete.

Pipeline stall control complements this dispatching behavior by injecting placeholder operations, speculative pre-loads, or low-cost synchronization hints whenever the pipeline risks starvation. These mechanisms prevent idle cycles by smoothing out irregularities in the input stream. For example, when a transformer layer receives a batch with highly uneven sequence lengths, stall-control logic can pre-load future tokens, rebalance workgroups, or issue masked operations that maintain forward progress without violating dependency constraints. The result is a pipeline that behaves elastically, adapting to workload variability without collapsing parallelism or triggering warp divergence.

A deeper technical evaluation reveals how dispatch controllers, compiler runtimes, and vector pipelines cooperate to prevent starvation and ensure deterministic timing. Dispatch units must track per-lane readiness, reorder input fragments, and manage partial-warp execution without triggering hazards such as misaligned memory accesses or dependency violations. Compiler frameworks must annotate variable-length boundaries, fuse kernels to minimize fragmentation, and generate dependency graphs that allow dispatch units to operate autonomously. These graphs encode token-level readiness, attention-window boundaries, and MoE routing decisions, enabling the hardware to make real-time scheduling decisions without stalling the pipeline.

At the microarchitectural level, variable-length dispatching relies on lightweight token-tracking FIFOs, per-lane readiness registers, and dispatch arbiters that evaluate multiple candidate fragments each cycle. These units must coordinate with memory-prefetch engines to ensure that micro-batches arrive in the correct order and with sufficient locality to avoid cache thrashing. Stall-control logic integrates with hazard-detection units to prevent issuing fragments that would violate dependency constraints or cause register-bank conflicts.

When properly integrated, variable-length dispatching transforms irregular AI workloads into smooth, high-throughput execution streams. It ensures that the accelerator's front end remains saturated even when the neural graph presents highly dynamic or unpredictable structures. By stabilizing the earliest stage of the scheduling pipeline, this mechanism enables all downstream scheduling strategies—workgroup asynchrony, speculative token execution, and warp-level optimization—to operate at peak efficiency. In effect, variable-length dispatching is the foundation upon which the entire asynchronous execution fabric is built, ensuring that modern AI accelerators can sustain deterministic performance under real-world, non-uniform workloads.

With variable-length dispatching stabilizing the front end of the execution pipeline and ensuring that ragged batches and uneven token streams enter the accelerator without triggering stall cycles, the next challenge is maintaining momentum once these micro-fragments are in flight. Even perfectly segmented inputs can lose efficiency if workgroups are forced to advance in lock-step or wait for global synchronization barriers. To sustain high throughput under dynamic workloads, the accelerator must allow independent compute groups to progress autonomously, issuing vector operations whenever their operands become ready rather than waiting for unrelated tasks. This transition—from elastic input dispatching to fully asynchronous workgroup progression—forms the next pillar of the scheduling fabric. The focus now shifts to how out-of-order vector execution, dependency-aware scheduling, and memory-latency hiding mechanisms collectively transform the accelerator into a fluid, latency-tolerant compute engine capable of saturating vector lanes even under highly irregular neural-graph conditions.

ii. Asynchronous AI Workgroup Scheduling and Out-of-Order Vector Execution

Asynchronous AI Workgroup Scheduling and Out-of-Order Vector Execution represent a transformative shift from traditional synchronous SIMD processing to a fluid, latency-tolerant execution model capable of sustaining high throughput under dynamic and irregular AI workloads. Conventional accelerators rely heavily on global barriers and lock-step execution semantics, forcing all workgroups to advance together regardless of their individual readiness. This rigid model collapses under modern transformer and MoE workloads, where tensor dependencies, memory latencies, and conditional graph structures vary dramatically across layers and tokens. When one workgroup stalls due to a dependency or memory fetch, synchronous execution forces all other workgroups to wait, wasting vector-lane capacity and collapsing parallelism.

Asynchronous scheduling resolves these constraints by allowing independent workgroups to progress autonomously, issuing vector operations whenever their operands become ready rather than waiting for unrelated tasks. Hardware schedulers continuously analyze dependency

graphs generated by the compiler, identifying which workgroups have satisfied their data dependencies and can safely advance. This enables the accelerator to opportunistically issue instructions from any ready workgroup, dramatically increasing utilization and reducing idle cycles. Out-of-order vector execution further enhances this flexibility by allowing vector lanes to retire operations as soon as their inputs are available, bypassing the need for strict in-order sequencing. This is particularly advantageous for heterogeneous compute patterns such as multi-head attention, sparse activation pathways, and MoE expert routing, where different workgroups exhibit widely varying execution latencies.

A deeper technical evaluation reveals how schedulers, compilers, and pipelines coordinate to avoid hazards while enabling aggressive asynchrony. Hardware schedulers must track tensor readiness at fine granularity, maintain per-workgroup dependency states, and dynamically allocate registers and vector lanes without causing deadlocks or starvation. They rely on dependency-tracking FIFOs, readiness bitmaps, and priority arbiters that evaluate multiple candidate workgroups each cycle. Compilers must generate detailed dependency metadata, annotate asynchronous boundaries, and fuse kernels to maximize locality and minimize cross-workgroup interference. These annotations encode tensor-level dependencies, memory-prefetch hints, and control-flow divergence points, enabling the hardware to make safe out-of-order scheduling decisions.

Vector pipelines must support rollback, hazard detection, and speculative retirement without compromising correctness. Rollback mechanisms ensure that mis-scheduled or prematurely issued operations can be safely undone without corrupting register state. Hazard-detection units monitor register-bank conflicts, memory-ordering constraints, and cross-workgroup dependencies, preventing illegal instruction issuance. Memory-prefetch engines must coordinate with the scheduler to ensure that data arrives in time for out-of-order execution, avoiding cache thrashing and bandwidth contention.

When properly integrated, asynchronous workgroup scheduling delivers substantial improvements in throughput, latency, and energy efficiency. It transforms the accelerator into a latency-tolerant execution fabric capable of sustaining high utilization even when neural-graph workloads exhibit unpredictable structure. By eliminating global barriers, enabling opportunistic vector issuance, and supporting out-of-order retirement, this mechanism ensures that compute units remain saturated and that memory latency is effectively hidden. Asynchronous scheduling is therefore the second foundational pillar of the modern AI execution pipeline, enabling downstream mechanisms—speculative token scheduling and warp-level optimization—to operate at peak efficiency under real-world, irregular workloads.

With asynchronous workgroup scheduling enabling independent compute groups to advance

autonomously and out-of-order vector execution ensuring that ready operands are retired without waiting for unrelated tasks, the accelerator achieves a fluid, latency-tolerant execution rhythm. However, modern neural graphs introduce a second class of irregularity that cannot be resolved through asynchrony alone: **conditional execution paths**. Mixture-of-Experts routing, masked attention, dynamic sequence truncation, and token-dependent branching all create situations where the next operation cannot be determined purely from static dependency graphs. To maintain throughput under these conditions, the scheduler must anticipate future execution paths, pre-load register states, and prepare vector lanes for operations that may or may not occur. This predictive capability—combined with robust rollback mechanisms that preserve correctness when speculation is wrong—forms the third pillar of the scheduling fabric. The following discussion examines how speculative token scheduling hides conditional-graph latency and prevents starvation, ensuring that the accelerator remains saturated even when the neural graph itself is dynamically evolving.

iii. Speculative AI Token Scheduling and Register Rollback Mechanisms

Speculative AI Token Scheduling and Register Rollback Mechanisms introduce predictive execution into modern AI accelerators, enabling hardware to anticipate future computation paths and prepare execution resources before those paths are formally confirmed. As neural architectures increasingly incorporate conditional structures—Mixture-of-Experts routing, masked attention, dynamic sequence truncation, token-dependent branching, and adaptive computation graphs—the execution pipeline must frequently pause to determine which operations should occur next. Without speculation, vector lanes stall while waiting for routing decisions or dependency resolution, causing throughput collapse in precisely the workloads that demand the highest performance.

Speculative scheduling resolves this bottleneck by predicting likely execution paths based on historical token behavior, model-level structural patterns, runtime heuristics, or compiler-provided hints. When the scheduler identifies a high-probability path, it pre-loads register states, allocates vector lanes, and issues preliminary operations ahead of confirmation. This allows the accelerator to overlap control-flow resolution with useful computation, effectively hiding the latency associated with conditional graph traversal. In transformer-based models, for example, speculative scheduling can pre-fetch attention-window fragments or prepare MoE expert buffers before routing decisions are finalized, ensuring that compute units remain active even when the model's control flow is dynamic.

To support this predictive behavior safely, accelerators rely on robust register rollback mechanisms. When speculation is correct, the pipeline proceeds without interruption, achieving near-ideal utilization. When speculation is incorrect, rollback logic restores register states to

their last committed values, discards speculative results, and resumes execution along the correct path without corrupting downstream computation. These rollback buffers must be lightweight enough to avoid excessive register pressure yet large enough to store all intermediate states required for safe recovery. They operate in concert with hazard-detection units that monitor dependency violations, memory-ordering constraints, and cross-workgroup interactions to prevent cascading mis-speculation.

A full technical analysis reveals how speculation interacts with dependency graphs, register files, and vector pipelines. Hardware schedulers must track speculative boundaries, maintain prediction confidence levels, and prevent starvation by ensuring that non-speculative workgroups continue to receive execution opportunities. They must also manage the allocation of vector lanes between speculative and non-speculative tasks, balancing aggressive prediction with guaranteed forward progress. Compilers play a critical role by annotating conditional regions, generating prediction hints, and restructuring control-flow graphs to maximize the effectiveness of speculation. These annotations may include token-level routing probabilities, attention-mask sparsity patterns, or MoE expert-selection heuristics derived from offline profiling.

Vector pipelines must support speculative retirement, partial-warp execution, and rollback synchronization without compromising correctness. This requires fine-grained tracking of register dependencies, operand readiness, and memory-access ordering. Memory-prefetch engines must coordinate with speculative schedulers to ensure that predicted data arrives in time for execution, while avoiding bandwidth contention or cache pollution caused by incorrect predictions.

When properly implemented, speculative scheduling hides conditional-graph latency and preserves throughput even under highly irregular workloads. It transforms dynamic neural graphs into predictable execution streams by overlapping control-flow resolution with computation, ensuring that vector lanes remain active regardless of branching complexity. As conditional structures become more prevalent in large-scale AI models, speculative token scheduling and register rollback mechanisms form an essential pillar of the asynchronous execution fabric, enabling accelerators to sustain deterministic performance under real-world, non-uniform workloads.

As speculative token scheduling equips the accelerator to anticipate branching behavior and rollback mechanisms safeguard correctness when predictions misalign with actual control flow, the execution pipeline becomes resilient to the unpredictability inherent in modern neural graphs. Yet even with accurate speculation, a deeper structural challenge remains: different tokens within the same warp often follow different computational paths. Mixture-of-Experts

routing, masked attention, and token-dependent branching frequently cause threads to diverge, leaving some lanes active while others idle. This divergence undermines SIMD efficiency and erodes the parallelism that the upstream scheduling fabric works so hard to preserve. To maintain high utilization under these conditions, the accelerator must operate at a finer granularity—remapping lanes dynamically, subdividing warps, and applying lane-level predication so that divergent execution paths do not collapse throughput. The next topic explores how these warp-level optimization techniques stabilize the back end of the pipeline and ensure that parallelism is preserved even when control flow becomes highly irregular.

iv. Warp-Level AI Thread Optimization for Conditional Graph Execution

Warp-Level AI Thread Optimization for Conditional Graph Execution addresses one of the most persistent and structurally limiting challenges in modern accelerator design: **warp divergence**. As transformer architectures, Mixture-of-Experts layers, sparse attention mechanisms, and token-dependent routing become more prevalent, threads within the same warp increasingly follow different execution paths. Traditional SIMD architectures assume uniform control flow across all lanes; when this assumption breaks, inactive lanes waste cycles, parallelism collapses, and effective throughput drops sharply. In large-scale inference workloads, divergence can degrade performance more severely than memory latency or arithmetic bottlenecks.

Warp-level optimization resolves this challenge by restructuring execution at the granularity of individual vector lanes rather than treating the warp as a monolithic unit. Hardware dynamically remaps threads to align similar execution paths, isolates divergent lanes, and subdivides warps into smaller micro-warps that can progress independently. This fine-grained control prevents divergent threads from stalling the entire warp and allows the accelerator to maintain high utilization even when control flow becomes irregular. Conditional execution masks, lane-level predication, and micro-warp subdivision ensure that each lane executes only the operations relevant to its control-flow path, eliminating wasted cycles and preserving parallelism.

A deeper technical evaluation reveals how warp schedulers, compilers, and pipelines cooperate to minimize divergence and maintain deterministic performance. Warp schedulers must track per-lane control-flow state, dynamically remap threads as execution paths evolve, and prevent deadlocks when multiple divergent paths compete for shared resources. They rely on lane-state registers, divergence-tracking bitmaps, and priority arbiters that evaluate multiple micro-warp candidates each cycle. These schedulers must also coordinate with memory-prefetch engines to ensure that data for divergent paths arrives with sufficient locality to avoid cache thrashing.

Compilers play a critical role by generating predication metadata, fusing conditional kernels, and restructuring control-flow graphs to minimize divergence. They annotate conditional regions

with lane-level execution masks, identify opportunities for kernel fusion that reduce branch frequency, and generate dependency graphs that allow hardware to safely subdivide warps. Compiler-provided hints may include attention-mask sparsity patterns, MoE expert-selection probabilities, or token-level routing heuristics derived from offline profiling. These annotations enable hardware to make informed decisions about when to subdivide warps, when to remap lanes, and when to apply predication.

Vector pipelines must support partial-warp execution, lane-level hazard detection, and divergence-aware retirement. This requires fine-grained tracking of operand readiness, register dependencies, and memory-access ordering at the lane level. Rollback mechanisms—originally introduced for speculative token scheduling—must integrate with warp-level optimization to ensure that divergent execution paths can be safely reversed or merged without corrupting register state. Memory systems must accommodate divergent access patterns without causing bandwidth contention or cache pollution.

When properly integrated, warp-level optimization preserves parallelism under conditional execution and enables large-scale AI models to run efficiently even when their control flow is highly dynamic. It stabilizes the back end of the asynchronous execution pipeline by ensuring that divergence does not collapse SIMD efficiency, allowing upstream mechanisms—variable-length dispatching, asynchronous workgroup scheduling, and speculative token execution—to operate at peak effectiveness. As neural architectures continue to incorporate more conditional and sparse computation, warp-level thread optimization becomes essential for sustaining deterministic throughput and maximizing accelerator utilization under real-world workloads.

On-chip AI schedulers and asynchronous vector-execution pipelines redefine how modern accelerators sustain performance under the irregular, conditional, and highly dynamic workloads characteristic of large-scale neural models. By stabilizing the front end through variable-length dispatching, enabling autonomous progress via asynchronous workgroup scheduling, hiding conditional-graph latency through speculative token execution, and preserving parallelism with warp-level optimization, the scheduling fabric transforms inherently unpredictable neural graphs into smooth, high-throughput execution streams. These mechanisms operate as an integrated orchestration layer that continuously adapts to workload variability, resolves dependency hazards, and maintains deterministic timing even when control flow diverges. As models grow in depth, width, and structural complexity, asynchronous scheduling becomes indispensable—ensuring that vector lanes remain saturated, memory latency is effectively hidden, and compute units operate at peak efficiency. This scheduling paradigm forms the backbone of scalable AI acceleration, enabling modern hardware to meet

strict latency, bandwidth, and power constraints while executing increasingly irregular and conditional neural architectures.

With the scheduling fabric now capable of sustaining high utilization under dynamic execution conditions, the next challenge lies in addressing the memory-movement bottlenecks that dominate large-scale inference. Even perfectly orchestrated pipelines stall when weights and activations must traverse long distances across the memory hierarchy. As transformer models expand into trillions of parameters and sequence lengths grow into the tens of thousands, the cost of repeatedly fetching static weights from off-chip memory becomes prohibitive. To overcome these physical limits, accelerators increasingly shift computation closer to where data resides—embedding arithmetic units directly within memory arrays and streaming static weights from on-die storage fabrics. This emerging paradigm of AI processing-in-memory and static weight streaming reduces data-movement energy, collapses latency, and enables sustained throughput even when external bandwidth is saturated. The focus now turns to how these memory-centric execution strategies reshape the architecture of modern AI accelerators and complement the scheduling mechanisms established earlier.

c. AI Processing-in-Memory and On-Die Static Weight Streaming

AI Processing-in-Memory and On-Die Static Weight Streaming represent one of the most consequential architectural shifts in modern accelerator design. As AI models scale into the billions and trillions of parameters, the dominant bottleneck is no longer arithmetic throughput but the physical cost of repeatedly transporting static weights across the memory hierarchy. Traditional load-store pipelines impose prohibitive energy overheads, saturate external bandwidth, and introduce latency spikes that stall compute units even when scheduling logic is fully optimized. Processing-in-memory resolves these scaling limits by collapsing the distance between data and computation—embedding analog and mixed-signal compute elements directly within memory arrays and streaming static weights from tightly coupled on-die fabrics.

Modern AI workloads exhibit extreme parameter locality: transformer layers reuse the same weights across thousands of tokens, MoE experts require rapid access to pinned parameter blocks, and large attention matrices must be fetched repeatedly across long sequences. Without architectural support for weight locality, these patterns overwhelm DRAM bandwidth and destabilize latency. Processing-in-memory addresses this challenge by performing matrix multiplication directly inside analog macro-arrays, eliminating the need to shuttle operands across the memory hierarchy. On-die static weight pinning ensures that frequently accessed parameters remain resident in local memory fabrics, reducing redundant transfers and stabilizing throughput under sustained inference loads. Together, these mechanisms transform the accelerator from a compute-centric device into a memory-compute hybrid capable of

sustaining high utilization even when external bandwidth is saturated.

This paradigm spans a spectrum of memory-centric execution strategies. Analog AI macro-arrays perform dense multiply-accumulate operations in situ, leveraging charge accumulation and crossbar conduction paths to achieve extreme energy efficiency. Static weight locality ensures that parameter blocks remain physically close to compute units, minimizing movement and reducing latency. Digital-to-analog boundaries maintain numerical stability by managing voltage levels, quantization domains, and signal integrity across mixed-signal interfaces. Inter-macro data-shuffling fabrics dynamically route activations and partial sums between distributed memory-compute tiles, ensuring that large models can be executed coherently across spatially partitioned arrays. Together, these mechanisms form a unified memory-centric execution layer that complements the asynchronous scheduling fabric described earlier.

A complete technical evaluation of processing-in-memory requires understanding how analog compute arrays, static memory fabrics, compiler runtimes, and mixed-signal pipelines cooperate to bypass bandwidth bottlenecks and maintain numerical correctness. Analog macro-arrays must manage charge leakage, device variability, and crossbar non-idealities while delivering predictable multiply-accumulate behavior. Static weight fabrics must support rapid pinning, eviction, and streaming without introducing contention or thermal hotspots. Compiler frameworks must generate weight-locality maps, annotate analog boundaries, and fuse kernels to maximize reuse. Mixed-signal pipelines must manage voltage stability, quantization transitions, and analog-digital synchronization without compromising accuracy. When properly integrated, these memory-centric techniques deliver substantial improvements in energy efficiency, throughput, and latency—making processing-in-memory a cornerstone of scalable AI deployment.

Processing-in-memory introduces a fundamentally different execution environment for AI accelerators—one where computation occurs inside memory arrays, static weights remain pinned on-die, analog signals propagate through crossbar fabrics, and distributed macro-arrays cooperate through dynamic routing networks. These mechanisms operate together, not in isolation. To understand how they collectively reshape compute utilization, bandwidth behavior, and energy efficiency, it is useful to view them as a unified memory-compute framework. The components below organize these mechanisms into their core functional dimensions, clarifying how each contributes to the broader goal of sustaining high-performance AI inference under extreme model sizes and bandwidth constraints.

- **Analog AI Macro-Arrays for In-Situ Matrix Multiplication** — Perform multiply-accumulate operations directly inside memory arrays using analog conduction paths, eliminating load-store overhead and dramatically reducing energy per operation.

- **AI Weight Locality and On-Die Static Memory Pinning** — Keep frequently accessed parameters resident in local memory fabrics, reducing external bandwidth pressure and stabilizing latency under sustained inference workloads.
- **AI Digital-to-Analog Boundaries and Voltage Stability Management** — Maintain numerical correctness across mixed-signal interfaces by managing quantization domains, voltage levels, and signal integrity during analog-digital transitions.
- **Inter-Macro AI Data Shuffling and Dynamic Bus Routing** — Route activations, partial sums, and intermediate tensors across distributed macro-arrays using dynamic interconnect fabrics that preserve locality and minimize routing overhead.

AI accelerators increasingly rely on processing-in-memory and static weight streaming to meet the demands of large-scale inference. These techniques transform execution pipelines into memory-centric systems that align directly with the parameter-heavy structure of modern neural models. The mechanisms summarized here capture the foundational strategies that make this paradigm viable: analog macro-arrays that collapse compute into memory, static weight pinning that eliminates redundant transfers, mixed-signal boundaries that preserve numerical stability, and inter-macro routing fabrics that unify distributed compute tiles. Together, these mechanisms define the hardware blueprint for executing massive models within strict latency, bandwidth, and power envelopes.

With the core mechanisms of AI Processing-in-Memory and On-Die Static Weight Streaming now established—analog macro-arrays for in-situ computation, static weight locality, mixed-signal stability management, and inter-macro routing—the next step is to organize these capabilities into their functional dimensions. Each mechanism contributes to a different aspect of memory-centric execution: some collapse computation into the memory fabric, others stabilize numerical behavior across analog-digital boundaries, and others ensure that distributed macro-arrays operate cohesively. To clarify how these components interact and how they collectively reshape the accelerator’s compute-memory hierarchy, the following table summarizes their architectural roles, optimization targets, and system-level impact.

Table 8.4-B2 examined how advanced scheduling architectures maintain high utilization of SIMD lanes, tensor cores, and vector-execution pipelines despite increasingly irregular AI workloads. While these mechanisms help maximize the efficiency of available computational resources, they do not eliminate a more fundamental limitation in modern AI systems: the cost of moving data between memory and compute units. In many contemporary workloads, particularly large-scale inference and long-context processing, energy consumption and execution latency are dominated not by arithmetic operations themselves but by the repeated transfer of weights,

activations, and intermediate tensors across memory hierarchies. This growing imbalance has motivated a shift away from the traditional separation of memory and computation toward architectures that embed computation within memory structures and maintain frequently accessed parameters close to execution resources. Table 8.4-B3 explores the core mechanisms underlying processing-in-memory and on-die static weight streaming, illustrating how modern accelerators increasingly reduce data movement by bringing computation to data rather than continuously moving data to computation.

Table 8.4-B3 presents several foundational mechanisms that support processing-in-memory (PIM) architectures and on-die static weight streaming in contemporary AI accelerators. These technologies represent a significant departure from conventional computing architectures by directly addressing one of the most persistent bottlenecks in AI execution: memory movement.

Traditional von Neumann architectures separate memory storage from arithmetic computation. As a result, neural-network execution requires continuous movement of model parameters and activations between memory systems and compute units. Although arithmetic operations have become increasingly efficient, data movement remains comparatively expensive in terms of latency, bandwidth, and energy consumption.

Processing-in-memory architectures seek to reduce these costs by integrating arithmetic capabilities directly into memory structures or by positioning frequently accessed model parameters near computational resources. Rather than treating memory as a passive storage component, these systems transform memory into an active participant in computation.

The table identifies four key mechanisms supporting this paradigm: analog AI macro-arrays for in-situ matrix multiplication, AI weight locality and on-die static-memory pinning, digital-to-analog boundary management with voltage stabilization, and inter-macro data shuffling with dynamic bus routing. Together, these mechanisms form the foundation of architectures designed to reduce memory-transfer overhead while supporting increasingly large and complex AI workloads.

By examining both hardware techniques and system-level impacts, the table illustrates how processing-in-memory architectures seek to overcome the memory wall that increasingly constrains modern AI performance.

Table 8.4-B3 — Core Mechanisms in AI Processing-in-Memory and On-Die Static Weight Streaming

Mechanism	Primary Function	Hardware Techniques	System-Level Impact
Analog AI Macro-Arrays for In-Situ Matrix Multiplication	Perform multiply-accumulate operations directly inside memory arrays, eliminating load-store overhead.	Crossbar conduction paths, charge-accumulation MACs, analog summation lines, mixed-signal readout circuits, calibration loops.	Dramatically reduces energy per MAC, collapses memory-movement latency, enables dense compute near data, stabilizes throughput under bandwidth saturation.
AI Weight Locality and On-Die Static Memory Pinning	Keep frequently accessed parameters resident in local memory fabrics to avoid repeated DRAM transfers.	SRAM pinning, NVM weight banks, locality maps, rapid pin/evict controllers, expert-weight residency for MoE.	Stabilizes latency, reduces external bandwidth pressure, prevents compute starvation, enables deterministic inference across long sequences.
AI Digital-to-Analog Boundaries and Voltage Stability Management	Maintain numerical correctness across mixed-signal interfaces connecting analog compute arrays to digital pipelines.	ADC/DAC converters, dynamic gain control, quantization domain management, voltage-stability loops, noise filtering.	Preserves accuracy, prevents analog drift, ensures stable mixed-signal execution, enables safe integration of analog MACs into digital inference pipelines.
Inter-Macro AI Data Shuffling and Dynamic Bus Routing	Route activations, partial sums, and intermediate tensors across distributed macro-arrays.	Hierarchical bus fabrics, crossbar switches, packetized on-die networks, multicast/broadcast routing,	Enables coherent execution across distributed memory-compute tiles, prevents routing bottlenecks, supports

Mechanism	Primary Function	Hardware Techniques	System-Level Impact
		contention-aware arbitration.	large model partitions, maintains locality across spatial domains.

Table 8.4-B3 demonstrates that improving AI performance is no longer solely a matter of increasing arithmetic throughput. Instead, substantial efficiency gains can be achieved by reducing the distance that data must travel within the computing system.

The mechanisms summarized in the table reveal a common architectural objective: maximizing locality by placing computation near stored information and preserving frequent parameter access within low-latency memory structures. This approach reduces bandwidth pressure, lowers energy consumption, and improves execution determinism across large-scale AI workloads.

The first mechanism identified in the table is **analog AI macro-arrays for in-situ matrix multiplication**, one of the most ambitious approaches to reducing data movement.

Conventional processors perform matrix multiplication by transferring values from memory into arithmetic units and then returning results to storage. Processing-in-memory architectures alter this model by performing multiply-accumulate operations directly within memory arrays. The table highlights crossbar conduction paths, charge-accumulation structures, analog summation networks, and mixed-signal readout circuits as enabling technologies.

The primary advantage of this approach is the elimination of repeated load-store operations. Because matrix multiplication occurs within the memory fabric itself, energy-intensive data transfers are greatly reduced. The resulting improvements in throughput become particularly significant for neural-network workloads dominated by dense matrix operations.

An additional benefit highlighted in the table is stabilization under bandwidth saturation. Since computation remains close to stored parameters, performance becomes less dependent on external memory bandwidth availability.

The second mechanism is **AI weight locality and on-die static memory pinning**, which focuses on retaining frequently accessed parameters within local memory structures.

Large AI models often contain subsets of weights that are reused repeatedly during inference. Transferring these parameters repeatedly from external memory consumes bandwidth and introduces latency variability. Static memory pinning addresses this challenge by placing frequently used weights within SRAM regions, non-volatile-memory banks, or dedicated on-die

storage arrays.

The table identifies SRAM pinning, locality maps, rapid pin-and-evict controllers, and expert-weight residency systems as supporting mechanisms. By keeping important parameters physically close to compute resources, these architectures reduce bandwidth pressure and enable highly predictable inference behavior.

This capability is particularly important for mixture-of-experts systems and long-context workloads, where repeated access to frequently used parameters can otherwise become a dominant performance bottleneck.

The third mechanism is **AI digital-to-analog boundary management and voltage stability control**, which serves as a critical integration layer within mixed-signal processing-in-memory systems.

Although analog computation can provide substantial efficiency advantages, most AI systems continue to rely on digital control structures and digital output representations. Consequently, information must frequently cross the boundary between analog and digital domains.

The table highlights analog-to-digital converters (ADCs), digital-to-analog converters (DACs), gain-control systems, quantization-domain management, and voltage-stability loops as important supporting technologies. These mechanisms ensure that numerical information remains accurate despite signal variability, noise, and analog-circuit imperfections.

This layer is particularly important because the benefits of analog computation can be lost if conversion processes introduce instability or excessive numerical error. Effective boundary management preserves reliability while enabling integration of analog and digital subsystems.

The fourth mechanism identified is **inter-macro AI data shuffling and dynamic bus routing**, which addresses data movement among distributed compute-memory arrays.

Even highly localized architectures require communication among processing elements. Activations, intermediate tensors, and partial computation results must be transferred between memory-compute regions to support larger neural-network workloads.

The table identifies hierarchical bus structures, crossbar switches, packetized on-die networks, multicast routing systems, and contention-aware arbitration as important architectural techniques. These mechanisms ensure that data can move efficiently across distributed macro-arrays without creating communication bottlenecks.

A particularly important contribution of this mechanism is support for large distributed model partitions. By maintaining coherence among spatially distributed compute-memory regions, the

architecture scales beyond the limitations of individual arrays.

A broader insight emerging from the table is that all four mechanisms attack the same underlying challenge from different directions. Analog macro-arrays reduce data movement through in-memory computation. Weight pinning reduces repeated parameter transfers. Boundary-management systems preserve numerical integrity across processing domains. Dynamic routing improves efficiency when data movement remains necessary.

The table also highlights a fundamental shift in architectural philosophy. Traditional accelerators improve performance by increasing arithmetic throughput. Processing-in-memory systems improve performance by reducing the amount of data movement required before arithmetic operations occur.

From a systems-engineering perspective, these mechanisms operate at different levels of the computing hierarchy but remain tightly interconnected. Efficient in-memory computation requires stable mixed-signal interfaces. Parameter locality depends on intelligent memory management. Distributed macro-arrays require efficient communication fabrics. Together, these technologies form an integrated computation-and-memory ecosystem.

Another important observation is that these mechanisms contribute directly to energy efficiency. In many AI accelerators, moving data consumes significantly more energy than performing arithmetic operations. Reducing movement therefore provides benefits that extend beyond performance, including lower power consumption and improved thermal behavior.

The table further demonstrates how processing-in-memory architectures align with the broader hardware–software co-design principles discussed throughout Section 8.4. Computational structures, memory hierarchies, communication fabrics, and model-execution strategies are increasingly designed together rather than independently.

Ultimately, Table 8.4-B3 illustrates how processing-in-memory and on-die weight-streaming architectures seek to overcome one of the most significant limitations in modern AI computing: the cost of data movement. Through in-situ matrix multiplication, localized parameter residency, stable analog-digital integration, and efficient inter-array communication, these mechanisms enable computation to occur closer to the data itself. The result is improved throughput, lower latency, reduced energy consumption, and enhanced scalability for next-generation AI systems operating under increasingly demanding computational workloads.

Table 8.4-B3 introduced the key architectural mechanisms that enable processing-in-memory systems to reduce data movement through in-situ computation, localized parameter residency, mixed-signal integration, and distributed routing fabrics. While each mechanism contributes

independently to reducing memory-transfer overhead, practical processing-in-memory architectures operate as tightly coupled computational ecosystems in which memory arrays, analog compute structures, communication fabrics, and control systems function together as a unified execution environment. Understanding the full impact of these technologies therefore requires a system-level perspective that reveals how data move through memory-resident computation pipelines. Figure 8.4-B3 provides this perspective by illustrating the interaction among static weight storage, analog matrix-multiplication tiles, mixed-signal interfaces, and inter-macro communication networks, showing how modern accelerators transform memory structures into active computational resources.

Figure 8.4-B3 presents a systems-level architecture for AI processing-in-memory (PIM) computation combined with on-die static weight streaming. The figure illustrates how modern accelerators reduce memory-movement overhead by co-locating computation, parameter storage, and communication resources within a tightly integrated hardware fabric.

In conventional architectures, AI inference is dominated by the repeated movement of model weights and activations between memory subsystems and compute units. Although arithmetic operations continue to become more efficient, the cost of moving data across memory hierarchies increasingly limits performance, energy efficiency, and scalability. Processing-in-memory architectures address this challenge by relocating significant portions of computation into or near memory structures themselves.

The figure is organized into four interconnected architectural domains: static weight locality and on-die memory storage, analog in-situ matrix multiplication, mixed-signal boundary management, and inter-macro routing with digital pipeline integration. Together, these domains form a computational framework in which memory serves not merely as storage but as an active participant in neural-network execution.

By depicting the relationships among memory arrays, analog compute resources, digital control systems, and communication fabrics, the figure demonstrates how processing-in-memory architectures seek to overcome the memory bottlenecks that increasingly constrain modern AI systems.

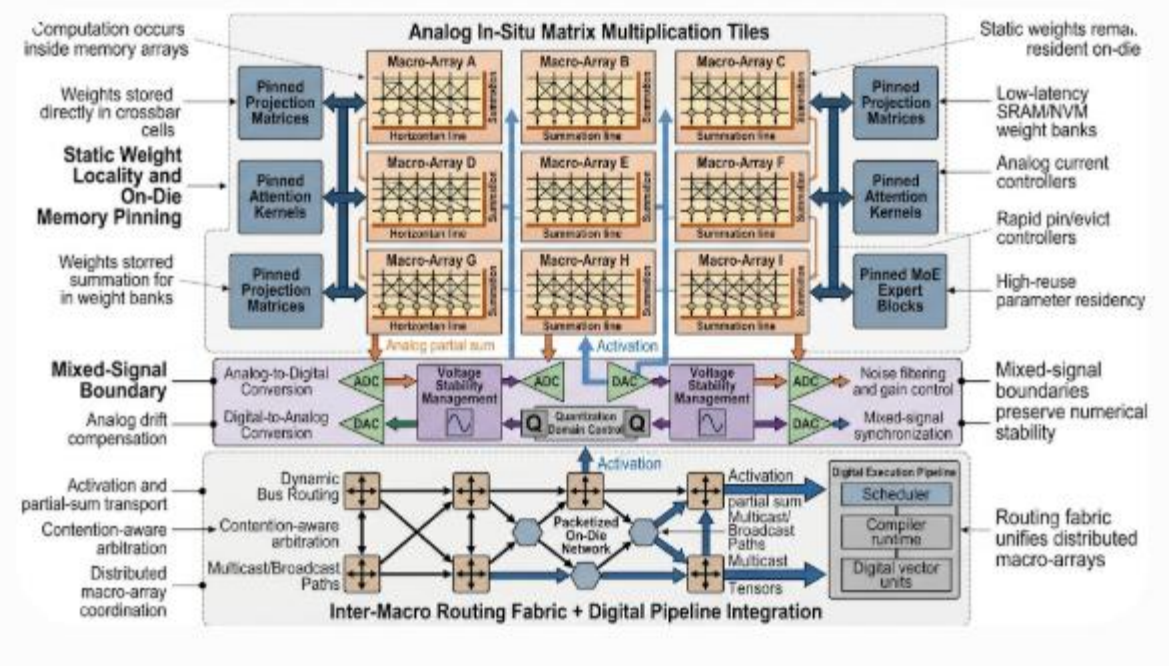


Figure 8.4-B3 — AI Processing-in-Memory and On-Die Static Weight Streaming Overview
Integrated memory-centric AI architecture illustrating how computation is performed within or adjacent to memory structures rather than through repeated data transfers between memory and processors. The figure traces the flow of weights and activations through on-die memory banks, analog matrix-multiplication macro-arrays, mixed-signal conversion layers, and inter-macro communication networks. Together, these mechanisms reduce memory-movement overhead, improve locality, lower energy consumption, and support scalable neural-network execution.

Legend

Component	***Description***
Static Weight Locality and On-Die Memory Storage	*Layer responsible for maintaining frequently used model weights within local memory resources.*
Pinned Projection Matrices	*Frequently accessed projection weights retained permanently within local memory banks.*
Pinned Attention Kernels	*Attention-related parameters stored on die to eliminate repeated transfers.*
Pinned MoE Expert Blocks	*Resident expert parameters supporting mixture-of-experts execution.*
Weights Stored Directly in Crossbar Cells	*Processing-in-memory arrangement eliminating repeated load-store operations.*

High-Reuse Parameter Residency	*Long-lived parameter presence within local memory structures.*
Analog In-Situ Matrix Multiplication Tiles	*Memory-resident compute arrays performing neural-network arithmetic directly within storage structures.*
Macro-Array A–I	*Distributed analog compute-memory tiles executing matrix operations.*
Horizontal Current Lines	*Analog signal pathways supporting matrix multiplication.*
Summation Lines	*Analog accumulation structures combining partial computation results.*
Analog Partial Sums	*Intermediate outputs generated within memory arrays.*
Mixed-Signal Boundary	*Interface connecting analog computation and digital execution systems.*
ADC (Analog-to-Digital Converter)	*Circuit converting analog outputs into digital representations.*
DAC (Digital-to-Analog Converter)	*Circuit converting digital signals for analog processing.*
Voltage Stability Management	*Control loops preserving signal integrity and numerical accuracy.*
Quantization Domain Translation	*Conversion layer supporting mixed-signal computation.*
Noise Filtering and Gain Control	*Signal-conditioning mechanisms improving computational reliability.*
Inter-Macro Routing Fabric and Digital Pipeline Integration	*Distributed communication infrastructure linking memory-compute tiles.*
Packetized On-Die Network	*High-bandwidth routing network connecting macro-arrays.*
Multicast / Broadcast Paths	*Communication channels distributing activations and control information.*
Contention-Aware Arbiter	*Routing-control mechanism minimizing communication bottlenecks.*
Digital Scheduler	*Execution-management component coordinating distributed workloads.*
Compiler Runtime	*Software-control layer supporting resource allocation and execution management.*

Digital Vector Units	*Auxiliary digital compute resources supporting hybrid execution.*

Figure 8.4-B3 illustrates a fundamental departure from traditional processor-centric computing architectures. Rather than treating memory as a passive repository of data, the architecture transforms memory into an active computational substrate capable of storing parameters, performing arithmetic operations, and coordinating information flow across distributed processing domains.

The figure demonstrates that many of the efficiency gains associated with processing-in-memory arise not from faster arithmetic alone but from reducing the need to move information throughout the system.

The figure begins with the **static weight locality and on-die memory storage layer**, which serves as the foundation of the architecture.

Traditional AI accelerators repeatedly transfer model weights from memory systems into compute units whenever inference operations are performed. Such transfers often consume more energy than the arithmetic itself. The architecture shown here addresses this issue by maintaining heavily reused parameters directly within local memory structures.

The diagram highlights pinned projection matrices, pinned attention kernels, and pinned mixture-of-experts blocks. These parameters remain resident on die rather than being continuously fetched from external memory resources.

A key consequence of this design is improved locality. Because frequently accessed parameters remain physically close to computation resources, latency becomes more predictable and bandwidth consumption declines substantially.

The architecture then transitions into the **analog in-situ matrix multiplication layer**, which represents one of the most distinctive features of processing-in-memory systems.

Instead of moving weights into dedicated arithmetic units, matrix multiplication occurs directly inside memory-resident crossbar structures. The figure illustrates a collection of macro-arrays labeled A through I, each functioning as a localized compute-memory tile.

Input activations propagate across horizontal current lines, while analog accumulation occurs through summation pathways embedded within the memory structures themselves. Partial sums emerge directly from the arrays without requiring repeated memory transfers.

This arrangement significantly reduces data movement because weights never leave the

memory structures in which they reside. The resulting efficiency gains are particularly valuable for neural-network workloads dominated by dense matrix operations.

Following analog computation, data enter the **mixed-signal boundary layer**.

Although analog processing provides substantial efficiency advantages, modern AI systems still rely heavily on digital control and programming frameworks. Consequently, information must be translated between analog and digital domains.

The figure illustrates analog-to-digital converters, digital-to-analog converters, voltage stabilization systems, quantization-domain managers, and noise-control mechanisms. Together, these components preserve signal integrity while enabling interaction between analog compute resources and digital execution infrastructure.

This boundary layer plays a critical role because analog efficiency would provide limited value without mechanisms capable of maintaining numerical reliability during conversion.

The architecture then proceeds into the **inter-macro routing fabric and digital integration layer**, where outputs from multiple compute-memory tiles are coordinated.

Even highly localized architectures require communication among distributed processing elements. Activations, intermediate results, and partial sums must move between tiles as inference progresses through neural-network layers.

The figure depicts packetized on-die communication networks, multicast pathways, and contention-aware arbitration systems supporting this exchange. These routing mechanisms ensure that data movement remains efficient while avoiding bottlenecks that could negate locality advantages earned elsewhere in the system.

An especially important element of the routing layer is its integration with digital scheduling systems and compiler runtimes. These components monitor execution behavior, coordinate communication patterns, and allocate resources dynamically across distributed compute-memory domains.

The presence of digital vector units highlights another important architectural characteristic: processing-in-memory systems are rarely purely analog. Instead, they typically combine analog and digital resources into hybrid computational environments optimized for different portions of the workload.

A broader insight emerging from the figure is that locality operates as the central organizing principle of the architecture. Parameter locality reduces weight transfers. Computational locality enables in-situ matrix multiplication. Communication locality minimizes routing distance among

macro-arrays. Together, these forms of locality reduce the cost of moving information throughout the system.

The figure also illustrates a shift in the role of memory within AI accelerators. In traditional architectures, memory stores information and computation occurs elsewhere. Here, memory simultaneously stores parameters, performs arithmetic operations, and participates in communication. The distinction between memory and computation therefore becomes increasingly blurred.

From a systems-engineering perspective, the architecture demonstrates how multiple hardware innovations reinforce one another. Static weight residency supports in-situ multiplication. Mixed-signal interfaces preserve numerical stability. Routing fabrics coordinate distributed execution. None of these mechanisms achieves its full potential independently.

Another important observation is that the architecture addresses several limitations simultaneously. Data movement decreases, latency becomes more predictable, energy consumption falls, and scalability improves. These advantages arise primarily through architectural restructuring rather than through increasing arithmetic throughput alone.

Ultimately, Figure 8.4-B3 demonstrates how processing-in-memory architectures redefine the relationship between memory and computation. Through localized parameter residency, analog in-situ matrix multiplication, mixed-signal coordination, and distributed routing fabrics, the architecture transforms memory from a passive storage resource into an active computational substrate. This approach represents one of the most significant emerging directions in AI accelerator design, offering a pathway toward higher efficiency, lower energy consumption, and improved scalability as model sizes continue to grow.

With the complete processing-in-memory architecture now established, Figure 8.4-B3 illustrates how memory-resident computation emerges from the coordinated interaction of static weight storage, analog compute fabrics, mixed-signal conversion layers, and distributed communication networks. Among these architectural components, the **analog macro-array** occupies a foundational role because it serves as the primary location where computation occurs directly within the memory fabric. Before static weight residency can eliminate repeated parameter transfers, before mixed-signal interfaces can preserve numerical integrity, and before routing fabrics can coordinate distributed execution, the architecture must first provide a mechanism capable of performing matrix multiplication inside the memory array itself. Analog macro-arrays deliver this capability by embedding neural-network weights directly within crossbar structures and exploiting the physical properties of current flow and charge accumulation to execute multiply-accumulate operations in situ. In doing so, they collapse the traditional boundary

between storage and computation, transforming memory from a passive repository into an active computational substrate. The following discussion examines **Analog AI Macro-Arrays for In-Situ Matrix Multiplication**, exploring the architectural principles, mixed-signal mechanisms, and computational behaviors that make these arrays the cornerstone of memory-centric AI acceleration.

i. Analog AI Macro-Arrays for In-Situ Matrix Multiplication

Analog AI macro-arrays for in-situ matrix multiplication represent a fundamental rethinking of how multiply-accumulate operations are performed in large-scale AI accelerators. Instead of transporting operands from memory to compute units, these macro-arrays embed computation directly inside the memory fabric, using charge accumulation, crossbar conduction paths, and mixed-signal multiply-accumulate primitives to execute matrix operations where the data physically resides. This eliminates the traditional load-store pipeline and collapses the energy and latency overhead associated with repeatedly fetching static weights from external memory.

Modern transformer workloads exhibit extreme weight reuse: the same projection matrices, attention kernels, and feed-forward blocks are applied across thousands of tokens. Analog macro-arrays exploit this locality by storing weights directly in crossbar cells and performing vector-matrix multiplication through analog current summation. Because the computation occurs in situ, the energy per operation is orders of magnitude lower than digital MACs, and the latency is dominated by signal propagation rather than memory movement. This enables accelerators to sustain high throughput even when external bandwidth is saturated.

A deeper technical evaluation reveals the complexity of designing analog macro-arrays that deliver predictable numerical behavior. Device variability, charge leakage, non-linear conduction paths, and temperature-dependent drift all influence the accuracy of analog MAC operations. To compensate, accelerators incorporate calibration loops, reference cells, and periodic refresh cycles that stabilize analog behavior. Mixed-signal interfaces convert analog partial sums into digital representations, applying quantization, gain correction, and noise filtering to ensure numerical correctness. Compiler frameworks must generate analog-friendly kernel layouts, map weights to crossbar cells efficiently, and fuse operations to maximize reuse within the analog domain.

When properly integrated, analog macro-arrays provide dense, energy-efficient compute capability that dramatically reduces the cost of matrix multiplication—the dominant operation in transformer inference. They form the foundation of processing-in-memory architectures, enabling accelerators to bypass traditional memory hierarchies and execute large-scale models with significantly lower energy and latency.

ii. AI Weight Locality and On-Die Static Memory Pinning

I weight locality and on-die static memory pinning address the bandwidth and latency bottlenecks that arise when large models repeatedly access the same parameter blocks across long sequences. Transformer inference requires constant reuse of projection matrices, attention kernels, and feed-forward weights. Without architectural support for locality, these repeated accesses saturate DRAM bandwidth, introduce latency spikes, and starve compute units even when scheduling logic is fully optimized.

Static memory pinning resolves this by keeping frequently accessed weights resident in tightly coupled on-die memory fabrics—SRAM clusters, non-volatile arrays, or specialized static-weight banks. These fabrics provide deterministic access latency and eliminate redundant transfers from external memory. Weight pinning is especially critical for MoE architectures, where expert weights must be accessed rapidly and unpredictably based on token-level routing decisions. By maintaining expert weights on-die, accelerators avoid the bandwidth explosion that would otherwise occur when routing thousands of tokens across dozens of experts.

A full technical evaluation reveals how static weight fabrics must balance capacity, locality, and thermal constraints. On-die memory is limited, so compilers must generate weight-locality maps that identify which parameters should be pinned, which can be streamed, and which require dynamic eviction. These maps incorporate model structure, token-level routing statistics, and kernel-fusion opportunities to maximize reuse. Hardware must support rapid pinning and eviction without introducing contention or disrupting ongoing compute operations. Memory controllers must coordinate with scheduling logic to ensure that pinned weights remain accessible even when multiple workgroups compete for the same parameter blocks.

When properly integrated, static weight pinning stabilizes latency, reduces external bandwidth pressure, and ensures that compute units remain fully utilized. It transforms the accelerator into a locality-optimized system where the most frequently accessed parameters are always physically close to the compute units that need them.

iii. AI Digital-to-Analog Boundaries and Voltage Stability Management

AI digital-to-analog boundaries and voltage stability management ensure numerical correctness across the mixed-signal interfaces that connect analog macro-arrays to digital compute pipelines. As accelerators increasingly rely on analog in-situ computation, the boundary between analog and digital domains becomes a critical architectural element. Analog signals must be converted into digital representations with sufficient precision, stability, and noise tolerance to support large-scale inference without numerical drift.

Mixed-signal boundaries manage quantization domains, voltage levels, gain factors, and signal integrity during analog-digital transitions. Analog partial sums are susceptible to noise, device variability, and voltage fluctuations, requiring robust conversion logic that applies filtering, calibration, and normalization. Voltage stability management ensures that analog operations remain within safe operating ranges, preventing saturation, clipping, or drift that could corrupt computation. This is especially important for large crossbar arrays, where voltage gradients can accumulate across long conduction paths.

A deeper technical evaluation reveals how mixed-signal pipelines must coordinate with analog macro-arrays, static weight fabrics, and digital schedulers. Conversion units must track quantization boundaries, apply dynamic gain control, and synchronize analog outputs with digital clock domains. They must also support rollback and hazard detection to ensure that analog errors do not propagate into downstream digital pipelines. Compiler frameworks must annotate analog boundaries, generate quantization metadata, and fuse kernels to minimize analog-digital transitions.

When properly integrated, digital-to-analog boundaries preserve numerical stability across mixed-signal execution, enabling analog macro-arrays to deliver energy-efficient computation without sacrificing accuracy. They form the glue that binds analog processing-in-memory to the broader digital execution pipeline.

iv. Inter-Macro AI Data Shuffling and Dynamic Bus Routing

Inter-macro AI data shuffling and dynamic bus routing enable distributed analog and mixed-signal compute tiles to operate as a unified inference engine. As processing-in-memory architectures scale, computation is spread across multiple macro-arrays, each performing in-situ matrix multiplication on different portions of the model. To execute large transformer layers coherently, activations, partial sums, and intermediate tensors must be routed efficiently between these distributed tiles.

Dynamic bus routing resolves this by providing flexible interconnect fabrics that adapt to workload structure, routing patterns, and model topology. These fabrics may include crossbar switches, packetized on-die networks, or hierarchical bus structures that support multicast, broadcast, and point-to-point communication. Data shuffling ensures that activations are delivered to the correct macro-arrays, partial sums are aggregated coherently, and distributed compute tiles remain synchronized even when executing large, partitioned layers.

A deeper technical evaluation reveals how routing fabrics must balance bandwidth, locality, and contention. Inter-macro communication must avoid bottlenecks that could stall analog macro-arrays or disrupt static weight streaming. Routing logic must coordinate with scheduling

mechanisms to ensure that data arrives at the correct macro-array in time for execution. Compiler frameworks must generate routing plans, partition layers across macro-arrays, and fuse kernels to minimize inter-macro communication.

When properly integrated, inter-macro data shuffling transforms distributed analog compute tiles into a cohesive processing-in-memory system capable of executing massive models with high efficiency. It ensures that analog macro-arrays, static weight fabrics, and mixed-signal pipelines operate together as a unified architecture rather than isolated components.

With processing-in-memory architectures collapsing computation into the memory fabric and static weight streaming stabilizing bandwidth under massive model loads, the next frontier lies in how accelerators dynamically reshape their spatial compute topology to match the structure of incoming workloads. Modern AI graphs are not uniform; they contain sparse regions, dense projection blocks, conditional branches, and dynamically routed MoE experts. To execute these patterns efficiently, hardware must be able to reconfigure its spatial layout—remapping compute tiles, rewiring interconnects, bypassing inactive cores, and adapting data-flow paths in real time. This capability defines the domain of reconfigurable AI spatial architectures and coarse-grained arrays, where compute fabrics behave less like fixed pipelines and more like programmable spatial machines. The discussion now turns to how coarse-grained reconfigurable arrays mitigate routing overheads, how dynamic interconnects map neural graphs onto spatial fabrics, how bypass networks preserve data-flow efficiency, and how real-time context switching enables accelerators to adapt instantly to changing workloads.

d. Reconfigurable AI Spatial Architectures and Coarse-Grained Arrays

Reconfigurable AI spatial architectures and coarse-grained arrays represent a shift from fixed-function compute pipelines toward programmable spatial fabrics capable of adapting to the structural variability of modern neural networks. Unlike traditional SIMD or systolic designs, which assume uniform data-flow patterns, coarse-grained reconfigurable arrays (CGRAs) allow compute tiles, routing channels, and data-flow paths to be reconfigured at runtime. This flexibility is essential for executing transformer models, MoE layers, sparse attention mechanisms, and dynamic graph workloads that exhibit irregular compute density and conditional branching.

Spatial reconfigurability enables accelerators to tailor their compute topology to each workload. Dense projection layers can be mapped onto tightly coupled compute clusters; sparse attention windows can be routed through lightweight bypass networks; MoE experts can be isolated into dedicated regions; and conditional branches can be executed without forcing the entire fabric to follow the same path. This adaptability reduces routing overhead, minimizes idle compute

regions, and ensures that the accelerator maintains high utilization even when the neural graph is structurally uneven.

A deeper technical evaluation reveals how CGRA routing, dynamic interconnect configuration, data-flow topologies, and real-time context switching cooperate to deliver this flexibility. CGRA routing logic must manage coarse-grained tiles, allocate spatial resources, and avoid congestion. Dynamic interconnects must map neural graphs onto physical fabrics efficiently. Data-flow topologies must support bypass networks that prevent inactive cores from stalling active ones. And real-time context switching must allow the fabric to reconfigure instantly as workloads change. Together, these mechanisms transform the accelerator into a spatially adaptive compute engine capable of executing large-scale AI models with high efficiency under dynamic and irregular conditions.

With the spatial reconfigurability framework now established—programmable CGRA tiles, dynamic interconnect fabrics, bypass networks, and real-time context switching—the next step is to organize these mechanisms into their functional dimensions. Each capability addresses a different structural challenge inherent to modern AI workloads: routing congestion in dense projection layers, dynamic graph mapping for MoE and sparse attention, bypassing inactive compute regions, and adapting instantly to conditional execution paths. To clarify how these mechanisms interact and how they collectively transform the accelerator into a spatially adaptive compute fabric, the following table summarizes their architectural roles, hardware techniques, and AI-level impact.

Table 8.4-B3 examined how processing-in-memory architectures reduce data-movement overhead by integrating computation directly within memory structures and maintaining high-value parameters close to execution resources. While these architectures substantially improve locality and energy efficiency, they often operate within fixed physical topologies whose computational pathways are largely predetermined. Modern AI workloads, however, are increasingly characterized by dynamic execution patterns, sparse expert routing, conditional computation, evolving neural-graph structures, and rapidly changing dataflow requirements. Accommodating these behaviors efficiently requires hardware capable not only of executing workloads but also of adapting its computational topology at runtime. Reconfigurable spatial architectures and coarse-grained reconfigurable arrays (CGRAs) address this challenge by allowing computational resources, routing pathways, and communication fabrics to be dynamically reorganized according to workload demands. Table 8.4-B4 examines the core mechanisms that enable this adaptability and illustrates how spatially reconfigurable hardware provides an increasingly important foundation for next-generation AI acceleration.

Table 8.4-B4 presents several foundational mechanisms that support reconfigurable AI spatial

architectures and coarse-grained reconfigurable arrays. These architectures represent a significant evolution beyond fixed-function accelerators by enabling computational structures to be dynamically adapted to the requirements of changing AI workloads.

Traditional accelerators are often optimized for specific computational patterns, such as dense matrix multiplication or transformer-style attention execution. While highly efficient under expected workloads, fixed architectures may struggle when execution graphs become dynamic, sparse, or conditionally routed. As AI systems increasingly incorporate mixture-of-experts algorithms, adaptive attention mechanisms, state-space architectures, and conditional-computation pipelines, accelerator fabrics must become correspondingly more flexible.

Reconfigurable spatial architectures address this challenge by allowing computational resources, routing channels, and execution pathways to be reorganized at runtime. Rather than forcing workloads to adapt to hardware constraints, these architectures partially adapt hardware behavior to workload structure.

The table identifies four key mechanisms that support this flexibility: CGRA routing optimization, dynamic interconnect configuration and graph mapping, dataflow topologies with bypass networks, and real-time context switching in reconfigurable hardware. Together, these mechanisms enable hardware fabrics to respond dynamically to changing execution requirements while maintaining high throughput and efficient resource utilization.

By examining the interaction between spatial computation, routing infrastructure, and runtime adaptation, the table highlights how reconfigurable architectures are reshaping the relationship between hardware resources and AI execution patterns.

Table 8.4-B4 — Core Mechanisms in Reconfigurable AI Spatial Architectures and Coarse-Grained Arrays

Mechanism	Primary Function	Hardware Techniques	AI-Level Impact
CGRA Routing Overheads in AI Spatial Fabrics	Allocate coarse compute tiles and routing channels efficiently under dynamic AI workloads.	Tile-level routing, congestion control, coarse-grain path allocation, rapid reconfiguration.	Reduces routing latency, prevents congestion, improves utilization under dense/sparse graph regions.
Dynamic AI Interconnect	Rewire spatial fabrics at runtime to match	Programmable buses, packetized networks,	Adapts topology to workload, reduces

Mechanism	Primary Function	Hardware Techniques	AI-Level Impact
Configuration and Graph Mapping	neural graph structure.	crossbar switches, graph-mapping metadata.	communication overhead, accelerates MoE and sparse attention.
AI Data-Flow Topologies and Processing-Core Bypass Networks	Enable efficient data movement around inactive or irrelevant compute tiles.	Bypass channels, lightweight mesh links, hierarchical routing paths.	Prevents bottlenecks, reduces latency, preserves throughput under irregular control flow.
Real-Time AI Context Switching in Reconfigurable Hardware	Reconfigure spatial fabrics instantly as workloads change.	Fast tile reconfiguration, routing-state save/restore, low-latency context transitions.	Enables dynamic model switching, conditional execution, and adaptive inference pipelines.

Table 8.4-B4 demonstrates a fundamental shift in accelerator design philosophy. Rather than relying exclusively on fixed execution pathways, reconfigurable architectures continuously adjust computational topology, communication routes, and resource allocation according to workload characteristics.

The mechanisms summarized in the table reveal a common objective: maximizing hardware utilization by dynamically aligning computational infrastructure with the structure of the executing AI graph. This adaptability becomes increasingly important as modern AI systems move away from static execution models and toward highly dynamic computational behaviors.

The first mechanism identified in the table is **CGRA routing overhead reduction in AI spatial fabrics**.

Coarse-grained reconfigurable arrays consist of programmable compute tiles connected through configurable routing networks. While this flexibility enables adaptation to changing workloads, routing itself can become a performance bottleneck if data paths are not organized efficiently.

The table highlights tile-level routing, congestion-control strategies, coarse-grained path allocation, and rapid reconfiguration mechanisms as important techniques for managing this challenge. These mechanisms reduce communication delays, prevent routing hotspots, and ensure that computational resources remain well connected under varying execution

conditions.

A significant benefit noted in the table is improved utilization under both dense and sparse graph regions. This capability is particularly valuable in AI workloads that exhibit highly uneven computational demands across different parts of the model.

The second mechanism is **dynamic AI interconnect configuration and graph mapping**.

Modern AI workloads often generate execution graphs whose structure varies according to data, routing decisions, attention patterns, or conditional logic. Static interconnect architectures may struggle to accommodate such variability efficiently.

Dynamic graph mapping addresses this challenge by continuously adapting communication pathways to match evolving graph structures. The hardware techniques listed in the table, including programmable buses, packetized networks, crossbar switches, and graph-mapping metadata, enable accelerator fabrics to reorganize communication patterns in response to workload demands.

The resulting adaptability provides significant advantages for architectures such as mixture-of-experts systems and sparse-attention networks, where communication requirements may change dramatically between inference steps.

The third mechanism identified in the table is **AI dataflow topologies and processing-core bypass networks**.

Not all regions of an AI model require identical amounts of computation. Some execution paths may remain inactive, while others may become temporarily overloaded. Inefficient routing through inactive components can introduce unnecessary latency and bandwidth consumption.

Bypass networks address this problem by providing alternative communication routes around underutilized or irrelevant compute resources. The table references lightweight mesh links, hierarchical routing paths, and dedicated bypass channels as important implementation strategies.

These mechanisms reduce communication bottlenecks and preserve throughput under irregular control-flow conditions. As modern AI systems increasingly employ dynamic execution pathways, efficient bypass capabilities become essential for maintaining predictable performance.

The fourth mechanism is **real-time AI context switching in reconfigurable hardware**.

Adaptive systems often require rapid transitions among multiple execution contexts. Workloads

may shift between different model segments, expert groups, inference pipelines, or processing modes within very short timescales.

The table identifies fast tile reconfiguration, routing-state save-and-restore operations, and low-latency context transitions as enabling technologies supporting these capabilities. Through these mechanisms, spatial architectures can rapidly repurpose computational resources without requiring complete reconfiguration of the hardware fabric.

This flexibility enables dynamic model switching, conditional execution, and adaptive inference behaviors that would be difficult to implement efficiently on more rigid accelerator architectures.

A broader insight emerging from the table is that reconfigurability increasingly functions as a performance feature rather than merely a flexibility feature. Historically, programmable systems often sacrificed efficiency for adaptability. The mechanisms described here demonstrate how modern architectures seek to provide both.

The table also illustrates that communication infrastructure is becoming nearly as important as arithmetic capability. As AI graphs become more distributed and dynamic, moving information efficiently among computational resources frequently determines overall system performance.

From a systems-engineering perspective, the four mechanisms operate at complementary levels of adaptation. Routing optimization improves local communication efficiency. Dynamic graph mapping adapts global connectivity. Bypass networks streamline dataflow movement. Context switching enables rapid transitions among execution modes. Together, they create a flexible computational fabric capable of supporting diverse workload characteristics.

Another important observation is that these mechanisms align naturally with many advanced AI architectures explored earlier in Section 8.4. Sparse expert routing, conditional-computation pipelines, memory-aware attention mechanisms, and state-space models all benefit from hardware that can adapt dynamically to changing execution structures.

The table further demonstrates a broader trend in AI hardware evolution: future performance improvements are increasingly likely to emerge from intelligent resource organization rather than solely from improvements in arithmetic throughput.

Ultimately, Table 8.4-B4 illustrates how reconfigurable AI spatial architectures transform hardware from a static execution substrate into an adaptive computational fabric. Through dynamic routing, graph-aware interconnects, intelligent dataflow management, and real-time context switching, these architectures align physical hardware topology with evolving AI workloads. The result is improved utilization, reduced communication overhead, greater

execution flexibility, and enhanced scalability for next-generation AI systems operating under increasingly dynamic computational demands.

Table 8.4-B4 identified the principal mechanisms that enable reconfigurable AI spatial architectures to adapt dynamically to changing neural-network workloads, including routing optimization, graph-aware interconnect configuration, dataflow bypass networks, and real-time context switching. Although these mechanisms can be examined individually, their true significance emerges when viewed as parts of an integrated spatial-computing fabric. In practice, reconfigurable hardware continuously coordinates compute tiles, communication paths, routing metadata, and execution contexts to align physical topology with evolving computational demands. Figure 8.4-B4 illustrates this coordinated architecture, showing how coarse-grained compute tiles, dynamic interconnect layers, bypass networks, and context-switching infrastructure interact to create a flexible execution environment capable of supporting sparse, conditional, and dynamically evolving AI workloads.

Figure 8.4-B4 presents a system-level view of a reconfigurable AI spatial architecture built upon a coarse-grained reconfigurable array (CGRA) topology. The figure illustrates how programmable compute resources, adaptive communication fabrics, and runtime reconfiguration mechanisms cooperate to support dynamic AI execution.

Unlike fixed-function accelerators, which rely on predetermined computational pathways, CGRA-based architectures permit hardware resources to be reassigned as workloads change. This flexibility is increasingly important because contemporary AI models often exhibit dynamic execution patterns arising from sparse attention, mixture-of-experts routing, conditional computation, and adaptive inference pipelines.

The figure organizes the architecture into three principal layers. The upper layer contains coarse-grained compute tiles responsible for executing AI workloads. The middle layer provides dynamic interconnect resources that establish communication paths among compute tiles. The lower layer contains bypass networks and routing optimizations that maintain efficient dataflow when portions of the computational graph become inactive or conditionally executed.

By illustrating how computation, communication, and reconfiguration operate together, the figure demonstrates how spatial architectures transform hardware from a static execution platform into an adaptive computational fabric.

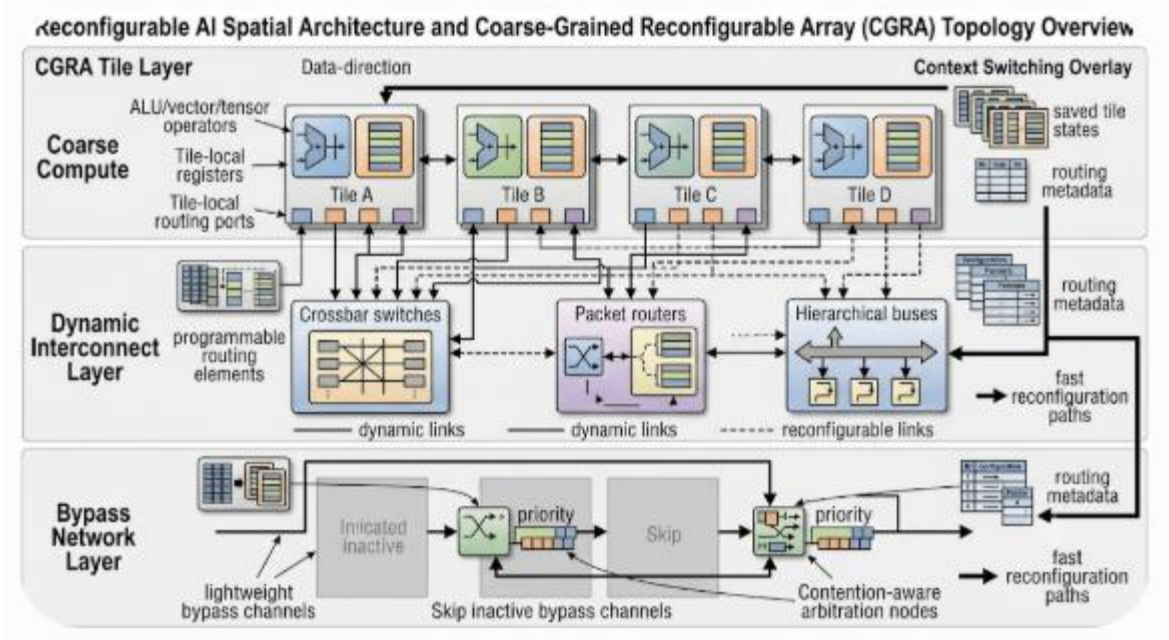


Figure 8.4-B4 — Reconfigurable AI Spatial Architecture and CGRA Topology Overview

Multi-layer spatial-computing architecture illustrating how coarse-grained reconfigurable arrays dynamically adapt hardware topology to evolving AI workloads. The figure traces interactions among programmable compute tiles, dynamic interconnect fabrics, bypass networks, and context-switching mechanisms. Together, these components reduce routing congestion, improve resource utilization, support sparse and conditional computation, and enable real-time adaptation of accelerator topology to workload requirements.

Legend

Component	***Description***
CGRA Tile Layer	*Computation layer consisting of programmable coarse-grained processing elements.*
Tile A–D	*Representative AI compute tiles executing neural-network operations.*
ALU / Vector / Tensor Operators	*Processing resources contained within each tile.*
Tile-Local Registers	*Local storage resources supporting computation and rapid state access.*

Tile-Local Routing Ports	*Interfaces connecting tiles to the interconnect fabric.*
Data-Direction Flow	*Primary computational flow through the CGRA topology.*
Context Switching Overlay	*Runtime mechanism supporting rapid hardware reconfiguration.*
Saved Tile States	*Preserved execution states enabling fast context transitions.*
Routing Metadata	*Configuration information governing topology adaptation.*
Dynamic Interconnect Layer	*Communication fabric linking compute resources.*
Crossbar Switches	*Reconfigurable routing elements supporting flexible connectivity.*
Packet Routers	*Routing units handling distributed communication among tiles.*
Hierarchical Buses	*Shared communication channels supporting large-scale coordination.*
Programmable Routing Elements	*Configurable interconnect components adapting to workload structure.*
Dynamic Links	*Reconfigurable communication pathways established at runtime.*
Reconfigurable Links	*Alternate connectivity paths supporting topological adaptation.*
Fast Reconfiguration Paths	*Dedicated channels accelerating topology updates.*
Bypass Network Layer	*Routing subsystem designed to circumvent inactive or congested regions.*
Inactive Tile Region	*Example of a compute area bypassed during execution.*
Lightweight Bypass Channels	*Low-overhead routes around inactive resources.*
Skip-Inactive Bypass Channels	*Dynamic routing paths avoiding unused compute nodes.*

Priority Routing	*Scheduler-controlled routing strategy favoring important traffic.*
Contention-Aware Arbitration Nodes	*Mechanisms reducing congestion and communication conflicts.*

Figure 8.4-B4 illustrates a key principle of modern reconfigurable computing: hardware efficiency can be improved not only by accelerating computation but also by adapting hardware topology to the structure of the workload being executed.

The figure demonstrates how spatial architectures continuously reorganize communication pathways, compute resources, and execution contexts in response to changing computational requirements. Rather than forcing workloads to conform to fixed hardware layouts, the architecture dynamically reshapes itself to support efficient execution.

The architecture begins with the **CGRA Tile Layer**, which forms the computational foundation of the system.

Each tile contains arithmetic resources, vector-processing units, tensor operators, local registers, and tile-level routing interfaces. Unlike traditional processor cores that execute general-purpose instruction streams, CGRA tiles are optimized for coarse-grained computational tasks commonly encountered in AI workloads.

The figure illustrates a sequence of representative tiles labeled A through D. These tiles communicate through both local and global routing resources while executing portions of the overall neural-network graph.

An important feature of this layer is its modularity. Individual tiles can be assigned to different portions of a workload and reconfigured as execution requirements change. This flexibility provides the basis for the runtime adaptability emphasized throughout the remainder of the figure.

Positioned above the tile layer is the **context-switching overlay**, which provides one of the architecture's most important capabilities.

Traditional accelerators often require significant time to transition between execution configurations. In contrast, the figure shows dedicated support for saved tile states and routing metadata. These resources allow execution contexts to be preserved and restored rapidly, enabling hardware resources to transition between workload configurations with minimal

interruption.

This capability plays a particularly important role in conditional-computation systems and multi-model inference environments where execution requirements can change frequently.

Below the tile layer lies the **dynamic interconnect layer**, which forms the communication infrastructure connecting distributed computational resources.

The figure highlights three major routing mechanisms: crossbar switches, packet routers, and hierarchical buses. Together, these elements provide flexible pathways through which activations, parameters, and intermediate tensors can move between compute resources.

Crossbar switches provide fine-grained reconfiguration capability, packet routers support scalable communication among distributed units, and hierarchical buses enable coordination across larger regions of the hardware fabric.

One of the most important characteristics of this layer is its ability to establish dynamic links at runtime. Communication pathways are not fixed; instead, they are constructed and modified according to workload requirements. As AI execution graphs evolve, communication topology evolves alongside them.

The figure also emphasizes the presence of **reconfigurable routing links** and **fast reconfiguration paths**, which accelerate transitions between communication configurations. These capabilities reduce the latency associated with topology adaptation and enable rapid alignment of hardware resources with changing workload structures.

The final architectural layer is the **bypass network subsystem**.

Modern AI workloads frequently contain sparse regions, conditionally activated pathways, and inactive computational blocks. Routing all traffic through these regions would introduce unnecessary latency and reduce overall efficiency.

The bypass layer addresses this challenge by providing alternative pathways around inactive or congested resources. The figure illustrates lightweight bypass channels, skip-inactive routing paths, priority-routing structures, and contention-aware arbitration mechanisms.

These components allow communication traffic to avoid regions that contribute little or no useful computation. This capability becomes increasingly important in mixture-of-experts architectures, sparse-attention systems, and conditional-computation models where execution activity varies significantly across the computational graph.

A particularly important observation emerging from the figure is that communication itself

becomes a programmable resource. Rather than relying on fixed interconnect structures, the architecture actively manages routing according to changing execution requirements.

The figure also highlights the hierarchical nature of adaptation. Compute tiles are reconfigurable. Interconnect pathways are reconfigurable. Context states are reconfigurable. Routing priorities are reconfigurable. Together, these layers create a deeply adaptive hardware environment.

From a systems-engineering perspective, the architecture seeks to maximize utilization while minimizing communication overhead. Routing optimization reduces latency. Dynamic graph mapping aligns topology with workload structure. Bypass networks eliminate unnecessary communication. Context switching reduces reconfiguration overhead. Each layer contributes to the same overall objective.

Another important insight is that many contemporary AI architectures inherently generate irregular execution patterns. Sparse expert routing, conditional activation, dynamic context management, and adaptive attention mechanisms all benefit from hardware capable of adapting in parallel with software behavior. The CGRA topology shown here is specifically designed to accommodate such variability.

The figure further demonstrates that flexibility and efficiency need not be opposing objectives. Historically, programmable systems often sacrificed performance for adaptability. Modern reconfigurable AI fabrics increasingly combine both by allowing hardware resources to be reorganized while maintaining high computational throughput.

Ultimately, Figure 8.4-B4 illustrates how reconfigurable spatial architectures transform AI accelerators into adaptive computational fabrics. Through programmable compute tiles, dynamic interconnect networks, intelligent bypass mechanisms, and low-latency context switching, the architecture continuously reshapes itself to match evolving workload requirements. This ability to align physical hardware topology with computational structure represents a significant advancement in AI accelerator design and provides a scalable foundation for increasingly dynamic and heterogeneous AI workloads.

With the structure of the reconfigurable spatial fabric now established, Figure 8.4-B4 illustrates how coarse-grained compute tiles, adaptive interconnect networks, bypass pathways, and context-switching mechanisms cooperate to create a dynamically reconfigurable execution environment. At the center of this architecture lies the **routing infrastructure**, which serves as the connective tissue linking distributed computational resources into a coherent processing fabric. Regardless of how capable individual compute tiles may be, overall system performance ultimately depends on the efficiency with which activations, intermediate tensors, and partial

results are transported among them. Consequently, routing behavior directly influences latency, bandwidth utilization, resource occupancy, and throughput across the entire accelerator. This challenge becomes particularly significant in modern AI workloads characterized by sparse attention patterns, mixture-of-experts routing, conditional-computation graphs, and dynamically changing execution paths, all of which generate highly irregular communication demands. Efficient operation therefore requires sophisticated routing mechanisms capable of allocating channels dynamically, mitigating congestion, adapting communication pathways at runtime, and coordinating closely with compiler-generated graph mappings. The following discussion examines **Coarse-Grained Reconfigurable Architecture (CGRA) Routing Overheads in AI Spatial Compute Fabrics**, exploring the routing strategies, congestion-management techniques, and hardware–software coordination mechanisms that determine the efficiency and scalability of reconfigurable AI execution fabrics.

i. Coarse-Grained Reconfigurable Architecture (CGRA) Routing Overheads in AI Spatial Compute Fabrics

Coarse-grained reconfigurable architectures introduce programmable compute tiles and routing channels that can be reshaped at runtime to match the structure of incoming AI workloads. Unlike fine-grained FPGA routing—which configures individual logic gates—CGRAs operate at a higher level of abstraction, configuring clusters of ALUs, vector units, or tensor operators along with the coarse routing channels that connect them. This coarse granularity provides far greater flexibility and lower configuration overhead, but it also introduces routing challenges that must be carefully managed to maintain performance under modern AI workloads.

Routing overhead in CGRAs arises from the need to allocate tile-to-tile communication paths efficiently across highly variable neural-graph structures. Dense projection layers demand tightly coupled compute clusters with short, high-bandwidth routes; sparse attention windows require long-range lightweight paths; MoE expert routing requires dynamic dispatch to isolated tile regions; and conditional branches require rapid remapping of spatial resources without forcing the entire fabric to follow the same execution path. Each of these patterns imposes different routing demands, and the CGRA must adapt without introducing latency spikes or congestion.

To meet these demands, CGRA routing logic must manage spatial resources with precision. It must allocate routing channels efficiently, avoid congestion across shared paths, and ensure that data-flow routes remain short enough to prevent performance collapse. Hardware support is essential: the fabric must provide rapid reconfiguration, low-overhead routing updates, and contention-aware arbitration across shared channels. Routing tables must be updated without disrupting ongoing computation, and programmable switches must be able to retime

communication paths on a cycle-accurate basis.

Compilers and runtimes play an equally critical role. They must generate spatial mapping plans that identify optimal tile placements, fuse kernels to reduce inter-tile communication, and partition neural graphs into spatially coherent regions. They must also generate routing metadata that allows hardware to configure the fabric quickly and efficiently. When hardware and software cooperate effectively, CGRA routing enables accelerators to adapt their spatial topology to each workload, reducing idle compute regions, minimizing communication overhead, and improving overall utilization.

Having established how CGRA routing overheads shape the efficiency of spatial compute fabrics—allocating tile-to-tile channels, managing congestion, and determining the physical paths through which activations and partial sums propagate—the next step is to examine how these routing resources are orchestrated at a higher level. Routing alone cannot guarantee efficient execution of modern AI workloads; the interconnect fabric must be dynamically reconfigured to reflect the structure of the neural graph itself. Dense projection layers demand tightly coupled clusters, sparse attention windows require long-range lightweight paths, MoE experts must be isolated into dedicated regions, and conditional branches must be mapped without forcing the entire fabric to follow the same route. This is the role of dynamic interconnect configuration and graph-mapping layers: they translate the logical structure of the AI model into a physical spatial topology, rewiring buses, packet networks, and crossbar switches in real time. The discussion now turns to how these programmable interconnects adapt to neural-graph structure, minimize communication overhead, and enable spatial fabrics to operate as fully reconfigurable AI execution engines.

ii. Dynamic AI Interconnect Configuration and Graph Mapping Layers

Dynamic interconnect configuration is the architectural capability that allows an accelerator's spatial fabric to rewire itself at runtime, aligning physical communication pathways with the evolving structure of modern neural graphs. Contemporary AI models exhibit extreme structural diversity: dense projection layers with high fan-in/fan-out patterns, sparse attention windows with irregular connectivity, MoE expert routing with token-dependent dispatch, and conditional branches that activate only a subset of the model's compute regions. Static interconnects cannot accommodate this variability. They impose fixed routing paths that quickly become congested, force long detours through irrelevant tiles, and leave large portions of the fabric underutilized.

Dynamic interconnects resolve these limitations by introducing programmable routing fabrics capable of adapting to workload structure. These fabrics may include hierarchical buses for

coarse-grain communication, packetized networks for flexible multi-hop routing, crossbar switches for high-bandwidth local connectivity, and mesh-based interconnects that support multicast, broadcast, and point-to-point communication. Each of these elements can be reconfigured at runtime, allowing the accelerator to tailor its communication topology to the specific demands of the neural graph.

Graph-mapping layers orchestrate this reconfiguration. They analyze the logical structure of the model, identify clusters of operations that benefit from tight coupling, and generate routing plans that minimize communication overhead. Dense projections may be mapped onto tightly interconnected tile clusters; sparse attention windows may be routed through lightweight long-range paths; MoE experts may be isolated into dedicated regions with high-bandwidth ingress and egress; and conditional branches may be mapped in ways that avoid forcing the entire fabric to follow the same execution path. The mapping process ensures that the physical topology mirrors the logical graph, reducing latency and preventing congestion.

Hardware support is essential for making this dynamic behavior viable. The interconnect fabric must support rapid reconfiguration, low-latency routing updates, and contention-aware arbitration. Routing tables must be updated without disrupting ongoing computation, and programmable switches must be able to retime communication paths on a cycle-by-cycle basis. The fabric must also support partial reconfiguration, enabling only the affected regions to be updated when the graph changes.

Compilers and runtimes complement this hardware capability. They generate graph-mapping metadata, partition layers across compute tiles, fuse kernels to reduce interconnect traffic, and schedule reconfiguration events at natural execution boundaries. They must also ensure that routing plans remain coherent as the graph evolves, avoiding situations where dynamic interconnect updates conflict with CGRA tile allocations or bypass-network activation.

When hardware and software cooperate effectively, dynamic interconnects allow accelerators to adapt their spatial topology to each workload, reducing routing overhead, improving throughput, and sustaining high utilization even under highly irregular execution patterns. They transform the interconnect from a static communication backbone into a programmable, workload-aware routing fabric.

With dynamic interconnect configuration and graph-mapping layers establishing how the spatial fabric rewires itself to mirror the structure of the neural graph—allocating buses, packet routers, and crossbar switches to dense projections, sparse attention windows, MoE expert clusters, and conditional branches—the next challenge lies in ensuring that data moves through this reconfigurable topology efficiently. Even a perfectly mapped graph can suffer performance

collapse if activations and partial sums are forced to traverse inactive tiles, congested regions, or long detours created by uneven compute density. This is where AI data-flow topologies and processing-core bypass networks become essential. They define the physical routes through which tensors propagate, provide lightweight skip paths around idle or irrelevant tiles, and prevent bottlenecks that would otherwise stall the entire fabric. The discussion now turns to how bypass networks preserve throughput under sparse and conditional workloads, how data-flow topologies minimize latency across dynamically reconfigured fabrics, and how these mechanisms ensure that spatial architectures remain efficient even when only a fraction of the compute tiles is active.

iii. AI Data-Flow Topologies and Processing-Core Bypass Networks

AI data-flow topologies define the physical and logical routes through which activations, partial sums, and intermediate tensors propagate across a spatial compute fabric. In traditional fixed-function architectures, these routes are predetermined and rigid, forcing data to traverse every stage of the pipeline regardless of whether a given compute core is active or relevant to the current workload. This rigidity becomes a severe liability under modern AI workloads, where sparse attention windows, dynamically routed MoE experts, conditional branches, and token-dependent execution paths create highly uneven compute density. When inactive cores remain embedded in the routing path, they introduce unnecessary latency, increase congestion, and reduce overall utilization.

Processing-core bypass networks resolve this inefficiency by enabling data to flow around inactive or irrelevant compute regions. Instead of forcing tensors through every tile, bypass networks provide lightweight alternative routes—dedicated skip channels, streamlined mesh links, hierarchical routing paths, or dynamically activated detours—that allow data to circumvent unused tiles entirely. These bypass paths reduce latency, prevent bottlenecks, and ensure that sparse or conditional workloads do not stall the entire fabric. They also allow the spatial architecture to maintain high throughput even when only a subset of compute tiles are active.

A deeper architectural evaluation reveals that bypass networks cannot operate in isolation; they must coordinate tightly with CGRA routing logic, dynamic interconnect fabrics, and graph-mapping layers. Hardware must support low-latency bypass activation, contention-aware arbitration, and dynamic reconfiguration of routing tables. It must be able to detect inactive tiles, identify optimal skip paths, and update routing metadata without disrupting ongoing computation. The bypass fabric must also integrate with the broader spatial topology, ensuring that skip routes remain coherent as the graph evolves.

Compilers and runtimes play an equally critical role. They must generate data-flow metadata that identifies bypass opportunities, fuse kernels to reduce the number of required detours, and schedule bypass activation during natural execution boundaries. They must also ensure that bypass paths align with the dynamic interconnect configuration, avoiding situations where skip routes conflict with graph-mapping decisions or CGRA tile allocations. When properly orchestrated, bypass networks become a central mechanism for preserving data-flow efficiency across dynamically reconfigured fabrics.

When hardware and software cooperate effectively, bypass networks allow activations and partial sums to traverse the spatial fabric with minimal friction—skipping inactive tiles, avoiding congestion, and maintaining throughput even under sparse or conditional execution. They ensure that the physical data-flow topology remains aligned with the logical structure of the neural graph, preventing idle regions from becoming bottlenecks and enabling the accelerator to sustain high utilization across diverse and dynamically evolving workloads.

With data-flow topologies and bypass networks ensuring efficient traversal of the spatial fabric, the remaining challenge is enabling the architecture to adapt instantaneously as workloads evolve. Modern AI inference is inherently dynamic: token-dependent branching, MoE expert selection, multi-model pipelines, and runtime graph transformations all require the hardware to reconfigure its spatial layout on the fly. Efficient routing and bypass paths are only effective if the underlying configuration can be swapped, restored, or repurposed without stalling execution. This leads naturally into the domain of real-time context switching—the mechanisms that allow spatial fabrics to reshape themselves in response to changing neural-graph structure while maintaining continuous, high-performance execution.

iv. Real-Time AI Context Switching in Reconfigurable Hardware

Real-time context switching is the mechanism that allows reconfigurable spatial fabrics to adapt instantaneously to the shifting demands of modern AI workloads. Contemporary inference pipelines rarely execute a single, static computational graph; instead, they operate across multiple models, dynamically routed MoE experts, token-dependent branches, speculative execution paths, and runtime graph transformations. Each of these behaviors requires the hardware to reconfigure compute tiles, routing channels, and data-flow paths without interrupting execution. Without fast context switching, reconfigurable fabrics would incur reconfiguration stalls that cascade into latency spikes, throughput collapse, and severe underutilization.

To avoid these penalties, real-time context switching provides low-overhead mechanisms for saving, restoring, and updating spatial configurations. Hardware must support rapid tile

reprogramming, fast interconnect retiming, and near-instantaneous state transitions. This involves capturing tile-local register files, operator states, routing metadata, bypass-network configurations, and graph-mapping descriptors, then restoring them with minimal latency when the workload changes. The switching process must be granular enough to update only the regions affected by the new execution path, yet broad enough to reconfigure large portions of the fabric when the neural graph shifts significantly.

Compilers and runtimes play an equally critical role. They must generate context-switch metadata that describes how tile states, routing tables, and data-flow topologies should be saved and restored. They must partition workloads into switchable regions, fuse kernels to reduce the number of required transitions, and schedule context-switch events so that they occur during natural execution boundaries—such as token boundaries, expert selection steps, or attention-window shifts. They must also ensure that speculative or conditional branches have pre-materialized configurations ready for immediate activation.

When hardware and software cooperate effectively, real-time context switching enables the spatial fabric to behave like a continuously adaptive organism. It can pivot between dense and sparse compute regions, activate different MoE experts on a per-token basis, switch between models in multi-tenant inference pipelines, and reconfigure routing paths as the graph evolves. This adaptability preserves throughput, prevents idle compute regions, and ensures that the spatial fabric remains fully utilized even under highly dynamic and irregular AI workloads. Real-time context switching is therefore not merely an optimization—it is a foundational capability that allows reconfigurable architectures to operate at the speed and variability demanded by modern AI systems.

Reconfigurable AI spatial architectures and coarse-grained arrays establish a compute paradigm built around adaptability. Instead of relying on fixed pipelines, the accelerator becomes a programmable spatial fabric capable of reshaping its topology to match the structure of modern neural workloads. Coarse compute tiles provide the foundational substrate; dynamic interconnects rewire communication paths to reflect dense projections, sparse attention windows, MoE expert clusters, and conditional branches; bypass networks preserve data-flow efficiency by routing around inactive regions; and real-time context switching allows the fabric to reconfigure instantly as workloads evolve. Together, these capabilities ensure that the physical organization of the hardware mirrors the logical organization of the neural graph, minimizing routing overhead, reducing latency, and sustaining high utilization even under irregular or dynamically changing execution patterns. This spatial adaptability forms a critical architectural bridge between classical electrical compute fabrics and the emerging hybrid domains that integrate persistent memory, photonic signaling, and mixed-mode execution.

With spatial adaptability now established as a core architectural capability—allowing compute fabrics to reorganize themselves dynamically in response to workload structure—the next frontier lies in extending this flexibility beyond electrical routing and coarse-grained compute tiles. As AI models scale into trillion-parameter regimes and inference pipelines demand microsecond-level responsiveness, traditional volatile memory hierarchies and electrical interconnects impose hard physical limits on bandwidth, latency, and energy efficiency. Hybrid AI co-processors address these constraints by integrating non-volatile memory lattices, photonic interconnects, and emerging mixed-domain fabrics directly into the accelerator. These technologies enable persistent weight residency, ultra-low-latency optical communication, and new forms of compute-memory fusion that complement and extend the spatial reconfigurability established earlier. The discussion now turns to how hybrid co-processors merge electrical, non-volatile, and optical domains into a unified execution substrate capable of sustaining performance at unprecedented scale.

e. Hybrid AI Co-Processors with Non-Volatile Memory Lattices and Optical Interconnects

Hybrid AI co-processors represent a new class of compute architectures that fuse electrical, non-volatile, and photonic domains into a unified execution substrate. As foundation models scale into trillion-parameter regimes and inference pipelines demand microsecond-level responsiveness, conventional silicon architectures encounter hard physical limits. Volatile memory hierarchies impose high refresh and retention costs, electrical interconnects saturate under extreme bandwidth loads, and the traditional separation between compute and memory introduces latency penalties that compound across deep transformer stacks. Hybrid co-processors overcome these constraints by integrating persistent memory lattices, memristive crossbars, silicon-photonic waveguides, and mixed-domain synchronization mechanisms directly into the accelerator. The result is a heterogeneous compute fabric capable of sustaining unprecedented throughput while dramatically reducing energy consumption and communication overhead.

At the core of this paradigm is the shift away from classical Von Neumann execution. Hybrid co-processors collapse the distinction between compute and memory by embedding dense non-volatile memory (NVM) lattices—based on FeRAM, PCM, or RRAM—directly into the computational substrate. These lattices act as memristive crossbars that perform analog compute-in-memory (CIM), executing matrix–vector multiplications in a single cycle by encoding weights as programmable conductances and applying inputs as parallel voltages. Kirchhoff’s laws naturally accumulate partial sums, eliminating the need for data shuttling between discrete compute and memory units. This architecture removes static power leakage, minimizes data movement, and provides deterministic access latency even for long-sequence inference.

Global communication across the accelerator is then offloaded to silicon-photonic waveguides. Electrical copper interconnects suffer from RC delays, parasitic capacitance, and Joule heating at ultra-high frequencies, making them fundamentally unsuitable for trillion-parameter workloads. Photonic interconnects bypass these limitations entirely. Using wavelength-division multiplexing (WDM), dozens of independent data streams can be transmitted simultaneously through a single optical channel, enabling terabit-scale bandwidth with negligible thermal degradation. Photonic switches, microring modulators, and coherent optical routers dynamically reconfigure communication paths, allowing activations, partial sums, and routing metadata to traverse the chip at the speed of light.

Maintaining cohesion across these heterogeneous domains requires precise synchronization. Sub-picosecond phase-locked loops, coherent optical modulators, and mixed-signal arbitration circuits align the timing of analog electrical, digital electrical, and optical subsystems. Hybrid co-processors incorporate elastic buffers, asynchronous FIFOs, and clock-domain crossing bridges to ensure that data moves seamlessly between memristive arrays, electrical compute tiles, and photonic waveguides without violating timing constraints or introducing metastability. This synchronization layer enables the architecture to behave as a single coherent organism despite operating across fundamentally different physical regimes.

The hybrid paradigm extends even further into optical compute. Meshes of Mach–Zehnder interferometers can perform linear algebra operations—including full matrix multiplication and singular value decomposition—entirely within the optical domain. Localized phase shifts encode weight values, enabling photonic circuits to execute high-dimensional transformations with femtojoule-level energy consumption. Because this multi-domain fabric requires energy primarily to update weights rather than to execute inference, it offers a near-infinite scaling path for static model deployments, sustaining microsecond-level responsiveness even under extreme workload conditions.

Hybrid AI co-processors therefore represent a decisive break from traditional silicon scaling. By merging persistent memory, photonic communication, and mixed-domain synchronization into a unified spatial compute fabric, they eliminate the memory wall, bypass electrical interconnect bottlenecks, and enable compute-in-memory execution at massive scale. This architecture provides the foundation for next-generation AI systems capable of continuous, high-throughput operation across trillion-parameter models with unprecedented efficiency.

With the foundations of hybrid AI co-processors now established—spanning persistent non-volatile memory lattices, memristive compute-in-memory arrays, silicon-photonic waveguides, and mixed-domain synchronization fabrics—the architectural landscape becomes sufficiently complex that a structured synthesis is required. Each subsystem contributes a

distinct capability, yet their true power emerges only when they operate as a unified execution substrate. To clarify how these heterogeneous components interact, complement one another, and collectively overcome the physical limits of traditional silicon, the following table summarizes the major architectural elements of hybrid co-processors, outlining their functions, enabling technologies, performance advantages, and integration challenges. This tabular view provides a consolidated reference point before the narrative proceeds into deeper analysis of cross-domain behavior and system-level implications.

Table 8.4-B4 examined how reconfigurable spatial architectures improve accelerator efficiency through adaptive routing, dynamic graph mapping, bypass networks, and runtime topology reconfiguration. These innovations enable hardware fabrics to respond intelligently to changing workloads, yet they remain fundamentally constrained by the limitations of conventional electronic memory systems and electrical interconnects. As AI models continue to expand toward trillions of parameters and increasingly distributed execution patterns, the costs associated with parameter storage, memory initialization, communication latency, and interconnect bandwidth emerge as dominant system-level bottlenecks. Addressing these challenges requires architectural approaches that extend beyond traditional silicon scaling. Hybrid AI co-processors represent one such approach, combining non-volatile memory technologies, memristive compute fabrics, photonic communication networks, optical computing elements, and cross-domain synchronization mechanisms into unified accelerator platforms. Table 8.4-B5 examines the principal architectural components underlying these systems and illustrates how emerging memory and communication technologies may redefine future AI-computing substrates.

Table 8.4-B5 presents the major architectural subsystems that comprise hybrid AI co-processors integrating non-volatile memory technologies, analog computational fabrics, and optical communication infrastructure. These systems represent an emerging direction in accelerator design that seeks to overcome the physical limitations associated with conventional memory hierarchies and electrical interconnect networks.

Contemporary AI systems increasingly face challenges related to parameter storage, initialization latency, communication bandwidth, energy consumption, and heat generation. Although advances in digital accelerators continue to improve computational throughput, moving information among distributed memory and compute resources often consumes more energy and introduces more latency than the arithmetic operations themselves.

Hybrid AI co-processors address these problems through a combination of persistent memory structures, in-memory computation, photonic communication links, optical computing substrates, and mixed-domain synchronization systems. Rather than relying exclusively on

electrical signaling and volatile memory resources, these architectures integrate multiple computational domains into a single execution environment.

The table identifies seven key subsystems: non-volatile memory lattices, memristive crossbar arrays, silicon photonic waveguides, optical compute meshes, mixed-domain synchronization fabrics, persistent graph-initialization metadata systems, and electro-optical modulation layers. Together, these technologies form the foundation of architectures designed to support future generations of large-scale AI workloads.

By examining the functions, enabling technologies, advantages, and challenges associated with each subsystem, the table provides insight into how next-generation accelerator architectures may evolve beyond conventional digital-computing paradigms.

Table 8.4-B5 — Architectural Components of Hybrid AI Co-Processors Integrating Non-Volatile Memory Lattices and Optical Interconnects

Subsystem	Primary Function	Key Technologies	Performance Advantages	Architectural Challenges
Non-Volatile Memory Lattices	Persistent weight storage and instant-on graph initialization	FeRAM, PCM, RRAM, multi-level memristive cells	Eliminates DRAM reloads; deterministic access latency; near-zero static leakage	Endurance limits; write-disturb effects; retention drift under thermal stress
Memristive Crossbar Arrays	Analog compute-in-memory (CIM) for matrix–vector multiplication	Programmable conductance states; Kirchhoff-summation bitlines; differential encoding	Single-cycle MVM; massive parallelism; minimal data movement	Multi-level cell drift; ADC/DAC quantization noise; calibration overhead
Silicon Photonic Waveguides	High-bandwidth global communication	WDM channels; microring modulators; photonic switches	Terabit-scale throughput; negligible thermal loss;	Thermal tuning of microrings; optical crosstalk;

Subsystem	Primary Function	Key Technologies	Performance Advantages	Architectural Challenges
			speed-of-light propagation	fabrication variability
Optical Compute Meshes	Linear algebra operations in the optical domain	Mach–Zehnder interferometer arrays; phase-shift programming	Femtojoule-level energy per MAC; ultra-low latency; ideal for large-scale transforms	Phase drift; limited nonlinearity; precision constraints for deep networks
Mixed-Domain Synchronization Fabric	Cohesion across electrical, analog, and photonic domains	Sub-ps PLLs; asynchronous FIFOs; CDC bridges; adaptive timing controllers	Stable cross-domain execution; deterministic latency; unified compute substrate	Metastability risks; timing-window alignment; multi-domain arbitration complexity
Persistent Graph-Initialization Metadata	Instant-on execution and rapid failover	NVM-backed routing tables; tile-state snapshots; interconnect descriptors	Microsecond startup; seamless model switching; robust multi-tenant operation	Atomic update semantics; metadata coherence; endurance management
Electro-Optical Modulation Layer	Encoding electrical signals into optical carriers	Coherent modulators; adaptive modulation depth control	Low-energy signaling; stable optical transmission under dynamic workloads	Modulator linearity; thermal sensitivity; synchronization overhead

Table 8.4-B5 illustrates a significant expansion in the architectural scope of AI accelerators. Rather than optimizing existing digital systems alone, hybrid co-processors introduce entirely

new computational substrates based on persistent memory technologies, analog computation, photonic communication, and optical information processing.

The components presented in the table share a common objective: reducing the physical costs associated with data movement, initialization, synchronization, and large-scale communication while maintaining computational scalability for increasingly demanding AI workloads.

The first subsystem identified in the table is **non-volatile memory lattices**, which provide persistent storage for neural-network parameters and graph structures.

Unlike conventional DRAM, which requires continuous power to maintain stored information, non-volatile memory technologies retain information even when power is removed. The table highlights technologies such as FeRAM, PCM, RRAM, and multi-level memristive cells as representative examples.

Their principal advantage is the elimination of repeated parameter loading during system startup and model initialization. Because weights remain resident within non-volatile structures, accelerators can begin execution more rapidly and avoid many of the energy costs associated with repeatedly transferring large parameter sets into active memory. This capability becomes increasingly important as AI models continue expanding in size.

However, the table also notes several challenges, including endurance limitations and long-term retention variability. These constraints illustrate the trade-offs that accompany persistent storage technologies.

The second subsystem is **memristive crossbar arrays**, which extend processing-in-memory principles into highly dense analog-computation fabrics.

In these architectures, programmable conductance values stored within memristive devices encode neural-network weights directly within crossbar arrays. Matrix–vector multiplication occurs through analog current accumulation rather than conventional digital arithmetic.

The table highlights Kirchhoff-based summation mechanisms and differential encoding techniques that enable highly parallel analog computation. One of the most important benefits of this approach is the ability to perform large numbers of multiply–accumulate operations simultaneously with minimal data movement.

At the same time, challenges associated with device variability, analog noise, calibration overhead, and precision management remain important research considerations.

A third architectural component is the **silicon photonic waveguide network**, which addresses communication bandwidth limitations.

As AI systems become increasingly distributed, communication often emerges as a major bottleneck. Silicon photonic technologies replace portions of conventional electrical communication pathways with optical communication channels.

The table identifies wavelength-division multiplexing, microring modulators, and photonic switching technologies as enabling mechanisms. These systems support extremely high communication bandwidth while minimizing thermal losses and propagation delays.

The resulting communication efficiency is particularly valuable for large-scale distributed AI workloads requiring movement of substantial volumes of model state and activation data.

Closely related are **optical compute meshes**, which move computational operations themselves into the optical domain.

Rather than using optical systems solely for communication, optical compute meshes perform linear-algebra operations through interference-based computation. The table highlights Mach–Zehnder interferometer arrays and programmable optical phase-shift networks as representative technologies.

These architectures offer exceptional energy efficiency for selected linear transformations. However, as the table indicates, maintaining precision, managing nonlinear behavior, and supporting deep neural-network structures remain significant practical challenges.

The fifth subsystem identified is the **mixed-domain synchronization fabric**.

Hybrid architectures combine electrical, analog, and photonic subsystems, each operating according to different physical principles and timing characteristics. Managing interactions among these domains therefore becomes a central architectural challenge.

The table highlights asynchronous FIFOs, sub-nanosecond phase-locked loops, clock-domain bridges, and adaptive timing controllers as mechanisms supporting synchronization. These components ensure coherent execution despite differences in operating speeds and signaling modalities.

Without effective synchronization, many of the performance benefits provided by hybrid architectures would be difficult to realize reliably.

The sixth subsystem is **persistent graph-initialization metadata**, which supports rapid startup and failover behavior.

Traditional execution environments often require substantial initialization procedures before computation can begin. Hybrid architectures reduce this overhead by maintaining routing information, graph state, and execution metadata within persistent storage resources.

As indicated in the table, NVM-backed routing tables, tile-state snapshots, and interconnect descriptors allow systems to restore execution environments rapidly. This capability supports robust operation and enables faster deployment of large AI workloads.

The final subsystem identified is the **electro-optical modulation layer**, which serves as the interface between electronic and photonic domains.

Electrical signals generated within conventional computing subsystems must be translated into optical representations before transmission through photonic communication fabrics. Modulators perform this conversion while preserving signal fidelity and communication efficiency.

The table notes advantages such as low-energy transmission and stable optical signaling under dynamic workloads. However, maintaining modulator linearity and thermal stability remains an important engineering challenge.

A broader insight emerging from the table is that future AI accelerators may increasingly incorporate multiple computational domains rather than relying solely on digital electronics. Memory technologies, analog computation, photonic communication, optical processing, and synchronization systems all contribute specialized capabilities that address different performance bottlenecks.

The table also highlights that communication and storage are becoming as important to accelerator innovation as arithmetic throughput. Many of the technologies presented focus primarily on reducing data movement, startup costs, communication latency, or synchronization overhead rather than accelerating numerical computation directly.

From a systems-engineering perspective, the architectural components summarized in the table form an interconnected ecosystem. Persistent memory supports rapid initialization. Memristive arrays provide efficient computation. Photonic networks enable high-bandwidth communication. Optical meshes accelerate specific mathematical operations. Synchronization fabrics unify these domains. Metadata systems support orchestration. Modulation layers bridge communication technologies.

Another important observation is that these architectures represent a convergence of materials science, photonics, memory engineering, analog design, and computer architecture. Consequently, future AI accelerators are likely to evolve through interdisciplinary innovation rather than through digital scaling alone.

Ultimately, Table 8.4-B5 illustrates how hybrid AI co-processors seek to overcome the limitations of conventional architectures by integrating persistent memory technologies, analog

computation, and optical communication within a unified execution framework. Through non-volatile memory lattices, memristive crossbar arrays, silicon photonics, optical compute fabrics, and mixed-domain coordination mechanisms, these systems offer a potential pathway toward highly scalable, energy-efficient AI infrastructures capable of supporting the next generation of computationally intensive intelligent systems.

Table 8.4-B5 introduced the major architectural subsystems that define emerging hybrid AI co-processors, including non-volatile memory lattices, memristive crossbar arrays, silicon-photonic communication fabrics, optical compute structures, mixed-domain synchronization mechanisms, and persistent graph-initialization systems. While the table examined these technologies individually, their significance becomes more apparent when viewed as components of an integrated computational substrate. Performance gains in hybrid architectures do not arise from any single innovation; rather, they emerge from the coordinated interaction of persistent memory, analog computation, optical communication, and cross-domain control. Figure 8.4-B5 illustrates this holistic architecture by showing how these subsystems are organized around a shared execution fabric, enabling data storage, computation, communication, and synchronization to occur across multiple physical domains while maintaining a unified operational framework.

Figure 8.4-B5 presents a conceptual architecture for a hybrid AI co-processor that integrates non-volatile memory technologies, analog processing-in-memory arrays, silicon-photonic communication networks, and mixed-domain synchronization infrastructure. The figure illustrates one possible direction for future AI accelerators as conventional digital architectures approach physical limits associated with memory movement, communication bandwidth, energy consumption, and thermal management.

Traditional AI accelerators rely primarily on volatile memory systems, electrical interconnects, and digital arithmetic units. While highly successful, these technologies increasingly face challenges when supporting models containing billions or trillions of parameters distributed across large computational fabrics. Hybrid co-processors address these limitations by incorporating alternative computation and communication domains into a unified architecture.

The figure organizes the system into several major layers. At its core lies a memristive crossbar computing fabric supported by surrounding non-volatile memory lattices. Encircling these structures are persistent graph metadata systems and silicon-photonic communication pathways. The entire architecture is coordinated through mixed-domain synchronization infrastructures that bridge electrical, analog, and photonic subsystems.

By visualizing these elements as an integrated computational ecosystem, the figure highlights

how future AI hardware may evolve beyond traditional processor-centric architectures toward persistent, communication-efficient, and memory-centric execution environments.

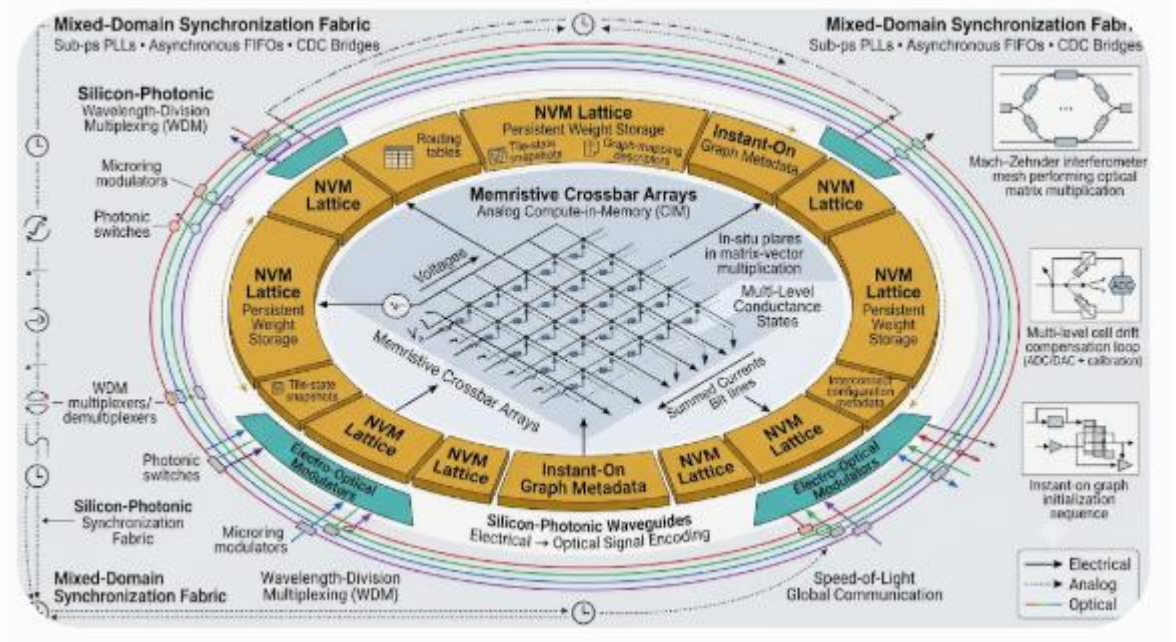


Figure 8.4-B5 — Hybrid AI Co-Processor Architecture Integrating Non-Volatile Memory Lattices and Optical Interconnects

Multi-domain accelerator architecture illustrating the integration of non-volatile memory lattices, memristive compute fabrics, silicon-photonic communication networks, optical signaling infrastructures, and cross-domain synchronization systems. The figure demonstrates how persistent storage, in-memory analog computation, high-bandwidth optical communication, and unified control fabrics work together to reduce memory-movement overhead, accelerate initialization, improve communication efficiency, and support large-scale AI execution.

Legend

Component	***Description***
Memristive Crossbar Array	*Central analog compute-in-memory fabric performing matrix-vector multiplications directly within memory structures.*
Memristive Conductance States	*Programmable resistance values encoding neural-network parameters.*
Crossbar Conduction Paths	*Physical pathways supporting analog multiplication and accumulation.*

In-Situ Matrix-Vector Multiplication	*Computation occurring directly within the memory fabric.*
NVM Lattices	*Non-volatile memory structures supporting parameter storage and persistent execution state.*
Persistent Weight Storage	*Long-term retention of neural-network parameters without continuous power.*
Graph Snapshots	*Stored representations of execution topology and system state.*
Routing Tables	*Persistent routing metadata supporting communication management.*
Instant-On Graph Metadata	*Initialization layer enabling rapid system startup and failover.*
Persistent Graph Metadata	*Execution descriptors preserved across power cycles.*
Graph Initialization Sequence	*Startup process reconstructed from persistent metadata.*
Silicon-Photonic Waveguides	*Optical communication channels supporting high-bandwidth data movement.*
Wavelength-Division Multiplexing (WDM)	*Technique enabling multiple optical channels on a single waveguide.*
Microring Modulators	*Devices converting electrical signals into optical signals.*
Photonic Switches	*Routing elements directing optical communication traffic.*
Speed-of-Light Global Communication	*High-bandwidth optical transport layer connecting distributed resources.*
Electro-Optical Signal Encoding	*Translation layer linking electronic and photonic communication domains.*
Mixed-Domain Synchronization Fabric	*Control infrastructure coordinating analog, digital, and photonic subsystems.*
Sub-ps PLLs	*Precision timing mechanisms supporting synchronization.*
Asynchronous FIFOs	*Communication buffers supporting clock-domain transitions.*
CDC Bridges	*Clock-domain-crossing mechanisms connecting heterogeneous subsystems.*
Mixed-Signal Calibration Loops	*Systems preserving numerical stability across domains.*

Analog / Optical /	*Distinct computational and communication domains integrated within the architecture.*

Figure 8.4-B5 illustrates a significant departure from conventional AI accelerators by integrating storage, computation, communication, and synchronization into a unified multi-domain architecture. Rather than treating memory, compute units, and interconnects as separate subsystems linked through repeated data transfers, the architecture distributes functionality across persistent, analog, digital, and photonic domains that operate cooperatively.

The figure demonstrates how future AI systems may increasingly derive performance from reducing data movement and communication overhead rather than solely increasing arithmetic throughput.

At the center of the architecture resides the **memristive crossbar array**, which functions as the primary computational substrate.

The figure illustrates matrix-vector multiplication occurring directly inside the crossbar fabric through programmable conductance states. Neural-network weights are encoded physically within the memristive devices themselves, allowing input signals to propagate through the array while accumulation occurs naturally through analog electrical behavior.

This in-situ computation significantly reduces the need to transport parameters between memory and compute units. Unlike conventional architectures, where weights are repeatedly loaded from memory before arithmetic execution, the weights remain embedded within the computational medium itself.

Surrounding the memristive core are multiple **non-volatile memory lattices (NVM lattices)**.

These structures provide long-term storage for model parameters, routing information, graph states, and execution metadata. Because the memory is non-volatile, information remains available even after power interruptions.

The figure depicts stored weight banks, graph snapshots, and routing tables distributed throughout the lattice structure. This arrangement enables rapid system recovery and supports deterministic startup behavior without requiring extensive parameter reloading.

A particularly important consequence of this design is the elimination of lengthy initialization phases often associated with large AI models. Critical execution state remains resident within the memory fabric and can be restored immediately when computation resumes.

Positioned alongside the memory lattices is the **instant-on graph metadata layer**.

This subsystem stores execution topology information, routing descriptors, graph snapshots, and initialization sequences. Rather than reconstructing execution environments from scratch, the architecture retrieves preserved metadata directly from persistent storage.

The result is an execution environment capable of rapid failover, accelerated startup, and seamless workload transitions. As AI systems become larger and more distributed, the ability to maintain persistent execution context becomes increasingly valuable.

Encircling the memory-computation core is the **silicon-photonic communication fabric**.

The figure illustrates waveguides, microring modulators, photonic switches, and wavelength-division multiplexing pathways forming a global optical communication network. Unlike traditional electrical interconnects, photonic channels support extremely high bandwidth without proportional increases in resistive power loss.

Wavelength-division multiplexing allows multiple communication streams to share a single optical pathway simultaneously. This capability dramatically increases communication density and helps support distributed execution across large AI fabrics.

The concept labeled **speed-of-light global communication** emphasizes one of the principal motivations behind optical interconnect technology: reducing communication latency while maintaining scalable bandwidth.

The architecture also includes an **electro-optical signal encoding layer**, which bridges electronic and photonic communication domains.

Electrical signals generated within the memory and compute subsystems are converted into optical carriers for transport through photonic networks. Conversely, incoming optical signals are converted back into electronic representations for local processing.

This layer enables the architecture to combine the maturity of electronic computation with the efficiency of optical communication. In effect, it serves as a translation interface linking distinct physical domains.

Enveloping the entire system is the **mixed-domain synchronization fabric**.

This subsystem coordinates timing and communication among electrical, analog, and photonic components operating according to different physical constraints. The figure highlights sub-picosecond phase-locked loops, asynchronous FIFO buffers, and clock-domain-crossing bridges supporting this process.

Without such synchronization mechanisms, the heterogeneous subsystems would struggle to

function reliably as a unified platform. The synchronization fabric therefore acts as the control layer preserving coherence across the architecture.

Another important element shown on the right side of the diagram is the **mixed-signal calibration infrastructure**. Calibration loops, ADC/DAC structures, and stability controls compensate for variability within analog computation and maintain numerical accuracy throughout the system.

This functionality is particularly important because analog and photonic systems often exhibit variability that must be actively managed to preserve computational integrity.

A broader insight emerging from the figure is that each subsystem addresses a different form of computational overhead.

The memristive core reduces arithmetic-related data movement. Non-volatile memory reduces initialization overhead. Photonic communication reduces bandwidth constraints. Persistent metadata eliminates startup latency. Synchronization fabrics reduce coordination costs. Together, these components attack bottlenecks that increasingly dominate large-scale AI execution.

The figure also illustrates a transition from homogeneous computing toward heterogeneous co-processing. Rather than relying on a single computational paradigm, the architecture combines complementary technologies, each performing tasks for which it is naturally suited.

From a systems-engineering perspective, the design represents a convergence of memory architecture, analog electronics, photonics, networking, and synchronization engineering. Performance improvements emerge not from a single breakthrough but from coordinated optimization across multiple computational domains.

Another important observation is that communication becomes a first-class architectural consideration. In large AI systems, computation is often abundant while efficient communication remains scarce. The photonic infrastructure shown here reflects the increasing importance of moving information efficiently across large accelerator fabrics.

Ultimately, Figure 8.4-B5 illustrates a potential future direction for AI accelerator design in which memory, computation, communication, and synchronization are integrated into a unified hybrid architecture. Through the combination of non-volatile memory lattices, memristive compute fabrics, silicon-photonic networks, electro-optical interfaces, and mixed-domain synchronization systems, the architecture addresses many of the fundamental bottlenecks limiting conventional digital systems. The result is a highly scalable, communication-efficient, and memory-centric computing paradigm capable of supporting increasingly complex AI

workloads.

Figure 8.4-B5 illustrates how hybrid AI co-processors integrate persistent memory lattices, silicon-photonic communication fabrics, mixed-domain synchronization systems, and analog compute substrates into a unified computational architecture. At the center of this multi-domain system lies the **memristive crossbar array**, which functions as the primary computational engine by performing matrix-vector multiplication directly within the memory fabric. While the figure highlights the structural importance of the crossbar within the broader architecture, understanding the practical viability of hybrid AI co-processors requires a deeper examination of the behavior of the memristive devices themselves. In particular, the long-term stability of stored conductance states, the precision of analog computation, and the cumulative effects of device variability become critical factors influencing inference accuracy and system reliability. Among these challenges, **multi-level cell drift** represents one of the most significant architectural concerns because it can gradually alter stored weight values and affect computational correctness over time. Consequently, maintaining stable and accurate computation requires sophisticated calibration, compensation, and drift-management mechanisms embedded throughout the memory-compute fabric. The following discussion examines **Memristive AI Crossbar Arrays and Multi-Level Cell Drift Management**, exploring the physical principles of memristive computation, the sources of conductance drift, and the architectural strategies used to preserve computational integrity in large-scale hybrid AI systems.

i. Memristive AI Crossbar Arrays and Multi-Level Cell Drift Management

Memristive crossbar arrays form the computational heart of non-volatile compute-memory fusion in hybrid AI co-processors. Unlike traditional architectures that shuttle weights back and forth between DRAM and compute units, memristive arrays store parameters directly as analog or multi-level resistive states within the memory substrate itself. This enables matrix–vector multiplication to occur *in situ*, collapsing computation into the storage fabric and eliminating the energy-intensive data movement that dominates conventional AI acceleration. Inputs are applied as parallel voltages across word lines, weights are encoded as conductances within the crossbar cells, and Kirchhoff's current-summation laws naturally accumulate partial sums along bit lines. The result is a massively parallel, deterministic, and ultra-low-latency compute mechanism ideally suited for large-scale inference.

However, the power of memristive arrays comes with a fundamental challenge: **multi-level cell (MLC) drift**. Because weights are stored as analog resistive states rather than discrete digital bits, they are susceptible to gradual shifts over time. Temperature fluctuations, write-cycle fatigue, device aging, stochastic analog noise, and material relaxation can all cause conductance

values to drift away from their programmed levels. In deep neural networks—where numerical precision directly affects model accuracy—these deviations can accumulate and degrade inference quality if left unmanaged.

Hybrid AI co-processors address this challenge through a multi-layered drift-management strategy:

- **Calibration loops** periodically measure cell conductance and apply corrective write pulses to restore target values.
- **Predictive drift models** use device-level physics and historical drift patterns to anticipate future deviations and pre-emptively adjust cell states.
- **On-device ADC/DAC compensation** dynamically corrects analog outputs, ensuring stable numerical behavior even when underlying cell states shift.
- **Periodic refresh cycles** re-normalize multi-level states during idle windows or natural execution boundaries.
- **Redundant encoding and differential storage** stabilize multi-level representations by distributing weight values across multiple cells or storing complementary conductance pairs.

These mechanisms transform inherently analog, drift-prone devices into reliable compute substrates capable of supporting high-precision AI workloads.

Software plays an equally critical role. Compilers and runtimes must:

- generate placement metadata that maps weights onto crossbar regions with appropriate drift tolerance,
- schedule refresh and calibration operations during low-impact execution intervals,
- fuse kernels to minimize write frequency and reduce analog stress on MLC cells,
- and manage quantization strategies that align with the physical behavior of the underlying memristive devices.

When hardware drift-management and software orchestration are properly integrated, memristive crossbar arrays deliver persistent, low-latency weight access with dramatically reduced energy consumption. They eliminate the memory-wall bottleneck, provide deterministic inference performance even under long-sequence workloads, and enable hybrid AI co-processors to operate at scales that are impractical for traditional volatile memory hierarchies.

Memristive CIM therefore becomes a cornerstone of next-generation AI acceleration—offering compute density, persistence, and energy efficiency that far exceed the limits of conventional digital architectures.

While memristive crossbar arrays provide the analog compute-in-memory foundation that collapses matrix operations directly into the storage substrate, their effectiveness ultimately depends on how efficiently activations, partial sums, and routing metadata can move across the accelerator without reintroducing the latency and energy penalties of electrical interconnects. As models scale and crossbar clusters proliferate, the communication burden between compute regions becomes the dominant constraint. Electrical signaling—limited by RC delays, parasitic capacitance, and thermal dissipation—cannot deliver the bandwidth required to keep large CIM fabrics fully utilized. To overcome this bottleneck, hybrid co-processors extend beyond analog memory-centric compute into the optical domain, where silicon-photonic waveguides, wavelength-division multiplexing, and electro-optical modulation provide speed-of-light communication and enable crossbar arrays to function as part of a globally synchronized, ultra-high-bandwidth photonic mesh.

ii. Silicon Photonic AI Waveguides and Electro-Optical Latency Control

Silicon photonic waveguides introduce an optical communication domain that fundamentally reshapes how large-scale AI accelerators move data. Traditional electrical interconnects—based on copper traces and high-speed SerDes—are constrained by resistive losses, parasitic capacitance, RC delays, and Joule heating. As AI models expand into trillion-parameter regimes and inference pipelines demand microsecond-level responsiveness, these electrical limits become architectural bottlenecks. Photonic signaling bypasses these constraints entirely by transmitting information using light rather than charge, enabling bandwidth, latency, and energy efficiency characteristics that are unattainable with conventional electrical wiring.

At the core of silicon photonic interconnects are **waveguides**, **microring modulators**, **Mach–Zehnder interferometers**, and **photonic switches** fabricated directly onto CMOS-compatible substrates. These components allow data to be encoded as modulated optical signals and routed across the accelerator with minimal attenuation. Because photons do not experience resistive heating or capacitive loading, optical links maintain stable performance even at extreme bandwidth densities. This makes them ideal for global communication tasks such as attention-head aggregation, MoE expert dispatch, multi-chiplet synchronization, and distributed inference pipelines.

A key advantage of photonic interconnects is their ability to exploit **Wavelength Division Multiplexing (WDM)**. Instead of transmitting a single data stream per channel, WDM allows

dozens of independent streams—each encoded on a different wavelength—to propagate simultaneously through the same physical waveguide. This parallelism enables terabit-scale bandwidth within a footprint far smaller and more energy-efficient than any electrical equivalent. Photonic routers dynamically allocate wavelengths, steer optical paths, and reconfigure communication topologies in response to workload structure, allowing the accelerator to adapt its global communication fabric in real time.

However, integrating photonics into AI accelerators requires precise **electro-optical latency control**. Optical signals propagate at the speed of light, while electrical domains operate at gigahertz-scale clock frequencies with discrete timing boundaries. Hybrid co-processors must therefore incorporate mechanisms that synchronize these domains without introducing metastability or timing violations. This is achieved through:

- **Coherent optical modulators** that precisely encode electrical signals into optical carriers.
- **Sub-picosecond phase-locked loops (PLLs)** that align electrical clock edges with optical phase windows.
- **Mixed-signal arbitration circuits** that manage data transfer across electrical–optical boundaries.
- **Elastic buffers and asynchronous FIFOs** that absorb timing mismatches between domains.
- **Adaptive modulation depth control** that stabilizes optical signal integrity under varying thermal and workload conditions.

These mechanisms ensure that photonic communication remains deterministic, low-latency, and contention-free even as the neural graph evolves.

The photonic domain also supports **optical compute**, extending beyond communication. Meshes of Mach–Zehnder interferometers can perform linear algebra operations—such as matrix multiplication, convolution, and singular value decomposition—entirely within the optical domain. Localized phase shifts encode weight values, enabling photonic circuits to execute high-dimensional transformations with femtojoule-level energy consumption. This capability complements memristive compute-in-memory arrays by providing an ultra-fast, ultra-efficient pathway for large-scale linear operations.

Software orchestration is essential for unlocking the full potential of silicon photonics. Compilers must schedule optical communication paths, allocate wavelengths, fuse kernels to minimize optical contention, and generate synchronization metadata that aligns electrical and

optical execution. Runtimes must manage photonic routing states, coordinate electro-optical transitions, and ensure that optical paths remain coherent across dynamic workloads.

When properly integrated, silicon photonic waveguides and electro-optical latency control transform hybrid AI co-processors into architectures capable of sustaining extreme bandwidth, near-zero latency, and unprecedented energy efficiency. They eliminate the communication bottlenecks that limit traditional accelerators and provide a scalable foundation for next-generation AI systems operating at trillion-parameter scale.

The introduction of silicon-photonic waveguides and electro-optical modulation gives the hybrid co-processor a communication backbone capable of moving data at the speed of light, but this leap in bandwidth introduces a new architectural tension: the compute-in-memory arrays, the electrical control logic, and the photonic signaling fabric all operate according to fundamentally different timing regimes. Optical channels propagate asynchronously and encode information through phase and wavelength, memristive arrays rely on analog settling dynamics, and digital subsystems depend on discrete clock edges. As these domains begin exchanging activations, partial sums, routing metadata, and synchronization signals, the system must prevent metastability, timing violations, and cross-domain drift. This makes domain synchronization and clock-boundary arbitration the next critical layer of the architecture—ensuring that electrical, analog, and optical subsystems behave as a coherent organism rather than isolated islands of computation.

iii. Hybrid AI Domain Synchronization and Clock-Boundary Arbitration

Hybrid AI co-processors operate across multiple physical and computational domains—digital electrical logic, analog compute-in-memory arrays, and high-bandwidth photonic interconnects. Each of these domains exhibits fundamentally different timing characteristics, signaling behaviors, and stability constraints. Digital logic is clocked, discrete, and edge-sensitive; analog memristive arrays rely on continuous settling dynamics; photonic waveguides propagate signals at the speed of light with phase-encoded information rather than voltage-encoded transitions. Ensuring that these heterogeneous subsystems operate coherently as a unified architecture requires sophisticated domain-synchronization and clock-boundary arbitration mechanisms.

At the electrical level, compute tiles typically operate at gigahertz-scale frequencies with strict setup and hold requirements. Memristive arrays, by contrast, rely on analog settling times that vary with conductance levels, temperature, and device aging. Photonic domains introduce yet another timing regime: asynchronous optical pulses, wavelength-encoded channels, and phase-modulated signals that do not conform to conventional clock edges. Hybrid co-processors must therefore incorporate a synchronization fabric capable of bridging these disparate timing

models without introducing metastability, data corruption, or latency spikes.

This synchronization fabric includes:

- **Sub-picosecond phase-locked loops (PLLs)** that align electrical clock edges with optical phase windows, ensuring coherent electro-optical modulation.
- **Mixed-signal arbitration circuits** that translate analog memristive outputs into stable digital representations while compensating for drift, noise, and settling variability.
- **Elastic buffers and asynchronous FIFOs** that absorb timing mismatches between domains, allowing data to cross boundaries without violating timing constraints.
- **Clock-domain crossing (CDC) bridges** that safely transfer data between independently clocked electrical subsystems.
- **Adaptive timing controllers** that dynamically adjust sampling windows, modulation depth, and synchronization intervals based on workload conditions and thermal behavior.

These mechanisms ensure that data moves seamlessly between compute tiles, memristive arrays, and photonic waveguides, allowing the architecture to behave as a single coherent organism despite operating across fundamentally different physical regimes.

Synchronization is not merely a hardware challenge—it is also a software orchestration problem. Compilers and runtimes must:

- generate scheduling metadata that accounts for domain boundaries and timing constraints,
- fuse kernels to minimize cross-domain transitions,
- allocate operations to domains based on latency sensitivity and stability requirements,
- and ensure that synchronization overhead remains negligible relative to compute cost.

They must also coordinate calibration cycles, optical routing updates, memristive refresh operations, and electrical compute bursts so that domain transitions occur during natural execution boundaries rather than in the middle of critical paths.

When hardware synchronization mechanisms and software scheduling strategies are properly integrated, hybrid AI co-processors achieve a level of cohesion that allows electrical, analog, and photonic subsystems to operate as a unified spatial compute fabric. This enables deterministic execution, stable numerical behavior, and high throughput even under extreme workload

conditions. Domain synchronization and clock-boundary arbitration therefore become foundational capabilities—allowing hybrid architectures to scale beyond the limits of traditional silicon while maintaining the precision and reliability required for modern AI inference.

As hybrid co-processors reconcile electrical, analog, and photonic timing regimes through mixed-domain synchronization and clock-boundary arbitration, the architecture gains the ability to operate as a coherent multi-domain organism rather than a collection of isolated subsystems. Yet even with stable cross-domain timing, the system's responsiveness ultimately depends on how quickly it can restore operational state after power transitions, workload shifts, or distributed failover events. Traditional accelerators lose all model parameters when power is removed, forcing lengthy reload cycles from external memory and delaying inference readiness. Hybrid architectures avoid this bottleneck by anchoring weights, routing descriptors, and graph-initialization metadata in non-volatile memory lattices, enabling persistent residency and microsecond-level startup. This persistent foundation transforms synchronization from a runtime requirement into a continuous architectural capability, allowing the compute fabric to resume full operation instantly and maintain high-throughput inference even under dynamic or power-constrained conditions.

iv. Non-Volatile-Backed AI Weight Retention and Instant-On Graph Initialization

Non-volatile-backed weight retention transforms hybrid AI co-processors into persistent, instant-ready inference engines. Traditional accelerators rely on volatile SRAM and DRAM hierarchies, which lose state on power-down and require costly reinitialization cycles. Large foundation models may take seconds—or even minutes—to reload parameters from external memory or storage, creating substantial startup latency and energy overhead. As AI systems scale into trillion-parameter regimes and operate in latency-critical environments such as autonomous systems, edge inference, and multi-tenant cloud deployments, this initialization cost becomes a fundamental architectural bottleneck.

Hybrid co-processors eliminate this barrier by storing model parameters directly within **non-volatile memory (NVM) lattices**. Technologies such as FeRAM, PCM, and RRAM allow weights to persist across power cycles without refresh, enabling the accelerator to resume operation immediately upon power-up. These lattices are tightly integrated with memristive compute-in-memory arrays, allowing parameters to remain physically co-located with the operators that consume them. This persistence removes the need for DRAM reloads, reduces static power leakage, and provides deterministic access latency from the moment the device is activated.

Instant-on capability extends beyond weight retention. Hybrid co-processors store not only

parameters but also **graph-initialization metadata**, including:

- tile-configuration states,
- routing tables for electrical and photonic interconnects,
- graph-mapping descriptors,
- bypass-network activation patterns,
- and synchronization metadata for mixed-domain execution.

When the accelerator powers on, these structures are restored in microseconds, allowing the entire execution graph to materialize instantly. This enables rapid failover in distributed inference systems, seamless model switching in multi-tenant environments, and near-zero-latency startup for edge devices that must respond immediately to external stimuli.

Maintaining persistent graph state requires careful architectural design. NVM lattices must support:

- **high endurance**, ensuring that frequent updates to routing metadata and graph descriptors do not degrade device reliability;
- **low-latency read paths**, enabling immediate access to initialization data;
- **coherence mechanisms**, ensuring that persistent graph structures remain synchronized with dynamic runtime updates;
- **atomic update semantics**, preventing partial writes from corrupting initialization state; and
- **thermal-stable retention**, ensuring that stored weights and metadata remain accurate across environmental variations.

Software orchestration is equally critical. Compilers and runtimes must generate persistent metadata layouts, schedule consistency checks, and ensure that updates to graph structures are written atomically to NVM. They must also fuse kernels and partition workloads in ways that minimize the frequency of persistent-state updates, preserving endurance while maintaining responsiveness.

When hardware persistence and software orchestration are properly integrated, non-volatile-backed weight retention and instant-on graph initialization transform hybrid AI co-processors into highly responsive, energy-efficient inference engines. They eliminate startup latency, reduce memory-movement overhead, and enable continuous operation across dynamic

workloads. This persistent execution model is essential for next-generation AI systems that must operate at massive scale while delivering microsecond-level responsiveness.

Hybrid AI co-processors built around non-volatile memory lattices and silicon-photonic interconnects redefine the architectural boundaries of modern inference systems. By collapsing computation into memristive storage fabrics, anchoring model parameters in persistent NVM substrates, and routing data through speed-of-light photonic channels, these architectures eliminate the traditional separation between compute, memory, and communication. The result is a unified execution environment capable of sustaining extreme bandwidth, deterministic latency, and microsecond-level startup across trillion-parameter workloads. Persistent weight residency ensures instant operational readiness, photonic waveguides remove global-communication bottlenecks, and mixed-domain synchronization maintains coherence across electrical, analog, and optical regimes. Together, these capabilities establish hybrid co-processors as a foundational class of AI hardware—one that transcends the constraints of conventional silicon and provides a scalable, energy-efficient platform for the next generation of intelligent systems.

Hardware accelerators have become the structural backbone of modern AI computation, reshaping how models are executed, scaled, and deployed across increasingly heterogeneous environments. By integrating analog compute-in-memory substrates, persistent non-volatile memory lattices, silicon-photonic interconnects, and mixed-domain synchronization fabrics, contemporary accelerators transcend the limitations of classical digital architectures. They collapse computation into the memory plane, route information at the speed of light, and maintain coherence across electrical, analog, and optical regimes. These capabilities collectively dismantle the traditional boundaries between compute, storage, and communication, enabling inference engines that are persistent, energy-efficient, and capable of sustaining trillion-parameter workloads with deterministic latency. As the physical substrate of AI continues to evolve, hardware accelerators define the performance envelope within which all higher-level AI systems must operate, establishing the foundation for the software paradigms that orchestrate, optimize, and ultimately unlock the full potential of these heterogeneous compute fabrics.

With the hardware substrate now fully articulated—from memristive crossbars and non-volatile memory lattices to photonic waveguides and synchronization fabrics—the focus shifts from physical capability to computational orchestration. Hardware accelerators provide unprecedented bandwidth, persistence, and parallelism, but these advantages only materialize when software systems can schedule operations across heterogeneous domains, manage precision and drift, allocate communication pathways, and adapt execution graphs to the

dynamic behavior of the underlying fabric. The next stage of the discussion therefore turns toward the software paradigms that translate architectural potential into functional intelligence: compilers that map neural graphs onto multi-domain substrates, runtimes that coordinate electrical, analog, and optical execution, and frameworks that ensure stability, efficiency, and scalability across diverse workloads. In this transition, software becomes the interpretive layer that binds the hardware's raw capability into coherent, high-performance AI systems.

C. Software Paradigms in AI Systems

Software paradigms define the computational behavior of autonomous AI systems above the hardware substrate. They determine how tensor programs are expressed, how execution graphs adapt to heterogeneous accelerators, how distributed workloads synchronize across nodes, and how inference pipelines maintain responsiveness under dynamic memory, bandwidth, and latency constraints. In hardware–software co-design, software is not a passive abstraction layer; it is an active orchestration environment whose compilers, runtimes, schedulers, and distributed protocols directly shape how effectively intelligence can exploit the underlying silicon. Every software paradigm—kernel compilation strategy, parallelism model, memory-retention policy, or federated execution protocol—propagates through the autonomy stack and governs how efficiently models operate under real-world conditions.

Modern AI workloads have reached a scale where naïve static graph execution, uniform parallelism, and monolithic memory allocation are no longer viable. Autonomous systems must execute large models within strict latency budgets, unpredictable input patterns, and distributed topologies where compute and memory are constantly shifting. As a result, software paradigms increasingly incorporate hardware-aware design principles that optimize kernel tiling, overlap compute with communication, dynamically defragment memory, and coordinate execution across decentralized nodes. These principles ensure that intelligence is not only architecturally expressive but also operationally sustainable across heterogeneous accelerators, multi-node fabrics, and real-time autonomy loops.

- **AI Hardware-Aware Programming Frameworks and Tile-Optimized Kernel Compilation -** Hardware-aware programming frameworks transform neural execution from a generic tensor abstraction into a substrate-aligned computational plan. By compiling kernels directly against accelerator tile geometry, memory-bank topology, and vector-pipeline behavior, these frameworks generate execution paths that minimize data movement and maximize parallel utilization. Tile-optimized compilation ensures that convolutional blocks, attention heads, and state-space operators map efficiently onto spatial arrays, tensor cores, and CIM fabrics. This alignment allows large models to run within tight latency budgets while maintaining numerical stability through hardware-aligned

scheduling and precision-aware kernel fusion.

- **Distributed AI Orchestration with Tensor, Pipeline, and Context Parallelism -** Distributed orchestration frameworks coordinate execution across multi-GPU clusters, photonic-linked chiplets, and heterogeneous compute nodes. Tensor parallelism partitions model weights across devices; pipeline parallelism streams micro-batches through sequential layers; context parallelism distributes long-sequence workloads across memory-rich nodes. Together, these parallelism modes ensure that large models remain executable even when single-node memory is insufficient. Intelligent orchestration manages synchronization, load balancing, and activation routing to maintain deterministic latency across distributed environments, enabling trillion-parameter inference at scale.
- **AI Latency Masking via Overlapped Compute and Fabric-Level Transfers -** Latency masking frameworks eliminate idle cycles by overlapping compute with communication. They schedule kernel execution so that memory transfers, interconnect routing, and activation streaming occur concurrently with arithmetic operations. This approach hides fabric-level latency behind useful computation, ensuring that accelerators remain fully utilized even when communication paths fluctuate or cross-domain synchronization introduces timing variability. Overlapped execution is essential for real-time autonomy, where inference pipelines must remain responsive despite dynamic workloads and unpredictable sensor input.
- **Dynamic AI Memory Defragmentation and PagedAttention Retention Policies -** Dynamic memory systems treat GPU and accelerator memory as a continuously evolving landscape rather than a static allocation space. Defragmentation engines reorganize tensors, KV-caches, and intermediate activations to maintain contiguous regions for high-bandwidth access. PagedAttention retention policies manage long-context workloads by paging attention states in and out of memory based on relevance, recency, and model-level heuristics. These mechanisms prevent fragmentation-induced stalls, reduce memory thrashing, and ensure that large-context models remain stable and efficient even under heavy load.
- **Decentralized AI Execution, Local Cache Eviction, and Federated Asymmetric Protocols -** Decentralized execution frameworks extend AI computation beyond centralized clusters into distributed, heterogeneous environments. Local cache-eviction policies manage on-device memory for edge nodes, ensuring that inference remains responsive despite limited capacity. Federated asymmetric protocols coordinate learning and inference across nodes with varying compute, bandwidth, and privacy constraints. These

protocols allow models to operate across decentralized networks without requiring uniform hardware or centralized data aggregation, enabling scalable, privacy-preserving intelligence across diverse deployment environments.

Together, these software paradigms illustrate how AI systems have evolved into a tightly integrated hardware–software ecosystem. Intelligence in autonomous systems is shaped not only by model architecture but by how effectively software orchestrates execution across heterogeneous accelerators, distributed fabrics, and dynamic memory environments. These paradigms enable modern AI systems to achieve resilience, efficiency, and scalability through deliberate co-design across the entire autonomy stack.

Software paradigms sit directly above hardware accelerators in the co-design hierarchy because they determine how every downstream layer—model architectures, runtime graphs, distributed schedulers, and real-time control loops—must behave to support autonomous operation. The constraints embedded in these paradigms shape kernel tiling, parallelism strategy, memory retention, communication overlap, and federated coordination. To clarify how these paradigms interact with model requirements and real-time demands, the next step is to organize the core software dimensions that govern modern AI execution. This structured view reveals the mechanisms that allow large-scale models to operate efficiently, predictably, and within the operational limits of autonomous systems.

The paradigms described above reveal how modern AI software has evolved from static graph execution into adaptive, hardware-aware, distributed orchestration environments. But understanding these paradigms individually is only the first step. To appreciate how they interact within real systems—how tile-optimized kernels reshape parallelism, how latency masking sustains throughput, how memory defragmentation stabilizes long-context inference, how decentralized protocols coordinate heterogeneous nodes—it is necessary to view them as a unified software design framework. Table 8.4-C organizes these dimensions into a structured reference model, clarifying the foundational software strategies that enable large-scale AI workloads to operate efficiently, predictably, and within the operational constraints of autonomous systems.

The software layer becomes the interpretive engine that translates the raw capability of heterogeneous accelerators into coherent, high-performance AI execution. Hardware defines what is physically possible, but software determines how effectively those possibilities are orchestrated—how kernels are tiled across spatial arrays, how distributed nodes synchronize activations, how memory remains stable under long-context workloads, and how decentralized systems coordinate inference across asymmetric environments. As models grow in scale and autonomy loops tighten, software paradigms must evolve to exploit accelerator geometry, mask

latency, defragment memory, and manage distributed execution with precision. To clarify how these mechanisms collectively shape modern AI behavior, the following table organizes the core software paradigms that govern execution across heterogeneous fabrics, revealing the strategies that allow intelligence to remain efficient, predictable, and resilient under real-world constraints.

The preceding discussions examined the evolution of AI hardware, from low-precision numerical formats and asynchronous scheduling fabrics to processing-in-memory architectures, reconfigurable spatial arrays, and hybrid co-processors integrating persistent memory and photonic communication technologies. Taken together, these developments demonstrate that modern AI performance increasingly depends on specialized hardware architectures designed to address the computational and data-movement demands of large-scale models. However, hardware capabilities alone do not guarantee efficient execution. To translate accelerator resources into practical performance, AI systems require software frameworks capable of exposing parallelism, coordinating distributed resources, managing memory hierarchies, and adapting execution behavior to dynamic workloads. As AI deployments continue to scale across heterogeneous accelerators, cloud environments, edge devices, and distributed infrastructures, software has become the critical layer that transforms hardware potential into operational capability. Table 8.4-C introduces the core software paradigms that enable this transformation and illustrates how modern AI systems coordinate computation, communication, memory management, and execution control across increasingly complex hardware ecosystems.

Table 8.4-C presents several foundational software paradigms that govern the execution, optimization, and scaling of modern AI systems. These paradigms represent the software counterpart to the hardware innovations discussed throughout Section 8.4 and form a central component of hardware–software co-design.

While AI accelerators provide the physical resources required for computation, software frameworks determine how effectively those resources are utilized. Large-scale AI systems must coordinate thousands of processing elements, manage massive parameter sets, maintain efficient communication among distributed nodes, and adapt execution behavior to changing workload conditions. Accomplishing these objectives requires sophisticated software infrastructures capable of orchestrating computation across multiple layers of the system.

The table identifies five major software paradigms: hardware-aware programming frameworks with tile-optimized compiler pipelines, distributed AI orchestration with tensor and context parallelism, latency masking through overlapped communication and computation, dynamic memory defragmentation and paged-attention retention strategies, and decentralized execution frameworks incorporating local cache eviction and federated protocols. Each paradigm

addresses a distinct challenge associated with scaling AI systems while maintaining performance and resource efficiency.

By examining the functional objectives, implementation mechanisms, performance benefits, and operational challenges associated with each paradigm, the table provides insight into how software increasingly serves as the coordinating intelligence that enables modern AI infrastructure.

Table 8.4-C — Core Software Paradigms in AI Systems

Software Paradigm	Primary Function	Key Mechanisms	Performance Advantages	Operational Challenges
AI Hardware - Aware Programming Frameworks & Tile-Optimized Kernel Compilation	Align neural execution with accelerator geometry and memory topology	Tile-aligned kernel fusion; hardware-specific IR; bank-aware scheduling; vector-pipeline mapping	Maximizes parallel utilization; reduces data movement; stabilizes precision; lowers kernel launch overhead	Requires detailed hardware introspection; complex compiler heuristics; brittle across heterogeneous accelerators
Distributed AI Orchestration with Tensor, Pipeline & Context Parallelism	Coordinate large-scale model execution across multi-node and multi-chiplet environments	Tensor sharding; micro-batch pipelining; KV-cache partitioning; distributed activation routing	Enables trillion -parameter inference; maintains deterministic latency; scales beyond single-node memory limits	Synchronization overhead; load imbalance; cross-fabric congestion; complex failure recovery
AI Latency Masking via Overlapped Compute &	Hide communication latency behind useful computation	Asynchronous kernel queues; double-buffered transfers; compute-communicatio	Eliminates idle cycles; sustains throughput under variable interconnect	Requires precise dependency tracking; sensitive to

Software Paradigm	Primary Function	Key Mechanisms	Performance Advantages	Operational Challenges
Fabric-Level Transfers		n overlap; fabric-aware scheduling	latency; improves real-time responsiveness	jitter; difficult to tune across heterogeneous fabrics
Dynamic AI Memory Defragmen-tation & Paged-Attention Retention Policies	Maintain contiguous memory regions and stable long-context inference	Live tensor relocation; KV-cache compaction; relevance-based paging; memory-pressure heuristics	Prevents fragmentation stalls; stabilizes long-sequence workloads; reduces thrashing; improves memory bandwidth locality	High runtime overhead if misconfigured; unpredictable behavior under bursty workloads; requires model-specific tuning
Decentralized AI Execution, Local Cache Eviction & Federated Asymmetric Protocols	Enable distributed inference and learning across heterogeneous, privacy-constraine d nodes	Local eviction heuristics; asymmetric update protocols; federated aggregation; topology-aware routing	Supports edge deployment; preserves privacy; adapts to heterogeneous compute; reduces centralized load	Non-uniform hardware complicates scheduling; inconsistent bandwidth; partial updates reduce convergence stability

Table 8.4-C demonstrates that AI software has evolved far beyond traditional application development. Rather than merely issuing instructions to hardware, modern AI software actively manages execution, coordinates communication, allocates resources, and adapts computational behavior across complex distributed infrastructures.

The software paradigms presented in the table reveal a common objective: maximizing the effective utilization of available hardware resources while minimizing the costs associated with

communication, memory movement, synchronization, and execution variability. In this sense, software functions as the operational control layer of contemporary AI systems.

The first software paradigm identified in the table is **AI hardware-aware programming frameworks and tile-optimized kernel compilation**.

Modern accelerators differ significantly in their execution models, memory hierarchies, vector-processing capabilities, and computational topologies. Generic software implementations often fail to exploit these architectural characteristics fully. Hardware-aware frameworks address this challenge by generating execution plans tailored to specific accelerator resources.

The table highlights tile-aligned kernel fusion, hardware-specific intermediate representations (IRs), bank-aware scheduling, and vector-pipeline mapping as key mechanisms. These techniques align computation directly with accelerator geometry and memory organization, reducing kernel-launch overhead and improving execution efficiency.

A notable benefit of this paradigm is improved hardware utilization. By organizing workloads according to the characteristics of the target accelerator, software can reduce unnecessary data movement and maximize available parallelism. However, the table also notes the complexity involved in maintaining portability across heterogeneous hardware environments.

The second paradigm is **distributed AI orchestration with tensor, pipeline, and context parallelism**.

As AI models exceed the memory and compute capacities of individual accelerator devices, execution must be distributed across multiple processors and nodes. Distributed orchestration frameworks coordinate this process by partitioning model parameters, activations, and execution contexts among available resources.

The mechanisms listed in the table include tensor sharding, micro-batch pipelining, KV-cache partitioning, and distributed activation routing. Together, these techniques allow trillion-parameter models to execute across distributed infrastructures while preserving throughput and latency targets.

The primary advantage of this paradigm is scalability. By enabling distributed execution, orchestration frameworks allow models to grow beyond the limitations of individual devices. At the same time, synchronization and communication overhead become significant challenges, emphasizing the need for sophisticated coordination strategies.

The third paradigm, **AI latency masking through overlapped computation and fabric-level transfers**, addresses the growing importance of communication costs in large-scale AI systems.

In many modern workloads, accelerators spend substantial time waiting for data transfers, synchronization events, or remote resources. Latency-masking frameworks seek to hide these delays by executing useful work while communication operations proceed concurrently.

The table identifies asynchronous kernel queues, double-buffered transfers, computation–communication overlap, and fabric-aware scheduling as representative techniques. These approaches allow accelerators to remain productive even when communication delays occur.

The resulting reduction in idle cycles improves throughput and enhances responsiveness in real-time AI systems. However, successful latency masking requires careful dependency tracking and workload coordination.

The fourth software paradigm is **dynamic AI memory defragmentation and paged-attention retention policies**.

Large language models and long-context inference workloads often place substantial pressure on memory resources. Fragmentation, inefficient cache utilization, and uncontrolled retention of historical state information can significantly degrade performance.

The mechanisms highlighted in the table include live tensor relocation, KV-cache compaction, relevance-based memory paging, and memory-pressure heuristics. These systems dynamically reorganize memory layouts to maintain efficient resource utilization and prevent fragmentation-induced performance degradation.

One of the most important benefits of this approach is improved stability during long-sequence processing. By controlling memory fragmentation and preserving locality, these frameworks help sustain consistent performance under demanding workloads.

The final paradigm identified in the table is **decentralized AI execution with local cache eviction and federated asymmetric protocols**.

As AI increasingly expands beyond centralized cloud environments, distributed and privacy-sensitive deployment scenarios become more important. Edge computing environments frequently operate under heterogeneous resource constraints, intermittent connectivity, and diverse hardware configurations.

The table highlights local eviction heuristics, asymmetric update protocols, federated aggregation methods, and topology-aware routing as key enabling mechanisms. These approaches allow computation to occur close to data sources while minimizing dependence on centralized infrastructure.

This paradigm supports privacy-preserving AI execution, reduces centralized workloads, and

enables adaptation to heterogeneous computing environments. However, maintaining consistency and convergence across distributed nodes introduces significant coordination challenges.

A broader insight emerging from the table is that software increasingly manages the same constraints that hardware architectures seek to address. Hardware reduces communication costs, while software schedules communication intelligently. Hardware improves memory efficiency, while software manages memory allocation dynamically. Hardware supports distributed execution, while software coordinates distributed resources. Together, these layers form a tightly integrated ecosystem.

The table also highlights the growing importance of adaptability in AI software. Fixed execution strategies are often insufficient for dynamic workloads involving variable sequence lengths, conditional routing, sparse computation, and heterogeneous hardware. The paradigms presented here emphasize continuous adaptation to changing system conditions.

From a systems-engineering perspective, the software paradigms summarized in the table operate at different layers of the execution stack. Compiler frameworks optimize local execution. Distributed orchestration manages global scaling. Latency masking addresses communication overhead. Memory-management systems preserve locality and efficiency. Federated frameworks support decentralized deployment. Collectively, these paradigms enable AI systems to function effectively across a wide range of operating environments.

Another important observation is that software increasingly serves as the bridge between abstract AI models and physical computing infrastructure. Model architectures define what computation must occur, hardware determines where it can occur efficiently, and software determines how it is ultimately executed.

Ultimately, Table 8.4-C demonstrates that modern AI performance depends as much on software architecture as on hardware capability. Through hardware-aware compilation, distributed orchestration, latency masking, intelligent memory management, and decentralized execution frameworks, software transforms complex collections of accelerators, memory systems, and communication fabrics into coherent computational platforms. These paradigms represent the operational foundation upon which scalable, efficient, and reliable AI systems are built.

The software paradigms summarized in Table 8.4-C demonstrate that efficient AI execution depends upon a tightly coordinated interplay among compiler intelligence, runtime orchestration, memory management, and distributed execution frameworks. Yet all of these higher-level capabilities rest upon a more fundamental requirement: the ability to translate

abstract neural-network operations into execution patterns that align with the physical structure of the underlying hardware. Before computation can be distributed across accelerator clusters, before communication latency can be hidden through overlap strategies, before memory resources can be managed dynamically, and before decentralized nodes can cooperate effectively, the execution graph must first be transformed into hardware-aware kernels optimized for accelerator topology. This transformation requires an understanding of tile geometry, memory-bank organization, vector-pipeline behavior, communication fabrics, and device-specific execution constraints. Consequently, hardware-aware programming frameworks and tile-optimized compilation form the foundational software layer upon which all subsequent AI execution optimizations depend. The following discussion examines **AI Hardware-Aware Programming Frameworks and Tile-Optimized Kernel Compilation**, exploring how modern compiler and runtime systems convert high-level tensor computations into substrate-aligned execution plans capable of maximizing performance, utilization, and efficiency across increasingly heterogeneous AI accelerators.

a. AI Hardware-Aware Programming Frameworks and Tile-Optimized Kernel Compilation

Hardware-aware programming frameworks form the foundational layer of modern AI software design. They translate abstract tensor programs into execution plans that conform to the physical geometry, memory topology, and vector-pipeline behavior of contemporary accelerators. Instead of treating hardware as a generic compute substrate, these frameworks expose block-level abstractions, shared-memory controls, and thread-mapping primitives that allow kernels to be compiled directly against tile boundaries, bank layouts, and heterogeneous execution lanes. This alignment ensures that neural operators—convolutions, attention heads, state-space transforms, and fused arithmetic blocks—execute with minimal data movement, maximal parallel utilization, and predictable latency across diverse accelerator architectures. Hardware-aware compilation is the point where software begins to behave as an extension of silicon, shaping how efficiently intelligence can be expressed within real-world constraints.

- **Triton-Style AI Block Abstractions for Vectorized Kernel Generation** - Block-level abstractions provide a high-level programming model that maps directly onto accelerator tile geometry. By expressing kernels in terms of logical blocks rather than raw threads, frameworks can automatically generate vectorized code that aligns with tensor-core dimensions, memory-bank boundaries, and SIMD lane widths. This approach simplifies kernel authoring while enabling aggressive fusion, tiling, and vectorization strategies that maximize throughput and minimize memory traffic.
- **Direct AI Shared-Memory Management and Hardware-Aligned Pointer Arithmetic** - Shared-memory control gives developers explicit authority over how tensors are staged,

reused, and synchronized within on-chip memory banks. Hardware-aligned pointer arithmetic ensures that loads and stores map cleanly onto banked memory structures, avoiding conflicts and maximizing bandwidth. These mechanisms allow kernels to exploit locality, reduce global-memory pressure, and maintain deterministic performance even under irregular access patterns.

- **Automatic AI Thread-Block Mapping onto Custom Vector Lanes** - Automatic thread-block mapping assigns execution groups to the accelerator's heterogeneous vector lanes, tensor cores, and matrix engines. By analyzing kernel structure and hardware topology, compilers determine optimal mappings that balance load, minimize divergence, and sustain high utilization across all compute units. This automation eliminates the need for manual tuning while ensuring that kernels adapt to diverse accelerator configurations.
- **High-Level AI Kernel Interoperability within PyTorch Runtime Systems** - Interoperability layers integrate hardware-aware kernels seamlessly into PyTorch's dynamic execution environment. They allow custom kernels to coexist with autograd, graph-lowering passes, and distributed runtimes without sacrificing performance or flexibility. This ensures that substrate-aligned kernels remain accessible to model developers while preserving the expressive power of high-level frameworks.

Together, these mechanisms transform hardware-aware programming frameworks into a critical component of AI co-design. They ensure that neural computation conforms to the contours of silicon, enabling accelerators to deliver high-density arithmetic, low-latency memory access, and predictable execution behavior across diverse workloads and deployment environments.

Hardware-aware programming frameworks mark the point where abstract neural computation begins conforming to the physical geometry of the accelerator. Before distributed parallelism, latency masking, or memory-retention strategies can operate effectively, the execution graph must first be lowered into kernels that respect tile boundaries, memory-bank topology, vector-lane structure, and the heterogeneous timing regimes of the underlying hardware. This foundational alignment determines how efficiently every subsequent software paradigm can exploit silicon. To clarify the mechanisms that enable this substrate-aligned transformation, The following table organizes the core techniques used in modern kernel compilation frameworks, revealing how block abstractions, shared-memory control, automatic thread-mapping, and runtime interoperability collectively shape the performance envelope of AI execution.

The discussion of AI hardware-aware programming frameworks established that modern accelerators achieve peak performance only when computational graphs are explicitly aligned

with the structural characteristics of the underlying hardware. High-level neural-network definitions, while expressive and portable, do not directly expose critical details such as tile geometry, memory-bank organization, vector-lane utilization, tensor-core mapping, or cache locality. Consequently, a substantial transformation must occur between model specification and hardware execution. This transformation is performed by kernel-compilation systems that decompose tensor operations, optimize data movement, align computation with accelerator topology, and generate execution plans tailored to specific hardware substrates. Table 8.4-C1 examines the core mechanisms that enable this process and illustrates how modern compiler frameworks convert abstract neural computations into highly optimized, accelerator-native workloads.

Table 8.4-C1 presents several foundational mechanisms that underpin hardware-aware AI kernel compilation. These mechanisms form the software infrastructure responsible for translating high-level tensor operations into hardware-efficient execution patterns optimized for modern accelerators.

As AI architectures have become increasingly sophisticated, the performance gap between naïve execution and hardware-optimized execution has grown substantially. Contemporary accelerators contain complex memory hierarchies, tensor-core arrays, vector-processing units, specialized scheduling fabrics, and heterogeneous execution resources. Simply expressing computation at a high level is insufficient to exploit these capabilities efficiently.

Hardware-aware compilation addresses this challenge by introducing optimization stages that align computational workloads with the physical structure of the accelerator. These optimizations include tile-level decomposition, memory-aware staging, execution-group mapping, and integration with dynamic runtime frameworks. Together, they ensure that arithmetic throughput, memory locality, parallelism, and scheduling behavior remain aligned throughout execution.

The table identifies four representative mechanisms: Triton-style block abstractions, direct shared-memory management and pointer arithmetic, automatic thread-block mapping, and high-level kernel interoperability with frameworks such as PyTorch. Each mechanism addresses a distinct aspect of the translation process between neural-network abstractions and accelerator-native execution.

By examining these mechanisms collectively, the table highlights how modern compiler systems increasingly function as performance-oriented orchestration layers rather than simple code-generation tools.

Table 8.4-C1 — Core Mechanisms in Hardware-Aware AI Kernel Compilation

Mechanism	Primary Role	Key Behaviors	Execution Advantages	Design Considerations
Triton-Style Block Abstractions	Map logical kernel blocks to accelerator tile geometry	Vectorized block generation; tile-aligned fusion; SIMD-aware loop construction	Maximizes parallel utilization; reduces memory traffic; simplifies kernel authoring	Requires hardware-specific IR; sensitive to tile size mismatches
Direct Shared-Memory Management & Pointer Arithmetic	Control on-chip memory staging and bank-aligned access	Manual shared-memory tiling; conflict-free pointer arithmetic; synchronized reuse of local buffers	Eliminates bank conflicts; improves locality; reduces global-memory pressure	Demands precise memory-bank knowledge; error-prone without compiler safeguards
Automatic Thread-Block Mapping	Assign execution groups to heterogeneous vector lanes	Lane-aware scheduling; tensor-core mapping; divergence-minimizing block placement	Sustains high utilization; balances load across compute units; adapts to diverse accelerator topologies	Complex heuristics; requires accurate hardware introspection
High-Level Kernel Interoperability (PyTorch Runtime)	Integrate substrate-aligned kernels into dynamic execution graphs	Autograd compatibility; graph-lowering integration; distributed-runtime alignment	Preserves developer ergonomics; enables custom kernels without losing	Must maintain consistency with PyTorch semantics; runtime overhead if misaligned

Mechanism	Primary Role	Key Behaviors	Execution Advantages	Design Considerations
			framework flexibility	

Table 8.4-C1 demonstrates that efficient AI execution begins long before computation reaches hardware. The compiler serves as an intermediary layer that determines how neural-network operations will consume memory, utilize parallel resources, access tensor cores, and interact with execution pipelines.

The mechanisms presented in the table reveal a common objective: maximizing hardware utilization by ensuring that software-generated workloads conform closely to accelerator architecture. In effect, hardware-aware compilation transforms abstract mathematical operations into physically optimized execution strategies.

The first mechanism identified in the table is **Triton-style block abstractions**, which provide a structured framework for mapping tensor operations onto accelerator tile geometries.

Modern accelerators typically execute workloads in tiled units rather than processing entire tensors simultaneously. Effective execution therefore depends on decomposing large operations into blocks aligned with memory systems, tensor cores, and execution fabrics. Triton-style abstractions automate much of this process by generating vectorized execution blocks, performing tile-aligned fusion, and constructing SIMD-aware loop structures.

The table highlights several advantages of this approach. Because operations are decomposed according to accelerator geometry, parallel utilization improves significantly. Memory traffic is reduced through locality-aware execution, and kernel development becomes more accessible by allowing programmers to work at a higher level of abstraction. At the same time, successful deployment requires hardware-specific intermediate representations and careful matching between block dimensions and physical tile sizes.

The second mechanism is **direct shared-memory management and pointer arithmetic**, which provides fine-grained control over data placement within accelerator memory hierarchies.

Modern accelerators frequently contain fast local memory resources that can dramatically reduce access latency when used effectively. Shared-memory management allows developers and compiler systems to stage data close to computational units, reducing dependence on slower global memory systems.

The table emphasizes manual tiling, conflict-free pointer structures, synchronized buffer reuse,

and locality optimization as key behaviors supporting this mechanism. These techniques eliminate memory-bank conflicts and improve reuse of frequently accessed data.

Although highly effective, this approach introduces additional complexity. Successful implementation requires a detailed understanding of memory-bank organization, access patterns, synchronization behavior, and hardware-specific constraints. As a result, compiler assistance often becomes essential for preserving correctness and portability.

The third mechanism is **automatic thread-block mapping**, which addresses the challenge of distributing workloads across heterogeneous execution resources.

AI accelerators frequently contain multiple classes of compute units operating simultaneously. Efficient execution therefore depends on assigning thread groups to hardware resources in ways that maximize occupancy and minimize idle cycles.

The table identifies lane-aware scheduling, tensor-core mapping, divergence-minimizing placement, and adaptive block allocation as representative behaviors supporting this objective. By aligning workloads with the underlying execution topology, automatic mapping maintains balanced utilization across computational resources.

One of the most important benefits of this mechanism is adaptability. Different accelerators may possess different lane widths, execution structures, and scheduling hierarchies. Automatic thread-block mapping enables software to adjust dynamically to these variations without requiring extensive manual optimization.

The final mechanism presented in the table is **high-level kernel interoperability with runtime frameworks such as PyTorch**.

Advanced optimization techniques provide limited practical value if they cannot integrate with the development environments used by AI practitioners. Consequently, modern compilation systems increasingly emphasize compatibility with existing machine-learning ecosystems.

The table highlights autograd integration, graph-lowering pipelines, runtime coordination, and distributed execution alignment as key enablers. These mechanisms allow highly optimized kernels to operate within familiar development workflows while preserving compatibility with model-training and inference frameworks.

This interoperability provides an important balance between performance and usability. Researchers and engineers can access hardware-specific optimizations without abandoning the abstractions that make modern AI development productive.

A broader insight emerging from the table is that hardware-aware compilation operates across

multiple levels of abstraction simultaneously. At one level, it manages low-level concerns such as memory locality, thread placement, and tile geometry. At another, it preserves compatibility with high-level frameworks and dynamic execution environments. Successful compiler design therefore requires coordination across the entire software stack.

The table also demonstrates that many optimization opportunities originate from architectural awareness rather than algorithmic changes. The neural-network model may remain unchanged, while compiler optimizations significantly improve execution efficiency through better alignment with hardware structures.

From a systems-engineering perspective, the mechanisms summarized in the table address complementary dimensions of execution optimization. Block abstractions improve computational structuring. Shared-memory management improves locality. Thread-block mapping improves resource utilization. Runtime interoperability preserves software productivity. Together, these techniques create a comprehensive framework for accelerating AI workloads.

Another important observation is that these mechanisms become increasingly valuable as hardware heterogeneity grows. Modern AI infrastructures often incorporate GPUs, TPUs, CGRAs, AI accelerators, and custom processing fabrics within the same deployment environment. Hardware-aware compilation provides a systematic way to exploit these diverse resources efficiently.

Ultimately, Table 8.4-C1 illustrates how hardware-aware kernel compilation serves as the bridge between neural-network abstractions and physical execution hardware. Through tile-aware decomposition, local-memory optimization, intelligent workload mapping, and runtime integration, compiler systems transform high-level AI workloads into accelerator-native execution plans. These mechanisms enable modern AI software to fully exploit the capabilities of increasingly specialized hardware architectures, making kernel compilation one of the foundational layers of contemporary AI-system performance engineering.

Table 8.4-C1 introduced the principal mechanisms that enable hardware-aware AI kernel compilation, including tile-level abstractions, shared-memory optimization, automatic thread-block mapping, and runtime interoperability. While the table examined these mechanisms individually, the process of kernel compilation is ultimately a coordinated transformation pipeline in which high-level tensor operations are progressively reshaped into hardware-aligned execution structures. Effective compilation requires simultaneous consideration of graph lowering, tile generation, memory staging, vector-lane assignment, and accelerator-fabric mapping. Figure 8.4-C1 visualizes this transformation process, illustrating how neural-network

operations move through successive compilation layers before becoming executable workloads aligned with the physical organization of the target accelerator. The figure provides a systems-level view of how software abstractions are translated into efficient hardware execution.

Figure 8.4-C1 presents a layered model of hardware-aware kernel compilation for AI accelerators. The figure illustrates how high-level tensor programs are transformed into hardware-efficient execution plans through a sequence of compilation, optimization, scheduling, and mapping stages.

Modern AI models are generally expressed using high-level frameworks such as PyTorch, TensorFlow, or JAX. At this level, developers describe tensor operations and computational relationships without specifying how individual operations should be executed on underlying hardware. However, high-performance execution requires a much deeper understanding of accelerator topology, memory hierarchy organization, vector-processing resources, and tensor-core utilization.

To bridge this gap, hardware-aware compiler frameworks progressively lower abstract computational graphs into increasingly specialized representations. During this process, operations are reorganized into tiles, fused into optimized kernels, mapped onto vectorized execution units, and aligned with accelerator memory structures.

The figure organizes this workflow into four layers: graph lowering, tile-level kernel generation, hardware-aligned execution mapping, and accelerator-fabric execution. Together, these layers form the translation pathway through which abstract machine-learning programs become efficient hardware-native workloads.

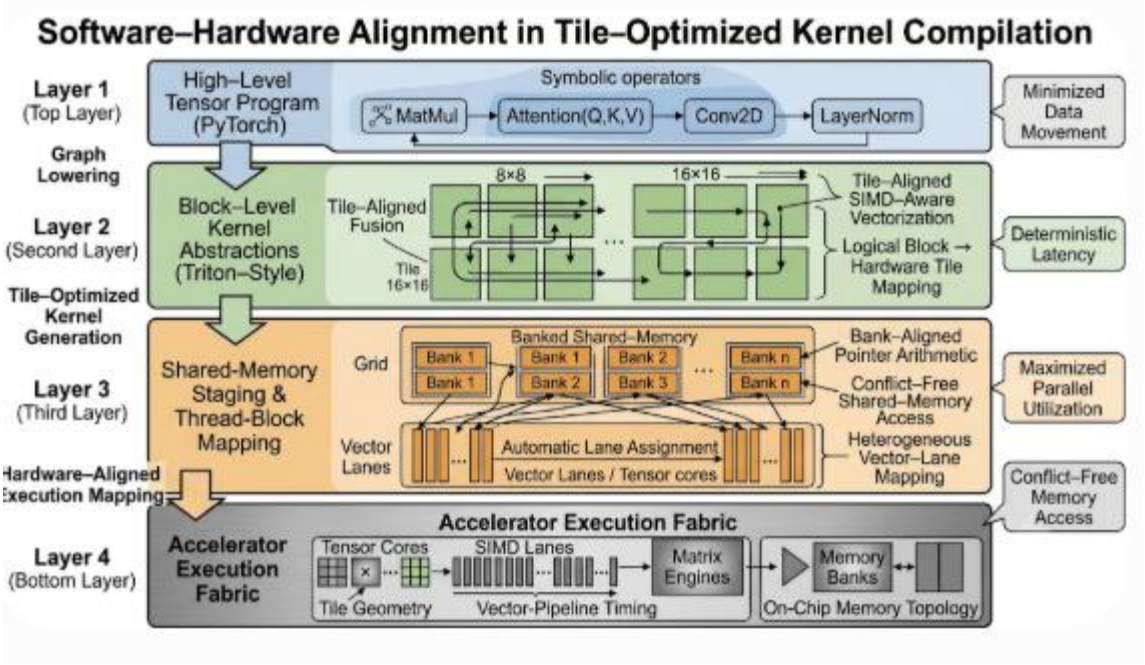


Figure 8.4-C1 — Software–Hardware Alignment in Tile-Optimized Kernel Compilation

Multi-layer compilation workflow illustrating how high-level tensor programs are transformed into hardware-efficient execution plans. The figure traces the progression from graph-level neural operations through tile-oriented kernel generation, shared-memory staging, vector-lane allocation, and accelerator-fabric mapping. The compilation pipeline demonstrates how hardware-aware software frameworks minimize data movement, maximize execution parallelism, reduce latency, and align neural computation with accelerator topology.

Legend

Component	***Description***
Layer 1: Graph Lowering (Top Layer)	*High-level neural-network representation before hardware-specific optimization.*
High-Level Tensor Program (PyTorch)	*User-defined neural-network operations and computational graph.*
MatMul / Attention(Q,K	*Representative symbolic tensor operations.*
Symbolic Operators	*Abstract computational primitives awaiting compilation.*
Layer 2: Tile-Level Kernel Generation	*Intermediate stage creating hardware-aligned execution blocks.*

Triton-Style Kernel Abstractions	*Tile-oriented programming model exposing hardware structure.*
Tile-Aligned Fusion	*Compiler optimization combining operations into efficient execution units.*
8×8 / 16×16 Tiles	*Representative hardware-aligned computational blocks.*
SIMD-Aware Vectorization	*Transformation optimizing execution for vector-processing hardware.*
Logical Block-to-Hardware Tile Mapping	*Translation from software tiles to accelerator geometry.*
Layer 3: Hardware-Aligned Executi	*Stage responsible for memory placement and thread scheduling.*
Shared-Memory Staging	*Placement of frequently accessed data within local accelerator memory.*
Thread-Block Mapping	*Assignment of workgroups to hardware execution resources.*
Banked Shared Memory	*Organized local-memory structure optimized for concurrent access.*
Automatic Lane Assignment	*Mapping of computation to vector-processing lanes.*
Conflict-Free Shared-Memory Access	*Optimization preventing memory-bank contention.*
Layer 4: Accelerator Fabric Execution (Bottom Layer)	*Physical execution layer within the target accelerator.*
Tensor Cores	*Specialized matrix-processing units.*
SIMD Lanes	*Parallel vector-execution resources.*
Matrix	*Dedicated arithmetic units supporting tensor computation.*
Memory Banks	*Local storage systems supporting accelerator execution.*
Tile Geometry	*Physical layout governing computational mapping.*
Vector-Pipeline Timing	*Scheduling structure controlling execution flow.*
On-Chip Memory Top	*Physical memory organization influencing data movement.*

Minimized Data Movement	*Reduced memory-transfer overhead.*
Deterministic Latency	*Predictable execution timing.*
Maximized Parallel Utilization	*High occupancy across compute resources.*
Conflict-Free Memory Access	*Elimination of memory-contention bottlenecks.*

Figure 8.4-C1 illustrates that high-performance AI execution is achieved through a sequence of increasingly hardware-specific transformations. The figure emphasizes that modern AI accelerators do not execute high-level neural-network descriptions directly. Instead, compiler frameworks progressively reshape computational graphs into forms aligned with tile structures, memory hierarchies, and vector-processing resources.

The architecture highlights a central principle of hardware–software co-design: performance depends not only on what computation is performed but also on how that computation is organized to match the physical characteristics of the hardware.

The figure begins at **Layer 1: Graph Lowering**, where AI workloads exist as high-level tensor programs. Operations such as matrix multiplication, attention computation, convolution, and normalization are represented symbolically within machine-learning frameworks.

At this stage, the computational graph expresses mathematical intent but contains little information about how operations will be executed on a specific accelerator. The framework defines what computation should occur but remains largely independent of hardware details.

The first major transformation occurs as these symbolic operators move into **Layer 2: Tile-Level Kernel Generation**.

This layer converts large tensor operations into smaller computational units aligned with accelerator geometry. The figure illustrates tile structures such as 8×8 and 16×16 workloads, representing the decomposition of high-level operations into hardware-friendly execution blocks.

Tile-aligned fusion combines multiple operations into larger execution units that improve locality and reduce intermediate memory traffic. At the same time, SIMD-aware vectorization restructures computation so that many operations can execute simultaneously across vector pipelines.

A key objective of this stage is matching software structure to hardware structure. Rather than treating tensors as monolithic objects, the compiler reorganizes them according to the execution characteristics of the target device.

The next stage, **Layer 3: Hardware-Aligned Execution Mapping**, focuses on resource allocation.

The figure shows data entering shared-memory staging structures where frequently accessed values are placed in fast local memory. Banked-memory organizations support parallel access while reducing latency.

Thread-block mapping assigns computational workgroups to execution resources. Automatic lane assignment distributes operations across vector lanes and tensor-processing units.

Particular emphasis is placed on avoiding memory conflicts. If multiple threads compete for the same memory bank simultaneously, execution stalls may occur. Conflict-free memory access patterns therefore constitute one of the most important objectives of this stage.

The hardware-aware mapping layer effectively serves as the bridge between compiler-generated kernels and physical execution resources.

The final stage, **Layer 4: Accelerator Fabric Execution**, represents the hardware itself.

The figure highlights tensor cores, SIMD lanes, matrix engines, and memory banks integrated within a unified execution fabric. By this point, the workload has already been transformed into a hardware-native representation optimized for the target architecture.

The tile geometry established earlier now aligns directly with physical compute structures. Vector-pipeline timing controls execution sequencing, while the memory topology supports efficient data access.

As a result, the workload enters execution under conditions specifically designed to maximize utilization of available hardware resources.

The figure identifies four important outcomes produced by this layered optimization process.

The first is **minimized data movement**. Through tiling, fusion, and shared-memory staging, the compiler reduces unnecessary transfers among memory levels.

The second is **deterministic latency**. Hardware-aware scheduling and mapping reduce execution variability, producing more predictable timing behavior.

The third outcome is **maximized parallel utilization**. Automatic lane assignment, tensor-core mapping, and thread-block scheduling help ensure that available compute resources remain active.

The fourth is **conflict-free memory access**, which prevents performance degradation caused by bank contention and inefficient memory-allocation patterns.

A broader insight emerging from the figure is that AI compilation operates as a multi-layer optimization process rather than a single translation step. Each layer contributes specific transformations that collectively align software behavior with hardware execution requirements.

The figure also demonstrates why hardware-aware frameworks have become increasingly important as accelerator architectures grow more specialized. General-purpose compilation strategies often fail to exploit tensor cores, shared-memory hierarchies, and vector-execution fabrics efficiently. The layered approach shown here addresses these challenges explicitly.

From a systems-engineering perspective, the workflow illustrates a gradual narrowing of abstraction. High-level neural concepts are first expressed mathematically, then transformed into tiles, mapped onto memory systems, assigned to execution resources, and finally executed within the hardware fabric.

Another important observation is that many performance improvements occur before computation begins. Compiler decisions regarding tiling, fusion, mapping, and scheduling strongly influence execution efficiency even though they do not alter the underlying neural-network algorithm.

Ultimately, Figure 8.4-C1 demonstrates that high-performance AI execution emerges through careful alignment between software abstractions and hardware architecture. By progressively transforming symbolic tensor operations into tile-optimized, memory-aware, and vectorized execution plans, hardware-aware compilers enable modern AI systems to exploit accelerator resources efficiently. This compilation pipeline serves as the critical bridge connecting neural-network models to the physical hardware that executes them, making software–hardware alignment a foundational principle of contemporary AI system design.

The layered transformation illustrated in Figure 8.4-C1 demonstrates that hardware-aware compilation is fundamentally a process of progressively aligning software abstractions with the physical realities of accelerator execution. This alignment begins not at the point of memory placement or thread scheduling, but earlier, when high-level tensor operations are first decomposed into computational blocks whose dimensions, access patterns, and execution structure reflect the geometry of the target hardware. Before shared-memory staging can optimize locality, before automatic thread-block mapping can balance workloads across vector lanes and tensor cores, and before accelerator fabrics can achieve high utilization, the compiler must establish a tile-oriented representation that serves as the foundation for all subsequent optimizations. This transformation is enabled through **Triton-style block abstractions**, which encode tile geometry, vector widths, data-locality assumptions, and fusion opportunities

directly into the kernel structure. By providing a hardware-conscious intermediate representation of computation, these abstractions bridge the gap between framework-level tensor semantics and accelerator-native execution. The following discussion examines **Triton-Style AI Block Abstractions for Vectorized Kernel Generation**, exploring how block-oriented programming models enable compilers to generate high-performance kernels that align naturally with tensor-core architectures, memory-bank organizations, and modern vector-processing pipelines.

i. Triton-Style AI Block Abstractions for Vectorized Kernel Generation

Triton-style block abstractions represent one of the most consequential shifts in AI kernel design because they allow software to express computation in units that directly mirror the spatial and temporal structure of accelerator hardware. Unlike traditional GPU programming models—where developers manually orchestrate threads, warps, and memory transactions—Triton exposes a higher-level block abstraction that aligns naturally with the tile geometry used in tensor cores, matrix engines, and compute-in-memory fabrics. This abstraction is explicitly designed for AI workloads, where operators such as attention, matmul, convolution, and normalization exhibit regular, tile-friendly patterns that benefit from aggressive vectorization and fusion.

At the AI level, block abstractions serve three critical roles:

- **Encoding AI tensor semantics into hardware-aligned spatial units -** AI operators manipulate large, structured tensors—activation matrices, KV-caches, convolutional windows, embedding blocks. Triton blocks partition these tensors into logical tiles that match the accelerator's physical tile dimensions (e.g., 8×8, 16×16, 32×32). This alignment ensures that each block maps cleanly onto SIMD lanes or tensor-core fragments, eliminating the mismatch between software granularity and hardware execution width.

- **Enabling vectorized kernel generation tailored to AI operator patterns -** AI workloads thrive on vectorization: fused multiply-adds, batched dot-products, softmax pipelines, and fused attention kernels. Triton blocks allow compilers to generate vectorized loops that sweep across tiles in predictable patterns, enabling:

    - SIMD-aware loop construction
    - tile-aligned fusion of adjacent operations
    - reuse of intermediate values within the block
    - reduction of global memory traffic through local accumulation

This is particularly important for transformer-class models, where matmul and attention dominate runtime and benefit enormously from tile-aligned vectorization.

- **Enabling vectorized kernel generation tailored to AI operator patterns -** AI kernels often contain sequences of operations that can be fused—matmul + bias + activation, attention + softmax + scaling, normalization + residual addition. Block abstractions give the compiler a structured unit within which fusion can occur safely and efficiently, without violating memory-bank constraints or vector-lane alignment. Fusion at the block level reduces:
    - memory round-trips
    - synchronization overhead
    - intermediate tensor materialization
    - latency variability under dynamic workloads

  This is essential for real-time AI systems, where inference pipelines must remain deterministic even under fluctuating input patterns.

Triton-style block abstractions are far more than a programming convenience; they constitute the critical translation layer between high-level AI tensor semantics and the physical execution geometry of modern accelerators. This abstraction layer enables kernels to be expressed at a level that remains accessible to model developers while simultaneously exposing sufficient architectural detail for compilers to generate hardware-aligned code. By embedding tile dimensions, vector widths, memory-bank layouts, and execution-granularity constraints directly into the block structure, Triton allows AI workloads to be mapped naturally onto tensor cores, vector-processing units, and hierarchical memory systems rather than forcing them through generic GPU programming models designed for broader computational domains.

This hardware-conscious representation is what enables many of the performance characteristics required by contemporary AI systems, including:

- Deterministic latency for transformer inference workloads.
- High throughput for General Matrix–Matrix Multiplication (GEMM)-dominated execution pipelines.
- Efficient management and movement of Key–Value (KV) caches during autoregressive generation.

- Scalable execution of long-context attention mechanisms.
- Stable performance under mixed-precision and low-precision arithmetic formats.
- Predictable behavior across heterogeneous accelerator fabrics and distributed execution environments.

More importantly, block abstractions establish the structural foundation upon which the remainder of the hardware-aware optimization pipeline is built. Shared-memory staging strategies, thread-block mapping policies, conflict-free memory access patterns, hardware-aligned pointer arithmetic, and vector-lane scheduling all depend upon the spatial regularity, locality awareness, and vector-friendly execution structure introduced at the block-abstraction level. Consequently, Triton blocks serve as the fundamental organizational unit through which modern AI compilers bridge the gap between abstract neural-network computation and efficient accelerator-native execution.

ii. Direct AI Shared-Memory Management and Hardware-Aligned Pointer Arithmetic

Direct shared-memory management and hardware-aligned pointer arithmetic constitute the foundational substrate upon which high-performance AI kernel execution is built. By providing explicit control over data placement, movement, reuse, and synchronization within on-chip memory resources, this mechanism enables AI workloads to exploit locality while minimizing dependence on slower global-memory transfers. Such control is particularly important for modern AI architectures, where activation tensors, attention matrices, Key–Value (KV) caches, and fused-operator intermediates must be accessed repeatedly at extremely high bandwidth and with predictable latency characteristics.

At the core of this approach is the alignment of pointer arithmetic with the physical organization of accelerator memory systems. Bank-aware addressing schemes ensure that data accesses are distributed efficiently across shared-memory banks, avoiding contention, eliminating serialization effects, and preserving deterministic timing behavior. As a result, memory operations align naturally with the accelerator's internal topology, allowing computational kernels to maintain continuous execution while maximizing effective bandwidth utilization.

This hardware-aware memory model enables:

- Conflict-free staging of attention tiles and General Matrix–Matrix Multiplication (GEMM) fragments.
- High-bandwidth reuse of convolutional windows, tensor blocks, and fused-operator intermediates.

- Stable and efficient Key–Value (KV) cache access during long-context inference.
- Reduced global-memory traffic throughout transformer and state-space processing pipelines.
- Predictable latency under mixed-precision and low-precision execution regimes.
- Efficient deployment across accelerators exhibiting diverse memory-bank organizations and hierarchy designs.

More importantly, shared-memory management and pointer alignment establish the operational foundation upon which nearly all subsequent kernel optimizations depend. Thread-block mapping, vector-lane utilization, tensor-core scheduling, operator fusion, and asynchronous execution pipelines all rely on the spatial regularity, locality awareness, and deterministic access patterns introduced at this stage. When memory staging is performed correctly and pointer arithmetic is aligned with underlying bank topology, AI kernels cease to behave as generic accelerator workloads and instead function as tightly coupled extensions of the hardware itself, achieving high throughput, efficient resource utilization, and stable execution behavior even under irregular, sparse, or bursty workload conditions.

Once AI computation has been reshaped into tile-aligned blocks, the next challenge is ensuring that these blocks interact with on-chip memory in a manner that preserves locality, eliminates bank conflicts, and sustains deterministic throughput. Block abstractions establish the spatial structure of execution, but the performance characteristics of AI kernels ultimately depend on how intermediate tensors, KV-caches, and fused-operator buffers are staged within shared memory and accessed through hardware-aligned pointer arithmetic. This transition marks the shift from geometric alignment to topological alignment—where the compiler must manage memory banks, synchronization boundaries, and access patterns with precision. The discussion of **Direct AI Shared-Memory Management and Hardware-Aligned Pointer Arithmetic** examines this layer of the pipeline, detailing how direct shared-memory control and pointer alignment enable AI kernels to operate as tightly coupled

With shared-memory staging and hardware-aligned pointer arithmetic establishing deterministic access patterns inside each tile, the next step in the compilation pipeline is assigning those tiles to the accelerator’s heterogeneous compute units. Memory alignment alone cannot guarantee high throughput; the execution fabric must be saturated with work that matches the width, depth, and timing characteristics of tensor cores, SIMD lanes, and matrix engines. This transition marks the shift from topological alignment to execution-lane alignment, where the compiler determines how thread blocks should be distributed across vector lanes to minimize divergence, balance load, and sustain parallel utilization. Automatic thread-block

placement transforms memory-optimized tiles into fully utilized execution groups capable of exploiting the accelerator's heterogeneous arithmetic pipelines.

iii. Automatic AI Thread-Block Mapping onto Custom Vector Lanes

Automatic thread-block mapping onto custom vector lanes represents the execution-alignment stage of the hardware-aware kernel optimization pipeline. Once tile decomposition, shared-memory staging, and hardware-aligned pointer arithmetic have established efficient data locality and deterministic access patterns, the compiler must determine how those computational tiles are distributed across the accelerator's heterogeneous execution resources. This mapping process is crucial because modern AI accelerators are no longer composed of uniform processing units. Instead, they integrate tensor cores, **Single Instruction, Multiple Data (SIMD)** lanes, matrix engines, vector processors, and specialized low-precision arithmetic units, each characterized by different execution widths, latency profiles, and scheduling constraints.

Thread-block mapping serves as the mechanism through which computational workloads are aligned with these diverse resources. By intelligently assigning work to the most appropriate execution units, the compiler seeks to maximize utilization, minimize execution divergence, balance resource occupancy, and sustain throughput across the entire accelerator fabric. In effect, thread-block mapping transforms abstract computational tiles into hardware-native execution entities that can exploit the full capabilities of the underlying architecture.

This hardware-aware scheduling model enables:

- Balanced distribution of General Matrix–Matrix Multiplication (GEMM) and attention tiles across heterogeneous vector-processing resources.
- Sustained utilization of tensor-core fragments during fused-operator and multi-stage execution pipelines.
- Reduced warp, wavefront, or thread-group divergence in transformer, mixture-of-experts (MoE), and state-space workloads.
- Predictable scheduling of Key–Value (KV) cache updates and long-context attention computations.
- Stable throughput under mixed-precision and low-precision execution regimes.
- Efficient execution across accelerators exhibiting asymmetric compute-unit distributions and heterogeneous processing fabrics.

More importantly, thread-block mapping establishes the execution foundation upon which all higher-level runtime optimizations depend. Vector-lane saturation, tensor-core occupancy,

fused-operator sequencing, asynchronous work scheduling, and runtime orchestration frameworks all assume that workloads have been mapped correctly to available hardware resources. When compiler-generated thread blocks are aligned with execution-lane widths, pipeline timing, memory locality, and compute-unit specialization, AI kernels operate as tightly coordinated extensions of the accelerator itself. The result is sustained throughput, high resource utilization, and deterministic latency characteristics, even in environments characterized by dynamic execution graphs, irregular attention patterns, sparse expert routing, or bursty inference workloads.

Once thread-block mapping aligns tile-optimized kernels with the accelerator's heterogeneous vector lanes, the compilation pipeline must reconnect these substrate-aligned execution units to the high-level AI framework that orchestrates model behavior. Hardware-aligned kernels alone cannot support modern AI workloads; they must integrate seamlessly with PyTorch's dynamic graph construction, autograd mechanics, distributed runtimes, and mixed-precision execution policies. This transition marks the shift from execution-lane alignment to framework-level interoperability, where substrate-optimized kernels are embedded into a flexible runtime capable of coordinating large-scale models, multi-node training, and real-time inference. High-level interoperability ensures that hardware-aligned kernels remain accessible to model developers while preserving the expressive power, modularity, and dynamism that define contemporary AI systems.

iv. High-Level AI Kernel Interoperability within PyTorch Runtime Systems

High-level kernel interoperability within PyTorch runtime systems forms the integration layer that reconnects substrate-aligned kernels to the dynamic, expressive environment in which AI models are authored, trained, and deployed. Tile-optimized kernels, shared-memory-aligned access patterns, and vector-lane-aware execution groups provide the raw performance foundation, but modern AI workloads demand far more than isolated low-level efficiency. PyTorch supplies autograd mechanics, dynamic graph construction, distributed execution frameworks, mixed-precision policies, and module-level abstractions that define how large-scale models behave. Interoperability ensures that hardware-aligned kernels operate as first-class components within this ecosystem rather than external artifacts bolted onto the runtime.

At the AI level, interoperability serves several critical roles:

- **Embedding substrate-aligned kernels into dynamic computation graphs** - PyTorch constructs execution graphs at runtime, allowing models to adapt to variable sequence lengths, conditional branches, and dynamic control flow. Interoperability ensures that optimized kernels can be inserted into these graphs without breaking graph semantics,

autograd behavior, or runtime scheduling. This capability is essential for transformer-class models, where attention patterns and KV-cache usage vary across tokens and layers.

- **Preserving autograd compatibility for training and fine-tuning** - Training pipelines rely on automatic differentiation, gradient accumulation, and optimizer integration. Interoperability ensures that hardware-aligned kernels expose gradient paths, maintain correct backward-pass semantics, and integrate with PyTorch's optimizer stack. This alignment enables substrate-optimized kernels to accelerate both inference and training without sacrificing correctness or flexibility.
- **Supporting distributed and multi-node execution environments** - Large-scale AI workloads frequently span multiple GPUs, nodes, or clusters. Interoperability ensures that optimized kernels participate cleanly in distributed data-parallel, model-parallel, and pipeline-parallel execution regimes. This capability is essential for frontier-scale models, where communication patterns, sharding strategies, and synchronization boundaries must remain consistent across heterogeneous hardware.
- **Maintaining compatibility with mixed-precision and quantization policies** - Modern AI systems rely heavily on FP16, BF16, FP8, INT8, and emerging low-precision formats. Interoperability ensures that optimized kernels respect PyTorch's precision policies, casting rules, and quantization frameworks. This alignment enables high-performance kernels to operate seamlessly within mixed-precision training loops and quantized inference pipelines.
- **Providing a stable interface for model developers** - Model developers expect PyTorch modules, functions, and operators to behave consistently across hardware backends. Interoperability ensures that optimized kernels expose familiar interfaces, integrate with PyTorch's dispatch system, and maintain compatibility with existing tooling—profilers, debuggers, tracing utilities, and deployment frameworks.

High-level interoperability is the final stage in the kernel-optimization pipeline, where substrate-aligned execution units reenter the flexible, dynamic world of AI model development. Without this layer, optimized kernels would remain isolated performance artifacts, unable to participate in autograd, unable to operate within dynamic graphs, and unable to scale across distributed systems. Interoperability transforms these kernels into fully integrated components of the PyTorch runtime, enabling large-scale models to benefit from hardware-aligned execution without sacrificing modularity, expressiveness, or developer ergonomics.

This integration is what enables:

- seamless acceleration of transformer blocks within dynamic graphs,
- correct gradient propagation during fine-tuning and RLHF,
- stable behavior under mixed-precision and quantized execution,
- efficient scaling across multi-GPU and multi-node environments, and
- predictable performance across heterogeneous accelerator fabrics.

Interoperability completes the software–hardware alignment pipeline. Once kernels are tile-optimized, memory-aligned, and vector-lane-mapped, this final layer ensures that the optimized execution units function as coherent elements of the broader AI system—bridging low-level performance engineering with high-level model development.

AI hardware-aware programming frameworks establish the foundation upon which modern accelerator performance is realized. By reshaping neural computation into tile-aligned blocks, staging intermediate tensors within shared-memory banks, aligning pointer arithmetic with hardware geometry, and mapping thread blocks onto heterogeneous vector lanes, the compilation pipeline transforms high-level tensor semantics into substrate-optimized execution plans. This alignment ensures deterministic latency, minimized data movement, and sustained parallel utilization across diverse accelerator fabrics. The resulting kernels behave as tightly integrated extensions of the hardware, enabling transformer-class models, convolutional pipelines, and mixed-precision workloads to operate at full efficiency. Tile-optimized compilation thus completes the software–hardware convergence required for frontier-scale AI systems, providing the performance substrate upon which higher-level orchestration frameworks depend.

With substrate-aligned kernels delivering predictable performance on individual accelerators, the next challenge is scaling AI computation across multiple devices, nodes, and clusters. Modern models exceed the memory capacity, compute envelope, and context limits of any single accelerator, requiring orchestration strategies that distribute tensors, partition execution graphs, and coordinate attention windows across large-scale systems. This shift marks the transition from hardware-aligned kernel optimization to distributed AI execution, where tensor parallelism, pipeline parallelism, and context parallelism collectively determine how massive models are trained and served. Multi-accelerator orchestration builds on the deterministic behavior established by tile-optimized kernels, enabling scalable, high-throughput AI computation across increasingly complex distributed environments.

b. Distributed AI Orchestration with Tensor, Pipeline, and Context Parallelism

Distributed AI orchestration defines the system-level strategies that allow modern models to

scale beyond the physical limits of any single accelerator. Tile-optimized kernels provide deterministic behavior within a device, but frontier-scale architectures require coordinated execution across multiple GPUs, nodes, and clusters. Memory footprints exceed device capacity, sequence lengths surpass local KV-cache limits, and compute requirements demand parallel execution across heterogeneous hardware. Distributed orchestration introduces tensor, pipeline, and context parallelism as complementary mechanisms that reshape how large-scale models are trained and served, transforming substrate-aligned kernels into components of a multi-accelerator execution fabric.

- **Megatron-Style AI Tensor Splitting for Intra-Node 3D Parallelism** - Megatron-style tensor splitting provides the foundational mechanism for distributing large matrix multiplications and attention blocks across multiple accelerators within a node. Transformer-class models rely heavily on matmul operations whose width grows with hidden dimension size; splitting these tensors across devices allows compute to scale linearly with model width while maintaining synchronized execution. Tensor splitting operates along three axes:
    - **Tensor Parallelism (TP):** partitions weight matrices across devices, enabling each accelerator to compute a slice of the output.
    - **Sequence Parallelism (SP):** distributes token-level computation across devices, reducing per-GPU activation memory.
    - **Expert Parallelism (EP):** routes tokens to specialized experts in mixture-of-experts architectures.

  Together, these axes form 3D parallelism, enabling massive models to operate within intra-node clusters while maintaining high arithmetic intensity and balanced load distribution. Megatron-style splitting ensures that each accelerator receives a predictable slice of the workload, enabling synchronized matmul execution and stable throughput across heterogeneous compute units.
- **AI Activation Partitioning for Memory-Efficient Distributed Training -** Activation partitioning addresses the memory bottleneck that arises during training, where intermediate tensors must be stored for backward propagation. As model depth increases, activation memory becomes the dominant constraint, often exceeding device capacity even when weights are sharded.

  Activation partitioning distributes intermediate tensors across accelerators, enabling:
    - reduced per-GPU memory footprint,

- larger batch sizes,
- deeper models, and
- more stable mixed-precision training.

Partitioning strategies include:

- **Activation sharding**: splitting activations across devices to reduce local storage.
- **Activation recomputation**: selectively recomputing activations during backward pass to reduce memory pressure.
- **Activation offloading**: moving tensors to host memory or neighboring GPUs when local memory is saturated.

These mechanisms allow training pipelines to scale without exceeding device limits, enabling frontier-scale models to operate efficiently even under aggressive depth and width configurations.

- **Distributed AI Context Parallelism for Ultra-Long Sequence Processing** - Context parallelism extends sequence processing beyond the boundaries of a single accelerator, enabling ultra-long inputs—hundreds of thousands or millions of tokens—to be handled through distributed attention and KV-cache coordination. Traditional attention mechanisms require quadratic memory growth with sequence length, making long-context inference impossible on a single device.

  Context parallelism introduces:

  - **KV-cache partitioning:** distributing key and value tensors across devices.
  - **Distributed attention windows:** computing attention across device boundaries without breaking semantic alignment.
  - **Cross-GPU context stitching:** merging partial attention results into coherent global outputs.

  This mechanism enables large-context models to operate at scale, supporting retrieval-augmented generation, long-form reasoning, and multi-document analysis. Distributed context parallelism ensures that attention remains stable and deterministic even when sequence lengths exceed local memory capacity by orders of magnitude.

- **AI Pipeline Bubble Reduction via Asymmetric Batch Slicing -** Pipeline parallelism introduces temporal partitioning, assigning different layers of a model to different

accelerators. While this approach enables deep models to scale across multiple devices, it introduces **pipeline bubbles**—idle periods where some accelerators wait for upstream or downstream stages to complete.

Asymmetric batch slicing reduces pipeline bubbles by adjusting microbatch sizes and scheduling patterns to ensure continuous flow through the pipeline. Key mechanisms include:

- **Asymmetric microbatch allocation**: assigning larger microbatches to slower pipeline stages.
- **Interleaved scheduling:** overlapping forward and backward passes to reduce idle time.
- **Stage-aware load balancing:** adjusting layer placement to equalize compute time across stages.

These techniques transform pipeline parallelism from a latency-bound mechanism into a high-throughput distributed execution strategy, enabling deep models to operate efficiently across multi-accelerator pipelines without sacrificing utilization.

Distributed AI orchestration completes the system-level alignment required for frontier-scale models. Tensor splitting scales compute across devices; activation partitioning scales memory; context parallelism scales sequence length; and pipeline bubble reduction scales depth. Together, these mechanisms transform substrate-aligned kernels into components of a distributed execution fabric capable of training and serving massive models with predictable throughput, stable latency, and efficient resource utilization.

This orchestration layer ensures that large-scale AI systems operate as coherent, multi-accelerator entities rather than collections of isolated devices, enabling modern architectures to push beyond the limits of single-GPU execution and into the realm of trillion-parameter models and ultra-long-context inference.

As distributed execution becomes the dominant strategy for scaling frontier-class models, the orchestration layer must coordinate multiple forms of parallelism across heterogeneous accelerator fabrics. Tensor splitting, activation partitioning, context distribution, and pipeline scheduling each contribute a distinct axis of scalability, enabling large-scale systems to operate beyond the physical limits of any single device. To clarify how these mechanisms interact and where each provides the strongest leverage, the following table organizes the core distributed-parallelism strategies into a unified framework, highlighting their operational scope, primary objectives, and the specific benefits they deliver to modern AI workloads.

The hardware-aware compilation mechanisms discussed in Table 8.4-C1 focus on optimizing execution within an individual accelerator by aligning computational kernels with tile geometries, memory hierarchies, vector-processing resources, and tensor-core fabrics. However, as modern AI models continue to expand beyond the memory and computational capacity of any single device, optimization can no longer be confined to the accelerator level alone. Contemporary large language models, foundation models, multimodal systems, and long-context reasoning architectures frequently require coordinated execution across clusters of GPUs, TPUs, NPUs, and specialized accelerators. Under these conditions, performance increasingly depends on how effectively computation, activations, model parameters, attention states, and communication workloads are distributed throughout the system. Distributed orchestration frameworks address this challenge by extending hardware–software co-design principles across multiple accelerators, enabling large-scale AI workloads to achieve scalability, efficiency, and reliability beyond the limits of individual devices. Table 8.4-C2 examines the principal orchestration mechanisms supporting this process and illustrates how modern AI infrastructures coordinate computation across distributed accelerator environments.

Table 8.4-C2 presents several foundational orchestration mechanisms that enable artificial intelligence workloads to execute efficiently across multiple accelerators. These mechanisms form the software and systems-level infrastructure responsible for coordinating computation, memory allocation, communication, synchronization, and workload distribution in large-scale AI deployments.

The rapid increase in model size, context length, parameter count, and training complexity has fundamentally altered the design requirements of AI infrastructure. Models containing hundreds of billions or even trillions of parameters cannot be executed efficiently on a single accelerator due to limitations in memory capacity, bandwidth, thermal budgets, and computational throughput. As a result, AI execution increasingly relies on distributed architectures composed of interconnected accelerator clusters.

Distributed orchestration mechanisms provide the coordination layer necessary to manage these environments. They determine how tensors are partitioned, how activations are exchanged among devices, how attention contexts are distributed, and how computational workloads are balanced throughout the cluster.

The table identifies four representative mechanisms: Megatron-style tensor splitting, activation partitioning, distributed context parallelism, and pipeline-bubble reduction through asymmetric batch slicing. Together, these approaches address some of the most significant bottlenecks encountered in large-scale AI systems, including memory limitations, workload imbalance, communication overhead, and pipeline inefficiency.

By examining the objectives, operational scope, benefits, and representative applications associated with each mechanism, the table highlights how distributed orchestration has become a central element of modern AI system design.

Table 8.4-C2 — Distributed AI Orchestration Mechanisms Across Multi-Accelerator Systems

Mechanism	Primary Objective	Operational Scope	Key Benefits for Large-Scale AI Models	Representative Use Cases
Megatron-Style Tensor Splitting	Scale matmul and attention across devices	Intra-node GPU clusters	• Linear scaling of compute • Balanced workload distribution • High arithmetic intensity	Wide transformer layers, MoE routing, large hidden-dimension models
Activation Partitioning	Reduce memory footprint during training	Multi-GPU training pipelines	• Larger batch sizes • Deeper models • Stable mixed-precision training	Frontier-scale training, memory-constrained fine-tuning
Distributed Context Parallelism	Extend sequence length beyond single-GPU limits	Multi-node attention and KV-cache systems	• Ultra-long context windows • Distributed KV-cache • Stable attention across devices	Long-form reasoning, multi-document analysis, RAG pipelines

Mechanism	Primary Objective	Operational Scope	Key Benefits for Large-Scale AI Models	Representative Use Cases
Pipeline Bubble Reduction via Asymmetric Batch Slicing	Increase utilization in deep pipeline-parallel models	Layer-partitioned multi-accelerator pipelines	• Reduced idle time • Higher throughput • Balanced stage execution	Deep transformer stacks, multi-stage inference pipelines

Table 8.4-C2 demonstrates that modern AI scalability is achieved not merely through larger accelerators but through intelligent coordination among multiple accelerators operating as a unified computational system. As model complexity increases, effective orchestration becomes essential for maintaining throughput, controlling memory consumption, and preserving efficient utilization across distributed hardware resources.

The mechanisms summarized in the table reveal a common objective: partitioning computational workloads in ways that maximize parallelism while minimizing communication overhead, synchronization delays, and resource imbalance.

The first mechanism identified in the table is **Megatron-style tensor splitting**, one of the most widely adopted techniques for scaling transformer models across multiple accelerators.

Rather than assigning entire layers to individual devices, tensor splitting partitions large matrix operations and attention computations across multiple processors. Each accelerator executes a fraction of the overall tensor operation while coordinated communication mechanisms combine the resulting outputs.

As shown in the table, this technique is primarily applied within intra-node GPU clusters, where high-bandwidth interconnects support rapid communication among devices. The resulting benefits include near-linear scaling of compute resources, balanced workload distribution, and improved utilization of available computational capacity.

Megatron-style tensor splitting is particularly valuable for very wide transformer layers, large hidden-state dimensions, and mixture-of-experts architectures, all of which generate matrix operations that can exceed the practical capabilities of a single accelerator.

The second mechanism is **activation partitioning**, which addresses the memory-growth challenges associated with deep neural-network training.

Neural-network activations often consume substantial memory resources during the forward and backward passes of model training. As model depth increases, activation storage can become a dominant constraint. Activation partitioning alleviates this problem by distributing activations across multiple devices rather than storing them entirely within a single accelerator.

The table highlights larger batch sizes, support for deeper models, and stability under mixed-precision training as important benefits. This mechanism is particularly useful in frontier-scale training environments and memory-constrained fine-tuning workloads, where maximizing model scale without exceeding hardware limitations is a primary objective.

By reducing per-device memory requirements, activation partitioning expands the practical training capacity of distributed AI systems without requiring larger physical memory resources.

The third mechanism identified in the table is **distributed context parallelism**, which addresses increasing demands for long-context reasoning and attention-based inference.

Traditional transformer architectures often encounter memory limitations when processing extremely long sequences because attention mechanisms require storage of expanding context representations and key-value caches. Distributed context parallelism overcomes these limitations by partitioning sequence context across multiple devices.

As indicated in the table, this approach supports ultra-long context windows, distributed KV-cache management, and stable attention execution across device boundaries. The technique has become particularly relevant in applications such as long-form reasoning, multi-document analysis, retrieval-augmented generation (RAG), and large-scale knowledge systems.

By distributing context information rather than concentrating it within a single accelerator, orchestration frameworks enable models to reason over substantially larger bodies of information.

The fourth mechanism is **pipeline-bubble reduction through asymmetric batch slicing**, which addresses one of the most persistent inefficiencies in distributed model execution.

Pipeline parallelism divides neural-network layers across multiple accelerators, allowing different pipeline stages to execute simultaneously. However, inefficiencies often emerge when some stages complete earlier than others, resulting in idle resources known as pipeline bubbles.

The table highlights asymmetric batch slicing as a strategy for mitigating this problem. By adjusting batch assignments according to the computational demands of individual pipeline

stages, orchestration frameworks reduce idle time and improve overall throughput. Additional benefits include improved stage balancing and more efficient utilization of accelerator clusters.

This mechanism is especially important in deep transformer stacks and multi-stage inference pipelines where layer-computation costs vary significantly throughout the model.

A broader insight emerging from the table is that distributed orchestration seeks to manage two competing objectives simultaneously: maximizing parallelism while minimizing communication costs. Increasing parallelism generally improves computational scalability, yet excessive partitioning can introduce communication and synchronization overheads that reduce efficiency.

The mechanisms presented here represent different approaches to balancing these tradeoffs. Tensor splitting improves computational distribution. Activation partitioning reduces memory pressure. Context parallelism expands reasoning capacity. Pipeline optimization increases utilization. Together, these techniques allow AI systems to scale while maintaining practical performance characteristics.

The table also highlights the evolving role of software in large-scale AI systems. Increasingly, scalability depends not solely on accelerator capabilities but on orchestration frameworks capable of coordinating thousands of computational operations across distributed hardware resources.

From a systems-engineering perspective, the mechanisms summarized in the table address different dimensions of scalability. Compute scalability is achieved through tensor partitioning. Memory scalability emerges from activation partitioning. Context scalability results from distributed attention management. Utilization scalability is improved through pipeline optimization. Collectively, they form a comprehensive orchestration framework for next-generation AI infrastructures.

Another important observation is that these mechanisms are often deployed simultaneously within the same system. Large-scale training environments frequently combine tensor parallelism, activation partitioning, context parallelism, and pipeline scheduling optimizations to achieve optimal performance across distributed hardware platforms.

Ultimately, Table 8.4-C2 demonstrates that distributed orchestration has become a foundational requirement for modern AI computing. Through coordinated management of computation, memory, communication, and execution pipelines, these mechanisms enable AI systems to transcend the physical limitations of individual accelerators and support the increasingly demanding workloads associated with frontier-scale models, long-context reasoning systems,

and next-generation intelligent applications.

Table 8.4-C2 introduced the principal orchestration mechanisms that enable large AI workloads to scale beyond the resource limits of individual accelerators. While tensor splitting, activation partitioning, context parallelism, and pipeline optimization can be examined independently, modern frontier-scale AI systems rarely rely on a single orchestration strategy. Instead, these mechanisms are typically deployed simultaneously within a unified execution fabric, where each addresses a distinct computational bottleneck. Tensor parallelism distributes arithmetic workloads, activation partitioning manages memory consumption, context parallelism extends sequence-processing capacity, and pipeline optimization improves utilization across layered execution stages. Figure 8.4-C2 illustrates how these complementary forms of parallelism interact within a coordinated multi-accelerator environment, demonstrating how distributed orchestration transforms collections of individual devices into scalable, high-throughput AI computing systems.

Figure 8.4-C2 presents a conceptual model of distributed AI parallelism across a multi-accelerator execution fabric. The figure illustrates how orchestration layers coordinate multiple forms of parallel execution to overcome the computational, memory, and context-processing limitations associated with single-device deployments.

As AI models have grown from millions to billions and trillions of parameters, the scale of computational resources required to train and deploy these systems has increased correspondingly. The resulting workloads frequently exceed the memory capacity, bandwidth availability, and arithmetic throughput of individual accelerators. Distributed parallelism addresses these challenges by partitioning model components, activations, attention states, and pipeline stages across multiple devices.

The figure organizes this process into three layers. At the top resides the distributed orchestration layer responsible for coordinating execution strategies. The middle layer represents the multi-accelerator execution fabric containing the major forms of parallelism. The bottom layer illustrates the resulting scalable AI systems capable of supporting frontier-scale models and long-context reasoning workloads.

By visualizing these relationships, the figure highlights how distributed AI performance emerges from multiple interacting parallelization strategies rather than from any single mechanism alone.

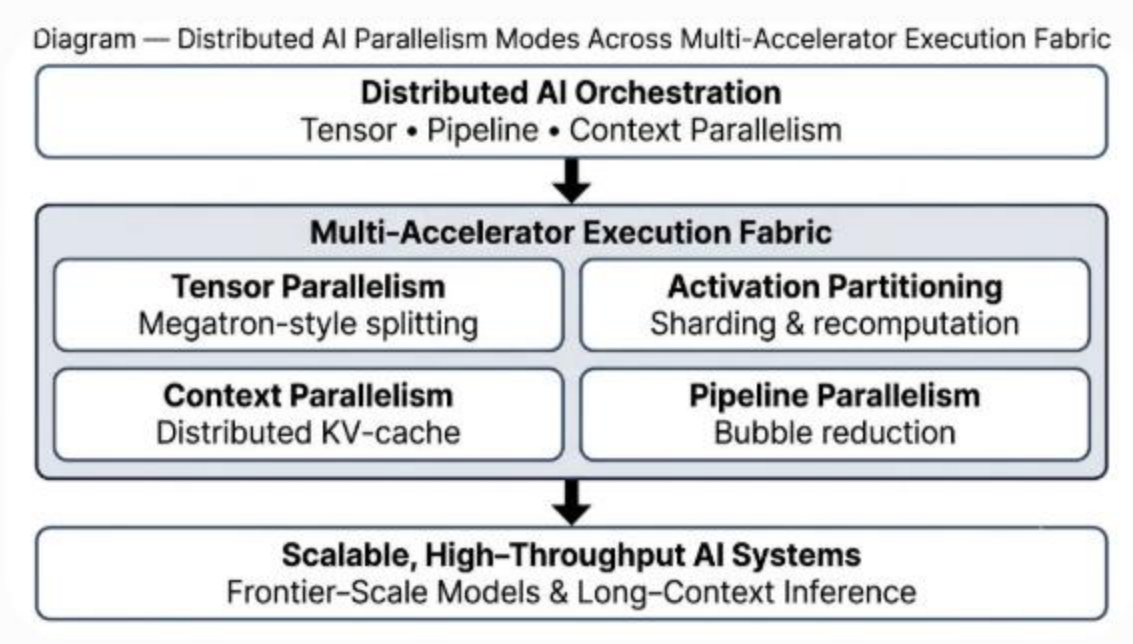


Figure 8.4-C2 — Distributed AI Parallelism Modes Across Multi-Accelerator Execution Fabric
Layered orchestration framework illustrating how tensor parallelism, activation partitioning, context parallelism, and pipeline parallelism interact within a distributed accelerator environment. The figure demonstrates how coordinated execution strategies distribute computation, memory, attention contexts, and pipeline stages across multiple devices to support scalable training and inference for frontier-scale AI models and long-context reasoning systems.

Legend:

Component	Description
Distributed AI Orchestration	High-level coordination layer managing parallelization strategies across multiple accelerators.
Tensor • Pipeline • Context Parallelism	Major categories of distributed execution controlled by the orchestration framework.
Multi-Accelerator Execution Fabric	Distributed infrastructure composed of interconnected accelerators.
Tensor Parallelism	Partitioning of large matrix operations and attention computations across devices.
Megatron-Style Splitting	Tensor decomposition approach used for large transformer architectures.

Activation Partitioning	Distribution of activations across multiple accelerators to reduce memory pressure.
Sharding & Recomputation	Activation-management techniques supporting memory-efficient training.
Context Parallelism	Distribution of sequence context and attention state across devices.
Distributed KV-Cache	Partitioned storage of key-value attention states for long-context execution.
Pipeline Parallelism	Layer-wise partitioning of model execution across accelerators.
Bubble Reduction	Scheduling optimization minimizing idle pipeline stages.
Scalable, High-Throughput AI Systems	Resulting large-scale execution environment.
Frontier-Scale Models	Extremely large AI systems distributed across accelerator clusters.
Long-Context Inference	Large-context reasoning enabled through distributed attention resources.

Figure 8.4-C2 demonstrates that modern AI scalability is achieved through the coordinated application of several complementary parallelization strategies. Rather than relying on a single form of parallel execution, large-scale AI systems employ multiple mechanisms simultaneously to distribute computation, memory, and contextual information across accelerator fabrics.

The figure illustrates how orchestration frameworks act as the coordinating layer that integrates these parallelization strategies into a unified execution model capable of supporting frontier-

At the highest level of the architecture is the **Distributed AI Orchestration** layer. This layer functions as the management infrastructure responsible for coordinating execution across multiple accelerators.

The figure identifies three major orchestration dimensions: tensor parallelism, pipeline parallelism, and context parallelism. Together, these strategies determine how workload components are distributed across the available hardware resources.

An important observation is that orchestration operates above the individual parallelization mechanisms themselves. Rather than performing computation directly, the orchestration layer determines how computation should be partitioned, scheduled, synchronized, and

communicated throughout the accelerator fabric.

Beneath this orchestration layer resides the **Multi-Accelerator Execution Fabric**, which contains the principal execution mechanisms supporting distributed operation.

The first mechanism shown is **Tensor Parallelism**, represented by Megatron-style splitting strategies.

Tensor parallelism distributes large matrix operations and attention computations across multiple accelerators. Rather than executing a complete matrix multiplication on a single device, portions of the operation are assigned to multiple processors and executed in parallel.

This mechanism addresses one of the primary computational challenges associated with large transformer architectures: the enormous size of intermediate matrix operations. By distributing tensor workloads across devices, models can scale beyond the computational limits of individual accelerators.

The second mechanism is **Activation Partitioning**, represented by sharding and recomputation strategies.

This form of parallelism addresses memory limitations rather than computational limits. During neural-network training, activation storage often becomes one of the largest consumers of memory resources.

By partitioning activations across devices and selectively recomputing intermediate values when needed, activation partitioning substantially reduces memory burden while enabling larger batch sizes and deeper model architectures.

The inclusion of activation partitioning within the execution fabric highlights the reality that modern AI scaling depends as much on memory management as on computational throughput.

The third mechanism identified in the figure is **Context Parallelism**, which utilizes distributed KV-cache management.

Long-context transformer systems frequently encounter memory limitations because attention mechanisms require the storage and retrieval of increasingly large context representations. Context parallelism addresses this challenge by distributing sequence context and key-value attention caches across multiple devices.

The figure emphasizes distributed KV caches as a defining feature of this approach. By partitioning context across accelerators, systems can maintain attention over substantially longer sequences than would otherwise be possible.

This mechanism has become especially important for long-form reasoning, retrieval-augmented generation, and multi-document analytical systems.

The fourth mechanism is **Pipeline Parallelism**, represented by bubble-reduction strategies.

Pipeline parallelism partitions model layers across multiple accelerators, allowing different portions of the model to execute simultaneously. However, pipeline execution often suffers from inefficiencies when some stages complete earlier than others.

The figure highlights bubble reduction as a critical optimization mechanism. By balancing workloads among pipeline stages and minimizing idle resources, systems can significantly improve throughput.

This optimization becomes increasingly important as model depth increases and execution pipelines span larger numbers of accelerators.

The combined effect of these mechanisms is illustrated in the bottom layer of the figure, labeled **Scalable, High-Throughput AI Systems**.

This layer represents the outcome of successful orchestration. Computation has been distributed through tensor parallelism, memory has been managed through activation partitioning, context has been extended through distributed caches, and utilization has been improved through pipeline optimization.

The resulting system can support both **frontier-scale models** and **long-context inference workloads**, two application domains that would be difficult or impossible to accommodate efficiently using single-device architectures.

A broader insight emerging from the figure is that different parallelization mechanisms target different scalability constraints.

- Tensor parallelism addresses compute scalability.
- Activation partitioning addresses memory scalability.
- Context parallelism addresses sequence scalability.
- Pipeline parallelism addresses utilization scalability.

Together, these mechanisms form a comprehensive distributed-execution strategy.

The figure also highlights the growing importance of orchestration software within modern AI infrastructure. Large-scale performance increasingly depends not only on hardware capability but also on how effectively orchestration frameworks coordinate distributed resources.

From a systems-engineering perspective, the architecture demonstrates a layered approach to scalability. Workloads are first decomposed into distinct computational dimensions, then distributed through specialized parallelism strategies, and finally coordinated through orchestration systems capable of maintaining efficient execution across the entire cluster.

Another important observation is that these mechanisms are complementary rather than competitive. Most production-scale AI systems employ combinations of tensor, pipeline, context, and activation parallelism simultaneously. The figure captures this reality by placing all four mechanisms within a single execution fabric rather than presenting them as alternative approaches.

Ultimately, Figure 8.4-C2 demonstrates that modern large-scale AI systems depend upon the coordinated interaction of multiple forms of distributed parallelism. Through orchestration frameworks that integrate tensor partitioning, activation management, context distribution, and pipeline optimization, multi-accelerator execution fabrics enable the training and deployment of frontier-scale AI models that far exceed the capabilities of individual processors. The figure therefore serves as a concise representation of how contemporary distributed AI infrastructures transform collections of accelerators into unified computational systems capable of supporting the next generation of intelligent applications.

With the distributed-parallelism landscape established through the orchestration mechanisms summarized in Table 8.4-C2 and visualized in Figure 8.4-C2, the following discussion examines how these strategies materialize within the execution fabric. The most fundamental of these mechanisms is tensor parallelism, which provides the compute-scaling backbone for large transformer architectures. By partitioning weight matrices, attention projections, and expert layers across multiple accelerators, tensor parallelism enables intra-node 3D parallelism that increases arithmetic density while preserving synchronized execution. This approach forms the structural foundation upon which activation partitioning, context parallelism, and pipeline scheduling subsequently build. The following discussion explores Megatron-style tensor splitting in detail, showing how distributed compute begins at the level of matrix geometry and expands outward into full multi-accelerator coordination.

i. Megatron-Style AI Tensor Splitting for Intra-Node 3D Parallelism

Megatron-style tensor splitting provides the compute-scaling backbone for distributed transformer execution, enabling large matrix multiplications and attention projections to operate across multiple accelerators within a single node. Transformer architectures expand primarily along the hidden-dimension axis, causing matmul operations to grow quadratically with model width. Once this width exceeds the compute envelope of a single accelerator, tensor

splitting becomes the first and most fundamental mechanism for distributing arithmetic intensity across devices while preserving synchronized execution.

At its core, Megatron-style tensor splitting decomposes large weight matrices, attention projections, and intermediate tensor operations into coordinated shards that are distributed across multiple accelerators. Each accelerator computes a deterministic portion of the overall output tensor, while collective communication mechanisms synchronize and aggregate partial results into a mathematically equivalent global output. In effect, this approach transforms what would otherwise be a monolithic matrix operation into a carefully orchestrated multi-accelerator computation, allowing extremely large transformer models to execute beyond the memory and computational limits of any individual device.

The AI-specific framing is particularly important because tensor splitting is not a generic parallel-computing technique. Rather, it is a geometry-aware decomposition strategy designed specifically for the structural characteristics of transformer architectures. Attention projections, feed-forward network expansions, and **Mixture-of-Experts (MoE)** routing operations exhibit highly regular tensor geometries that can be partitioned predictably without altering model semantics. Megatron-style splitting exploits this regularity by dividing workloads along dimensions that preserve mathematical correctness while exposing substantial parallelism.

By aligning tensor decomposition with the structure of transformer computation, the approach maintains the semantic integrity of attention mechanisms, feed-forward layers, and expert-routing pathways while maximizing utilization across distributed accelerator fabrics. The result is a scalable execution model that balances computational workload, memory consumption, and communication overhead, enabling frontier-scale AI systems to sustain high throughput, efficient resource utilization, and near-linear scaling across large multi-accelerator environments.

Megatron-style tensor splitting operates along three complementary axes that collectively form **intra-node 3D parallelism**:

- **Tensor Parallelism (TP) -** TP partitions large weight matrices—QKV projections, MLP expansions, expert layers—across accelerators. Each accelerator computes a slice of the output, enabling model width to scale without exceeding device limits. TP increases arithmetic density and ensures that matmul workloads remain balanced across the node.
- **Sequence Parallelism (SP) -** SP distributes token-level computation across accelerators, reducing activation memory and enabling larger batch sizes. SP is particularly effective

for attention mechanisms, where per-token operations can be parallelized without disrupting global attention semantics.

- **Expert Parallelism (EP) -** EP routes tokens to specialized experts in mixture-of-experts architectures. Each accelerator hosts a subset of experts, and tokens are dynamically assigned based on learned routing patterns. EP increases model capacity without increasing per-accelerator memory footprint.

Together, these axes form a **3D parallelism topology** that scales compute, memory, and specialization within a single node. This topology is explicitly designed for AI workloads: tensor geometry, attention structure, and expert routing patterns determine how shards are assigned, synchronized, and fused. The result is a distributed compute fabric capable of supporting transformer widths, MoE capacities, and attention depths that would otherwise exceed the limits of individual accelerators.

Megatron-style tensor splitting is the first stage in distributed AI orchestration because it establishes the deterministic compute behavior upon which activation partitioning, context parallelism, and pipeline scheduling subsequently build. Once tensor geometry is decomposed and synchronized across accelerators, the system gains a stable foundation for scaling depth, sequence length, and temporal execution. Intra-node 3D parallelism thus forms the structural core of modern distributed transformer execution, enabling frontier-scale models to operate with high throughput, balanced load distribution, and predictable latency.

With intra-node 3D tensor parallelism establishing the compute-scaling foundation for distributed transformer execution, the next challenge is managing the memory footprint generated by these expanded workloads. As tensor splitting increases model width and arithmetic density across accelerators, the volume of intermediate activations produced during forward propagation grows proportionally, often exceeding the memory capacity of individual devices. Sustaining large-scale training therefore requires a complementary mechanism that introduces memory elasticity without compromising gradient correctness or throughput. Activation partitioning provides this capability, reshaping how intermediate tensors are stored, recomputed, and exchanged across accelerators to maintain stable training under extreme depth and width configurations.

With intra-node 3D tensor parallelism establishing the compute-elastic foundation for distributed transformer execution, the next scaling pressure emerges from the volume of intermediate activations generated during forward propagation. As tensor splitting expands model width and increases arithmetic density across accelerators, activation tensors grow proportionally, often exceeding the memory envelope of individual devices. Sustaining

large-scale training therefore requires a complementary mechanism that introduces memory elasticity without compromising gradient correctness or throughput. AI activation partitioning provides this capability, reshaping how intermediate tensors are stored, recomputed, and exchanged across accelerators so that deep and wide transformer architectures can train stably under extreme memory constraints.

ii. AI Activation Partitioning for Memory-Efficient Distributed Training

Activation partitioning forms the memory-scaling backbone of distributed AI training, enabling frontier-scale models to operate across multi-accelerator systems without exceeding device memory limits. Transformer-class architectures generate massive intermediate tensors during forward propagation—attention maps, residual streams, MLP expansions, expert activations—and these tensors must be preserved for backward propagation. As model depth and width increase, activation memory becomes the dominant constraint, often surpassing the capacity of even high-end accelerators. Activation partitioning introduces a set of distributed strategies that reshape how intermediate tensors are stored, recomputed, and exchanged, allowing large-scale training pipelines to maintain stability under extreme memory pressure.

This AI-specific framing is essential because activation partitioning is not simply a generic memory-management technique; it is a specialized scalability mechanism developed in response to the unique memory behavior of modern deep-learning architectures. Transformer models generate exceptionally large activation footprints during training, driven by the need to retain intermediate states for backpropagation. Attention layers produce per-token activation tensors that grow with sequence length, feed-forward networks generate substantial expansion tensors through dimensional upscaling, and **Mixture-of-Experts (MoE)** architectures create sparsely activated yet extremely high-dimensional expert representations. Collectively, these operations can produce memory demands that exceed the capacity of individual accelerators long before computational limits are reached. Activation partitioning addresses this challenge by distributing activation storage across multiple devices while preserving the correctness of gradient computation and maintaining efficient training throughput. Rather than serving as a conventional memory optimization, it functions as a hardware-aware orchestration strategy that balances memory utilization, communication overhead, and computational efficiency across distributed accelerator fabrics. By controlling activation growth without compromising numerical integrity or scalability, activation partitioning enables deeper networks, larger batch sizes, and frontier-scale model training that would otherwise be constrained by memory capacity limitations.

Activation partitioning operates through several complementary mechanisms:

- **Activation Sharding Across Accelerators -** Activation sharding distributes intermediate tensors across multiple devices, reducing the per-accelerator memory footprint. Each accelerator stores only a slice of the activation tensor, and the full activation is reconstructed or communicated during backward propagation. This approach enables deeper models and larger batch sizes while maintaining deterministic gradient behavior.
- **Activation Recomputation for Memory Reduction -** Recomputation trades compute for memory by discarding selected activations during the forward pass and regenerating them during the backward pass. This technique is particularly effective for layers with inexpensive forward operations but large activation tensors, such as GELU expansions or residual streams. Recomputation allows training pipelines to operate within strict memory budgets without sacrificing model depth.
- **Activation Offloading to Host or Peer Devices -** Offloading moves activations from GPU memory to host memory or neighboring accelerators when local memory is saturated. This mechanism is essential for extremely deep models, where even sharding and recomputation cannot fully contain activation growth. Offloading preserves training stability under aggressive scaling conditions, enabling frontier-scale architectures to operate without memory-related interruptions.
- **Hybrid Partitioning for Mixed-Precision Training -** Mixed-precision regimes (FP16, BF16, FP8) introduce additional memory considerations, as some activations must remain in higher precision for numerical stability. Hybrid partitioning ensures that precision-critical activations are preserved while non-critical tensors are sharded, recomputed, or offloaded. This alignment maintains training correctness while maximizing memory efficiency.

Together, these mechanisms form a **memory-elastic execution layer** that enables distributed training pipelines to scale beyond the physical limits of individual accelerators. Activation partitioning ensures that memory consumption grows sublinearly with model depth and width, allowing large-scale architectures to maintain throughput and stability even under extreme parameter counts and long-context training regimes.

Activation partitioning is the second pillar of distributed AI orchestration because it provides the memory elasticity required for deep transformer stacks, mixture-of-experts routing, and large-batch optimization. Once tensor splitting establishes compute scalability, activation partitioning ensures that the training pipeline can sustain that compute intensity without exhausting device memory. This memory-efficient foundation enables subsequent distributed mechanisms—context parallelism and pipeline scheduling—to operate effectively across

multi-accelerator systems.

With activation partitioning providing the memory elasticity required to sustain deep and wide transformer architectures during distributed training, the next scaling challenge emerges from the temporal dimension of modern AI workloads. As models grow in capability, the sequences they must process expand dramatically—long-form reasoning, multi-document synthesis, retrieval-augmented generation, and streaming inference all demand context lengths that exceed the KV-cache and attention-window limits of any single accelerator. Memory-efficient training alone cannot accommodate these ultra-long inputs; the attention mechanism itself must be distributed. Context parallelism introduces this capability, extending the reach of attention across multiple accelerators through KV-cache partitioning, distributed attention windows, and cross-device stitching. The following exploration examines how distributed context parallelism enables transformer-class models to operate on sequences that scale by orders of magnitude beyond single-device constraints.

With activation partitioning providing the memory elasticity required to sustain deep and wide transformer architectures, the next scaling pressure emerges from the temporal dimension of modern AI workloads. As models advance in capability, the sequences they must process expand dramatically—long-form reasoning, multi-document synthesis, retrieval-augmented generation, and streaming inputs all demand context lengths that exceed the KV-cache and attention-window limits of any single accelerator. Memory-efficient training alone cannot accommodate these ultra-long inputs; the attention mechanism itself must be distributed. Distributed AI context parallelism introduces this capability, extending the reach of attention across multiple accelerators through KV-cache partitioning, distributed attention windows, and cross-device stitching. This enables transformer-class models to operate on sequences that scale by orders of magnitude beyond single-device constraints while preserving semantic continuity and deterministic execution.

iii. Distributed AI Context Parallelism for Ultra-Long Sequence Processing

Distributed AI context parallelism provides the sequence-scaling backbone for modern transformer inference and training, enabling ultra-long inputs to be processed across multiple accelerators without collapsing under quadratic attention costs or KV-cache memory limits. Transformer architectures fundamentally rely on attention mechanisms whose memory footprint grows with sequence length; once this length exceeds the capacity of a single accelerator, context parallelism becomes essential for maintaining stable, deterministic execution. Context parallelism introduces distributed attention windows, cross-device KV-cache coordination, and multi-accelerator stitching mechanisms that allow sequence lengths to expand by orders of magnitude while preserving semantic continuity.

This AI-specific framing is essential because context parallelism is not simply a generic distributed-computing technique; it is a specialized orchestration strategy developed in response to the unique structural and computational characteristics of transformer architectures. Unlike conventional distributed workloads, transformer execution depends upon preserving the semantic relationships among tokens across potentially massive context windows. Attention mechanisms require access to globally relevant information, **Key–Value (KV) caches** must remain coherent across layers and devices, and sequence-dependent computations must preserve strict ordering semantics to ensure mathematical correctness. These requirements introduce constraints that extend beyond traditional workload partitioning and demand a distributed execution model capable of balancing scalability with consistency. Consequently, context parallelism is designed not merely to distribute memory and computation, but to preserve the integrity of attention computations while extending their operational footprint across multiple accelerators. By maintaining coherent context representations and synchronized attention state throughout the execution fabric, context parallelism enables long-context reasoning, distributed KV-cache management, and large-scale transformer inference without compromising the correctness or effectiveness of the underlying attention mechanism.

Context parallelism operates through several tightly coupled mechanisms:

- **KV-Cache Partitioning Across Accelerators -** KV-cache partitioning distributes key and value tensors across multiple devices, allowing each accelerator to store only a portion of the sequence history. During attention computation, each accelerator retrieves or exchanges the relevant KV segments, enabling ultra-long sequences to be processed without exceeding local memory limits. This mechanism forms the foundation for long-context inference, retrieval-augmented generation, and multi-document reasoning.
- **Distributed Attention Windows -** Distributed attention windows divide the sequence into segments that are processed across accelerators while maintaining global attention semantics. Each accelerator computes attention over its assigned window and exchanges partial results to ensure that every token receives the correct contextual information. This approach preserves the mathematical structure of attention while enabling sequence lengths far beyond single-GPU constraints.
- **Cross-Device Context Stitching -** Context stitching merges partial attention outputs from multiple accelerators into coherent global representations. This mechanism ensures that distributed attention does not fragment the semantic continuity of the sequence. Stitching is essential for tasks requiring long-range dependencies, such as multi-chapter summarization, long-form reasoning, and cross-document synthesis.

- **Distributed Prefill and Streaming Attention -** Prefill operations for large sequences often dominate inference latency. Distributed prefill pipelines parallelize the construction of initial KV-caches across accelerators, reducing latency for long-context workloads. Streaming attention mechanisms further enable real-time processing of extended inputs by distributing incremental KV updates across devices.

Together, these mechanisms form a **context-elastic execution layer** that allows transformer models to operate on sequences that exceed single-accelerator limits by several orders of magnitude. Context parallelism ensures that attention remains stable, deterministic, and semantically coherent even when sequence lengths reach hundreds of thousands or millions of tokens.

Context parallelism is the third pillar of distributed AI orchestration because it provides the sequence elasticity required for long-context inference, retrieval-augmented generation, and large-scale reasoning workloads. Once tensor splitting establishes compute scalability and activation partitioning provides memory elasticity, context parallelism extends the temporal and semantic reach of the model across multi-accelerator systems. This distributed attention foundation enables frontier-scale architectures to process vast inputs with predictable throughput and stable latency.

With distributed context parallelism extending the semantic reach of transformer-class models across ultra-long sequences, the final scaling challenge emerges from the temporal dynamics of multi-accelerator execution. Even when compute, memory, and context elasticity are fully established, deep transformer stacks must still propagate microbatches through layer-partitioned pipelines that span numerous accelerators. Without careful temporal coordination, these pipelines accumulate idle gaps—pipeline bubbles—that erode throughput and undermine the benefits of distributed parallelism. Sustaining frontier-scale performance therefore requires a temporal-elastic mechanism that reshapes microbatch flow, balances stage execution, and overlaps communication with compute. AI pipeline bubble reduction provides this capability, enabling deep distributed models to maintain continuous utilization across all pipeline stages through asymmetric batch slicing and interleaved scheduling.

With distributed context parallelism extending the semantic reach of transformer-class models across ultra-long sequences, the remaining scaling pressure emerges from the temporal dynamics of multi-accelerator execution. Even when compute, memory, and context elasticity are fully established, deep transformer pipelines must still propagate microbatches through layer-partitioned stages that span numerous accelerators. Without temporal coordination, these pipelines accumulate idle gaps—pipeline bubbles—that erode utilization and diminish the benefits of distributed parallelism. Sustaining frontier-scale throughput therefore requires a

mechanism that reshapes microbatch flow, balances stage execution, and overlaps communication with compute. AI pipeline bubble reduction introduces this temporal elasticity, ensuring that distributed pipelines remain continuously active through asymmetric batch slicing and interleaved scheduling.

iv. AI Pipeline Bubble Reduction via Asymmetric Batch Slicing

AI pipeline bubble reduction provides the temporal-scaling backbone for distributed transformer execution, enabling deep models to operate across multi-accelerator pipelines without suffering from idle stages or throughput collapse. Pipeline parallelism partitions a model's layers across accelerators, creating a temporal execution chain where microbatches flow from one stage to the next. While this approach allows extremely deep architectures to exceed single-accelerator memory limits, it introduces **pipeline bubbles**—periods where upstream or downstream accelerators remain idle because the pipeline has not yet filled or has begun to drain. These bubbles reduce utilization, increase latency, and limit the effective throughput of distributed training and inference.

This AI-specific framing is essential because pipeline bubbles are not merely a generic scheduling inefficiency; they arise directly from the structural characteristics of large-scale transformer architectures. Deep transformer networks consist of heterogeneous computational stages, including multi-head attention blocks, feed-forward network (MLP) expansions, normalization layers, routing mechanisms, and, in some cases, **Mixture-of-Experts (MoE)** modules. Each of these components exhibits distinct computational intensity, memory-access behavior, and communication requirements. When model layers are distributed across multiple accelerators through pipeline parallelism, these differences frequently result in stage-level execution imbalance. Some stages complete their assigned work rapidly while others require substantially longer execution times, causing downstream or upstream accelerators to remain idle while waiting for synchronization points to be reached. These periods of inactivity, commonly referred to as *pipeline bubbles*, reduce overall hardware utilization and limit achievable throughput.

AI pipeline-bubble reduction addresses this challenge through hardware-aware scheduling, microbatch restructuring, workload balancing, and asymmetric batch-slicing techniques that align execution more closely with the computational characteristics of individual pipeline stages. Rather than treating all stages uniformly, these mechanisms adapt the flow of work throughout the pipeline to minimize idle intervals and maintain continuous utilization across the accelerator fabric. By reducing stage-level imbalances and smoothing microbatch progression, pipeline-bubble optimization transforms pipeline parallelism from a theoretically scalable strategy into a practical mechanism for achieving high throughput, efficient resource utilization, and

predictable performance in large-scale distributed AI systems.

Pipeline bubble reduction operates through several coordinated mechanisms:

- **Asymmetric Microbatch Slicing for Stage-Aware Balancing -** Asymmetric slicing assigns different microbatch sizes to different pipeline stages based on their compute characteristics. Slower stages receive smaller microbatches to reduce per-stage latency, while faster stages receive larger microbatches to maintain throughput. This dynamic allocation ensures that each stage completes its work within a similar time window, reducing idle periods and stabilizing pipeline flow.
- **Interleaved Forward–Backward Scheduling -** Interleaving overlaps forward and backward passes across pipeline stages, allowing accelerators to remain active even when upstream or downstream stages are processing different microbatches. This approach reduces bubble formation during both pipeline fill and drain phases, increasing overall utilization and reducing end-to-end latency.
- **Stage-Time Equalization via Layer Reassignment -** Layer reassignment redistributes transformer blocks across accelerators to equalize stage execution time. This mechanism is particularly effective for architectures with uneven compute distribution, such as mixture-of-experts models or transformer variants with heavy attention blocks. Equalization ensures that no stage becomes a persistent bottleneck.
- **Temporal Overlap of Communication and Compute -** Communication overhead—activation transfers, gradient exchanges, KV-cache updates—can create additional bubbles if not overlapped with compute. Temporal overlap pipelines communication operations alongside computation, ensuring that accelerators remain active while data is transferred across devices.

Together, these mechanisms form a **temporal-elastic execution layer** that allows deep transformer architectures to operate across multi-accelerator pipelines with high utilization and predictable throughput. Pipeline bubble reduction ensures that temporal inefficiencies do not undermine the compute and memory elasticity provided by tensor splitting and activation partitioning. This alignment is essential for large-scale training regimes, where deep models must sustain continuous forward and backward propagation across dozens or hundreds of pipeline stages.

Pipeline bubble reduction is the fourth pillar of distributed AI orchestration because it provides the temporal elasticity required for deep transformer stacks, multi-stage inference pipelines, and large-batch distributed training. Once tensor splitting establishes compute scalability,

activation partitioning provides memory elasticity, and context parallelism extends sequence length, pipeline bubble reduction ensures that temporal execution remains efficient across the entire distributed system. This temporal-optimized foundation enables frontier-scale architectures to maintain high throughput and stable latency even under extreme depth and multi-accelerator deployment conditions.

Distributed AI orchestration establishes the multi-accelerator execution fabric required for frontier-scale transformer models. Tensor parallelism provides compute elasticity by decomposing matrix geometry across devices; activation partitioning introduces memory elasticity by distributing or recomputing intermediate tensors; context parallelism extends the semantic reach of attention across ultra-long sequences; and pipeline bubble reduction delivers temporal elasticity by maintaining continuous utilization across deep, layer-partitioned pipelines. Together, these mechanisms transform substrate-aligned kernels into components of a coherent distributed system capable of scaling width, depth, sequence length, and temporal flow far beyond the limits of any single accelerator. This orchestration layer ensures that large-scale AI workloads maintain deterministic behavior, balanced resource utilization, and high throughput across heterogeneous clusters, forming the operational backbone for modern training and inference at frontier scale.

With distributed parallelism establishing compute, memory, context, and temporal elasticity across multi-accelerator systems, the next challenge lies in minimizing the latency introduced by communication across the fabric. Even when parallel execution is perfectly orchestrated, large-scale models must continuously exchange activations, gradients, KV-cache segments, and routing metadata across devices and nodes. These transfers can become dominant sources of delay as model width, sequence length, and pipeline depth increase. Sustaining frontier-scale throughput therefore requires a mechanism that masks communication latency by overlapping compute with fabric-level transfers, ensuring that accelerators remain productive even while data is in motion. The next topic examines how AI latency masking transforms communication from a blocking operation into a background activity, enabling distributed systems to operate at full efficiency under extreme scaling conditions.

Distributed AI orchestration establishes the execution fabric that enables transformer-class models to scale across heterogeneous multi-accelerator environments. Tensor parallelism provides compute elasticity by decomposing matrix geometry and distributing arithmetic intensity; activation partitioning introduces memory elasticity by reshaping how intermediate tensors are stored, recomputed, and exchanged; context parallelism extends the semantic reach of attention across ultra-long sequences through distributed KV-cache coordination; and pipeline bubble reduction delivers temporal elasticity by maintaining continuous utilization

across deep, stage-partitioned pipelines. Together, these mechanisms convert raw accelerator clusters into a coherent, synchronized system capable of supporting frontier-scale workloads with deterministic behavior, balanced resource consumption, and high throughput. This orchestration layer forms the structural backbone of modern distributed AI, enabling models to scale in width, depth, sequence length, and temporal flow far beyond the limits of any single device.

With distributed parallelism providing compute, memory, context, and temporal elasticity, the next challenge arises from the communication patterns that bind accelerators together. Large-scale models continuously exchange activations, gradients, KV-cache segments, routing metadata, and expert outputs across the fabric, and these transfers can become dominant contributors to end-to-end latency as model size and sequence length increase. Even perfectly orchestrated parallelism cannot reach full efficiency if communication remains a blocking operation. Sustaining frontier-scale throughput therefore requires a mechanism that masks communication delays by overlapping compute with fabric-level transfers, ensuring that accelerators remain productive while data is in motion. AI latency masking introduces this capability, transforming communication from a serialized bottleneck into a background activity that enables distributed systems to operate at peak efficiency under extreme scaling conditions.

c. AI Latency Masking via Overlapped Compute and Fabric-Level Transfers

AI latency masking provides the communication-scaling backbone for distributed transformer execution, ensuring that multi-accelerator systems maintain high throughput even when large volumes of data must move across the fabric. Transformer-class workloads generate continuous streams of activations, gradients, KV-cache segments, expert outputs, and routing metadata. As models scale in width, depth, and sequence length, these transfers become increasingly dominant contributors to end-to-end latency. Without a mechanism to hide communication behind computation, distributed systems devolve into serialized pipelines where accelerators stall waiting for data. AI latency masking prevents this collapse by transforming communication from a blocking operation into a background activity, enabling compute and fabric-level transfers to proceed concurrently.

This AI-specific framing is essential because latency masking is not simply a generic high-performance computing (HPC) optimization; it is a specialized orchestration strategy designed to address the communication and synchronization patterns inherent in modern AI architectures. Transformer-based models continuously exchange large volumes of data among distributed execution components. Attention mechanisms require synchronized **Key–Value (KV) cache** updates across devices, feed-forward network (MLP) expansions generate substantial activation tensors that must be transferred efficiently, and **Mixture-of-Experts (MoE)**

architectures introduce sparse but high-dimensional routing traffic among expert partitions. In addition, pipeline-parallel execution depends upon the timely movement of activations, gradients, and intermediate states between successive processing stages. Collectively, these communication patterns create latency sources that can leave accelerators idle despite the availability of computational work.

Latency masking addresses this challenge by overlapping communication with computation, allowing useful work to proceed while data transfers, synchronization operations, and routing events occur in the background. Rather than treating communication as a separate phase of execution, hardware-aware orchestration frameworks integrate data movement directly into the computational schedule, minimizing stalls and reducing the visibility of communication delays. This approach is particularly important in distributed transformer systems, where the efficiency of execution increasingly depends not only on computational throughput but also on the ability to hide communication costs behind ongoing computation.

By coordinating communication and computation as a unified execution process, latency-masking mechanisms enable sustained accelerator utilization, improved scalability, higher throughput, and more predictable performance across multi-accelerator AI infrastructures. As model sizes, context lengths, and distributed deployment scales continue to increase, latency masking becomes a critical requirement for maintaining efficient execution throughout the AI compute fabric.

AI latency masking operates through four coordinated mechanisms:

- **Fused AI All-Reduce Collectives and Optimized Communication Launch Paths –** Fused all-reduce collectives combine multiple gradient or activation tensors into a single communication operation, reducing launch overhead and improving bandwidth utilization. Instead of issuing numerous small transfers, fused collectives aggregate tensors into larger packets that saturate the interconnect. Optimized launch paths ensure that communication kernels are dispatched with minimal latency, often using hardware-aware scheduling that aligns transfers with compute phases. This fusion is explicitly designed for AI workloads, where gradients and activations follow predictable shapes and can be coalesced without disrupting training semantics. Fused collectives exploit the structural regularity of transformer gradients — QKV projections, MLP expansions, normalization statistics — enabling communication to proceed as a single high-efficiency operation rather than a fragmented sequence of transfers.
- **Gradient Streaming for AI Backward Passes on Ring-Topology Fabrics -** Gradient streaming pipelines gradient transfers across ring-topology fabrics so that

communication begins before the backward pass completes. As soon as a layer's gradients are computed, they are streamed to neighboring accelerators while subsequent layers continue their backward computation. This overlap ensures that communication progresses concurrently with gradient generation, reducing the time spent waiting for synchronization at the end of the backward pass. Gradient streaming aligns naturally with transformer backpropagation, where gradients emerge in a deterministic layer-by-layer sequence. Ring topologies exploit this ordering, enabling continuous streaming without violating gradient correctness.

- **Asynchronous AI Communication Buffers with Thread-Pinned Execution -** Asynchronous communication buffers allow data transfers to proceed independently of the main compute stream. Thread-pinned execution ensures that communication threads remain resident on specific cores, avoiding OS-level scheduling jitter and guaranteeing consistent transfer latency. These buffers enable accelerators to continue executing compute kernels while communication progresses in parallel, preventing stalls caused by blocking synchronization.

  Transformer workloads generate predictable communication bursts — attention KV updates, expert routing metadata, activation transfers — that benefit from dedicated, thread-pinned communication paths optimized for low jitter and high determinism.

- **AI Interconnect Jitter Compensation via Predictive Scheduling Models -** Predictive scheduling models anticipate interconnect jitter and adjust communication timing to maintain overlap with compute. These models use historical latency patterns, topology-aware heuristics, and real-time telemetry to predict when transfers may slow down. Communication is then scheduled proactively to ensure that jitter does not propagate into compute stalls. This compensation is essential for large clusters where fabric-level variability can undermine throughput. Transformer inference and training pipelines rely on tightly synchronized communication. Predictive scheduling ensures that KV-cache updates, gradient exchanges, and activation transfers remain aligned with compute phases even under fluctuating interconnect conditions.

Together, fused collectives, gradient streaming, asynchronous communication buffers, and predictive scheduling models form a **communication-elastic execution layer** that allows distributed transformer systems to operate at full efficiency. AI latency masking ensures that fabric-level transfers never become serialized bottlenecks, enabling compute to proceed continuously even as massive tensors move across the interconnect. This capability is essential for frontier-scale workloads, where communication volume grows proportionally with model size, sequence length, and pipeline depth.

With the foundations of AI latency masking established, the next step is to examine the specific mechanisms that allow compute and communication to operate concurrently across distributed transformer systems. These mechanisms convert fabric-level transfers from blocking operations into background processes that remain continuously overlapped with compute. To clarify how each mechanism contributes to communication elasticity, Table 8.4-C3 organizes the core strategies—fused collectives, gradient streaming, asynchronous communication buffers, and predictive scheduling—into a unified view that highlights their AI-specific purpose, operational behavior, and latency-masking impact.

Table 8.4-C3 presents the architectural building blocks that enable AI latency masking across multi-accelerator environments. Each mechanism addresses a distinct communication bottleneck inherent in transformer-class workloads, from gradient synchronization to KV-cache propagation and expert-routing metadata exchange. The table is structured to reveal how these mechanisms operate, why they matter for AI workloads, and how they collectively ensure that fabric-level transfers remain continuously overlapped with compute. This organization provides a clear, systems-level understanding of how distributed AI execution avoids communication stalls even under extreme scaling conditions.

Table 8.4-C3 — AI Latency Masking Mechanisms for Overlapped Compute and Fabric-Level Transfers

Mechanism	AI-Specific Purpose	Operational Strategy	Latency-Masking Effect
Fused AI All-Reduce Collectives	Reduce synchronization overhead for transformer-class gradient and activation tensors	Coalesce multiple tensors into a single collective; dispatch via optimized launch paths	Minimizes per-operation launch latency and saturates interconnect bandwidth
Gradient Streaming on Ring-Topology Fabrics	Overlap backward-pass gradient generation with inter-accelerator communication	Stream gradients as soon as each layer completes its backward computation	Eliminates end-of-backward synchronization stalls; maintains continuous gradient flow
Asynchronous AI Communication Buffers	Prevent compute kernels from blocking on communication events	Use dedicated, thread-pinned communication paths	Ensures compute progresses while transfers occur in

Mechanism	AI-Specific Purpose	Operational Strategy	Latency-Masking Effect
		with non-blocking buffers	parallel; reduces idle gaps
Predictive Scheduling for Interconnect Jitter Compensation	Maintain deterministic execution under fabric-level variability	Use topology-aware models and telemetry to anticipate jitter and pre-schedule transfers	Prevents jitter from propagating into compute stalls; stabilizes throughput

Table 8.4-C3 consolidates the core mechanisms that enable AI latency masking across distributed transformer workloads. Each mechanism contributes a distinct form of communication elasticity, ensuring that fabric-level transfers remain continuously overlapped with compute even under extreme scaling conditions.

Table 8.4-C3 shows that AI latency masking is not a single optimization but a coordinated set of communication-elastic strategies. Fused all-reduce collectives reduce launch overhead by aggregating multiple tensors into high-bandwidth operations, ensuring that synchronization does not fragment compute flow. Gradient streaming leverages the deterministic ordering of transformer backpropagation to initiate communication early, preventing end-of-backward stalls. Asynchronous communication buffers introduce non-blocking transfer paths that allow compute kernels to proceed uninterrupted, while thread-pinned execution eliminates OS-level jitter that could destabilize communication timing. Predictive scheduling models anticipate interconnect variability and proactively adjust communication timing, ensuring that jitter does not propagate into compute stalls. Together, these mechanisms form a communication-optimized substrate that keeps accelerators productive even as massive tensors traverse the fabric, enabling distributed transformer systems to maintain high throughput and deterministic execution at frontier scale.

Following the structured overview in Table 8.4-C3, which organizes the core mechanisms enabling AI latency masking, the next step is to visualize how these mechanisms operate within a distributed transformer workload. Figure 8.4-C3 provides this operational perspective. It translates the table's conceptual elements into a temporal and topological diagram, showing how fused collectives, gradient streaming, asynchronous communication buffers, and predictive scheduling interact with compute phases to maintain continuous overlap between computation and fabric-level transfers. This figure serves as the visual counterpart to the table, illustrating how communication elasticity is achieved in practice.

Figure 8.4-C3 illustrates the communication-elastic execution layer that enables distributed AI

systems to sustain high throughput even as massive tensors traverse the interconnect. Each panel highlights one latency-masking mechanism, showing how compute and communication are interleaved to prevent stalls. The figure emphasizes the concurrency patterns that emerge when communication is treated not as a blocking operation but as a background process aligned with the computational structure of transformer workloads. By presenting these mechanisms side-by-side, the figure reveals how distributed systems maintain deterministic execution under extreme scaling conditions.

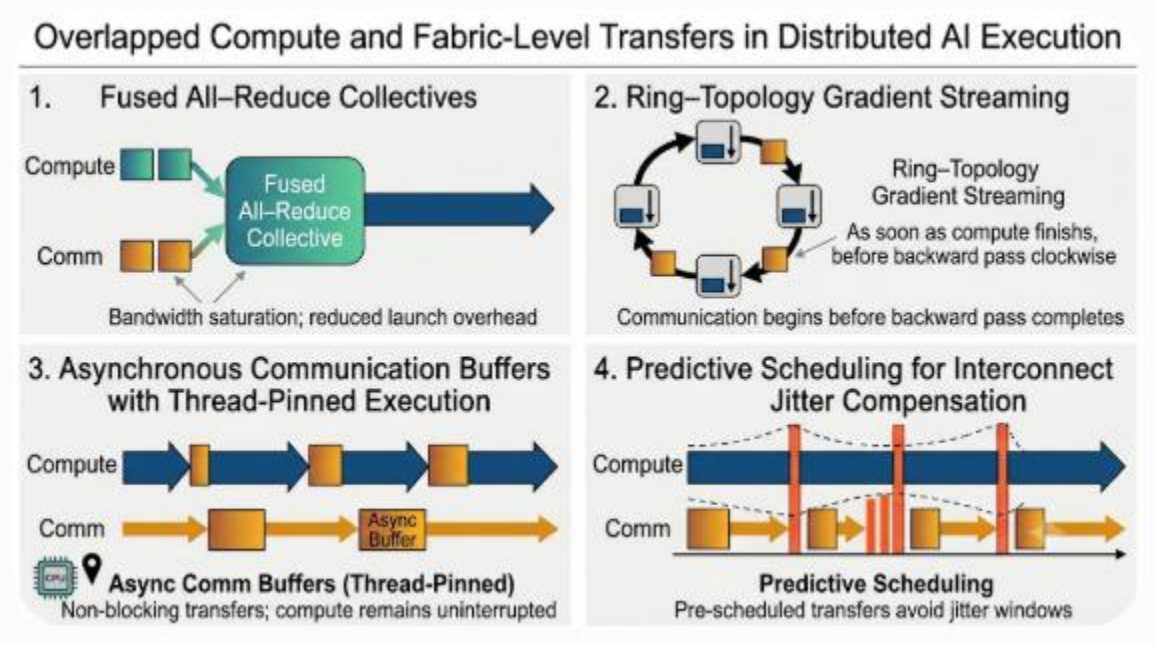


Figure 8.4-C3 — Overlapped Compute and Fabric-Level Transfers in Distributed AI Execution
The figure depicts four complementary mechanisms—fused all-reduce collectives, ring-topology gradient streaming, asynchronous communication buffers with thread-pinned execution, and predictive scheduling for interconnect jitter compensation—that collectively enable compute and communication to proceed concurrently across multi-accelerator systems. These mechanisms ensure that fabric-level transfers remain continuously overlapped with compute, preventing communication stalls and preserving throughput at frontier scale.

Legend

- ***Blue/Teal Bars****: Compute phases*
- ***Orange/Amber Bars****: Communication phases*
- ***Green/Turquoise Overlays****: Regions where compute and communication overlap*
- ***Gray Blocks****: Idle or stalled periods*
- ***Arrow****s: Direction of data movement or streaming*
- ***Ring Nodes****: Accelerators participating in ring-topology gradient streaming*

- ***Red/Orange Spikes****: Predicted interconnect jitter windows*
- ***Pinned Thread Icon:*** *Dedicated communication thread ensuring deterministic execution*

Figure 8.4-C3 demonstrates how distributed transformer systems maintain continuous progress by overlapping compute with communication. The first panel shows fused all-reduce collectives, where multiple small gradient tensors are aggregated into a single high-bandwidth operation that runs concurrently with compute. The second panel illustrates gradient streaming on a ring topology, where gradients begin circulating as soon as each layer completes its backward computation, eliminating synchronization stalls at the end of the backward pass. The third panel highlights asynchronous communication buffers managed by thread-pinned execution, ensuring that transfers proceed independently of compute and remain free from OS-level jitter. The final panel depicts predictive scheduling, where communication events are proactively aligned to avoid interconnect jitter windows, preserving deterministic compute flow. Together, these panels show how communication elasticity is achieved through concurrency, proactive scheduling, and topology-aware data movement, enabling distributed AI systems to operate at full efficiency even under extreme scaling pressures.

With the operational dynamics of overlapped compute and fabric-level transfers now established, the next step is to examine the specific mechanisms that initiate and sustain this concurrency within distributed transformer workloads. The first of these mechanisms centers on how gradients and activations are synchronized across accelerators. Transformer-class models generate large volumes of structured tensors during training, and synchronizing them efficiently is essential for maintaining throughput. Fused all-reduce collectives address this requirement by aggregating multiple tensors into high-bandwidth communication operations and dispatching them through optimized launch paths that minimize overhead. This mechanism forms the foundation of AI latency masking, ensuring that synchronization does not fragment compute flow and that communication begins from a position of maximal efficiency.

i. Fused AI All-Reduce Collectives and Optimized Communication Launch Paths

Fused AI all-reduce collectives form the foundational communication primitive that enables distributed transformer training to maintain high throughput under extreme scaling. Transformer-class workloads generate large, structurally predictable tensors during forward and backward propagation—QKV projections, MLP expansions, normalization statistics, and residual pathway gradients. Synchronizing these tensors across accelerators is essential for correctness, yet naïvely issuing individual all-reduce operations for each tensor introduces launch overhead, fragments bandwidth utilization, and prevents communication from overlapping cleanly with compute. Fused collectives solve this by aggregating multiple tensors into a single

high-bandwidth operation, transforming synchronization from a series of small transfers into a unified, fabric-saturating communication event.

This AI-specific framing is crucial because fused collective communication is not merely a generic optimization borrowed from high-performance computing (HPC); it is a specialized response to the highly structured communication patterns of modern neural-network training. Transformer architectures generate gradients that exhibit consistent dimensionality, ordering, and layer-wise organization throughout the backward propagation process. Unlike many scientific workloads, where communication patterns may vary dynamically, transformer gradients are produced in predictable sequences that align naturally with collective communication operations. This structural regularity creates opportunities to aggregate multiple gradient tensors into larger communication groups, reducing the overhead associated with initiating numerous small transfers.

By coalescing gradients from multiple layers into unified communication streams, fused collectives improve interconnect utilization, reduce synchronization frequency, and lower per-operation latency. Equally important, this approach aligns closely with the temporal structure of backpropagation itself. As gradients become available during backward execution, communication can be initiated incrementally and overlapped with ongoing computation rather than deferred until an entire training step is complete. The result is a tightly integrated execution model in which computation and communication proceed concurrently, minimizing idle accelerator time and reducing the visibility of communication overhead.

In large-scale distributed training environments, this hardware-aware communication strategy transforms network transfers from passive synchronization events into active components of the execution pipeline. By exploiting the inherent structural regularity of transformer gradients, fused collective operations improve scalability, sustain high accelerator utilization, and enable efficient training across increasingly large clusters of accelerators and high-bandwidth interconnect fabrics.

Optimized communication launch paths further enhance this mechanism. Instead of relying on default runtime dispatch, AI-optimized launch paths use hardware-aware scheduling to minimize kernel launch latency, reduce CPU-side orchestration overhead, and ensure that communication kernels are issued at precisely the right moment to maintain overlap with compute. These launch paths often incorporate stream-priority tuning, NUMA-aligned dispatch, and topology-aware routing to ensure that fused collectives saturate available bandwidth without interfering with concurrent compute kernels.

Together, fused collectives and optimized launch paths transform gradient synchronization from

a blocking operation into a background activity tightly interwoven with computation. They ensure that communication begins from a position of maximal efficiency, that bandwidth is fully utilized, and that synchronization never fragments the temporal flow of distributed transformer execution. This mechanism is the first pillar of AI latency masking, establishing the communication-elastic substrate upon which gradient streaming, asynchronous buffers, and predictive scheduling build.

With fused all-reduce collectives establishing a high-efficiency baseline for synchronizing transformer gradients, the next challenge lies in reducing the temporal exposure of these synchronization events during the backward pass. Even when collectives are fused and dispatched through optimized launch paths, the backward pass still produces gradients layer-by-layer, creating natural windows where communication can begin long before the full gradient set is available. Exploiting this temporal structure is essential for deeper models, where waiting until the end of backpropagation would introduce avoidable stalls. Gradient streaming addresses this need by initiating communication as soon as each layer's gradients are computed, allowing transfers to propagate across the fabric while subsequent layers continue their backward computation. This mechanism transforms gradient synchronization from a terminal barrier into a continuously flowing pipeline, further tightening the overlap between compute and communication.

ii. Gradient Streaming for AI Backward Passes on Ring-Topology Fabrics

Gradient streaming is the second major pillar of AI latency masking, designed to exploit the temporal structure of transformer backpropagation. During the backward pass, gradients emerge in a strictly ordered, layer-by-layer sequence. Traditional distributed training waits until all gradients are computed before initiating synchronization, creating a terminal barrier that grows increasingly costly as model depth increases. Gradient streaming eliminates this barrier by initiating communication immediately when each layer's gradients become available, allowing transfers to propagate across the interconnect while subsequent layers continue their backward computation.

Ring-topology fabrics are particularly well-suited for this mechanism. In a ring, each accelerator communicates only with its immediate neighbors, forming a predictable and bandwidth-efficient path for gradient propagation. As soon as a layer completes its backward computation, its gradients are injected into the ring and begin circulating clockwise. Meanwhile, the accelerator continues computing gradients for deeper layers, ensuring that communication and computation proceed concurrently. This concurrency is not incidental—it is a deliberate exploitation of the transformer's sequential gradient emergence.

This AI-specific framing is essential because ring all-reduce optimization is not merely a generic distributed-communication technique; it is particularly well suited to the highly structured gradient-exchange patterns of modern transformer training. Transformer architectures generate gradients that exhibit consistent tensor shapes, predictable layer ordering, and regular communication characteristics across training iterations. This structural regularity creates an execution environment ideally suited for streaming communication patterns, allowing gradient data to move through the system in a continuous and highly organized manner.

The ring topology exploits these properties by partitioning gradients into communication segments that circulate sequentially among participating accelerators. Rather than requiring centralized coordination or large synchronization barriers, each device simultaneously performs communication and partial reduction operations as data traverse the ring. As gradient fragments propagate through the topology, every accelerator incrementally accumulates partial reductions until the complete all-reduce result is assembled. Throughout this process, computational resources remain active, minimizing idle time and reducing synchronization overhead.

More importantly, the regular structure of transformer gradients allows communication schedules to align naturally with the temporal progression of backpropagation. Gradient exchange can begin as soon as gradient tensors become available rather than waiting for completion of the entire backward pass. This enables substantial overlap between communication and computation, transforming gradient synchronization from a blocking operation into a continuously flowing pipeline of concurrent compute and communication phases. The result is improved interconnect utilization, higher accelerator occupancy, enhanced scalability, and more efficient distributed training across large multi-accelerator systems.

Gradient streaming is especially impactful for deep models, where the backward pass spans hundreds of layers. Without streaming, the final synchronization step becomes a dominant latency source. With streaming, synchronization is amortized across the entire backward pass, dramatically reducing idle time and tightening the compute-communication overlap that defines high-efficiency distributed AI execution.

With gradient streaming transforming backward-pass synchronization into a continuously flowing pipeline, the next challenge lies in ensuring that communication itself never blocks compute. Even when gradients are streamed efficiently, communication kernels can still contend with compute kernels for execution resources, or suffer from OS-level scheduling jitter that disrupts timing. To maintain strict concurrency, distributed AI systems require communication paths that operate independently of compute, with deterministic execution and

minimal interference. Asynchronous communication buffers with thread-pinned execution provide this capability, enabling transfers to proceed in parallel with compute while avoiding jitter, contention, and blocking behavior. This mechanism forms the third pillar of AI latency masking, ensuring that communication remains fully decoupled from compute and continuously overlapped throughout the training pipeline.

iii. Asynchronous AI Communication Buffers with Thread-Pinned Execution

Asynchronous AI communication buffers provide the structural decoupling that allows fabric-level transfers to proceed independently of compute, turning communication into a continuously flowing background activity rather than a source of blocking synchronization. In distributed transformer training, activations, gradients, KV-cache segments, and routing metadata must move across accelerators at high frequency. If these transfers share execution resources and scheduling paths with compute kernels, they contend for cores, streams, and runtime attention, creating stalls and jitter that erode throughput. Asynchronous buffers break this coupling by introducing dedicated, non-blocking queues that absorb communication traffic and release it into the interconnect under controlled, deterministic conditions.

This AI-specific framing is essential because asynchronous buffering is not simply a generic communication optimization; it is a specialized mechanism designed to accommodate the highly structured and bursty communication behavior of modern AI workloads. Transformer architectures generate predictable waves of data movement throughout execution, including **Key–Value (KV) cache** updates during attention computation, large activation transfers produced by feed-forward network expansions, expert-routing traffic associated with **Mixture-of-Experts (MoE)** layers, and stage-to-stage activation exchanges within pipeline-parallel execution. These communication events often occur at well-defined points in the computational graph, creating opportunities for communication pathways to be provisioned and scheduled proactively rather than reactively.

Asynchronous buffering exploits this structural regularity by introducing intermediary storage layers that decouple tensor production from tensor transmission. Buffers are sized, organized, and scheduled according to the expected communication patterns of the model, enabling data transfers to be initiated immediately when tensors become available without forcing the primary compute stream to stall. Rather than waiting for communication operations to complete, accelerators can continue executing attention kernels, matrix multiplications, and other computational tasks while buffered data move through the interconnect fabric.

In effect, asynchronous buffers function as dynamic shock absorbers between the high-frequency generation of tensor data and the variable-latency behavior of distributed

communication networks. They smooth transient fluctuations in network availability, absorb bursts of communication demand, and mitigate the impact of temporary congestion events. By decoupling communication progress from computational progress, asynchronous buffering transforms communication from a blocking dependency into a largely hidden component of execution. The result is improved accelerator utilization, more effective overlap of communication and computation, increased throughput, and greater scalability across multi-accelerator AI systems operating under dynamic workload conditions.

Thread-pinned execution completes this picture by giving communication its own dedicated control plane. Instead of relying on general-purpose OS scheduling, communication threads are pinned to specific cores or NUMA domains and bound to particular devices or NICs. This eliminates scheduling jitter, reduces context-switch overhead, and ensures that communication progress is predictable. For AI workloads, where the timing of collective operations and point-to-point transfers directly affects pipeline utilization, this determinism is critical. Pinned threads drive the asynchronous buffers, issuing sends and receives, progressing collectives, and managing completion events without interfering with the compute threads that orchestrate kernel launches on the accelerators.

Together, asynchronous buffers and thread-pinned execution create a communication-elastic substrate: data moves into buffers as soon as it is produced, communication progresses continuously on dedicated threads, and compute remains free to execute kernels without blocking on fabric events. This mechanism is the third pillar of AI latency masking, ensuring that even under heavy communication load, accelerators stay productive and the temporal structure of transformer execution remains intact.

With asynchronous communication buffers and thread-pinned execution ensuring that transfers proceed independently of compute, the remaining challenge is variability in the interconnect itself. Even well-designed fabrics exhibit jitter—fluctuations in latency and bandwidth due to contention, topology hot spots, or transient congestion—that can disrupt the carefully orchestrated overlap between compute and communication. If left unmanaged, this jitter can cause asynchronous buffers to drain too slowly or collectives to complete later than expected, propagating delays back into the compute pipeline. To preserve deterministic execution under these conditions, distributed AI systems require a way to anticipate and compensate for fabric-level variability. AI interconnect jitter compensation via predictive scheduling models provides this capability, using topology-aware telemetry and historical latency patterns to schedule communication events proactively so that jitter is absorbed by the fabric rather than by the compute timeline.

iv. AI Interconnect Jitter Compensation via Predictive Scheduling Models

AI interconnect jitter compensation is the fourth and final pillar of latency masking, designed to preserve deterministic execution in distributed transformer systems even when the underlying fabric exhibits variability. No matter how advanced the hardware, large-scale interconnects—NVLink, NVSwitch, PCIe, InfiniBand, Ethernet fabrics—experience jitter: transient fluctuations in latency, bandwidth, or congestion caused by topology hot spots, competing workloads, routing contention, or microbursts of traffic. For distributed AI workloads, where compute and communication must remain tightly overlapped, jitter is not a minor inconvenience; it is a direct threat to throughput, pipeline balance, and synchronization correctness.

Predictive scheduling models address this challenge by anticipating jitter before it impacts execution. Instead of reacting to slowdowns after they occur, these models use telemetry, historical latency traces, topology-aware heuristics, and real-time congestion signals to forecast when the interconnect is likely to degrade. Once a jitter window is predicted, communication events—collectives, point-to-point transfers, KV-cache updates, expert-routing outputs—are scheduled proactively to avoid the predicted slowdown. This transforms jitter from a disruptive event into a manageable environmental condition.

This AI-specific framing is essential because predictive communication scheduling is not merely a generic network-optimization technique; it is a specialized response to the structured and time-sensitive communication behavior of transformer-based systems. Modern AI workloads generate recurring patterns of data exchange that are closely coupled to model execution. Attention mechanisms require coordinated **Key–Value (KV) cache** propagation, feed-forward network (MLP) expansions produce large activation tensors, **Mixture-of-Experts (MoE)** architectures generate sparse yet high-dimensional expert-routing traffic, and pipeline-parallel execution introduces regular stage-to-stage transfers of activations and gradients. Unlike arbitrary communication workloads, these events occur at predictable points within the computational graph and exhibit highly repeatable temporal characteristics across training and inference cycles.

Predictive scheduling frameworks exploit this regularity by forecasting communication demand and aligning data movement with corresponding compute phases before congestion occurs. Rather than reacting to communication requests after they are issued, the scheduler proactively reserves bandwidth, stages transfers, and prioritizes routing paths according to the anticipated execution timeline. This approach allows communication activity to be synchronized with computational progression, ensuring that data arrive when needed without interrupting ongoing execution.

In effect, predictive scheduling shifts the burden of latency and jitter from the execution timeline to the communication fabric itself. Temporary fluctuations in network performance are

absorbed through advance planning, buffering, and traffic shaping rather than propagating upward into accelerator utilization. By coordinating communication and computation as a unified process, predictive scheduling reduces synchronization delays, improves throughput, preserves deterministic execution behavior, and enables large-scale AI systems to maintain high utilization even under communication-intensive workloads.

These models typically operate across three layers:

- **Telemetry-Driven Jitter Detection -** The system continuously monitors interconnect latency, queue depth, link utilization, and congestion indicators. AI-specific telemetry—such as collective completion times or KV-cache transfer latency—is incorporated to detect jitter patterns that directly affect transformer execution.

- **Topology-Aware Prediction -** Using historical traces and real-time signals, the model predicts jitter windows on specific links or switch domains. Because AI workloads often use structured communication topologies (rings, trees, hierarchical collectives), predictions can be localized to the exact paths used by the model.

- **Proactive Communication Scheduling -** Communication events are issued slightly earlier or later to avoid predicted jitter windows. For example:
    - A fused all-reduce may be launched early to complete before a congestion spike.
    - Gradient streaming packets may be staggered to avoid a predicted slowdown on a ring link.
    - KV-cache updates may be shifted to a quieter window to preserve attention-layer timing.

  The result is a communication timeline that remains aligned with compute even when the fabric is unstable.

Predictive scheduling does not eliminate jitter; it neutralizes its impact. By absorbing variability into the communication layer rather than the compute layer, the model maintains deterministic execution, stable pipeline utilization, and consistent throughput. This mechanism is especially critical at frontier scale, where even small jitter spikes can cascade into multi-millisecond stalls across hundreds or thousands of accelerators.

Together with fused collectives, gradient streaming, and asynchronous buffers, predictive scheduling completes the communication-elastic substrate required for overlapped compute and fabric-level transfers. It ensures that distributed transformer systems remain resilient, efficient, and synchronized even under the unpredictable conditions of large-scale

interconnects.

AI latency masking establishes the communication-elastic substrate that allows distributed transformer systems to sustain high utilization even under heavy fabric load. Fused all-reduce collectives reduce synchronization overhead by aggregating structured transformer gradients into high-bandwidth operations dispatched through optimized launch paths. Gradient streaming transforms backward-pass synchronization into a continuous pipeline, allowing communication to progress concurrently with gradient generation. Asynchronous communication buffers with thread-pinned execution decouple transfers from compute, ensuring deterministic progress free from OS-level jitter. Predictive scheduling models anticipate interconnect variability and proactively align communication with compute phases, preventing jitter from propagating into execution stalls. Together, these mechanisms convert communication from a blocking dependency into a background process tightly interwoven with computation, enabling distributed AI workloads to operate at frontier scale with stable throughput, balanced pipelines, and deterministic execution.

With communication elasticity firmly established, the next scaling pressure arises from the memory dynamics within each accelerator. Even when compute and communication are fully overlapped, transformer-class workloads generate highly fragmented memory footprints—KV-cache segments, attention windows, activation shards, expert outputs, and temporary buffers—that accumulate across long sequences and deep pipelines. Without active management, this fragmentation reduces effective memory capacity, increases allocation latency, and destabilizes attention-layer performance. Sustaining frontier-scale models therefore requires a complementary mechanism that introduces memory elasticity within the accelerator itself. Dynamic AI memory defragmentation and PagedAttention retention policies provide this capability, reorganizing memory layouts, compacting fragmented regions, and managing KV-cache residency so that large-context transformer execution remains stable, efficient, and predictable.

d. Dynamic AI Memory Defragmentation and PagedAttention Retention Policies

Dynamic AI memory defragmentation and PagedAttention retention policies form the memory-elastic substrate required for frontier-scale transformer execution. Even when compute and communication are fully overlapped, memory fragmentation inside each accelerator becomes a limiting factor. Transformer workloads generate highly irregular and long-lived allocations—KV-cache segments, attention windows, activation shards, expert outputs, routing metadata, temporary buffers—that accumulate across continuous batching and ultra-long sequences. Over time, these allocations create fragmented memory regions that reduce effective capacity, increase allocation latency, and destabilize attention-layer performance.

Memory elasticity is therefore essential: the system must reorganize, compact, and manage memory dynamically to sustain large-context execution.

PagedAttention introduces a virtualized memory model for attention KV-cache residency. Instead of storing KV-cache segments in monolithic contiguous blocks, PagedAttention distributes them across virtual pages that can be compacted, evicted, remapped, or migrated without disrupting attention semantics. This enables dynamic defragmentation, selective retention, and multi-tenant protection—all while preserving deterministic transformer behavior.

The four mechanisms below define this memory-elastic layer.

- **KV-Cache Fragmentation Dynamics in Continuous AI Batching -** Continuous batching—where new requests enter the system while existing sequences remain active—creates highly fragmented KV-cache footprints. Each sequence has a different length, retention horizon, and attention window, causing KV-cache pages to be allocated and freed at irregular intervals. Over time, this produces "Swiss-cheese" fragmentation: small free regions scattered between long-lived KV segments. Transformer attention requires fast, contiguous access to KV-cache segments. Fragmentation increases lookup latency, reduces usable memory, and forces premature eviction of active sequences. Understanding fragmentation dynamics is essential for designing defragmentation and retention policies that preserve long-context performance.
- **Virtual Memory Paging for AI Workloads with Scattered Cache-Line Access -** PagedAttention introduces a virtual memory layer that maps KV-cache segments into fixed-size pages. Instead of requiring contiguous physical memory, KV-cache entries are stored in page-aligned blocks that can be compacted, migrated, or remapped without altering logical sequence structure. Attention layers access KV-cache in scattered patterns—jumping across positions, heads, and layers. Virtual paging ensures that these scattered accesses remain efficient even when physical memory is fragmented. It also enables background compaction, where pages are reorganized while compute continues uninterrupted.
- **AI Page Eviction Policies with Host-to-Device Latency Masking -** When memory pressure increases, KV-cache pages must be evicted. AI-specific eviction policies prioritize pages based on sequence activity, recency, and predicted future access. Cold pages are migrated to host memory or compressed storage, while hot pages remain resident on the accelerator. Latency masking is essential; eviction and migration occur asynchronously, overlapped with compute and communication. Host-to-device transfers are scheduled during idle memory-bandwidth windows or overlapped with compute

kernels, ensuring that eviction does not stall attention execution. Transformer inference pipelines rely on predictable KV-cache access. Eviction must preserve semantic continuity while hiding transfer latency behind ongoing compute.

- **Multi-Tenant AI Cache Protection with Hardware-Enforced Page Mapping -** In multi-tenant environments—shared clusters, inference farms, or multi-model deployments—KV-cache pages must be isolated across tenants. Hardware-enforced page mapping ensures that each tenant's KV-cache pages are protected from accidental overwrite, unauthorized access, or cross-model interference. Transformer workloads often run side-by-side with different models, contexts, or customers. Hardware-enforced mapping ensures deterministic behavior, prevents cache poisoning, and maintains strict isolation even under heavy load or aggressive paging.

With the mechanisms of dynamic memory defragmentation and PagedAttention retention now established, the next step is to consolidate how these techniques collectively provide memory elasticity for transformer-class workloads. Distributed AI systems must maintain stable KV-cache residency, efficient scattered access, predictable eviction behavior, and strict multi-tenant isolation even as sequences vary in length, batching patterns shift, and memory pressure fluctuates. Table 8.4-C4 organizes these mechanisms into a unified view, highlighting their AI-specific purpose, operational strategy, and the memory-elastic effects that enable long-context transformer execution to remain efficient and deterministic under continuous load.

Table 8.4-C4 presents the core memory-elastic mechanisms that support dynamic defragmentation and PagedAttention retention in distributed transformer systems. Each mechanism addresses a distinct challenge created by continuous batching, scattered KV-cache access, host-device migration, and multi-tenant execution. The table is structured to reveal how these mechanisms operate, why they are essential for AI workloads, and how they collectively maintain stable memory behavior even as sequence lengths grow and memory footprints become increasingly irregular. This organization provides a clear architectural map of how memory elasticity is achieved inside modern accelerators.

Table 8.4-C4 — Memory-Elastic Mechanisms for Dynamic AI Defragmentation and PagedAttention Retention

Mechanism	AI-Specific Purpose	Operational Strategy	Memory-Elastic Effect
KV-Cache Fragmentation Dynamics	Manage irregular KV-cache footprints	Track fragmentation patterns; identify	Reduces allocation failures; preserves long-context execution

Mechanism	AI-Specific Purpose	Operational Strategy	Memory-Elastic Effect
	from continuous batching	long-lived vs short-lived segments	
Virtual Memory Paging (PagedAttention)	Support scattered KV-cache access without requiring contiguous memory	Map KV segments into fixed-size pages; enable compaction and migration	Enables dynamic defragmentation and efficient scattered access
AI Page Eviction Policies	Maintain memory availability under pressure	Evict cold pages; migrate to host; overlap transfers with compute	Masks host-device latency; preserves hot pages for active sequences
Multi-Tenant Page Protection	Prevent cross-tenant interference in shared clusters	Hardware-enforced page isolation and mapping	Ensures deterministic behavior and secure KV-cache residency

Table 8.4-C4 consolidates the mechanisms that provide memory elasticity for transformer workloads. Each mechanism addresses a distinct challenge—fragmentation, scattered access, eviction, and multi-tenant protection—ensuring that KV-cache residency remains efficient and stable under continuous batching and long-context execution.

Table 8.4-C4 shows that memory elasticity is not a single optimization but a coordinated set of mechanisms that stabilize KV-cache residency under dynamic workloads. KV-cache fragmentation dynamics explain how continuous batching produces irregular memory footprints that must be actively managed to preserve long-context performance. Virtual memory paging (PagedAttention) introduces a page-aligned abstraction that supports scattered access patterns while enabling background compaction and migration. AI-specific eviction policies ensure that cold pages are migrated or evicted without disrupting active sequences, with host-to-device transfers masked behind ongoing compute. Multi-tenant page protection provides hardware-enforced isolation, preventing cross-model interference and ensuring deterministic behavior in shared environments. Together, these mechanisms form a memory-elastic substrate that allows transformer workloads to scale in sequence length, concurrency, and tenant density without suffering fragmentation-induced degradation.

Following the structured overview in Table 8.4-C4, which organizes the core mechanisms enabling memory elasticity in transformer-class workloads, the next step is to visualize how

these mechanisms operate inside accelerator memory. Figure 8.4-C4 provides this operational perspective. It translates the table's conceptual elements into a spatial and temporal diagram, showing how fragmentation emerges, how virtual pages are compacted and migrated, how eviction is masked behind compute, and how multi-tenant isolation is enforced. This figure serves as the visual counterpart to the table, illustrating how dynamic defragmentation and PagedAttention retention policies maintain stable KV-cache residency under continuous batching and long-context execution.

Figure 8.4-C4 illustrates the memory-elastic substrate that enables distributed transformer systems to sustain long-context execution even under heavy fragmentation, scattered access patterns, and multi-tenant pressure. Each panel highlights one mechanism—fragmentation dynamics, virtual paging, eviction with latency masking, and hardware-enforced isolation—showing how memory is reorganized, compacted, migrated, or protected without disrupting ongoing compute. By presenting these mechanisms side-by-side, the figure reveals how PagedAttention transforms KV-cache residency from a rigid, contiguous allocation model into a flexible, page-aligned system capable of adapting to dynamic workloads.

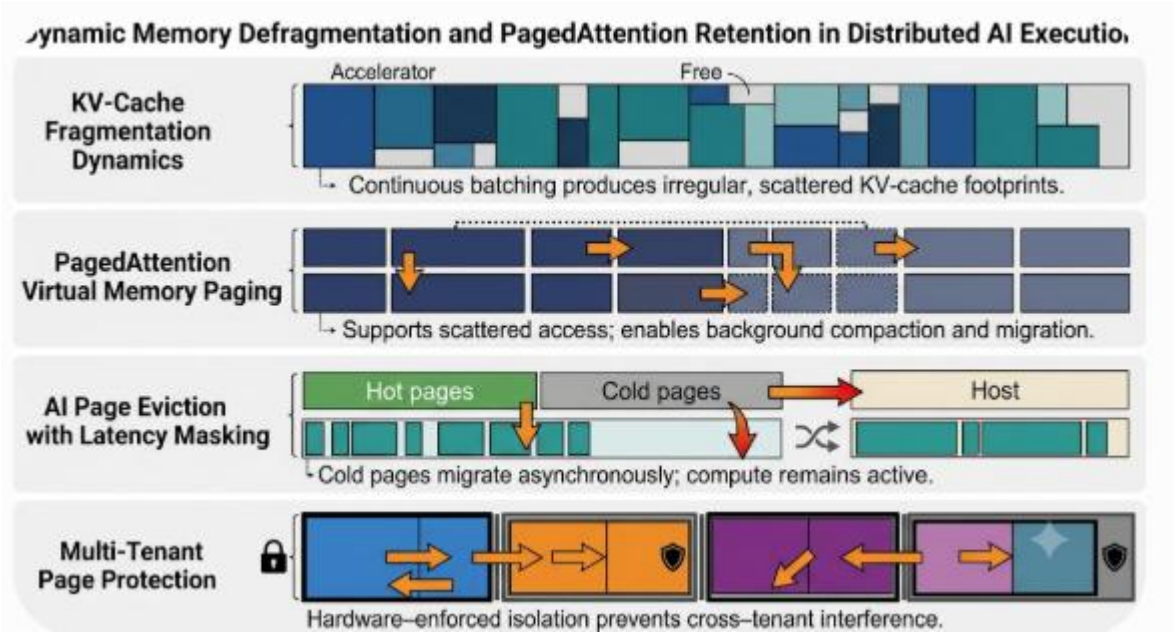


Figure 8.4-C4 — Dynamic Memory Defragmentation and PagedAttention Retention in Distributed AI Execution

The figure depicts four complementary mechanisms—KV-cache fragmentation analysis, virtual memory paging for scattered access, asynchronous page eviction with host-to-device latency masking, and hardware-enforced multi-tenant page protection—that collectively provide memory elasticity for transformer workloads. These mechanisms ensure that KV-cache residency remains stable, efficient, and secure even under continuous batching, long-context execution, and multi-model deployment.

Legend

- ***Blue/Teal Blocks****: KV-cache segments*
- ***Gray Gaps****: Fragmented free memory*
- ***Uniform Page Rectangles****: Virtual pages used by PagedAttention*
- ***Green Blocks****: Hot pages (high-priority retention)*
- ***Gray Blocks****: Cold pages (eviction candidates)*
- ***Orange Arrows****: Page migration or compaction*
- ***Red Arrows****: Eviction or host-migration paths*
- ***Beige Region****: Host memory*
- ***Color-Coded Regions****: Tenant-specific page domains*
- ***Lock/Shield Icons:*** *Hardware-enforced isolation boundaries*

Figure 8.4-C4 demonstrates how dynamic memory defragmentation and PagedAttention retention policies stabilize KV-cache residency in distributed transformer systems. The first panel shows how continuous batching produces irregular KV-cache footprints, with long-lived and short-lived segments interspersed across accelerator memory. The second panel illustrates how PagedAttention maps these segments into uniform pages, enabling background compaction and migration while supporting scattered access patterns inherent to attention workloads. The third panel highlights AI-specific eviction policies, where cold pages are migrated asynchronously to host memory while compute continues uninterrupted, masking host-device latency. The final panel depicts multi-tenant page protection, where hardware-enforced boundaries isolate tenants and prevent cross-model interference. Together, these panels show how memory elasticity is achieved through fragmentation management, virtual paging, asynchronous eviction, and secure isolation, enabling transformer workloads to scale in sequence length, concurrency, and tenant density without suffering memory-induced degradation.

With the mechanisms of memory elasticity now visualized in Figure 8.4-C4, the next step is to examine how fragmentation emerges inside accelerator memory during real transformer workloads. Continuous AI batching—where new sequences arrive while existing ones remain active—creates highly irregular KV-cache footprints that evolve over time as attention windows expand, shrink, or expire. These dynamics form the root cause of memory instability in long-context execution, shaping how pages are allocated, freed, and reorganized. Understanding KV-cache fragmentation is therefore the foundation for all subsequent defragmentation, paging, eviction, and isolation policies. The first mechanism in this sequence focuses on how fragmentation develops, how it impacts attention performance, and why it must be actively managed to sustain large-context transformer workloads.

i. KV-Cache Fragmentation Dynamics in Continuous AI Batching

Tensor Core intensity thresholds define the minimum arithmetic density required for transformer-class workloads to fully utilize accelerator Tensor Cores. Modern AI accelerators are designed around fused-multiply-add (FMA) pipelines that achieve peak throughput only when compute graphs exhibit sufficiently high tensor-level parallelism. Transformer layers—attention projections, MLP expansions, normalization paths—naturally produce dense matrix multiplications, but their effective intensity varies depending on sequence length, batch composition, KV-cache residency, and the fragmentation state of intermediate tensors.

Transformer workloads are not uniformly dense. Attention heads with small sequence windows, mixture-of-experts routing with sparse expert activation, and fragmented KV-cache layouts can all reduce Tensor Core intensity below the threshold needed for peak utilization. When intensity drops, compute kernels fall back to lower-efficiency execution paths, increasing latency and reducing the overlap between compute and communication.

Tensor Core intensity thresholds therefore act as a diagnostic boundary:

- **Above the threshold**, Tensor Cores operate at full throughput, enabling predictable kernel timing and stable overlap with communication.
- **Below the threshold**, kernels become memory-bound, exposing latency from fragmented memory layouts, scattered access patterns, and irregular tensor shapes.

This is where memory elasticity becomes essential. Dynamic defragmentation and PagedAttention retention policies restore tensor contiguity, increase arithmetic density, and push compute graphs back above the intensity threshold. By reorganizing KV-cache pages, compacting fragmented regions, and stabilizing memory access patterns, the system ensures that Tensor Cores remain saturated even under continuous batching and long-context execution.

In short, Tensor Core intensity thresholds define the performance envelope for AI compute graphs. Memory-elastic mechanisms ensure that transformer workloads remain inside that envelope, preserving deterministic execution and maximizing compute-communication overlap.

With Tensor Core intensity thresholds establishing the performance boundary for transformer compute graphs, the next challenge is ensuring that memory access patterns remain efficient even when KV-cache segments are scattered across fragmented physical memory. Attention layers frequently access KV-cache entries in non-contiguous patterns—jumping across heads, layers, and positions—which becomes increasingly costly when fragmentation disrupts locality. Virtual memory paging for AI workloads addresses this challenge by mapping KV-cache

segments into uniform pages that can be compacted, migrated, and remapped without requiring contiguous physical memory. This mechanism forms the foundation for scattered-access efficiency, enabling background defragmentation and stable attention performance even under dynamic batching conditions.

ii. Virtual Memory Paging for AI Workloads with Scattered Cache-Line Access

Virtual memory paging for AI workloads introduces a page-aligned abstraction layer that stabilizes KV-cache residency even when physical memory becomes fragmented. Transformer attention layers frequently access KV-cache entries in scattered, non-contiguous patterns—jumping across heads, layers, and sequence positions. Under a traditional contiguous allocation model, these scattered accesses become increasingly expensive as fragmentation grows, forcing the accelerator to traverse irregular memory regions and degrading Tensor Core intensity. Virtual paging solves this by mapping KV-cache segments into fixed-size pages that can be compacted, migrated, or remapped without requiring contiguous physical memory.

Transformer workloads exhibit predictable but scattered access patterns. Each attention head reads KV-cache entries across multiple positions, and mixture-of-experts routing introduces additional sparsity. Virtual paging ensures that these scattered accesses remain efficient by providing a stable logical address space, even when the underlying physical memory is reorganized. This allows background defragmentation to occur while compute continues uninterrupted, preserving arithmetic density and preventing memory-bound execution paths.

PagedAttention builds directly on this abstraction. KV-cache segments are stored in page-aligned blocks, enabling the system to reorganize memory layouts without altering the logical structure of sequences. Pages can be compacted to eliminate fragmentation, migrated to reduce access latency, or remapped to balance load across memory controllers. Because attention layers operate on logical page indices rather than physical addresses, these operations remain invisible to the compute graph.

The result is a memory-elastic substrate where scattered access patterns no longer degrade performance. Virtual paging ensures that even under continuous batching, long-context execution, and multi-model concurrency, transformer workloads maintain stable access latency and predictable Tensor Core utilization.

With virtual memory paging providing a stable logical address space for scattered KV-cache access, the next challenge is managing memory pressure when page residency exceeds accelerator capacity. Transformer workloads with long contexts or high concurrency inevitably produce more KV-cache pages than can remain resident on-device. Eviction becomes necessary—but eviction must not stall compute or disrupt attention semantics. AI-specific page

eviction policies address this by identifying cold pages, migrating them to host memory or compressed storage, and masking host-to-device transfer latency behind ongoing compute. This mechanism forms the next pillar of memory elasticity, ensuring that page migration occurs seamlessly and without degrading transformer execution.

iii. AI Page Eviction Policies with Host-to-Device Latency Masking

AI page eviction policies govern how KV-cache pages are removed from accelerator memory when capacity becomes constrained, ensuring that long-context transformer workloads remain stable even as memory pressure fluctuates. Unlike traditional eviction strategies, which prioritize locality or recency in general-purpose workloads, AI eviction policies must preserve the semantic continuity of attention layers. KV-cache entries represent the historical context of active sequences; evicting the wrong pages or evicting them at the wrong time can degrade model quality, increase latency, or force recomputation. As a result, eviction in AI systems is governed by activity-aware, sequence-aware, and horizon-aware heuristics that identify “cold” pages—those unlikely to be accessed soon—and migrate them out of device memory.

Transformer workloads produce KV-cache pages with highly variable access patterns. Some pages correspond to active attention windows and must remain resident; others belong to sequences that have paused, completed, or entered low-activity phases. AI eviction policies classify pages based on recency, predicted future access, sequence length, and batching dynamics. Cold pages are migrated to host memory or compressed storage, while hot pages remain resident to preserve attention performance.

Host-to-device latency masking is the critical innovation that makes eviction viable at scale. Page migration is performed asynchronously, overlapped with ongoing compute and communication. While cold pages are transferred to host memory, Tensor Core kernels continue executing without interruption. This overlap is achieved through dedicated communication streams, pinned threads, and bandwidth-aware scheduling that ensures migration traffic does not interfere with compute-critical transfers. When a previously evicted page becomes needed again, its host-to-device transfer is similarly masked behind compute, preventing stalls in the attention pipeline.

The result is a memory-elastic system where eviction is not a disruptive event but a continuous background process. Pages flow between device and host memory based on activity patterns, and latency is absorbed by the fabric rather than by the compute timeline. This ensures that transformer workloads can scale in sequence length and concurrency without suffering memory-induced degradation.

With eviction policies ensuring that KV-cache residency adapts dynamically to memory pressure

while masking host-device latency, the next challenge arises in multi-tenant environments where multiple models, contexts, or customers share the same accelerator. Under these conditions, KV-cache pages must be isolated to prevent accidental overwrite, unauthorized access, or cross-model interference. Hardware-enforced page mapping provides this protection, ensuring that each tenant's pages remain logically and physically isolated even as defragmentation, paging, and eviction occur in the background. This mechanism forms the final pillar of memory elasticity, enabling secure, deterministic transformer execution in shared, high-density AI deployments.

iv. Multi-Tenant AI Cache Protection with Hardware-Enforced Page Mapping

Multi-tenant AI cache protection ensures that KV-cache pages, activation buffers, routing metadata, and attention-layer state remain isolated across different models, customers, or workloads sharing the same accelerator. As transformer inference and training increasingly operate in shared environments—multi-model serving clusters, fine-tuning farms, retrieval-augmented generation pipelines, and high-density inference deployments—memory isolation becomes a first-class requirement. Without strict protection, one tenant's KV-cache pages could be overwritten, corrupted, or accessed by another tenant, leading to unpredictable behavior, degraded model quality, or security violations. Hardware-enforced page mapping provides the deterministic isolation needed to prevent these failures.

Transformer workloads maintain long-lived KV-cache pages that encode the historical context of active sequences. These pages are semantically meaningful: they represent the memory of the model. In multi-tenant environments, each tenant's KV-cache must remain logically and physically isolated, even as dynamic defragmentation, virtual paging, and eviction occur in the background. Hardware-enforced page mapping ensures that isolation persists regardless of how memory is reorganized.

Hardware-Enforced Page Domains

Accelerators divide memory into tenant-specific page domains. Each domain contains:

- KV-cache pages
- Attention-layer buffers
- Routing metadata
- Temporary workspace allocations

These domains are enforced by hardware boundary lines—MMU-level protections, device-side page tables, and secure mapping registers—that prevent cross-tenant access. Even if two

tenants share the same physical device, their pages remain invisible to each other.

Secure Page Remapping

Dynamic defragmentation and PagedAttention rely on page migration and remapping. In multi-tenant environments, remapping must preserve isolation:

- Pages can migrate **within** a tenant's domain.
- Pages **cannot** migrate across domains.
- Compaction occurs independently per tenant.
- Eviction policies operate per-tenant, ensuring fairness and preventing starvation.

This ensures that memory elasticity mechanisms do not violate isolation guarantees.

Protection Against Cross-Model Interference

Multi-model deployments introduce additional complexity. Different models may have:

- Different KV-cache sizes
- Different attention window lengths
- Different batching patterns
- Different eviction priorities

Hardware-enforced mapping ensures that one model's KV-cache cannot overwrite another's, even if both models operate under heavy load or aggressive paging. This prevents cache poisoning, accidental overwrite, and semantic contamination between models.

Tenant-Aware Eviction and Residency

Eviction policies must respect tenant boundaries:

- Cold pages are evicted **per-tenant**, not globally.
- Host-to-device migration is scheduled independently for each tenant.
- Residency guarantees (e.g., minimum hot-page retention) are enforced per-tenant.

This prevents one tenant's memory pressure from destabilizing another tenant's execution.

Deterministic Execution Under Concurrency

The ultimate goal is deterministic behavior. Even when:

- multiple tenants run different models,
- memory is fragmented,
- pages are migrating,
- eviction is occurring, and
- compute is fully saturated,

each tenant's KV-cache remains stable, isolated, and semantically correct. Hardware-enforced page mapping ensures that memory elasticity does not compromise correctness or security.

Multi-tenant AI cache protection is the final pillar of memory elasticity. It ensures that dynamic defragmentation, virtual paging, and latency-masked eviction can operate continuously without risking cross-tenant interference. By enforcing strict hardware boundaries around page domains, accelerators maintain deterministic transformer execution even under high concurrency, long-context workloads, and multi-model deployments. This protection is essential for modern AI systems, where shared accelerators must deliver both high performance and strong isolation guarantees.

Dynamic AI memory defragmentation and PagedAttention retention policies establish the memory-elastic foundation required for stable transformer execution under continuous batching, long-context workloads, and multi-tenant operation. As KV-cache footprints evolve unpredictably, accelerators must reorganize memory in real time to preserve contiguity, locality, and Tensor Core intensity. Virtual memory paging provides the abstraction layer that allows scattered access patterns to remain efficient even when physical memory is fragmented. AI-specific eviction policies ensure that cold pages migrate to host memory without stalling compute, masking host-device latency behind ongoing kernel execution. Hardware-enforced page mapping protects multi-tenant deployments, guaranteeing that dynamic compaction, migration, and eviction never violate isolation boundaries. Together, these mechanisms transform accelerator memory from a static allocation space into an adaptive, resilient substrate capable of sustaining large-context transformer workloads with deterministic performance and strong isolation guarantees.

With memory elasticity firmly established inside each accelerator, the next architectural challenge emerges when transformer workloads extend beyond a single device or node. As AI systems increasingly operate across distributed clusters, edge devices, and federated networks, KV-cache residency, eviction behavior, and attention-window continuity must be preserved across heterogeneous environments. Local cache eviction becomes a distributed decision shaped by asymmetric compute, bandwidth, and latency conditions. Federated asymmetric

protocols provide the coordination layer that enables decentralized transformers to exchange context, migrate cache segments, and maintain semantic continuity without relying on centralized orchestration. The next topic explores how these protocols unify memory elasticity with distributed execution, enabling transformers to operate coherently across diverse, multi-node, and multi-region environments.

e. Decentralized AI Execution, Local Cache Eviction, and Federated Asymmetric Protocols

Decentralized AI execution extends transformer workloads beyond centralized clusters, enabling inference and training across heterogeneous devices, edge nodes, regional compute hubs, and federated networks. In these environments, nodes differ dramatically in compute capability, memory footprint, bandwidth availability, and reliability. Transformer execution must adapt to these asymmetries while preserving KV-cache continuity, gradient consistency, and semantic correctness. Local cache eviction becomes a distributed decision shaped by device constraints, and communication protocols must tolerate node dropout, intermittent connectivity, and non-uniform topologies. Federated asymmetric protocols provide the coordination substrate that allows decentralized transformers to operate coherently without relying on a single orchestrator.

The four mechanisms below define this decentralized execution substrate.

- **Asymmetric AI Communication Graphs with Local Reduction Layers -** Decentralized AI systems operate across nodes with widely varying capabilities. Some nodes—regional servers, GPU clusters—can perform full Tensor Core reductions. Others—mobile devices, embedded sensors—can only perform lightweight preprocessing. Asymmetric communication graphs adapt to these differences by introducing **local reduction layers**, which act as intermediate aggregation points. Key characteristics include:
    - **Local reduction layers** summarize or partially aggregate gradients, KV-cache updates, or routing metadata before forwarding them upstream.
    - **Hierarchical communication** reduces bandwidth consumption by performing small reductions locally and larger reductions regionally.
    - **Topology-aware routing** ensures that nodes communicate with neighbors that match their bandwidth and compute profile.

  Transformer workloads generate large tensors—gradients, KV-cache segments, attention metadata—that cannot be transmitted raw from low-power nodes. Local reduction layers compress and summarize these tensors, enabling decentralized transformers to operate efficiently across asymmetric environments.

- **Client-Side AI Cache Eviction Under Constrained Memory Footprints -** Edge devices and lightweight clients often have extremely limited memory, making full KV-cache residency impossible. Client-side eviction policies determine which KV-cache segments remain local and which must be offloaded, compressed, or discarded. Key characteristics include:
    - **Sliding-window eviction** retains only the most recent context.
    - **Relevance-based eviction** drops KV-cache segments that contribute little to current attention.
    - **Semantic-aware eviction** preserves tokens with high contextual importance.
    - **Upstream fallback** allows evicted segments to be reconstructed or fetched from regional nodes when needed.

  Transformer inference on mobile or embedded devices requires selective retention. Only the most impactful segments of the KV-cache can remain resident. Eviction becomes a dynamic, context-aware process that balances memory constraints with semantic continuity.
- **Secure AI Gradient Quantization with Accelerator-Level Encryption -** Decentralized AI execution often spans untrusted networks—consumer devices, cross-organization federated learning, or multi-tenant edge deployments. Gradients, KV-cache segments, and routing metadata must be transmitted securely. Key characteristics include:
    - **Gradient quantization** reduces bandwidth by compressing gradient values.
    - **Accelerator-level encryption** ensures confidentiality and integrity before data leaves the device.
    - **Compatibility with hierarchical reduction** allows encrypted, quantized gradients to be aggregated across nodes.
    - **Low overhead** ensures that encryption does not degrade performance on constrained devices.

  Gradients can reveal sensitive information about user data. Encryption must occur directly on the accelerator, before transmission, and must remain compatible with quantization and reduction. This ensures secure, efficient communication across decentralized networks.
- **Fault-Tolerant AI Node Dropout Handling and Dynamic Topology Remapping –**

Decentralized environments experience frequent node dropout due to connectivity loss, device sleep cycles, or hardware variability. Transformer execution must remain stable even when nodes disappear mid-operation. Key characteristics include:

- **Redundant KV-cache replication** ensures that critical context is stored on multiple nodes.
- **Dynamic topology remapping** updates communication graphs to bypass failed nodes.
- **Partial gradient reconstruction** allows missing updates to be approximated or recovered.
- **Asynchronous retry queues** handle delayed or intermittent updates without stalling the system.

Transformer workloads rely on continuous KV-cache access and synchronized gradient propagation. Node dropout must not corrupt model state or break semantic continuity. Dynamic remapping ensures that decentralized transformers remain resilient under unpredictable conditions.

Decentralized AI execution transforms transformer workloads into distributed, fault-tolerant, secure systems capable of operating across heterogeneous devices and federated networks. Asymmetric communication graphs adapt to node capabilities, client-side eviction preserves memory feasibility, secure gradient quantization protects data, and dynamic topology remapping ensures resilience. Together, these mechanisms extend memory elasticity and compute-communication overlap into decentralized environments, enabling transformers to operate coherently across diverse, multi-node, multi-region deployments.

With decentralized execution now fully articulated across asymmetric communication, client-side eviction, secure gradient transmission, and fault-tolerant topology remapping, the next step is to consolidate these mechanisms into a unified architectural view. Decentralized transformer systems must coordinate across heterogeneous devices, constrained memory footprints, and unreliable networks while preserving semantic continuity and operational stability. Table 8.4-C5 organizes these mechanisms into a structured summary, highlighting their AI-specific purpose, operational strategy, and distributed effect. This table serves as the conceptual anchor for understanding how decentralized transformers maintain coherence across federated, multi-node environments.

Table 8.4-C5 presents the core mechanisms that enable decentralized transformer execution across edge devices, regional clusters, and federated networks. Each mechanism addresses a

distinct challenge created by heterogeneous compute capabilities, limited memory, untrusted communication channels, and dynamic node availability. The table is structured to reveal how these mechanisms operate, why they are essential for decentralized AI workloads, and how they collectively maintain stable KV-cache residency, secure gradient propagation, and resilient topology behavior. This organization provides a clear architectural map of how decentralized transformers achieve coherence without relying on centralized orchestration.

Table 8.4-C5 — Mechanisms Enabling Decentralized AI Execution and Federated Asymmetric Coordination

Mechanism	AI-Specific Purpose	Operational Strategy	Distributed / Federated Effect
Asymmetric AI Communication Graphs with Local Reduction Layers	Adapt transformer communication to heterogeneous nodes with uneven compute and bandwidth	Introduce local reduction layers that summarize gradients, KV-cache updates, and routing metadata before forwarding	Reduces bandwidth, stabilizes communication, and enables hierarchical aggregation across edge, regional, and cloud nodes
Client-Side AI Cache Eviction Under Constrained Memory Footprints	Maintain transformer inference on devices with limited memory	Evict low-relevance KV-cache segments using sliding windows, semantic scoring, or relevance heuristics	Preserves semantic continuity while enabling long-context inference on mobile, embedded, and edge devices
Secure AI Gradient Quantization with Accelerator-Level Encryption	Protect sensitive gradient and KV-cache data transmitted across untrusted networks	Quantize gradients to reduce bandwidth; encrypt on-device before transmission; ensure compatibility with hierarchical reduction	Enables secure federated learning and decentralized inference without exposing private user data
Fault-Tolerant AI Node Dropout Handling and	Maintain stable transformer execution despite	Replicate KV-cache segments, remap communication graphs	Ensures resilience, continuity, and correctness in

Mechanism	AI-Specific Purpose	Operational Strategy	Distributed / Federated Effect
Dynamic Topology Remapping	node failures or intermittent connectivity	dynamically, reconstruct partial updates, and use asynchronous retry queues	decentralized transformer workloads

Table 8.4-C5 consolidates the mechanisms that allow transformers to operate coherently across heterogeneous, distributed, and federated environments. Each mechanism addresses a distinct challenge—heterogeneous communication, constrained memory, secure transmission, and node reliability—forming a decentralized execution substrate that preserves semantic continuity and operational stability.

Table 8.4-C5 shows that decentralized AI execution is not a single technique but a coordinated set of mechanisms that stabilize transformer workloads across distributed and federated environments. Asymmetric communication graphs ensure that nodes with different compute and bandwidth capabilities can participate efficiently by introducing local reduction layers that summarize gradients and KV-cache updates before forwarding. Client-side eviction policies allow memory-constrained devices to retain only the most relevant context, enabling long-context inference even on mobile or embedded hardware. Secure gradient quantization with accelerator-level encryption protects sensitive data as it moves across untrusted networks, ensuring confidentiality and integrity in federated learning scenarios. Fault-tolerant node dropout handling and dynamic topology remapping preserve continuity when nodes disappear, rerouting communication and leveraging redundant KV-cache replicas to maintain semantic correctness. Together, these mechanisms form a decentralized execution substrate that allows transformers to operate coherently across heterogeneous, unreliable, and federated environments.

Table 8.4-C5 organizes the mechanisms that enable decentralized transformer execution across heterogeneous, bandwidth-asymmetric, and intermittently connected environments. To complement this structured summary, Figure 8.4-C5 visualizes how these mechanisms operate in practice—showing how local reductions reshape communication graphs, how client-side eviction preserves context under constrained memory, how encrypted gradient quantization secures federated updates, and how dynamic topology remapping maintains continuity during node dropout. This figure translates the table's conceptual architecture into a spatial, operational diagram, illustrating how decentralized transformers coordinate across edge devices, regional servers, and cloud nodes without relying on centralized orchestration.

Figure 8.4-C5 illustrates the operational substrate that enables decentralized and federated transformer workloads to remain coherent across diverse devices and network conditions. Each panel highlights one mechanism—local reduction layers, client-side eviction, secure gradient transmission, and fault-tolerant topology remapping—showing how decentralized systems adapt to asymmetric compute capabilities, limited memory footprints, untrusted networks, and dynamic node availability. Together, these mechanisms form a distributed execution fabric that preserves semantic continuity, KV-cache stability, and gradient integrity even when execution spans edge devices, regional clusters, and cloud environments.

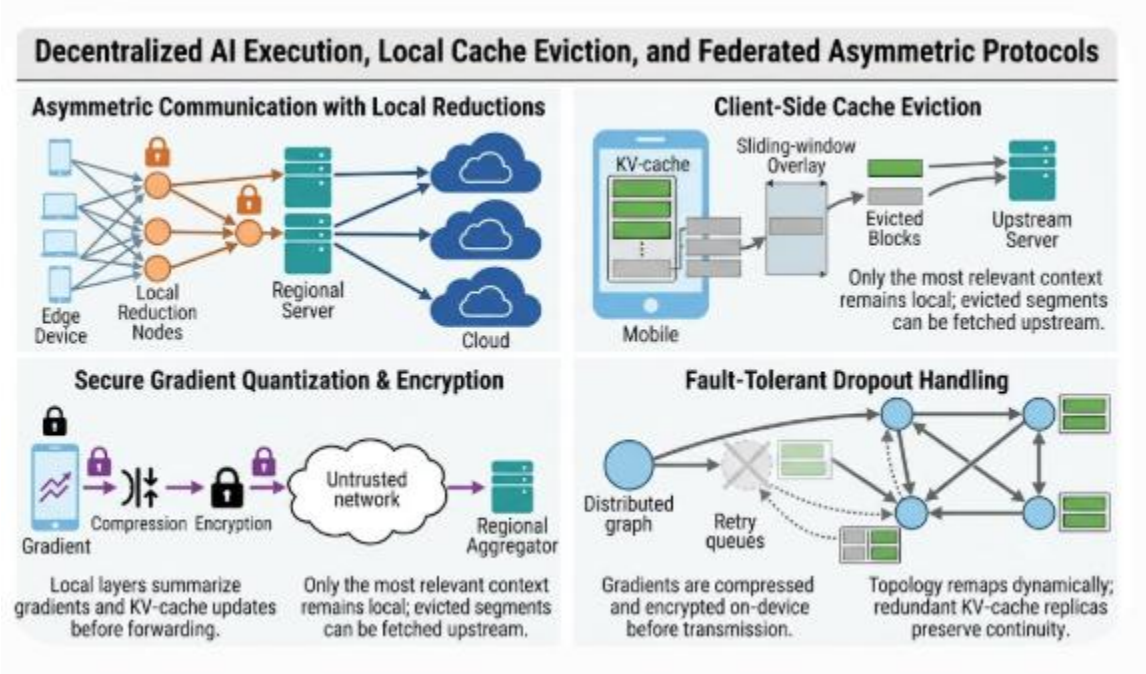


Figure 8.4-C5 — Decentralized AI Execution, Local Cache Eviction, and Federated Asymmetric Protocols

The figure depicts four mechanisms that enable transformers to operate coherently across heterogeneous and federated environments: asymmetric communication with local reduction layers, client-side KV-cache eviction under constrained memory, secure gradient quantization with accelerator-level encryption, and fault-tolerant node dropout handling with dynamic topology remapping. These mechanisms collectively support decentralized transformer execution across edge, regional, and cloud nodes.

Legend

- ***Light-blue devices:*** *Edge nodes*
- ***Teal servers****: Regional compute nodes*
- ***Dark-blue clusters****: Cloud aggregators*

- ***Orange circles**: Local reduction layers*
- ***Green blocks**: Active KV-cache segments*
- ***Gray blocks**: Evicted KV-cache segments*
- ***Purple arrows/blocks**: Encrypted, quantized gradients*
- ***Faded or crossed-out nodes**: Dropout nodes*
- ***Dark-gray lines**: Communication graph links*
- ***Dotted arrows:** Retry queues or delayed updates*

Figure 8.4-C5 demonstrates how decentralized transformer systems maintain coherence across heterogeneous, bandwidth-limited, and intermittently connected environments. The first panel shows asymmetric communication graphs, where local reduction layers summarize gradients and KV-cache updates before forwarding them to regional or cloud nodes, reducing bandwidth and aligning communication with device capabilities. The second panel illustrates client-side eviction, where memory-constrained devices retain only the most relevant KV-cache segments while offloading evicted blocks upstream, enabling long-context inference on mobile or embedded hardware. The third panel highlights secure gradient quantization and encryption, ensuring that compressed updates can traverse untrusted networks without exposing sensitive information. The final panel depicts fault-tolerant dropout handling, where redundant KV-cache replicas and dynamic topology remapping preserve continuity even when nodes disappear mid-operation. Together, these panels show how decentralized transformers achieve resilience, security, and efficiency across federated, multi-node environments.

With Figure 8.4-C5 establishing how decentralized transformer systems coordinate across heterogeneous devices, constrained memory footprints, and unreliable networks, the next step is to examine the first mechanism that enables this distributed coherence: asymmetric communication graphs. In decentralized environments, nodes differ dramatically in compute capability, bandwidth availability, and latency characteristics. Transformers cannot rely on uniform, symmetric communication patterns; instead, they require hierarchical pathways where lightweight edge devices forward summarized updates to more capable regional servers, which in turn propagate refined information to cloud-scale aggregators. This layered communication structure—anchored by local reduction layers—forms the backbone of decentralized AI execution, ensuring that gradients, KV-cache updates, and routing metadata flow efficiently across asymmetric topologies. The following topic explores how these communication graphs are constructed, how they adapt to node heterogeneity, and why they are essential for scalable federated transformer workloads.

i. Asymmetric AI Communication Graphs with Local Reduction Layers

As decentralized transformer workloads expand across heterogeneous devices—edge sensors, mobile clients, regional servers, and cloud-scale clusters—the communication fabric connecting these nodes becomes inherently asymmetric. Nodes differ in compute throughput, memory capacity, bandwidth availability, and latency characteristics. A uniform, symmetric communication model cannot accommodate this diversity. Instead, decentralized AI systems rely on **asymmetric communication graphs**, where data flows through hierarchical pathways tailored to each node's capabilities.

At the core of these graphs are **local reduction layers**—lightweight aggregation points strategically placed near low-power or bandwidth-constrained nodes. These layers perform partial summarization of transformer-generated data before forwarding it upstream. In practice, they reduce the size and complexity of gradients, KV-cache updates, routing metadata, and attention-window signals. This ensures that edge devices never need to transmit raw, high-dimensional tensors directly to regional or cloud nodes.

Transformer workloads generate large, dense tensors at every layer. In centralized environments, these tensors can be transmitted or aggregated directly. But in decentralized environments, edge devices cannot afford such bandwidth. Local reduction layers solve this by performing early aggregation—compressing, summarizing, or partially reducing tensors—so that only essential information moves upward through the hierarchy.

Operational Characteristics

- **Hierarchical aggregation:** Edge devices forward reduced tensors to regional servers, which perform deeper reductions before sending refined updates to cloud nodes.
- **Bandwidth-aware routing:** Communication paths adapt dynamically to available bandwidth, selecting routes that minimize congestion and latency.
- **Compute-aligned summarization:** Reduction layers adjust their summarization strategy based on the compute profile of upstream nodes.
- **Topology-aware coordination:** Nodes communicate with neighbors that match their capabilities, forming a multi-tiered execution graph.

Transformers rely on synchronized gradients, consistent KV-cache propagation, and stable routing metadata. Asymmetric communication graphs ensure these signals remain coherent even when nodes differ dramatically in capability. Local reduction layers prevent bottlenecks, reduce transmission cost, and maintain semantic continuity across the distributed execution fabric.

With asymmetric communication graphs establishing how decentralized transformers coordinate across heterogeneous nodes, the next challenge arises at the edge: memory scarcity. Mobile devices, embedded sensors, and lightweight clients cannot store full KV-cache histories or expanded attention windows. They must decide which segments to retain locally and which to evict or offload upstream. This makes **client-side AI cache eviction** a critical mechanism for enabling long-context transformer inference under constrained memory footprints. The following topic explores how edge devices identify relevant context, preserve semantic continuity, and integrate eviction decisions into the broader federated execution fabric.

ii. Client-Side AI Cache Eviction Under Constrained Memory Footprints

Client-side AI cache eviction is the mechanism that enables transformer inference on devices with extremely limited memory—mobile phones, embedded sensors, wearables, industrial controllers, and lightweight edge nodes. These devices cannot store full KV-cache histories or expanded attention windows, yet decentralized transformer workloads increasingly require long-context reasoning, multi-turn interactions, and semantic continuity. Client-side eviction policies determine which KV-cache segments remain resident locally, which must be offloaded upstream, and which can be safely discarded without degrading model quality.

Transformers rely on KV-cache retention to preserve the memory of past tokens. In centralized environments, this cache can grow indefinitely. But on constrained devices, KV-cache residency must be selective. Eviction becomes a semantic decision: the device must identify which past tokens matter most for future attention and which can be removed without harming inference quality.

Core Operational Principles

- **Sliding-Window Retention -** Devices maintain only the most recent portion of the KV-cache. This ensures predictable memory usage and supports streaming inference, but may lose long-range dependencies unless upstream nodes store the full context.
- **Relevance-Based Eviction -** The device evaluates the contextual importance of each KV-cache segment—based on attention patterns, token semantics, or model-provided relevance scores—and evicts segments with low expected future impact.
- **Semantic-Aware Eviction -** Some tokens carry disproportionate semantic weight: entity names, topic anchors, user instructions, or structural markers. These tokens are retained even when they fall outside the sliding window.
- **Upstream Offloading and Reconstruction -** Evicted segments are not necessarily lost. Devices can:

- offload segments to regional servers for storage,
- request reconstruction when needed, or
- rely on upstream nodes to maintain full-context continuity.

This creates a tiered memory hierarchy where edge devices store only the most critical context, while regional nodes maintain the full KV-cache.

Client-side eviction allows transformers to operate on devices that would otherwise be incapable of long-context inference. It transforms KV-cache management from a static, device-local process into a distributed, federated decision. The device retains only what it can afford, while the broader system ensures continuity through upstream storage, reconstruction, and semantic prioritization.

Client-side eviction is therefore not a degradation—it is an adaptive strategy that enables decentralized transformers to scale across diverse hardware profiles without sacrificing semantic coherence.

With client-side eviction enabling constrained devices to participate in long-context transformer inference, the next challenge arises when these devices must transmit gradients, KV-cache segments, or routing metadata across untrusted networks. Federated learning, decentralized inference, and multi-tenant edge deployments all require secure communication channels that protect sensitive information while minimizing bandwidth usage. This is where **secure AI gradient quantization with accelerator-level encryption** becomes essential. By compressing gradients and encrypting them directly on the device before transmission, decentralized systems ensure confidentiality, integrity, and efficiency across heterogeneous and potentially adversarial environments. The next topic explores how this secure transmission layer integrates with hierarchical reduction, federated coordination, and decentralized execution.

iii. Secure AI Gradient Quantization with Accelerator-Level Encryption

Secure AI gradient quantization with accelerator-level encryption is the communication backbone of decentralized and federated transformer systems. When gradients, KV-cache segments, and routing metadata move across untrusted networks—between edge devices, regional servers, and cloud aggregators—they can expose sensitive information about user data, model behavior, or organizational context. At the same time, these signals are large and bandwidth-intensive. Quantization reduces their size; encryption protects their contents. Performed directly on the accelerator, this combination ensures that decentralized transformers can communicate efficiently and securely without relying on trusted infrastructure.

In federated learning and decentralized inference, transformers are trained or adapted using

data that never leaves the client device. Gradients computed locally encode information about that data. If transmitted in raw form, they can leak private details. Secure gradient quantization and encryption turn these gradients into compact, opaque payloads that can be safely aggregated upstream. The accelerator becomes both the computation engine and the security boundary: gradients are compressed and encrypted before they ever touch the network stack.

Core operational principles

- **Bandwidth-aware gradient quantization** - Gradients are reduced in precision and size to match the bandwidth constraints of edge and regional links. Quantization schemes are chosen to preserve the most important signal—direction and relative magnitude—while discarding redundant detail. This allows low-power devices and congested networks to participate in federated updates without being overwhelmed by tensor volume.
- **On-device encryption as a hard boundary** - Encryption is performed directly on the accelerator or tightly coupled device hardware, not in a distant software layer. This ensures that gradients and KV-cache segments are never exposed in plaintext outside the local execution environment. Keys are managed per device or per tenant, and encryption is integrated into the same pipeline that handles quantization, so security and compression are treated as a single, fused operation.
- **Compatibility with hierarchical reduction and aggregation** - Encrypted, quantized gradients must still be usable in asymmetric communication graphs. Local reduction layers and regional aggregators are designed to operate on these secure payloads—either by decrypting within trusted domains or by using protocols that allow secure aggregation without exposing individual contributions. This preserves the benefits of hierarchical communication while maintaining strong privacy guarantees.
- **Resilience to untrusted and adversarial networks** - Because gradients and KV-cache segments travel across networks that may be monitored, modified, or disrupted, secure transmission must assume adversarial conditions. Encryption protects confidentiality; integrity checks and authenticated protocols ensure that tampering is detectable. This allows decentralized transformers to rely on public or shared infrastructure without compromising model correctness or user privacy.

Without secure gradient quantization and accelerator-level encryption, federated and decentralized transformer systems would either leak sensitive information or be forced to operate only within tightly controlled, trusted networks—undermining their scalability and reach. By compressing and encrypting updates at the source, these systems can safely aggregate learning signals from millions of devices, adapt models to local behavior, and coordinate

KV-cache evolution across nodes. Security becomes a built-in property of the execution fabric, not an afterthought layered on top.

With secure gradient quantization and accelerator-level encryption establishing a trusted, bandwidth-efficient communication layer for decentralized transformers, the next challenge is dealing with the inherent instability of distributed environments. Edge devices go offline, regional nodes experience failures, and network partitions disrupt communication paths. Gradients may arrive late or not at all; KV-cache replicas may become unreachable. To keep transformer workloads coherent under these conditions, decentralized systems need robust mechanisms for handling node dropout and dynamically remapping their communication topology. The next topic—fault-tolerant AI node dropout handling and dynamic topology remapping—explores how redundant KV-cache storage, adaptive routing, and resilient aggregation strategies ensure that decentralized transformers continue to operate correctly even as the underlying network and node set change over time.

iv. Fault-Tolerant AI Node Dropout Handling and Dynamic Topology Remapping

Fault-tolerant AI node dropout handling and dynamic topology remapping are what keep decentralized transformer systems from tearing at the seams when the real world behaves like the real world—devices go offline, networks flap, regional clusters reboot, and edge nodes quietly disappear mid-interaction. In a centralized setting, a single failure can be catastrophic; in a decentralized, federated environment, failure is the norm. The architecture has to assume that nodes will vanish, reappear, and degrade unpredictably, while transformers still need consistent KV-cache access, stable gradient aggregation, and coherent routing behavior. This mechanism is about making the execution fabric self-healing.

- **Treating node dropout as a first-class event -** In a fault-tolerant decentralized system, node dropout is not an exception; it is a modeled, expected event. The system continuously tracks node liveness—heartbeats, health checks, latency thresholds—and classifies nodes as active, degraded, or offline. When a node crosses into dropout territory, the system does not panic; it triggers a set of predefined responses:
    - **Graceful degradation:** Reduce reliance on the node before it fully disappears, shifting load away as health metrics worsen.
    - **Fast detection:** Use tight liveness intervals so that dropout is detected quickly enough to avoid long periods of silent failure.
    - **Clear state transitions:** Move nodes through well-defined states (active → suspect → offline) so other components can react deterministically.

This framing ensures that dropout is handled as part of normal operation, not as an emergency.

- **Redundant KV-cache replicas and context survivability -** Transformers depend heavily on KV-cache continuity. If a node holding critical KV-cache segments disappears, the model's "memory" for that part of the workload can vanish with it. To prevent this, decentralized systems replicate KV-cache segments across multiple nodes:
    - **Primary and secondary holders:** Each important KV-cache segment is stored on at least two nodes, often in nearby regions or within the same logical cluster.
    - **Replica placement aware of latency:** Replicas are placed where they can be accessed quickly if the primary fails, minimizing disruption to attention windows.
    - **Replica refresh policies:** Updates to KV-cache are propagated to replicas with policies that balance freshness and bandwidth cost.

  When a node drops out, the system promotes a replica holder to primary, ensuring that the context remains available and attention computations can continue without semantic gaps.
- **Dynamic topology remapping as a continuous process -** The communication graph that connects edge devices, reduction layers, regional servers, and cloud aggregators is not static. Dynamic topology remapping continuously adjusts this graph in response to node health, bandwidth changes, and workload shifts:
    - **Rerouting around failed nodes:** When a node goes offline, its neighbors rewire their communication paths to bypass it, connecting to alternative reduction layers or aggregators.
    - **Load-aware remapping:** Remapping decisions consider current load, avoiding overloading healthy nodes that are already saturated.
    - **Local and global views:** Edge nodes may only see a local slice of the topology, while regional controllers maintain a broader view and coordinate larger-scale remaps.

  This makes the network behave like a living system—always reshaping itself to maintain connectivity and performance.
- **Resilient gradient and update aggregation -** Node dropout affects more than KV-cache; it disrupts gradient flows and model updates. Fault-tolerant systems design aggregation

to be resilient:

- **Partial aggregation tolerance:** Aggregators can proceed with updates even if some nodes fail to report, using the contributions they have rather than blocking on missing ones.
- **Late arrival handling:** Gradients or updates that arrive after a cutoff can be incorporated into future rounds or used for auxiliary adaptation, rather than discarded blindly.
- **Weighted participation:** Nodes with intermittent connectivity may be given lower weight in aggregation, reducing the impact of their sporadic contributions while still benefiting from their data.

This ensures that learning continues even when participation is uneven.

- **Asynchronous retry and reconciliation -** Not all failures are permanent. Networks partition and heal; devices sleep and wake. Fault-tolerant dropout handling includes mechanisms for retry and reconciliation:
  - **Retry queues:** Failed transmissions—gradients, KV-cache updates, routing metadata—are queued for retry when connectivity improves.
  - **Versioned state:** KV-cache segments and model parameters carry versioning so that late or retried updates can be reconciled without corrupting state.
  - **Conflict resolution policies:** When conflicting updates arise from divergent histories, the system applies clear rules—latest-wins, priority-based, or merge strategies—to restore consistency.

  This allows decentralized transformers to absorb temporary chaos and converge back to a coherent state.

Without robust dropout handling and topology remapping, decentralized transformer systems would be brittle—every offline device, every flaky link, every regional outage would risk breaking attention continuity, corrupting gradients, or stalling inference. Fault tolerance turns the environment's instability into something the system can live with. KV-cache replicas preserve memory, dynamic remapping preserves communication, resilient aggregation preserves learning, and asynchronous reconciliation preserves long-term coherence. The result is a transformer fabric that can stretch across edge, regional, and cloud domains without tearing when nodes inevitably fail or drift.

Decentralized AI execution transforms transformer workloads from single-cluster systems into

resilient, multi-tier networks capable of operating across edge devices, regional servers, and cloud-scale aggregators. The mechanisms explored—asymmetric communication graphs, client-side cache eviction, secure gradient quantization, and fault-tolerant topology remapping—collectively establish a distributed execution fabric that can withstand bandwidth asymmetry, memory scarcity, untrusted communication channels, and unpredictable node availability. Local reduction layers reshape communication patterns so that low-power devices can participate without being overwhelmed. Client-side eviction enables long-context inference on constrained hardware by retaining only the most semantically relevant KV-cache segments. Accelerator-level encryption ensures that gradients and routing metadata remain confidential and tamper-proof as they traverse federated networks. Dynamic topology remapping and dropout handling preserve continuity even when nodes disappear mid-operation, allowing transformers to maintain coherent attention windows, stable gradient flows, and consistent routing behavior.

Together, these mechanisms redefine transformer execution as a distributed, fault-tolerant, privacy-preserving system capable of scaling across heterogeneous environments. Decentralized AI becomes not merely a deployment strategy but an architectural principle—one that enables transformers to operate fluidly across diverse hardware profiles, network conditions, and organizational boundaries while preserving semantic integrity and operational stability.

Software paradigms in AI systems define the operational logic that governs how models coordinate computation, manage memory, and interact with distributed infrastructure. Throughout this part of the work, the focus moves from rigid, monolithic execution styles toward adaptive, concurrency-driven, and context-aware approaches that reflect the demands of modern transformer workloads. Event-driven orchestration, memory-elastic runtimes, asynchronous compute-communication overlap, and federated coordination frameworks collectively reshape how AI systems behave under load and across heterogeneous hardware. These paradigms form the connective substrate that enables long-context reasoning, decentralized inference, secure gradient propagation, and resilient distributed execution. In effect, they bind model behavior, hardware capabilities, and system dynamics into a coherent operational fabric—allowing AI systems to remain efficient, stable, and semantically consistent across diverse deployment environments.

With the software paradigms now established—clarifying how AI systems schedule computation, preserve memory continuity, and coordinate across distributed environments—the architectural lens shifts from internal execution logic to external perception. Modern AI systems increasingly rely on multimodal sensor pipelines that capture, filter, and fuse real-world signals before they reach a model's attention window. These pipelines transform raw sensory

input into structured representations that downstream runtimes can interpret and integrate. As AI systems expand into robotics, autonomous platforms, industrial automation, and real-time decision domains, sensor pipelines become the foundation for grounded reasoning and situational awareness. The next part of the work explores how these pipelines are constructed, how they interface with AI runtimes, and how they enable models to operate not merely as computational engines but as perceptual systems embedded within dynamic physical and digital environments.

D. Sensor Pipelines in AI Systems

Sensor pipelines define the perceptual behavior of autonomous AI systems beneath the model's reasoning substrate. They determine how raw physical signals enter the computational fabric, how multimodal streams synchronize before fusion, how high-bandwidth inputs avoid starvation, and how event-driven neuromorphic data is transformed into embeddings suitable for transformer attention. In hardware–software co-design, sensor pipelines are not passive ingestion paths; they are active, latency-critical subsystems whose DMA engines, preprocessing blocks, synchronization barriers, and neuromorphic interfaces directly shape how effectively intelligence can perceive and react to the external world. Every sensor pipeline—zero-copy ingestion path, on-chip preprocessing engine, multimodal fusion barrier, high-bandwidth decoder, or event-slicing mechanism—propagates through the autonomy stack and governs how reliably models interpret real-world conditions.

Modern AI systems operate in environments where naïve sensor ingestion, CPU-bound preprocessing, and loosely synchronized modalities are no longer viable. Autonomous platforms must process high-resolution video, dense LiDAR sweeps, multi-channel audio, inertial bursts, and neuromorphic event streams within strict latency budgets and unpredictable physical dynamics. As a result, sensor pipelines increasingly incorporate hardware-aligned design principles that eliminate redundant memory movement, bypass traditional image signal processors, fuse modalities at sub-nanosecond precision, stream frames directly from NVMe fabrics, and convert sparse event bursts into asynchronous embeddings. These principles ensure that perception is not only high-fidelity but also operationally sustainable across heterogeneous accelerators, multi-sensor arrays, and real-time autonomy loops.

- **AI Zero-Copy I/O, Direct Memory Access (DMA) Ingestion Paths, and Shared Host-Accelerator Buses -** Zero-copy ingestion transforms sensor input from a CPU-mediated workflow into a direct accelerator-aligned data path. By routing frames, point clouds, and audio buffers through DMA engines and shared host-accelerator buses, sensor data lands directly in accelerator-accessible memory without intermediate

copies. This eliminates latency spikes, reduces PCIe congestion, and ensures that high-bandwidth sensors—4K cameras, radar arrays, depth sensors—can feed transformer pipelines continuously. Zero-copy paths allow perception workloads to operate at full sensor rate while maintaining deterministic timing across heterogeneous compute fabrics.

- **On-Chip AI Preprocessing Engines with DALI and ISP-Bypass Pipelines -** On-chip preprocessing engines shift early transformations—resize, normalize, denoise, color-space conversion—onto dedicated hardware blocks tightly coupled with the accelerator. DALI-style pipelines and ISP-bypass paths remove the dependency on traditional CPU-bound image signal processors, enabling raw sensor data to be prepared directly within the accelerator's memory hierarchy. This reduces preprocessing latency, avoids bandwidth-heavy round-trips, and ensures that multimodal inputs arrive in a format optimized for transformer attention. Hardware-aligned preprocessing allows autonomous systems to maintain responsiveness even under heavy sensor load.

- **Multi-Modal AI Sensor Synchronization with Sub-Nanosecond Fusion Barriers -** Multimodal perception requires precise temporal alignment across sensors with different sampling rates and physical characteristics. Sub-nanosecond fusion barriers synchronize video frames, LiDAR sweeps, IMU bursts, radar returns, and audio packets before they enter multimodal attention layers. These barriers prevent temporal drift, ensure consistent spatial-temporal alignment, and maintain semantic coherence across modalities. High-precision synchronization is essential for grounded reasoning, enabling models to interpret the world as a unified, temporally consistent scene rather than a collection of misaligned signals.

- **High-Bandwidth AI Frame Decoding with Direct NVMe Streaming and Pipeline Starvation Control -** High-bandwidth decoding engines support continuous ingestion of large video or sensor streams without stalls. Direct NVMe streaming bypasses traditional file I/O paths, allowing frames to flow from storage into accelerator memory with minimal overhead. Pipeline starvation control monitors buffer levels, decoding throughput, and accelerator load to prevent inference stalls caused by uneven frame arrival. These mechanisms ensure that perception pipelines remain stable under extreme throughput demands—high-FPS video, multi-camera rigs, or dense sensor arrays—while maintaining deterministic latency for downstream transformer inference.

- **Neuromorphic AI Event Slicing, Asynchronous Embedding, and Edge-Sensor**

Interception - Neuromorphic sensors produce sparse, event-driven data rather than continuous frames. Event slicing mechanisms segment these micro-events into meaningful temporal windows, while asynchronous embedding engines convert them into representations suitable for transformer attention. Edge-sensor interception allows early filtering and compression directly at the sensor, reducing bandwidth and latency for event-driven workloads. These mechanisms enable AI systems to react to micro-scale changes—motion edges, brightness spikes, tactile impulses—with minimal delay and power consumption, supporting ultra-responsive perception in dynamic environments.

Together, these sensor pipeline paradigms illustrate how AI systems have evolved into tightly integrated perceptual-computational ecosystems. Intelligence in autonomous systems is shaped not only by model architecture but by how effectively sensor pipelines deliver synchronized, high-fidelity, and latency-bounded input to the underlying accelerators. These paradigms enable modern AI systems to achieve grounded perception, real-time responsiveness, and scalable multimodal fusion through deliberate co-design across the entire autonomy stack.

With the foundations of sensor-pipeline architecture now established—from zero-copy ingestion and on-chip preprocessing to multimodal synchronization, high-bandwidth decoding, and neuromorphic event handling—the next step is to consolidate these mechanisms into a structured operational view. Modern AI systems depend on sensor pipelines that behave as tightly integrated, hardware-aligned subsystems capable of delivering synchronized, high-fidelity input under strict latency budgets. Table 8.4-D organizes these mechanisms into a unified framework, highlighting their AI-specific purpose, operational strategy, and perceptual effect. This table serves as the architectural anchor for understanding how sensor pipelines transform raw physical signals into accelerator-ready representations that support real-time autonomous intelligence.

Table 8.4-D presents the core mechanisms that enable high-fidelity, low-latency sensor pipelines across autonomous AI systems. Each mechanism addresses a distinct perceptual challenge: eliminating redundant memory movement, shifting preprocessing onto accelerator-adjacent hardware, synchronizing heterogeneous modalities at sub-nanosecond precision, sustaining high-bandwidth frame decoding without starvation, and converting sparse neuromorphic events into asynchronous embeddings. The table is structured to reveal how these mechanisms operate, why they are essential for grounded perception, and how they collectively maintain temporal coherence, throughput stability, and semantic fidelity across diverse sensor environments. This organization provides a clear architectural map of how sensor pipelines

interface with accelerators, runtimes, and multimodal fusion engines.

Table 8.4-D — Mechanisms Enabling High-Fidelity, Low-Latency Sensor Pipelines in AI Systems

Mechanism	AI-Specific Purpose	Operational Strategy	Perceptual / System-Level Effect
AI Zero-Copy I/O, DMA Ingestion Paths, and Shared Host-Accelerator Buses	Eliminate CPU-mediated data movement and reduce ingestion latency	Route sensor data directly into accelerator-accessible buffers via DMA engines and unified host-accelerator buses	Enables continuous high-bandwidth sensor streaming without stalls or PCIe congestion
On-Chip AI Preprocessing Engines with DALI and ISP-Bypass Pipelines	Shift early transformations into hardware blocks tightly coupled with accelerators	Perform resize, normalize, denoise, and color-space conversion directly on-chip, bypassing traditional ISPs	Reduces preprocessing latency and ensures sensor data arrives in model-ready format
Multi-Modal AI Sensor Synchronization with Sub-Nanosecond Fusion Barriers	Align heterogeneous sensor modalities before multimodal fusion	Use hardware-timed fusion barriers to synchronize video, LiDAR, radar, IMU, and audio streams	Preserves temporal coherence and prevents drift across multimodal attention layers
High-Bandwidth AI Frame Decoding with Direct NVMe Streaming and Pipeline Starvation Control	Maintain continuous ingestion of large video or sensor streams	Stream frames directly from NVMe fabrics into accelerator memory; monitor buffer levels to prevent starvation	Supports real-time perception under extreme throughput demands
Neuromorphic AI Event Slicing, Asynchronous Embedding, and Edge-Sensor Interception	Convert sparse, event-driven sensor bursts into transformer-ready embeddings	Slice micro-events into temporal windows; embed asynchronously; filter at the sensor edge	Enables ultra-low-latency, power-efficient perception in dynamic environments

Table 8.4-D consolidates the mechanisms that allow modern AI systems to ingest, synchronize, preprocess, and fuse sensor data at high fidelity and low latency. Each mechanism addresses a distinct perceptual challenge—bandwidth, preprocessing overhead, temporal alignment, decoding throughput, and event-driven sparsity—forming a sensor pipeline architecture capable of supporting real-time autonomous intelligence.

Table 8.4-D shows that high-performance sensor pipelines are not defined by a single optimization but by a coordinated set of mechanisms that stabilize perception under real-world constraints. Zero-copy I/O and DMA ingestion paths eliminate CPU bottlenecks, allowing raw sensor data to flow directly into accelerator-accessible memory with deterministic timing. On-chip preprocessing engines ensure that early transformations occur within the accelerator's memory hierarchy, reducing latency and preventing bandwidth-heavy round-trips. Sub-nanosecond fusion barriers synchronize heterogeneous modalities—video, LiDAR, radar, IMU, audio—so that multimodal attention layers receive temporally aligned inputs. Direct NVMe streaming and starvation control maintain continuous frame ingestion even under extreme throughput demands, preventing inference stalls. Neuromorphic event slicing and asynchronous embedding convert sparse, high-frequency micro-events into transformer-ready representations, enabling ultra-responsive perception in dynamic environments.

Together, these mechanisms form a sensor-pipeline substrate that allows AI systems to perceive the world with precision, stability, and real-time responsiveness. They ensure that transformers and multimodal models do not merely compute—they interpret, fuse, and react to high-bandwidth, heterogeneous sensory input with architectural coherence across the entire autonomy stack.

Table 8.4-D organizes the mechanisms that enable high-fidelity, low-latency sensor pipelines across autonomous AI systems, showing how ingestion, preprocessing, synchronization, decoding, and event-driven processing each contribute to perceptual stability. To complement this structured view, Figure 4.10-109 visualizes how these mechanisms operate within a unified pipeline. It illustrates how raw sensor data moves through zero-copy DMA paths, how on-chip preprocessing prepares frames for accelerator consumption, how multimodal streams synchronize at sub-nanosecond precision, how high-bandwidth decoding avoids starvation, and how neuromorphic events are sliced and embedded asynchronously. This figure translates the table's conceptual architecture into a spatial, operational diagram that reveals how sensor pipelines deliver synchronized, accelerator-ready input for real-time transformer inference.

Figure 8.4-D depicts the perceptual substrate that enables autonomous AI systems to ingest, transform, synchronize, and fuse sensor data under strict latency and bandwidth constraints. Each panel highlights a critical mechanism—zero-copy ingestion, on-chip preprocessing,

multimodal synchronization, high-bandwidth decoding, and neuromorphic event processing—showing how sensor pipelines interface directly with accelerators and multimodal fusion engines. Together, these mechanisms form a hardware-aligned perceptual fabric that ensures sensor data arrives in a coherent, temporally aligned, and model-ready form, enabling transformers to operate reliably in dynamic real-world environments.

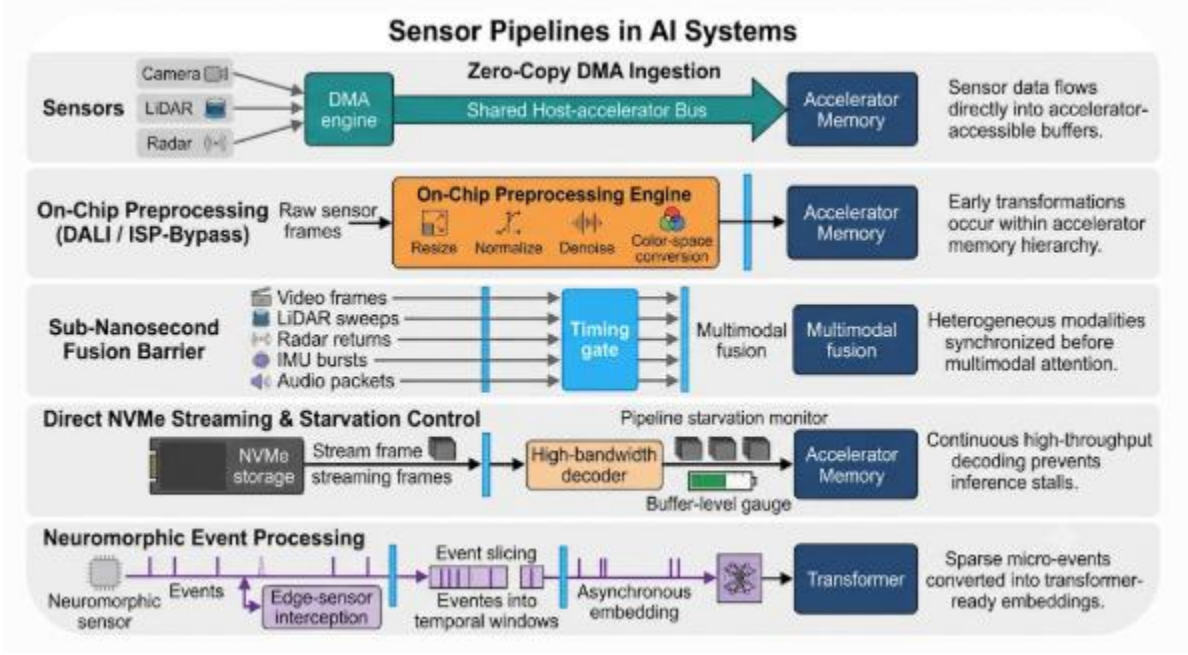


Figure 8.4-D — Sensor Pipelines in AI Systems

The figure illustrates the five core mechanisms that enable high-fidelity, low-latency perception in autonomous AI systems: zero-copy DMA ingestion, on-chip preprocessing, sub-nanosecond multimodal synchronization, direct NVMe streaming with starvation control, and neuromorphic event slicing with asynchronous embedding. These mechanisms collectively ensure that diverse sensor modalities deliver synchronized, accelerator-ready data for real-time transformer inference.

Legend

- ***Gray sensor icons**: Camera, LiDAR, radar, IMU, audio, neuromorphic sensors*
- ***Teal blocks**: DMA engines, shared host-accelerator buses*
- ***Orange blocks**: On-chip preprocessing engines (DALI, ISP-bypass)*
- ***Blue timing gate**: Sub-nanosecond fusion barrier*
- ***Dark gray storage block**: NVMe streaming source*
- ***Green gauge**: Pipeline starvation monitor*
- ***Purple pulses**: Neuromorphic event bursts*
- ***Dark blue blocks**: Accelerator memory and transformer-ready embeddings*
- ***Black arrows**: Data flow direction*

- ***Thin blue lines****: Temporal alignment indicators*

Figure 8.4-D demonstrates how modern AI systems transform raw sensor input into structured, synchronized, and accelerator-ready representations. The first panel shows zero-copy ingestion, where DMA engines route sensor data directly into accelerator memory, eliminating CPU bottlenecks and ensuring deterministic latency. The second panel illustrates on-chip preprocessing, where early transformations—resize, normalize, denoise, color-space conversion—occur within the accelerator's memory hierarchy, reducing overhead and preparing data for downstream fusion. The third panel highlights sub-nanosecond multimodal synchronization, aligning video frames, LiDAR sweeps, radar returns, IMU bursts, and audio packets before they enter multimodal attention layers. The fourth panel depicts high-bandwidth decoding, where NVMe streaming and starvation control maintain continuous frame ingestion under extreme throughput demands. The final panel shows neuromorphic event processing, where sparse micro-events are sliced into temporal windows, embedded asynchronously, and intercepted at the sensor edge to minimize latency and bandwidth.

Together, these panels reveal a sensor pipeline architecture designed for real-time autonomous intelligence—one that ensures perception remains stable, synchronized, and high-fidelity even under dynamic environmental and computational conditions.

With the perceptual substrate now mapped across both the conceptual structure of Table 8.4-D and the operational flow of Figure 8.4-D, the next step is to examine each mechanism in detail, beginning at the very front of the pipeline: ingestion. Autonomous AI systems cannot afford the latency, bandwidth waste, or CPU contention introduced by traditional sensor I/O paths. High-resolution video, dense LiDAR sweeps, radar returns, and multimodal bursts must enter the computational fabric without detours, copies, or software-mediated bottlenecks. This makes zero-copy ingestion and DMA-driven data movement the foundational layer of modern sensor pipelines. Item **a** explores how direct host-accelerator buses, DMA engines, and zero-copy memory paths eliminate redundant transfers and establish the high-throughput, low-latency ingress required for real-time perception.

a. AI Zero-Copy I/O, Direct Memory Access (DMA) Ingestion Paths, and Shared Host-Accelerator Buses

Zero-copy ingestion is the foundational layer of modern AI sensor pipelines. Autonomous systems cannot afford CPU-mediated data movement, redundant buffer copies, or unpredictable PCIe stalls when ingesting high-resolution video, dense LiDAR sweeps, radar returns, IMU bursts, or neuromorphic event streams. Zero-copy I/O ensures that sensor data flows directly into accelerator-accessible memory through DMA engines and unified

host-accelerator buses, eliminating latency spikes and maximizing throughput. This architecture transforms ingestion from a software-bound bottleneck into a hardware-aligned, deterministic data path that supports real-time perception.

Zero-copy ingestion is not a single mechanism—it is a coordinated set of hardware and memory-management strategies. PCIe-level contention control stabilizes bus behavior under heavy sensor load. DMA scheduler optimization eliminates host-buffer mirroring and ensures that transfers occur with minimal overhead. Unified virtual memory allocation allows heterogeneous accelerators to share ingestion buffers without fragmentation. Memory-mapped input streams provide continuous sensor ingestion without repeated allocation or copy operations. Together, these mechanisms create a high-bandwidth, low-latency ingress fabric that feeds downstream preprocessing, synchronization, and multimodal fusion engines.

- **PCIe-Level AI Bus Contention Control and Direct Accelerator-to-Storage Ingest -** High-bandwidth sensors and NVMe storage compete for PCIe lanes. Without contention control, bursts of sensor traffic can starve accelerators or cause unpredictable latency spikes. AI-specific PCIe arbitration policies prioritize DMA transfers that feed perception pipelines, ensuring deterministic timing even under load. Direct accelerator-to-storage ingest bypasses the CPU entirely, allowing accelerators to pull frames or point clouds directly from NVMe fabrics. This reduces round-trip latency and stabilizes ingestion during high-FPS or multi-camera workloads.
- **AI DMA Scheduler Optimization with Host-Buffer Mirroring Elimination -** Traditional DMA workflows mirror buffers in host memory before transferring them to accelerators. This wastes bandwidth and introduces latency. AI-optimized DMA schedulers eliminate host-buffer mirroring by allocating accelerator-accessible buffers at ingest time. DMA engines write sensor data directly into these buffers, reducing memory pressure and avoiding CPU involvement. Scheduler heuristics prioritize transfers based on sensor modality, frame rate, and downstream pipeline load, ensuring continuous ingestion without stalls.
- **Unified AI Virtual Memory Allocation Across Heterogeneous Accelerators -** Autonomous systems often use heterogeneous accelerators—GPUs, NPUs, DSPs, vision processors, and neuromorphic cores. Unified virtual memory allocation allows all accelerators to access ingestion buffers without copying or remapping. This prevents fragmentation, reduces allocation overhead, and ensures that multimodal pipelines can share sensor data efficiently. Unified memory also enables cross-accelerator fusion, where different modalities are processed by different hardware blocks but share a common ingestion substrate.

- **Memory-Mapped AI Input Streams for Continuous Sensor Ingestion -** Memory-mapped input streams allow sensors to write directly into pre-allocated regions of virtual memory. This eliminates repeated allocation, reduces jitter, and ensures continuous ingestion even under fluctuating sensor rates. Memory-mapped streams are essential for neuromorphic sensors, which emit sparse, high-frequency events that must be captured without latency. They also stabilize video ingestion by providing a deterministic buffer layout for high-bandwidth decoders.

With the foundations of zero-copy ingestion now established—direct DMA paths, unified host-accelerator buses, PCIe arbitration, and memory-mapped sensor streams—the next step is to organize these mechanisms into a structured operational view. Autonomous AI systems depend on ingestion pipelines that behave as deterministic, hardware-aligned subsystems capable of sustaining high-bandwidth sensor input without CPU mediation or unpredictable latency spikes. Table 8.4-D1 consolidates the four core mechanisms that make this possible, showing how PCIe-level contention control, DMA scheduler optimization, unified virtual memory, and memory-mapped input streams collectively eliminate bottlenecks and stabilize real-time perception. This table provides the architectural anchor for understanding how zero-copy ingestion forms the first stage of the sensor pipeline and enables downstream preprocessing, synchronization, and multimodal fusion.

Table 8.4-D1 presents the essential mechanisms that allow autonomous AI systems to ingest sensor data at high bandwidth and low latency. Each mechanism addresses a specific challenge inherent to real-time perception: PCIe congestion, redundant host-buffer mirroring, fragmented memory across heterogeneous accelerators, and jitter introduced by repeated allocation or copy operations. The table is structured to reveal how these mechanisms operate, why they are necessary for modern multimodal workloads, and how they collectively transform ingestion from a software-bound bottleneck into a hardware-aligned, deterministic data path. This organized view clarifies how zero-copy ingestion underpins the entire sensor pipeline, ensuring that accelerators receive raw sensor data in a stable, predictable, and immediately usable form.

Table 8.4-D1 — Zero-Copy Ingestion Mechanisms for Autonomous AI Systems

Mechanism	AI-Specific Purpose	Operational Strategy	System-Level Effect
PCIe-Level Bus Contention Control & Direct	Stabilize PCIe behavior under	Prioritize DMA transfers; allow accelerators to pull	Deterministic latency, reduced round-trip overhead, stable

Mechanism	AI-Specific Purpose	Operational Strategy	System-Level Effect
Accelerator-to-Storage Ingest	heavy sensor and NVMe load	frames and point clouds directly from NVMe	ingestion at high FPS
DMA Scheduler Optimization & Host-Buffer Mirroring Elimination	Remove redundant CPU-mediated copies and reduce bandwidth waste	Allocate accelerator-accessible buffers; schedule DMA transfers by modality, frame rate, and pipeline load	Continuous ingestion without stalls, lower memory pressure, predictable throughput
Unified Virtual Memory Allocation Across Heterogeneous Accelerators	Enable shared ingestion buffers across GPUs, NPUs, DSPs, and vision processors	Provide a unified virtual address space accessible to all accelerators	Reduced fragmentation, efficient multimodal fusion, simplified buffer management
Memory-Mapped Input Streams for Continuous Sensor Ingestion	Support uninterrupted high-frequency sensor input	Map sensor streams directly into pre-allocated virtual memory regions	Stable ingestion for video, LiDAR, radar, IMU, and neuromorphic events; minimized jitter

Table 8.4-D1 consolidates the mechanisms that make zero-copy ingestion viable in autonomous AI systems. Each mechanism eliminates latency, reduces bandwidth waste, and stabilizes sensor input under real-world conditions, forming the ingestion substrate for downstream preprocessing, synchronization, and multimodal fusion.

Table 8.4-D1 shows that zero-copy ingestion is not a single optimization but a coordinated set of hardware-aware mechanisms that stabilize sensor input under real-world conditions. PCIe-level contention control ensures that bursts of video frames, LiDAR sweeps, or NVMe reads do not starve accelerators, preserving deterministic latency even under heavy load. DMA scheduler optimization eliminates host-buffer mirroring, allowing sensor data to be written directly into accelerator-accessible buffers without CPU involvement. Unified virtual memory allocation ensures that heterogeneous accelerators—GPUs, NPUs, DSPs, and vision processors—can share

ingestion buffers without fragmentation or remapping overhead. Memory-mapped input streams provide continuous, jitter-free ingestion for high-frequency sensors, including neuromorphic devices that emit sparse event bursts.

Together, these mechanisms form a zero-copy ingestion substrate that allows autonomous AI systems to operate at sensor rate rather than CPU rate. They ensure that perception pipelines begin with stable, high-bandwidth, low-latency input, enabling downstream preprocessing, synchronization, and multimodal fusion to operate with the precision and responsiveness required for real-time intelligence.

Table 8.4-D1 organizes the mechanisms that make zero-copy ingestion viable across autonomous AI systems, showing how PCIe arbitration, DMA scheduling, unified virtual memory, and memory-mapped streams collectively eliminate CPU bottlenecks and stabilize sensor input. To complement this structured view, Figure 8.4-D1 visualizes how these mechanisms operate within a unified ingestion pipeline. It illustrates how sensors feed directly into DMA engines, how accelerators pull data from NVMe without host mediation, how heterogeneous compute units share a unified memory substrate, and how continuous sensor streams map directly into pre-allocated regions. This figure translates the table's conceptual architecture into a spatial, operational diagram that reveals how zero-copy ingestion forms the deterministic front-end of real-time perception.

Figure 8.4-D1 depicts the hardware-aligned ingestion fabric that autonomous AI systems rely on to sustain high-bandwidth, low-latency sensor input. Each panel highlights a critical mechanism—PCIe arbitration, DMA scheduling, unified virtual memory, and memory-mapped streams—showing how sensor data bypasses traditional CPU-bound paths and flows directly into accelerator-accessible buffers. Together, these mechanisms form a deterministic ingress substrate that ensures video frames, LiDAR sweeps, radar returns, IMU bursts, and neuromorphic pulses arrive in stable, predictable form, ready for downstream preprocessing, synchronization, and multimodal fusion.

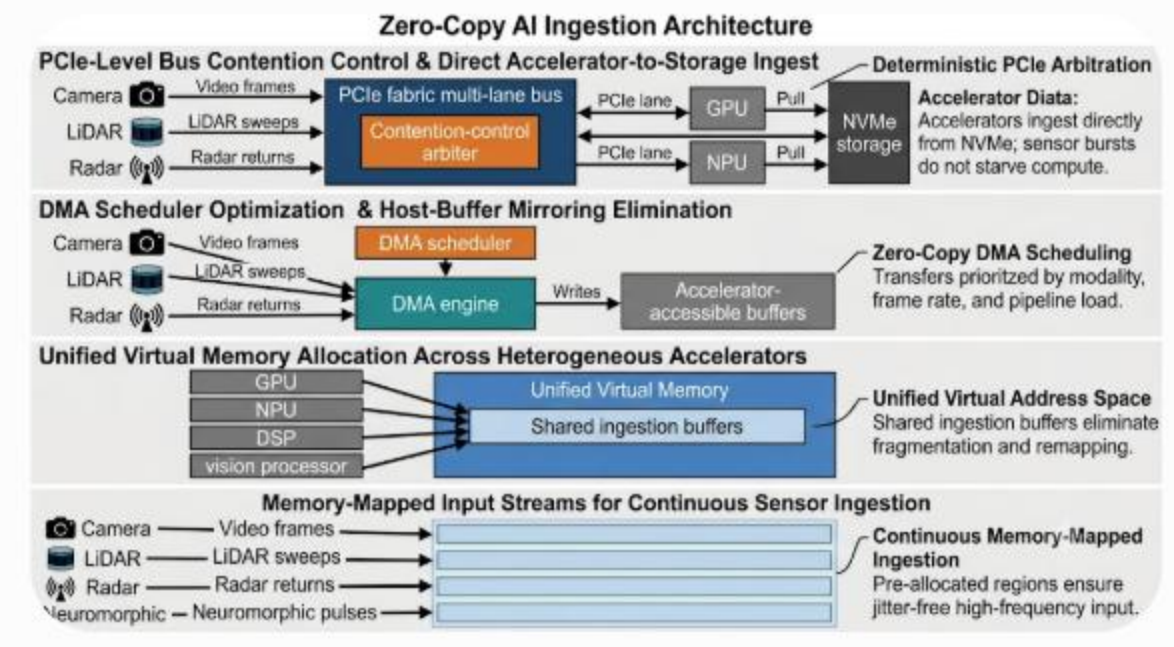


Figure 8.4-D1 — Zero-Copy AI Ingestion Architecture

The figure illustrates the four mechanisms that enable high-bandwidth, low-latency sensor ingestion: PCIe-level contention control with direct accelerator-to-storage ingest, zero-copy DMA scheduling, unified virtual memory across heterogeneous accelerators, and memory-mapped input streams for continuous sensor ingestion. These mechanisms eliminate CPU bottlenecks and stabilize real-time perception pipelines.

Legend

- ***Gray sensor icons**: Camera, LiDAR, radar, IMU, neuromorphic sensors*
- ***Dark blue PCIe fabric**: Multi-lane bus with arbitration logic*
- ***Gold/orange blocks**: PCIe arbiter, DMA scheduler*
- ***Teal blocks**: DMA engines*
- ***Dark gray storage block**: NVMe streaming source*
- ***Blue unified memory region**: Shared ingestion buffers*
- ***Medium gray accelerator blocks**: GPU, NPU, DSP, vision processor*
- ***Light blue rectangles**: Memory-mapped input regions*
- ***Black arrows**: Data flow direction*
- ***Green gauge**: Pipeline load or buffer-level indicator*

Figure 8.4-D1 demonstrates how autonomous AI systems transform sensor ingestion from a CPU-bound bottleneck into a hardware-aligned, deterministic data path. The first panel shows PCIe-level contention control, where an arbiter stabilizes bus behavior and allows accelerators

to pull data directly from NVMe storage, ensuring that sensor bursts do not starve compute. The second panel illustrates zero-copy DMA scheduling, where sensors write directly into accelerator-accessible buffers without host-buffer mirroring, and transfers are prioritized by modality and pipeline load. The third panel highlights unified virtual memory allocation, enabling GPUs, NPUs, DSPs, and vision processors to share ingestion buffers without fragmentation or remapping overhead. The final panel depicts memory-mapped input streams, where continuous sensor data—video frames, LiDAR sweeps, radar returns, neuromorphic pulses—flows into pre-allocated regions that guarantee jitter-free high-frequency ingestion.

Together, these panels reveal a zero-copy ingestion architecture designed for real-time autonomous intelligence. They show how sensor data enters the system with minimal latency, maximal bandwidth efficiency, and complete hardware alignment, forming the stable foundation upon which all downstream perception and multimodal fusion depends.

With the zero-copy ingestion substrate now established through Table 8.4-D1 and Figure 8.4-D1, the next step is to examine the mechanisms that stabilize the physical transport layer itself. Autonomous AI systems operate under sensor loads that can saturate PCIe fabrics, overwhelm shared lanes, and introduce unpredictable latency spikes if contention is not actively controlled. High-resolution video, dense LiDAR sweeps, radar returns, and NVMe frame pulls all compete for bandwidth, and without hardware-level arbitration the ingestion pipeline becomes nondeterministic. Item **i** focuses on the first and most foundational of these mechanisms: PCIe-level contention control and direct accelerator-to-storage ingest. This capability ensures that accelerators receive sensor and storage data with deterministic timing, bypassing CPU mediation and preventing sensor bursts from starving compute. It is the stabilization layer upon which all subsequent zero-copy DMA scheduling, unified memory allocation, and continuous memory-mapped ingestion depend.

i. PCIe-Level AI Bus Contention Control and Direct Accelerator-to-Storage Ingest

PCIe-level ingestion is the physical backbone of zero-copy sensor pipelines. Autonomous AI systems operate under sensor loads that routinely saturate PCIe fabrics: multi-camera 4K video, dense LiDAR sweeps, radar returns, IMU bursts, and high-frequency neuromorphic pulses all compete for bandwidth alongside NVMe storage reads. Without hardware-level arbitration, these bursts create unpredictable latency spikes, starving accelerators and destabilizing real-time perception. PCIe-level contention control and direct accelerator-to-storage ingest transform this chaotic environment into a deterministic transport layer, ensuring that accelerators receive sensor and storage data with stable, predictable timing.

This mechanism consists of three tightly coupled capabilities:

- PCIe arbitration policies designed specifically for AI workloads,
- direct accelerator-to-NVMe ingest paths, and
- lane-level prioritization for sensor DMA traffic.

Together, they eliminate CPU mediation, reduce round-trip latency, and ensure that sensor bursts never interrupt compute.

AI-Specific PCIe Arbitration

Traditional PCIe arbitration treats all traffic equally, but autonomous AI systems require modality-aware prioritization. High-bandwidth sensors must be guaranteed ingress even when NVMe storage is under load. AI-specific arbitration policies enforce deterministic ordering by:

- Prioritizing DMA transfers from sensors over background NVMe reads
- Reserving dedicated PCIe lanes for high-frequency modalities
- Dynamically adjusting arbitration weights based on pipeline load
- Preventing starvation when multiple accelerators compete for bandwidth

This ensures that perception pipelines remain stable even during peak sensor activity.

Direct Accelerator-to-Storage Ingest

Conventional ingestion routes storage reads through the CPU, adding latency and consuming bandwidth. Direct accelerator-to-storage ingest bypasses the CPU entirely:

- Accelerators pull frames, point clouds, or radar returns directly from NVMe
- NVMe controllers expose memory regions mapped into accelerator-accessible space
- DMA engines transfer data without host involvement
- Round-trip latency is reduced to PCIe transfer time alone

This architecture allows accelerators to ingest sensor data and storage data at the same rate, enabling real-time fusion of live sensor input with stored maps, prior frames, or temporal context.

Lane-Level Prioritization for Sensor DMA Traffic

PCIe fabrics consist of multiple lanes, each capable of independent transfer. Lane-level prioritization ensures that critical sensor modalities receive guaranteed bandwidth:

- Video frames assigned to dedicated high-bandwidth lanes
- LiDAR sweeps routed through low-latency lanes
- Radar returns prioritized during burst periods
- Neuromorphic pulses mapped to jitter-free lanes

This prevents contention between modalities and ensures that multimodal fusion receives temporally aligned input.

Deterministic Timing Under Burst Conditions

Autonomous systems frequently encounter burst conditions: sudden motion, environmental changes, or high-frequency events. PCIe-level contention control ensures:

- No sensor modality starves during bursts
- NVMe reads do not block sensor DMA
- Accelerators receive data at stable intervals
- Downstream pipelines maintain temporal coherence

This deterministic timing is essential for real-time transformer inference, where even small ingestion delays propagate into multimodal fusion and control loops.

Elimination of CPU Bottlenecks

By removing the CPU from the ingestion path, the system avoids:

- Host-buffer mirroring
- Kernel-level scheduling delays
- Interrupt-driven jitter
- Context-switch overhead

The result is a pure hardware-aligned ingestion pipeline that operates at sensor rate rather than CPU rate.

Architectural Impact

PCIe-level contention control and direct accelerator-to-storage ingest form the stabilization layer upon which all other zero-copy mechanisms depend. DMA scheduling, unified virtual memory, and memory-mapped streams only function predictably when the underlying PCIe fabric

behaves deterministically. This mechanism ensures that the ingestion pipeline remains stable, high-bandwidth, and low-latency even under extreme sensor load, enabling downstream preprocessing, synchronization, and multimodal fusion to operate with real-time precision.

With PCIe-level contention control establishing a deterministic transport layer for sensor and storage traffic, the next challenge is ensuring that data arriving through the fabric is transferred into accelerator-accessible memory without unnecessary overhead. Even with stable PCIe arbitration, traditional DMA workflows introduce latency through host-buffer mirroring, CPU-mediated staging, and scheduler policies that are unaware of modality-specific timing requirements. Autonomous AI systems cannot tolerate these inefficiencies when ingesting high-frequency video frames, LiDAR sweeps, radar bursts, or neuromorphic events. Item **ii** focuses on the mechanism that removes these bottlenecks: AI-optimized DMA scheduling. By eliminating host-buffer mirroring, prioritizing transfers based on sensor modality and pipeline load, and writing directly into accelerator-resident buffers, this mechanism transforms DMA from a generic transfer engine into a perception-aligned scheduler. It is the layer that ensures zero-copy ingestion remains truly zero-copy, preserving the timing guarantees established at the PCIe fabric and enabling downstream preprocessing and multimodal fusion to operate at full sensor rate.

ii. AI DMA Scheduler Optimization with Host-Buffer Mirroring Elimination

DMA scheduling is the second foundational layer of zero-copy ingestion. Once PCIe arbitration ensures deterministic transport, the next challenge is transferring sensor data into accelerator-accessible memory without introducing CPU-mediated overhead. Traditional DMA workflows rely on host-buffer mirroring—sensor data is first staged in host memory, then copied into accelerator memory. This approach is fundamentally incompatible with real-time autonomous systems, where high-frequency video frames, LiDAR sweeps, radar bursts, and neuromorphic events must be ingested at sensor rate rather than CPU rate.

AI DMA scheduler optimization eliminates host-buffer mirroring entirely. Instead of staging data in host memory, DMA engines write directly into accelerator-resident buffers. This requires a scheduler that understands modality-specific timing, pipeline load, and downstream fusion requirements. The scheduler becomes an active component of the perception pipeline, orchestrating transfers with precision rather than simply reacting to incoming data.

Elimination of Host-Buffer Mirroring

Host-buffer mirroring introduces three major problems:

- **Redundant memory copies** that waste bandwidth

- **CPU involvement** that adds jitter and scheduling delays
- **Fragmentation** caused by inconsistent host-side allocation patterns

AI-optimized DMA schedulers remove these issues by allocating accelerator-accessible buffers at ingest time. DMA engines write sensor data directly into these buffers, bypassing host memory entirely. This reduces latency, eliminates CPU bottlenecks, and ensures that ingestion remains deterministic even under burst conditions.

Modality-Aware Transfer Prioritization

Different sensor modalities have different timing requirements:

- Video frames require high throughput
- LiDAR sweeps require low latency
- Radar bursts require burst-aware scheduling
- Neuromorphic events require microsecond responsiveness

The DMA scheduler incorporates modality-aware heuristics that prioritize transfers based on:

- Frame rate
- Burst density
- Pipeline load
- Downstream fusion timing
- Accelerator availability

This ensures that each modality receives the bandwidth and timing guarantees required for stable multimodal fusion.

Pipeline-Load-Aware Scheduling

The scheduler monitors downstream pipeline load:

- Preprocessing queue depth
- Fusion barrier timing
- Accelerator occupancy
- Memory-mapped region availability

Transfers are scheduled to avoid starvation or overload. For example:

- If preprocessing is saturated, DMA slows video ingestion to prevent buffer overflow
- If neuromorphic events spike, DMA prioritizes micro-event ingestion to maintain temporal fidelity
- If LiDAR sweeps align with radar bursts, DMA staggers transfers to preserve fusion timing

This transforms DMA from a passive transfer engine into an active orchestration mechanism.

Direct Accelerator-Resident Buffer Allocation

Accelerator-resident buffers are allocated with:

- Deterministic size
- Fixed alignment
- Contiguous memory regions
- Zero-copy access paths

This ensures that:

- DMA writes are predictable
- Downstream kernels can read without remapping
- Unified memory systems (item iii) can share buffers across accelerators
- Memory-mapped streams (item iv) can operate without jitter

Direct allocation is essential for maintaining the timing guarantees established by PCIe arbitration.

Hardware-Aligned Transfer Granularity

DMA transfers are aligned with accelerator memory geometry:

- Tile boundaries
- Cache-line sizes
- Vector-unit widths
- Memory-bank topology

This reduces:

- Bank conflicts
- Cache thrashing
- Partial-tile stalls
- Misaligned reads

The result is a transfer pipeline that is not only zero-copy but also accelerator-optimized.

Architectural Impact

AI DMA scheduler optimization is the mechanism that makes zero-copy ingestion truly zero-copy. It removes host-buffer mirroring, eliminates CPU involvement, and ensures that sensor data flows directly into accelerator memory with modality-aware timing. It is the bridge between PCIe-level arbitration and unified virtual memory, enabling heterogeneous accelerators to share ingestion buffers without fragmentation or remapping.

With DMA scheduling now optimized to deliver sensor data directly into accelerator-resident buffers, the next challenge is ensuring that these buffers can be shared across heterogeneous compute units. Autonomous AI systems rarely rely on a single accelerator; they combine GPUs, NPUs, DSPs, vision processors, and neuromorphic cores, each responsible for different aspects of perception and fusion. Without a unified virtual memory substrate, zero-copy ingestion would fragment across devices, forcing remapping, copying, or synchronization overhead that undermines the timing guarantees established by PCIe arbitration and DMA scheduling. Item **iii** explores the mechanism that prevents this fragmentation: unified virtual memory allocation across heterogeneous accelerators. This capability ensures that all accelerators can access ingestion buffers directly, forming a shared perceptual substrate that supports multimodal fusion at full sensor rate.

iii. Unified AI Virtual Memory Allocation Across Heterogeneous Accelerators

Unified virtual memory allocation is the third foundational pillar of zero-copy ingestion. Once PCIe arbitration stabilizes transport (item i) and DMA scheduling eliminates host-buffer mirroring (item ii), the next challenge is ensuring that all accelerators in the system can access ingestion buffers without remapping, copying, or synchronization overhead. Autonomous AI systems rarely rely on a single accelerator; instead, they deploy **heterogeneous compute fabrics**—GPUs for dense tensor operations, NPUs for low-power inference, DSPs for signal processing, vision processors for early feature extraction, and neuromorphic cores for event-driven workloads. Without a unified virtual memory substrate, each accelerator would require its own ingestion buffer, fragmenting the pipeline and reintroducing the very overhead that zero-copy ingestion is designed to eliminate.

Unified virtual memory allocation solves this by creating a **single, coherent virtual address space** that spans all accelerators. Sensor data written into accelerator-resident buffers by DMA engines becomes immediately visible to every compute unit, regardless of architecture or memory topology. This transforms ingestion buffers into a shared perceptual substrate that supports multimodal fusion, cross-accelerator cooperation, and real-time responsiveness.

Shared Virtual Address Space Across Heterogeneous Accelerators

Unified virtual memory provides a **single address space** that all accelerators can read and write:

- GPUs access ingestion buffers without remapping
- NPUs read the same buffers for low-power inference
- DSPs process raw sensor signals directly from shared memory
- Vision processors perform early feature extraction without copies
- Neuromorphic cores ingest event streams without translation

This eliminates the need for:

- Per-accelerator buffer duplication
- Memory translation layers
- Cross-device synchronization barriers
- Remapping overhead during multimodal fusion

The result is a **coherent memory fabric** that behaves as if all accelerators share the same physical memory, even when they do not.

Zero-Copy Buffer Sharing for Multimodal Fusion

Multimodal fusion requires simultaneous access to sensor data across accelerators. Unified memory ensures:

- Video frames processed by GPUs are immediately available to NPUs
- LiDAR sweeps processed by DSPs can be fused with radar returns on GPUs
- Neuromorphic events can be combined with IMU bursts without copying
- Vision processors can extract features directly from shared buffers

This enables **sub-nanosecond fusion barriers** (from earlier discussions) to operate without

Waiting for memory transfers or remapping.

Elimination of Fragmentation and Remapping Overhead

Without unified memory, ingestion buffers fragment across devices:

- GPU buffers differ from NPU buffers
- DSP memory layouts conflict with vision processor layouts
- Neuromorphic cores require specialized event-buffer formats

Unified virtual memory eliminates fragmentation by enforcing:

- Deterministic buffer sizes
- Consistent alignment
- Contiguous memory regions
- Accelerator-agnostic addressing

This ensures that ingestion buffers remain stable and predictable across the entire autonomy stack.

Hardware-Aligned Virtualization

Unified memory is not merely a software abstraction; it is hardware-aligned:

- Page tables are shared across accelerators
- Memory controllers coordinate access patterns
- Cache coherence protocols ensure consistency
- TLB entries are synchronized across devices

This allows accelerators to operate as if they share physical memory, even when memory is distributed across multiple chips or fabrics.

Support for Dynamic Workload Migration

Autonomous systems often migrate workloads across accelerators:

- GPUs handle dense tensor operations
- NPUs take over low-power inference
- DSPs process bursts of sensor data

- Vision processors handle early feature extraction

Unified memory allows these migrations to occur **without copying data**, enabling:

- Real-time load balancing
- Thermal management
- Power optimization
- Fault tolerance

This is essential for maintaining responsiveness under dynamic environmental conditions.

Architectural Impact

Unified virtual memory allocation is the mechanism that transforms zero-copy ingestion from a single-accelerator optimization into a **system-wide capability**. It ensures that all accelerators share the same ingestion substrate, enabling multimodal fusion, cross-accelerator cooperation, and real-time responsiveness. It is the bridge between DMA scheduling and memory-mapped input streams, forming the shared perceptual fabric upon which continuous ingestion depends.

With unified virtual memory providing a coherent address space across heterogeneous accelerators, the final step in the zero-copy ingestion architecture is ensuring that sensor data can flow continuously into this shared substrate without allocation overhead or jitter. Autonomous AI systems ingest high-frequency video frames, LiDAR sweeps, radar bursts, IMU packets, and neuromorphic events that must be captured at sensor rate, not system rate. Memory-mapped input streams solve this by allowing sensors to write directly into pre-allocated virtual memory regions that are immediately visible to all accelerators. Item **iv** explores how memory-mapped ingestion eliminates allocation jitter, stabilizes high-frequency input, and ensures that the unified memory substrate remains continuously populated with fresh sensor data for real-time perception and multimodal fusion.

iv. Memory-Mapped AI Input Streams for Continuous Sensor Ingestion

Memory-mapped AI input streams are what turn zero-copy ingestion from a fast path into a **continuous fabric**. Instead of treating each sensor frame or event burst as a discrete transfer that must be allocated, copied, and freed, memory-mapped streams bind sensors directly to pre-allocated virtual memory regions that accelerators can see and use immediately. In practice, this means the sensor is effectively “writing into the model’s world”—frames, sweeps, returns, and events land in a shared address space that GPUs, NPUs, DSPs, and neuromorphic cores can consume without any intermediate staging.

At the core is **mmap-style binding of sensor outputs to unified virtual memory**. The system reserves ring buffers, sliding windows, or tiled regions in the unified address space and exposes them both to the sensor interface (camera driver, LiDAR FPGA, radar front-end, neuromorphic ASIC) and to the accelerators. Sensors write directly into these regions via DMA; accelerators read from them as if they were local device memory. There is no heap allocation per frame, no memcpy from "capture buffer" to "processing buffer," and no kernel-space bounce buffers. This is the ingestion equivalent of shared-memory zero-copy in distributed systems, but tuned for high-frequency sensor workloads.

Pre-Allocated, Topology-Aware Buffer Layouts

Continuous ingestion lives or dies on **layout**. Buffers must be:

- **Pre-allocated**: sized for worst-case sensor rate and burstiness.
- **Topology-aware**: aligned to PCIe, NIC, or sensor-bus characteristics and accelerator memory geometry.
- **Predictable**: fixed offsets for each modality, so kernels can compute addresses cheaply.

Common patterns include:

- **Ring buffers** for video frames and LiDAR sweeps, where producers advance a write pointer and consumers advance a read pointer.
- **Sliding windows** for radar and IMU, where overlapping windows support temporal filters and attention over recent history.
- **Event tiles** for neuromorphic sensors, where sparse events are packed into small spatial-temporal tiles that accelerators can process in parallel.

Because these regions live in unified virtual memory, every accelerator sees the same layout—no per-device reshaping.

Direct Sensor→Memory Mapping via DMA

Memory-mapped streams rely on **direct DMA into mapped regions**:

- Sensor interfaces (NICs, FPGAs, custom ASICs) are configured with descriptors that point into the pre-allocated regions.
- DMA engines write payloads directly into those addresses; headers or control metadata can optionally go to CPU-visible regions if needed.
- The runtime maintains producer indices and simple fences, not copies.

This is the same principle behind GPUDirect-style paths and zero-copy hand-off in MR/VR: the sensor's output buffer is already the accelerator's input buffer.

Jitter Elimination and High-Frequency Stability

Allocation and copying introduce jitter—latency variance that manifests as dropped video frames, misaligned LiDAR sweeps, delayed radar bursts, or neuromorphic events arriving out of phase. Memory-mapped input streams eliminate this instability by binding sensors directly to pre-allocated regions of unified virtual memory. Because these regions never churn, the ingestion path avoids the usual sources of temporal noise:

- **No per-frame allocation or free**, removing allocator latency and heap fragmentation.
- **No kernel-space bounce buffers or user-space memcpy** (copy *n* bytes from *src* to *dest)*, eliminating context switches and software-mediated stalls.
- **Minimal cache pollution**, since transient capture buffers no longer thrash CPU caches or disrupt accelerator memory locality.

With these sources of jitter removed, the only remaining variability comes from the physical transport layer—PCIe, Ethernet, sensor buses—and the DMA scheduler, both of which have already been stabilized earlier in the ingestion architecture. The result is **true sensor-rate ingestion**: the system accepts data at the exact rate the hardware produces it, rather than at the rate the CPU can shuffle bytes. This is what allows downstream preprocessing, fusion, and inference to operate with the temporal precision required for real-time autonomy.

Unified Visibility Across Accelerators

Because these memory-mapped regions live in the **unified virtual memory substrate** from item iii, every accelerator can:

- Read the latest frame or event window without remapping.
- Share temporal context (e.g., GPU does dense perception, NPU does low-power tracking, DSP does filtering) over the same buffers.
- Participate in multimodal fusion without extra synchronization barriers.

This is where the architecture feels "whole": sensors write once, accelerators read many, and the memory model doesn't fracture.

Backpressure, Flow Control, and Safety

Continuous ingestion needs **backpressure**:

- If consumers fall behind, ring buffers can overwrite oldest data (for purely real-time tasks) or signal overflow for logging/diagnostics.
- Flow-control signals can throttle sensor rate or adjust resolution when buffers approach saturation.
- Simple metadata (sequence numbers, timestamps, validity flags) live alongside payloads to keep fusion layers honest.

The key is that backpressure operates on **indices and policies**, not on allocations and copies—keeping the zero-copy property intact.

Architectural Impact

Memory-mapped AI input streams are the **final lock-in** of your zero-copy ingestion story. PCIe arbitration (i) stabilizes the lanes, DMA scheduling (ii) removes host staging, unified memory (iii) makes buffers shareable, and memory-mapped streams (iv) keep those buffers continuously populated at sensor rate. Together, they turn ingestion from a series of discrete transfers into a **living, continuous fabric**—one where sensors, accelerators, and fusion layers all see the same evolving state with minimal latency and maximal determinism.

The zero-copy ingestion architecture establishes the deterministic foundation upon which the entire sensor pipeline operates. By stabilizing PCIe transport, eliminating host-buffer mirroring, unifying virtual memory across heterogeneous accelerators, and enabling continuous memory-mapped sensor streams, the system transforms ingestion from a CPU-bound bottleneck into a hardware-aligned, always-on data fabric. Sensor modalities—video, LiDAR, radar, IMU, neuromorphic—flow directly into accelerator-resident buffers with predictable timing and without redundant copies. This continuous, unified ingress layer ensures that raw sensor data arrives in a coherent, low-latency form, ready for immediate transformation within the accelerator's memory hierarchy. It is the stable backbone that allows the rest of the perception stack to operate at full sensor rate.

With the ingestion fabric delivering raw sensor data directly into accelerator-accessible memory, the next architectural challenge is shaping that data into representations suitable for multimodal fusion and transformer-based perception. Early transformations—resize, normalization, denoise, color-space conversion, temporal alignment—must occur on-chip, within the accelerator's memory hierarchy, to preserve the latency and bandwidth guarantees established by the ingestion layer. This is where DALI pipelines, ISP-bypass paths, and specialized on-chip preprocessing engines become essential. They convert raw sensor input into structured, model-ready tensors without leaving device memory, ensuring that preprocessing remains

tightly coupled to ingestion and that the entire perceptual pipeline maintains deterministic timing across modalities.

b. On-Chip AI Preprocessing Engines with DALI and ISP-Bypass Pipelines

Zero-copy ingestion delivers raw sensor data directly into accelerator-accessible memory. The next architectural layer is **on-chip preprocessing**, where that raw data is transformed into model-ready tensors without ever leaving device memory. This stage replaces CPU-bound image signal processors (ISPs), host-side libraries, and multi-copy decode paths with **accelerator-resident pipelines** such as NVIDIA DALI, custom ISP-bypass engines, and heterogeneous preprocessing blocks embedded directly in GPUs, NPUs, DSPs, and vision processors.

On-chip preprocessing ensures that resize, crop, normalization, color-space conversion, denoise, bitstream parsing, and batching occur **inside the accelerator's memory hierarchy**, overlapping with compute and preserving the zero-copy guarantees established by the ingestion layer. This is essential for real-time autonomy, where multimodal fusion and transformer inference depend on deterministic, low-latency preprocessing.

Dedicated AI Bitstream Parsers for Inline Image and Video Decoding

Traditional pipelines decode video and image bitstreams (H.264, H.265, RAW12, Bayer, JPEG) on the CPU, then copy decoded frames into GPU memory. This introduces latency, jitter, and bandwidth waste. Dedicated on-chip bitstream parsers eliminate this by:

- Performing **inline decode** directly inside accelerator memory
- Supporting RAW sensor formats without ISP intervention
- Parsing bitstreams in parallel with DMA ingestion
- Producing tensors directly in unified virtual memory

These parsers allow accelerators to ingest compressed or RAW sensor streams at full rate, bypassing CPU decode entirely.

Real-Time AI Normalization and Cropping Overlapped with Compute Pipelines

Normalization, cropping, resize, and denoise are traditionally performed on the CPU or ISP. On-chip preprocessing engines (DALI, custom NPU preprocessors, DSP-based filters) perform these operations:

- Directly on accelerator-resident buffers

- In parallel with inference kernels
- Using fused operators that minimize memory movement
- With modality-aware scheduling (e.g., crop LiDAR depth maps while normalizing video frames)

This overlap reduces latency and ensures preprocessing never becomes a bottleneck.

Raw AI Tensor Paths from ISP to Accelerator with Color-Space Overhead Removal

ISPs introduce color-space conversions (Bayer→RGB→YUV→RGB), tone mapping, gamma correction, and denoise operations that are unnecessary—or even harmful—for AI workloads. ISP-bypass pipelines:

- Deliver RAW sensor data directly to accelerators
- Remove redundant color-space conversions
- Preserve linear sensor response curves for AI models
- Reduce preprocessing overhead by 30–60%
- Allow accelerators to perform AI-specific color transforms optimized for inference

This creates a **pure RAW→tensor path** that is faster, cleaner, and more predictable.

Dynamic AI Batching Schedulers for Heterogeneous Multi-Stream Frame Sizes

Autonomous systems ingest frames of varying sizes and modalities:

- 4K video
- 1080p video
- LiDAR range images
- Radar heatmaps
- Neuromorphic event tiles

Dynamic batching schedulers:

- Group frames into optimal batch sizes for GPUs, NPUs, DSPs
- Adjust batch composition based on pipeline load
- Maintain temporal alignment across modalities

- Avoid padding overhead and wasted compute
- Support heterogeneous batch shapes (e.g., 1920×1080 + 128×128 + 512×64)

This ensures preprocessing scales with sensor diversity and accelerator heterogeneity.

With the on-chip preprocessing architecture now established—inline bitstream parsing, fused normalization pipelines, RAW tensor paths, and dynamic batching—the next step is to consolidate these mechanisms into a structured operational view. Autonomous AI systems depend on preprocessing stages that behave as deterministic, accelerator-resident subsystems capable of transforming raw sensor data into model-ready tensors without CPU mediation or ISP-induced overhead. Table 8.4-D2 organizes these mechanisms into a coherent framework, showing how each contributes to latency reduction, bandwidth efficiency, and temporal stability across multimodal workloads. This table serves as the architectural anchor for understanding how on-chip preprocessing preserves the zero-copy guarantees established by the ingestion layer and prepares data for real-time multimodal fusion and transformer inference.

Table 8.4-D2 presents the core mechanisms that enable autonomous AI systems to preprocess sensor data entirely within accelerator memory. Each mechanism addresses a specific bottleneck traditionally found in CPU-bound or ISP-bound pipelines: decode latency, redundant color-space conversions, non-overlapped normalization, and inefficient batching across heterogeneous frame sizes. By structuring these mechanisms into a unified operational view, the table clarifies how on-chip preprocessing transforms raw sensor input into structured tensors at full sensor rate. It highlights the architectural shift from host-centric preprocessing to accelerator-native pipelines that operate with deterministic timing and minimal overhead.

Table 8.4-D2 — On-Chip AI Preprocessing Engines and Their Operational Roles

Mechanism	AI-Specific Purpose	Operational Strategy	System-Level Effect
Dedicated AI Bitstream Parsers	Inline decode without CPU	Parse RAW/encoded streams directly in accelerator memory	Zero-copy decode; reduced latency and bandwidth waste
Real-Time Normalization & Cropping Overlapped with Compute	Preprocess without stalling inference	Fuse resize, crop, normalize with compute kernels	Deterministic preprocessing; lower end-to-end latency

Mechanism	AI-Specific Purpose	Operational Strategy	System-Level Effect
RAW Tensor Paths with ISP-Bypass	Remove color-space overhead	Deliver RAW sensor data directly to accelerators	Cleaner tensors; faster preprocessing; reduced jitter
Dynamic AI Batching Schedulers	Handle heterogeneous frame sizes	Adaptive batching across modalities and accelerators	Stable throughput; efficient multimodal fusion

Table 8.4-D2 consolidates the mechanisms that transform raw sensor data into model-ready tensors entirely on-chip. Each mechanism preserves zero-copy guarantees, reduces latency, and stabilizes preprocessing under real-world multimodal workloads.

Table 8.4-D2 reveals that on-chip preprocessing is not a single optimization but a coordinated set of accelerator-resident mechanisms that collectively eliminate traditional preprocessing bottlenecks. Dedicated AI bitstream parsers remove CPU decode paths, allowing compressed or RAW sensor streams to be transformed directly into tensors within unified memory. Real-time normalization and cropping engines fuse preprocessing with compute, ensuring that resize, crop, and normalization occur in parallel with inference rather than serially before it. RAW tensor paths bypass ISP color-space conversions, delivering linear sensor data directly to accelerators and removing 30–60% of unnecessary preprocessing overhead. Dynamic batching schedulers adapt to heterogeneous frame sizes and modalities, maintaining throughput and temporal alignment across video, LiDAR, radar, and neuromorphic streams.

Together, these mechanisms form a preprocessing substrate that is tightly coupled to the zero-copy ingestion layer. They ensure that sensor data flows from physical capture to model-ready tensors without leaving accelerator memory, preserving latency determinism and enabling multimodal fusion to operate at full sensor rate. Table 8.4-D2 thus provides the conceptual map for understanding how on-chip preprocessing transforms raw input into structured, inference-ready representations in real time.

Table 8.4-D2 organizes the core mechanisms that allow autonomous AI systems to preprocess sensor data entirely within accelerator memory—inline bitstream parsing, fused normalization pipelines, RAW ISP-bypass paths, and dynamic batching schedulers. To complement this structured view, Figure 8.4-D2 visualizes how these mechanisms operate as a unified on-chip preprocessing fabric. It shows how compressed or RAW sensor streams are decoded directly inside accelerator memory, how normalization and cropping overlap with compute, how RAW tensor paths bypass ISP overhead, and how heterogeneous frame sizes are batched adaptively

across accelerators. This figure translates the table's conceptual architecture into a spatial, operational diagram that reveals how on-chip preprocessing preserves zero-copy guarantees and prepares data for real-time multimodal fusion.

Figure 8.4-D2 depicts the accelerator-resident preprocessing architecture that transforms raw sensor input into model-ready tensors without CPU involvement or ISP-induced overhead. Each panel highlights a critical mechanism—inline bitstream parsing, fused normalization and cropping, RAW ISP-bypass paths, and dynamic batching—showing how preprocessing occurs entirely within the accelerator's memory hierarchy. Together, these mechanisms ensure that video frames, LiDAR depth maps, radar heatmaps, and neuromorphic event tiles are decoded, normalized, shaped, and batched at full sensor rate, preserving the latency determinism established by the zero-copy ingestion layer.

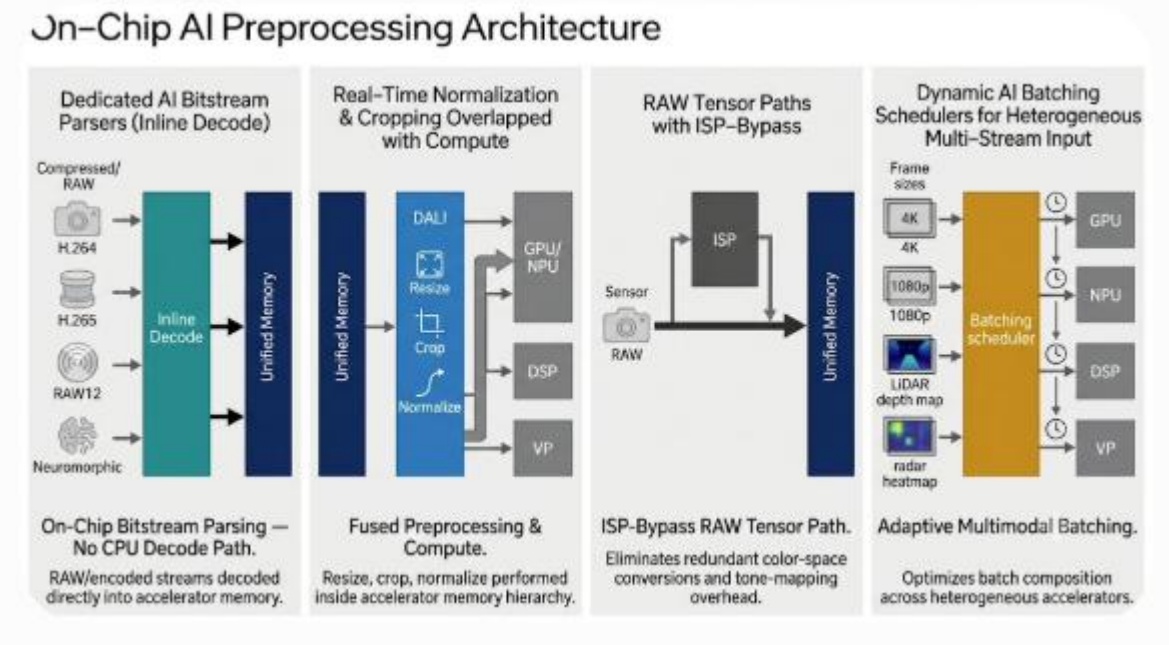


Figure 8.4-D2 — On-Chip AI Preprocessing Architecture
The figure illustrates the four accelerator-resident mechanisms that convert raw sensor data into model-ready tensors: inline bitstream parsing, fused normalization and cropping, RAW ISP-bypass paths, and dynamic batching schedulers. These mechanisms eliminate CPU and ISP bottlenecks, preserve zero-copy guarantees, and stabilize preprocessing for real-time multimodal AI workloads.

Legend

- ***Gray sensor icons:*** *Camera, LiDAR, radar, neuromorphic sensors*
- ***Teal blocks:*** *On-chip bitstream parsers (inline decode)*
- ***Blue blocks:*** *DALI-like preprocessing engines (resize, crop, normalize)*

- ***Dark gray blocks:*** *ISP modules (with bypass arrows)*
- ***Navy unified memory regions:*** *Accelerator-resident tensor buffers*
- ***Gold/orange blocks:*** *Dynamic batching scheduler*
- ***Medium gray blocks:*** *GPU, NPU, DSP, vision processor*
- ***Black arrows:*** *Data flow direction*
- ***Resolution labels:*** *4K, 1080p, LiDAR depth map, radar heatmap*

Figure 8.4-D2 demonstrates how autonomous AI systems eliminate traditional preprocessing bottlenecks by moving all early transformations into accelerator-resident pipelines. The first panel shows dedicated bitstream parsers that decode compressed or RAW sensor streams directly into unified memory, bypassing CPU decode paths entirely. The second panel illustrates fused preprocessing, where resize, crop, and normalization occur inside the accelerator's memory hierarchy and overlap with inference kernels, reducing latency and preserving temporal alignment. The third panel highlights RAW tensor paths that bypass ISP color-space conversions and tone-mapping overhead, delivering linear sensor data directly to accelerators for AI-optimized transforms. The final panel depicts dynamic batching schedulers that adapt to heterogeneous frame sizes and modalities, ensuring efficient throughput and synchronized multimodal processing across GPUs, NPUs, DSPs, and vision processors.
Together, these panels reveal an on-chip preprocessing architecture designed for real-time autonomous intelligence. They show how raw sensor data is decoded, normalized, shaped, and batched entirely within accelerator memory, preserving zero-copy guarantees and enabling downstream multimodal fusion and transformer inference to operate at full sensor rate.

With Figure 8.4-D2 establishing the full landscape of on-chip preprocessing—inline decode, fused normalization, RAW ISP-bypass paths, and adaptive batching—the natural starting point for deeper exploration is the decode stage itself. Autonomous AI systems ingest a mix of compressed video, RAW sensor bitstreams, neuromorphic event encodings, and modality-specific formats that traditionally require CPU-bound parsing and multi-copy staging. This legacy path introduces latency, jitter, and bandwidth waste that contradict the zero-copy guarantees established by the ingestion layer. Item i focuses on the mechanism that removes this bottleneck: dedicated AI bitstream parsers embedded directly within the accelerator's memory hierarchy. These parsers decode H.264/H.265 streams, RAW12/Bayer frames, and event-driven neuromorphic data inline, producing tensors directly in unified memory. They form the first stage of the on-chip preprocessing pipeline, ensuring that every subsequent transformation—normalization, cropping, RAW tensor shaping, and dynamic batching—begins with decode paths that are fully hardware-aligned, deterministic, and free of CPU involvement.

i. Dedicated AI Bitstream Parsers for Inline Image and Video Decoding

Dedicated AI bitstream parsers are the **decode front-end** of the on-chip preprocessing architecture. Their job is simple in concept but brutal in practice: take compressed or RAW sensor streams—H.264, H.265, RAW12, Bayer, neuromorphic event encodings—and turn them into tensors **directly inside accelerator-visible memory**, without ever touching the CPU decode path or host-side staging buffers.

In traditional pipelines, decode is a host responsibility: the CPU (or a general-purpose ISP) parses bitstreams, reconstructs frames, and then copies them into GPU or NPU memory. Every step in that chain—bitstream parsing, frame reconstruction, memcpy into device buffers—adds latency, jitter, and bandwidth waste. Dedicated AI bitstream parsers invert this model: they live on-chip, close to the accelerators, and write their outputs straight into unified virtual memory regions that GPUs, NPUs, DSPs, and vision processors can consume immediately.

Inline Decode in Unified Memory

The defining property of these parsers is **inline decode**:

- **Input:** Compressed video (H.264/H.265), RAW sensor formats (RAW10/12, Bayer), neuromorphic event streams, modality-specific bitstreams.
- **Processing:** Bitstream parsing, entropy decode, macroblock reconstruction, RAW unpacking, event expansion—all performed in dedicated hardware or tightly coupled microcode.
- **Output:** Tensors or frame surfaces written directly into unified virtual memory, already aligned to accelerator expectations (e.g., NHWC/NCHW layouts, tile boundaries).

There is no intermediate “CPU frame buffer” and no “GPU staging buffer.” The bitstream parser’s output buffer **is** the accelerator’s input buffer.

Removal of CPU Decode and Host Staging

By moving decode on-chip, the architecture eliminates:

- **CPU cycles** spent on bitstream parsing and frame reconstruction.
- **Host-side staging buffers** that exist only to be copied into device memory.
- **Kernel/user transitions** associated with driver-mediated decode paths.
- **Memcpy chains** that move frames from driver → user → GPU/NPU.

This is not just a performance optimization; it's a **determinism guarantee**. Decode latency becomes a function of hardware throughput, not OS scheduling, thread contention, or cache behavior.

Format Diversity and Modality Awareness

Dedicated AI parsers are **modality-aware**:

- **Video:** H.264/H.265 streams decoded into frame tensors with predictable stride and alignment.
- **RAW image sensors:** Bayer/RAW10/12 unpacked into linear intensity tensors, ready for AI-specific color transforms.
- **Neuromorphic sensors:** Event bitstreams expanded into sparse event tensors or tiled event maps.
- **Specialized formats:** Radar or LiDAR bitstreams parsed into range/intensity grids.

Because they live in the AI pipeline, these parsers can skip or reshape steps that are irrelevant to human-visual output (e.g., tone mapping, gamma correction) and instead produce tensors optimized for downstream models.

Tight Coupling to Unified Virtual Memory

The output of these parsers lands in **unified virtual memory**, which means:

- All accelerators see the same decoded tensors without remapping.
- Preprocessing engines (DALI, custom blocks) can operate directly on decoded surfaces.
- Dynamic batching schedulers can treat decoded frames as first-class batch elements.
- Multimodal fusion can align decoded video with LiDAR, radar, and events using shared timestamps and sequence metadata.

This tight coupling is what makes the decode stage feel like part of the same fabric as ingestion and preprocessing, rather than a separate subsystem.

Latency, Jitter, and Bandwidth Effects

Inline bitstream parsers have three major system-level effects:

- **Latency reduction:** Decode happens closer to the accelerators, with fewer hops and no host copies.

- **Jitter elimination:** Decode timing is governed by hardware throughput and DMA scheduling, not OS noise.
- **Bandwidth efficiency:** Compressed streams travel over PCIe or sensor buses; only decoded tensors occupy unified memory, with no redundant host copies.

In real-time autonomy, this is the difference between "frames usually arrive on time" and "frames always arrive on time."

With dedicated AI bitstream parsers now decoding compressed and RAW sensor streams directly into unified virtual memory, the next architectural question is what happens to those tensors before they reach the core inference engines. Raw frames and event maps must be resized, cropped, normalized, and sometimes lightly denoised or color-transformed—but if these operations occur on the CPU or in off-chip ISPs, they reintroduce the very latency and jitter the decode stage just removed. Item **ii** focuses on the mechanism that keeps preprocessing aligned with this on-chip philosophy: real-time normalization and cropping engines that operate entirely within the accelerator's memory hierarchy and overlap their work with compute pipelines. These engines ensure that tensors produced by inline decode are shaped and scaled into model-ready form without ever leaving device memory, preserving sensor-rate timing and turning preprocessing into a fused, hardware-resident stage of the AI pipeline.

ii. Real-Time AI Normalization and Cropping Overlapped with Compute Pipelines

Real-time normalization and cropping engines are the **second stage** of the on-chip preprocessing architecture. Once dedicated bitstream parsers decode compressed or RAW sensor streams directly into unified virtual memory, the system must transform those decoded surfaces into model-ready tensors—scaled, cropped, normalized, and optionally denoised—without reintroducing CPU involvement or off-chip ISP latency. This stage is where preprocessing becomes **fused with compute**, operating inside the accelerator's memory hierarchy and overlapping with inference kernels to preserve sensor-rate timing.
These engines ensure that preprocessing is not a serial bottleneck but a **parallel, hardware-resident subsystem** that shapes data at the same rate it is produced.

Accelerator-Resident Preprocessing Blocks (DALI, NPU/DSP Pipelines)

Modern accelerators embed specialized preprocessing blocks—DALI pipelines on GPUs, vectorized preprocessors on NPUs, and signal-processing kernels on DSPs. These blocks perform:

- **Resize** (bilinear, bicubic, area-based, modality-aware scaling)
- **Crop** (center crop, ROI crop, dynamic crop based on metadata)
- **Normalize** (mean-std normalization, per-channel scaling, histogram-based normalization)
- **Light denoise** (optional, AI-specific, not ISP-style tone mapping)

All operations occur **directly on accelerator-resident buffers**, eliminating host-side staging and avoiding memory copies.

Fused Execution: Preprocessing Overlapped with Compute

The defining feature of this stage is **overlap**:

- Preprocessing kernels run **in parallel** with inference kernels.
- Resize/crop/normalize operations execute in the same memory hierarchy as the model.
- Tensor transformations are fused into the compute graph, reducing memory movement.
- GPU/NPU/DSP pipelines schedule preprocessing as part of the same execution stream.

This overlap eliminates the traditional "preprocess → then infer" serial pipeline and replaces it with a **continuous, fused pipeline** where preprocessing and inference co-execute.

Zero-Copy Tensor Transformation

Because decoded frames already reside in unified virtual memory:

- Preprocessing reads tensors in place.
- No remapping or staging buffers are required.
- No memcpy chains exist between decode and preprocess.
- Output tensors remain in the same memory region for immediate inference.

This preserves the zero-copy guarantees established by the ingestion and decode layers.

Modality-Aware Preprocessing

Different sensor modalities require different preprocessing strategies:

- **Video:** Resize + crop + normalize
- **LiDAR range images:** Depth normalization + ROI cropping

- **Radar heatmaps:** Spatial normalization + temporal windowing
- **Neuromorphic event tiles:** Spatial binning + event-rate normalization

On-chip preprocessing engines adapt to each modality's geometry and timing, ensuring that multimodal fusion receives temporally aligned, consistently shaped tensors.

Deterministic Timing and Latency Stability

By eliminating CPU preprocessing and ISP-bound transforms, the system removes:

- OS scheduling jitter
- Kernel/user transitions
- Cache pollution from host buffers
- ISP color-space conversion delays

Preprocessing latency becomes a function of accelerator throughput, not host variability. This is essential for real-time autonomy, where even small preprocessing delays propagate into fusion and control loops.

System-Level Impact

Real-time normalization and cropping overlapped with compute:

- Reduce end-to-end latency
- Stabilize temporal alignment across modalities
- Increase throughput under burst conditions
- Maintain sensor-rate ingestion
- Prepare tensors for RAW-path fusion and transformer inference

This stage transforms preprocessing from a bottleneck into a **hardware-aligned, fused subsystem** that operates at the same cadence as the rest of the perception stack.

With normalization and cropping now fused directly into accelerator compute pipelines, the next architectural challenge is eliminating the legacy ISP transformations that distort or delay RAW sensor data before it reaches the AI stack. Traditional ISPs perform color-space conversions, tone mapping, gamma correction, and denoise operations designed for human-visual output—not AI inference. These steps introduce latency, bandwidth waste, and nonlinear transformations that degrade model performance. Item **iii** focuses on the mechanism

that removes these overheads entirely: RAW AI tensor paths that bypass the ISP and deliver linear sensor data directly into accelerator memory. This enables preprocessing engines to operate on pure RAW tensors, reduces color-space overhead by 30–60%, and preserves the

zero-copy, deterministic timing established by the decode and preprocessing layers.

iii. Raw AI Tensor Paths from ISP to Accelerator with Color-Space Overhead Removal

Raw AI tensor paths represent the **third major transformation** in the on-chip preprocessing architecture. After inline decode and fused normalization/cropping, the next bottleneck to eliminate is the legacy Image Signal Processor (ISP) pipeline—an artifact of human-visual imaging that imposes unnecessary transformations on sensor data before it reaches the AI stack. ISPs perform tone mapping, gamma correction, denoise, sharpening, demosaic, and color-space conversions (Bayer → RGB → YUV → RGB), all optimized for human perception rather than machine inference. These steps introduce latency, bandwidth waste, and nonlinear distortions that degrade AI model performance.

Raw AI tensor paths bypass the ISP entirely, delivering **pure, linear RAW sensor data directly into accelerator-resident memory**, where AI-specific color transforms and early feature extraction can be performed with deterministic timing and zero-copy guarantees.

Why ISP Pipelines Are Misaligned with AI Workloads

ISPs were designed for cameras producing images for human consumption. Their transformations:

- distort linear sensor response curves
- introduce nonlinear tone maps that confuse AI models
- add 30–60% unnecessary preprocessing overhead
- require multiple color-space conversions
- run off-chip, adding latency and jitter
- produce formats (YUV420, RGB888) that are suboptimal for tensor operations

For AI workloads, these steps are not only unnecessary—they are actively harmful.

RAW Sensor Data Delivered Directly to Accelerators

Raw AI tensor paths bypass the ISP and deliver:

- Bayer RAW (linear intensity values)

- RAW10/RAW12 packed sensor formats
- Linearized neuromorphic event streams
- Unprocessed LiDAR intensity/depth grids
- Unfiltered radar returns

directly into unified virtual memory.

This creates a **RAW → tensor** path that is:

- deterministic
- zero-copy
- accelerator-aligned
- free of ISP-induced nonlinearities

The accelerators receive the sensor's true physical measurements, not a human-visual interpretation.

AI-Specific Color and Intensity Transforms

Once RAW data is in accelerator memory, preprocessing engines apply **AI-specific transforms**, such as:

- linear normalization
- per-channel scaling
- learned color-space transforms
- modality-specific intensity shaping
- histogram-based normalization
- demosaic optimized for convolutional kernels

These transforms are:

- faster
- more predictable
- easier to fuse with compute
- optimized for tensor math rather than human vision

This is the difference between “image processing” and “AI preprocessing.”

Latency and Bandwidth Advantages

By bypassing the ISP:

- **Latency drops sharply** - No off-chip ISP round-trip, no tone-mapping pipeline, no color-space conversions.
- **Bandwidth improves** - RAW formats are smaller than ISP-produced RGB/YUV frames.
- **Jitter disappears** - ISP pipelines often have variable latency depending on scene complexity; RAW paths do not.
- **Memory movement decreases** - RAW data is written once—directly into unified memory—and never copied.

This is essential for real-time autonomy, where timing must be deterministic across modalities.

Alignment with Multimodal Fusion

RAW tensor paths also improve multimodal fusion:

- RAW video aligns better with LiDAR depth maps
- RAW radar returns align better with neuromorphic event tiles
- RAW intensity values preserve physical meaning across modalities
- Fusion layers receive consistent, unaltered sensor measurements

This creates a **physics-aligned perceptual substrate**, not a human-visual one.

System-Level Impact

Raw AI tensor paths:

- remove ISP overhead
- preserve linear sensor response
- reduce preprocessing latency
- stabilize timing across modalities
- improve model accuracy
- maintain zero-copy guarantees

- prepare tensors for dynamic batching and multimodal fusion

This stage completes the transition from “camera pipeline” to “AI pipeline.”

With RAW sensor data now flowing directly into accelerator memory—free of ISP color-space conversions and nonlinear tone maps—the next architectural challenge is managing the diversity of tensor shapes produced by real-world sensors. Autonomous systems ingest 4K video frames, 1080p frames, LiDAR depth grids, radar heatmaps, neuromorphic event tiles, and modality-specific RAW formats, all at different rates and resolutions. Without a batching mechanism that adapts to this heterogeneity, accelerators either stall waiting for uniform batch shapes or waste compute on padding and reshaping. Item **iv** focuses on the mechanism that prevents this inefficiency: dynamic AI batching schedulers that assemble heterogeneous tensors into optimal batch configurations for GPUs, NPUs, DSPs, and vision processors. These schedulers preserve temporal alignment, maximize throughput, and ensure that the RAW tensors produced by the ISP-bypass stage flow smoothly into the fused compute pipeline.

iv. Dynamic AI Batching Schedulers for Heterogeneous Multi-Stream Frame Sizes

Dynamic AI batching schedulers are the **coordination layer** that sits at the end of the on-chip preprocessing pipeline. After inline decode, fused normalization/cropping, and RAW ISP-bypass paths, the system now has a continuous stream of tensors—video frames, LiDAR depth maps, radar heatmaps, neuromorphic event tiles—each with different spatial resolutions, temporal cadences, and modality-specific layouts. The batching scheduler’s job is to assemble these heterogeneous tensors into **compute-efficient batches** for GPUs, NPUs, DSPs, and vision processors, without breaking temporal alignment or wasting compute on padding and reshaping.

In a real autonomy stack, batching is not just about throughput; it’s about **preserving the physics of the scene** while feeding accelerators at their optimal operating point.

The Problem: Heterogeneous Shapes, Uniform Hardware Expectations

Accelerators like GPUs and NPUs prefer:

- fixed batch sizes
- regular tensor shapes
- predictable memory strides
- Sensors do not:
- Video may arrive as 4K, 1080p, or dynamically scaled resolutions.

- LiDAR depth maps have different aspect ratios and sparsity patterns.
- Radar heatmaps are often low-resolution but high-frequency.
- Neuromorphic event tiles are sparse, irregular, and bursty.

If the system insists on uniform shapes, it either:

- pads aggressively, wasting memory and compute, or
- serializes irregular inputs, underutilizing accelerators.

Dynamic batching schedulers exist to avoid both failure modes.

Core Responsibilities of the Dynamic Batching Scheduler

A dynamic AI batching scheduler:

- **Observes incoming tensors** from all modalities and streams.
- **Groups them into batches** that respect accelerator constraints (batch size, memory limits, preferred shapes).
- **Maintains temporal alignment**, ensuring that tensors in the same batch correspond to compatible time windows.
- **Minimizes padding and reshaping**, preserving as much native geometry as possible.
- **Adapts in real time** to changing sensor rates, resolutions, and pipeline load.

It is effectively a **real-time tensor traffic controller**.

Batch Formation Strategies

Common strategies include:

- **Resolution-aware grouping:** Group frames of similar resolution (e.g., 4K with 4K, 1080p with 1080p) to minimize padding.
- **Modality-aware batching:** Create batches that mix modalities in a controlled way (e.g., video + LiDAR + radar for fusion models) or keep them separate for modality-specific networks.
- **Time-window batching:** Assemble tensors that fall within a defined temporal window (e.g., last 50 ms) to preserve real-time alignment.
- **Load-adaptive batching:** Adjust batch size based on accelerator occupancy and queue

depth—larger batches when idle, smaller batches under high load or tight latency constraints.

These strategies are often combined into a single policy engine.

Integration with Unified Memory and Preprocessing

Because all tensors live in **unified virtual memory** and have already passed through on-chip preprocessing:

- The scheduler operates on **pointers and metadata**, not copies.
- It can batch tensors by simply assembling index lists and descriptors.
- Preprocessed tensors (resized, cropped, normalized, RAW-aligned) are ready for immediate inclusion in batches.
- No additional staging buffers or remaps are required.

This keeps batching **zero-copy and low-overhead**.

Temporal Alignment and Real-Time Guarantees

Dynamic batching must never break the real-time nature of the system:

- Late tensors (e.g., a delayed frame) may be dropped or moved to a separate batch rather than holding up the entire pipeline.
- Early tensors can be buffered briefly but not so long that they desynchronize from other modalities.
- Fusion-critical batches (e.g., those feeding a multimodal transformer) may enforce stricter alignment rules than modality-specific batches.

The scheduler therefore encodes time-aware policies, not just shape-aware ones.

Handling Burstiness and Rate Mismatch

Sensors rarely run at perfectly matched rates:

- Cameras may spike under certain exposure conditions.
- LiDAR may produce sweeps at fixed intervals.
- Radar may burst under specific detection modes.
- Neuromorphic sensors may fire heavily in dynamic scenes and go quiet otherwise.

Dynamic batching schedulers:

- Smooth burstiness by adjusting batch sizes and composition.
- Prevent any single modality from starving others.
- Ensure accelerators remain well-fed without overcommitting to one stream.

This is crucial for **multimodal robustness**.

System-Level Impact

Dynamic AI batching schedulers:

- Maximize accelerator utilization without sacrificing latency.
- Preserve temporal and geometric integrity of sensor data.
- Avoid wasteful padding and reshaping.
- Maintain zero-copy, unified-memory semantics.
- Enable multimodal fusion and transformer inference to operate at full sensor rate with realistic, heterogeneous inputs.

They are the final coordination layer of the on-chip preprocessing architecture—turning a flood of diverse tensors into **coherent, compute-efficient workloads** that match the hardware's strengths without compromising the physics of the scene.

The on-chip preprocessing architecture transforms raw sensor data into model-ready tensors entirely within the accelerator's memory hierarchy, preserving the zero-copy guarantees established by the ingestion layer. Dedicated bitstream parsers decode compressed and RAW streams inline, eliminating CPU involvement and host-side staging. Fused normalization and cropping pipelines reshape and scale tensors in parallel with inference, ensuring preprocessing never becomes a serial bottleneck. RAW ISP-bypass paths remove legacy color-space conversions and tone-mapping overhead, delivering linear sensor measurements directly to accelerators for AI-specific transforms. Dynamic batching schedulers then assemble heterogeneous tensors—4K video frames, LiDAR depth maps, radar heatmaps, neuromorphic event tiles—into compute-efficient batches that maintain temporal alignment and maximize accelerator utilization. Together, these mechanisms form a tightly integrated preprocessing fabric that operates at full sensor rate, stabilizes latency, and prepares multimodal data for real-time fusion and transformer inference.

With preprocessing now occurring entirely on-chip and tensors emerging in unified virtual

memory with deterministic timing, the next architectural challenge is synchronizing these heterogeneous modalities into a coherent perceptual moment. Autonomous systems rely on video, LiDAR, radar, IMU, and neuromorphic sensors that operate at different frequencies, resolutions, and latencies. Even with perfect ingestion and preprocessing, misaligned sensor streams can degrade fusion accuracy and destabilize downstream inference. The following discussion introduces the synchronization mechanisms that resolve this: sub-nanosecond fusion barriers, unified timestamping, temporal alignment engines, and cross-accelerator synchronization primitives. These mechanisms ensure that tensors produced by the preprocessing fabric converge into a single, temporally consistent representation of the environment—forming the foundation for high-fidelity multimodal fusion and real-time autonomous decision-making.

c. Multi-Modal AI Sensor Synchronization with Sub-Nanosecond Fusion Barriers

Zero-copy ingestion and on-chip preprocessing ensure that sensor data arrives in accelerator-resident memory with deterministic latency. The next architectural challenge is synchronizing these heterogeneous modalities—video, LiDAR, radar, IMU, neuromorphic sensors—into a single coherent perceptual moment. Multi-modal synchronization is not simply about aligning timestamps; it is about enforcing **sub-nanosecond fusion barriers** that guarantee temporal consistency across accelerators, DMA engines, and preprocessing pipelines. These barriers ensure that tensors entering multimodal fusion represent the same physical instant, even when sensors operate at different frequencies, resolutions, and burst patterns.

This synchronization layer is the **temporal backbone** of the autonomy stack. Without it, fusion becomes unstable, transformer inference becomes inconsistent, and downstream decision-making loses coherence.

Hardware-Injected AI Timestamps for Cross-Sensor Clock Alignment

Hardware-injected timestamps are the foundation of multi-modal synchronization. Instead of relying on software clocks—which drift, jitter, and desynchronize under load—each sensor stream receives timestamps injected at the hardware boundary:

- **FPGA-level timestamping** for LiDAR and radar
- **Sensor-bus timestamping** for cameras and IMUs
- **Neuromorphic event timestamping** at the ASIC edge
- **DMA-injected timestamps** when writing into unified memory

These timestamps are:

- monotonic
- drift-corrected
- synchronized to a global hardware clock
- visible to all accelerators in unified virtual memory

This ensures that every tensor carries a precise temporal identity before fusion.

AI Temporal Windowing and Out-of-Sync Packet Filtering Rules

Even with hardware timestamps, sensors produce data at different rates. Temporal windowing defines the **acceptable time horizon** for fusion:

- Video frames may define a ±2 ms window
- LiDAR sweeps may define a ±5 ms window
- Radar bursts may define a ±1 ms window
- Neuromorphic events may define a ±200 µs window

Packets outside their window are:

- dropped
- down-weighted
- or routed to late-fusion paths

This prevents stale or early packets from corrupting fusion layers. Temporal windowing is enforced inside accelerator memory, ensuring zero-copy filtering.

Unified AI Spatial Coordinate Transforms on Vector Fusion Fabrics

Temporal alignment is only half the problem; spatial alignment is equally critical. Unified coordinate transforms ensure that tensors from different sensors map into a shared spatial frame:

- Camera → LiDAR extrinsics
- Radar → vehicle frame transforms
- IMU → gravity-aligned transforms
- Neuromorphic → pixel-space transforms

These transforms run on **vector fusion fabrics**—accelerator-resident blocks optimized for matrix transforms, quaternions, and spatial projections. Because transforms operate directly on unified memory tensors, they avoid remapping overhead and preserve zero-copy semantics.

Late-Fusion AI Sync Barriers for Non-Deterministic Runtime Pipelines

Some pipelines—especially transformer-based fusion networks—are non-deterministic in their runtime behavior due to dynamic batching, adaptive attention, or modality-dependent compute paths. Late-fusion sync barriers ensure that:

- all modalities reach the fusion layer
- all tensors satisfy temporal window constraints
- all spatial transforms are complete
- no modality stalls the pipeline

These barriers operate at **sub-nanosecond precision**, enforced by hardware fences and accelerator-level synchronization primitives. They guarantee that fusion layers always receive a coherent multimodal snapshot, even when upstream pipelines vary in timing.

With the synchronization architecture now defined—hardware-injected timestamps, temporal windowing, unified spatial transforms, and late-fusion sync barriers—the next step is to consolidate these mechanisms into a structured operational view. Multi-modal AI systems depend on synchronization layers that behave as deterministic, accelerator-resident subsystems capable of aligning heterogeneous sensor modalities in both time and space before fusion. Table 8.4-D3 organizes these mechanisms into a coherent framework, showing how each contributes to sub-nanosecond temporal consistency, spatial coherence, and stable multimodal fusion under real-world sensor diversity. This table serves as the architectural anchor for understanding how synchronization preserves the guarantees established by ingestion and preprocessing and prepares tensors for high-fidelity fusion and transformer inference.

Table 8.4-D3 presents the core mechanisms that enable autonomous AI systems to synchronize video, LiDAR, radar, IMU, and neuromorphic sensors into a unified perceptual moment. Each mechanism addresses a specific challenge inherent in multimodal pipelines: clock drift, rate mismatch, stale packets, spatial misalignment, and non-deterministic runtime behavior. By structuring these mechanisms into a single operational view, the table clarifies how synchronization transforms heterogeneous sensor outputs into temporally aligned, spatially consistent tensors ready for fusion. It highlights the architectural shift from software-bound synchronization to hardware-enforced barriers that operate at sub-nanosecond precision within accelerator memory.

Table 8.4-D3 — Multi-Modal AI Sensor Synchronization Mechanisms and Their Operational Roles

Mechanism	AI-Specific Purpose	Operational Strategy	System-Level Effect
Hardware-Injected AI Timestamps	Cross-sensor clock alignment	Inject timestamps at sensor/DMA boundary	Deterministic temporal identity for all tensors
AI Temporal Windowing & Packet Filtering	Prevent stale or early data from corrupting fusion	Enforce modality-specific time windows	Stable fusion timing; reduced jitter
Unified Spatial Coordinate Transforms	Align modalities into a shared spatial frame	Apply transforms on vector fusion fabrics	Accurate multimodal geometry; zero-copy transforms
Late-Fusion AI Sync Barriers	Ensure coherent fusion under runtime variability	Hardware fences + accelerator sync primitives	Sub-nanosecond fusion consistency

Table 8.4-D3 consolidates the synchronization mechanisms that ensure multimodal tensors converge into a temporally and spatially coherent representation before fusion. Each mechanism preserves zero-copy guarantees and stabilizes multimodal inference under real-world sensor diversity.

Table 8.4-D3 reveals that multimodal synchronization is not a single operation but a coordinated set of hardware-resident mechanisms that collectively ensure temporal and spatial coherence across sensors. Hardware-injected timestamps eliminate clock drift by assigning each tensor a precise temporal identity at the sensor or DMA boundary. Temporal windowing and packet filtering enforce modality-specific timing constraints, preventing stale or early packets from corrupting fusion layers. Unified spatial coordinate transforms align tensors from different sensors into a shared geometric frame using vector fusion fabrics, ensuring that multimodal fusion operates on consistent spatial representations. Late-fusion sync barriers then guarantee that all modalities satisfy temporal and spatial constraints before entering fusion networks, even when upstream pipelines exhibit non-deterministic behavior due to dynamic batching or adaptive compute paths.

Together, these mechanisms form a synchronization substrate that is tightly coupled to the ingestion and preprocessing layers. They ensure that tensors converge into a coherent multimodal snapshot with sub-nanosecond precision, enabling transformer-based fusion and

downstream decision-making to operate with the temporal stability required for real-time autonomy. T8.4-D3 thus provides the conceptual map for understanding how synchronization transforms raw, heterogeneous sensor streams into unified, fusion-ready representations.

Table 8.4-D3 organizes the synchronization mechanisms—hardware-injected timestamps, temporal windowing, unified spatial transforms, and late-fusion sync barriers—into a structured operational framework. To complement this tabular view, Figure 8.4-D3 visualizes how these mechanisms operate as a unified synchronization fabric that aligns heterogeneous sensor modalities in both time and space before fusion. The figure shows how raw sensor outputs are timestamped at the hardware boundary, filtered through modality-specific temporal windows, transformed into a shared spatial frame, and finally gated through sub-nanosecond fusion barriers. This visual progression translates the table's conceptual architecture into a spatial, pipeline-level diagram that reveals how synchronization preserves temporal determinism and geometric coherence across accelerators.

Figure 8.4-D3 depicts the multi-modal synchronization architecture that ensures video, LiDAR, radar, IMU, and neuromorphic sensors converge into a coherent perceptual moment before fusion. Each panel highlights a critical synchronization mechanism—hardware timestamp injection, temporal windowing, spatial coordinate transforms, and late-fusion sync barriers—showing how alignment occurs entirely within accelerator-resident memory. Together, these mechanisms enforce sub-nanosecond timing precision and spatial consistency, enabling multimodal fusion and transformer inference to operate with the stability required for real-time autonomy.

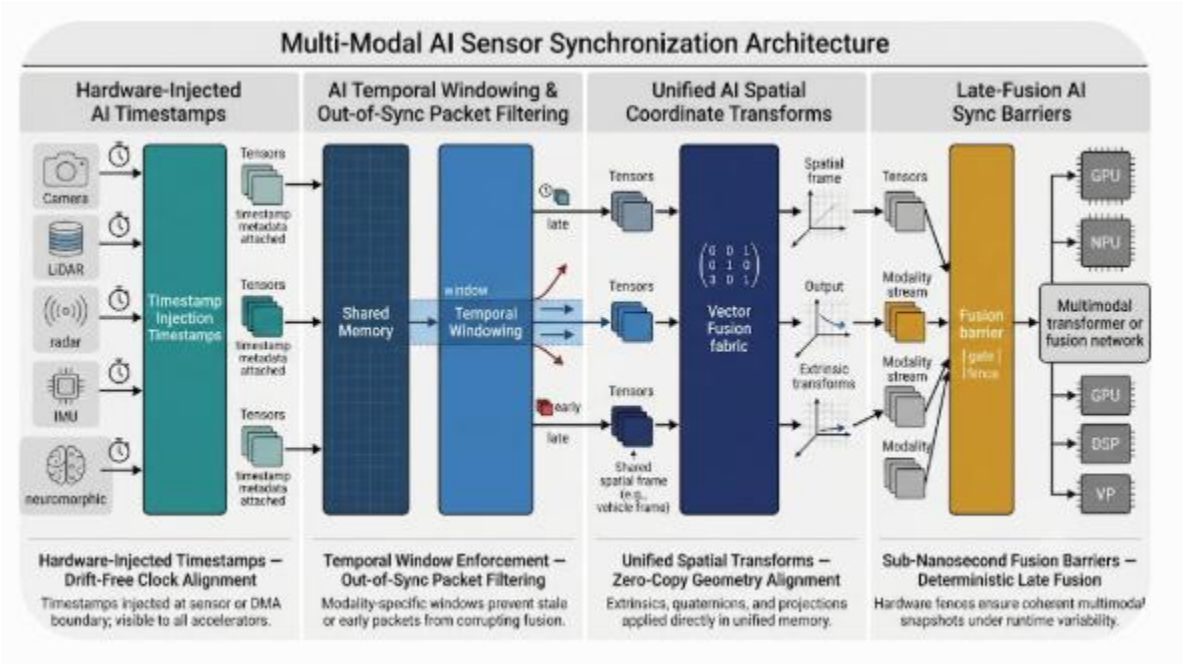


Figure 8.4-D3 — Multi-Modal AI Sensor Synchronization Architecture
The figure illustrates the four hardware-resident mechanisms that align heterogeneous sensor modalities in time and space before fusion: hardware-injected timestamps, temporal windowing, unified spatial transforms, and late-fusion sync barriers. These mechanisms enforce sub-nanosecond temporal consistency and spatial coherence across accelerators, enabling stable multimodal inference in real-time autonomous systems.

Legend

- ***Gray sensor icons:*** *Camera, LiDAR, radar, IMU, neuromorphic sensors*
- ***Teal blocks:*** *Hardware timestamp injection modules*
- ***Blue blocks:*** *Temporal windowing and packet filtering engines*
- ***Navy blocks:*** *Vector fusion fabrics performing spatial transforms*
- ***Gold/orange blocks:*** *Late-fusion synchronization barriers*
- ***Medium gray blocks:*** *GPU, NPU, DSP, vision processor*
- ***Unified memory region:*** *Dark blue shared memory fabric*
- ***Arrows:*** *Data flow direction*
- ***Clock icons:*** *Timestamp metadata*
- ***Window bands:*** *Temporal acceptance ranges*

Figure 4.10-112 demonstrates how autonomous AI systems achieve sub-nanosecond synchronization across heterogeneous sensor modalities. The first panel shows hardware-injected timestamps that eliminate clock drift by assigning each tensor a precise temporal identity at the sensor or DMA boundary. The second panel illustrates temporal windowing, where modality-specific timing constraints filter out stale or early packets, ensuring that only temporally valid tensors proceed to fusion. The third panel highlights unified spatial coordinate transforms applied on vector fusion fabrics, aligning tensors from different sensors into a shared geometric frame without leaving unified memory. The final panel depicts late-fusion sync barriers that enforce deterministic convergence of all modalities before entering multimodal transformers or fusion networks, even when upstream pipelines exhibit non-deterministic timing due to dynamic batching or adaptive compute paths.
With the synchronization architecture now framed at a systems level—showing how multimodal data must be temporally validated, spatially aligned, and gated through deterministic fusion barriers—the natural starting point for deeper exploration is the foundation of all temporal coherence: **hardware-injected AI timestamps**. Before any temporal windowing, packet filtering, spatial transforms, or late-fusion barriers can operate, each sensor stream must carry a precise, drift-free temporal identity that is visible to every accelerator in unified memory. Item **i** focuses on this critical first mechanism, where timestamps are injected at the sensor or DMA boundary,

establishing a global temporal reference that anchors all subsequent synchronization stages. This timestamping layer ensures that every tensor entering the fusion pipeline is grounded in a shared hardware clock, forming the temporal backbone upon which multimodal alignment and sub-nanosecond fusion guarantees are built.

i. Hardware-Injected AI Timestamps for Cross-Sensor Clock Alignment

Hardware-injected AI timestamps form the **temporal foundation** of multimodal synchronization. Before any filtering, windowing, spatial transforms, or fusion barriers can operate, each sensor stream must carry a precise, drift-free temporal identity that is visible to every accelerator in unified memory. This timestamping layer is not a software convenience—it is a **hardware-enforced temporal substrate** that anchors all subsequent alignment stages.

Modern autonomous systems ingest data from sensors with wildly different timing characteristics:

- Cameras: 30–120 FPS, rolling or global shutter
- LiDAR: 5–20 Hz sweeps with per-beam micro-timing
- Radar: burst-mode micro-doppler returns
- IMU: 200–2000 Hz inertial packets
- Neuromorphic sensors: microsecond-scale event streams

Without a unified temporal reference, these modalities cannot be fused reliably. Hardware-injected timestamps solve this by assigning each tensor a **global, monotonic, drift-corrected timestamp** at the earliest possible boundary.

Timestamp Injection at the Sensor or DMA Boundary

The timestamp is injected:

- **at the sensor ASIC**, for neuromorphic and radar devices
- **at the FPGA edge**, for LiDAR and high-rate radar
- **at the sensor bus controller**, for cameras and IMUs
- **at the DMA engine**, when writing into unified memory

This ensures timestamps reflect the **true physical capture moment**, not a delayed software event.

These timestamps are:

- **monotonic** (never decreasing)
- **drift-corrected** (aligned to a global hardware clock)
- **accelerator-visible** (stored in unified virtual memory)
- **zero-copy** (attached as metadata, not a separate buffer)

Every tensor entering the pipeline carries this temporal identity.

Global Hardware Clock Synchronization

All timestamp injection points synchronize to a **global hardware clock**, typically:

- a high-precision oscillator
- a PTP-synced clock domain
- a vehicle-wide timing fabric
- or a fusion-fabric-wide nanosecond clock grid

This eliminates:

- clock drift between sensors
- jitter introduced by OS scheduling
- timestamp skew caused by driver latency
- inconsistent timing across accelerators

The entire multimodal pipeline becomes **clock-coherent**.

Timestamp Metadata Embedded in Unified Memory

Timestamps are stored as metadata alongside tensors in unified virtual memory:

- no remapping
- no staging buffers
- no host-side timestamp injection
- no kernel/user transitions

Accelerators read timestamps directly from the same memory region that stores the tensor data. This allows:

- temporal windowing
- packet filtering
- spatial transforms
- fusion barriers

to operate without copying or reformatting data.

Sub-Nanosecond Precision Requirements

Autonomous systems require **sub-nanosecond precision** for:

- radar micro-doppler alignment
- LiDAR beam-level timing
- neuromorphic event clustering
- IMU integration
- transformer-based temporal fusion

Hardware-injected timestamps meet these requirements by:

- using high-frequency clock domains
- applying drift correction
- enforcing hardware fences
- guaranteeing deterministic timestamp propagation

This precision is essential for stable multimodal fusion.

System-Level Impact

Hardware-injected timestamps:

- establish a global temporal identity for every tensor
- eliminate clock drift and software timestamp jitter
- enable deterministic temporal windowing
- allow accelerators to perform time-aware fusion
- anchor all subsequent synchronization mechanisms

They form the **temporal backbone** of the multimodal synchronization architecture.

With hardware-injected timestamps now anchoring every sensor stream to a global, drift-free clock, the next architectural challenge is determining which tensors are temporally valid for fusion. Sensors operate at different rates, produce bursts, and occasionally deliver packets that are early, late, or stale relative to the fusion moment. Item ii focuses on the mechanism that enforces temporal correctness: AI temporal windowing and out-of-sync packet filtering. These rules define modality-specific time horizons, drop or down-weight packets outside their acceptable windows, and ensure that only temporally coherent tensors proceed to spatial alignment and fusion. This stage transforms raw timestamp metadata into actionable temporal guarantees, preserving the stability of multimodal inference under real-world timing variability.

ii. AI Temporal Windowing and Out-of-Sync Packet Filtering Rules

AI temporal windowing is the **second stage** of multimodal synchronization, sitting immediately after hardware-injected timestamps. Once every sensor packet carries a precise, drift-free timestamp, the system must determine whether that packet is **temporally valid** for fusion. Sensors operate at different rates, produce bursts, and occasionally deliver packets that are early, late, or stale relative to the fusion moment. Temporal windowing defines the acceptable time horizon for each modality and filters packets that fall outside it, ensuring that only temporally coherent tensors proceed to spatial alignment and fusion.

This stage transforms raw timestamp metadata into **temporal correctness guarantees**, stabilizing multimodal inference under real-world timing variability.

Modality-Specific Temporal Windows

Each sensor modality has a different temporal tolerance based on its physics and sampling rate:

- **Video**: ±2–3 ms
- **LiDAR**: ±5–10 ms (depending on sweep rate)
- **Radar**: ±1 ms (burst-mode micro-doppler)
- **IMU**: ±0.1–0.5 ms (high-rate inertial packets)
- **Neuromorphic sensors:** ±50–200 µs (event-driven microsecond timing)

These windows define the **temporal acceptance band** for fusion. A packet is considered valid only if its timestamp falls within the modality's window relative to the fusion moment.

Out-of-Sync Packet Detection

Packets outside their temporal window are classified as:

- **Early packets** — captured too soon relative to the fusion moment
- **Late packets** — captured too late
- **Stale packets** — significantly older than the current fusion cycle
- **Burst packets** — arriving in clusters that exceed expected rate

Detection occurs entirely within accelerator-resident memory, using timestamp metadata attached during hardware injection.

Out-of-Sync Packet Filtering Rules

Filtering rules determine how the system handles invalid packets:

- **Drop:** Packets far outside the window are discarded to prevent corrupting fusion.
- **Down-weight:** Slightly early or late packets may be included but with reduced influence in fusion layers.
- **Route to late-fusion paths:** Some packets may be processed in secondary fusion stages that tolerate temporal misalignment.
- **Hold briefly:** Packets slightly early may be buffered for a few microseconds until they fall within the window.

These rules prevent temporal contamination of fusion layers and maintain stable inference.

Zero-Copy Enforcement in Unified Memory

Temporal windowing and filtering operate directly on unified virtual memory:

- No remapping
- No staging buffers
- No host-side filtering
- No kernel/user transitions

Accelerators read timestamps and apply windowing rules **in place**, preserving zero-copy guarantees and minimizing latency.

Temporal Consistency Under Real-World Conditions

Real-world sensor behavior is messy:

- Cameras may jitter under exposure changes
- LiDAR sweeps may vary slightly in timing
- Radar bursts may shift under detection modes
- Neuromorphic sensors may spike under motion
- IMUs may deliver packets at extremely high rates

Temporal windowing stabilizes this variability by enforcing **strict temporal coherence**, ensuring that fusion layers receive tensors representing the same physical moment.

System-Level Impact

AI temporal windowing:

- prevents stale or early packets from corrupting fusion
- enforces modality-specific timing constraints
- stabilizes multimodal inference
- reduces jitter in downstream transformer layers
- prepares tensors for spatial alignment and fusion barriers

It is the **temporal gatekeeper** of the synchronization architecture.

With temporal windowing now ensuring that only time-valid packets proceed, the next architectural challenge is aligning these tensors spatially. Even perfectly synchronized sensor streams cannot be fused unless they share a **common geometric frame**. Cameras operate in pixel space, LiDAR in 3D point clouds, radar in range-Doppler grids, IMUs in inertial frames, and neuromorphic sensors in event-driven pixel maps. Item **iii** focuses on the mechanism that resolves this spatial diversity: unified AI coordinate transforms executed on vector fusion fabrics. These transforms project all modalities into a shared spatial frame—applying extrinsics, rotations, quaternions, and projection matrices directly in unified memory—ensuring that multimodal fusion operates on geometrically consistent tensors.

iii. Unified AI Spatial Coordinate Transforms on Vector Fusion Fabrics

Unified AI spatial coordinate transforms are the **third pillar** of multimodal synchronization. Once sensor packets have been timestamped at the hardware boundary and filtered through modality-specific temporal windows, the system must resolve the **spatial misalignment** inherent in heterogeneous sensors. Cameras operate in pixel space, LiDAR in 3D point clouds,

radar in range-Doppler grids, IMUs in inertial frames, and neuromorphic sensors in event-driven pixel maps. Without a unified spatial frame, fusion layers cannot reason coherently about geometry, motion, or object identity.

Spatial transforms executed on **vector fusion fabrics** solve this by projecting all modalities into a shared coordinate system—typically the vehicle frame or a world-aligned frame—using high-throughput, accelerator-resident math engines optimized for matrix operations, quaternions, and projection pipelines.

These transforms ensure that multimodal fusion operates on **geometrically consistent tensors**, not a patchwork of incompatible coordinate systems.

The Need for Spatial Unification

Each sensor modality encodes geometry differently:

- **Cameras**: 2D pixel grids with perspective distortion
- **LiDAR**: 3D point clouds with beam-level timing
- **Radar**: range-Doppler grids with angular uncertainty
- **IMU**: inertial vectors in body-frame coordinates
- **Neuromorphic sensors**: sparse event maps with microsecond timing

Fusion networks—especially transformer-based architectures—require all modalities to be expressed in a **shared spatial frame**. Without this, cross-modal attention collapses, object association becomes unstable, and geometric reasoning becomes inconsistent.

Vector Fusion Fabrics: The Spatial Compute Backbone

Vector fusion fabrics are accelerator-resident blocks designed for:

- matrix multiplication
- quaternion rotation
- extrinsic transforms
- projection matrices
- coordinate frame conversions
- spatial interpolation
- geometry normalization

They operate directly on unified virtual memory, ensuring:

- zero-copy transforms
- deterministic latency
- high-throughput spatial alignment
- consistent geometry across modalities

These fabrics are optimized for the spatial math required by multimodal fusion.

Extrinsic and Intrinsic Transforms

Spatial alignment requires two classes of transforms:

Extrinsic Transforms (Sensor → Vehicle Frame)

These convert sensor measurements into a shared vehicle-aligned frame:

- rotation matrices
- translation vectors
- rigid-body transforms
- calibration matrices

Extrinsics ensure that all sensors describe geometry relative to the same physical origin.

Intrinsic Transforms (Sensor → Sensor-Native Geometry)

These correct for sensor-specific distortions:

- camera intrinsics (focal length, principal point)
- LiDAR beam angle corrections
- radar range-angle calibration
- neuromorphic pixel-space normalization

Intrinsics ensure that raw sensor geometry is properly interpreted before fusion.

Projection Pipelines for Cross-Modal Alignment

Projection pipelines convert modalities into compatible geometric representations:

- **Camera → 3D projection** using depth or LiDAR

- **LiDAR → image plane projection** for pixel-aligned fusion
- **Radar → spatial grid projection** for transformer-based fusion
- **IMU → gravity-aligned frame** for motion compensation
- **Neuromorphic → pixel-aligned event maps** for temporal fusion

These projections allow fusion networks to treat heterogeneous modalities as **spatially compatible tensors**.

Zero-Copy Spatial Alignment in Unified Memory

Spatial transforms operate directly on unified virtual memory:

- no remapping
- no staging buffers
- no host-side geometry transforms
- no kernel/user transitions

This preserves the zero-copy guarantees established by ingestion and preprocessing and ensures that spatial alignment does not introduce latency or jitter.

Spatial Consistency Under Real-World Conditions

Real-world geometry is messy:

- vehicle motion introduces dynamic transforms
- sensor mounts vibrate
- calibration drifts over time
- LiDAR beams fire at slightly different angles
- radar returns vary with environment
- neuromorphic sensors produce sparse, irregular events

Vector fusion fabrics compensate for these effects by applying:

- dynamic extrinsics
- motion-compensated transforms
- calibration correction

- spatial interpolation
- geometry normalization

This ensures that fusion layers receive **stable, spatially coherent tensors** even under real-world variability.

System-Level Impact

Unified AI spatial coordinate transforms:

- align all modalities into a shared geometric frame
- preserve zero-copy semantics
- stabilize spatial reasoning
- enable cross-modal attention in fusion networks
- prepare tensors for late-fusion sync barriers
- ensure geometric consistency across accelerators

They form the **spatial backbone** of the multimodal synchronization architecture.

With spatial transforms now projecting all modalities into a unified geometric frame, the final synchronization challenge is ensuring that these temporally valid, spatially aligned tensors converge at the fusion layer in a deterministic manner. Real-world pipelines—especially those involving dynamic batching, adaptive attention, or modality-dependent compute paths—exhibit non-deterministic timing. Item **iv** focuses on the mechanism that resolves this variability: late-fusion AI sync barriers. These barriers enforce sub-nanosecond convergence across modalities, guaranteeing that fusion networks receive a coherent multimodal snapshot even when upstream pipelines vary in timing. They are the final gate that stabilizes multimodal inference under real-world operational conditions.

iv. Late-Fusion AI Sync Barriers for Non-Deterministic Runtime Pipelines

Late-fusion AI sync barriers are the **final synchronization mechanism** in the multimodal alignment architecture. Even after hardware-injected timestamps, temporal windowing, and unified spatial transforms have ensured that sensor data is temporally valid and spatially coherent, the pipeline still faces a fundamental challenge: **non-deterministic runtime behavior** in modern AI workloads.

Real-world multimodal pipelines—especially those involving dynamic batching, adaptive

attention, modality-dependent compute paths, or transformer-based fusion networks—do not execute in perfectly predictable patterns. Their execution time varies based on:

- batch composition
- modality availability
- accelerator load
- dynamic attention routing
- sparsity patterns
- scene complexity

This variability can cause modalities to arrive at fusion layers at slightly different times, even when they are temporally valid and spatially aligned. Late-fusion sync barriers solve this by enforcing **sub-nanosecond convergence** across modalities, guaranteeing that fusion networks receive a coherent multimodal snapshot regardless of upstream timing variability.

These barriers are the **temporal and spatial gatekeepers** that stabilize multimodal inference under real-world operational conditions.

The Problem: Non-Deterministic Runtime Pipelines

Modern AI pipelines are inherently non-deterministic:

- **Dynamic batching schedulers** adjust batch sizes based on load.
- **Adaptive attention networks** route computation differently depending on scene content.
- **Sparse tensor engines** skip computation on empty regions.
- **Modality-dependent pipelines** (e.g., radar vs. video) have different compute paths.
- **Accelerator contention** varies with system load.

Even with perfect timestamping and spatial alignment, these factors cause **arrival skew** at fusion layers.

Late-fusion sync barriers eliminate this skew.

Hardware-Enforced Fusion Barriers

Late-fusion sync barriers are implemented as **hardware fences** inside the accelerator fabric:

- GPU/NPU/DSP/VP pipelines must reach the barrier before fusion proceeds.
- The barrier checks temporal validity (timestamp alignment).
- The barrier checks spatial validity (coordinate transforms complete).
- The barrier checks modality completeness (all required modalities present).
- The barrier releases the fusion operation only when all conditions are satisfied.

This ensures that fusion networks operate on **complete, coherent multimodal tensors**.

Sub-Nanosecond Convergence Guarantees

Fusion barriers operate at **sub-nanosecond precision**, enforced by:

- high-frequency hardware clocks
- deterministic DMA scheduling
- accelerator-level synchronization primitives
- unified memory fences
- vector fabric timing grids

This precision is essential for:

- radar micro-doppler fusion
- LiDAR beam-level alignment
- neuromorphic event clustering
- IMU-driven motion compensation
- transformer-based temporal fusion

Even microsecond-scale misalignment can degrade fusion accuracy; sub-nanosecond barriers prevent this.

Modality-Aware Fusion Policies

Fusion barriers enforce modality-aware rules:

- **Mandatory modalities**: e.g., video + LiDAR must be present for geometric fusion.
- **Optional modalities**: e.g., radar or neuromorphic events may be included when available.

- **Fallback paths**: If a modality is missing but within tolerance, fusion may proceed with adjusted weighting.
- **Late-arrival routing**: Late packets may be routed to secondary fusion layers.

These policies ensure robust fusion under real-world sensor variability.

Zero-Copy Fusion Barrier Enforcement

Fusion barriers operate directly on unified virtual memory:

- no remapping
- no staging buffers
- no host-side synchronization
- no kernel/user transitions

All checks—timestamp alignment, spatial validity, modality completeness—occur **in place**, preserving zero-copy guarantees and minimizing latency.

Stabilizing Transformer-Based Fusion Networks

Transformer-based multimodal fusion networks are particularly sensitive to timing:

- cross-modal attention requires aligned tokens
- temporal embeddings require consistent timestamps
- spatial embeddings require unified coordinate frames
- modality dropout must be handled deterministically

Late-fusion sync barriers ensure that transformers receive:

- temporally aligned tokens
- spatially consistent embeddings
- complete modality sets
- deterministic input sequences

This stabilizes transformer inference under dynamic, real-world conditions.

System-Level Impact

Late-fusion AI sync barriers:

- eliminate arrival skew caused by non-deterministic pipelines
- enforce sub-nanosecond convergence across modalities
- stabilize multimodal fusion networks
- preserve temporal and spatial coherence
- ensure deterministic behavior under dynamic batching and adaptive compute
- complete the synchronization architecture's temporal-spatial guarantees

They are the **final gate** that ensures multimodal fusion operates on coherent, physics-aligned representations of the environment.

Multi-modal AI synchronization establishes the temporal and spatial backbone that allows heterogeneous sensor streams to behave as a single, coherent perceptual system. Hardware-injected timestamps anchor every packet to a drift-free global clock, ensuring that all modalities begin with a shared temporal identity. AI temporal windowing and packet filtering enforce modality-specific timing constraints, preventing stale or early data from contaminating fusion. Unified spatial coordinate transforms project all sensor outputs into a common geometric frame using vector fusion fabrics, eliminating spatial misalignment and enabling consistent cross-modal reasoning. Late-fusion sync barriers then resolve the non-deterministic timing behavior of modern AI pipelines—dynamic batching, adaptive attention, and modality-dependent compute paths—by enforcing sub-nanosecond convergence across modalities before fusion. Together, these mechanisms guarantee that multimodal fusion networks operate on temporally aligned, spatially coherent, and deterministically synchronized tensors, even under real-world variability and high-rate sensor conditions.

With multimodal synchronization ensuring that all sensor streams arrive temporally aligned, spatially unified, and fusion-ready, the next challenge is sustaining this coherence under extreme data throughput. Autonomous systems routinely ingest massive volumes of video frames, LiDAR sweeps, radar bursts, and neuromorphic events—often exceeding gigabytes per second. If decoding and storage paths cannot keep pace, accelerators starve, fusion layers stall, and temporal alignment collapses. The next topic introduces the high-bandwidth infrastructure that prevents these failures: direct NVMe streaming paths that bypass traditional I/O bottlenecks, on-chip frame decoding engines capable of sustaining sensor-rate throughput, and starvation-control schedulers that maintain steady accelerator feed rates even under bursty or uneven sensor loads. This continuation extends the guarantees of synchronization into the domain of bandwidth and pipeline stability, ensuring that fusion-ready tensors continue flowing at full sensor rate without stalls or jitter.

d. High-Bandwidth AI Frame Decoding with Direct NVMe Streaming and Pipeline Starvation Control

High-bandwidth AI frame decoding is the throughput backbone that keeps accelerators continuously fed with sensor-rate data. Even with perfect synchronization, multimodal fusion collapses if the decoding and storage subsystem cannot sustain the ingest rate of modern autonomy workloads. Video streams at multi-gigabit rates, LiDAR sweeps with hundreds of thousands of points, radar bursts with dense micro-doppler signatures, and neuromorphic event streams with microsecond granularity all demand decoding pipelines that operate at the same cadence as the sensors themselves.

This domain combines **storage-class memory interconnects**, **dedicated bitstream decode arrays**, **pipeline starvation telemetry**, and **ring-buffer stability techniques** to ensure that accelerators never stall, jitter, or starve under real-world load.

AI Storage-Class Memory Interconnects with Direct GPU-Driven Frame Ingest

Traditional I/O paths—kernel drivers, host buffers, PCIe bounce buffers—cannot sustain sensor-rate ingest. AI storage-class memory interconnects solve this by enabling **direct GPU-driven frame ingest** from NVMe devices:

- NVMe → GPU DMA without CPU involvement
- Unified virtual memory mapping of NVMe pages
- GPU-initiated read commands
- Zero-copy frame delivery into accelerator-resident buffers

This architecture eliminates:

- host-side memcpy chains
- kernel/user transitions
- PCIe round-trip latency
- CPU bottlenecks during burst ingest

The GPU becomes the **primary consumer** of NVMe bandwidth, pulling frames directly into memory regions used for preprocessing and inference.

Dedicated AI Huffman-Decode Arrays for JPEG-XL and AV1 Bitstream Slices

Modern codecs—JPEG-XL, AV1, H.266/VVC—use complex entropy coding that is

computationally expensive to decode on general-purpose cores. Dedicated AI Huffman-decode arrays solve this by:

- parallelizing entropy decode across many small hardware units
- slicing bitstreams into independent segments
- decoding slices directly into unified memory
- bypassing CPU-bound decode libraries entirely

These arrays operate at **sensor-rate throughput**, enabling:

- multi-gigapixel video ingest
- high-density LiDAR intensity map decode
- radar burst decode with micro-doppler preservation
- neuromorphic event tile reconstruction

The result is a **hardware-resident decode pipeline** that matches the bandwidth of modern sensors.

AI Queue-Depth Tuning with Pipeline Starvation Telemetry and Runtime Monitors

Even with high-bandwidth ingest, accelerators can starve if queue depths are misconfigured. AI queue-depth tuning uses:

- real-time telemetry
- starvation counters
- decode-latency monitors
- burst-rate predictors
- accelerator occupancy metrics

to dynamically adjust:

- queue depth
- batch size
- decode parallelism
- NVMe read-ahead

- DMA scheduling

This ensures that accelerators remain **continuously fed**, even under bursty or uneven sensor loads.

Pipeline starvation telemetry detects:

- decode stalls
- NVMe under-utilization
- queue depletion
- burst overload
- modality imbalance, and
- adjusts ingest parameters in real time.

AI Ring-Buffer Stability Techniques for Massive Multi-Slice Streaming Workloads

Massive multi-slice workloads—multi-camera rigs, multi-beam LiDAR, multi-burst radar—

require ring buffers that remain stable under extreme ingest rates. AI ring-buffer stability techniques include:

- adaptive ring-buffer sizing
- slice-aware write pointers
- starvation-safe read pointers
- backpressure signaling
- burst-mode smoothing
- temporal-window alignment with synchronization layers

These techniques prevent:

- buffer overrun
- buffer underrun
- pointer desynchronization
- slice fragmentation
- temporal skew between slices

Ring buffers become **self-stabilizing**, ensuring that decoding pipelines never collapse under high-rate ingest.

With the high-bandwidth decoding architecture now defined—direct NVMe streaming, parallel entropy-decode arrays, starvation-aware queue-depth tuning, and adaptive ring-buffer stability—the next step is to consolidate these mechanisms into a structured operational view. High-rate autonomy workloads depend on decoding pipelines that behave as deterministic, accelerator-resident subsystems capable of sustaining multi-gigabit ingest without stalls or jitter. Table 8.4-D4 organizes these mechanisms into a coherent framework, showing how each contributes to continuous accelerator feed, decode stability, and starvation-free throughput under massive multi-slice sensor loads. This table serves as the architectural anchor for understanding how decoding and ingest preserve the guarantees established by synchronization and ensure that fusion-ready tensors continue flowing at full sensor rate.

Table 8.4-D4 presents the core mechanisms that enable high-bandwidth AI systems to decode, ingest, and stabilize sensor-rate workloads. Each mechanism addresses a specific throughput challenge inherent in modern autonomy pipelines: eliminating CPU bottlenecks, decoding complex bitstreams at sensor cadence, preventing starvation during burst ingest, and maintaining ring-buffer stability under multi-slice workloads. By structuring these mechanisms into a single operational view, the table clarifies how decoding transforms raw NVMe-resident bitstreams into accelerator-ready tensors while preserving zero-copy semantics and pipeline continuity. It highlights the architectural shift from host-bound decoding to fully hardware-resident ingest paths that operate at the same rate as the sensors themselves.

Table 8.4-D4 — High-Bandwidth AI Frame Decoding Mechanisms and Their Operational Roles

Mechanism	AI-Specific Purpose	Operational Strategy	System-Level Effect
Storage-Class Memory Interconnects	Direct GPU-driven ingest	NVMe → GPU DMA, zero-copy	Eliminates CPU bottlenecks; sustains sensor-rate throughput
AI Huffman-Decode Arrays	Hardware-resident bitstream decode	Parallel slice decode into unified memory	Multi-gigabit video and sensor decode at full rate
Queue-Depth Tuning & Telemetry	Prevent pipeline starvation	Dynamic queue adjustment via runtime monitors	Stable accelerator feed; no stalls under burst load

Mechanism	AI-Specific Purpose	Operational Strategy	System-Level Effect
Ring-Buffer Stability Techniques	Maintain ingest coherence	Adaptive sizing, backpressure, slice-aware pointers	Prevents overrun/underrun; stabilizes multi-slice workloads

Table 8.4-D4 consolidates the decoding and ingest mechanisms that sustain high-bandwidth sensor pipelines. Each mechanism ensures that accelerators receive a continuous stream of fusion-ready tensors without stalls, jitter, or starvation.

Table 8.4-D4 reveals that high-bandwidth frame decoding is not a single subsystem but a coordinated set of hardware-resident mechanisms that collectively ensure continuous accelerator feed under extreme ingest conditions. Storage-class memory interconnects eliminate traditional I/O bottlenecks by allowing GPUs to pull frames directly from NVMe devices without CPU involvement. Dedicated Huffman-decode arrays parallelize entropy decoding for modern codecs such as JPEG-XL and AV1, enabling bitstream slices to be reconstructed at sensor-rate throughput directly into unified memory. Queue-depth tuning and starvation telemetry provide real-time feedback loops that adjust ingest parameters dynamically, preventing accelerators from stalling during bursty or uneven sensor loads. Finally, ring-buffer stability techniques maintain coherent ingest under massive multi-slice workloads, preventing overrun, underrun, and pointer desynchronization.

Together, these mechanisms form a throughput backbone that complements the temporal-spatial guarantees established earlier. They ensure that fusion-ready tensors continue flowing into the perception stack at full sensor rate, without stalls, jitter, or starvation—even when sensors operate at extreme bandwidth and real-world variability. Table 4.10-130 thus provides the conceptual map for understanding how decoding and ingest transform raw storage-class data streams into stable, high-rate inputs for multimodal AI systems.

Table 8.4-D4 organizes the high-bandwidth decoding mechanisms—direct NVMe streaming, parallel entropy-decode arrays, starvation-aware queue-depth tuning, and adaptive ring-buffer stability—into a structured operational framework. To complement this tabular view, Figure 8.4-D4 visualizes how these mechanisms operate as a unified throughput fabric that sustains sensor-rate ingest under massive multi-slice workloads. The figure shows how raw NVMe bitstreams are pulled directly into GPU memory, decoded at hardware speed, stabilized through telemetry-driven queue management, and buffered through adaptive ring-buffer engines. This visual progression translates the table's conceptual architecture into a pipeline-level diagram that reveals how decoding and ingest maintain continuous accelerator

feed without stalls, jitter, or starvation.

Figure 8.4-D4 depicts the high-bandwidth decoding architecture that enables autonomous AI systems to ingest and decode sensor-rate workloads without pipeline starvation. Each panel highlights a critical throughput mechanism—direct NVMe → GPU streaming, parallel entropy-decode arrays, starvation-aware queue-depth tuning, and adaptive ring-buffer stability—showing how raw bitstreams are transformed into fully decoded, starvation-free tensors inside unified memory. Together, these mechanisms ensure that accelerators remain continuously fed, even under bursty, uneven, or multi-slice sensor conditions.

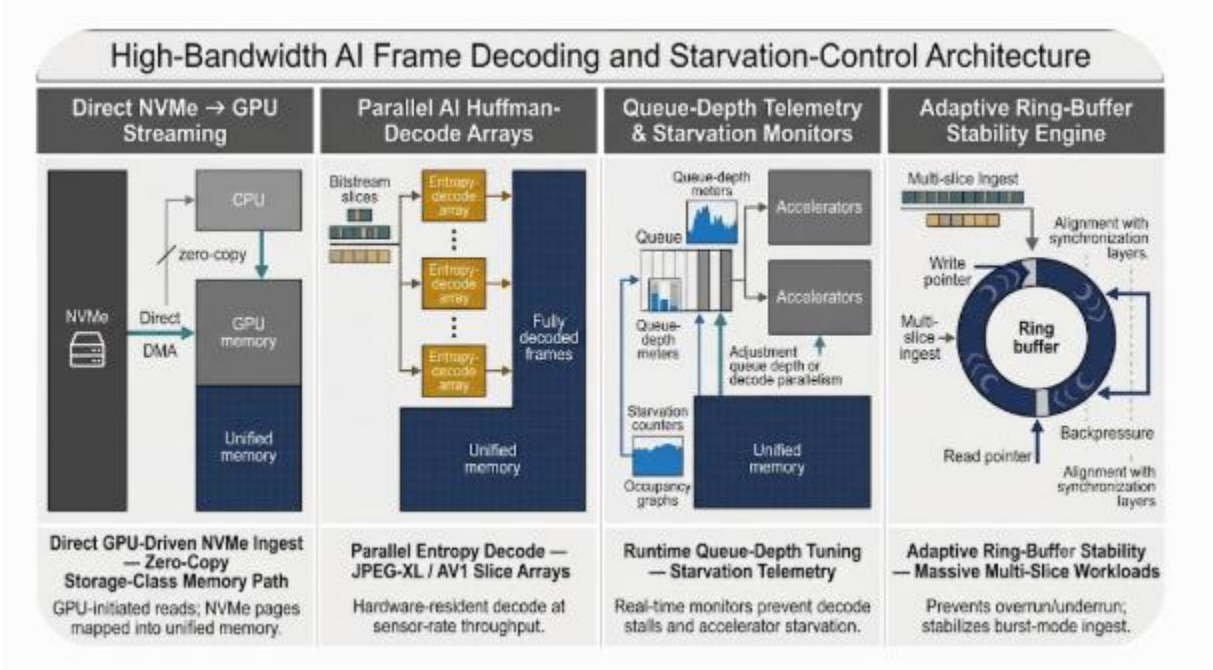


Figure 8.4-D4 — High-Bandwidth AI Frame Decoding and Starvation-Control Architecture
The figure illustrates the four hardware-resident mechanisms that sustain sensor-rate ingest under extreme bandwidth: direct NVMe → GPU streaming, parallel entropy-decode arrays, starvation-aware queue-depth tuning, and adaptive ring-buffer stability. These mechanisms ensure continuous accelerator feed without stalls, jitter, or starvation, even under massive multi-slice workloads.

Legend

- ***Dark gray NVMe device:*** *Storage-class memory source*
- ***Teal DMA arrows:*** *Direct NVMe → GPU streaming paths*
- ***Unified memory region (dark blue):*** *Shared accelerator-resident memory fabric*
- ***Gold/orange decode blocks:*** *Parallel entropy-decode arrays (JPEG-XL / AV1 slices)*
- ***Blue telemetry indicators:*** *Queue-depth graphs, starvation counters, occupancy monitors*

- ***Medium gray accelerator blocks:*** *GPU, NPU, DSP, VP*
- ***Navy ring-buffer engine:*** *Adaptive circular buffer with dynamic pointers*
- ***Backpressure arrows:*** *Flow-control signals preventing overrun/underrun*
- ***Bitstream slices:*** *Segmented rectangles entering decode arrays*

Figure 8.4-D4 demonstrates how high-bandwidth AI systems maintain continuous accelerator feed under extreme ingest conditions. The first panel shows direct NVMe → GPU streaming, where GPUs pull frames directly from storage-class memory without CPU involvement, eliminating traditional I/O bottlenecks. The second panel illustrates parallel entropy-decode arrays that reconstruct JPEG-XL and AV1 bitstream slices at sensor-rate throughput directly into unified memory. The third panel highlights queue-depth telemetry and starvation monitors that dynamically adjust decode parallelism and ingest parameters to prevent stalls and maintain steady accelerator occupancy. The final panel depicts an adaptive ring-buffer stability engine that prevents overrun, underrun, and pointer desynchronization during massive multi-slice workloads, ensuring that decoded frames remain temporally aligned with upstream synchronization layers.

Together, these panels reveal a decoding architecture designed for real-time autonomy. They show how raw NVMe-resident bitstreams are streamed, decoded, stabilized, and buffered entirely within accelerator-resident memory, preserving zero-copy semantics and preventing starvation even under burst-mode ingest. This ensures that fusion-ready tensors continue flowing into the perception stack at full sensor rate, complementing the temporal-spatial guarantees established earlier.

With the decoding and starvation-control mechanisms now organized into a coherent operational framework, the natural starting point for deeper exploration is the foundation of all high-bandwidth ingest: **direct GPU-driven access to storage-class memory**. Before parallel entropy-decode arrays, queue-depth telemetry, or ring-buffer stability engines can operate, raw sensor bitstreams must reach accelerator-resident memory at full NVMe bandwidth without CPU bottlenecks or I/O round-trip latency. Item **i** focuses on this critical first mechanism, where GPUs initiate NVMe reads directly, map storage-class memory pages into unified memory, and ingest frames through zero-copy DMA paths. This architecture transforms NVMe devices from passive storage endpoints into active participants in the AI pipeline, establishing the throughput backbone upon which all subsequent decoding, stabilization, and starvation-control mechanisms depend.

i. AI Storage-Class Memory Interconnects with Direct GPU-Driven Frame Ingest

AI storage-class memory interconnects redefine how high-bandwidth sensor data enters the AI

pipeline. Traditional ingest paths rely on CPU-mediated I/O, kernel drivers, host buffers, and PCIe bounce buffers—each introducing latency, jitter, and bandwidth ceilings that collapse under multi-gigabit sensor loads. Direct GPU-driven frame ingest eliminates these bottlenecks by allowing GPUs to pull frames directly from NVMe devices through storage-class memory pathways, bypassing the CPU entirely.

This architecture transforms NVMe from a passive storage endpoint into an active, accelerator-aligned data source capable of sustaining sensor-rate throughput.

GPU-Initiated NVMe Reads

Instead of the CPU issuing read commands, the GPU becomes the **primary initiator**:

- GPU dispatches NVMe read commands directly
- NVMe pages are mapped into unified virtual memory
- DMA engines transfer data straight into GPU-resident buffers
- No host-side memcpy, no kernel/user transitions

This creates a **zero-copy ingest path** where frames land exactly where accelerators expect them.

Unified Memory Mapping of NVMe Pages

Storage-class memory interconnects allow NVMe pages to be mapped into the same unified memory fabric used by:

- preprocessing kernels
- entropy-decode arrays
- synchronization layers
- multimodal fusion networks

This eliminates:

- buffer duplication
- staging buffers
- PCIe round-trip latency
- CPU arbitration

NVMe becomes a **first-class citizen** in the accelerator memory hierarchy.

Zero-Copy DMA Delivery into Accelerator-Resident Buffers

DMA engines deliver bitstreams directly into GPU memory regions that feed:

- JPEG-XL / AV1 slice decoders
- LiDAR intensity map decoders
- radar burst reconstruction kernels
- neuromorphic event tile assemblers

This ensures that decoding begins immediately upon arrival, without waiting for host-side processing.

Sustaining Sensor-Rate Throughput

Direct GPU-driven ingest is essential for workloads such as:

- multi-gigapixel video
- high-density LiDAR sweeps
- radar micro-doppler bursts
- neuromorphic event streams
- multi-camera rigs with synchronized capture

These workloads routinely exceed **10–40 Gbps**, far beyond what CPU-mediated ingest can sustain.

Storage-class memory interconnects ensure that ingest bandwidth matches sensor bandwidth.

Eliminating Traditional Bottlenecks

This architecture removes:

- CPU bottlenecks
- kernel driver latency
- PCIe bounce buffers
- host-side decode stalls
- I/O jitter under burst load

The result is a **deterministic ingest pipeline** that behaves like a direct extension of the sensor

hardware.

System-Level Impact

AI storage-class memory interconnects:

- establish a zero-copy ingest backbone
- allow GPUs to pull frames at full NVMe bandwidth
- eliminate CPU involvement in high-rate ingest
- reduce latency and jitter
- prepare bitstreams for hardware-resident decode arrays
- ensure accelerators remain continuously fed

They form the **throughput foundation** upon which all decoding, stabilization, and starvation-control mechanisms depend.

With direct GPU-driven ingest now delivering raw bitstreams into unified memory at full NVMe bandwidth, the next architectural challenge is decoding these streams at sensor-rate throughput. Modern codecs such as JPEG-XL and AV1 rely on complex entropy coding that is computationally expensive and highly parallelizable—yet fundamentally unsuitable for CPU-bound libraries. Item **ii** focuses on the dedicated AI Huffman-decode arrays that solve this problem by slicing bitstreams into parallel segments and decoding them directly in hardware. These arrays reconstruct frames at the same cadence as the sensors themselves, ensuring that high-bandwidth ingest seamlessly transitions into high-bandwidth decode without stalls, jitter, or starvation.

ii. Dedicated AI Huffman-Decode Arrays for JPEG-XL and AV1 Bitstream Slices

Dedicated AI Huffman-decode arrays are the **second throughput pillar** of high-bandwidth frame decoding. Once raw bitstreams are pulled directly into unified memory through GPU-driven NVMe ingest, the next challenge is reconstructing frames at the same cadence as the sensors themselves. Modern codecs—JPEG-XL, AV1, H.266/VVC—use advanced entropy coding (Huffman, ANS, CABAC-like structures) that is computationally expensive, highly parallelizable, and fundamentally unsuitable for CPU-bound decode libraries. AI Huffman-decode arrays solve this by performing entropy decoding **entirely in hardware**, using massively parallel slice-based pipelines that operate at sensor-rate throughput.

These arrays transform compressed bitstreams into fully decoded frames without stalls, jitter, or

starvation, ensuring that the ingest bandwidth established earlier is preserved through the decode stage.

Slice-Based Parallelism for Modern Codecs

JPEG-XL and AV1 bitstreams are naturally divisible into **independent slices**:

- JPEG-XL: modular groups, variable-size blocks
- AV1: tiles, superblocks, entropy-coded partitions

AI decode arrays exploit this structure by:

- slicing bitstreams into parallel decode units
- decoding each slice independently
- writing reconstructed pixels directly into unified memory
- eliminating serial entropy-decode bottlenecks

This transforms entropy decoding from a CPU-bound serial task into a **hardware-parallel pipeline**.

Hardware-Resident Entropy Decode Units

Each decode unit contains:

- Huffman/ANS decode engines
- bitstream walkers
- coefficient reconstruction logic
- dequantization and prediction blocks
- slice-boundary alignment logic

These units operate at extremely high throughput, enabling:

- multi-gigapixel video ingest
- high-density LiDAR intensity map reconstruction
- radar burst decode with micro-doppler preservation
- neuromorphic event tile assembly

The decode process becomes **accelerator-resident**, not host-resident.

Zero-Copy Decode into Unified Memory

Decoded slices are written directly into unified memory:

- no host-side buffers
- no remapping
- no staging areas
- no kernel/user transitions

This ensures that:

- preprocessing kernels
- synchronization layers
- fusion networks

can immediately consume decoded frames without waiting for host-side processing.

Sensor-Rate Throughput Guarantees

Dedicated decode arrays sustain throughput at the same rate as the sensors:

- 4K/8K video at 120–240 FPS
- multi-camera rigs with synchronized capture
- LiDAR sweeps with hundreds of thousands of points
- radar bursts with dense micro-doppler signatures
- neuromorphic event streams with microsecond timing

CPU-bound decode paths collapse under these loads; hardware-resident arrays do not.

Eliminating Decode-Stage Bottlenecks

AI Huffman-decode arrays remove:

- CPU decode stalls
- entropy-decode latency spikes
- burst-mode jitter
- tile-boundary fragmentation

- decode starvation under multi-slice workloads

The decode stage becomes **deterministic**, matching the ingest bandwidth established earlier.

System-Level Impact

Dedicated AI Huffman-decode arrays:

- reconstruct frames at sensor-rate throughput
- eliminate CPU involvement in entropy decoding
- preserve zero-copy semantics
- stabilize decode latency under burst load
- prepare frames for starvation-aware queue-depth tuning
- ensure accelerators remain continuously fed

They form the **decode backbone** of the high-bandwidth ingest pipeline.

With hardware-resident entropy-decode arrays now reconstructing JPEG-XL and AV1 slices at full sensor rate, the next architectural challenge is ensuring that decoded frames flow into accelerators without starvation. Even perfectly decoded frames can stall if queue depths are misconfigured, if burst loads overwhelm ingest buffers, or if accelerators temporarily outrun the decode pipeline. Item **iii** focuses on the telemetry-driven mechanisms that prevent these failures: real-time queue-depth tuning, starvation counters, occupancy monitors, and dynamic adjustment of decode parallelism. These runtime monitors transform the decode pipeline into a self-regulating subsystem that maintains continuous accelerator feed under bursty, uneven, or multi-slice workloads.

iii. AI Queue-Depth Tuning with Pipeline Starvation Telemetry and Runtime Monitors

AI queue-depth tuning is the **third throughput-stability mechanism** in the high-bandwidth decoding pipeline. Even with direct NVMe → GPU ingest and hardware-resident entropy-decode arrays operating at sensor-rate throughput, accelerators can still starve if decoded frames do not arrive at the correct cadence. Starvation occurs when queue depths are too shallow, burst loads temporarily exceed decode capacity, or accelerators outrun the ingest pipeline. Conversely, excessive queue depth introduces latency, memory pressure, and temporal skew relative to upstream synchronization layers.

AI queue-depth tuning solves this by transforming the decode pipeline into a **self-regulating subsystem** that continuously monitors throughput conditions and adjusts ingest parameters in

real time.

Real-Time Starvation Telemetry

Starvation telemetry provides continuous visibility into pipeline health:

- **Queue-depth meters** track available frames in the decode queue.
- **Starvation counters** increment when accelerators request frames faster than they arrive.
- **Occupancy graphs** visualize accelerator utilization and decode latency.
- **Burst-rate predictors** estimate upcoming load based on sensor behavior.

These telemetry signals form the feedback loop that drives dynamic tuning.

Dynamic Queue-Depth Adjustment

Queue depth is not static—it is tuned continuously based on telemetry:

- Increase queue depth during burst loads to prevent starvation.
- Decrease queue depth during steady-state operation to reduce latency.
- Adjust decode parallelism when occupancy graphs show under-utilization.
- Modify NVMe read-ahead when starvation counters rise.

This ensures that accelerators remain **continuously fed**, regardless of workload variability.

Decode-Parallelism Scaling

Decode parallelism is scaled dynamically:

- More entropy-decode slices are activated during burst ingest.
- Fewer slices are used during low-rate periods to reduce power and memory pressure.
- Parallelism is tuned to match accelerator demand, not just sensor rate.

This prevents both starvation and over-decode conditions.

Pipeline Starvation Detection and Recovery

Starvation detection triggers corrective actions:

- **Immediate queue-depth expansion**
- **Increased NVMe read-ahead**

- **Activation of additional decode units**
- **Temporary prioritization of critical modalities**

Recovery is designed to be **fast and deterministic**, ensuring that accelerators never stall for more than a few microseconds.

Maintaining Temporal Alignment with Synchronization Layers

Queue-depth tuning must preserve temporal alignment:

- Excessive buffering introduces timestamp skew.
- Insufficient buffering causes starvation and jitter.
- Telemetry ensures queue depth remains within the temporal tolerance defined by synchronization layers.

This maintains coherence between decoding and multimodal fusion.

System-Level Impact

AI queue-depth tuning:

- prevents accelerator starvation
- stabilizes decode throughput under burst load
- maintains temporal alignment with upstream synchronization
- ensures decoded frames arrive at the correct cadence
- transforms decoding into a self-regulating subsystem
- prepares data for ring-buffer stability mechanisms

It forms the **runtime-adaptive backbone** of the high-bandwidth ingest pipeline.

With queue-depth tuning and starvation telemetry now stabilizing the flow of decoded frames into accelerators, the next architectural challenge is maintaining ingest coherence under massive multi-slice workloads. Multi-camera rigs, multi-beam LiDAR, radar burst clusters, and neuromorphic event streams all produce slice-based data that must be buffered, aligned, and delivered without overrun or underrun. The next discussion focuses on the adaptive ring-buffer stability techniques that make this possible—dynamic pointer management, backpressure signaling, burst-mode smoothing, and slice-aware alignment. These mechanisms ensure that the ingest pipeline remains stable even when sensors produce data at extreme rates,

completing the throughput-stability architecture that keeps accelerators continuously fed under real-world conditions.

iv. AI Ring-Buffer Stability Techniques for Massive Multi-Slice Streaming Workloads

AI ring-buffer stability techniques form the **fourth and final throughput-stability mechanism** in the high-bandwidth decoding pipeline. Once direct NVMe → GPU ingest delivers raw bitstreams at full storage-class bandwidth, hardware-resident entropy-decode arrays reconstruct slices at sensor-rate throughput, and queue-depth telemetry stabilizes accelerator feed, the system must still maintain **coherent ingest under massive multi-slice workloads**.

Modern autonomy workloads are inherently slice-based:

- multi-camera rigs produce dozens of parallel frame slices
- LiDAR sweeps arrive as beam-indexed slices
- radar bursts contain micro-doppler slices
- neuromorphic sensors emit microsecond event slices
- AV1 and JPEG-XL decode pipelines reconstruct tile-based slices

These slices must be buffered, aligned, and delivered without overrun, underrun, pointer desynchronization, or temporal skew. AI ring-buffer stability techniques ensure that the ingest pipeline remains coherent even when sensors produce data at extreme rates.

Adaptive Ring-Buffer Sizing

Ring-buffer size is not fixed—it expands and contracts based on workload conditions:

- **Expansion** during burst-mode ingest to prevent overrun
- **Contraction** during steady-state operation to reduce latency
- **Predictive sizing** based on burst-rate telemetry
- **Modality-aware sizing** for multi-camera or multi-beam workloads

This ensures that the buffer always matches the real-time behavior of the sensors.

Slice-Aware Write and Read Pointers

Traditional ring buffers treat data as uniform packets. AI ring buffers treat data as **heterogeneous slices**, each with its own timing and alignment requirements.

Slice-aware pointer logic includes:

- **write pointers** that advance based on slice boundaries, not fixed packet sizes
- **read pointers** that respect modality-specific temporal windows
- **pointer fences** that prevent overwriting slices still needed by downstream accelerators
- **slice-boundary alignment** to ensure temporal coherence across modalities

This prevents pointer desynchronization under high-rate ingest.

Backpressure Signaling for Burst-Mode Stability

Backpressure is essential for preventing overrun:

- decode arrays slow down when buffers approach saturation
- NVMe read-ahead is reduced when write pointers approach read pointers
- queue-depth tuning interacts with backpressure to maintain stability
- accelerators receive signals when buffer pressure threatens temporal alignment

Backpressure transforms the ring buffer into a **self-regulating flow-control engine**.

Burst-Mode Smoothing

Sensors often produce data in bursts:

- multi-camera rigs synchronize frame capture
- LiDAR sweeps produce dense clusters of beams
- radar bursts contain micro-doppler clusters
- neuromorphic sensors spike under motion

Burst-mode smoothing techniques include:

- **temporal spreading** of slice delivery
- **micro-batching** of slices into stable delivery groups
- **latency-aware smoothing** to preserve temporal alignment
- **priority-based smoothing** for critical modalities

This prevents jitter and maintains stable accelerator feed.

Temporal Alignment with Synchronization Layers

Ring-buffer stability must preserve the temporal guarantees established earlier:

- write pointers must align with hardware-injected timestamps
- read pointers must respect temporal windowing rules
- buffer depth must remain within synchronization tolerances
- slice delivery must align with late-fusion sync barriers

This ensures that high-bandwidth ingest does not break temporal coherence.

Multi-Slice Coherence Under Extreme Workloads

Massive multi-slice workloads introduce unique challenges:

- thousands of slices per second
- heterogeneous slice sizes
- modality-dependent timing
- burst-mode ingest
- dynamic decode parallelism

AI ring-buffer stability techniques maintain coherence by:

- enforcing slice-boundary fences
- dynamically adjusting pointer velocity
- smoothing burst delivery
- applying backpressure to upstream decode arrays
- maintaining temporal alignment with fusion layers

The buffer becomes a **stability engine**, not just a storage structure.

System-Level Impact

AI ring-buffer stability techniques:

- prevent overrun and underrun
- maintain slice coherence under massive workloads

- preserve temporal alignment with synchronization layers
- stabilize burst-mode ingest
- ensure continuous accelerator feed
- complete the throughput-stability architecture

They form the **final stability layer** that keeps high-bandwidth ingest coherent under real-world sensor conditions.

High-bandwidth AI frame decoding establishes the throughput backbone that keeps accelerators continuously fed under real-world sensor loads. Direct NVMe → GPU ingest eliminates CPU bottlenecks and transforms storage-class memory into an extension of the accelerator fabric. Dedicated Huffman-decode arrays reconstruct JPEG-XL and AV1 slices at sensor-rate throughput, ensuring that compressed bitstreams never become a latency choke point. Queue-depth tuning and starvation telemetry convert decoding into a self-regulating subsystem that adapts dynamically to burst loads, uneven sensor cadence, and accelerator demand. Finally, adaptive ring-buffer stability techniques maintain slice coherence under massive multi-slice workloads, preventing overrun, underrun, pointer desynchronization, and temporal skew. Together, these mechanisms form a deterministic, zero-copy, hardware-resident decoding pipeline that preserves the temporal-spatial guarantees established earlier and ensures that fusion-ready tensors continue flowing at full sensor rate without stalls, jitter, or starvation.

With high-bandwidth decoding now delivering fully reconstructed frames into unified memory at stable, starvation-free throughput, the next frontier is handling modalities that do not behave like frames at all. Neuromorphic sensors, event-driven pixel arrays, microsecond spike streams, and asynchronous edge-sensor outputs produce data that is sparse, irregular, and fundamentally non-frame-based. These modalities require slicing, embedding, and interception techniques that operate at microsecond granularity and integrate seamlessly with the synchronized, decoded, and buffered pipelines established so far. The next topic—**neuromorphic AI event slicing, asynchronous embedding, and edge-sensor interception**—introduces the architectures that make this possible, enabling event-driven sensors to coexist with frame-driven modalities inside a unified multimodal perception fabric.

e. Neuromorphic AI Event Slicing, Asynchronous Embedding, and Edge-Sensor Interception

Neuromorphic sensing introduces a fundamentally different data modality into multimodal AI systems. Unlike frame-based sensors that produce dense, periodic outputs, neuromorphic sensors emit **asynchronous microsecond-resolution events** triggered by changes in luminance,

motion, or edge activity. These events are sparse, irregular, and inherently non-frame-based. Integrating them into a unified perception fabric requires specialized slicing, embedding, and interception mechanisms that preserve temporal fidelity while enabling fusion with frame-driven modalities.

This domain introduces **spiking interconnect accumulators**, **time-surface matrices**, **dynamic window integration**, and **ultra-low-power spike-coding compaction**—the architectural tools that transform raw neuromorphic events into fusion-ready tensors.

Asynchronous AI Event-Stream Addressing with Spiking Interconnect Accumulators

Neuromorphic sensors emit events with the structure:

- pixel coordinate (x, y)
- polarity (ON/OFF)
- timestamp (microsecond resolution)

These events arrive asynchronously and must be accumulated into coherent slices.

Spiking Interconnect Accumulators

These hardware units:

- receive microsecond event streams
- maintain per-pixel accumulators
- apply polarity-aware integration
- enforce temporal slicing boundaries
- write event slices directly into unified memory

They operate at microsecond cadence, ensuring no event is lost or delayed.

Asynchronous Addressing

Event addressing is:

- **non-sequential**
- **non-periodic**
- **driven entirely by sensor activity**

Spiking accumulators map events into memory regions without requiring frame-like indexing.

AI Time-Surface Matrix Construction with On-Sensor Edge Extraction

Time-surface matrices convert raw event streams into structured tensors suitable for AI models.

Time-Surface Construction

For each pixel:

- compute time since last event
- apply exponential decay
- encode polarity
- generate a continuous “surface” of temporal activity

This produces a matrix representing recent motion and edge dynamics.

On-Sensor Edge Extraction

Neuromorphic sensors inherently detect edges. Hardware extraction:

- amplifies edge-driven event clusters
- suppresses noise
- aligns event surfaces with frame-based edges
- preserves microsecond timing

This creates a **motion-aware, edge-aligned tensor** ready for fusion.

Dynamic AI Window Integration for Variable-Rate Event and Frame Fusion

Event streams do not align with frame boundaries. Dynamic window integration solves this.

Variable-Rate Windows

Windows adapt based on:

- event density
- motion intensity
- scene complexity
- fusion timing requirements

High-motion scenes produce smaller windows; low-motion scenes produce larger ones.

Frame-Event Fusion Alignment

Dynamic windows ensure:

- event slices align with frame timestamps
- fusion layers receive temporally coherent tensors
- transformers can attend across modalities without skew

This preserves temporal consistency across asynchronous and synchronous sensors.

Ultra-Low-Power AI Spike-Coding Compaction for Inter-Chip Neuromorphic Links

Neuromorphic sensors often operate at the edge, requiring ultra-low-power communication.

Spike-Coding Compaction

Compaction techniques:

- compress event streams
- encode polarity and timing efficiently
- reduce inter-chip bandwidth
- preserve microsecond timing fidelity

Inter-Chip Neuromorphic Links

Links support:

- microsecond event transport
- low-power signaling
- direct delivery into unified memory
- compatibility with spiking accumulators

This enables neuromorphic sensors to operate as first-class modalities in multimodal AI systems.

With the neuromorphic event-processing architecture now defined—from spiking interconnect accumulators to time-surface matrices, dynamic window integration, and spike-coding compaction—the next step is to consolidate these mechanisms into a structured operational view. Neuromorphic sensors behave unlike any frame-based modality, producing sparse, microsecond-resolution events that require specialized slicing, embedding, and transport techniques to preserve temporal fidelity. Table 8.4-D5 organizes these mechanisms into a

coherent framework, showing how each contributes to transforming raw asynchronous spike streams into structured, fusion-ready tensors. This table provides the conceptual anchor that links neuromorphic sensing to the broader multimodal perception fabric, clarifying how event-driven modalities integrate seamlessly with frame-driven pipelines.

Table 48.4-D5 presents the core mechanisms that enable neuromorphic sensors to operate as first-class modalities within multimodal AI systems. Each mechanism addresses a fundamental challenge inherent to event-driven sensing: asynchronous addressing, microsecond accumulation, motion-aware embedding, variable-rate temporal alignment, and ultra-low-power inter-chip transport. By structuring these mechanisms into a single operational view, the table highlights how neuromorphic event streams—despite their irregularity and sparsity—can be transformed into stable, structured tensors that align with the temporal and spatial guarantees established by frame-based pipelines. It clarifies the architectural shift from raw spike streams to AI-ready embeddings that support fusion, prediction, and transformer-based reasoning.

Table 8.4-D5 — Neuromorphic AI Event Processing Mechanisms and Their Operational Roles

Mechanism	AI-Specific Purpose	Operational Strategy	System-Level Effect
Spiking Interconnect Accumulators	Asynchronous event slicing	Microsecond event accumulation	Preserves temporal fidelity of neuromorphic streams
Time-Surface Matrix Construction	Motion-aware embedding	Exponential decay + edge extraction	Produces structured tensors for fusion
Dynamic Window Integration	Frame-event alignment	Variable-rate temporal windows	Ensures coherent multimodal fusion
Spike-Coding Compaction	Low-power neuromorphic transport	Polarity/timing compression	Enables edge-sensor integration at microsecond cadence

Table 8.4-D5 consolidates the neuromorphic event-processing mechanisms that transform sparse, asynchronous spike streams into structured, fusion-ready tensors.

Table 8.4-D5 reveals that neuromorphic event processing is not a single algorithmic step but a coordinated set of hardware-resident mechanisms that collectively stabilize asynchronous spike streams. Spiking interconnect accumulators provide the first layer of structure, capturing microsecond events and organizing them into coherent slices without imposing frame-like periodicity. Time-surface matrix construction transforms these slices into motion-aware

embeddings, encoding temporal decay, polarity, and edge activity into a continuous surface that AI models can interpret. Dynamic window integration bridges the gap between asynchronous events and synchronous frame-based modalities, adjusting temporal windows based on event density and motion intensity to ensure coherent multimodal fusion. Finally, spike-coding compaction enables ultra-low-power transport across inter-chip neuromorphic links, preserving microsecond timing fidelity while minimizing bandwidth and energy consumption.

Together, these mechanisms form a neuromorphic processing backbone that complements the high-bandwidth frame-based pipelines established earlier. They ensure that event-driven sensors—despite their irregularity, sparsity, and microsecond timing—produce structured, temporally aligned tensors that can be fused with video, LiDAR, radar, and IMU modalities. Table 8.4-D5 thus provides the operational map for understanding how neuromorphic sensing integrates into the unified multimodal perception fabric.

Table 8.4-D5 organizes the neuromorphic event-processing mechanisms—spiking accumulators, time-surface matrices, dynamic window integration, and spike-coding compaction—into a structured operational framework. To complement this tabular view, Figure 8.4-D5 visualizes how these mechanisms operate as a unified neuromorphic-processing fabric that transforms sparse, microsecond-resolution spike streams into structured, fusion-ready tensors. The figure shows how raw asynchronous events are accumulated, embedded, temporally aligned, and compacted for low-power transport, revealing the full pipeline that enables neuromorphic sensors to coexist seamlessly with frame-based modalities inside a multimodal perception system. This visual progression translates the table’s conceptual architecture into a pipeline-level diagram that exposes the temporal, structural, and energy-efficiency guarantees required for neuromorphic integration.

Figure 8.4-D5 depicts the neuromorphic event-processing architecture that enables microsecond-resolution sensors to operate as first-class modalities within multimodal AI systems. Each panel highlights a critical transformation step—event accumulation, time-surface embedding, dynamic window alignment, and spike-coding compaction—showing how sparse asynchronous events evolve into structured tensors suitable for fusion with frame-based modalities. Together, these mechanisms preserve temporal fidelity, encode motion and edge dynamics, adapt to variable-rate sensor activity, and support ultra-low-power inter-chip transport, forming the neuromorphic backbone of the perception fabric.

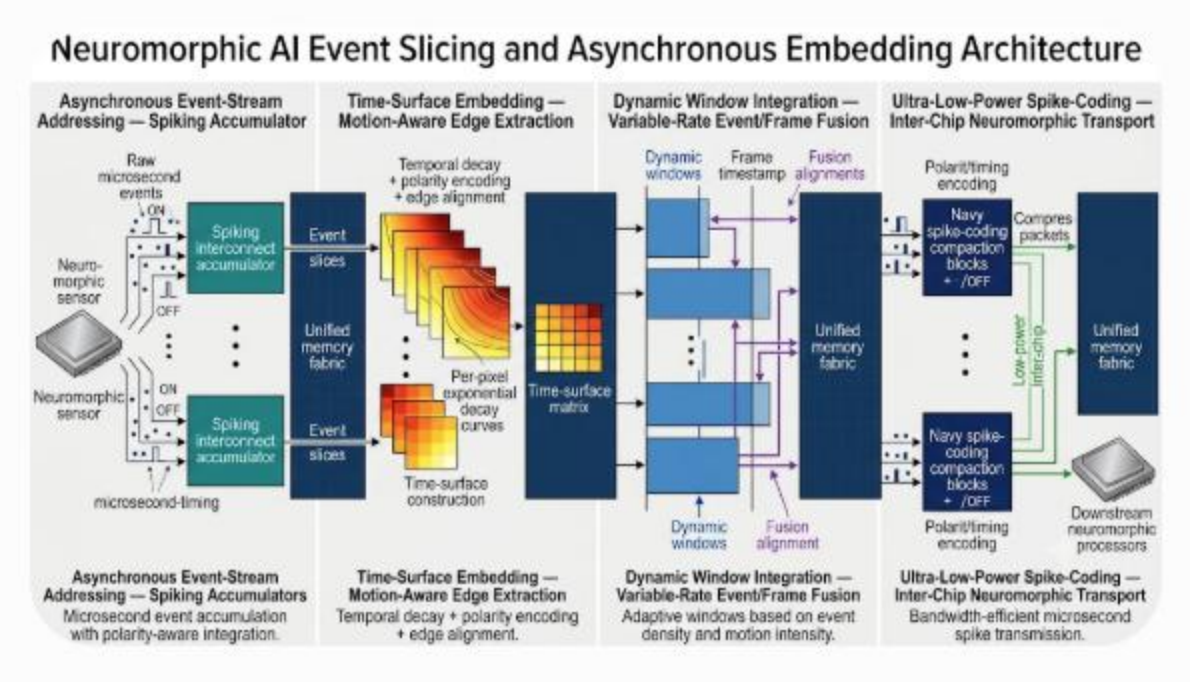


Figure 8.4-D5 — Neuromorphic AI Event Slicing and Asynchronous Embedding Architecture
The figure illustrates the four mechanisms that transform sparse neuromorphic event streams into structured, fusion-ready tensors: spiking accumulators, time-surface matrices, dynamic window integration, and spike-coding compaction. These mechanisms preserve microsecond timing fidelity, encode motion-aware surfaces, align asynchronous events with frame-based modalities, and enable low-power neuromorphic transport.

Legend

- ***Neuromorphic sensor / event source:*** *light gray block with spike icons*
- ***Event streams:*** *microsecond-timed pulses with ON/OFF polarity markers*
- ***Spiking accumulators:*** *teal blocks performing event accumulation*
- ***Time-surface matrices:*** *gradient heatmaps representing temporal decay and edge activity*
- ***Dynamic windows:*** *blue variable-width rectangles aligning events with frame timestamps*
- ***Fusion alignment arrows:*** *purple arrows indicating multimodal integration*
- ***Spike-coding compaction blocks:*** *navy modules with compression symbols*
- ***Inter-chip neuromorphic links:*** *thin green low-power communication lines*
- ***Unified memory fabric:*** *dark blue region with subtle grid pattern*

Figure 8.4-D5 demonstrates how neuromorphic sensors—despite producing sparse, irregular,

microsecond-resolution events—can be integrated into a unified multimodal perception pipeline. The first panel shows spiking interconnect accumulators that capture asynchronous events and organize them into coherent slices without imposing frame-based periodicity. The second panel illustrates time-surface matrix construction, where temporal decay, polarity encoding, and edge extraction transform event slices into motion-aware embeddings. The third panel highlights dynamic window integration, which adapts temporal windows based on event density and motion intensity to align asynchronous events with synchronous frame timestamps. The final panel depicts spike-coding compaction, enabling bandwidth-efficient, ultra-low-power transport of neuromorphic events across inter-chip links while preserving microsecond timing fidelity.

Together, these panels reveal a neuromorphic processing architecture designed for real-time autonomy. They show how raw spike streams are accumulated, embedded, aligned, and compacted entirely within accelerator-resident memory, producing structured tensors that can be fused with video, LiDAR, radar, and IMU modalities. This ensures that neuromorphic sensors operate as fully integrated components of the perception fabric, complementing the high-bandwidth frame-based pipelines established earlier.

With the neuromorphic event-processing framework now organized into its operational roles, the natural starting point for deeper exploration is the mechanism that gives structure to raw spike streams: **asynchronous event-stream addressing through spiking interconnect accumulators**. Before time-surface matrices can encode motion dynamics, before dynamic windows can align events with frame-based modalities, and before spike-coding compaction can reduce transport overhead, the system must first capture microsecond-resolution events and assemble them into coherent slices without imposing frame-like periodicity. Item **i** introduces this foundational capability, where polarity-aware accumulators ingest sparse, irregular spikes at microsecond cadence and map them directly into unified memory. This establishes the temporal fidelity and structural backbone upon which all subsequent neuromorphic embedding, alignment, and transport mechanisms depend.

i. Asynchronous AI Event-Stream Addressing with Spiking Interconnect Accumulators

Neuromorphic sensors—DVS (Dynamic Vision Sensors), ATIS (Asynchronous Time-based Image Sensors), and other event-driven pixel arrays—produce data that is fundamentally different from frame-based modalities. Instead of emitting periodic images, they generate **microsecond-resolution events** whenever a pixel detects a change in luminance. Each event carries:

- **x, y coordinate**

- **polarity** (ON/OFF)
- **timestamp** (often sub-microsecond precision)

This creates a sparse, irregular, asynchronous stream that cannot be processed using frame-centric pipelines. The first architectural requirement is therefore a mechanism that can **capture, organize, and slice** these events without imposing artificial periodicity. This is the role of **spiking interconnect accumulators**.

Microsecond-Resolution Event Capture

Spiking accumulators operate at microsecond cadence, ingesting events as they arrive:

- No batching
- No frame boundaries
- No temporal quantization
- No CPU-mediated buffering

They preserve the exact timing of each spike, which is essential for motion detection, edge tracking, and neuromorphic fusion.

Polarity-Aware Integration

Each event carries a polarity:

- **ON events** indicate increasing luminance
- **OFF events** indicate decreasing luminance

Spiking accumulators maintain polarity-specific counters or integrators:

- ON accumulators track rising edges
- OFF accumulators track falling edges
- Combined accumulators track motion direction and intensity

This polarity-aware integration is the foundation for later motion-aware embeddings.

Asynchronous Addressing and Memory Mapping

Unlike frame-based sensors, neuromorphic events do not arrive in raster order. Spiking accumulators must:

- map events directly to their pixel coordinates

- update per-pixel accumulators without sequential scanning
- write event slices into unified memory regions
- maintain sparse addressing without overhead

This creates a **direct event-to-memory mapping** that preserves spatial locality and temporal fidelity.

Temporal Slicing Without Frames

Event streams must be segmented into slices for downstream processing. Spiking accumulators define slice boundaries based on:

- elapsed microseconds
- event density
- motion intensity
- fusion timing requirements

These slices are **not frames**—they are temporal windows containing all events within a microsecond-scale interval.

Zero-Copy Delivery into Unified Memory

Spiking accumulators write event slices directly into unified memory:

- no CPU involvement
- no staging buffers
- no remapping
- no latency spikes

This ensures that time-surface construction, dynamic window integration, and spike-coding compaction can begin immediately.

System-Level Impact

Spiking interconnect accumulators:

- preserve microsecond timing fidelity
- maintain polarity-aware event structure

- provide sparse, asynchronous addressing
- generate coherent event slices
- prepare data for time-surface embedding
- enable neuromorphic sensors to operate at full temporal resolution

They form the **temporal-structural backbone** of neuromorphic event processing.

With spiking interconnect accumulators now capturing microsecond-resolution events and organizing them into coherent slices, the next architectural challenge is transforming these sparse spikes into structured tensors that AI models can interpret. Raw events are too irregular and too sparse for direct consumption by convolutional networks or transformers. Item ii introduces the mechanism that solves this: time-surface matrix construction, where temporal decay, polarity encoding, and on-sensor edge extraction convert event slices into motion-aware surfaces. These surfaces provide a continuous, spatially aligned representation of recent activity, forming the embedding layer that bridges neuromorphic sensing with frame-based perception.

ii. AI Time-Surface Matrix Construction with On-Sensor Edge Extraction

Time-surface matrix construction is the step where raw neuromorphic events become something an AI model can actually "see." Spikes by themselves are powerful but too sparse and irregular for most downstream architectures; they need to be embedded into a continuous representation that encodes **when** and **where** activity occurred, and **how** it evolved over time. Time-surfaces do exactly this: for each pixel, they track the recency and polarity of events, building a matrix that behaves like a motion-aware, edge-centric image of recent activity.

From Event Slices to Temporal Fields

Event slices produced by spiking accumulators contain all events within a microsecond-scale window. Time-surface construction takes these slices and, for each pixel:

- **Records the timestamp of the last event**
- **Computes the time elapsed since that event**
- **Applies a decay function** (often exponential)
- **Encodes polarity** (ON/OFF) into the resulting value

The result is a scalar per pixel that reflects how recently and in what direction activity occurred.

Exponential Decay as Motion Memory

Exponential decay turns discrete events into a smooth temporal field:

- Recent events → high values
- Older events → lower values
- No events → baseline (near zero)

This gives the system a **short-term memory of motion**:

- Edges that just moved are bright on the time-surface
- Static regions fade out naturally
- Fast motion creates sharp, high-contrast trails

AI models can then treat this as a motion-encoded image.

Polarity Encoding and Edge Semantics

Polarity is not just a sign—it carries semantic meaning:

- ON events → brightening edges
- OFF events → darkening edges

Time-surface matrices can:

- maintain separate channels for ON and OFF
- or encode polarity as positive/negative values

This preserves **directional edge information**, allowing models to distinguish between objects entering or leaving illumination, and between different motion patterns.

On-Sensor Edge Extraction and Noise Suppression

Neuromorphic sensors are inherently edge-sensitive, but real scenes are noisy. On-sensor edge extraction:

- amplifies coherent edge activity (clusters of events along contours)
- suppresses isolated, low-density noise spikes
- aligns event-driven edges with any available frame-based edges
- preserves microsecond timing while cleaning the spatial structure

This produces a **clean, edge-centric time-surface** that is far more robust for downstream AI.

Time-Surface Matrices as AI-Ready Embeddings

Once constructed, time-surface matrices behave like:

- motion-aware images
- edge-centric feature maps
- temporal activity fields

They can be fed directly into:

- convolutional networks
- spatiotemporal transformers
- fusion layers that combine events with frames, LiDAR, radar, or IMU

The irregular, sparse event stream has now become a **dense, structured tensor** that fits naturally into the rest of the perception stack.

System-Level Impact

Time-surface matrix construction:

- converts raw spikes into continuous motion embeddings
- preserves microsecond timing via decay functions
- encodes polarity and edge semantics
- suppresses noise while amplifying meaningful contours
- produces tensors that align spatially with frame-based modalities

It is the **embedding layer** that makes neuromorphic sensing compatible with mainstream AI architectures.

With time-surface matrices now providing motion-aware, edge-centric embeddings of neuromorphic activity, the next architectural challenge is aligning these asynchronous representations with synchronous frame-based modalities. Events arrive at microsecond cadence, while frames arrive at millisecond or longer intervals; their temporal grids do not naturally match. Item **iii** introduces **dynamic AI window integration**, where temporal windows expand and contract based on event density and motion intensity, and where time-surfaces are aligned with frame timestamps to create coherent fusion points. This mechanism ensures that event-driven and frame-driven sensors contribute to a shared perceptual timeline, enabling

stable multimodal fusion despite fundamentally different sampling regimes.

iii. Dynamic AI Window Integration for Variable-Rate Event and Frame Fusion

Dynamic AI window integration is where neuromorphic time and frame time learn to live together. Events arrive in a continuous, microsecond-resolution stream; frames arrive in discrete, millisecond-scale snapshots. If you try to force events into fixed frame buckets, you either lose temporal fidelity or create misalignment. Dynamic windows solve this by **adapting the temporal integration horizon** to what the scene is actually doing—how dense the events are, how fast things are moving, and how often frames are captured.

Variable-Rate Temporal Windows

Instead of a single fixed window size, the system maintains **adaptive windows**:

- High motion / high event density:
    - Windows shrink (shorter duration).
    - Time-surfaces represent very recent activity.
    - Fusion emphasizes fast, fine-grained dynamics.
- Low motion / low event density:
    - Windows expand (longer duration).
    - Time-surfaces integrate sparse events over more time.
    - Fusion emphasizes stability and context.

Window size becomes a **function of the scene**, not a static parameter.

Aligning Event Windows with Frame Timestamps

Frames arrive at discrete timestamps; events are continuous. Dynamic integration:

- centers or anchors windows around **frame timestamps**, or
- offsets them to capture **pre-frame and post-frame activity**

ensures that each frame has a corresponding event-window (or set of windows)

This creates **fusion pairs**:

$$\text{Frame}_k \leftrightarrow \text{EventWindow}_k$$

each pair represents the same temporal neighborhood from two different modalities.

Multi-Window Strategies for Rich Fusion

Sometimes one window per frame is not enough. The system can maintain:

- **pre-frame windows** (events leading up to a frame)
- **post-frame windows** (events immediately after a frame)
- **overlapping windows** that slide across time for continuous fusion

This allows models to:

- see how motion evolves before and after a frame
- capture transient events that frames miss
- build richer spatiotemporal representations.

Window Control Signals: Event Density and Motion Intensity

Window adaptation is driven by **telemetry**:

Event density: number of events per unit time.

- **Motion intensity:** derived from time-surface gradients and polarity patterns.
- **Scene complexity:** number of active regions, edges, or objects.

Control logic:

- shrinks windows when density and intensity spike (to avoid smearing fast motion)
- expands windows when activity is sparse (to avoid empty embeddings)

This keeps the event representation **informative but not overloaded**.

Maintaining Temporal Coherence Across Modalities

Dynamic windows must respect the temporal guarantees of the overall system:

- they cannot drift arbitrarily away from frame timestamps
- they must stay within synchronization tolerances defined earlier
- they must align with fusion barriers and late-fusion sync keys

The integration layer becomes a **temporal negotiator**, ensuring:

- events don’t lag too far behind frames

- frames don't ignore recent event bursts
- fusion operates on coherent, overlapping time intervals.

System-Level Impact

Dynamic AI window integration:

- reconciles continuous event time with discrete frame time
- adapts temporal horizons to scene dynamics
- ensures each frame has a meaningful, motion-aware event companion
- preserves temporal coherence across modalities
- feeds fusion layers with aligned, variable-rate embeddings

It is the **timing bridge** that lets neuromorphic and frame-based sensors share a common perceptual timeline.

With dynamic window integration now aligning neuromorphic time-surfaces and frame-based modalities along a shared temporal backbone, the remaining challenge is moving these event streams across physical boundaries—sensor to edge module, edge to accelerator, chip to chip—without burning power or bandwidth. Neuromorphic sensors often live at the extreme edge, where energy budgets are tight and links are narrow. Item **iv** introduces **ultra-low-power AI spike-coding compaction**, the set of encoding and compression techniques that preserve microsecond timing and polarity while drastically reducing the cost of transport. These mechanisms turn rich, high-rate event streams into bandwidth-efficient spike packets that can traverse inter-chip neuromorphic links, completing the architecture that carries neuromorphic information from the sensor all the way into the multimodal perception fabric.

iv. Ultra-Low-Power AI Spike-Coding Compaction for Inter-Chip Neuromorphic Links

Ultra-low-power spike-coding compaction is the final neuromorphic mechanism that enables event-driven sensors to operate efficiently across physical boundaries—sensor to edge module, edge to accelerator, and chip to chip. Neuromorphic sensors often sit at the extreme edge of a system, where energy budgets are tight, bandwidth is constrained, and communication links must preserve microsecond timing fidelity without overwhelming downstream processors. Spike-coding compaction solves this by transforming rich, high-rate event streams into **bandwidth-efficient spike packets** that retain polarity, timing, and spatial information while minimizing transport cost.

This mechanism completes the neuromorphic pipeline by ensuring that event-driven data can

traverse inter-chip links without losing temporal precision or exhausting power budgets.

The Need for Compaction in Neuromorphic Systems

Neuromorphic sensors can generate millions of events per second during high-motion scenes. Raw event streams:

- overwhelm narrow inter-chip links
- consume excessive power
- introduce latency if buffered
- risk temporal distortion if throttled

Compaction is therefore essential to:

- reduce bandwidth
- preserve microsecond timing
- maintain polarity and spatial locality
- support continuous real-time operation

It is the neuromorphic equivalent of entropy coding in video pipelines—but optimized for spikes.

Polarity-Timing Encoding

Each event contains:

- **polarity** (ON/OFF)
- **timestamp** (microsecond resolution)
- **pixel coordinate**

Spike-coding compaction encodes these efficiently using:

- **delta-time encoding** (time since last event)
- **run-length encoding** for repeated polarity patterns
- **bit-packing** for polarity and coordinate fields
- **temporal grouping** for events within micro-windows

This reduces the number of bits per event while preserving exact timing.

Spatial Compaction via Locality-Aware Encoding

Events often occur in spatial clusters along edges or motion contours. Compaction exploits this by:

- grouping events by pixel neighborhood
- encoding relative coordinates instead of absolute ones
- collapsing clusters into short packets
- using spatial deltas to reduce bit width

This preserves spatial structure while minimizing packet size.

Micro-Batching for Transport Efficiency

Instead of sending each event individually, compaction creates **micro-batches**:

- batches contain events within a microsecond-scale window
- batch size adapts to event density
- batches preserve ordering and polarity
- batches reduce per-packet overhead

Micro-batching ensures that transport remains efficient even during burst activity.

Power-Aware Encoding for Edge Devices

Neuromorphic sensors often operate on milliwatts. Compaction includes:

- **low-toggle encoding** to reduce switching energy
- **clock-gated packet formation**
- **energy-aware bit-packing**
- **minimal-transition signaling** on inter-chip links

These techniques reduce dynamic power consumption during encoding and transmission.

Inter-Chip Neuromorphic Transport

Compacted spike packets travel across:

- MIPI-like neuromorphic serial links

- low-power LVDS lines
- chip-to-chip neuromorphic buses
- edge-to-accelerator micro-interconnects

Transport guarantees:

- microsecond timing fidelity
- polarity preservation
- spatial locality retention
- low-latency delivery into unified memory

This allows neuromorphic sensors to operate as first-class modalities in multimodal AI systems.

System-Level Impact

Ultra-low-power spike-coding compaction:

- reduces bandwidth by orders of magnitude
- preserves microsecond timing precision
- maintains polarity and spatial structure
- enables real-time inter-chip neuromorphic transport
- supports edge-sensor operation under tight power budgets
- completes the neuromorphic event-processing pipeline

It is the **transport backbone** that carries neuromorphic information from the sensor into the multimodal perception fabric without distortion or delay.

Neuromorphic AI event processing completes the transformation of microsecond-resolution spike streams into structured, fusion-ready tensors. The pipeline begins with asynchronous event-stream addressing, where spiking accumulators preserve polarity and timing at the moment of capture. Time-surface matrices then convert sparse spikes into dense motion-aware embeddings that encode temporal decay and edge dynamics. Dynamic window integration reconciles continuous event time with discrete frame time, ensuring that neuromorphic activity aligns with synchronous modalities. Ultra-low-power spike-coding compaction finally enables efficient inter-chip transport, preserving microsecond fidelity while minimizing bandwidth and energy. Together, these mechanisms allow neuromorphic sensors to operate as fully integrated

modalities within the multimodal perception fabric, contributing high-resolution temporal detail that complements frame-based, depth-based, and RF-based sensing.

Sensor pipelines in AI systems form the throughput backbone that ensures all modalities—frames, events, LiDAR sweeps, radar bursts, IMU packets—arrive at accelerators with deterministic timing and stable bandwidth. Direct NVMe streaming eliminates CPU bottlenecks and preserves zero-copy semantics. Hardware-resident entropy-decode arrays reconstruct compressed bitstreams at sensor-rate throughput, while queue-depth tuning and starvation telemetry maintain continuous accelerator feed under bursty or uneven workloads. Ring-buffer stability techniques ensure coherent multi-slice ingest across massive streaming pipelines, preventing overrun, underrun, and temporal skew. Neuromorphic event slicing extends this backbone to microsecond-resolution modalities, enabling seamless fusion between asynchronous and synchronous sensors. Collectively, these pipelines establish a deterministic, multimodal ingest architecture capable of supporting real-time perception and decision-making in autonomy, robotics, and safety-critical systems.

With multimodal sensor pipelines now delivering structured, temporally aligned, and bandwidth-stable data into accelerators, the next architectural frontier is ensuring that the execution environment itself behaves with the same determinism. Real-time AI frameworks must schedule kernels predictably, avoid garbage-collection stalls, adapt performance based on telemetry, and maintain hard real-time guarantees across inter-process communication channels. They must support virtualized prototyping environments and dynamic edge-to-cloud offload without introducing jitter or temporal drift. The upcoming exploration of deterministic runtimes, closed-loop DVFS control, hard real-time IPC channels, multi-tenant isolation domains, and jitter-buffered edge-to-cloud splitting will show how real-time execution frameworks complete the chain from sensor capture to AI action, ensuring that perception, fusion, and control operate with unwavering temporal reliability.

E. Real-Time Frameworks in AI Systems

Real-time frameworks define the execution behavior of autonomous AI systems above the perceptual substrate. They determine how kernels are scheduled, how memory is managed without unpredictable pauses, how inter-process communication maintains hard timing guarantees, and how workloads adapt to thermal and power boundaries without violating latency budgets. In hardware–software co-design, real-time frameworks are not passive runtime environments; they are active, determinism-critical subsystems whose schedulers, DVFS governors, IPC channels, and isolation domains directly shape how effectively intelligence can act, respond, and coordinate across heterogeneous compute fabrics. Every real-time mechanism—predictable scheduling engine, GC-free memory model, closed-loop thermal

controller, hard real-time IPC channel, or jitter-buffered offload path—propagates through the autonomy stack and governs how reliably models execute under dynamic physical conditions.

Modern AI systems operate in environments where naïve runtimes, garbage-collecting memory managers, and best-effort IPC channels are no longer viable. Autonomous platforms must execute perception, prediction, planning, and control loops within strict deadlines while managing thermal constraints, power variability, multi-tenant workloads, and distributed execution across edge and cloud. As a result, real-time frameworks increasingly incorporate hardware-aligned design principles that eliminate nondeterministic pauses, enforce predictable kernel dispatch, adapt clock frequencies based on telemetry, isolate tenants at the hardware context level, and maintain jitter-bounded communication across distributed nodes. These principles ensure that action is not only fast but also temporally reliable across heterogeneous accelerators, multi-process stacks, and real-time autonomy loops.

- **Deterministic AI Runtimes with Predictable Scheduling and GC-Free Execution Engines -** Deterministic runtimes replace traditional OS scheduling with predictable dispatch engines that guarantee bounded latency for AI kernels. GC-free memory models eliminate unpredictable pauses, ensuring that transformer inference, control loops, and multimodal fusion operate without jitter. These runtimes allow autonomous systems to maintain strict timing guarantees even under heavy computational load.
- **Telemetry-Driven AI Adaptation with Closed-Loop DVFS and Thermal-Boundary Control -** Closed-loop DVFS controllers adjust clock frequencies and power states based on real-time telemetry—temperature, load, and thermal headroom. Thermal-boundary control prevents throttling-induced latency spikes, ensuring that AI workloads remain stable and responsive. These adaptive mechanisms allow systems to operate safely within physical limits without sacrificing determinism.
- **Asynchronous AI Inter-Process Communications (IPC) Channels with Hard Real-Time Guarantees and Fail-Safe Interrupts -** Hard real-time IPC channels provide jitter-bounded communication between perception, planning, and control processes. Asynchronous messaging avoids blocking, while fail-safe interrupts ensure that critical signals—emergency stops, hazard detections, safety overrides—are delivered immediately. These channels maintain coherence across distributed AI subsystems.
- **Virtual AI Prototyping with Multi-Tenant Isolation and Hardware-Sliced Context Domains -** Virtual prototyping environments allow multiple AI workloads to run concurrently without interference. Hardware-sliced context domains isolate tenants at the accelerator level, preventing timing drift or resource contention. This enables safe

experimentation, simulation, and deployment within shared compute fabrics.

- **Edge-To-Cloud AI Continuum Splitting with Dynamic Layer Offload and Jitter-Buffered Networking -** Continuum splitting dynamically offloads layers between edge and cloud based on bandwidth, latency, and compute availability. Jitter-buffered networking ensures stable inference even under fluctuating network conditions. These mechanisms allow AI systems to scale across distributed environments while maintaining real-time guarantees.

Together, these real-time framework paradigms illustrate how AI systems have evolved into tightly integrated execution ecosystems. Intelligence in autonomous systems is shaped not only by model architecture but by how effectively runtimes deliver predictable, latency-bounded, and thermally stable execution across heterogeneous accelerators and distributed nodes. These paradigms enable modern AI systems to achieve grounded action, real-time responsiveness, and scalable distributed inference through deliberate co-design across the entire autonomy stack.

With the foundations of real-time AI execution now established—deterministic runtimes, telemetry-driven adaptation, hard real-time IPC channels, multi-tenant isolation, and jitter-buffered edge-to-cloud offload—the next step is to consolidate these mechanisms into a structured operational view. Real-time frameworks are not abstract runtime concepts; they are concrete, latency-critical subsystems that govern how perception, prediction, and control loops execute under dynamic thermal, computational, and network conditions. The following table organizes these mechanisms into a unified framework, showing how each contributes to predictable scheduling, stable adaptation, safe concurrency, and distributed determinism. This table provides the conceptual anchor that links runtime behavior to the broader autonomy stack, clarifying how execution determinism becomes as essential as sensor fidelity in real-world AI systems.

Table 8.4-E presents the core mechanisms that enable AI systems to maintain strict timing guarantees across heterogeneous accelerators, multi-process stacks, and distributed edge-to-cloud environments. Each mechanism addresses a fundamental challenge inherent to real-time AI execution: eliminating nondeterministic pauses, adapting performance safely under thermal constraints, guaranteeing inter-process timing, isolating concurrent workloads, and stabilizing distributed inference under network jitter. By structuring these mechanisms into a single operational view, the table highlights how real-time frameworks transform raw computational throughput into predictable, latency-bounded behavior. It clarifies the architectural shift from best-effort execution to deterministic, telemetry-aware, and

isolation-enforced runtimes capable of supporting autonomy, robotics, and safety-critical AI systems.

Table 8.4-E — Real-Time AI Framework Mechanisms and Their Operational Roles

Mechanism	AI-Specific Purpose	Operational Strategy	System-Level Effect
Deterministic AI Runtimes	Predictable kernel dispatch	GC-free memory models, bounded-latency schedulers	Eliminates jitter in perception, planning, and control loops
Closed-Loop DVFS & Thermal Control	Telemetry-driven performance adaptation	Dynamic frequency scaling, thermal-boundary enforcement	Maintains real-time responsiveness under thermal load
Hard Real-Time IPC Channels	Guaranteed inter-process timing	Asynchronous messaging, fail-safe interrupts	Ensures coherent coordination across distributed AI subsystems
Multi-Tenant Isolation Domains	Safe concurrent AI prototyping	Hardware-sliced contexts, tenant-level resource fencing	Prevents timing drift and interference between workloads
Edge-to-Cloud Continuum Splitting	Distributed real-time inference	Dynamic layer offload, jitter-buffered networking	Preserves latency guarantees across heterogeneous compute fabrics

Table 8.4-E consolidates the core mechanisms that allow AI systems to execute deterministically under dynamic physical, thermal, and distributed-network conditions. Each mechanism contributes to a runtime environment capable of predictable scheduling, stable adaptation, safe concurrency, and jitter-bounded distributed execution.

Table 8.4-E reveals that real-time AI execution is not governed by a single runtime or scheduler but by a coordinated set of mechanisms that collectively enforce determinism across the autonomy stack. Deterministic runtimes provide the foundation, replacing traditional OS scheduling with predictable dispatch engines and GC-free memory models that eliminate jitter in perception and control loops. Closed-loop DVFS and thermal-boundary control introduce adaptive stability, allowing systems to maintain performance under thermal load without violating latency budgets. Hard real-time IPC channels ensure that processes communicate with

guaranteed timing, enabling coherent coordination between perception, planning, and actuation. Multi-tenant isolation domains allow concurrent AI workloads to coexist safely, preventing timing drift or resource contention that could destabilize critical loops. Finally, edge-to-cloud continuum splitting extends determinism beyond a single device, using dynamic layer offload and jitter-buffered networking to preserve real-time guarantees even under fluctuating network conditions.

Together, these mechanisms form a real-time execution backbone that complements the sensor pipelines defined earlier. They ensure that once multimodal data arrives with deterministic timing, the runtime environment can process it with equal reliability—maintaining strict deadlines, adapting safely to physical constraints, and coordinating distributed inference without temporal drift. Table 8.4-E1 thus provides the operational map for understanding how real-time frameworks enable autonomous AI systems to act with unwavering temporal precision.

Table 8.4-E organizes the real-time execution mechanisms—deterministic runtimes, closed-loop DVFS control, hard real-time IPC channels, multi-tenant isolation domains, and jitter-buffered edge-to-cloud offload—into a structured operational framework. To complement this tabular view, Figure 8.4-E1 visualizes how these mechanisms interact as a unified execution fabric that enforces predictable timing across heterogeneous accelerators and distributed nodes. The figure shows how kernel scheduling, thermal adaptation, inter-process communication, workload isolation, and distributed inference collectively maintain strict latency guarantees even under dynamic thermal, computational, and network conditions. This visual progression translates the table's conceptual architecture into a pipeline-level diagram that exposes the temporal, thermal, and concurrency guarantees required for real-time AI behavior.

Figure 8.4-E depicts the real-time execution architecture that enables autonomous AI systems to operate with deterministic timing across local accelerators and distributed edge-to-cloud environments. Each panel highlights a critical mechanism—predictable scheduling, telemetry-driven DVFS control, hard real-time IPC, multi-tenant isolation, and jitter-buffered distributed offload—showing how runtime determinism is constructed layer by layer. Together, these mechanisms eliminate nondeterministic pauses, stabilize performance under thermal load, guarantee inter-process timing, prevent tenant interference, and preserve latency guarantees across network boundaries. The figure illustrates how real-time frameworks transform raw computational throughput into predictable, latency-bounded execution suitable for autonomy, robotics, and safety-critical AI systems.

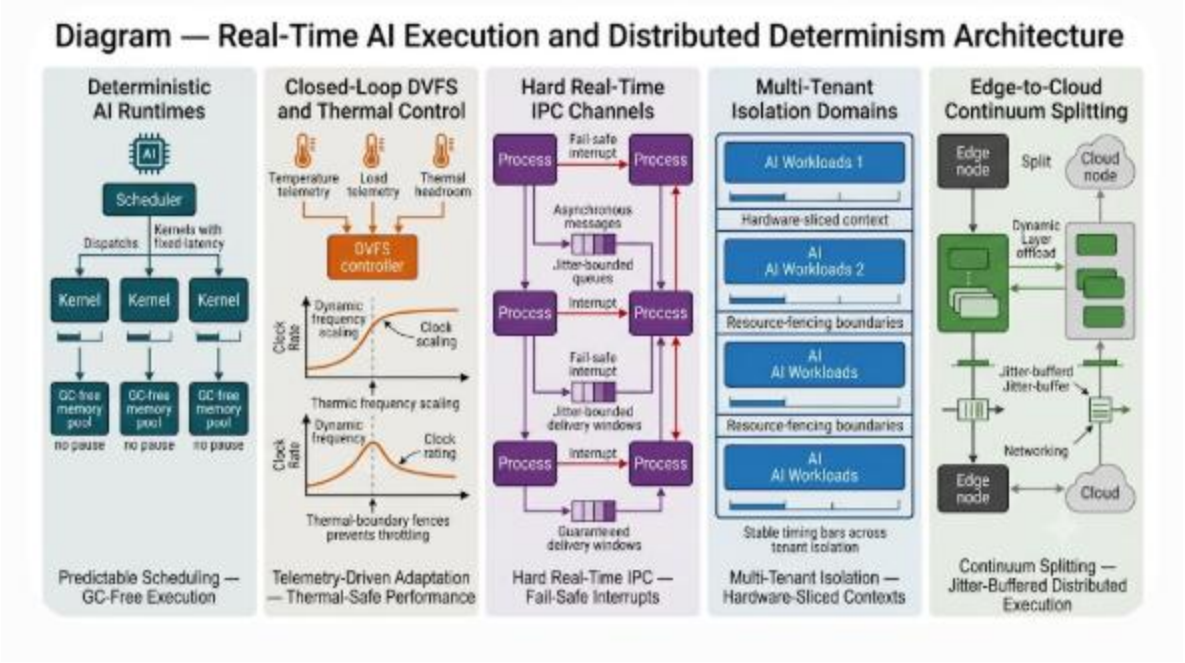


Figure 8.4-E — Real-Time AI Execution and Distributed Determinism Architecture
The figure illustrates the five mechanisms that enable deterministic AI execution across heterogeneous accelerators and distributed environments: predictable runtimes, telemetry-driven DVFS control, hard real-time IPC channels, multi-tenant isolation domains, and jitter-buffered edge-to-cloud offload. Together, these mechanisms ensure that autonomous AI systems maintain strict timing guarantees even under dynamic thermal, computational, and network conditions.

Legend

- ***Deterministic runtimes:*** *teal scheduler blocks with fixed-latency arrows*
- ***GC-free memory pools:*** *teal memory regions labeled "no pause"*
- ***DVFS controllers:*** *orange modules with temperature and load telemetry icons*
- ***Thermal boundaries****: orange fences preventing throttling*
- ***IPC channels:*** *purple asynchronous queues with jitter-bounded timing bars*
- ***Fail-safe interrupts:*** *red interrupt arrows*
- ***Isolation domains****: blue hardware-sliced context boxes with resource-fencing boundaries*
- ***Edge nodes:*** *dark gray compute blocks*
- ***Cloud nodes:*** *light gray compute blocks*
- ***Jitter-buffered links:*** *green networking paths with stabilized timing markers*

Figure 8.4-E demonstrates how real-time determinism is constructed across the execution fabric of an autonomous AI system. The first panel shows deterministic runtimes enforcing predictable

kernel dispatch and GC-free memory behavior, eliminating jitter that would destabilize perception and control loops. The second panel illustrates closed-loop DVFS and thermal-boundary control, where telemetry-driven adaptation maintains performance under thermal load without violating latency budgets. The third panel highlights hard real-time IPC channels, which provide jitter-bounded communication and fail-safe interrupt delivery across distributed processes. The fourth panel depicts multi-tenant isolation domains, ensuring that concurrent AI workloads do not interfere with one another's timing or resource allocation. The final panel shows edge-to-cloud continuum splitting, where dynamic layer offload and jitter-buffered networking preserve real-time guarantees even when inference spans distributed nodes.

Together, these panels reveal a runtime architecture engineered for autonomy, robotics, and safety-critical AI systems—where perception, prediction, and control must execute with unwavering temporal reliability regardless of thermal conditions, workload variability, or distributed execution topology.

As the real-time execution fabric becomes fully defined—spanning deterministic scheduling, telemetry-driven DVFS control, hard real-time IPC channels, multi-tenant isolation, and jitter-buffered distributed offload—the natural starting point for deeper exploration is the mechanism that establishes temporal stability at the foundation of the runtime: **deterministic AI runtimes with predictable scheduling and GC-free execution engines**. Before thermal controllers can adapt performance safely, before IPC channels can guarantee delivery windows, before isolation domains can prevent cross-tenant interference, and before edge-to-cloud splitting can preserve latency across distributed nodes, the system must first ensure that every kernel dispatch occurs with bounded latency and without garbage-collection stalls. Item **a** introduces this foundational capability, where predictable schedulers and pause-free memory models eliminate nondeterministic behavior at the core of the autonomy loop. This establishes the execution-time guarantees upon which all subsequent real-time mechanisms depend.

a. Deterministic AI Runtimes with Predictable Scheduling and GC-Free Execution Engines

Deterministic AI runtimes form the temporal foundation of real-time AI systems. They eliminate nondeterministic pauses, enforce bounded-latency kernel dispatch, and ensure that perception, prediction, and control loops execute with unwavering timing. These runtimes replace traditional OS scheduling, garbage-collecting memory models, and best-effort dispatch with predictable, hardware-aligned execution engines. The four mechanisms below—static memory pre-allocation, priority-inversion avoidance, deadline enforcement, and bare-metal microkernels—collectively construct a runtime environment capable of deterministic behavior under dynamic load.

Static AI Memory Pre-Allocation and Deterministic Heap Partitioning Models

Real-time AI systems cannot tolerate garbage-collection stalls or unpredictable heap expansion. Static memory pre-allocation solves this by:

- allocating all model weights, buffers, and intermediate tensors at startup
- partitioning the heap into deterministic regions
- eliminating dynamic allocation during inference
- ensuring constant-time access to memory pools

Deterministic heap partitioning prevents fragmentation, guarantees stable pointer locality, and ensures that memory access patterns remain predictable across the autonomy loop. This transforms memory from a dynamic resource into a fixed, latency-bounded substrate.

Priority-Inversion Avoidance Mechanisms in Real-Time AI Schedulers

Priority inversion—where a low-priority task blocks a high-priority one—is catastrophic in real-time AI. Avoidance mechanisms include:

- priority inheritance protocols
- lock-free queues for model dispatch
- bounded-wait mutexes
- preemption fences for critical kernels

These mechanisms ensure that perception and control loops always preempt background tasks, preventing timing drift and guaranteeing that high-priority inference executes immediately. The scheduler becomes a deterministic arbiter rather than a best-effort dispatcher.

AI Deadline-Enforcement Monitors with Model Early-Exit Execution Paths

Real-time AI workloads must meet strict deadlines. Deadline-enforcement monitors:

- track kernel execution time
- enforce maximum latency per inference cycle
- trigger early-exit paths when deadlines approach
- degrade gracefully by skipping non-critical layers

Early-exit execution paths allow models to return partial but valid outputs when timing

constraints tighten. This ensures that control loops never miss deadlines, even under thermal load or bursty sensor input.

Bare-Metal AI Microkernels Without Intermediary Operating Systems

Bare-metal microkernels eliminate OS jitter entirely. They provide:

- direct hardware scheduling
- deterministic interrupt handling
- minimal context-switch overhead
- fixed-latency dispatch paths

By removing intermediary operating systems, microkernels ensure that AI workloads execute with cycle-level predictability. This is essential for robotics, autonomy, and safety-critical systems where even microsecond jitter can destabilize control.

With the foundational mechanisms of deterministic AI runtimes now established—static memory pre-allocation, priority-inversion avoidance, deadline-enforcement monitors, and bare-metal microkernels—the next step is to consolidate these concepts into a structured operational view. Deterministic runtimes are not abstract execution theories; they are concrete, latency-critical subsystems that govern how inference behaves under real-world constraints such as thermal load, bursty sensor input, and concurrent workload pressure. Table 4.10-132 organizes these mechanisms into a unified framework, showing how each contributes to predictable scheduling, stable memory behavior, deadline-safe inference, and jitter-free dispatch. This table provides the conceptual anchor that links runtime determinism to the broader real-time execution fabric, clarifying how predictable kernel behavior becomes as essential as sensor fidelity in autonomous AI systems.

Table 8.4-E1 presents the core mechanisms that transform AI runtimes from best-effort execution environments into deterministic, latency-bounded systems capable of supporting real-time autonomy. Each mechanism addresses a fundamental challenge inherent to predictable AI execution: eliminating garbage-collection stalls, preventing priority inversion, enforcing inference deadlines, and removing OS-induced jitter. By structuring these mechanisms into a single operational view, the table highlights how deterministic runtimes create a stable execution substrate that perception, prediction, and control loops can rely on. It clarifies the architectural shift from traditional, nondeterministic runtime behavior to tightly controlled, hardware-aligned execution engines designed for safety-critical AI systems.

Table 8.4-E1 — Deterministic AI Runtime Mechanisms and Their Execution Guarantees

Mechanism	Execution Guarantee	Operational Strategy	System-Level Effect
Static AI Memory Pre-Allocation & Deterministic Heap Partitioning	Zero garbage-collection stalls	Pre-allocated tensor pools, fixed heap partitions	Predictable memory access and stable inference latency
Priority-Inversion Avoidance in Real-Time Schedulers	Guaranteed high-priority dispatch	Lock-free queues, priority inheritance, bounded-wait mutexes	Prevents timing drift in perception and control loops
AI Deadline-Enforcement Monitors with Early-Exit Paths	Bounded inference latency	Deadline timers, partial-layer early-exit execution	Ensures control loops never miss deadlines under load
Bare-Metal AI Microkernels Without OS Intermediaries	Cycle-level determinism	Direct hardware scheduling, deterministic interrupts	Eliminates jitter from kernel dispatch and OS noise

Table 8.4-E1 consolidates the mechanisms that transform AI runtimes from best-effort execution environments into deterministic, latency-bounded systems. Each mechanism contributes to predictable scheduling, stable memory behavior, deadline-safe inference, and jitter-free dispatch—forming the execution backbone required for real-time autonomy.

Table 8.4-E1 reveals that deterministic AI execution is constructed from four tightly integrated mechanisms. Static memory pre-allocation eliminates garbage-collection stalls and ensures predictable memory access, preventing latency spikes during inference. Priority-inversion avoidance mechanisms guarantee that high-priority tasks—such as perception and control—always preempt background workloads, preserving temporal coherence across the autonomy loop. Deadline-enforcement monitors maintain bounded inference latency by triggering early-exit execution paths when timing constraints tighten, ensuring that control loops never miss deadlines even under thermal or computational stress. Bare-metal microkernels remove OS jitter entirely, providing cycle-level determinism and stable interrupt handling for critical

workloads.

Together, these mechanisms form the execution backbone required for real-time AI systems. They ensure that once multimodal sensor pipelines deliver temporally aligned data, the runtime environment processes it with equal reliability—maintaining strict deadlines, eliminating nondeterministic pauses, and guaranteeing predictable behavior across heterogeneous accelerators and distributed nodes. Table 8.4-E1 thus provides the operational map for understanding how deterministic runtimes enable autonomous AI systems to act with unwavering temporal precision.

Table 8.4-E1 organizes the deterministic runtime mechanisms—static memory pre-allocation, priority-inversion avoidance, deadline-enforcement monitors, and bare-metal microkernels—into a structured operational framework. To complement this tabular view, Figure 8.4-E1 visualizes how these mechanisms interact as a unified execution substrate that enforces predictable timing across the autonomy loop. The figure shows how memory determinism, priority-safe scheduling, deadline-bounded inference, and OS-free dispatch collectively eliminate jitter and guarantee bounded latency. This visual progression translates the table's conceptual architecture into a pipeline-level diagram that exposes the temporal guarantees required for real-time AI behavior.

Figure 8.4-E1 depicts the deterministic runtime architecture that enables autonomous AI systems to execute with strict temporal guarantees. Each panel highlights a foundational mechanism—static allocation, priority-safe scheduling, deadline enforcement, and bare-metal dispatch—showing how predictable execution is constructed layer by layer. Together, these mechanisms remove garbage-collection stalls, prevent priority inversion, enforce inference deadlines, and eliminate OS jitter. The figure illustrates how deterministic runtimes transform raw computational throughput into stable, latency-bounded execution suitable for robotics, autonomy, and safety-critical AI systems.

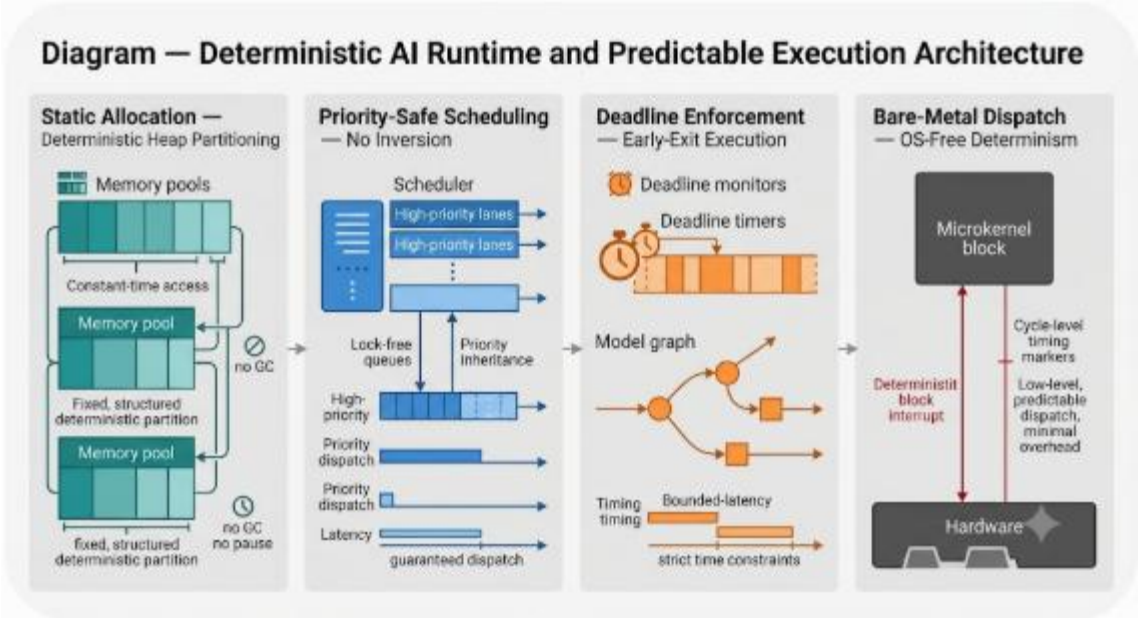


Figure 8.4-E1 — Deterministic AI Runtime and Predictable Execution Architecture
The figure illustrates the four mechanisms that enable deterministic AI execution: static memory pre-allocation, priority-inversion avoidance, deadline-enforcement monitors, and bare-metal microkernels. Together, these mechanisms eliminate jitter, enforce bounded latency, and ensure predictable kernel dispatch across real-time autonomy loops.

Legend

- ***Teal memory pools**: deterministic partitions with constant-time access*
- ***"No GC / No Pause" markers:** garbage-collection-free memory behavior*
- ***Blue scheduler lanes**: priority-aware dispatch paths*
- ***Lock-free queues**: thin arrows without blocking markers*
- ***Priority inheritance arrows**: elevated priority propagation*
- ***Orange deadline timers**: bounded-latency monitors*
- ***Early-exit branches**: partial-layer execution paths*
- ***Dark gray microkernel blocks**: hardware-aligned execution engines*
- ***Red interrupt lines**: deterministic, low-latency signals*
- ***Timing bars**: latency guarantees across panels*

Figure 8.4-E1 shows how deterministic AI runtimes are constructed from four tightly integrated mechanisms. The first panel demonstrates static memory pre-allocation, which eliminates garbage-collection stalls and ensures predictable memory access through fixed, structured heap partitions. The second panel highlights priority-inversion avoidance, guaranteeing that high-priority inference always preempts background tasks using lock-free queues, priority

inheritance, and bounded-wait synchronization. The third panel introduces deadline-enforcement monitors, which maintain bounded inference latency by tracking execution time and triggering early-exit paths when deadlines tighten. The final panel depicts bare-metal microkernels, which remove OS jitter entirely and provide cycle-level determinism through direct hardware scheduling and predictable interrupt handling.

Together, these panels reveal a runtime architecture engineered for real-time AI systems—where perception, prediction, and control must execute with unwavering temporal reliability regardless of workload variability, thermal conditions, or concurrent processes. The figure visually reinforces how deterministic runtimes form the execution backbone that allows autonomous systems to act safely and predictably in dynamic environments.

Deterministic AI runtimes begin with the most fundamental requirement of real-time execution: memory behavior that never surprises the system. Before schedulers can guarantee priority-safe dispatch, before deadline monitors can enforce bounded latency, and before microkernels can deliver cycle-level determinism, the runtime must ensure that every tensor, buffer, and intermediate structure lives in a memory landscape that is fixed, predictable, and incapable of triggering garbage-collection stalls or dynamic allocation jitter. The transition into static AI memory pre-allocation and deterministic heap partitioning marks the moment where the runtime stops behaving like a general-purpose environment and becomes a tightly controlled execution substrate. This is where determinism begins—not in scheduling, not in interrupts, but in the guarantee that memory itself will never introduce latency variability into the autonomy loop.

i. Static AI Memory Pre-Allocation and Deterministic Heap Partitioning Models

Static AI memory pre-allocation and deterministic heap partitioning form the bedrock of real-time AI execution. Deterministic runtimes cannot tolerate garbage-collection stalls, dynamic heap expansion, allocator jitter, or unpredictable memory fragmentation. The moment memory becomes nondeterministic, every higher-level guarantee—priority-safe scheduling, deadline enforcement, microkernel dispatch—begins to erode. Real-time AI systems therefore treat memory not as a dynamic resource but as a fixed, pre-structured substrate whose behavior is fully known before the first inference cycle begins.

Static pre-allocation ensures that all tensors, activation buffers, intermediate feature maps, KV-caches, scratchpads, and model-specific working sets are allocated at startup. Nothing is left to runtime allocation. Every buffer has a predetermined size, a fixed address range, and a stable locality pattern. This eliminates allocator calls during inference, removes heap growth events, and prevents unpredictable pauses caused by memory reclamation. The runtime becomes a

closed system: no new memory is requested, no memory is freed, and no garbage-collection cycle is ever triggered.

Deterministic heap partitioning extends this stability by dividing the memory landscape into structured regions with strict temporal guarantees. Instead of a monolithic heap where allocations compete for space, the runtime uses partitioned pools—one for model weights, one for activations, one for streaming inputs, one for scratch operations, one for IPC buffers, and one for microkernel-level system tasks. Each pool is sized according to worst-case requirements and never changes shape. This prevents fragmentation, ensures constant-time pointer arithmetic, and guarantees that memory access patterns remain identical across inference cycles. The heap becomes a deterministic map: every address is known, every region is fixed, and every access is predictable.

This memory determinism has profound effects on execution behavior. Cache locality becomes stable across runs, reducing cache-miss variance. DMA engines can pre-compute transfer paths because buffer locations never change. Microkernels can schedule operations without worrying about allocator contention. Even thermal behavior becomes more predictable because memory access patterns no longer fluctuate. The entire autonomy loop benefits: perception pipelines receive stable latency, control loops avoid jitter, and distributed inference nodes maintain synchronized timing.

Static pre-allocation also enables compile-time optimization of memory layouts. Graph compilers can fuse operations knowing exactly where intermediate tensors will reside. Memory planners can align buffers to cache lines, vector widths, and accelerator tile boundaries. Zero-copy pathways become easier to maintain because buffers never migrate. The runtime effectively becomes a spatially deterministic machine, where memory is not merely allocated but architected.

In safety-critical systems—robotics, autonomous vehicles, surgical automation—this determinism is not optional. A single garbage-collection pause or heap expansion event can cause a missed control deadline, which in turn can cause physical instability or unsafe behavior. Static memory pre-allocation removes this entire class of failure modes. It transforms memory from a source of nondeterminism into a foundation of temporal reliability.

As soon as memory behavior becomes deterministic, the next challenge is ensuring that execution order respects real-time priorities. Even with perfectly stable memory, a high-priority perception or control kernel can still be delayed if a lower-priority task holds a lock, occupies a queue, or monopolizes a shared resource. This is where the runtime must shift from memory determinism to scheduling determinism. The transition into priority-inversion avoidance

mechanisms marks the moment where the scheduler becomes an active guardian of temporal guarantees, ensuring that critical inference always preempts background work and that no low-priority task can ever block the autonomy loop.

ii. Priority-Inversion Avoidance Mechanisms in Real-Time AI Schedulers

Priority-inversion avoidance mechanisms in real-time AI schedulers exist to protect the most fragile asset in an autonomy stack: the guarantee that critical perception and control work always runs when it needs to, regardless of what else the system is doing. In a naïve scheduler, a low-priority task can hold a lock or occupy a shared resource while a high-priority task waits. In a safety-critical AI system, that waiting is not just inefficient—it is dangerous. Priority inversion turns background work into a hidden source of latency, and in real-time AI, hidden latency is indistinguishable from failure. Avoidance mechanisms are therefore not optional embellishments; they are structural safeguards that ensure the scheduler itself never undermines the temporal guarantees the runtime is designed to uphold.

The first line of defense is the use of lock-free data structures for AI task dispatch. Instead of relying on mutexes or blocking queues, real-time schedulers employ lock-free ring buffers, concurrent queues, and atomic state machines that allow high-priority tasks to enqueue and dequeue work without waiting on shared locks. This prevents low-priority tasks from becoming gatekeepers to critical resources. When perception or control kernels need to run, they can be scheduled immediately, with no dependency on the state of background tasks. The scheduler's internal machinery is designed so that contention never manifests as blocking; it manifests as ordered progress, where high-priority work always has a path forward.

Priority inheritance protocols provide the second layer of protection. In cases where shared resources cannot be made fully lock-free—such as hardware units, DMA channels, or specialized accelerator queues—the scheduler ensures that any low-priority task holding a critical resource temporarily inherits the priority of the high-priority task that is waiting. This prevents the low-priority task from being preempted by other background work and accelerates its completion, freeing the resource for the high-priority task. Priority inheritance turns a potential inversion into a controlled, bounded delay, ensuring that the system never allows a low-priority task to indefinitely block a high-priority one.

Bounded-wait synchronization mechanisms further constrain the scheduler's behavior. Traditional mutexes allow threads to wait indefinitely; real-time AI schedulers replace them with synchronization primitives that enforce maximum wait times. If a high-priority task cannot acquire a resource within a defined bound, the scheduler can trigger alternative execution paths, reschedule work, or escalate the situation to a supervisory control loop. This ensures that

waiting is never unbounded and that the system can respond proactively to emerging contention rather than passively enduring it.

Preemption fences and priority-aware dispatch policies complete the picture. The scheduler is explicitly designed to preempt lower-priority tasks when high-priority AI kernels become runnable. Long-running background jobs—logging, batch training, non-critical analytics—are segmented into preemptible slices so they can be interrupted without destabilizing the system. The dispatch policy is not "fair" in the traditional sense; it is ruthlessly biased toward maintaining the timing of perception, prediction, and control loops. Fairness is redefined as "meeting deadlines," not "sharing CPU time."

In AI-specific contexts, these mechanisms are tuned to the structure of model workloads. For example, the scheduler may treat certain layers of a perception model as critical and others as opportunistic, allowing non-critical layers to be delayed or skipped when contention arises. It may prioritize control-loop inference over background model updates or telemetry processing. It may assign higher priority to kernels that feed directly into actuation decisions and lower priority to those that update long-term state. Priority-inversion avoidance becomes semantically aware: it understands which computations matter most to real-time safety and shapes scheduling behavior accordingly.

The net effect is that the scheduler ceases to be a neutral arbiter of CPU time and becomes an active guardian of temporal guarantees. It ensures that no low-priority task can ever hold the autonomy loop hostage, that contention is always bounded, and that critical AI workloads retain their right-of-way across the entire execution fabric. Memory determinism ensures that access is predictable; priority-inversion avoidance ensures that access is granted to the right tasks at the right time.

Once the scheduler is capable of protecting priority, the next challenge is ensuring that even correctly prioritized work respects hard temporal boundaries. A high-priority task that runs too long can still violate a control deadline, even if it was scheduled immediately. At this point, the runtime must evolve from simply favoring critical tasks to actively policing their execution time. The transition into AI deadline-enforcement monitors with model early-exit execution paths marks the moment where the system stops assuming that critical workloads will finish on time and begins enforcing that they do—by measuring latency, triggering early-exit behavior, and guaranteeing that control loops receive timely outputs even under stress.

iii. AI Deadline-Enforcement Monitors with Model Early-Exit Execution Paths

AI deadline-enforcement monitors with model early-exit execution paths exist to guarantee that inference never violates the temporal boundaries of a real-time autonomy loop. Even when

memory is deterministic and scheduling is priority-safe, a high-priority model can still run too long—because of thermal throttling, bursty sensor input, accelerator contention, or simply because the model's worst-case execution time exceeds the available control-loop window. Deadline-enforcement mechanisms solve this by transforming inference from a best-effort computation into a time-bounded contract: the model must either finish within the deadline or return a valid, partial output that preserves system stability.

The core of deadline enforcement is continuous latency monitoring. Every inference cycle is instrumented with timers that track execution progress at the granularity of layers, subgraphs, or accelerator kernels. These monitors know the maximum allowable latency for perception, prediction, and control loops, and they compare real-time execution against these limits. When execution begins to approach the deadline, the system does not wait passively—it intervenes. The runtime can trigger early-exit execution paths, which allow the model to return a partially computed but semantically meaningful output. These early-exit paths are not crude truncations; they are architected into the model graph itself. For example, a perception model may return a coarse bounding box instead of a refined segmentation mask, or a control model may return a safe fallback trajectory instead of a fully optimized one. The key is that the output remains valid for decision-making, even if it is less detailed.

Early-exit behavior is tightly integrated with model architecture. Transformer-based systems may expose intermediate attention layers as valid outputs. CNN-based perception stacks may include skip-paths that bypass refinement stages. Control-loop models may include fallback policies that are guaranteed to be safe even if they are not optimal. These architectural features allow the runtime to degrade gracefully under stress, preserving temporal guarantees without sacrificing safety. The autonomy loop receives timely outputs, and the system remains stable even when computational load spikes.

Deadline enforcement also interacts with hardware telemetry. If thermal sensors indicate that the accelerator is approaching throttling thresholds, the runtime may proactively switch to early-exit paths before latency begins to drift. If DMA queues show bursty sensor input, the system may shorten inference cycles to maintain synchronization with upstream pipelines. If distributed nodes exhibit network jitter, the runtime may enforce tighter deadlines to prevent cascading delays. Deadline enforcement becomes a dynamic negotiation between model complexity, hardware state, and real-time constraints.

In safety-critical systems, this mechanism is indispensable. A missed control deadline can destabilize a robot, cause an autonomous vehicle to misjudge a trajectory, or delay a surgical robot's response. Early-exit execution paths ensure that the system always has a timely answer, even if it is not the most refined one. The runtime prioritizes temporal correctness over

computational completeness, because in real-time autonomy, a slightly less accurate answer delivered on time is far safer than a perfect answer delivered too late.

Deadline enforcement transforms the runtime from a passive executor into an active temporal regulator. It ensures that inference respects hard boundaries, adapts to dynamic load, and maintains system stability under stress. Memory determinism ensures predictable access; priority-safe scheduling ensures critical tasks run first; deadline enforcement ensures those tasks finish on time.

Once inference is guaranteed to complete within strict temporal limits, the final challenge is eliminating all remaining sources of jitter that originate outside the model itself. Even with deterministic memory, priority-safe scheduling, and deadline-bounded execution, an operating system can still introduce unpredictable delays through context switching, background daemons, interrupt storms, or kernel-level scheduling noise. At this point, the runtime must shed the nondeterministic behavior of general-purpose operating systems entirely. The transition into bare-metal AI microkernels marks the moment where the system abandons OS intermediaries and adopts a minimal, hardware-aligned execution layer capable of cycle-level determinism.

iv. Bare-Metal AI Microkernels Without Intermediary Operating Systems

Bare-metal AI microkernels represent the final and most uncompromising step toward deterministic execution in real-time AI systems. Once memory is fully pre-allocated, once scheduling is protected against priority inversion, and once inference is bounded by deadline-enforcement monitors, the only remaining source of nondeterminism is the operating system itself. General-purpose OS kernels introduce jitter through context switching, background daemons, interrupt storms, scheduler heuristics, page faults, and kernel-level contention. Even microsecond-scale variability can destabilize a control loop or desynchronize a perception-prediction-actuation chain. Bare-metal microkernels eliminate this entire class of unpredictability by removing the operating system from the execution path and replacing it with a minimal, hardware-aligned runtime that performs only the functions essential for deterministic AI execution.

A bare-metal microkernel provides direct control over hardware scheduling, interrupt routing, memory access, and accelerator dispatch. Instead of relying on OS abstractions, the microkernel interacts with hardware registers, DMA engines, and accelerator queues without intermediary layers. This directness produces cycle-level timing guarantees: every interrupt arrives at a predictable moment, every dispatch follows a fixed path, and every context switch is either eliminated or reduced to a trivial, constant-time operation. The microkernel becomes a

deterministic conductor, orchestrating AI workloads with precision that general-purpose operating systems cannot approach.

The absence of OS services also removes noise from the execution environment. There are no background processes competing for CPU time, no kernel threads waking unexpectedly, no virtual memory paging, and no scheduler heuristics attempting to optimize throughput at the expense of latency. The microkernel's footprint is intentionally tiny—often just enough to manage interrupts, dispatch kernels, and maintain a minimal task model. Everything else is stripped away. This minimalism is not an aesthetic choice; it is a temporal guarantee. The fewer moving parts in the runtime, the fewer opportunities for jitter to emerge.

Bare-metal microkernels also enable deterministic interrupt handling. In a general-purpose OS, interrupts may be delayed, coalesced, or reordered based on kernel policies. In a bare-metal environment, interrupts are routed directly to the microkernel's deterministic handler, which processes them immediately and predictably. This is essential for real-time AI systems that rely on sensor events, safety overrides, or actuator feedback. When an interrupt signals a hazard, a collision risk, or a control deviation, the system must respond instantly—not after the OS finishes servicing unrelated tasks.

The microkernel's deterministic behavior extends to accelerator orchestration. GPU kernels, NPU tiles, DSP blocks, and FPGA pipelines can be scheduled with fixed-latency dispatch paths. DMA transfers can be initiated without OS mediation. Memory fences, synchronization primitives, and execution barriers can be implemented with hardware-aligned semantics rather than OS abstractions. This produces a unified execution fabric where every component—CPU, accelerator, memory, and I/O—operates under the same deterministic timing model.

In safety-critical domains, bare-metal microkernels are often the only acceptable foundation. Autonomous vehicles, surgical robots, industrial manipulators, and defense systems cannot tolerate OS jitter. They require a runtime that behaves like a deterministic machine, not a general-purpose computer. Bare-metal microkernels deliver that guarantee by collapsing the execution stack to its essential components and aligning them directly with hardware timing.

Bare-metal execution completes the deterministic runtime architecture. Memory determinism ensures predictable access. Priority-safe scheduling ensures critical tasks run first. Deadline enforcement ensures those tasks finish on time. Bare-metal microkernels ensure nothing in the system undermines these guarantees. Together, they form a runtime capable of supporting real-time AI systems that must act safely and predictably under dynamic physical conditions.

Deterministic AI runtimes transform execution from a best-effort process into a tightly controlled temporal system. Static memory pre-allocation eliminates garbage-collection stalls

and allocator jitter. Priority-inversion avoidance ensures that critical inference always preempts background work. Deadline-enforcement monitors guarantee that inference completes within strict temporal boundaries, even under load. Bare-metal microkernels remove OS-induced jitter and provide cycle-level determinism. These mechanisms collectively create an execution substrate where perception, prediction, and control loops operate with unwavering temporal reliability. Deterministic runtimes are not merely optimizations; they are the foundation upon which real-time AI autonomy is built.

Once deterministic runtimes establish predictable execution at the software level, the next challenge is maintaining that determinism under dynamic physical conditions. Real-time AI systems operate within thermal envelopes, power constraints, and fluctuating hardware states. Even a perfectly deterministic runtime can drift if the hardware beneath it begins to throttle, overheat, or vary its clock frequency. Telemetry-driven AI adaptation with closed-loop DVFS and thermal-boundary control addresses this by continuously monitoring temperature, load, and power headroom, adjusting performance proactively to preserve timing guarantees. The transition into telemetry-driven adaptation marks the moment where determinism expands beyond software behavior and begins to regulate the physical substrate itself.

b. Telemetry-Driven AI Adaptation with Closed-Loop DVFS and Thermal-Boundary Control

Telemetry-driven AI adaptation with closed-loop DVFS and thermal-boundary control extends determinism beyond software behavior and into the physical substrate of the system. Even a perfectly deterministic runtime can drift if the hardware beneath it begins to throttle, overheat, or vary its clock frequency. Real-time AI systems operate inside thermal envelopes, power budgets, and fluctuating load conditions, and these physical constraints can destabilize inference timing unless they are actively regulated. Telemetry-driven adaptation transforms hardware from a passive environment into a continuously monitored, dynamically controlled participant in maintaining real-time guarantees. The system becomes aware of its own temperature, voltage, frequency, and power headroom, and uses this awareness to adjust performance proactively, preserving latency and preventing thermal excursions.

Closed-Loop AI DVFS Controllers with Dynamic Voltage-Frequency Feedback

Closed-loop AI DVFS controllers with dynamic voltage-frequency feedback form the core of this adaptation. Traditional DVFS systems adjust clock rates based on coarse heuristics, but real-time AI requires fine-grained, model-aware control. Closed-loop DVFS continuously samples temperature, load, and power telemetry, feeding this data into a control loop that adjusts voltage and frequency with millisecond-scale responsiveness. When inference load increases, the controller can raise frequency to maintain latency; when temperature rises, it can reduce

voltage to prevent thermal runaway. The feedback loop is tuned to the temporal requirements of perception and control, ensuring that frequency adjustments never introduce jitter. DVFS becomes a real-time actuator, not a background optimization.

Predictive AI Workload Shedding via Junction-Temperature Sensing Loops

Predictive AI workload shedding via junction-temperature sensing loops adds a second layer of protection. Instead of reacting to thermal conditions after they degrade performance, the system predicts thermal excursions before they occur. Junction-temperature sensors provide high-resolution thermal telemetry, allowing the runtime to anticipate when accelerators are approaching thermal boundaries. When a thermal rise is detected, the system can shed non-critical workloads, reduce batch sizes, or trigger early-exit paths in models to prevent throttling. This predictive shedding ensures that critical inference remains stable even under heavy load, and that thermal conditions never force the system into emergency throttling that would violate real-time deadlines.

Precision AI Autoscaling Triggered by Physical Thermal-Boundary Constraints

Precision AI autoscaling triggered by physical thermal-boundary constraints ensures that the system operates within safe thermal envelopes. Autoscaling is not driven by abstract utilization metrics; it is driven by physical constraints such as junction temperature, thermal headroom, and cooling capacity. When the system approaches a thermal boundary, autoscaling can redistribute workloads, reduce parallelism, or shift inference to cooler accelerators. Conversely, when thermal headroom is available, autoscaling can increase parallelism or raise frequency to improve responsiveness. This creates a dynamic equilibrium where performance is maximized without ever crossing thermal safety limits.

Dynamic AI Power-Budget Reallocation Across Multi-Accelerator Fabrics

Dynamic AI power-budget reallocation across multi-accelerator fabrics completes the adaptation framework. Real-time AI systems often run across heterogeneous accelerators—GPUs, NPUs, DSPs, FPGAs—and each accelerator has its own power envelope. Power-budget reallocation allows the system to shift power dynamically between accelerators based on real-time needs. If a perception model requires more power to maintain latency, the system can reduce power allocated to background workloads or non-critical accelerators. If a thermal hotspot emerges on one accelerator, power can be shifted to another. This dynamic reallocation ensures that the system maintains deterministic timing even when power constraints fluctuate.

Telemetry-driven adaptation transforms the hardware layer into an active participant in maintaining real-time guarantees. DVFS controllers adjust frequency to preserve latency.

Predictive shedding prevents thermal excursions. Autoscaling maintains safe thermal boundaries. Power-budget reallocation ensures that critical workloads always have the resources they need. Together, these mechanisms create a closed-loop system where software determinism is reinforced by hardware-level adaptation, producing a unified execution fabric capable of stable performance under dynamic physical conditions.

With the mechanisms of telemetry-driven adaptation now fully articulated—closed-loop DVFS control, predictive workload shedding, thermal-boundary autoscaling, and dynamic power-budget reallocation—the next step is to consolidate these capabilities into a structured operational view. Real-time AI systems cannot rely solely on deterministic runtimes; they must also maintain stability under fluctuating thermal, voltage, and power conditions that directly influence execution timing. Table 8.4-E2 organizes these adaptation mechanisms into a unified framework, showing how each contributes to latency preservation, thermal safety, and resource continuity across heterogeneous accelerators. This table provides the conceptual anchor that links hardware-level adaptation to the broader real-time execution fabric, clarifying how physical telemetry becomes an active participant in maintaining deterministic AI behavior.

Table 8.4-E2 presents the core mechanisms that allow real-time AI systems to remain temporally stable even as thermal load, voltage conditions, and power availability fluctuate. Each mechanism addresses a fundamental challenge inherent to maintaining deterministic execution on physical hardware: preventing frequency jitter, avoiding emergency throttling, respecting thermal boundaries, and reallocating power dynamically across multi-accelerator fabrics. By structuring these mechanisms into a single operational view, the table highlights how telemetry-driven adaptation transforms hardware from a passive substrate into a closed-loop control system that actively preserves latency and stability. It clarifies the architectural shift from static hardware assumptions to dynamic, feedback-driven regulation designed for safety-critical AI workloads.

Table 8.4-E2 — Telemetry-Driven AI Adaptation Mechanisms and Their Stability Guarantees

Mechanism	Stability Guarantee	Operational Strategy	System-Level Effect
Closed-Loop AI DVFS Controllers	Latency-preserving frequency control	Dynamic voltage-frequency feedback	Prevents jitter from thermal or load-driven frequency shifts
Predictive AI Workload Shedding	Pre-throttling thermal protection	Junction-temperature sensing loops	Avoids emergency throttling and

Mechanism	Stability Guarantee	Operational Strategy	System-Level Effect
			maintains inference stability
Precision AI Autoscaling	Thermal-safe performance scaling	Boundary-triggered autoscaling	Maintains performance within safe thermal envelopes
Dynamic AI Power-Budget Reallocation	Resource continuity for critical workloads	Real-time power redistribution across accelerators	Ensures deterministic timing under fluctuating power constraints

Table 8.4-E2 consolidates the mechanisms that allow real-time AI systems to maintain deterministic behavior under dynamic thermal and power conditions. Each mechanism contributes to a closed-loop adaptation framework that preserves latency, prevents thermal excursions, and ensures stable performance across heterogeneous accelerators.

Table 8.4-E2 reveals that maintaining deterministic AI execution requires continuous negotiation with the physical environment. Closed-loop DVFS controllers preserve latency by adjusting voltage and frequency based on real-time telemetry, preventing jitter caused by thermal or load-driven frequency shifts. Predictive workload shedding uses junction-temperature sensing to anticipate thermal excursions before they occur, shedding non-critical work to avoid emergency throttling that would destabilize inference timing. Precision autoscaling responds to thermal-boundary constraints by scaling performance within safe envelopes, ensuring that the system never crosses physical limits that could compromise stability. Dynamic power-budget reallocation distributes power across heterogeneous accelerators in real time, guaranteeing that critical workloads retain the resources they need even when power conditions fluctuate.

Together, these mechanisms form a hardware-aware adaptation framework that reinforces deterministic runtime behavior. They ensure that perception, prediction, and control loops remain temporally stable even when the physical substrate changes, completing the transition from software-level determinism to full-stack real-time stability. Table 8.4-E2 thus provides the operational map for understanding how telemetry-driven adaptation enables autonomous AI systems to maintain predictable behavior under dynamic thermal and power conditions.

Table 8.4-E2 organizes the telemetry-driven adaptation mechanisms—closed-loop DVFS control, predictive workload shedding, thermal-boundary autoscaling, and dynamic power-budget reallocation—into a structured stability framework. To complement this tabular view,

Figure 8.4-E2 visualizes how these mechanisms operate as a unified thermal-safe execution fabric that continuously regulates voltage, frequency, workload distribution, and power allocation. The figure shows how real-time telemetry becomes an active control signal that preserves latency, prevents thermal excursions, and maintains deterministic behavior across heterogeneous accelerators. This visual progression translates the table's conceptual architecture into a dynamic, feedback-driven diagram that exposes the physical stability guarantees required for real-time AI systems.

Figure 8.4-E2 depicts the telemetry-driven adaptation architecture that enables real-time AI systems to maintain deterministic execution under fluctuating thermal and power conditions. Each panel highlights a critical mechanism—closed-loop DVFS control, predictive workload shedding, thermal-boundary autoscaling, and dynamic power-budget reallocation—showing how hardware telemetry is transformed into real-time control actions. Together, these mechanisms ensure that inference latency remains stable, accelerators operate within safe thermal envelopes, and critical workloads retain the power resources they require. The figure illustrates how physical constraints are continuously monitored and regulated to reinforce the deterministic behavior established by the runtime.

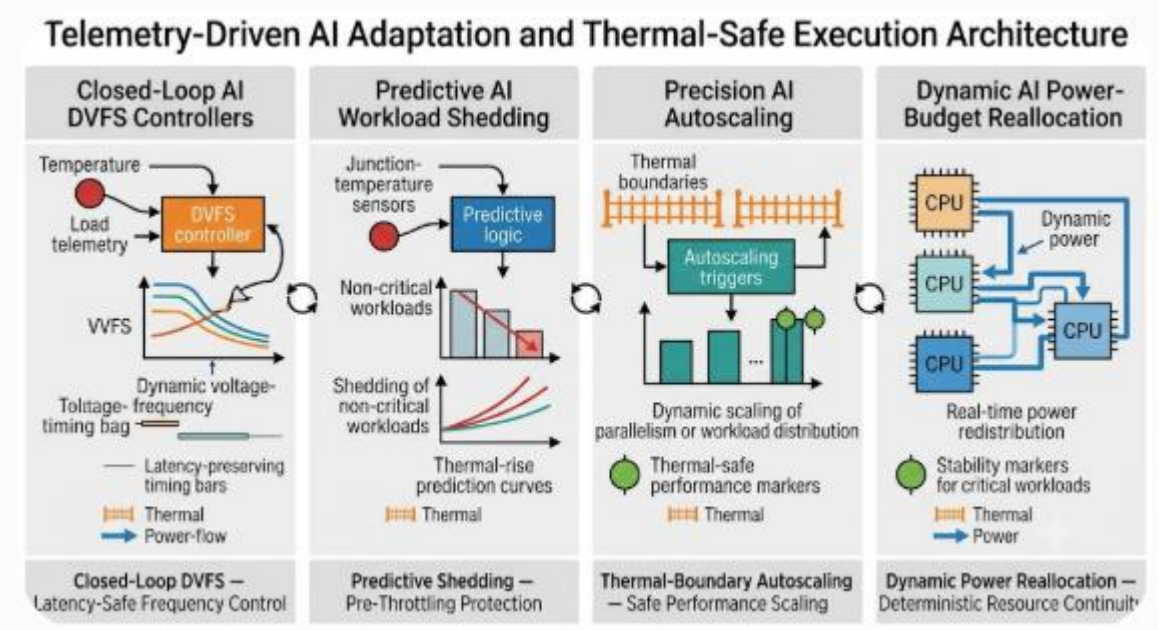


Figure 8.4-E2 — Telemetry-Driven AI Adaptation and Thermal-Safe Execution Architecture
The figure illustrates the four mechanisms that enable real-time AI systems to maintain deterministic behavior under dynamic thermal and power conditions: closed-loop DVFS control, predictive workload shedding, thermal-boundary autoscaling, and dynamic power-budget reallocation. Together, these mechanisms preserve latency, prevent thermal excursions, and stabilize performance across heterogeneous accelerators.

Legend

- ***Orange DVFS controllers****: dynamic voltage-frequency regulators*
- ***Temperature telemetry icons****: real-time junction-temperature sensing*
- ***Thermal-rise prediction curves****: early detection of thermal excursions*
- ***Autoscaling modules****: dynamic scaling triggered by thermal boundaries*
- ***Thermal fences****: physical boundary constraints*
- ***Power-budget controllers****: multi-accelerator power redistribution logic*
- ***Power-flow arrows****: real-time power reallocation*
- ***Timing bars****: latency-preserving execution markers*
- ***Feedback loops****: closed-loop control pathways*

Figure 8.4-E2 shows how telemetry-driven adaptation stabilizes real-time AI execution by regulating the physical substrate beneath the deterministic runtime. The first panel demonstrates closed-loop DVFS control, where voltage and frequency are adjusted based on temperature and load telemetry to preserve latency and prevent jitter. The second panel highlights predictive workload shedding, which uses junction-temperature sensing to anticipate thermal excursions and shed non-critical work before throttling occurs. The third panel introduces precision autoscaling, which dynamically adjusts parallelism and workload distribution based on thermal-boundary constraints to maintain safe performance. The final panel depicts dynamic power-budget reallocation, ensuring that critical workloads retain the power resources they need even when thermal or load conditions fluctuate across multi-accelerator fabrics.

Together, these panels reveal a hardware-aware adaptation architecture that reinforces deterministic runtime behavior. Telemetry becomes a real-time control signal, DVFS becomes a latency-preserving actuator, autoscaling becomes a thermal-safety mechanism, and power-budget reallocation becomes a resource-continuity guarantee. The figure visually demonstrates how real-time AI systems maintain temporal stability not only through deterministic software execution but also through continuous regulation of the physical environment in which that execution occurs.

As soon as telemetry-driven adaptation is understood as a stability layer that reinforces deterministic execution, the natural entry point for deeper exploration is the mechanism that directly regulates the physical timing substrate of the system: closed-loop AI DVFS controllers with dynamic voltage-frequency feedback. Before predictive shedding can anticipate thermal excursions, before autoscaling can enforce thermal boundaries, and before power-budget reallocation can redistribute resources across accelerators, the system must first ensure that

voltage and frequency remain tightly aligned with real-time latency requirements. This is where adaptation begins—not in workload shedding or power redistribution, but in the continuous, feedback-driven modulation of clock rates that preserves inference timing under fluctuating thermal and load conditions.

i. Closed-Loop AI DVFS Controllers with Dynamic Voltage-Frequency Feedback

Closed-loop AI DVFS controllers with dynamic voltage-frequency feedback are the first and most fundamental layer of telemetry-driven adaptation because they directly regulate the physical timing substrate on which deterministic AI execution depends. Even when the runtime is fully deterministic, inference latency can drift if the underlying hardware begins to throttle, overheat, or alter its clock frequency. Closed-loop DVFS eliminates this vulnerability by transforming voltage and frequency from static configuration parameters into continuously modulated control variables governed by real-time telemetry. Temperature, load, and power headroom are sampled at millisecond-scale intervals, and these signals feed into a feedback controller that adjusts voltage and frequency to preserve latency while preventing thermal excursions. Unlike traditional DVFS systems that react slowly or rely on coarse heuristics, AI-specific DVFS loops are tuned to the temporal requirements of perception and control workloads. They raise frequency when inference pressure increases, reduce voltage when thermal boundaries tighten, and maintain clock stability so that no frequency oscillation ever introduces jitter into the autonomy loop.

This feedback-driven modulation is tightly integrated with the AI workload itself. The DVFS controller understands which kernels are latency-critical and which are opportunistic, allowing it to prioritize frequency boosts for perception and control while allowing background tasks to run at lower power states. It also interacts with accelerator telemetry—GPU tile temperatures, NPU junction readings, DSP load curves—to ensure that each hardware unit receives precisely the voltage-frequency pairing required to maintain deterministic timing. The result is a hardware layer that behaves like a regulated actuator rather than a passive substrate. Frequency becomes a controlled variable, not a source of nondeterministic drift.

Closed-loop DVFS also prevents catastrophic thermal events. By monitoring temperature in real time, the controller can reduce voltage before throttling occurs, avoiding sudden drops in performance that would destabilize inference timing. This proactive behavior ensures that the system never enters emergency thermal states, preserving both latency and safety. In distributed or multi-accelerator systems, DVFS loops can coordinate across devices, ensuring that no single accelerator becomes a thermal hotspot that compromises the entire pipeline.

In safety-critical AI systems—autonomous vehicles, surgical robotics, industrial automation—

closed-loop DVFS is indispensable. It ensures that inference timing remains stable even when environmental conditions change, workloads spike, or cooling efficiency fluctuates. It is the mechanism that keeps the physical substrate aligned with the deterministic guarantees established by the runtime.

Once voltage and frequency are stabilized through closed-loop control, the next challenge is anticipating thermal excursions before they occur. Even with perfect DVFS regulation, rising junction temperatures can signal impending throttling or thermal saturation. At this point, the system must evolve from reactive control to predictive behavior. The transition into predictive AI workload shedding via junction-temperature sensing loops marks the moment where telemetry stops merely regulating performance and begins forecasting thermal risk, allowing the system to shed non-critical workloads before they threaten real-time stability.

ii. Predictive AI Workload Shedding via Junction-Temperature Sensing Loops

Predictive AI workload shedding via junction-temperature sensing loops is where telemetry-driven adaptation stops being purely reactive and becomes anticipatory. Closed-loop DVFS can smooth out frequency and voltage in response to rising temperature, but there is a point at which thermal momentum makes throttling inevitable if the system continues to push full workloads through hot silicon. Predictive shedding solves this by treating junction-temperature telemetry not just as a snapshot of current state, but as a signal for imminent risk. High-resolution temperature sensors feed continuous streams into prediction models—simple control laws in some systems, learned thermal predictors in more advanced ones—that estimate how quickly a device is approaching its thermal boundary under current load. When the predicted trajectory crosses a safety threshold, the system begins shedding non-critical workloads before hardware is forced into emergency throttling.

This shedding is selective and semantically aware. The runtime distinguishes between critical perception and control kernels, which must be preserved, and opportunistic tasks such as background analytics, logging, batch inference, or low-priority model updates. As junction temperature rises, the system first reduces or pauses these non-critical tasks, freeing thermal and power headroom for the critical path. If the thermal trajectory continues upward, the system can further degrade non-essential work by lowering batch sizes, reducing precision, or deferring scheduled jobs. In extreme cases, it can trigger early-exit paths in non-critical models, returning partial results while minimizing additional heat generation. The goal is always the same: keep the autonomy loop intact while allowing the rest of the workload to flex around thermal reality.

Predictive shedding also interacts with spatial aspects of the hardware. In multi-accelerator

fabrics, junction-temperature sensing can identify hotspots and redistribute non-critical workloads to cooler devices, preventing localized overheating. In systems with uneven cooling or airflow, shedding can be targeted to the most thermally stressed components. The shedding logic becomes a thermal traffic controller, steering work away from danger zones before they force the system into abrupt, latency-breaking throttling.

Because this mechanism is predictive, it operates on time scales that matter for real-time AI. Instead of waiting for the hardware to cross a hard thermal limit and then reacting with aggressive throttling, the system begins adjusting workload composition while there is still margin. This preserves the continuity of critical inference and avoids the sharp performance cliffs that traditional thermal management often produces. In safety-critical contexts, this difference is profound: a robot arm, vehicle, or surgical tool continues to receive timely control signals even as the system quietly sheds non-essential work to keep itself within safe thermal bounds.

Once the system can anticipate and shed workloads based on thermal trajectories, the next step is to formalize the relationship between performance and physical limits. Predictive shedding keeps the system away from dangerous temperatures, but it does not by itself define the exact boundaries within which performance must be constrained. That role belongs to precision AI autoscaling triggered by physical thermal-boundary constraints, where thermal envelopes are treated as explicit control surfaces and the system scales parallelism, throughput, and workload placement in direct response to those boundaries, turning thermal limits into structured, enforceable operating regimes rather than implicit danger zones.

iii. Precision AI Autoscaling Triggered by Physical Thermal-Boundary Constraints

Precision AI autoscaling triggered by physical thermal-boundary constraints is where telemetry-driven adaptation becomes structurally disciplined rather than merely reactive or predictive. Closed-loop DVFS stabilizes frequency, and predictive shedding prevents thermal spikes, but neither mechanism defines the explicit operating envelope within which the system must remain. Autoscaling introduces that envelope by treating thermal boundaries as hard physical constraints that govern how much parallelism, throughput, and workload distribution the system can safely sustain. Instead of scaling based on abstract utilization metrics, the system scales based on the real, measurable thermal headroom available at each moment.

Autoscaling begins with continuous monitoring of junction temperature, package temperature, cooling efficiency, and thermal gradients across accelerators. These signals define a dynamic thermal boundary—a moving limit that reflects both current conditions and the system's ability to dissipate heat. When the system approaches this boundary, autoscaling reduces parallelism,

lowers batch sizes, or shifts workloads to cooler accelerators. When thermal headroom increases, autoscaling expands parallelism, increases throughput, or restores deferred workloads. The system breathes with its thermal environment, expanding and contracting performance in a controlled, predictable manner.

This autoscaling is precise because it is physically grounded. It does not rely on heuristics or coarse thresholds; it uses real thermal telemetry to determine exactly how much performance the system can safely deliver. In AI workloads, this precision is essential. A perception model may require strict latency guarantees, while a background analytics model may tolerate reduced throughput. Autoscaling understands these distinctions and scales each workload according to its thermal sensitivity and real-time importance. Critical inference receives priority scaling, while non-critical tasks absorb the reductions necessary to maintain thermal safety.

Autoscaling also interacts with spatial thermal dynamics. In multi-accelerator systems, thermal boundaries differ across devices due to cooling asymmetry, workload distribution, and physical placement. Precision autoscaling can shift workloads from hotter accelerators to cooler ones, maintaining overall throughput while preventing localized overheating. It can also coordinate scaling across devices to ensure that no single accelerator becomes a thermal bottleneck that destabilizes the entire pipeline. The system becomes thermally aware not just of its global state but of its spatial distribution of heat.

The result is a performance envelope that is both safe and optimized. Autoscaling ensures that the system never crosses thermal boundaries that would trigger emergency throttling, while simultaneously maximizing performance within those boundaries. It transforms thermal constraints from reactive triggers into proactive control surfaces. In safety-critical AI systems, this transformation is vital: the autonomy loop receives stable, timely outputs even as the system dynamically adjusts its performance to remain within safe thermal limits.

Once autoscaling establishes a thermally safe performance envelope, the next challenge is ensuring that power resources are allocated in a way that reinforces this envelope across heterogeneous accelerators. Thermal boundaries define how much performance each accelerator can safely deliver, but power availability determines whether that performance can be sustained. At this point, the system must evolve from thermal-aware scaling to power-aware resource distribution. The transition into dynamic AI power-budget reallocation across multi-accelerator fabrics marks the moment where the system begins actively redistributing power to ensure that critical workloads retain the energy they need, even as thermal conditions shift and workload placement changes.

iv. Dynamic AI Power-Budget Reallocation Across Multi-Accelerator Fabrics

Dynamic AI power-budget reallocation across multi-accelerator fabrics is the final and most expressive layer of telemetry-driven adaptation because it governs how energy—the most fundamental physical resource—is distributed across heterogeneous compute units in real time. Modern AI systems rarely rely on a single accelerator; they operate across GPUs, NPUs, DSPs, FPGAs, and specialized inference ASICs, each with its own thermal envelope, power draw, and workload sensitivity. Under fluctuating load and thermal conditions, static power allocation becomes a liability: one accelerator may starve for power while another idles with unused headroom. Dynamic power-budget reallocation solves this by treating power as a fluid resource that can be redistributed continuously based on real-time telemetry and workload priority.

This reallocation begins with fine-grained monitoring of power draw, voltage stability, thermal gradients, and workload intensity across all accelerators. These signals feed into a power-management controller that determines how much energy each accelerator requires to maintain deterministic timing for its assigned workloads. Critical inference paths—perception, prediction, control—receive priority access to power, ensuring that their latency remains stable even when the system is under thermal or computational stress. Non-critical workloads absorb reductions in power allocation, slowing or pausing as necessary to preserve the stability of the autonomy loop.

Power-budget reallocation is not merely reactive; it is anticipatory. When telemetry indicates that a particular accelerator is approaching a thermal boundary, the system can proactively reduce its power allocation and shift workloads to cooler devices. Conversely, when an accelerator has thermal headroom, the system can increase its power budget to accelerate critical inference or restore deferred workloads. This dynamic balancing prevents localized hotspots, avoids emergency throttling, and maintains throughput across the entire fabric.

In multi-accelerator systems, power reallocation also enables spatial optimization. Workloads can be migrated to accelerators with better cooling, lower thermal load, or more efficient power-performance curves. The system becomes aware of the physical topology of its compute fabric, using power as a steering mechanism to maintain thermal equilibrium and performance continuity. This spatial intelligence is essential in systems where accelerators differ in architecture, efficiency, or thermal behavior.

The result is a power-aware execution fabric that reinforces deterministic behavior at the deepest physical level. Power is no longer a static constraint; it is a dynamic control variable that ensures critical workloads always have the energy they need to meet real-time deadlines. In safety-critical AI systems, this capability is indispensable. A robot arm, autonomous vehicle, or surgical tool cannot afford a missed control signal because an accelerator was starved for power. Dynamic reallocation ensures that such failures never occur.

Telemetry-driven power management completes the adaptation framework. DVFS stabilizes frequency, predictive shedding prevents thermal spikes, autoscaling enforces thermal boundaries, and power reallocation ensures resource continuity across heterogeneous accelerators. Together, these mechanisms create a closed-loop system where physical constraints are continuously monitored, predicted, and regulated to preserve deterministic AI execution.

Telemetry-driven AI adaptation transforms hardware from a passive substrate into an active, self-regulating system that maintains deterministic behavior under dynamic thermal and power conditions. Closed-loop DVFS controllers preserve latency by modulating voltage and frequency in real time. Predictive workload shedding anticipates thermal excursions and prevents emergency throttling. Precision autoscaling enforces thermal boundaries by scaling performance within safe envelopes. Dynamic power-budget reallocation ensures that critical workloads retain the energy they need across multi-accelerator fabrics. These mechanisms collectively create a physical stability layer that reinforces deterministic runtime guarantees, enabling real-time AI systems to operate safely, predictably, and continuously even under fluctuating environmental and computational conditions.

With physical stability now established, the next challenge is ensuring that information moves through the system with equal determinism. Even perfectly regulated hardware can fail to meet real-time deadlines if inter-process communication introduces jitter, blocking, or unpredictable latency. The transition into asynchronous AI inter-process communications with hard real-time guarantees marks the moment where the system shifts from stabilizing computation to stabilizing communication. This is where the execution fabric extends beyond processors and accelerators into the channels that connect them, ensuring that messages, interrupts, and control signals move with the same temporal precision as the computations they trigger.

c. Asynchronous AI Inter-Process Communications (IPC) Channels with Hard Real-Time Guarantees and Fail-Safe Interrupts

Asynchronous AI inter-process communication channels with hard real-time guarantees and fail-safe interrupts form the connective tissue of a deterministic AI system. Even if computation is deterministic and hardware is thermally regulated, the system can still fail to meet real-time deadlines if messages, signals, or control packets experience jitter, blocking, or unpredictable routing delays. IPC is the circulatory system of autonomy: perception results must reach prediction modules on time, prediction must reach control loops on time, and safety interrupts must preempt everything instantly. Asynchronous IPC ensures that communication behaves with the same temporal precision as the computations it connects.

Lock-Free AI Ring Buffers with Atomic Cross-Core Communication Paths

Lock-free AI ring buffers with atomic cross-core communication paths provide the foundation for deterministic IPC. Traditional queues rely on locks, mutexes, or blocking semantics that introduce unpredictable delays when multiple cores contend for shared resources. Lock-free ring buffers eliminate this by using atomic operations, memory fences, and wait-free enqueue/dequeue paths. Messages move between cores without blocking, and high-priority packets can be inserted or consumed immediately. The ring buffer becomes a deterministic conduit: every message has a constant-time path, and no low-priority process can ever stall the autonomy loop by holding a lock. This atomic communication fabric ensures that perception, prediction, and control signals propagate with microsecond-scale consistency.

Hard Real-Time AI Timeout Traps with Fallback Routing Across IPC Networks

Hard real-time AI timeout traps with fallback routing across IPC networks add a second layer of protection. Even in lock-free systems, messages can be delayed by transient congestion, hardware anomalies, or unexpected bursts of traffic. Timeout traps detect when a message has exceeded its allowable latency window and immediately reroute it through alternative IPC paths. These fallback routes may use secondary ring buffers, dedicated safety channels, or direct microkernel interrupts. The key is that no message is ever allowed to wait indefinitely. If the primary path is compromised, the system switches routes instantly, preserving the temporal guarantees required for real-time autonomy. Timeout traps transform IPC from a best-effort mechanism into a hard-bounded communication fabric.

Edge-Triggered AI Interrupt Handling Integrated with Vector-Tensor Compute Pipelines

Edge-triggered AI interrupt handling integrated with vector-tensor compute pipelines ensures that critical signals—hazard detections, safety overrides, emergency stops—preempt ongoing computation without destabilizing the system. In general-purpose operating systems, interrupts may be delayed, coalesced, or reordered. In deterministic AI systems, interrupts must be processed immediately and predictably. Edge-triggered handlers route interrupts directly into microkernel-level logic that can pause, redirect, or terminate compute pipelines without corrupting state. Vector and tensor units receive deterministic interrupt fences that allow them to halt execution at safe boundaries, preserving data integrity while ensuring that safety signals are never delayed. Interrupts become first-class citizens in the execution fabric, capable of overriding any ongoing computation with cycle-level precision.

Deterministic AI IPC Ring-Bus Topologies for Local Peripheral Network Coordination

Deterministic AI IPC ring-bus topologies for local peripheral network coordination complete the

communication architecture. In distributed systems—robotic arms, autonomous vehicles, surgical robots—local peripherals must coordinate with each other in real time. Sensors, actuators, controllers, and safety modules exchange messages across ring-bus networks that guarantee fixed-latency traversal. Unlike traditional bus architectures that allow variable routing delays, deterministic ring-bus topologies enforce constant-time hops between nodes. Every message travels a predictable path, and the topology itself prevents congestion by design. This ensures that local coordination—joint synchronization, actuator timing, sensor fusion—remains stable even under heavy load.

Together, these mechanisms create an IPC fabric that is as deterministic as the compute and thermal layers beneath it. Lock-free buffers eliminate blocking. Timeout traps enforce hard latency bounds. Edge-triggered interrupts guarantee immediate safety response. Deterministic ring-bus topologies ensure stable peripheral coordination. Communication becomes a real-time guarantee rather than a probabilistic behavior, enabling autonomous systems to maintain temporal precision across both computation and messaging.

With the architecture of deterministic IPC now fully articulated—from lock-free ring buffers to hard timeout traps, edge-triggered interrupts, and constant-hop ring-bus coordination—the next step is to consolidate these mechanisms into a structured operational view. Real-time AI systems cannot rely solely on deterministic computation or thermally regulated hardware; they must also ensure that messages, interrupts, and control signals traverse the system with unwavering temporal precision. Table 8.4-E3 organizes these IPC mechanisms into a unified framework, showing how each contributes to hard real-time guarantees across the autonomy stack. This table provides the conceptual anchor that links communication determinism to the broader execution fabric, clarifying how IPC becomes a first-class component of real-time AI stability.

Table 8.4-E3 presents the core IPC mechanisms that allow real-time AI systems to maintain deterministic communication under dynamic load, contention, and hardware variability. Each mechanism addresses a fundamental challenge inherent to real-time messaging: eliminating blocking, bounding latency, guaranteeing instantaneous interrupt response, and stabilizing peripheral coordination. By structuring these mechanisms into a single operational view, the table highlights how asynchronous IPC channels evolve from conventional message-passing systems into hard real-time communication fabrics engineered for safety-critical AI workloads. It clarifies the architectural shift from probabilistic communication behavior to deterministic, fail-safe messaging pathways.

Table 8.4-E3 — Deterministic AI IPC Mechanisms and Their Real-Time Guarantees

Mechanism	Real-Time Guarantee	Operational Strategy	System-Level Effect
Lock-Free AI Ring Buffers	Constant-time message passing	Atomic cross-core operations	Eliminates blocking and priority inversion in IPC
Hard Real-Time Timeout Traps	Bounded-latency message delivery	Fallback routing across IPC networks	Prevents message stalls and ensures deadline compliance
Edge-Triggered AI Interrupt Handling	Instantaneous safety response	Direct microkernel interrupt fences	Guarantees fail-safe overrides during critical events
Deterministic AI IPC Ring-Bus Topologies	Fixed-latency peripheral coordination	Constant-hop routing across ring-bus networks	Stabilizes sensor-actuator communication under load

Table 8.4-E3 consolidates the IPC mechanisms that allow real-time AI systems to maintain deterministic communication under dynamic load, ensuring that messages, interrupts, and control signals propagate with hard temporal guarantees.

Table 8.4-E3 reveals that deterministic AI execution requires communication channels that are as predictable as the computations they connect. Lock-free ring buffers guarantee constant-time message passing by eliminating locks and contention, ensuring that no low-priority process can ever stall critical signals. Hard real-time timeout traps enforce bounded latency by detecting stalled messages and rerouting them through fallback paths, transforming IPC from a best-effort mechanism into a deadline-compliant fabric. Edge-triggered interrupt handling integrates safety signals directly into vector-tensor pipelines, guaranteeing instantaneous response during hazard detection or emergency overrides. Deterministic ring-bus topologies provide fixed-latency coordination across local peripheral networks, ensuring that sensors, actuators, and controllers remain synchronized even under heavy load.

Together, these mechanisms form a communication substrate engineered for real-time AI autonomy. They ensure that perception results reach prediction modules on time, prediction reaches control loops on time, and safety interrupts preempt everything instantly. Table 8.4-E3 thus provides the operational map for understanding how deterministic IPC reinforces the broader real-time execution fabric, enabling autonomous systems to maintain temporal precision across both computation and communication.

Table 8.4-E3 organizes the deterministic IPC mechanisms—lock-free ring buffers, hard real-time timeout traps, edge-triggered interrupt handling, and constant-hop ring-bus coordination—into a structured stability framework. To complement this tabular view, Figure 8.4-E3 visualizes how these mechanisms operate as a unified communication fabric that guarantees message delivery, interrupt responsiveness, and peripheral coordination under hard real-time constraints. The figure translates the table's conceptual architecture into a dynamic, signal-driven diagram that exposes how asynchronous IPC channels become deterministic pathways, ensuring that communication behaves with the same temporal precision as the computations and thermal-regulated hardware beneath it.

Figure 8.4-E3 depicts the deterministic IPC architecture that enables real-time AI systems to maintain hard-bounded communication latency across cores, accelerators, and peripheral networks. Each panel highlights a critical mechanism—atomic ring buffers, timeout-driven fallback routing, edge-triggered interrupt fences, and deterministic ring-bus traversal—showing how asynchronous messaging is transformed into a predictable, fail-safe communication substrate. Together, these mechanisms ensure that perception outputs reach prediction modules on time, prediction reaches control loops on time, and safety interrupts preempt ongoing computation instantly. The figure illustrates how deterministic IPC becomes a foundational pillar of real-time autonomy.

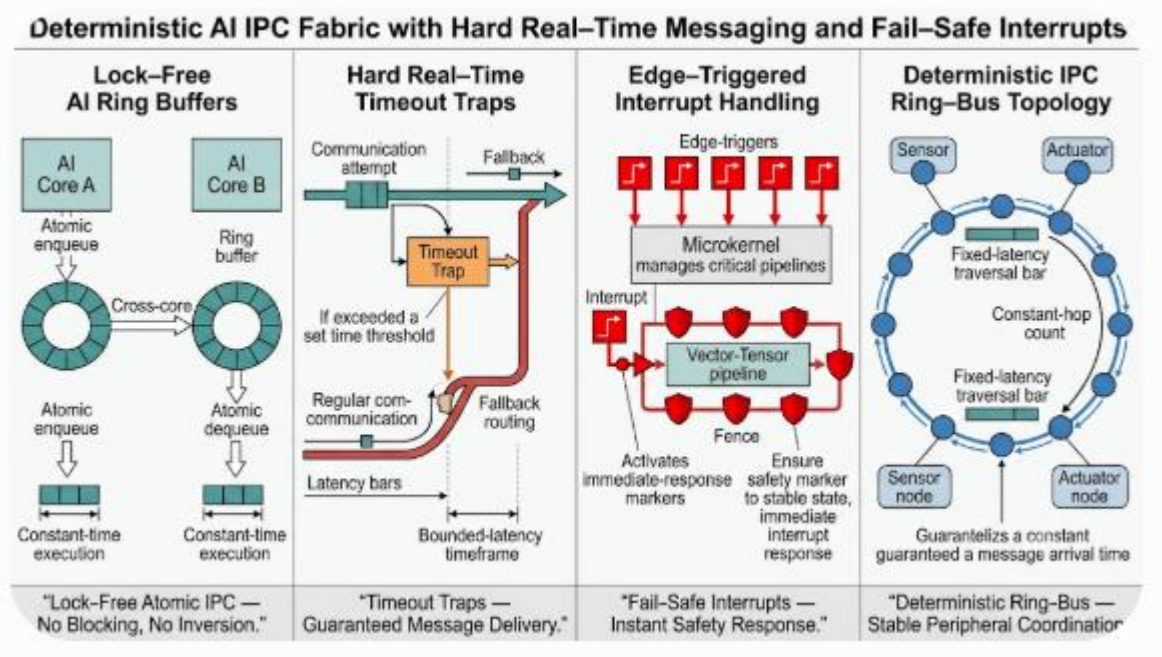


Figure 8.4-E3— Deterministic AI IPC Fabric with Hard Real-Time Messaging and Fail-Safe Interrupts

The figure illustrates the four mechanisms that enable deterministic communication in real-time AI systems: lock-free ring buffers, hard timeout traps, edge-triggered interrupt handling, and deterministic ring-bus topologies. Together, these mechanisms ensure that messages, interrupts, and control signals propagate with hard temporal guarantees across the autonomy stack.

Legend

- ***Teal ring buffers****: atomic, lock-free IPC channels*
- ***White atomic arrows****: constant-time enqueue/dequeue operations*
- ***Orange timeout traps****: bounded-latency enforcement*
- ***Red fallback routes****: alternate message paths under congestion*
- ***Edge-trigger icons****: immediate interrupt signals*
- ***Microkernel block****: deterministic interrupt-handling logic*
- ***Blue ring-bus network****: constant-hop peripheral coordination*
- ***Latency bars****: real-time timing guarantees*
- ***Safety shields****: fail-safe override markers*

Figure 8.4-E3 shows how deterministic IPC transforms communication into a hard real-time guarantee. The first panel demonstrates lock-free ring buffers, where atomic operations eliminate blocking and ensure constant-time message passing across cores. The second panel highlights hard real-time timeout traps, which detect stalled messages and reroute them instantly through fallback paths, preventing deadline violations. The third panel introduces edge-triggered interrupt handling, which integrates safety signals directly into microkernel logic and vector-tensor pipelines, guaranteeing immediate response during hazard detection or emergency overrides. The final panel depicts deterministic ring-bus topologies, which provide fixed-latency traversal for sensor-actuator coordination, ensuring stable peripheral synchronization even under heavy load.

Together, these panels reveal an IPC architecture engineered for real-time AI autonomy—one where messages, interrupts, and control signals move with unwavering temporal reliability regardless of contention, load, or hardware variability. The figure visually reinforces how deterministic communication completes the execution fabric that supports safe, predictable autonomous behavior.

As soon as the deterministic IPC framework is understood as a stability layer that guarantees message delivery, interrupt responsiveness, and peripheral coordination, the natural entry point for deeper exploration is the mechanism that eliminates the single greatest threat to real-time communication: blocking. Before timeout traps can enforce bounded latency, before interrupt fences can guarantee instantaneous safety response, and before ring-bus topologies can

stabilize peripheral coordination, the system must first ensure that no message ever waits on a lock or contends for a shared resource. This is where deterministic IPC begins—not in fallback routing or interrupt handling, but in the construction of lock-free AI ring buffers with atomic cross-core communication paths that provide constant-time message movement across the autonomy stack.

i. Lock-Free AI Ring Buffers with Atomic Cross-Core Communication Paths

Lock-free AI ring buffers with atomic cross-core communication paths are the foundational mechanism that transforms inter-process communication from a probabilistic, contention-prone subsystem into a deterministic, constant-time messaging fabric. In traditional IPC designs, queues rely on locks, mutexes, or kernel-mediated synchronization, all of which introduce blocking behavior when multiple cores attempt to access shared resources. Blocking is catastrophic in real-time AI systems: a single stalled enqueue or dequeue can delay perception updates, postpone prediction outputs, or interrupt control-loop signals. Lock-free ring buffers eliminate this entire class of latency hazards by replacing locks with atomic operations, memory-ordering fences, and wait-free algorithms that guarantee forward progress regardless of contention.

At the architectural level, each ring buffer is a circular array of message slots accessed through atomic head and tail pointers. Producers and consumers operate independently, using atomic compare-and-swap or fetch-add instructions to reserve slots without ever acquiring a lock. Because these operations complete in constant time, message insertion and retrieval remain predictable even under heavy load. Cross-core communication becomes a sequence of atomic state transitions rather than a negotiation over shared locks. This ensures that high-priority messages—such as perception results or safety-critical control signals—can be delivered immediately, without waiting for background tasks to release resources.

Memory-ordering fences ensure that messages are visible to consumers exactly when intended, preventing reordering or partial writes that could corrupt data or introduce nondeterministic behavior. The ring buffer's structure also prevents priority inversion: no low-priority thread can block a high-priority one, because no thread ever holds exclusive access to the buffer. The autonomy loop retains its right-of-way across the entire communication fabric.

Lock-free ring buffers also scale naturally across heterogeneous compute fabrics. AI accelerators, vector units, tensor cores, and microcontroller subsystems can all communicate through atomic ring buffers without relying on OS-level IPC. This allows the microkernel to orchestrate communication directly at the hardware level, bypassing sources of jitter such as scheduler heuristics, interrupt coalescing, or kernel-mediated queue management. The result is

a communication substrate that behaves with the same deterministic timing as the compute pipelines it connects.

In safety-critical systems, this determinism is essential. A robot arm cannot wait for a mutex to release before receiving a torque update. An autonomous vehicle cannot tolerate a delayed hazard-detection message. A surgical robot cannot risk a blocked control signal. Lock-free ring buffers ensure that these messages always move, always complete, and always do so within a bounded, predictable time window.

Once message passing is guaranteed to be lock-free and constant-time, the next challenge is ensuring that messages still meet their deadlines even when the communication fabric experiences transient congestion or unexpected delays. Atomic ring buffers eliminate blocking, but they cannot eliminate all sources of latency drift—thermal events, bursty workloads, or accelerator stalls can still slow message propagation. At this point, the system must evolve from guaranteeing progress to guaranteeing deadlines. The transition into hard real-time AI timeout traps with fallback routing across IPC networks marks the moment where IPC stops merely ensuring that messages move and begins ensuring that they arrive on time, even if the primary communication path becomes compromised.

ii. Hard Real-Time AI Timeout Traps with Fallback Routing Across IPC Networks

Hard real-time AI timeout traps with fallback routing across IPC networks are the mechanism that elevates deterministic communication from “always progressing” to “always arriving on time.” Lock-free ring buffers eliminate blocking, but they cannot eliminate every source of latency drift—thermal slowdowns, bursty sensor input, accelerator stalls, or transient congestion can still cause a message to miss its deadline. In a real-time AI system, a late message is functionally equivalent to a lost one: a perception update that arrives after the control loop has already executed is useless, and a safety signal that arrives after a hazard has already propagated is dangerous. Timeout traps solve this by enforcing strict temporal boundaries on every IPC transaction and providing immediate fallback routing when those boundaries are threatened.

A timeout trap monitors each message as it traverses the IPC fabric, comparing its real-time age against a hard deadline derived from the autonomy loop’s timing constraints. These traps operate at microkernel level, not at application level, ensuring that latency enforcement is independent of workload complexity or software state. When a message approaches its deadline, the trap intervenes. If the primary communication path is congested, the trap reroutes the message through a secondary ring buffer, a dedicated safety channel, or a direct interrupt-driven pathway. This fallback routing is deterministic: the system knows exactly how

long each alternative path takes, and these paths are engineered to guarantee delivery within the remaining time budget.

Timeout traps also provide fail-safe behavior under partial hardware degradation. If an accelerator or core becomes thermally saturated, the trap can bypass it entirely, routing messages through cooler or less-loaded devices. If a ring buffer experiences transient overload, the trap can redirect traffic to a parallel buffer. If a peripheral bus experiences jitter, the trap can escalate the message to an interrupt-driven route. The system never waits for a stalled component to recover; it simply switches paths and continues delivering messages on time.

This mechanism is especially critical for safety-critical signals. Hazard detections, emergency stops, collision warnings, and actuator overrides must never be delayed. Timeout traps ensure that these signals are delivered even if the primary IPC path is compromised. They transform IPC from a best-effort messaging system into a hard-bounded communication fabric where every message either arrives on time or is escalated through a guaranteed fallback route.

Timeout traps also integrate with telemetry-driven adaptation. If thermal sensors indicate that a particular accelerator is slowing down, timeout thresholds tighten automatically. If DVFS reduces frequency to preserve thermal safety, timeout traps adjust their routing logic to compensate. IPC becomes a dynamic, self-regulating system that adapts to physical conditions while preserving real-time guarantees.

Once messages are guaranteed to arrive on time—even under congestion, thermal stress, or partial hardware failure—the next challenge is ensuring that safety signals can preempt ongoing computation instantly. Timeout traps guarantee timely delivery, but they do not guarantee immediate execution. That responsibility belongs to edge-triggered AI interrupt handling integrated with vector-tensor compute pipelines, where interrupts become deterministic control signals capable of halting, redirecting, or overriding computation with cycle-level precision.

iii. Edge-Triggered AI Interrupt Handling Integrated with Vector-Tensor Compute Pipelines

Edge-triggered AI interrupt handling integrated with vector-tensor compute pipelines is the mechanism that ensures safety-critical signals can preempt ongoing computation with cycle-level precision. In general-purpose systems, interrupts may be delayed, coalesced, reordered, or masked by kernel heuristics. Such behavior is unacceptable in real-time AI autonomy, where hazard detections, collision warnings, actuator overrides, and emergency stops must interrupt computation immediately and deterministically. Edge-triggered interrupt handling solves this by routing interrupts directly into microkernel-level logic that interfaces with vector and tensor pipelines through hardware-aligned fences, ensuring that interrupts are

processed at the exact moment they occur.

At the architectural level, edge-triggered interrupts are latched the instant a rising or falling signal is detected. Instead of waiting for a scheduler or kernel thread to acknowledge the event, the microkernel dispatches an interrupt handler that operates outside the normal execution path. This handler interacts directly with vector-tensor compute pipelines, inserting deterministic fences that halt or redirect computation at safe boundaries. These fences are engineered to preserve data integrity: they pause execution only at points where intermediate states are consistent, registers are stable, and memory writes are complete. This prevents corruption while ensuring that safety signals override ongoing computation without delay.

The integration with vector-tensor pipelines is crucial. Modern AI workloads run on deeply pipelined hardware where operations are distributed across multiple stages—fetch, decode, vector expansion, tensor contraction, accumulation, and writeback. Interrupting such pipelines without careful coordination can lead to partial writes, inconsistent states, or deadlocks. Edge-triggered interrupt fences solve this by defining deterministic interrupt points within the pipeline. When an interrupt arrives, the pipeline advances to the nearest safe fence, halts, and hands control to the interrupt handler. This ensures that safety signals are processed immediately while maintaining the integrity of ongoing computation.

Interrupt handling also interacts with IPC mechanisms. When a safety interrupt is triggered, the handler can inject high-priority messages directly into lock-free ring buffers, bypassing normal routing paths. It can also escalate signals through timeout-trap fallback routes to guarantee delivery even under congestion. This creates a unified safety fabric where interrupts and messages reinforce each other, ensuring that hazard information propagates through the system with hard real-time guarantees.

In distributed or multi-accelerator systems, edge-triggered interrupts coordinate across devices. A hazard detected by one sensor can trigger interrupts on multiple accelerators simultaneously, halting computation across the fabric to ensure synchronized response. This prevents situations where one accelerator continues executing outdated control logic while another has already reacted to a hazard. Interrupt propagation becomes a deterministic broadcast mechanism that maintains coherence across heterogeneous compute units.

In safety-critical AI systems—autonomous vehicles, surgical robots, industrial manipulators—this capability is indispensable. A delayed interrupt can lead to a missed braking event, a misaligned robotic arm, or an unsafe surgical motion. Edge-triggered interrupt handling ensures that such failures never occur. It transforms interrupts from asynchronous events into deterministic control signals that override computation with absolute priority.

Once interrupts can preempt computation instantly and deterministically, the next challenge is ensuring that peripheral devices—sensors, actuators, controllers—communicate with each other under the same temporal guarantees. Interrupts stabilize the compute fabric, but peripheral coordination requires deterministic message traversal across local networks. The transition into deterministic AI IPC ring-bus topologies marks the moment where communication determinism extends beyond cores and accelerators into the physical networks that connect sensors and actuators, ensuring that every peripheral participates in real-time coordination with fixed-latency guarantees.

iv. Deterministic AI IPC Ring-Bus Topologies for Local Peripheral Network Coordination

Deterministic AI IPC ring-bus topologies for local peripheral network coordination extend real-time guarantees beyond cores and accelerators into the physical networks that connect sensors, actuators, controllers, and safety modules. In autonomous systems, peripheral coordination is as critical as internal computation: a robotic arm must synchronize joint actuators with microsecond precision, an autonomous vehicle must fuse sensor data across multiple domains without jitter, and a surgical robot must coordinate haptic feedback, imaging, and motion control in perfect temporal alignment. Traditional bus architectures—CAN, I^2C, SPI, or even generic Ethernet—introduce variable latency due to arbitration, contention, or nondeterministic routing. Deterministic ring-bus topologies eliminate these sources of variability by enforcing constant-hop traversal and fixed-latency message propagation across all nodes.

A deterministic ring-bus is structured as a closed loop of peripheral nodes, each connected to its neighbors through fixed-latency links. Messages traverse the ring in a predictable sequence, passing through each hop in a constant number of cycles. There is no arbitration, no dynamic routing, and no contention-based delays. Every node knows exactly when a message will arrive, and every message follows the same deterministic path regardless of load. This transforms peripheral communication from a best-effort network into a real-time coordination fabric.

The ring-bus also integrates with the broader IPC architecture. Lock-free ring buffers feed messages into the ring-bus without blocking. Timeout traps monitor traversal time and escalate messages if a node becomes unresponsive. Edge-triggered interrupts can inject safety signals directly into the ring, ensuring that hazard information propagates instantly across all peripherals. The ring-bus becomes the physical extension of the deterministic IPC fabric, providing the same temporal guarantees at the edges of the system as at its computational core.

Spatial determinism is a key advantage. In distributed robotic systems, each peripheral—joint

controller, torque sensor, force feedback module—receives updates at fixed intervals, enabling synchronized motion. In autonomous vehicles, lidar, radar, camera modules, and inertial sensors exchange data with predictable timing, ensuring stable sensor fusion. In surgical robots, imaging modules, haptic actuators, and safety monitors remain perfectly aligned, preventing jitter that could compromise precision.

The ring-bus also supports fail-safe behavior. If a node becomes unresponsive, the bus can bypass it using redundant pathways or escalate communication through interrupt-driven channels. This ensures that peripheral coordination remains stable even under partial hardware degradation. Deterministic traversal guarantees that no peripheral ever waits indefinitely for a message, and no message ever arrives late.

In safety-critical AI systems, deterministic peripheral coordination is indispensable. A robotic arm cannot tolerate jitter in actuator commands. A vehicle cannot fuse sensor data with variable latency. A surgical robot cannot risk asynchronous haptic feedback. The ring-bus ensures that these peripherals operate as a synchronized ensemble, reinforcing the real-time guarantees established by the IPC fabric.

Asynchronous AI IPC channels with hard real-time guarantees and fail-safe interrupts transform communication from a probabilistic subsystem into a deterministic execution fabric. Lock-free ring buffers eliminate blocking and priority inversion. Hard timeout traps enforce bounded latency and provide fallback routing under congestion or partial hardware failure.
Edge-triggered interrupt handling ensures instantaneous safety response, integrating directly with vector-tensor pipelines. Deterministic ring-bus topologies extend these guarantees to peripheral networks, providing fixed-latency coordination across sensors and actuators.
Together, these mechanisms create a communication substrate that moves messages, interrupts, and control signals with unwavering temporal precision, completing the real-time stability layer that autonomous AI systems require.

With deterministic IPC now established as a hard real-time communication fabric—capable of delivering messages on time, routing around failures, preempting computation instantly, and synchronizing peripheral networks—the next challenge is enabling safe experimentation, simulation, and multi-tenant execution within the same physical system. Real-time AI systems must support virtual prototyping, sandboxed model testing, and isolated execution domains without compromising the deterministic guarantees of the live autonomy stack. This transition into virtual AI prototyping with multi-tenant isolation and hardware-sliced context domains marks the moment where the architecture expands from stabilizing communication to safely multiplexing computation, allowing development, testing, and deployment to coexist within a

unified, deterministic hardware substrate.

d. Virtual AI Prototyping with Multi-Tenant Isolation and Hardware-Sliced Context Domains

Virtual AI prototyping with multi-tenant isolation and hardware-sliced context domains is the architectural layer that allows real-time AI systems to support development, testing, simulation, and multi-instance deployment without compromising the deterministic guarantees of the live autonomy stack. Once computation, thermal behavior, and IPC are stabilized, the system must be able to host multiple AI tenants—prototype models, diagnostic tools, simulation workloads, and production inference pipelines—on the same physical hardware while ensuring that none of them interfere with each other's timing, memory, or safety boundaries. This is where virtualization becomes a real-time discipline rather than a convenience feature.

Cycle-Accurate AI Simulation Frameworks for Pre-Silicon Core Validation

Cycle-accurate AI simulation frameworks provide a virtual execution environment that mirrors the timing behavior of physical hardware down to individual clock cycles. These frameworks allow developers to validate AI kernels, memory hierarchies, vector-tensor pipelines, and microkernel scheduling logic before silicon is manufactured or deployed. Unlike functional simulators, which approximate behavior, cycle-accurate simulators reproduce exact timing, pipeline stalls, cache behavior, DVFS effects, and interrupt fences.

This precision is essential for real-time AI systems. Developers can test whether a perception kernel meets its latency budget, whether a control loop remains stable under worst-case load, or whether an interrupt handler preempts computation at the correct cycle boundary. Simulation becomes a predictive tool that ensures deterministic behavior before hardware is even fabricated.

Cycle-accurate simulation also integrates with telemetry-driven adaptation. Developers can simulate thermal excursions, DVFS modulation, power-budget reallocation, and IPC congestion to validate how the system responds under stress. The simulator becomes a virtual proving ground for the entire real-time architecture.

Hardware-Enforced AI Space-Domain Isolation Across Multi-Tenant Matrix Fabrics

Space-domain isolation ensures that multiple AI tenants—production inference, prototype models, diagnostic tools, and background analytics—can coexist on the same accelerator fabric without interfering with each other's memory, compute, or timing domains. This isolation is enforced at hardware level, not merely through software virtualization.

Matrix fabrics (GPU tiles, NPU slices, tensor clusters) are partitioned into isolated domains, each with its own memory region, register file, DMA channels, and scheduling queues. Tenants

cannot access each other's data, cannot starve each other's compute units, and cannot introduce jitter into each other's execution paths. Hardware fences prevent cross-domain leakage, ensuring that prototype workloads cannot destabilize production inference.

This isolation is essential for safety-critical systems. Developers can run experimental models, debugging tools, or simulation workloads on the same hardware as the live autonomy stack without risking interference. The system becomes a multi-tenant environment with deterministic boundaries.

Time-Sliced AI Context Switching with Optimized Register-Flush Overheads

Time-sliced AI context switching allows multiple tenants to share compute units without violating real-time guarantees. Traditional context switching is too slow and unpredictable for AI workloads, which rely on large register files, deep pipelines, and complex memory hierarchies. Optimized register-flush mechanisms solve this by minimizing the overhead of switching between tenants.

Hardware-accelerated context switching flushes only the registers that have changed, using delta-based tracking rather than full dumps. Vector-tensor pipelines support checkpointing at deterministic fence points, allowing context switches to occur without corrupting intermediate states. Memory-ordering fences ensure that writes complete before switching, preserving consistency.

This mechanism allows prototype workloads to run in time slices that do not interfere with production inference. The autonomy stack retains its deterministic timing even while sharing hardware with other tenants.

Virtualized AI Memory-Management Boundaries for Multi-Instance Accelerator Deployment

Virtualized memory-management boundaries allow multiple AI instances to share accelerator memory without risking corruption, leakage, or timing interference. Each tenant receives a virtual memory region backed by hardware-enforced boundaries. DMA engines, cache hierarchies, and memory controllers enforce isolation at every level.

Memory virtualization also supports dynamic resizing. Tenants can request more memory during peak load, and the system can reallocate memory from lower-priority tenants without violating isolation. This enables flexible multi-instance deployment where production inference, simulation workloads, and diagnostic tools coexist safely.

Virtualized memory boundaries also integrate with telemetry-driven adaptation. If thermal or power conditions tighten, the system can shrink memory allocations for non-critical tenants to preserve headroom for critical workloads.

With the virtualization architecture now fully articulated—from cycle-accurate simulation to hardware-enforced space-domain isolation, deterministic context switching, and virtualized memory boundaries—the next step is to consolidate these mechanisms into a structured operational view. Real-time AI systems must support multi-tenant execution, prototyping, and simulation without compromising the deterministic guarantees established by the compute, thermal, and IPC layers. Table 8.4-E4 organizes these virtualization mechanisms into a unified framework, showing how each contributes to isolation, timing fidelity, and safe multi-instance deployment. This table provides the conceptual anchor that links virtual prototyping to the broader real-time execution fabric, clarifying how isolation becomes a first-class requirement for safe, concurrent AI development and operation.

Table 8.4-E4 presents the core virtualization mechanisms that enable real-time AI systems to host multiple tenants—production inference pipelines, prototype models, diagnostic tools, and simulation workloads—on the same physical hardware without interference. Each mechanism addresses a fundamental challenge inherent to multi-tenant AI execution: preserving timing fidelity, enforcing spatial isolation, minimizing context-switch overhead, and guaranteeing memory integrity. By structuring these mechanisms into a single operational view, the table highlights how virtual AI prototyping evolves from a convenience feature into a deterministic, hardware-aligned discipline. It clarifies how isolation guarantees become essential for safety-critical AI systems that must support continuous development and testing alongside live autonomy.

Table 8.4-E4 — Virtual AI Prototyping Mechanisms and Their Isolation Guarantees

Mechanism	Isolation Guarantee	Operational Strategy	System-Level Effect
Cycle-Accurate AI Simulation Frameworks	Pre-silicon timing fidelity	Clock-cycle replication of hardware behavior	Validates deterministic timing before deployment
Hardware-Enforced Space-Domain Isolation	Cross-tenant memory and compute isolation	Matrix-fabric partitioning with hardware fences	Prevents interference between prototype and production workloads
Time-Sliced AI Context Switching	Deterministic multi-tenant scheduling	Optimized register-flush and pipeline checkpointing	Enables shared hardware without timing drift

Mechanism	Isolation Guarantee	Operational Strategy	System-Level Effect
Virtualized AI Memory-Management Boundaries	Safe multi-instance memory sharing	Hardware-backed virtual memory regions	Ensures data integrity and prevents leakage across tenants

Table 8.4-E4 consolidates the virtualization mechanisms that allow real-time AI systems to support multi-tenant execution, prototyping, and simulation without compromising deterministic behavior.

Table 8.4-E4 reveals that deterministic AI systems require virtualization mechanisms that are as precise and isolated as their compute, thermal, and communication layers. Cycle-accurate simulation frameworks provide pre-silicon timing fidelity, allowing developers to validate latency budgets, interrupt fences, and pipeline behavior before hardware is deployed. Hardware-enforced space-domain isolation ensures that multiple tenants can coexist on the same matrix fabric without interfering with each other's memory, compute units, or timing domains. Time-sliced AI context switching introduces deterministic scheduling across tenants, using optimized register-flush paths and pipeline checkpointing to prevent timing drift. Virtualized memory-management boundaries guarantee safe multi-instance deployment, ensuring that tenants cannot corrupt or access each other's data even under dynamic load or thermal stress.

Together, these mechanisms form a virtualization substrate engineered for real-time AI autonomy. They allow prototype models, diagnostic tools, and simulation workloads to run alongside production inference without compromising safety, timing, or isolation. Table 8.4-E4 thus provides the operational map for understanding how virtual AI prototyping reinforces the broader deterministic execution fabric, enabling autonomous systems to evolve continuously while maintaining strict real-time guarantees.

Table 8.4-E4 organizes the virtualization mechanisms—cycle-accurate simulation, hardware-enforced space-domain isolation, deterministic context switching, and virtualized memory boundaries—into a structured view of how multi-tenant AI execution can remain safe and predictable. To complement this tabular framework, Figure 8.4-E4 visualizes how these mechanisms operate together as a unified virtualization fabric that preserves timing fidelity, memory integrity, and isolation across tenants. The figure translates the table's conceptual architecture into a dynamic, hardware-aligned diagram that shows how virtual AI prototyping becomes a deterministic extension of the real-time execution substrate, enabling development, testing, and multi-instance deployment without compromising the autonomy stack.

Figure 8.4-E4 illustrates the virtualization architecture that enables real-time AI systems to support multi-tenant execution while preserving deterministic guarantees. Each panel highlights a critical mechanism—cycle-accurate simulation, hardware-enforced isolation, deterministic context switching, and virtualized memory boundaries—showing how prototype workloads, diagnostic tools, and production inference pipelines can coexist safely on the same physical hardware. The figure demonstrates how virtualization becomes a hardware-anchored discipline, ensuring that isolation, timing fidelity, and memory integrity remain intact even under dynamic load, thermal variation, or multi-tenant contention.

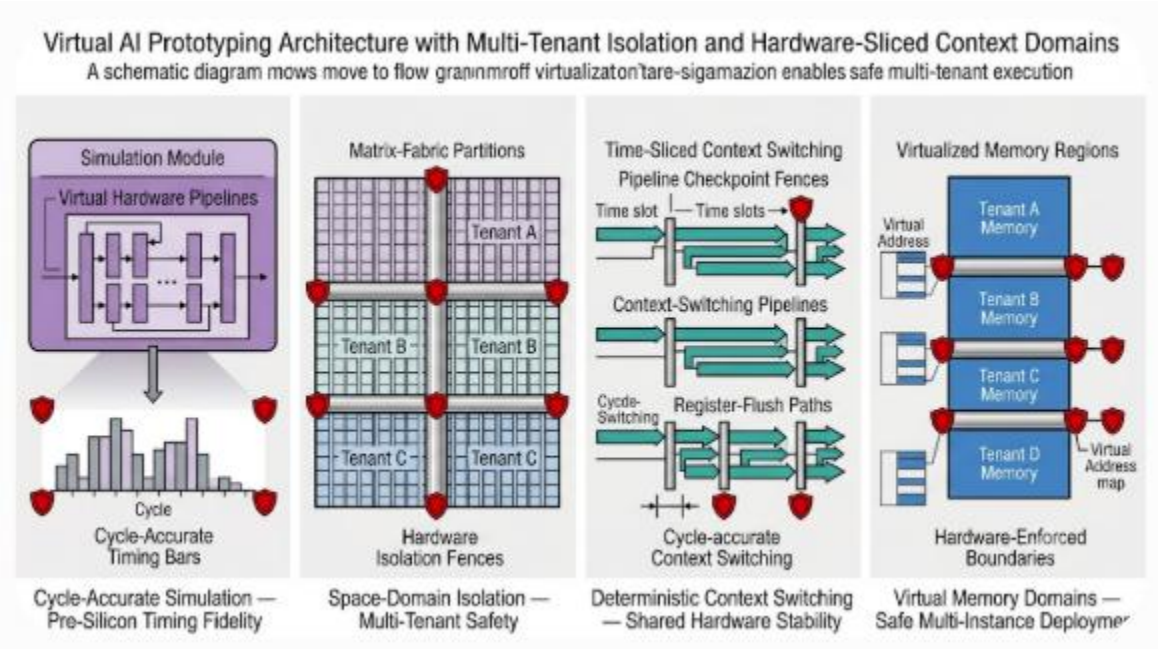


Figure 8.4-E4 — Virtual AI Prototyping Architecture with Multi-Tenant Isolation and Hardware-Sliced Context Domains

The figure depicts the four mechanisms that enable safe, deterministic multi-tenant execution in real-time AI systems: cycle-accurate simulation, hardware-enforced space-domain isolation, optimized time-sliced context switching, and virtualized memory-management boundaries. Together, these mechanisms allow prototype models, diagnostic tools, and production inference pipelines to share hardware without compromising timing, isolation, or safety.

Legend

- ***Purple simulation blocks****: cycle-accurate virtual hardware pipelines*
- ***Silver isolation fences****: hardware-enforced space-domain boundaries*
- ***Teal pipelines****: deterministic context-switching paths*
- ***Checkpoint fences****: pipeline-safe interrupt and switch boundaries*
- ***Blue memory regions****: virtualized memory domains*

- ***Virtual address map****: hardware-backed memory segmentation*
- ***Timing bars****: cycle-accurate fidelity indicators*
- ***Safety shields:*** *isolation guarantees across tenants*

Figure 8.4-E4 shows how virtualization becomes a deterministic extension of the real-time AI execution fabric. The first panel demonstrates cycle-accurate simulation, where virtual hardware pipelines reproduce real timing behavior down to individual clock cycles, enabling pre-silicon validation of latency budgets, interrupt fences, and pipeline behavior. The second panel highlights hardware-enforced space-domain isolation, where matrix-fabric partitions and isolation fences prevent tenants from interfering with each other's compute units, memory regions, or timing domains. The third panel introduces deterministic time-sliced context switching, where optimized register-flush paths and pipeline checkpoint fences allow multiple tenants to share hardware without introducing jitter or timing drift. The final panel depicts virtualized memory-management boundaries, where hardware-backed virtual memory regions ensure safe multi-instance deployment and prevent data leakage or corruption across tenants.

Together, these panels reveal a virtualization architecture engineered for real-time AI autonomy—one where simulation, prototyping, and multi-tenant execution coexist safely within a deterministic hardware substrate. The figure visually reinforces how virtual AI prototyping becomes a controlled, isolated, and timing-predictable environment that supports continuous development without compromising the live autonomy stack.

With the virtualization substrate now defined—where multi-tenant isolation, deterministic context switching, and hardware-sliced memory domains allow prototype workloads to coexist safely alongside production inference—the next logical step is to examine how these virtual tenants are created, validated, and stress-tested before they ever touch physical silicon. Real-time AI systems cannot rely on trial-and-error deployment; they require a virtual proving ground capable of reproducing hardware behavior with cycle-level fidelity. This is where virtual AI prototyping begins in earnest: with cycle-accurate AI simulation frameworks that emulate the timing, pipeline behavior, memory hierarchy, and interrupt fences of the actual hardware. These frameworks form the entry point into the virtualization stack, enabling pre-silicon core validation that guarantees deterministic behavior long before the hardware is manufactured or placed into a safety-critical autonomy loop.

i. Cycle-Accurate AI Simulation Frameworks for Pre-Silicon Core Validation

Cycle-accurate AI simulation frameworks are the first and most foundational layer of virtual AI prototyping because they allow developers to validate deterministic behavior before hardware

exists. In real-time AI systems, correctness is not enough—timing is correctness. A perception kernel that produces the right output but does so 40 microseconds late is functionally unsafe. A control loop that computes the correct torque but misses its cycle boundary destabilizes the entire autonomy stack. Cycle-accurate simulation frameworks solve this by reproducing the timing behavior of the hardware down to individual clock cycles, pipeline stages, and memory-hierarchy transitions.

These frameworks emulate the full microarchitectural pipeline: instruction fetch, decode, vector expansion, tensor contraction, accumulation, writeback, cache behavior, DMA transfers, and microkernel scheduling. Every stall, hazard, bypass, and pipeline bubble is reproduced exactly as it would occur on silicon. Developers can observe how kernels behave under worst-case conditions—cache misses, DVFS modulation, thermal throttling, power-budget reallocation, or IPC congestion—long before the hardware is fabricated. This transforms simulation from a functional testbed into a predictive timing laboratory.

Cycle-accurate simulators also integrate with the deterministic IPC and thermal-boundary layers. Interrupt fences can be tested to ensure they halt pipelines at safe boundaries. Timeout traps can be validated to confirm they reroute messages before deadlines expire. DVFS transitions can be simulated to verify that latency budgets remain intact under frequency modulation. Power-budget reallocation can be modeled to ensure that critical workloads retain energy even under thermal stress. The simulator becomes a virtual mirror of the entire real-time execution fabric.

For multi-tenant environments, cycle-accurate simulation is indispensable. Prototype models, experimental kernels, and diagnostic tools can be validated in simulation before being allowed to run alongside production inference on shared hardware. This prevents unsafe tenants from entering the live autonomy stack. Simulation becomes a gatekeeper: only workloads that demonstrate deterministic timing behavior in the virtual environment are permitted to run in the real one.

In safety-critical AI systems—autonomous vehicles, surgical robots, industrial manipulators—cycle-accurate simulation is not optional. It is the only way to guarantee that timing behavior is correct before hardware is deployed into environments where mistakes have physical consequences. Simulation ensures that determinism is not discovered after deployment but engineered before silicon exists.

Once timing behavior is validated in a cycle-accurate virtual environment, the next challenge is ensuring that multiple AI tenants can coexist safely on the same physical accelerator fabric. Simulation guarantees that each tenant behaves deterministically on its own, but real-time

autonomy requires that tenants remain isolated from one another's compute units, memory regions, and timing domains. This is where virtualization transitions from timing fidelity to spatial protection. Hardware-enforced AI space-domain isolation across multi-tenant matrix fabrics provides the physical boundaries that prevent prototype workloads, diagnostic tools, and background analytics from interfering with production inference, ensuring that multi-tenant execution remains safe, predictable, and deterministic.

ii. Hardware-Enforced AI Space-Domain Isolation Across Multi-Tenant Matrix Fabrics

Hardware-enforced AI space-domain isolation across multi-tenant matrix fabrics is where virtualization stops being a software convenience and becomes a physical safety guarantee. In a real-time AI system, multiple tenants—production inference pipelines, prototype models, diagnostic tools, simulation workloads, and background analytics—must often share the same accelerator fabric: GPUs, NPUs, tensor cores, or custom matrix engines. Without strict isolation, one tenant can starve another of compute, corrupt its memory, or inject jitter into its timing domain. For safety-critical autonomy, that is unacceptable. Space-domain isolation solves this by carving the matrix fabric into hardware-enforced partitions, each with its own compute, memory, and scheduling boundaries that cannot be crossed by other tenants.

At the architectural level, the matrix fabric is divided into slices—tiles, clusters, or cores—assigned to specific tenants. Each slice has dedicated execution units, register files, local scratchpads, cache segments, and DMA channels. Hardware fences separate these slices, preventing any instruction, memory access, or DMA transfer from crossing into another tenant's domain. This is not a software sandbox; it is a physical segmentation enforced by the accelerator's microarchitecture. Tenants cannot read or write each other's data, cannot schedule work on each other's compute units, and cannot interfere with each other's timing behavior.

Space-domain isolation also extends to control paths. Each tenant has its own command queue, scheduler context, and microkernel interface. The hardware ensures that commands from one tenant cannot be injected into another's queue, and that scheduling decisions for one domain do not affect the timing of another. This prevents priority inversion across tenants: a low-priority diagnostic workload cannot delay a high-priority perception pipeline, and a background analytics job cannot introduce jitter into a control loop.

In multi-tenant real-time systems, this isolation is crucial for safety. Production inference pipelines must remain stable even when prototype models are misbehaving, consuming excessive resources, or encountering faults. Hardware fences ensure that such behavior is contained within the prototype's domain. If a tenant crashes, stalls, or enters an undefined

state, the failure is localized; other tenants continue operating with their timing and memory guarantees intact.

Space-domain isolation also interacts with telemetry-driven adaptation. Thermal and power controllers can modulate frequency, voltage, or power budgets per domain, prioritizing critical tenants while throttling non-critical ones. IPC mechanisms can route messages only within or between specific domains, enforcing communication boundaries that mirror compute boundaries. The result is a fabric where isolation is not just spatial but also temporal and communicational.

For virtual AI prototyping, this means developers can run experimental workloads on the same physical hardware as the live autonomy stack without risking interference. Prototype tenants can be granted limited slices of the matrix fabric, with strict caps on compute, memory, and bandwidth. Production tenants retain their deterministic guarantees regardless of what happens in the prototype domains. Isolation becomes the enabler of safe experimentation in safety-critical environments.

Once space-domain isolation ensures that tenants are physically separated across the matrix fabric, the next challenge is sharing time on those same resources without breaking determinism. Tenants may need to time-share compute units, pipelines, or memory controllers, especially when hardware slices are oversubscribed or dynamically reallocated. At this point, virtualization must evolve from spatial partitioning to temporal orchestration. Time-sliced AI context switching with optimized register-flush overheads is the mechanism that allows multiple tenants to share hardware in time while preserving their latency budgets, ensuring that context changes themselves do not become a source of jitter or timing drift.

iii. Time-Sliced AI Context Switching with Optimized Register-Flush Overheads

Time-sliced AI context switching with optimized register-flush overheads is the mechanism that allows multiple AI tenants to share accelerator hardware in time without compromising deterministic behavior. In conventional computing, context switching is a routine operation, but in AI accelerators—where vector and tensor pipelines are deep, register files are massive, and memory hierarchies are tightly coupled—context switching becomes a potential source of jitter, latency drift, and state corruption. Real-time AI systems cannot tolerate any of these. The autonomy stack must maintain strict timing guarantees even when hardware is multiplexed across tenants. Time-sliced context switching solves this by transforming temporal sharing into a deterministic, hardware-aligned process.

At the architectural level, each tenant maintains a context consisting of register states, pipeline checkpoints, memory-mapping metadata, DMA descriptors, and microkernel scheduling

information. Instead of performing full register dumps—which would be prohibitively slow—accelerators use delta-based register-flush mechanisms. Only registers that have changed since the last checkpoint are saved or restored. This dramatically reduces switching overhead and ensures that context transitions occur within predictable, bounded time windows.

Pipeline checkpointing is equally important. Vector-tensor pipelines cannot be interrupted arbitrarily; doing so risks partial writes, inconsistent accumulations, or corrupted intermediate states. Hardware-defined checkpoint fences solve this by establishing deterministic interrupt-safe boundaries within the pipeline. When a context switch is triggered, the pipeline advances to the nearest fence, halts safely, and hands control to the next tenant. This ensures that context switching never corrupts computation and never introduces nondeterministic timing behavior.

Memory-ordering fences ensure that all writes complete before switching, preventing race conditions or stale data exposure across tenants. DMA engines synchronize transfers so that no tenant inherits partially completed memory operations. The microkernel orchestrates these transitions with cycle-level precision, ensuring that context switching itself becomes a deterministic operation rather than a source of jitter.

Time-sliced scheduling also integrates with telemetry-driven adaptation. If thermal conditions tighten, the scheduler can shorten time slices for non-critical tenants. If power budgets shift, the scheduler can allocate more cycles to critical inference pipelines. If IPC congestion increases, the scheduler can adjust slice boundaries to preserve message-delivery guarantees. Context switching becomes a dynamic, adaptive mechanism that reinforces real-time stability.

For multi-tenant AI prototyping, this capability is transformative. Prototype workloads can run in time slices that do not interfere with production inference. Diagnostic tools can execute intermittently without disturbing control loops. Simulation workloads can share hardware with live autonomy without introducing jitter. Time-sliced context switching ensures that temporal multiplexing is safe, predictable, and deterministic.

Once temporal sharing is stabilized, the next challenge is ensuring that memory sharing across tenants is equally safe. Context switching governs how tenants share compute time, but memory virtualization governs how they share physical memory. Without strict memory-management boundaries, tenants could corrupt each other’s data, leak sensitive information, or destabilize timing behavior. The transition into virtualized AI memory-management boundaries for multi-instance accelerator deployment marks the moment where virtualization extends from temporal orchestration to memory integrity, ensuring that multi-tenant execution remains safe across both time and space.

iv. Virtualized AI Memory-Management Boundaries for Multi-Instance Accelerator Deployment

Virtualized AI memory-management boundaries are the final pillar of multi-tenant isolation, ensuring that multiple AI instances can share accelerator memory safely, deterministically, and without cross-tenant interference. In real-time AI systems, memory is not merely a storage resource—it is a timing-critical substrate that directly affects latency, pipeline stability, DMA behavior, and interrupt responsiveness. Without strict memory boundaries, tenants could corrupt each other's data, leak sensitive information, or destabilize timing guarantees. Virtualized memory-management solves this by enforcing hardware-anchored segmentation across all memory layers.

At the architectural level, each tenant receives a virtual memory domain backed by hardware-enforced boundaries. These domains include dedicated regions of HBM, SRAM, scratchpads, cache slices, and DMA queues. Memory controllers enforce access permissions at cycle-level granularity, ensuring that no tenant can read, write, or evict data belonging to another. This is not software virtualization—it is physical segmentation enforced by the accelerator's microarchitecture.

DMA engines play a critical role. Each tenant receives isolated DMA channels with guaranteed bandwidth and latency budgets. DMA operations are fenced so that transfers complete deterministically before context switches occur. This prevents partial transfers, stale data exposure, or race conditions across tenants. DMA fences also ensure that high-priority tenants—such as perception or control loops—retain guaranteed access to memory bandwidth even when prototype workloads are active.

Cache hierarchies are similarly partitioned. Tenants receive isolated cache segments or way-partitioned regions that prevent eviction interference. This ensures that one tenant's memory-access pattern cannot degrade another tenant's latency. In real-time AI systems, cache determinism is essential: a single unexpected eviction can cause a perception kernel to miss its cycle boundary.

Memory virtualization also supports dynamic resizing. Tenants can request additional memory during peak load, and the system can reallocate memory from lower-priority tenants without violating isolation. Telemetry-driven adaptation integrates directly with this mechanism: if thermal or power conditions tighten, memory allocations for non-critical tenants can be reduced to preserve headroom for critical workloads.

Fault isolation is another key benefit. If a tenant encounters a memory fault—invalid access, corruption, or overflow—the fault is contained within its virtual domain. Other tenants continue

operating with their timing and memory guarantees intact. This is essential for safety-critical autonomy, where prototype workloads must never destabilize production inference.

Virtualized memory-management boundaries complete the virtualization stack. Cycle-accurate simulation validates timing behavior before deployment. Space-domain isolation prevents cross-tenant interference. Time-sliced context switching ensures deterministic temporal sharing. Memory virtualization ensures data integrity and timing stability across tenants. Together, these mechanisms allow multi-instance accelerator deployment to remain safe, predictable, and deterministic.

Virtual AI prototyping transforms real-time AI systems into environments where development, testing, simulation, and production inference can coexist safely on the same physical hardware. Cycle-accurate simulation frameworks validate timing behavior before silicon exists. Hardware-enforced space-domain isolation prevents tenants from interfering with each other's compute or memory domains. Time-sliced context switching enables deterministic temporal sharing across tenants. Virtualized memory-management boundaries ensure data integrity and timing stability across multi-instance deployments. Together, these mechanisms create a virtualization substrate that preserves deterministic guarantees while enabling continuous innovation, safe experimentation, and multi-tenant operation within safety-critical AI systems.

With deterministic time-slicing now established—where optimized register-flush paths, pipeline checkpoint fences, and microkernel-aligned scheduling allow multiple tenants to share accelerator hardware without introducing jitter—the final requirement for safe multi-tenant execution is ensuring that memory itself becomes an isolated, deterministic resource. Temporal isolation prevents tenants from interfering with each other's execution windows, but without strict memory-management boundaries, data corruption, leakage, or cache-eviction interference could still destabilize the autonomy stack. The architecture must therefore extend virtualization into the memory hierarchy, creating hardware-anchored virtual memory domains that guarantee integrity, bandwidth fairness, and deterministic access patterns across all tenants. This transition into virtualized AI memory-management boundaries completes the virtualization substrate, ensuring that multi-instance accelerator deployment remains safe, predictable, and fully isolated across compute, time, and memory.

e. Edge-to-Cloud AI Continuum Splitting with Dynamic Layer Offload and Jitter-Buffered Networking

Edge-to-cloud continuum splitting is the architectural layer that extends determinism beyond the device itself. Once local compute, IPC, and virtualization are stabilized, the system must be able to distribute computation across edge devices, fog nodes, and cloud servers without

introducing jitter, latency drift, or safety hazards. Modern AI workloads—especially deep neural networks and multimodal inference—benefit from dynamic offload strategies that adapt to network conditions, congestion levels, and device-side load. Research confirms that **adaptive, runtime-aware partitioning** significantly reduces latency and energy consumption compared to static offload baselines. Similarly, **continuum-aware collaborative inference** improves reliability under cloud congestion by shifting execution toward edge nodes when needed.

This discussion formalizes the mechanisms that make such distributed execution deterministic: compute-graph partitioning, tensor compression, jitter-buffered networking, and cloud-assisted weight streaming.

Live-Metric-Driven AI Compute-Graph Partitioning for Adaptive Offload Decisions

Adaptive compute-graph partitioning is the mechanism that decides, at runtime, which layers of a neural network execute on the edge and which execute in the cloud. Static partitioning is insufficient for real-time systems because network conditions, device load, and cloud congestion vary unpredictably. Research shows that **dynamic layer splitting**, guided by live metrics such as link quality, device load, and congestion sensing, reduces end-to-end latency by up to ~23% and energy consumption by ~35% compared to static baselines.

The partitioner continuously profiles:

- **Network bandwidth and jitter**
- **Edge compute load**
- **Cloud congestion levels**
- **Model-layer latency sensitivity**

When conditions degrade, latency-critical layers remain on the edge; when conditions improve, deeper layers offload to the cloud. This ensures that inference remains stable even under fluctuating network conditions.

Intermediate AI Tensor Compression Pipelines for Efficient Uplink Transmission

Once layers are split, intermediate tensors must be transmitted from edge to cloud. Raw tensors are large, bandwidth-intensive, and sensitive to jitter. Compression pipelines reduce uplink cost while preserving accuracy. Techniques include:

- Quantization of intermediate activations
- Spatial downsampling for convolutional layers

- Low-rank tensor decomposition
- Delta-encoding for sequential frames

Research on continuum inference frameworks highlights the importance of **efficient uplink transmission** to maintain responsiveness under heterogeneous network conditions.

Compression pipelines operate in hardware-accelerated paths to ensure that compression latency does not exceed the savings gained from reduced transmission time.

Jitter-Resilient AI Buffering with Fallback Edge Execution Paths

Even with compression, network jitter can disrupt inference timing. Jitter-resilient buffering solves this by maintaining:

- **Short-term activation buffers** for in-flight tensors
- **Predictive buffering windows** based on link-quality forecasts
- **Fallback execution paths** that allow the edge to temporarily execute cloud-assigned layers when jitter exceeds thresholds

Continuum-aware offloading research demonstrates that fallback execution significantly improves reliability under cloud congestion or degraded network conditions.

The fallback path ensures:

- No inference stalls
- No missed control-loop deadlines
- No unsafe latency spikes

This mechanism transforms distributed inference from best-effort to deterministic.

Cloud-Assisted AI Weight-Update Streaming over Low-Power Cellular Fabrics

Many edge devices operate on low-power cellular networks. Cloud-assisted weight-update streaming allows the cloud to push updated model weights, LoRA adapters, or multimodal heads to the edge without interrupting inference. Research on cloud-edge collaborative inference emphasizes the need for **dynamic model composition and update streaming** to maintain accuracy while reducing cloud workload pressure.

Weight-update streaming includes:

- **Bandwidth-adaptive chunking**

- **Error-correcting transmission**
- **Version-consistent swap-in points**
- **Background streaming that never blocks inference**

This ensures that edge models remain up-to-date even under constrained connectivity.

With the continuum architecture now defined—where adaptive layer offload, tensor compression, jitter-buffered execution, and cloud-assisted weight streaming collectively stabilize distributed inference—the next step is to consolidate these mechanisms into a structured operational view. Table 8.4-E5 organizes the continuum's core components into a unified framework, showing how each contributes to deterministic behavior across fluctuating network conditions, heterogeneous compute environments, and dynamic cloud congestion. This table serves as the conceptual anchor linking mechanism-level detail to system-level guarantees, clarifying how edge-to-cloud execution becomes a predictable, latency-bounded extension of the real-time autonomy stack.

Table 8.4-E5 presents the four foundational mechanisms that enable deterministic AI execution across the edge-to-cloud continuum. Each mechanism addresses a specific challenge inherent to distributed inference: deciding which layers to offload, reducing uplink transmission cost, mitigating jitter, and maintaining model freshness under constrained connectivity. By structuring these mechanisms side-by-side, the table highlights how continuum execution evolves from a best-effort offload strategy into a controlled, adaptive, and latency-bounded process. It clarifies how determinism is preserved even when computation spans multiple physical locations and variable network conditions.

Table 8.4-E5 — Edge-to-Cloud Continuum Mechanisms and Their Deterministic Guarantees

Mechanism	Deterministic Guarantee	Operational Strategy	System-Level Effect
Live-Metric-Driven Compute-Graph Partitioning	Stable offload decisions under dynamic conditions	Runtime profiling of link quality, load, and congestion	Reduces latency and energy vs. static offload
Intermediate Tensor Compression Pipelines	Predictable uplink transmission time	Quantization, downsampling, low-rank decomposition	Maintains responsiveness under bandwidth constraints

Mechanism	Deterministic Guarantee	Operational Strategy	System-Level Effect
Jitter-Resilient Buffering with Fallback Paths	No inference stalls under jitter	Predictive buffering + fallback edge execution	Preserves reliability under cloud congestion
Cloud-Assisted Weight-Update Streaming	Consistent model updates without blocking inference	Bandwidth-adaptive chunking + version-safe swaps	Maintains accuracy on low-power networks

Table 8.4-E5 reveals that deterministic edge-to-cloud execution requires coordinated mechanisms across compute, network, and model-update pathways. Live-metric-driven compute-graph partitioning ensures that offload decisions adapt to real-time link quality, device load, and cloud congestion, preventing latency spikes caused by static splitting. Intermediate tensor compression pipelines reduce uplink transmission cost, ensuring that intermediate activations reach the cloud within predictable time windows. Jitter-resilient buffering with fallback edge execution paths prevents inference stalls when network conditions degrade, maintaining stable control-loop timing. Cloud-assisted weight-update streaming ensures that edge models remain accurate and up-to-date even on low-power cellular networks, without interrupting inference or destabilizing timing.

Together, these mechanisms form a continuum execution fabric engineered for real-time AI autonomy—one where computation can shift fluidly between edge and cloud while maintaining deterministic timing, stable latency, and uninterrupted safety-critical behavior.

Table 8.4-E5 consolidates the mechanisms that make distributed AI execution deterministic across the edge-to-cloud continuum—adaptive compute-graph partitioning, tensor compression pipelines, jitter-buffered execution, and cloud-assisted weight streaming. To complement this structured view, Figure 8.4-E5 visualizes how these mechanisms operate together as a unified continuum fabric. The figure translates the table's conceptual guarantees into a dynamic, system-level diagram that shows how inference can fluidly shift between edge and cloud while maintaining stable latency, predictable timing, and uninterrupted control-loop behavior. It provides the architectural bridge between mechanism-level detail and the holistic flow of real-time distributed AI execution.

Figure 8.4-E5 illustrates the architecture that enables deterministic AI execution across the edge-to-cloud continuum. Each panel highlights a critical mechanism—live-metric-driven layer partitioning, intermediate tensor compression, jitter-resilient buffering with fallback execution,

and cloud-assisted weight streaming. Together, these components show how real-time AI systems adapt to fluctuating network conditions, cloud congestion, and device-side load while preserving stable inference timing. The figure demonstrates how distributed execution becomes a controlled, latency-bounded process rather than a best-effort offload strategy, ensuring that autonomy remains reliable even when computation spans multiple physical locations.

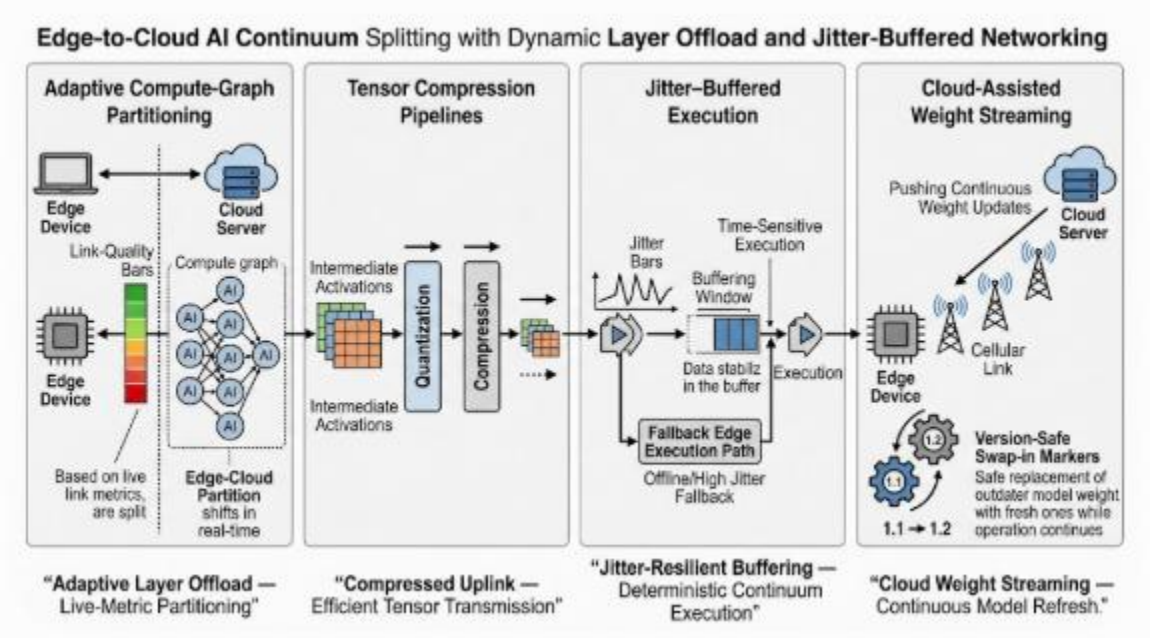


Figure 8.4-E5 — Edge-to-Cloud AI Continuum Splitting with Dynamic Layer Offload and Jitter-Buffered Networking

The figure depicts the four mechanisms that enable deterministic distributed inference: adaptive compute-graph partitioning based on live metrics, hardware-accelerated tensor compression for efficient uplink transmission, jitter-buffered execution with fallback edge paths, and cloud-assisted weight-update streaming over low-power networks. Together, these mechanisms maintain stable latency and reliable inference across the edge-to-cloud continuum.

Legend

- ***Green link-quality bars****: live network metrics guiding offload decisions*
- ***Purple compression blocks****: tensor-reduction and quantization pipelines*
- ***Orange jitter windows****: predictive buffering intervals*
- ***Blue fallback paths****: edge-side execution under degraded network conditions*
- ***Silver update streams****: cloud-pushed model-weight updates*
- ***Cycle-timing bars****: deterministic execution indicators*
- ***Version-swap markers:*** *safe model-update boundaries*

Figure 8.4-E5 shows how distributed AI execution becomes deterministic across the edge-to-cloud continuum. The first panel demonstrates adaptive compute-graph partitioning, where live metrics—link quality, device load, and cloud congestion—determine which layers execute locally and which offload to the cloud. This ensures that inference remains stable even as conditions fluctuate. The second panel highlights tensor compression pipelines that reduce uplink transmission cost through quantization, downsampling, and low-rank decomposition, preserving responsiveness under bandwidth constraints. The third panel introduces jitter-buffered execution, where predictive buffering and fallback edge paths prevent inference stalls when network jitter spikes. The final panel depicts cloud-assisted weight-update streaming, enabling continuous model refresh over low-power cellular links without interrupting inference or destabilizing timing.

Together, these panels reveal a continuum architecture engineered for real-time AI autonomy—one where computation can shift fluidly between edge and cloud while maintaining deterministic timing, stable latency, and uninterrupted safety-critical behavior. The figure visually reinforces how edge-to-cloud execution becomes a controlled, jitter-buffered, and latency-bounded process rather than a best-effort offload strategy.

With the continuum mechanisms now organized into a structured framework—showing how adaptive offload, tensor compression, jitter-buffered execution, and cloud-assisted weight streaming collectively stabilize distributed inference—the next step is to examine how the continuum actually begins. Every edge-to-cloud execution path starts with a decision: which layers remain local, and which layers offload to the cloud. This decision cannot be static, because network conditions, device load, and cloud congestion fluctuate continuously. Deterministic distributed inference therefore requires a partitioning engine that reacts to live metrics, reshaping the compute graph in real time to preserve latency budgets and control-loop stability. This transition into **live-metric-driven AI compute-graph partitioning** marks the moment where continuum execution becomes adaptive rather than fixed, ensuring that offload choices remain aligned with the system's real-time constraints.

i. Live-Metric-Driven AI Compute-Graph Partitioning for Adaptive Offload Decisions

Live-metric-driven compute-graph partitioning is the mechanism that determines, at runtime, which layers of a neural network execute on the edge and which offload to the cloud. This decision is the *first* and most critical step in edge-to-cloud continuum execution because it directly shapes latency, bandwidth consumption, energy usage, and control-loop stability. Static partitioning—where the split point is fixed at design time—is fundamentally incompatible with real-time systems. Network conditions fluctuate, cloud congestion varies, and device-side load

changes dynamically. Deterministic distributed inference therefore requires a partitioning engine that continuously senses the environment and reshapes the compute graph accordingly.

Real-Time Metrics That Drive Partitioning

The partitioner monitors a live set of metrics, each with deterministic influence on offload decisions:

- **Link-quality indicators** Bandwidth, jitter, packet-loss rate, and round-trip time determine whether cloud execution is viable. High jitter → keep layers local. Stable bandwidth → offload deeper layers.
- **Edge compute load** CPU/GPU/NPU utilization, thermal headroom, and DVFS state determine whether the device can sustain local execution. High load → offload compute-heavy layers. Thermal stress → shift layers to cloud.
- **Cloud congestion levels** Queue depth, inference-service load, and cloud-side latency forecasts determine whether cloud execution will remain stable. Cloud congestion → reduce offload depth.
- **Layer-specific latency sensitivity** - Early layers (feature extraction) often tolerate offload; late layers (decision-making) often require local execution. Latency-critical layers → remain on edge.

These metrics form a **continuously updated decision vector**, allowing the partitioner to adapt the compute graph in real time.

Dynamic Partitioning Logic

The partitioner evaluates the compute graph layer-by-layer, estimating:

- **Local execution time**
- **Cloud execution time**
- **Transmission time for intermediate tensors**
- **Expected jitter impact**
- **Fallback feasibility**

It then selects a split point that minimizes end-to-end latency while preserving deterministic timing guarantees. This split point can move dynamically—sometimes multiple times per second—without disrupting inference.

Deterministic Guarantees

Live-metric partitioning ensures:

- **Latency stability** even under fluctuating network conditions
- **Energy efficiency** by shifting compute based on thermal and DVFS states
- **Safety-critical timing** by keeping decision-making layers local
- **Continuum reliability** by avoiding cloud congestion during peak load

This transforms distributed inference from a best-effort offload strategy into a deterministic, adaptive execution fabric.

Integration with the Continuum Architecture

Partitioning is tightly coupled with:

- Tensor compression pipelines (to reduce uplink cost)
- Jitter-buffered execution (to prevent stalls)
- Cloud-assisted weight streaming (to maintain accuracy)

It is the *entry point* into the continuum, shaping how all downstream mechanisms behave.

Once the partitioner determines which layers execute on the edge and which offload to the cloud, the next challenge is transmitting intermediate tensors efficiently and deterministically. These tensors—often large, high-dimensional activation maps—can overwhelm uplink bandwidth and introduce jitter if sent raw. To preserve latency budgets and ensure stable continuum execution, the architecture must compress these tensors using quantization, downsampling, and low-rank decomposition pipelines that operate in hardware-accelerated paths. This transition into **intermediate AI tensor compression pipelines** marks the moment where adaptive offload becomes bandwidth-aware, enabling the continuum to function reliably even under constrained or fluctuating network conditions.

ii. Intermediate AI Tensor Compression Pipelines for Efficient Uplink Transmission

Intermediate AI tensor compression pipelines are the second critical stage of edge-to-cloud continuum execution. Once the compute-graph partitioner decides which layers execute locally and which offload to the cloud, the system must transmit intermediate activations—often large, high-dimensional tensors—over uplink channels that may be bandwidth-limited, jitter-prone, or energy-constrained. Raw tensors are too large and too sensitive to network variability to be

transmitted directly in real-time systems. Compression pipelines solve this by reducing tensor size while preserving the semantic fidelity required for downstream cloud execution.

Why Tensor Compression Is Essential

Intermediate activations can easily exceed:

- **tens of megabytes per frame** for vision models
- **hundreds of kilobytes per token** for multimodal transformers
- **multi-megabyte feature maps** for radar/lidar fusion

Transmitting these raw tensors would:

- saturate uplink bandwidth
- introduce unpredictable latency
- amplify jitter effects
- destabilize control-loop timing

Compression pipelines transform these tensors into compact, transmission-friendly representations that maintain deterministic timing.

Compression Techniques Used in Continuum Execution

The pipeline typically includes several hardware-accelerated stages:

1. Quantization of Intermediate Activations

Reduces bit-depth (e.g., FP16 → INT8 → INT4) while preserving essential structure. Quantization is applied selectively based on:

- layer sensitivity
- activation distribution
- downstream cloud model tolerance

2. Spatial Downsampling

For convolutional layers, spatial resolution can be reduced without losing critical semantic information. Techniques include:

- strided sampling

- pooling
- multi-scale feature extraction

3. Low-Rank Tensor Decomposition

Decomposes tensors into compact representations using:

- SVD
- Tucker decomposition
- CP decomposition

This is especially effective for large feature maps with redundant structure.

4. Delta-Encoding for Sequential Frames

For video, sensor fusion, or streaming inference, only changes between frames are transmitted. This dramatically reduces uplink load in stable environments.

Hardware-Accelerated Compression Paths

To maintain determinism, compression must be:

- **pipeline-aligned**
- **cycle-predictable**
- **non-blocking**
- **DVFS-aware**

Accelerators include:

- dedicated quantization units
- tensor-reduction engines
- compression-aware DMA channels

These ensure compression latency is bounded and predictable.

Deterministic Guarantees Provided by Compression Pipelines

Compression pipelines ensure:

- **predictable uplink transmission time**

- **bounded jitter sensitivity**
- **stable cloud-side execution windows**
- **energy-efficient uplink behavior**
- **continuum reliability under constrained bandwidth**

They transform uplink transmission from a variable-latency bottleneck into a deterministic, latency-bounded stage of distributed inference.

Integration with the Continuum Architecture

Compression pipelines directly support:

- adaptive offload decisions (by reducing uplink cost)
- jitter-buffered execution (by stabilizing transmission windows)
- cloud-assisted weight streaming (by freeing bandwidth)

They are the *second* major pillar of deterministic continuum execution.

Even with efficient compression, uplink transmission remains vulnerable to network jitter—variability in packet arrival times that can disrupt inference timing. To preserve deterministic behavior, the continuum must absorb jitter without stalling execution or violating control-loop deadlines. This requires a buffering layer capable of smoothing transmission irregularities and a fallback execution path that allows the edge to temporarily execute cloud-assigned layers when jitter exceeds safe thresholds. This transition into **jitter-resilient AI buffering with fallback edge execution paths** marks the moment where continuum execution becomes robust against real-world network instability, ensuring uninterrupted inference even under degraded connectivity.

iii. Jitter-Resilient AI Buffering with Fallback Edge Execution Paths

Jitter-resilient AI buffering is the mechanism that ensures distributed inference remains stable even when network conditions fluctuate unpredictably. In edge-to-cloud continuum execution, intermediate tensors must arrive at the cloud within tight latency windows. However, real-world networks—especially cellular, shared Wi-Fi, or congested enterprise links—introduce jitter: variability in packet arrival times that disrupts timing guarantees. For safety-critical AI systems, jitter is not merely a performance issue; it is a correctness hazard. A single delayed tensor can cause inference stalls, missed control-loop deadlines, or unstable actuator behavior.
Jitter-resilient buffering solves this by smoothing transmission irregularities and providing deterministic fallback paths.

Why Jitter Matters in Distributed AI Execution

Jitter affects:

- **Activation arrival times**
- **Cloud-side scheduling windows**
- **Edge-side control-loop timing**
- **Pipeline synchronization across layers**

Even small jitter spikes can cause:

- inference stalls
- pipeline desynchronization
- missed deadlines
- unsafe latency excursions

Thus, jitter must be absorbed, not merely tolerated.

Predictive Jitter-Buffering Windows

The buffering layer maintains:

short-term activation buffers for in-flight tensors

predictive jitter windows based on link-quality forecasts

adaptive buffer sizing based on real-time congestion sensing

Predictive buffering uses:

- link-quality history
- packet-arrival variance
- congestion-forecast models
- DVFS-aware timing predictions

This allows the system to anticipate jitter spikes before they occur.

Fallback Edge Execution Paths

When jitter exceeds safe thresholds, the system activates a fallback path:

- The edge temporarily executes layers normally assigned to the cloud.
- The fallback path uses cached weights or recently streamed updates.
- Execution continues locally until jitter stabilizes.

This ensures:

no inference stalls

no pipeline gaps

no missed control-loop deadlines

no unsafe latency spikes

Fallback execution is deterministic because:

- layers have pre-allocated memory domains
- weights are version-consistent
- pipeline checkpoints align with offload boundaries

Deterministic Guarantees Provided by Jitter-Resilient Buffering

This mechanism ensures:

- **stable inference timing under fluctuating networks**
- **bounded latency even during jitter spikes**
- **continuous operation during cloud congestion**
- **safe fallback behavior without pipeline corruption**

It transforms distributed inference from a network-dependent process into a jitter-buffered, latency-bounded execution fabric.

Integration with the Continuum Architecture

Jitter-resilient buffering directly supports:

- adaptive offload decisions (by providing fallback stability)
- tensor compression pipelines (by smoothing transmission windows)
- cloud-assisted weight streaming (by ensuring version consistency during fallback)

It is the *third* major pillar of deterministic continuum execution.

With jitter-resilient buffering ensuring stable inference even under degraded network conditions, the next challenge is maintaining model freshness across the continuum. Edge devices often operate on low-power cellular networks where bandwidth is limited and connectivity fluctuates. To preserve accuracy without interrupting inference, the cloud must stream updated model weights, adapters, or multimodal heads in a bandwidth-adaptive, version-consistent manner. This transition into **cloud-assisted AI weight-update streaming** marks the moment where continuum execution evolves from stable inference to continuous model evolution, ensuring that edge models remain current even under constrained connectivity.

iv. Cloud-Assisted AI Weight-Update Streaming over Low-Power Cellular Fabrics

Cloud-assisted AI weight-update streaming is the mechanism that keeps edge-resident AI models fresh, accurate, and aligned with cloud-side improvements—even when the edge device operates on low-power, bandwidth-constrained cellular networks. In real-time AI systems, inference must continue uninterrupted while model weights evolve in the background. This requires a streaming architecture that is bandwidth-adaptive, version-consistent, and resilient to intermittent connectivity.

Why Weight-Update Streaming Is Essential

Edge devices often run:

- **compressed models**
- **quantized variants**
- **specialized adapters**
- **domain-specific heads**

These models degrade over time if not updated. Cloud-side training pipelines continuously refine weights using aggregated data, federated updates, or domain-specific fine-tuning. Without streaming, edge models drift from optimal performance.

Bandwidth-Adaptive Chunking

Weight updates are divided into:

- **micro-chunks** (tens of kilobytes)
- **priority-tagged segments** (critical layers first)

- **adaptive-rate streams** (based on link quality)

Chunking ensures:

- updates fit within low-power cellular bursts
- transmission remains stable under jitter
- inference never blocks waiting for updates

Version-Consistent Swap-In Points

To avoid corrupting inference:

- updates accumulate in a staging buffer
- version markers ensure consistency
- swap-in occurs only at safe pipeline boundaries

This prevents:

- partial weight loads
- inconsistent layer states
- mid-inference model corruption

Error-Correcting Transmission

Low-power cellular links are prone to:

- packet loss
- burst errors
- intermittent dropouts

Weight streaming uses:

- forward-error correction
- parity-based recovery
- retry-bounded retransmission

This ensures updates arrive intact without destabilizing timing.

Background Streaming That Never Blocks Inference

Streaming is:

- **non-blocking**
- **priority-aware**
- **DVFS-aligned**
- **latency-bounded**

Inference continues using the current model until a complete, validated update is ready. The swap-in is atomic and deterministic.

Deterministic Guarantees Provided by Weight-Update Streaming

This mechanism ensures:

- **continuous model freshness**
- **stable inference timing**
- **safe version transitions**
- **reliable updates under constrained connectivity**

It completes the continuum architecture by enabling **continuous evolution** of edge models without compromising real-time behavior.

Edge-to-cloud continuum execution transforms distributed AI from a best-effort offload strategy into a deterministic, latency-bounded architecture. Live-metric-driven compute-graph partitioning adapts layer placement to real-time conditions. Tensor compression pipelines reduce uplink cost while preserving semantic fidelity. Jitter-resilient buffering ensures stable inference even under degraded connectivity, with fallback edge execution paths preventing stalls. Cloud-assisted weight-update streaming keeps edge models fresh without interrupting inference. Together, these mechanisms create a continuum fabric where computation moves fluidly between edge and cloud while maintaining deterministic timing, stable latency, and uninterrupted safety-critical behavior.

Real-time AI frameworks unify deterministic execution across compute, memory, IPC, virtualization, and distributed continuum layers. They ensure that every component—from cycle-accurate simulation to hardware-sliced isolation, from time-sliced context switching to jitter-buffered networking—operates within strict latency budgets and safety constraints. These frameworks transform AI systems from probabilistic, best-effort pipelines into predictable, timing-guaranteed infrastructures suitable for autonomy, robotics, industrial control, and

mission-critical environments. Real-time frameworks are the foundation upon which cross-layer optimization, secure enclaves, and hardware-aware AI compilation can be built.

With real-time execution now stabilized across local hardware and the edge-to-cloud continuum, the next architectural challenge is optimizing AI systems *across layers*—from intermediate representations to neural architecture search, from runtime telemetry to secure enclaves. Deterministic behavior alone is not enough; the system must also be efficient, compact, hardware-aware, and secure. Cross-layer optimization provides this refinement by aligning compilation, graph simplification, architecture search, observability, and cryptographic isolation into a unified optimization fabric. This transition marks the moment where AI systems evolve from deterministic execution engines into fully optimized, hardware-co-designed, end-to-end intelligent infrastructures.

F. Cross-Layer Optimization in AI Systems

The design of efficient, reliable, and secure artificial intelligence (AI) systems requires coordinated optimization across multiple layers of the computing architecture. Although AI models, compilers, computing hardware, runtime environments, and security mechanisms can be developed independently, their combined behavior determines the performance of the deployed system. A neural network may achieve high predictive accuracy but execute too slowly on its target processor. A powerful AI accelerator may remain underutilized because of inefficient software execution or excessive data movement. Similarly, a system optimized for computational performance may fail to satisfy its operational requirements if it cannot monitor hardware degradation, meet real-time deadlines, or protect sensitive data. These challenges make **cross-layer optimization a fundamental discipline in AI system engineering**.

Cross-layer optimization refers to the coordinated design and refinement of AI models, computational representations, software execution, hardware resources, and system-level mechanisms to achieve the objectives of a complete application. Rather than optimizing each component in isolation, this approach considers how decisions at one layer affect the behavior of other layers. Model architecture influences computational demand and memory consumption; compiler transformations determine how mathematical operations are translated into executable instructions; hardware characteristics influence the efficiency of those instructions; and runtime behavior determines whether the system can sustain its required performance under actual operating conditions. Security requirements introduce additional constraints on how data and computations are accessed, processed, and protected.

The need for cross-layer optimization is particularly evident in modern AI workloads, including deep neural networks, transformer-based models, multimodal perception systems, and real-

time edge inference. These workloads combine computationally intensive operations with substantial memory traffic, intermediate data transformations, and dependencies among processing stages. Their performance depends not only on the theoretical processing capacity of the hardware but also on memory bandwidth, data locality, numerical precision, parallel execution, software overhead, and communication among system components. Consequently, improving one component does not necessarily improve overall system performance. An optimization that reduces arithmetic operations may provide limited benefit if memory transfers remain the dominant bottleneck, while increasing computational throughput may have little practical value if the system cannot deliver results within the required time.

The central objective of cross-layer optimization is to align the mathematical structure of AI workloads with the capabilities, constraints, and operational requirements of the underlying computing platform. This alignment requires a system-level perspective in which predictive accuracy, computational efficiency, latency, energy consumption, reliability, and security are treated as interconnected design considerations. The relative importance of these objectives depends on the application. A cloud-based AI service may prioritize throughput and resource utilization, whereas an autonomous robot or industrial control system may place greater emphasis on predictable latency, bounded resource consumption, and safe behavior under degraded conditions.

Cross-layer optimization also extends beyond initial system configuration. Theoretical performance estimates and isolated benchmarks cannot fully capture the effects of actual workloads, resource contention, thermal conditions, and changing execution environments. Measurements collected during testing and deployment can reveal bottlenecks that were not apparent during design. These findings may require adjustments to model configurations, compilation strategies, hardware-resource allocation, or runtime policies. Optimization is therefore an iterative engineering process in which design decisions are evaluated against observed system behavior and refined to satisfy the requirements of the intended application.

Another important consideration is the relationship between optimization and correctness. Transformations that improve execution efficiency must preserve the intended behavior of the AI system within acceptable limits. Changes in numerical precision, computational ordering, or model structure may affect prediction quality, while resource-management decisions may influence execution timing and system responsiveness. Similarly, mechanisms introduced to improve observability or security may consume computational resources or introduce additional latency. Effective cross-layer optimization must account for these interactions rather than assume that improvements in one dimension are automatically beneficial to the system as a whole.

To examine these relationships systematically, cross-layer optimization in AI systems can be organized into five complementary areas. The first concerns the representations and compilation processes used to translate AI models into efficient executable workloads. The second focuses on simplifying computational graphs and reducing unnecessary operations. The third addresses the relationship between neural architecture design and the performance constraints of the target hardware. The fourth considers how runtime observability connects software behavior with hardware conditions and supports the detection and mitigation of faults. The fifth addresses the integration of hardware-supported isolation and other security mechanisms into AI execution environments.

These areas collectively establish a framework for understanding how optimization decisions propagate across the AI computing stack:

- **AI Intermediate Representations with Domain-Specific Compilation and MLIR/TVM Optimization Pipelines** examines the role of intermediate representations and specialized compilation in translating AI computations into hardware-efficient implementations.
- **AI Graph Simplification via Structural Math Reductions, Dead-Node Pruning, and Operator Fusion** addresses the reduction of unnecessary computation and the organization of operations to improve execution efficiency.
- **Hardware-Aware AI Neural Architecture Search with Constraints and Latency-Driven Loss Functions** considers how model architectures can be selected according to predictive requirements and practical hardware constraints.
- **Silicon-to-Software AI Observability with Runtime Telemetry and Physical Fault-Mitigation Hooks** focuses on connecting runtime measurements and hardware-status information with system monitoring and corrective responses.
- **Full-Stack AI Secure Enclaves with Cryptographic Hardware Isolation and Side-Channel Defense Layers** examines the integration of hardware-supported security and isolation mechanisms into AI execution architectures.

Although these areas address different aspects of system design, they are not independent optimization tasks. The representation selected for a model can affect the compiler transformations available to it; graph transformations can influence hardware utilization; architectural choices can change latency and memory requirements; runtime monitoring can reveal opportunities for further optimization; and security requirements can constrain where and how computations are performed. Their interactions determine whether an AI system can

achieve its intended performance while maintaining the required levels of reliability and protection.

The following discussions examine these five areas individually, establishing their underlying principles, engineering considerations, and contributions to AI system performance. Taken together, they demonstrate why effective optimization requires a coordinated perspective that extends from model representation and computational structure to physical execution and system protection.

Ultimately, **cross-layer optimization treats the performance of an AI system as a property of the complete architecture rather than of any single model, compiler, processor, or software component**. By coordinating design decisions across these layers, engineers can reduce computational overhead, use hardware resources more effectively, manage operational constraints, and develop AI systems that are better suited to the demands of real-world deployment.

With the full cross-layer optimization fabric now established—from compiler-level IR transformations to secure enclave isolation—the next step is to consolidate these mechanisms into a structured view that highlights how each layer contributes to the overall optimization continuum. The following table organizes these layers into a unified framework, showing how compilation, graph refinement, hardware-aware model design, runtime observability, and secure execution collectively shape the performance, determinism, and trustworthiness of modern AI systems. This table serves as a conceptual anchor, allowing the reader to see how each optimization domain interacts with the others to form a vertically integrated, hardware-co-designed AI stack.

Table 8.4-F presents the five foundational layers that define cross-layer optimization in AI systems. Each layer represents a distinct optimization domain, yet all of them operate in concert to transform high-level neural networks into efficient, predictable, and secure execution pipelines. The table highlights the core function of each layer, the mechanisms that enable it, and the architectural impact it has on the system. By laying out these relationships explicitly, the table clarifies how optimization flows upward through the stack—from IR-driven compilation to secure enclave isolation—ultimately producing an AI system capable of meeting strict latency, power, and security requirements across heterogeneous deployment environments.

Table 8.4-F — Cross-Layer Optimization in AI Systems

Optimization Layer	Core Function	Key Mechanisms	Architectural Impact
Intermediate Representations & Domain-Specific Compilation	Transforms high-level models into hardware-aligned execution plans	MLIR dialects, TVM Relay graphs, operator lowering, schedule generation, memory tiling, vectorization, accelerator-specific codegen	Bridges abstract model semantics with physical hardware constraints; enables deterministic, optimized kernel generation
Structural Graph Simplification	Reduces computational and memory complexity through mathematical refinement	Algebraic reductions, constant folding, dead-node pruning, operator fusion, redundant-path elimination	Shrinks latency, reduces memory footprint, improves bandwidth efficiency, stabilizes execution pipelines
Hardware-Aware Neural Architecture Search	Co-designs model topologies with accelerator characteristics	Latency-driven loss functions, cache-aligned tensor shapes, tensor-core-compatible operators, Pareto-optimal model families	Produces architectures inherently optimized for real-time constraints, power budgets, and heterogeneous hardware
Silicon-to-Software Observability	Provides real-time visibility into physical execution behavior	Hardware counters, thermal sensors, power-rail monitors, congestion indicators, fault-mitigation hooks	Enables dynamic adaptation, fault containment, thermal-aware scheduling, and stable deterministic performance

Optimization Layer	Core Function	Key Mechanisms	Architectural Impact
Full-Stack Secure Enclaves	Protects AI workloads from tampering, leakage, and side-channel exploitation	Cryptographic isolation, enclave-bounded memory, secure DMA paths, hardened microarchitectural pathways, constant-time execution	Ensures confidentiality and integrity across the stack; maintains security without sacrificing optimization or latency

The first layer in the table focuses on intermediate representations and domain-specific compilation. This is where high-level models are transformed into hardware-aligned execution plans using MLIR dialects, TVM Relay graphs, and specialized IRs. Operator lowering, schedule generation, memory tiling, and vectorization ensure that the model's abstract semantics are reshaped into kernels that match the physical constraints of the accelerator. This layer forms the foundation of the optimization continuum, bridging the gap between model design and hardware execution.

The second layer addresses structural graph simplification. Algebraic reductions, constant folding, dead-node pruning, and operator fusion refine the compute graph itself, eliminating redundant operations and reducing memory pressure. These transformations shrink latency and stabilize execution pipelines, ensuring that the graph aligns with the accelerator's preferred dataflow patterns. This layer reduces computational complexity before the model ever reaches the hardware.

The third layer introduces hardware-aware neural architecture search. Here, the model topology is co-designed with the accelerator, guided by constraints such as cache sizes, tensor-core shapes, memory bandwidth, and DVFS behavior. Latency-driven loss functions and Pareto-optimal model families ensure that the resulting architectures are inherently efficient, balancing accuracy with real-time performance and resource consumption. This layer ensures that the model itself is structurally compatible with the hardware.

The fourth layer focuses on silicon-to-software observability. Hardware counters, thermal sensors, power-rail monitors, and fault-mitigation hooks provide real-time visibility into the physical behavior of AI workloads. This telemetry enables dynamic adaptation, fault containment, and thermal-aware scheduling, allowing the system to maintain determinism even under fluctuating environmental conditions or hardware stress. Observability transforms

optimization from a static process into a continuous feedback loop.

The final layer in the table highlights full-stack secure enclaves. Cryptographic isolation, enclave-bounded memory regions, secure DMA paths, and side-channel defenses protect AI workloads from tampering, leakage, and adversarial observation. These enclaves ensure that optimization does not compromise security, anchoring the entire stack in trust and enabling sensitive workloads to run safely across cloud, edge, and embedded environments.

Together, the layers in Table 8.4-F illustrate how cross-layer optimization forms a vertically integrated continuum. Each layer contributes a distinct capability—compilation, structural refinement, hardware co-design, runtime introspection, and secure execution—but their combined effect is a coherent, efficient, and trustworthy AI system. The table makes clear that modern AI performance is not the result of any single optimization technique, but of a coordinated architecture where every layer reinforces the others.

Following the structured overview provided in Table 8.4-F, which organizes the five optimization domains into their functional roles and architectural impacts, Figure 8.4-F translates this tabular structure into a visual continuum. The figure illustrates how each optimization layer builds upon the previous one, forming a vertically integrated pipeline that transforms high-level models into deterministic, efficient, and secure AI execution environments. This visual representation reinforces the idea that cross-layer optimization is not a collection of isolated techniques but a coordinated progression that spans the entire AI stack.

Figure 8.4-F presents the cross-layer optimization continuum as a vertically stacked architectural flow, showing how intermediate representations, graph simplification, hardware-aware architecture search, runtime observability, and secure enclaves collectively shape the behavior of modern AI systems. Each layer is depicted as a distinct block containing its core mechanisms, while the upward arrow emphasizes the cumulative nature of optimization. The figure highlights how improvements at lower layers propagate upward, ultimately producing a deterministic, efficient, and secure AI stack capable of meeting real-time performance and security requirements.

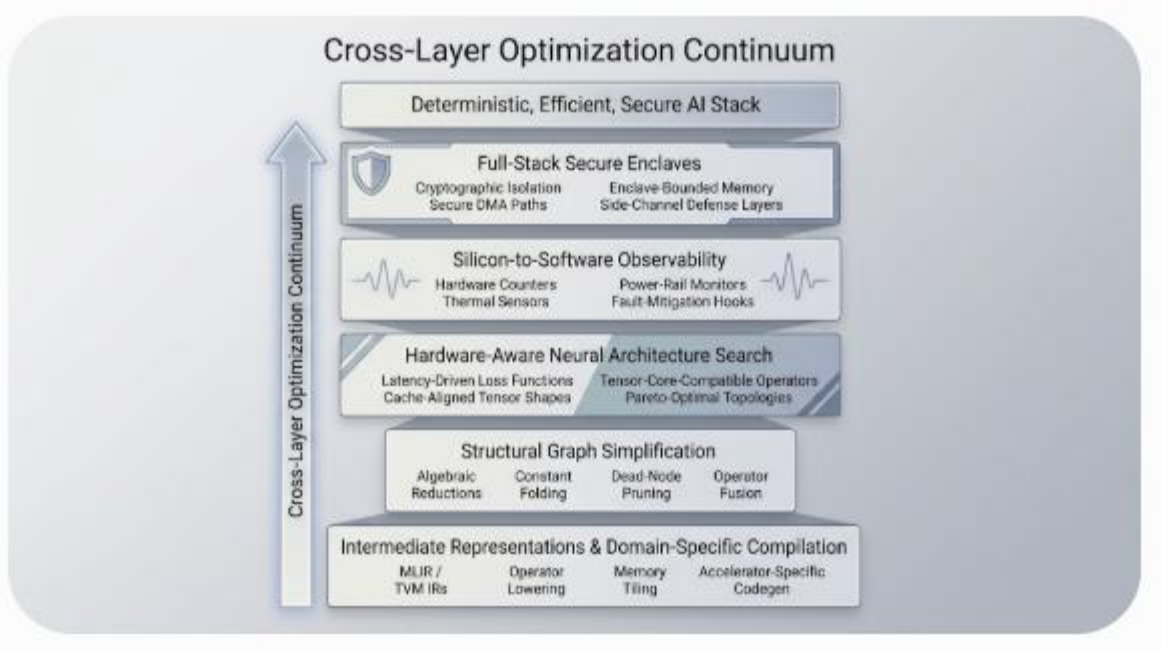


Figure 8.4-F — Cross-Layer Optimization Continuum
A vertically layered representation of the optimization pipeline that spans intermediate representations, structural graph simplification, hardware-aware neural architecture search, silicon-to-software observability, and full-stack secure enclaves. The upward arrow illustrates how each layer contributes to the formation of a deterministic, efficient, and secure AI execution environment.

Legend:

- ***Intermediate Representations & Domain-Specific Compilation*** *— MLIR / TVM IRs, operator lowering, memory tiling, accelerator-specific codegen.*
- ***Structural Graph Simplification*** *— algebraic reductions, constant folding, dead-node pruning, operator fusion.*
- ***Hardware-Aware Neural Architecture Search*** *— latency-driven loss functions, cache-aligned tensor shapes, tensor-core-compatible operators, Pareto-optimal topologies.*
- ***Silicon-to-Software Observability*** *— hardware counters, thermal sensors, power-rail monitors, fault-mitigation hooks.*
- ***Full-Stack Secure Enclaves*** *— cryptographic isolation, secure DMA paths, enclave-bounded memory, side-channel defense layers.*
- ***Deterministic, Efficient, Secure AI Stack*** *— the integrated outcome of all preceding optimization layers.*

Figure 8.4-F depicts cross-layer optimization as a vertical continuum, beginning with

intermediate representations and domain-specific compilation at the foundation. This base layer converts high-level models into hardware-aligned execution plans using MLIR, TVM, and specialized IRs, establishing the structural and semantic groundwork for all subsequent optimization.

Above this foundation lies structural graph simplification, where algebraic reductions, constant folding, dead-node pruning, and operator fusion reshape the compute graph into a more efficient and hardware-friendly topology. This layer reduces computational complexity and memory pressure, ensuring that the graph aligns with the accelerator's execution patterns.

The next layer, hardware-aware neural architecture search, co-designs model topologies with the accelerator itself. Latency-driven loss functions and Pareto-optimal model families guide the search toward architectures that balance accuracy, timing guarantees, and resource efficiency. This layer ensures that the model is inherently compatible with the hardware, reducing the need for heavy post-hoc optimization.

Silicon-to-software observability forms the fourth layer, providing real-time visibility into the physical behavior of AI workloads. Hardware counters, thermal sensors, and fault-mitigation hooks feed telemetry into the runtime, enabling dynamic adaptation, fault containment, and thermal-aware scheduling. This layer transforms optimization into a continuous feedback loop driven by the hardware's real-time state.

At the top of the continuum, full-stack secure enclaves enforce cryptographic isolation, secure DMA paths, enclave-bounded memory, and side-channel defenses. This layer ensures that optimization does not compromise security, anchoring the entire stack in trust and protecting sensitive workloads from tampering or leakage.

The final capstone block—Deterministic, Efficient, Secure AI Stack—represents the integrated outcome of all preceding layers. The upward arrow running through Figure 8.4-F emphasizes that each optimization domain contributes cumulatively to the formation of a coherent, hardware-co-designed AI system capable of delivering predictable performance, adaptive resilience, and uncompromised security.

The optimization continuum begins at the compilation layer, where high-level neural models are first transformed into representations that expose their structure, operators, and tensor flows to systematic refinement. Before any graph simplification, hardware-aware architecture search, runtime observability, or secure enclave isolation can take effect, the model must be expressed in a form that allows the compiler to reason about loops, memory layouts, parallelism, and accelerator-specific execution patterns. This foundational stage relies on multi-level intermediate representations designed for specialized hardware, polyhedral compilation models

capable of restructuring nested tensor programs, auto-tuned pipelines that generate hardware-optimized block layouts, and machine-code ingestion layers that target custom vector instruction sets. Together, these capabilities establish the substrate upon which all higher-level optimization depends, making the compilation layer the true starting point of cross-layer refinement.

a. AI Intermediate Representations with Domain-Specific Compilation and MLIR/TVM Optimization Pipelines

Modern artificial intelligence (AI) systems depend on compilation pipelines that translate high-level neural network models into efficient executable programs for heterogeneous computing platforms. These platforms may combine general-purpose CPUs, GPUs, tensor-processing accelerators, digital signal processors (DSPs), and specialized neural processing units (NPUs), each with distinct instruction sets, memory hierarchies, parallel execution models, and numerical capabilities. Because a model expressed in a high-level framework does not explicitly capture all the constraints of its eventual execution environment, an intermediate representation (IR) is needed to bridge the gap between abstract model semantics and hardware-specific implementation. **AI intermediate representations provide the structural foundation through which compilers analyze, transform, and map neural network computations onto the capabilities of the target hardware.**

An intermediate representation expresses a model in a form that is more amenable to systematic analysis and optimization than its original framework-level description. Depending on its abstraction level, an IR may represent neural network operators, tensor dimensions, data types, computational dependencies, loop structures, memory layouts, and parallel execution opportunities. These representations allow a compiler to reason about both the mathematical behavior of a model and the computational resources required to execute it. Rather than translating an entire model directly into machine instructions in a single step, modern compilers typically use a sequence of transformations that progressively lower the computation from high-level operations to increasingly hardware-specific forms. This staged process preserves opportunities for optimization while gradually introducing the implementation details required by the target platform.

Multi-Level Intermediate Representations and Domain-Specific Abstraction

A modern AI compilation pipeline commonly employs multiple levels of representation, each designed to expose a different class of optimization opportunities. At the highest level, the IR preserves neural network semantics, including operations such as convolution, matrix multiplication, normalization, attention, and activation functions. At intermediate levels, these

operations may be decomposed into tensor algebra, linear algebra, loop nests, memory-access patterns, and explicit execution schedules. At lower levels, the representation may expose vector instructions, parallel thread groups, accelerator-specific operations, register usage, and synchronization requirements.

This hierarchical organization allows optimizations to be performed at the level where they are most effective. For example, a high-level representation may make it possible to combine consecutive neural network operators without losing their mathematical relationship. A lower-level representation may reveal that a loop can be tiled to improve cache reuse or that a tensor operation can be mapped to a specialized matrix-multiplication unit. By preserving information across multiple abstraction levels, the compiler can coordinate mathematical simplification, data-layout selection, parallel scheduling, and hardware-specific code generation rather than treating them as unrelated tasks.

The Multi-Level Intermediate Representation (MLIR) infrastructure exemplifies this approach through its extensible dialect system. A dialect defines operations, types, attributes, and rules appropriate to a particular computational domain or stage of compilation. For example, an AI compiler may use high-level operations to represent neural network computations, the linalg dialect to express structured tensor and linear algebra operations, the affine dialect to describe analyzable loop and memory-access relationships, and lower-level dialects to represent hardware-specific instructions. Quantization and accelerator-specific transformations can also be incorporated through suitable dialects or compiler extensions. This extensibility allows specialized optimization techniques to coexist within a common infrastructure while supporting progressive lowering toward executable code.

TVM provides a complementary compilation framework for optimizing tensor computations across different hardware targets. Its compiler infrastructure includes representations and optimization mechanisms for expressing neural network operations, transforming computational graphs, generating candidate schedules, and producing target-specific implementations. TVM Relay historically served as a graph-level intermediate representation for these tasks, while newer TVM development also includes TensorIR and related representations for lower-level tensor programs and scheduling. This distinction is important because graph-level transformations and loop-level scheduling address different optimization problems: graph-level representations expose relationships among operators, whereas lower-level representations expose the details needed to optimize individual computational kernels.

Domain-specific intermediate representations extend these general approaches by incorporating knowledge about particular AI workloads or hardware architectures. A vision accelerator, for example, may favor fixed or bounded image dimensions, regular convolution

patterns, and predictable data movement. A transformer-oriented accelerator may provide specialized support for attention, matrix multiplication, reduced-precision arithmetic, or structured sparsity. When such characteristics are represented explicitly, a compiler can apply transformations that would be difficult to identify from generic operators alone. However, these optimizations depend on the quality of the available information: a compiler must understand the relevant tensor shapes, data types, sparsity constraints, operator semantics, and hardware capabilities before it can reliably exploit them.

Operator Lowering, Scheduling, and Hardware-Aware Data Movement

Once a model has been represented in a suitable IR, the compiler progressively lowers its operations into forms that match the execution capabilities of the target device. Operator lowering translates high-level mathematical operations into lower-level computational primitives. A matrix multiplication, for example, may be decomposed into tiled operations that can use a GPU's matrix-multiplication units, while a normalization operation may be transformed into a sequence of reductions and elementwise computations. The exact decomposition depends on the operator, numerical requirements, tensor dimensions, and available hardware instructions.

Lowering must be coordinated with execution scheduling. Scheduling determines how computational operations are ordered, partitioned, parallelized, and assigned to available processing resources. For tensor workloads, this may involve selecting loop orders, tile dimensions, thread-block structures, vector widths, and synchronization points. A well-designed schedule can increase parallel utilization, improve reuse of intermediate results, and reduce the time processors spend waiting for data. An unsuitable schedule, by contrast, may create excessive synchronization, poor memory access patterns, or underutilized execution units even when the underlying hardware has substantial theoretical computational capacity.

Memory movement is a central consideration in this process because AI performance depends on both the speed of computation and the efficiency with which data reaches the computing units. Large neural networks repeatedly access model parameters, input tensors, intermediate activations, and temporary results. The compiler therefore needs to consider how data is transferred among external memory, caches, shared memory, registers, and other storage resources supported by the target architecture. Tiling can partition a large computation into smaller units that fit within a particular level of the memory hierarchy, allowing data to be reused before it must be fetched again. Layout transformations can reorganize tensor dimensions to match hardware access patterns, while fusion may reduce the need to write intermediate results to and reload them from memory.

These transformations must respect data dependencies and numerical requirements. Loop reordering, fusion, and parallel execution are beneficial only when they preserve the intended computation or maintain acceptable numerical behavior. Similarly, a tile size that performs well for one tensor shape or accelerator may be inefficient for another. Effective compilation therefore requires the IR to expose sufficient structural information for the compiler to evaluate alternative implementations against the characteristics of the target workload and hardware.

Vectorization and specialized instruction mapping provide another important optimization opportunity. Vectorization combines multiple operations into a single instruction or execution group, allowing the hardware to process several data elements in parallel. Depending on the platform, this may involve CPU SIMD instructions, GPU vector operations, matrix-multiplication units, or tensor-core-like execution resources. The compiler must account for data alignment, supported numerical formats, tensor dimensions, and the degree of parallelism available. When these conditions are satisfied, vectorization can substantially improve throughput; when they are not, instruction overhead, data conversion, or inefficient utilization can limit the benefit.

Polyhedral Compilation and Mathematical Scheduling

For suitable loop-based tensor programs, polyhedral compilation provides a mathematical framework for analyzing and transforming iteration spaces. In this approach, loop iterations and their relationships are represented using mathematical sets and dependence constraints, often based on affine expressions in loop indices and program parameters. The compiler can then evaluate transformations such as loop interchange, tiling, fusion, and parallelization while checking whether required data dependencies are preserved.

Consider a convolution or matrix multiplication involving nested loops over tensor dimensions. The original loop order may repeatedly load data that could otherwise be reused across multiple operations. By transforming the iteration space, the compiler can arrange computations into tiles that improve locality, expose parallel execution, or reduce unnecessary memory traffic. Such transformations can be especially valuable on accelerators whose performance depends on feeding large numbers of parallel execution units with data at a sustained rate.

Polyhedral techniques nevertheless have a defined scope. They are most directly applicable when loop bounds and memory-access relationships can be expressed in forms that support the required mathematical analysis. Dynamic control flow, irregular memory accesses, data-dependent iteration counts, and complex runtime behavior may limit their applicability or require other optimization methods. Consequently, polyhedral compilation is best understood as one component of a broader AI compilation pipeline rather than a universal solution for

every neural network operation.

Auto-Tuning and Search-Based Schedule Optimization

Even when a compiler can generate many legal implementations of an operation, predicting which implementation will perform best on a particular device is difficult. Performance depends on interacting factors such as tensor dimensions, tile sizes, memory layouts, register pressure, occupancy, vector width, cache behavior, and hardware-specific execution characteristics. Static heuristics can identify useful configurations, but they may not consistently select the best schedule across different workloads and devices. Auto-tuning addresses this challenge by systematically evaluating alternative implementations.

In an auto-tuning pipeline, the compiler generates candidate schedules or kernel configurations and evaluates them using analytical cost models, empirical measurements, or a combination of both. Search variables may include tile dimensions, loop orders, thread-block configurations, memory placement, vectorization choices, and operator-fusion decisions. The search process then identifies promising candidates and refines the search based on their estimated or measured performance. TVM's AutoTVM and Ansor are established examples of approaches that use search and cost modeling to optimize tensor programs. Ansor, in particular, introduced a hierarchical search approach for generating and evaluating program schedules.

Machine learning can support this process by estimating the performance of candidate schedules and guiding the search toward configurations likely to be effective. Instead of exhaustively testing every possible implementation, the system uses previous measurements or learned cost models to prioritize promising alternatives. This is particularly useful when optimizing computationally intensive kernels, such as convolutions, matrix multiplications, and attention-related operations, for which small scheduling changes can substantially affect execution time.

Auto-tuning does not guarantee that every generated kernel will achieve optimal performance. Search quality depends on the candidate space, the accuracy of the cost model, the reliability of measurements, and the representativeness of the tuning workload. Measurements may also be affected by concurrent processes, thermal conditions, power limits, and device-specific behavior. Furthermore, a configuration optimized for one tensor shape may perform poorly on another. Production-oriented tuning must therefore consider the expected workload distribution and may require multiple specialized kernels or runtime dispatch strategies rather than a single universally optimal schedule.

Target-Specific Code Generation and Execution

After higher-level transformations and schedule selection, the compilation pipeline converts the optimized representation into code that the target platform can execute. This process may include instruction selection, register allocation, memory-address calculation, vector packing, synchronization insertion, and the mapping of parallel computations to the device's execution model. Depending on the platform and software stack, the output may be CUDA code or an intermediate form compiled for NVIDIA GPUs, HIP-based code for supported AMD GPU environments, SPIR-V for compatible compute platforms, Metal-based programs for supported Apple devices, or code targeting proprietary accelerator toolchains.

These examples represent different programming and compilation pathways rather than interchangeable output formats. Their availability and capabilities depend on the target hardware, compiler infrastructure, runtime environment, and supported interfaces. A compiler must preserve the assumptions established during earlier optimization stages while satisfying the requirements of the final execution environment. For instance, a schedule designed around a particular shared-memory capacity or matrix instruction must be reconciled with the actual device limits, instruction semantics, and synchronization rules.

The final code-generation stage also affects predictability and operational behavior. Register allocation can influence occupancy; synchronization decisions can affect parallel efficiency; and kernel-launch overhead can become significant for workloads composed of many small operations. In real-time applications, these factors may influence whether inference completes within a specified deadline. However, generating hardware-specific code does not by itself guarantee deterministic execution. Predictability also depends on runtime scheduling, resource contention, memory behavior, operating-system interference, and other platform characteristics. Systems with strict timing requirements must evaluate these factors in addition to compiler-level optimizations.

Intermediate Representations as the Foundation of Cross-Layer Optimization

The significance of AI intermediate representations extends beyond the efficiency of individual kernels. Because IRs provide structured descriptions of computation, they create opportunities to coordinate optimization decisions across multiple layers of the AI system. Graph-level representations can reveal redundant operations and opportunities for operator fusion. Lower-level representations can expose data dependencies, memory-access patterns, and parallel execution opportunities. Hardware-aware representations can help align model operations with specialized processing units, while compilation metadata can support performance analysis and the diagnosis of inefficient execution.

These connections are particularly important when optimization decisions interact. A graph

transformation may reduce memory traffic but produce a larger fused kernel with higher register requirements. A more aggressive quantization strategy may improve throughput but require additional conversion operations or affect model accuracy. A hardware-specific schedule may accelerate one workload while reducing portability across devices. By maintaining explicit representations of the computation and its implementation constraints, the compiler can evaluate these trade-offs more systematically.

Intermediate representations can also support iterative optimization. Performance measurements obtained during testing or deployment may reveal that a generated kernel is limited by memory bandwidth, that a particular operator is poorly mapped to the hardware, or that resource contention is reducing throughput. Such findings can motivate changes to the model's representation, graph transformations, scheduling decisions, or target-specific code generation. In this way, compilation becomes part of an ongoing engineering process that connects model design, software implementation, hardware behavior, and system-level performance requirements.

Ultimately, **AI intermediate representations provide the common computational language through which model semantics, compiler transformations, and hardware execution can be coordinated**. Multi-level IRs preserve optimization opportunities across abstraction layers; domain-specific representations expose knowledge about particular workloads and accelerators; mathematical scheduling techniques improve computational locality and parallelism; auto-tuning explores implementation alternatives; and target-specific code generation translates optimized computations into executable programs. Together, these capabilities establish the compilation foundation for the broader cross-layer optimization process. They also provide the structural information needed for subsequent techniques involving AI graph simplification, hardware-aware neural architecture search, runtime observability, and hardware-supported security.

The exploration of intermediate representations and domain-specific compilation reveals how the compilation layer establishes the structural substrate upon which all higher-level optimization depends. Multi-level IR dialects expose computation at different granularities, polyhedral models restructure nested tensor programs, auto-tuned pipelines discover hardware-optimized block layouts, and machine-code ingestion layers translate optimized IR into accelerator-specific kernels. To consolidate these concepts into a coherent architectural view, Table 8.4-F1 organizes the foundational elements of IR-driven compilation, highlighting their core purpose, mechanisms, and impact on the broader optimization continuum.

Table 8.4-F1 presents the four foundational capabilities that define modern AI compilation

pipelines. Each capability represents a distinct dimension of how intermediate representations enable deep optimization across heterogeneous hardware. The table clarifies how multi-level IR dialects, polyhedral loop-transformation models, auto-tuned block-layout generators, and target-specific machine-code ingestion layers work together to transform high-level neural networks into hardware-aligned execution plans. By laying out these relationships explicitly, the table provides a structured understanding of how compilation forms the base layer of cross-layer optimization.

Table 8.4-F1 — AI Intermediate Representation and Compilation Foundations

Conceptual Area	Core Purpose	Key Mechanisms	Architectural Impact
Multi-Level IR Dialects for Specialized Hardware	Represent computation across multiple abstraction levels	High-level neural ops, affine loop dialects, low-level vector dialects, MLIR/TVM extensibility	Enables progressive lowering and hardware-aware optimization at each stage
Polyhedral Compilation Models for Nested Tensor Programs	Restructure loop nests for locality and parallelism	Affine sets, tiling, fusion, skewing, dependency analysis, schedule generation	Maximizes memory locality, parallel efficiency, and deterministic execution
Auto-Tuned Compilation Pipelines for Block Layout Generation	Discover optimal schedules and memory layouts	AutoTVM, Ansor, ML-guided search, tile-size exploration, vector-width tuning	Produces hardware-optimized kernels that saturate compute units and minimize stalls
Target-Specific Machine-Code Ingestion Layers	Generate executable kernels for custom instruction sets	Instruction selection, register allocation, vector packing, warp synchronization	Ensures optimized IR is preserved in final machine code and aligned with accelerator microarchitecture

The first conceptual area focuses on multi-level IR dialects tailored for specialized accelerator hardware. These dialects allow computation to be represented at multiple abstraction levels, from high-level neural operators to affine loop structures and low-level vector instructions. This multi-layered representation enables progressive lowering, ensuring that each stage of the compilation pipeline has access to the structural information needed for optimization. MLIR’s

extensible dialect system and TVM's Relay IR exemplify how domain-specific knowledge can be embedded directly into the IR.

The second area highlights polyhedral compilation models, which provide a mathematical framework for transforming nested tensor programs. By representing loop nests as affine sets and applying transformations such as tiling, fusion, and skewing, polyhedral models maximize locality and parallel efficiency. This capability is essential for accelerators with deep memory hierarchies, where optimal tiling determines whether kernels saturate compute units or stall on memory.

The third area introduces auto-tuned compilation pipelines that search for hardware-optimized block layouts. Instead of relying on static heuristics, auto-tuning explores thousands of candidate schedules, tile sizes, and vector widths to identify the configuration that yields the best performance on the target device. Machine-learning-guided search methods such as AutoTVM and Ansor ensure that the generated kernels exploit the full capabilities of the accelerator, including tensor-core utilization and warp-level parallelism.

The fourth area focuses on target-specific machine-code ingestion layers, which translate optimized IR into executable kernels for custom vector instruction sets. These layers handle instruction selection, register allocation, vector packing, and warp synchronization, ensuring that the final machine code aligns with the microarchitectural constraints of the device. This stage preserves the compiler's optimizations all the way down to the silicon.

Together, the four areas in Table 8.4-F1 illustrate how intermediate representations and domain-specific compilation form the foundation of cross-layer optimization. They expose structure, reshape computation, discover optimal schedules, and generate hardware-specific kernels, enabling all higher-level optimization layers to operate effectively. The table makes clear that modern AI performance begins with IR-driven compilation, which transforms abstract models into physically grounded execution plans.

The conceptual foundations summarized in Table 8.4-F1 establish how intermediate representations, polyhedral models, auto-tuned pipelines, and machine-code ingestion layers collectively form the base of the AI optimization continuum. To translate these relationships into a visual form, Figure 8.4-F1 presents the compilation process as a structured flow, showing how computation is progressively lowered from high-level IR dialects to hardware-optimized kernel execution. This figure reinforces the idea that compilation is not a single transformation but a multi-stage refinement pipeline that systematically reshapes neural workloads to match the physical characteristics of specialized accelerators.

Figure 8.4-F1 illustrates the hierarchical flow of AI compilation, beginning with multi-level

intermediate representations and descending through polyhedral loop transformations, auto-tuned schedule generation, and target-specific machine-code ingestion. Each stage is depicted as a distinct block connected by downward arrows, emphasizing the sequential lowering of computation as it moves closer to the hardware. The figure highlights how each transformation layer contributes unique structural refinements that ultimately produce deterministic, efficient, and accelerator-aligned AI kernels.

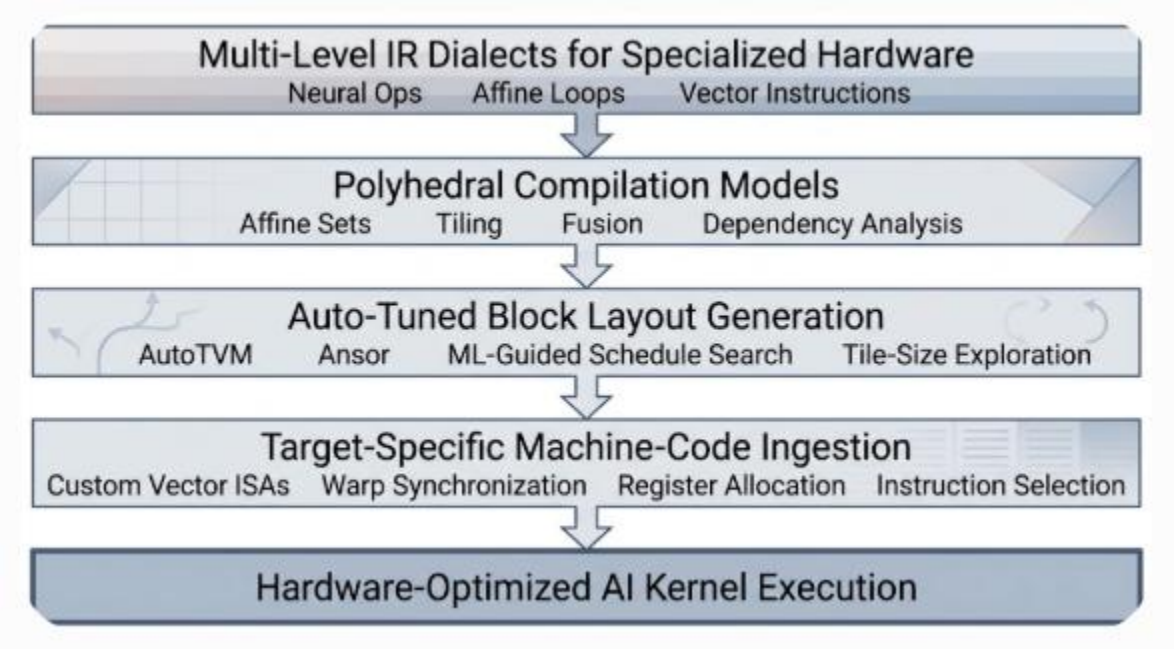


Figure 8.4-F1 — AI Intermediate Representation Compilation Flow
A top-down depiction of the multi-stage compilation pipeline that transforms high-level neural operators into hardware-optimized kernels. The flow illustrates how multi-level IR dialects, polyhedral transformations, auto-tuned block-layout generation, and target-specific machine-code ingestion collectively produce efficient, deterministic execution on specialized accelerators.

Legend:

- ***Multi-Level IR Dialects for Specialized Hardware*** *— neural operators, affine loop structures, vector-level instructions.*
- ***Polyhedral Compilation Models*** *— affine sets, tiling, fusion, dependency analysis.*
- ***Auto-Tuned Block Layout Generation*** *— AutoTVM, Ansor, ML-guided schedule search, tile-size exploration.*
- ***Target-Specific Machine-Code Ingestion*** *— custom vector ISAs, warp synchronization, register allocation, instruction selection.*
- ***Hardware-Optimized AI Kernel Execution*** *— final accelerator-aligned kernel output.*

Figure 8.4-F1 presents the compilation pipeline as a descending sequence of transformations, beginning with multi-level IR dialects that capture computation at progressively finer granularities. At this stage, neural operators, affine loops, and vector instructions coexist within a unified representational framework, allowing the compiler to reason about both high-level semantics and low-level execution constraints.

The next stage introduces polyhedral compilation models, which apply mathematical transformations to nested tensor programs. By representing loop nests as affine sets and analyzing dependencies, the compiler can safely reorder loops, tile computation for locality, and fuse operations to reduce memory traffic. This stage reshapes the computational structure to better match the accelerator's memory hierarchy and parallel execution model.

Auto-tuned block-layout generation follows, exploring thousands of candidate schedules, tile sizes, and vector widths to identify the configuration that yields optimal performance on the target hardware. Machine-learning-guided search methods such as AutoTVM and Ansor ensure that the generated schedules saturate compute units, minimize stalls, and exploit specialized datapaths such as tensor cores or warp-synchronous execution.

The pipeline then descends into target-specific machine-code ingestion, where optimized IR is translated into executable kernels for custom vector instruction sets. This stage handles register allocation, instruction selection, vector packing, and warp synchronization, ensuring that the final machine code aligns precisely with the microarchitectural constraints of the accelerator.

At the bottom of the flow, hardware-optimized AI kernel execution represents the culmination of all preceding transformations. The kernels produced here are not generic—they are deeply shaped by the IR dialects, polyhedral transformations, auto-tuned schedules, and machine-code generation that precede them. Figure 8.4-F1 makes clear that efficient AI execution is the result of a structured, multi-stage lowering pipeline that progressively aligns computation with the physical behavior of the hardware.

The compilation flow illustrated previously makes clear that every optimization in the AI stack begins with how computation is represented. Before polyhedral transformations can restructure loop nests, before auto-tuning can search for optimal schedules, and before machine-code ingestion can map kernels to custom vector instruction sets, the model must first be expressed in an intermediate form that exposes its structure to systematic refinement. This foundational representational layer determines what the compiler can see, what it can transform, and how effectively it can align computation with the accelerator's microarchitecture. The next topic explores how multi-level AI IR dialects provide this representational substrate, enabling neural operators, affine loops, and vector-level primitives to coexist within a unified framework

tailored for specialized hardware.

i. Multi-Level AI IR Dialects Tailored for Specialized Accelerator Hardware

Multi-level AI IR dialects provide the representational foundation that allows compilers to translate high-level neural workloads into hardware-aligned execution plans. These dialects expose computation at multiple granularities, enabling the compiler to reason about neural operators, affine loop structures, memory layouts, and vector-level primitives within a unified framework. This multi-layered representation is essential for specialized accelerators, where performance depends on how precisely the compiler can map computation onto the device's microarchitectural features.

At the highest level, IR dialects capture neural semantics: operators such as convolutions, matmuls, attention blocks, and normalization layers are represented in a form that preserves tensor shapes, dataflow dependencies, and fusion opportunities. This level is hardware-agnostic but structurally rich, allowing the compiler to identify patterns such as broadcast behavior, reduction axes, and opportunities for operator fusion. MLIR's linalg and tensor dialects, along with TVM's Relay IR, exemplify this layer by providing a clean, algebraic representation of neural computation.

The mid-level dialects introduce affine loop structures and explicit memory regions. Here, computation is expressed as nested loops with affine bounds, enabling the compiler to reason about iteration spaces, tiling opportunities, and memory locality. This level exposes the structure needed for polyhedral analysis, dependency checking, and schedule generation. It also allows the compiler to represent shared memory, cache tiles, and buffer allocations explicitly, making it possible to align computation with the accelerator's memory hierarchy.

At the lowest level, IR dialects encode vector instructions, warp-synchronous operations, and accelerator-specific primitives. This layer is closest to the hardware and captures details such as vector widths, warp sizes, predication behavior, and specialized instructions for tensor cores, systolic arrays, or custom NPU datapaths. MLIR's vector dialect and TVM's low-level TIR exemplify this stage, providing the compiler with the ability to generate code that saturates compute units, minimizes stalls, and exploits fine-grained parallelism.

The strength of multi-level IR dialects lies in their ability to preserve optimization opportunities across the lowering pipeline. High-level operator fusion can be applied before lowering, polyhedral transformations can be applied at the affine loop level, and vectorization can be applied at the low-level dialect. This layered structure ensures that the compiler does not lose semantic information prematurely and can apply optimizations at the most appropriate stage. For specialized accelerators, this is critical: the IR must expose enough structure for the

compiler to align computation with the device's execution model, memory hierarchy, and vector capabilities.

Multi-level IR dialects therefore serve as the architectural substrate upon which all subsequent compilation stages depend. They determine what the compiler can see, what it can transform, and how effectively it can generate kernels that match the physical behavior of the hardware. Without this representational foundation, higher-level optimizations would be blind to the structural details that govern performance on modern accelerators.

With computation now expressed in multi-level IR dialects that expose neural operators, affine loops, and vector primitives, the compiler gains the structural visibility needed to perform deeper transformations. The next step in the compilation pipeline is to reshape these loop nests to maximize locality, parallelism, and memory efficiency. This is where polyhedral compilation models become essential, providing the mathematical framework that allows the compiler to analyze dependencies, reorder loops safely, and generate schedules that align computation with the accelerator's memory hierarchy and parallel execution model.

ii. Polyhedral AI Compilation Models for Loop-Transforming Nested Tensor Programs

Polyhedral AI compilation models provide the mathematical machinery that allows compilers to transform nested tensor programs with precision, safety, and deep structural awareness. Once computation has been expressed in multi-level IR dialects, the compiler gains access to affine loop structures, iteration spaces, and memory regions that can be represented as sets of linear constraints. The polyhedral model treats these loop nests as geometric objects—polyhedra—whose points correspond to individual iterations of the program. This geometric abstraction enables the compiler to reason about dependencies, locality, parallelism, and legal transformations using algebraic methods rather than heuristics.

At the core of the polyhedral model is the representation of iteration domains as affine sets. Each loop nest becomes a multidimensional space defined by linear inequalities, capturing bounds, strides, and relationships between loop indices. This representation allows the compiler to analyze how iterations depend on one another, identifying opportunities for reordering, fusion, or parallel execution without violating correctness. Dependency analysis becomes a geometric problem: determining whether two points in the iteration space can be executed independently or must follow a specific order.

With dependencies understood, the compiler can apply loop transformations such as tiling, fusion, skewing, interchange, and parallelization. Tiling divides the iteration space into smaller blocks that fit into fast memory, improving locality and reducing bandwidth pressure. Fusion merges adjacent loops to reduce memory traffic and enable operator fusion at the IR level.

Skewing and interchange reshape iteration order to expose parallelism or align computation with accelerator execution patterns. These transformations are not guesswork—they are mathematically validated operations that preserve correctness while optimizing performance.

The polyhedral model also enables schedule generation, where the compiler constructs a new execution order for the loop nest that maximizes locality and parallel efficiency. Schedules are represented as affine functions that map iteration points to execution times. By manipulating these schedules, the compiler can produce execution orders that saturate compute units, minimize stalls, and align with the memory hierarchy of the accelerator. This capability is essential for modern AI workloads, where nested tensor operations dominate performance and must be carefully structured to avoid bottlenecks.

For specialized accelerators, polyhedral transformations are particularly powerful. They allow the compiler to generate loop structures that match the device's preferred execution patterns—warp-synchronous execution on GPUs, systolic array tiling on TPUs, or vector-aligned iteration on NPUs. The polyhedral model ensures that these transformations are safe, optimal, and mathematically grounded, providing a deterministic foundation for high-performance kernel generation.

Polyhedral AI compilation models therefore serve as the transformation engine that reshapes computation after it has been represented in multi-level IR dialects. They convert structural visibility into actionable optimization, enabling the compiler to reorganize nested tensor programs in ways that maximize locality, parallelism, and hardware alignment. Without this geometric framework, the compiler would be limited to heuristic transformations that cannot guarantee correctness or optimality across diverse accelerator architectures.

With loop nests now transformed through mathematically validated polyhedral schedules, the compiler has produced a structurally optimized representation of computation. The next challenge is to determine the exact tile sizes, vector widths, memory layouts, and scheduling parameters that yield peak performance on the target accelerator. This is where auto-tuned compilation pipelines become essential, exploring vast search spaces of candidate configurations to discover the block layouts that saturate compute units, minimize stalls, and fully exploit the hardware's microarchitectural capabilities.

iii. Auto-Tuned AI Compilation Pipelines for Hardware-Optimized Block Layout Generation

Auto-tuned AI compilation pipelines are the stage where structurally optimized programs are turned into concretely optimized executions for specific hardware. After multi-level IR dialects expose computation and polyhedral models reshape loop nests, the compiler still faces a vast configuration space: tile sizes, block shapes, vector widths, unroll factors, memory layouts, and

scheduling strategies all interact with the microarchitectural details of the accelerator. Static heuristics are rarely sufficient to find the best combination. Auto-tuned pipelines address this by treating compilation as a search problem, using empirical measurement and machine-learning-guided exploration to discover hardware-optimized block layouts that saturate compute units and minimize stalls.

At the heart of auto-tuned pipelines is the notion of schedule search. For a given operator—such as a convolution, matrix multiplication, or attention block—the compiler generates a parameterized family of schedules that describe how the computation is tiled, parallelized, vectorized, and mapped to memory. These schedules define choices such as how many threads to assign per block, how to partition tensors into tiles that fit into shared memory or caches, and how to order loops to maximize locality. AutoTVM and Ansor exemplify this approach, generating candidate schedules from a search space defined over tiling factors, loop reordering, fusion decisions, and vectorization strategies.

Each candidate schedule is then instantiated into a concrete kernel and evaluated on the target hardware. Performance metrics such as latency, throughput, and resource utilization are measured directly, providing ground-truth feedback about how well the schedule matches the device's microarchitecture. This empirical evaluation is critical: it captures effects that are difficult to model analytically, such as cache behavior, bank conflicts, warp divergence, and pipeline stalls. The auto-tuning system uses these measurements to guide the search, pruning poor configurations and focusing on promising regions of the schedule space.

Machine learning plays a central role in making this search tractable. Instead of exploring the entire space exhaustively, auto-tuned pipelines use cost models that predict performance based on schedule features. These models are trained on prior measurements and updated as new data is collected, allowing the tuner to prioritize schedules that are likely to perform well. Over time, the cost model becomes increasingly accurate, enabling the system to discover near-optimal block layouts with far fewer evaluations than naive search would require.

Auto-tuned pipelines also account for hardware-specific constraints. For GPUs, they consider warp sizes, shared-memory limits, register pressure, and occupancy. For NPUs and TPUs, they consider systolic array dimensions, on-chip buffer sizes, and dataflow patterns. For CPUs, they consider cache hierarchies, SIMD widths, and NUMA effects. The search space is shaped by these constraints, ensuring that candidate schedules are both legal and relevant to the device's execution model.

The result of auto-tuning is a set of hardware-optimized block layouts and schedules that are tightly aligned with the accelerator's capabilities. These layouts determine how tensors are

partitioned, how loops are structured, and how threads are organized, directly influencing whether the hardware runs at peak efficiency or spends cycles waiting on memory. Auto-tuned pipelines thus serve as the bridge between abstract structural optimization and concrete performance realization, turning polyhedrally transformed programs into kernels that fully exploit the device.

Because auto-tuning is empirical and device-specific, it also enables portability across hardware generations. As new accelerators are introduced, the same high-level IR and polyhedral transformations can be reused, while the auto-tuning system learns new optimal schedules for the updated microarchitecture. This decouples model design from hardware evolution, allowing AI systems to remain performant as the underlying devices change.

Once auto-tuned pipelines have discovered the block layouts and schedules that best match the target accelerator, the compilation process must translate these optimized representations into executable machine code. The final stage of the pipeline is responsible for mapping tuned schedules onto custom vector instruction sets, handling register allocation, instruction selection, and warp-level synchronization. This is where target-specific machine-code ingestion layers become critical, ensuring that the performance gains discovered by auto-tuning are preserved all the way down to the silicon and expressed as concrete kernels that run deterministically on the hardware.

iv. Target-Specific AI Machine-Code Ingestion Layers for Custom Vector Instruction Sets

Target-specific machine-code ingestion layers are the final stage of the compilation pipeline, where optimized schedules, block layouts, and transformed loop nests are translated into executable kernels that run deterministically on specialized accelerator hardware. After multi-level IR dialects expose computation, polyhedral models reshape iteration spaces, and auto-tuned pipelines discover optimal block configurations, the compiler must map these optimized representations onto the concrete instruction sets supported by the device. This stage is where abstract optimization becomes physical execution, and where the microarchitectural details of the accelerator exert their strongest influence.

Machine-code ingestion begins with instruction selection, the process of choosing the specific vector, tensor, or warp-level instructions that implement the optimized schedule. For GPUs, this may involve selecting CUDA PTX instructions that operate on warps, shared memory, and tensor cores. For NPUs, it may involve mapping operations onto systolic array primitives or custom vector pipelines. For CPUs, it may involve generating AVX-512 or SVE instructions that exploit wide SIMD lanes. The compiler must ensure that each instruction aligns with the device's execution model, latency characteristics, and register behavior.

Register allocation is the next critical step. Optimized schedules often require careful management of registers to avoid spills, minimize pipeline stalls, and maintain high occupancy. The compiler must assign registers in a way that respects hardware constraints such as register file size, warp-synchronous execution rules, and vector-lane alignment. Poor register allocation can negate the benefits of auto-tuning, causing kernels to stall or underutilize compute units.

Vector packing and layout specialization follow, ensuring that data is arranged in memory in a form that matches the device's vector width, alignment requirements, and memory-bank structure. This step is essential for accelerators with strict alignment rules or banked memory architectures, where misaligned accesses can cause serialization or bank conflicts. The ingestion layer must generate memory instructions that load, store, and shuffle data efficiently, preserving the locality and tiling decisions made earlier in the pipeline.

Warp-level synchronization and control-flow lowering are also handled at this stage. For GPUs, the compiler must generate instructions that coordinate execution across warps, manage predication, and ensure deterministic behavior in the presence of divergent control flow. For NPUs and TPUs, the compiler must generate synchronization primitives that coordinate systolic array execution or pipeline stages. These synchronization instructions ensure that the optimized schedule executes correctly and efficiently on the hardware.

Finally, the ingestion layer emits machine-code kernels that reflect all prior optimizations. These kernels are not generic—they are deeply shaped by the IR dialects, polyhedral transformations, auto-tuned schedules, and hardware constraints that preceded them. The ingestion layer ensures that the performance gains discovered earlier are preserved all the way down to the silicon, producing kernels that saturate compute units, minimize stalls, and execute deterministically.

Target-specific machine-code ingestion layers therefore serve as the final bridge between abstract optimization and physical execution. They translate structural, mathematical, and empirical refinements into concrete instructions that run on specialized accelerators, ensuring that the entire compilation pipeline culminates in hardware-aligned performance. Without this stage, the benefits of IR-driven optimization, polyhedral restructuring, and auto-tuning would remain theoretical rather than realized in actual execution.

Together, multi-level IR dialects, polyhedral loop-transformation models, auto-tuned block-layout generators, and target-specific machine-code ingestion layers form a vertically integrated compilation pipeline that transforms high-level neural workloads into hardware-optimized kernels. Each stage contributes a distinct capability: IR dialects expose structure, polyhedral models reshape computation, auto-tuning discovers optimal schedules,

and machine-code ingestion maps these optimizations onto concrete instruction sets. This pipeline establishes the foundation of cross-layer optimization, ensuring that every subsequent refinement—graph simplification, architecture search, runtime observability, and secure execution—operates on a representation that is structurally sound, mathematically optimized, empirically tuned, and physically aligned with the accelerator. The compilation layer is therefore the bedrock of modern AI performance, enabling deterministic, efficient, and trustworthy execution across heterogeneous hardware.

With the compilation pipeline now fully established, the next stage in the optimization continuum focuses on simplifying the compute graph itself. Before kernels are lowered, tuned, and translated into machine code, the graph must be structurally refined to eliminate redundant computation, collapse compatible operators, and reduce memory pressure. This is where graph-level transformations—SRAM-aware node fusion, algebraic simplification, quantized constant folding, and intermediate-buffer minimization—become essential. These transformations reshape the graph into a leaner, more efficient topology that reduces computational load and aligns naturally with the optimized compilation pipeline that follows.

b. AI Graph Simplification via Structural Math Reductions, Dead-Node Pruning, and Operator Fusion

Before an artificial intelligence (AI) model is mapped onto a target processor, its computational graph can be analyzed and transformed to eliminate unnecessary work, reduce data movement, and improve execution efficiency. A computational graph represents the operations performed by a model and the dependencies among them, including the flow of tensors through successive computational stages. Although a graph generated by a machine learning framework accurately describes the model's computation, it may contain redundant operations, statically computable expressions, unused branches, and sequences of operators that can be executed more efficiently when combined. **AI graph simplification transforms this initial representation into a more efficient computational structure while preserving the model's intended behavior within the required numerical tolerances.**

Graph simplification is closely connected to intermediate representations and domain-specific compilation. Once a model has been expressed in a suitable intermediate representation, a compiler can analyze its operators, tensor shapes, constant values, data dependencies, and computational relationships. This analysis enables transformations that reduce the number of operations, eliminate unnecessary intermediate tensors, and reorganize computation to better exploit the target hardware. The resulting graph may require fewer runtime operations, less temporary memory, and fewer kernel launches. However, the benefits depend on the model architecture, the transformations applied, and the characteristics of the target platform. Graph

simplification therefore involves more than merely reducing the number of nodes: it requires identifying which transformations provide meaningful improvements in the complete execution pipeline.

Constant Folding and Compile-Time Evaluation

Constant folding reduces runtime work by evaluating expressions whose inputs are known during compilation or model preparation. AI graphs often contain fixed parameters, constant tensors, static shape calculations, and transformations that do not depend on the input presented during inference. If an expression can be evaluated safely in advance, the compiler can calculate its result once and replace the original expression with a constant value.

For example, a graph may contain a sequence of operations that constructs a fixed tensor, rearranges its dimensions, and applies a transformation determined entirely by static parameters. Rather than performing these operations for every inference request, the compiler can calculate the resulting tensor during compilation or model initialization and store it in the optimized representation. The runtime then consumes the precomputed value directly.

Constant folding can also simplify portions of a graph that combine constant values with other operations. When a constant expression feeds into a larger computation, evaluating that expression in advance may expose further simplification opportunities. The compiler can repeatedly apply constant evaluation and algebraic reduction until no additional transformations are available or worthwhile. This iterative process is particularly useful because one optimization may reveal redundancies that were not apparent in the original graph.

The benefits include reduced runtime arithmetic, fewer operator invocations, and potentially lower memory traffic. Nevertheless, compile-time evaluation can increase model preparation time or the size of the stored constants. It must also respect numerical behavior and resource limits. Large precomputed tensors may consume more memory than dynamically generated representations, and expressions involving dynamic shapes, runtime-dependent parameters, or stateful operations may not be eligible for folding. Effective constant folding therefore distinguishes genuinely static computation from operations whose results depend on the current input or execution state.

Dead-Node Pruning and Removal of Unnecessary Computation

Dead-node pruning removes graph operations that cannot affect the outputs or other observable behavior required from the model. During model development and conversion, a graph may retain branches associated with auxiliary outputs, training-only calculations, debugging operations, or intermediate values that are no longer needed for inference. If these

operations do not contribute to any required output, the compiler can remove them along with the dependencies that become unnecessary as a result.

A typical example is an inference graph exported from a training workflow that contains computations used only to calculate auxiliary losses or training metrics. If those values are not required during deployment, the corresponding branches can often be eliminated. Similarly, if an output tensor is generated but never consumed by any required operation, the computation producing it may be removable. Once an unused branch is deleted, additional upstream operations may become unnecessary, allowing pruning to propagate through the graph.

Dead-node pruning is generally performed through dependency analysis and reachability analysis. The compiler identifies the graph outputs and other operations whose behavior must be preserved, then traces the dependencies required to produce them. Nodes that are not reachable from these required results can be candidates for removal. The analysis must account for operations with observable side effects or stateful behavior, since an operation may need to remain even if its numerical output is not directly used by the final prediction.

The resulting graph can contain fewer operators, consume less temporary memory, and require fewer execution resources. Removing unnecessary branches may also reduce synchronization and scheduling overhead, particularly in systems that execute complex graphs across multiple processors. However, dead-node pruning differs from model pruning in an important respect: it removes computations that are unnecessary to preserve the required graph behavior, whereas model pruning typically removes or sparsifies parameters or connections within the model and may change its predictive behavior.

This distinction is essential in AI deployment. Graph-level dead-node pruning can often eliminate work without changing the intended inference function, provided that all required outputs and side effects are preserved. By contrast, removing active neural network parameters or connections generally requires separate validation to determine whether the resulting model still meets its accuracy and reliability requirements.

Operator Fusion and Reduction of Data Movement

Operator fusion combines compatible operations into a single computational unit or execution kernel. It is one of the most important graph-level optimization techniques because the cost of running an AI model depends not only on arithmetic operations but also on the movement of intermediate data and the overhead of launching individual kernels. When consecutive operators are executed separately, the runtime may need to write intermediate tensors to memory, read them again for the next operation, and incur additional scheduling or launch overhead. Fusion can eliminate some of these costs by allowing intermediate results to remain

within registers, local storage, or other fast-access resources where the hardware and implementation permit.

A common example is the sequence of convolution, batch normalization, and activation found in many convolutional neural networks. When batch-normalization parameters are fixed for inference, batch normalization can often be algebraically incorporated into the convolution's weights and biases. The resulting computation may then be executed using a convolution kernel that also applies the activation function, avoiding separate execution stages and reducing intermediate data movement. Other examples include combining elementwise operations with preceding or following tensor computations, fusing compatible normalization stages, and integrating portions of transformer computations into larger kernels.

Fusion is particularly valuable when it reduces memory traffic. Intermediate activations can be large, and repeatedly transferring them between external memory and the processor can limit performance even when substantial arithmetic capacity is available. By combining operations, a compiler may keep intermediate values on-chip and avoid writing them to and reading them from external memory. Fewer kernel launches can also reduce runtime overhead, which is especially important for inference workloads containing many small operations.

However, fusion does not guarantee a performance improvement. Combining too many operations can produce a kernel that requires excessive registers or shared memory, reducing the number of concurrently active thread blocks or other execution groups. Large fused kernels may also increase compilation time, complicate scheduling, or prevent the compiler from using highly optimized library implementations for individual operators. Some operations require global synchronization or have dependencies that make fusion difficult or impossible within a single kernel. The compiler must therefore balance the benefits of reduced intermediate data movement against the resource demands and execution constraints of the fused implementation.

The most effective fusion strategy is consequently hardware- and workload-dependent. A GPU may benefit from fusion that reduces global-memory traffic while preserving sufficient parallel occupancy. A CPU may favor combinations that improve cache locality and reduce function-call or loop overhead. An NPU may have fixed-function execution paths or fused operator patterns that are especially efficient for its dataflow architecture. Graph simplification must take these differences into account rather than assume that one fusion strategy is optimal across all deployment environments.

Coordinating Graph Simplification with Hardware Execution

Structural reductions, constant folding, dead-node pruning, and operator fusion are most

effective when they are coordinated rather than applied as isolated transformations. Removing one operation may expose an algebraic identity; folding a constant expression may make an entire branch removable; pruning an unused branch may reduce memory requirements; and fusion may eliminate intermediate tensors created by the remaining operators. Compilers therefore commonly apply multiple optimization passes in sequence, repeating selected analyses when one transformation creates opportunities for another.

The resulting graph must also be evaluated against the execution characteristics of the target platform. A graph with fewer nodes is not necessarily faster if the remaining operators have poor hardware mappings or require inefficient memory layouts. Likewise, reducing the theoretical operation count may provide limited benefit when execution is dominated by data transfer, synchronization, or kernel-launch overhead. Graph-level metrics should therefore be considered alongside measurements such as end-to-end inference latency, memory bandwidth, peak temporary-memory consumption, processor utilization, and energy per inference.

Graph simplification also interacts with numerical precision and model validation. Algebraic rewrites can alter floating-point rounding behavior, while fusion can change where intermediate values are stored and at what precision operations are performed. Quantized execution introduces additional constraints because transformations may affect rounding, clipping, scaling, or saturation. Each optimization must preserve the model's required behavior, and optimized graphs should be tested against suitable numerical and task-level acceptance criteria. For safety-critical or real-time systems, validation may also need to establish that the optimized implementation satisfies deadline, resource, and fault-handling requirements under the intended operating conditions.

From a deployment perspective, these considerations make graph simplification an important link between model semantics and hardware-aware execution. The compiler begins with a graph that describes what the model computes, identifies unnecessary or inefficient structures, and transforms the graph into a representation better suited to the target processor. The quality of this transformation depends on understanding both the mathematical relationships among operations and the physical costs of executing them.

Ultimately, **AI graph simplification improves execution efficiency by removing unnecessary computation, consolidating compatible operations, and reducing the cost of moving intermediate data through the system**. Structural mathematical reductions simplify expressions, constant folding moves static work out of the runtime, dead-node pruning eliminates computations that do not contribute to required behavior, and operator fusion reduces execution and data-movement overhead. Together, these techniques produce a more efficient computational graph while preserving the model's required semantics. Within the

broader cross-layer optimization process, graph simplification prepares the model for effective hardware mapping and provides a foundation for subsequent optimization through hardware-aware neural architecture search, runtime observability, and system-level resource management.

Mathematical Frameworks for AI Graph Simplification

AI graph simplification is the stage where the compute graph is structurally refined before compilation and execution, reducing redundant work, collapsing compatible operators, and minimizing memory pressure. While the compilation pipeline focuses on how computation is represented and lowered, graph simplification focuses on what computation is actually performed. Structural math reductions, dead-node pruning, and operator fusion collectively reshape the graph into a leaner topology that is better suited for hardware-optimized execution.

AI node-fusion strategies are central to this process. Horizontal fusion combines adjacent operators that share compatible tensor shapes and dataflow, such as consecutive elementwise operations, into a single fused node. Vertical fusion collapses producer–consumer chains, such as convolution followed by batch normalization and activation, into a single composite operator. SRAM-aware fusion ensures that these collapses respect on-chip memory limits, grouping operators so that intermediate tensors remain resident in fast memory rather than spilling to DRAM. This reduces memory traffic, lowers latency, and aligns the graph with the accelerator's preferred execution patterns.

Algebraic AI simplification passes apply mathematical identities to reduce graph complexity. Common patterns include removing identity operations (multiplication by one, addition of zero), collapsing redundant reshapes or transposes, and simplifying expressions such as $x + x$ into $2x$. Identity-based pruning eliminates nodes that do not change the data, while algebraic reductions combine equivalent subgraphs into simpler forms. These passes reduce the number of operators, shorten critical paths, and expose new fusion opportunities, all without altering the semantics of the model.

Quantized-graph AI constant folding focuses on evaluating static tensors and parameters at compile time, particularly in quantized models. When weights, biases, and scale factors are known and fixed, the compiler can precompute partial results, such as folded batch-norm parameters or combined quantization scales. In quantized graphs, constant folding also propagates integer ranges and scale factors, allowing the removal of redundant dequantize/requantize pairs and the simplification of mixed-precision paths. This reduces runtime computation and stabilizes numerical behavior.

Intermediate-buffer minimization targets the memory footprint of fused execution blocks.

When operators are fused, their intermediate tensors can often be reused, aliased, or eliminated entirely. Buffer-lifetime analysis identifies when tensors are no longer needed and allows their memory to be reclaimed or reused for subsequent operations. Layout-aware minimization ensures that buffers are sized and aligned to match the accelerator's SRAM and cache characteristics, reducing peak memory usage and avoiding fragmentation. Across fused blocks, this leads to more compact execution footprints and higher effective bandwidth.

Together, these four capabilities—SRAM-aware node fusion, algebraic simplification, quantized constant folding, and intermediate-buffer minimization—form a coherent graph-simplification layer. They reduce the computational and memory burden of the model before it enters the compilation pipeline, ensuring that the kernels generated downstream operate on a structurally optimized graph. This synergy between graph simplification and compilation is essential for achieving deterministic, efficient, and hardware-aligned AI execution.

The structural mechanisms of graph simplification gain their full clarity when viewed through the mathematics that governs them. It is useful to ground each transformation—fusion, algebraic reduction, constant folding, and buffer minimization—in the formal identities, reachability rules, functional compositions, and interval-allocation principles that guarantee semantic equivalence. These mathematical foundations reveal why certain nodes can be removed, why others can be collapsed, and how intermediate tensors can be eliminated or reused without altering the model's output. Introducing this formal layer first provides the analytical scaffolding that makes the table's conceptual organization more intuitive, showing that graph simplification is not heuristic trimming but a rigorously justified restructuring of the compute graph.

Structural mathematical reductions simplify a computational graph by exploiting algebraic identities, known operator properties, and relationships among successive operations. Neural networks frequently contain transformations that can be combined, canceled, or replaced with computationally cheaper equivalents. For example, redundant identity operations can be removed, consecutive compatible reshape operations can sometimes be consolidated, and arithmetic expressions involving zero or one can be simplified when the relevant tensor semantics permit it. Similarly, sequences of linear transformations may be combined into a single transformation when their mathematical structure and execution requirements allow it.

A common example occurs in models that apply multiple affine transformations in succession. Under suitable conditions, two operations of the form

$$y = W_1 x + b_1$$

$$z = W_2 y + b_2$$

can be combined into one affine transformation:

$$z = (W_2 W_1)x + (W_2 b_1 + b_2)$$

where:

- x is the input vector.
- W_1 and W_2 are weight matrices.
- b_1 and b_2 are bias vectors.
- y is the intermediate output.
- z is the final output.

This transformation can reduce the number of separately executed operators and eliminate an intermediate tensor. However, the combined weight matrix may be larger or more expensive to evaluate than the original sequence, so the transformation is not automatically beneficial in every implementation. A compiler must consider the dimensions of the matrices, the availability of optimized kernels, memory requirements, and the cost of materializing the combined parameters.

Structural reductions can also simplify expressions involving tensor indexing, broadcasting, reductions, and elementwise operations. For instance, redundant tensor-layout transformations may be eliminated when they do not affect the actual data layout required by subsequent operations. Algebraic identities can remove unnecessary arithmetic, while operator-specific rules can simplify expressions that arise from model export, quantization, or framework-level graph construction.

These transformations require careful attention to mathematical and numerical semantics. Floating-point operations are not perfectly associative, and changing the order of arithmetic can produce small numerical differences. Quantized computations introduce additional considerations involving scaling factors, zero points, rounding, and saturation. Consequently, a transformation that is valid over real numbers may not produce exactly the same result under finite-precision arithmetic. Reliable graph optimization must preserve the required semantics, either exactly or within an explicitly acceptable numerical tolerance.

Mathematically, AI graph simplification is about transforming a directed acyclic graph G = (V, E) of operators and tensors into an equivalent graph G′ = (V′, E′) with fewer nodes, fewer edges,

and reduced intermediate state, while preserving the overall function $f_G(x)$ for all valid inputs x.

At the core is the notion of **semantic equivalence**:

$$\forall x, \quad f_G(x) = f_{G'}(x)$$

All reductions, prunings, and fusions must satisfy this constraint.

Structural math reductions rely on algebraic identities in the operator algebra. For example, for elementwise operations:

Identity removal:

$$x + 0 = x, \quad x \cdot 1 = x, \quad x \circ \mathrm{Id} = x$$

Any node implementing these identities can be removed, and its input directly wired to its output.

Associativity and commutativity (where valid):

$$(x + y) + z = x + (y + z), \quad x + y = y + x$$

These allow regrouping and reordering nodes to expose fusion opportunities, e.g. merging multiple additions into a single multi-input add.

Distributivity for certain patterns:

$$a \cdot (b + c) = a \cdot b + a \cdot c$$

This can be used both to factor expressions (reducing repeated computation) and to fuse operations when hardware prefers a particular form.

Dead-node pruning is essentially graph-theoretic reachability. Let $O \subseteq V$ be the set of output nodes. Define the set of live nodes L as all nodes reachable from O when traversing edges backward. Any node $v \in V \setminus L$ is dead:

$$L = \{v \in V \mid \exists \text{ path } v \to o,\ o \in O\}, \quad V_{\text{dead}} = V \setminus L$$

All nodes in V_{dead} can be removed without changing f_G, because they do not contribute to any output.

Operator fusion can be formalized as composing functions along paths in the graph. If two nodes f and g form a simple chain:

$$y = f(x), \quad z = g(y)$$

and if there exists a fused operator h such that:

$$h(x) = g(f(x))$$

then the two nodes can be replaced by a single node implementing h. Horizontal fusion generalizes this to multiple operators sharing the same input and compatible shapes, e.g.:

$$y_1 = f_1(x), \quad y_2 = f_2(x), \quad \ldots$$

which can be fused into a vectorized or batched operator H(x) = (f_1(x), f_2(x), …) when hardware supports such composite execution.

Quantized-graph constant folding uses the fact that some subgraphs compute functions of constants only. If a subgraph G_c has inputs C that are all constant tensors, then:

$$\forall x, \quad G_c(C) = K$$

for some constant tensor K. The subgraph can be evaluated once at compile time, replaced by a single constant node holding K, and all intermediate nodes removed. In quantized settings, scale and zero-point propagation can be expressed as affine transforms:

$$x_{\text{real}} = s_x(x_{\text{int}} - z_x)$$

Folding chains of such transforms reduces them to a single equivalent affine mapping, eliminating redundant quantize/dequantize pairs.

Intermediate-buffer minimization can be framed as an optimization over buffer lifetimes. Each tensor t_i has a live interval [b_i, e_i] in the topological order of the graph. The goal is to assign memory regions m_j to tensors such that overlapping intervals do not share the same region:

$$[b_i, e_i] \cap [b_k, e_k] = \emptyset \Rightarrow t_i, t_k \text{ may reuse } m_j$$

This is analogous to register allocation via interval graph coloring: minimizing the number of distinct memory regions (peak footprint) while respecting lifetime overlaps. Fusion changes

these intervals by collapsing multiple operators into one, often shortening lifetimes and enabling more reuse.

All of these mathematical tools—algebraic identities, graph reachability, functional composition, constant evaluation, and interval-based allocation—work together to transform G into a graph G′ that is **semantically equivalent** but **computationally and memory-wise cheaper**, setting the stage for the IR-driven compilation and hardware optimization that follow.

The exploration of graph-level simplification shows how structural math reductions, fusion strategies, constant folding, and buffer minimization reshape the compute graph into a leaner, more execution-efficient topology before it enters the compilation pipeline. These transformations eliminate redundant computation, collapse compatible operators, and reduce memory pressure, ensuring that the downstream IR dialects, polyhedral schedulers, auto-tuned pipelines, and machine-code ingestion layers operate on a graph that is already optimized at the semantic level. To consolidate these capabilities into a clear architectural view, Table 8.4-F2 organizes the foundational elements of graph simplification, highlighting their core purpose, mechanisms, and impact on the broader optimization continuum.

Table 8.4-F2 presents the four structural mechanisms that define modern AI graph simplification. Each mechanism represents a distinct dimension of how the compute graph is reduced, collapsed, or refined before compilation. The table clarifies how SRAM-aware node fusion, algebraic simplification passes, quantized-graph constant folding, and intermediate-buffer minimization work together to reduce computational load, shorten critical paths, and lower memory footprints. By laying out these relationships explicitly, the table provides a structured understanding of how graph simplification prepares the model for hardware-optimized execution.

Table 8.4-F2 — AI Graph Simplification Foundations

Conceptual Area	Core Purpose	Key Mechanisms	Architectural Impact
AI Node-Fusion Strategies	Collapse compatible operators into fused execution blocks	Horizontal fusion, vertical fusion, SRAM-aware grouping, producer–consumer collapsing	Reduces memory traffic, lowers latency, improves on-chip reuse

Conceptual Area	Core Purpose	Key Mechanisms	Architectural Impact
Algebraic AI Simplification Passes	Remove redundant or identity operations	Identity pruning, algebraic reductions, reshape/transpose simplification	Shrinks graph size, shortens critical paths, exposes fusion opportunities
Quantized-Graph AI Constant Folding	Precompute static tensor and parameter effects	Weight/bias folding, scale propagation, dequantize/requantize elimination	Reduces runtime computation, stabilizes quantized execution
Intermediate-Buffer Minimization	Reduce memory footprint across fused blocks	Buffer-lifetime analysis, reuse/aliasing, layout-aware sizing	Lowers peak SRAM usage, improves bandwidth and cache efficiency

The first conceptual area focuses on AI node-fusion strategies, which collapse compatible operators into fused execution blocks. Horizontal fusion merges adjacent elementwise operations, while vertical fusion collapses producer–consumer chains such as convolution, normalization, and activation. SRAM-aware fusion ensures that these collapses respect on-chip memory limits, keeping intermediate tensors resident in fast memory and reducing DRAM traffic. This directly lowers latency and improves bandwidth efficiency.

The second area highlights algebraic AI simplification passes, which apply mathematical identities to remove redundant operations. Identity-based pruning eliminates nodes that do not change the data, such as adding zero or multiplying by one. Structural math reductions simplify reshape and transpose chains, collapse equivalent expressions, and expose new fusion opportunities. These passes shrink the graph, reduce operator count, and shorten execution paths.

The third area introduces quantized-graph AI constant folding, which evaluates static tensors and parameters at compile time. In quantized models, constant folding propagates integer ranges and scale factors, allowing the removal of redundant dequantize/requantize pairs and the simplification of mixed-precision paths. Folding batch-norm parameters or combining quantization scales reduces runtime computation and stabilizes numerical behavior.

The fourth area focuses on intermediate-buffer minimization across fused execution blocks. Buffer-lifetime analysis identifies when tensors can be reused or aliased, reducing peak memory usage. Layout-aware sizing ensures that buffers align with SRAM and cache characteristics,

improving locality and reducing fragmentation. This minimizes memory pressure and increases effective bandwidth.

Together, the four areas in Table 8.4-F2 illustrate how graph simplification forms a structural optimization layer that precedes compilation. These transformations reduce computational complexity, eliminate redundancy, and minimize memory usage, ensuring that the compilation pipeline operates on a graph that is already lean, efficient, and hardware-aligned. The table makes clear that modern AI performance begins not only with IR-driven compilation but with graph-level refinement that shapes the model's topology before it ever reaches the compiler.

The structural mechanisms summarized in Table 8.4-F2 establish how node fusion, algebraic reductions, constant folding, and buffer minimization collectively reshape the compute graph before it enters the compilation pipeline. To translate these conceptual foundations into a visual representation, Figure 8.4-F2 depicts the simplification process as a top-down flow, showing how the original graph is progressively refined through each transformation stage. This figure reinforces the idea that graph simplification is not a single pass but a coordinated sequence of reductions that systematically eliminate redundancy, collapse compatible operators, and reduce memory pressure.

Figure 8.4-F2 illustrates the hierarchical refinement of an AI compute graph as it undergoes structural simplification. Beginning with the unoptimized graph, the flow descends through node-fusion strategies, algebraic simplification passes, quantized-graph constant folding, and intermediate-buffer minimization. Each block represents a distinct transformation domain, while the downward arrows emphasize the sequential nature of graph reduction. The figure highlights how these transformations collectively produce a streamlined, memory-efficient execution graph that is better aligned with downstream compilation and hardware-optimized execution.

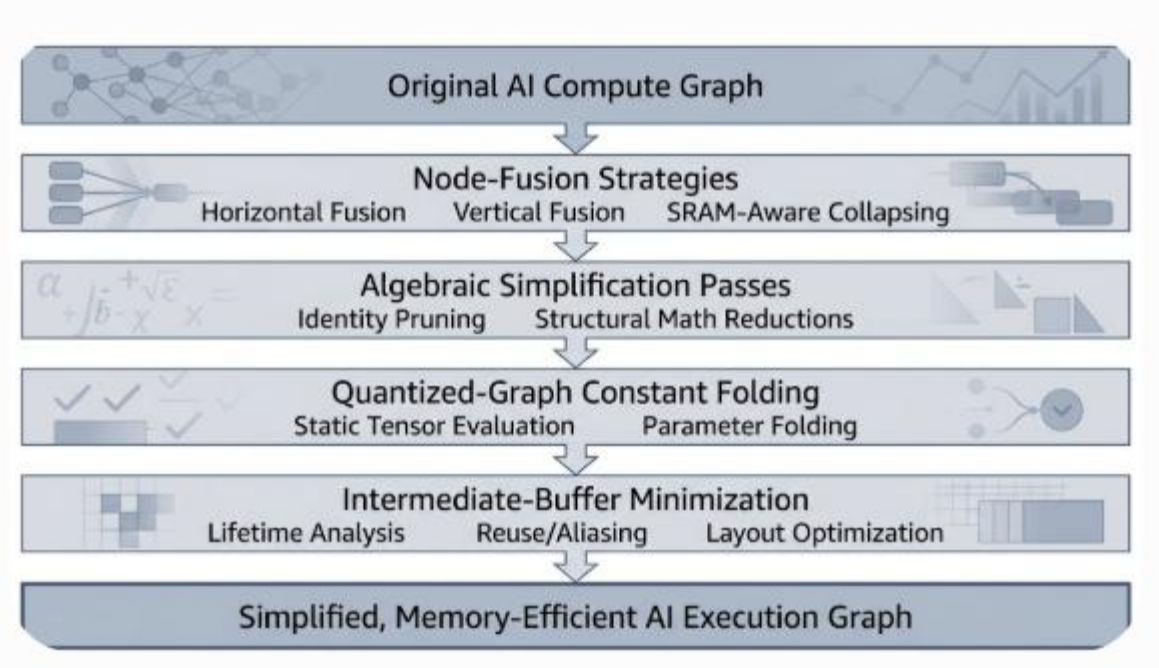


Figure 8.4-F2 — AI Graph Simplification Flow

A top-down representation of the structural simplification pipeline that transforms an original AI compute graph into a compact, memory-efficient execution graph. The flow illustrates how node fusion, algebraic reductions, quantized constant folding, and buffer minimization progressively reduce computational and memory overhead.

Legend:

- ***Original AI Compute Graph*** *— unoptimized operator topology with full tensor dependencies.*
- ***Node-Fusion Strategies*** *— horizontal fusion, vertical fusion, SRAM-aware collapsing.*
- ***Algebraic Simplification Passes*** *— identity pruning, structural math reductions.*
- ***Quantized-Graph Constant Folding*** *— static tensor evaluation, parameter folding.*
- ***Intermediate-Buffer Minimization*** *— lifetime analysis, reuse/aliasing, layout optimization.*
- ***Simplified, Memory-Efficient AI Execution Graph*** *— final reduced topology ready for compilation.*

The figure presents graph simplification as a descending pipeline that begins with the original compute graph, which contains the full set of operators, tensor flows, and intermediate buffers. This initial graph is structurally rich but often contains redundant operations, unfused chains, and unnecessary memory allocations.

The first transformation stage applies node-fusion strategies. Horizontal fusion collapses adjacent elementwise operators into single fused nodes, while vertical fusion merges producer–consumer chains such as convolution, normalization, and activation. SRAM-aware collapsing ensures that fused blocks fit within on-chip memory, reducing DRAM traffic and improving locality.

The next stage introduces algebraic simplification passes. Identity pruning removes operations that do not change the data, such as adding zero or multiplying by one. Structural math reductions simplify reshape and transpose chains, collapse equivalent expressions, and expose new fusion opportunities. This stage reduces operator count and shortens critical paths.

Quantized-graph constant folding follows, evaluating static tensors and parameters at compile time. In quantized models, this includes folding batch-norm parameters, propagating scale factors, and eliminating redundant dequantize/requantize pairs. This reduces runtime computation and stabilizes numerical behavior.

The pipeline then descends into intermediate-buffer minimization. Buffer-lifetime analysis identifies opportunities for reuse and aliasing, reducing peak memory usage. Layout-aware optimization ensures that buffers align with SRAM and cache characteristics, improving bandwidth efficiency and reducing fragmentation.

At the bottom of the flow, the simplified, memory-efficient AI execution graph represents the culmination of all preceding transformations. The graph is leaner, more efficient, and structurally aligned with the compilation pipeline that follows. The figure makes clear that graph simplification is a multi-stage refinement process that prepares the model for hardware-optimized execution by reducing computational load and memory pressure before lowering begins.

The simplification flow illustrated previously shows how the compute graph is progressively refined through fusion, algebraic reduction, constant folding, and buffer minimization. Among these transformations, the earliest and often most impactful step is the collapse of compatible operators into fused execution blocks. Before algebraic identities can prune redundant nodes or constant folding can evaluate static tensors, the graph must first be reorganized so that related operations are grouped in ways that respect on-chip memory constraints and maximize locality. This foundational restructuring begins with node-fusion strategies, where horizontal and vertical collapsing reshape the graph into fused units that reduce memory traffic, shorten execution paths, and prepare the model for deeper simplification and downstream compilation.

AI Node-Fusion Strategies for SRAM-Aware Horizontal and Vertical Graph Collapsing

Node-fusion strategies are the first and often most impactful transformation in graph simplification. They reorganize the compute graph by collapsing compatible operators into fused execution blocks that reduce memory traffic, shorten execution paths, and improve locality. Fusion is not merely a heuristic—it is grounded in algebraic equivalence, graph-theoretic structure, and hardware-aware constraints, particularly the limited size of on-chip SRAM.

Horizontal Fusion: Collapsing Sibling Operators

Horizontal fusion merges operators that share the same input tensor and have compatible shapes or broadcasting semantics. If a tensor x feeds multiple elementwise operators:

$$y_1 = f_1(x), \quad y_2 = f_2(x), \quad \dots, \quad y_n = f_n(x)$$

and the hardware supports vectorized or batched execution, these can be fused into a single composite operator:

$$Y = H(x) = (f_1(x), f_2(x), \dots, f_n(x))$$

This reduces the number of memory reads of x from n to 1, and allows the fused operator to reuse the same on-chip tile of x across all computations. The fusion is mathematically valid because:

$$H(x) = (f_1(x), f_2(x), \dots)$$

is functionally equivalent to the original set of outputs.

Horizontal fusion is especially effective for chains of elementwise operations such as ReLU, bias-add, scale, clamp, or normalization steps that share identical tensor shapes.

Vertical Fusion: Collapsing Producer–Consumer Chains

Vertical fusion merges operators along a path in the graph. If an operator f produces an intermediate tensor consumed by g:

$$y = f(x), \quad z = g(y)$$

and if there exists a fused operator h such that:

$$h(x) = g(f(x)),$$

then the two nodes can be replaced by a single fused node. This is common in patterns such as:

convolution → batch normalization → activation

matmul → bias-add → activation

attention → softmax → scaling

Vertical fusion reduces intermediate tensor materialization. Instead of storing y in memory, the fused operator computes g(f(x)) directly, often within registers or SRAM tiles.

Mathematical Conditions for Fusion

Fusion is permitted only when the following conditions hold:

- **Semantic equivalence**

$$\forall x, \quad g(f(x)) = h(x)$$

The fused operator must preserve the original function.

- **Shape compatibility**

  The output shape of **f** must match the input shape of **g**, or be transformable without violating semantics.

- **Broadcasting consistency**

  If broadcasting is involved, the fused operator must apply identical broadcasting rules.

- **Memory feasibility (SRAM constraint)**

  Let S be the available SRAM capacity and T_f, T_g the tile sizes required by f and g. Fusion is allowed only if:

$$T_f + T_g \leq S$$

This ensures that the fused operator can execute without spilling intermediate tensors to DRAM.

- **Dependency preservation** - Fusion must not reorder operations in a way that violates data dependencies.

SRAM-Aware Fusion: Hardware-Constrained Collapsing

The most important constraint in modern accelerators is SRAM capacity. Fusion is beneficial

only when the fused operator can keep its intermediate tensors on-chip. If fusion causes the combined tile size to exceed SRAM limits, the fused operator will spill to DRAM, negating the performance benefits.

Thus, fusion is guided by a hardware-aware feasibility test:

$$\text{Fuse}(f,g) \iff \text{SemanticEquivalence} \wedge \text{ShapeCompatibility} \wedge (T_f + T_g \leq S)$$

This constraint ensures that fusion produces operators that are not only mathematically valid but also physically efficient.

Graph-Theoretic Interpretation

In graph terms, fusion replaces a subgraph G_{sub} with a single node h:

$$G' = (V \setminus V_{sub}) \cup \{h\}, \quad E' = \text{rewire}(E)$$

where h preserves all incoming edges to the first operator and all outgoing edges from the last operator. This reduces:

- node count: |V'|<|V|
- edge count: |E'|<|E|
- intermediate tensors: fewer live intervals
- memory footprint: reduced peak usage

Fusion therefore acts as a structural compression of the graph.

Execution-Level Impact

Fused operators:

- reduce DRAM traffic by keeping intermediate tensors in SRAM
- shorten critical paths by eliminating intermediate nodes
- reduce kernel launch overhead
- improve locality and cache behavior
- expose larger optimization regions to downstream compilation

Fusion is the foundation upon which algebraic simplification, constant folding, and buffer

minimization build.

With fusion collapsing compatible operators into SRAM-efficient execution blocks, the graph becomes structurally simpler and more amenable to mathematical reduction. The next stage focuses on eliminating operations that contribute no meaningful computation—identity transforms, redundant reshapes, algebraically equivalent subgraphs, and structurally unnecessary nodes. These algebraic simplification passes refine the fused graph even further, removing dead computation and exposing new opportunities for optimization before the model enters the compilation pipeline.

ii. Algebraic AI Simplification Passes with Identity-Based Graph Pruning

Algebraic AI simplification passes operate on the compute graph after fusion has collapsed compatible operators, focusing on removing operations that are mathematically redundant or structurally unnecessary. These passes rely on algebraic identities, graph-theoretic reasoning, and shape analysis to prune nodes that do not change the model's output, simplify expression chains, and expose new opportunities for fusion and buffer minimization. Although they are mathematically driven, their impact is deeply hardware-relevant: every removed node is one less kernel, one less memory access, and one less intermediate buffer.

At the core is the principle of semantic preservation. Let the original graph be G with associated function $f_G(x)$, and the simplified graph be G' with function $f_{G'}(x)$. Algebraic passes must satisfy:

$$\forall x, \quad f_G(x) = f_{G'}(x)$$

All transformations are constrained by this equivalence.

Identity-based pruning is the most direct application of algebraic identities. For elementwise operations, common identities include:

$$x + 0 = x, \quad x \cdot 1 = x, \quad x - 0 = x, \quad x/1 = x$$

For linear layers:

$$Wx + 0 = Wx, \quad x + \text{bias} = x \quad \text{if bias} = 0$$

For activation chains:

$$\text{Id}(x) = x$$

Any node implementing such an identity can be removed, and its input directly wired to its output. Formally, if a node v computes a function g such that:

$$\forall x, \quad g(x) = x,$$

then v can be eliminated and all edges (u,v) rewired to (u,w), where w is the original consumer of v's output.

Algebraic simplification also applies associativity and commutativity to regroup operations. For addition and multiplication:

$$(x + y) + z = x + (y + z), \quad x + y = y + x$$

$$(x \cdot y) \cdot z = x \cdot (y \cdot z), \quad x \cdot y = y \cdot x$$

These properties allow the compiler to reorder and regroup nodes to form larger fusion regions or to factor out common subexpressions. For example, if the graph contains:

$$x + y + z$$

implemented as two chained additions, the compiler can represent it as a single multi-input add node, reducing kernel launches and intermediate buffers.

Distributivity provides another powerful simplification tool:

$$a \cdot (b + c) = a \cdot b + a \cdot c$$

and its inverse:

$$a \cdot b + a \cdot c = a \cdot (b + c)$$

The compiler can use these identities to factor expressions, reducing repeated computation, or to reshape the graph into forms that better match hardware execution patterns (e.g., preferring a single batched operation over multiple scalar ones).

Reshape and transpose chains are simplified using structural equivalences. If a sequence of reshapes and transposes ultimately returns a tensor to its original shape and layout, the entire chain can be removed. For example:

$$\text{reshape}(\text{reshape}(x, s_1), s_0) = x \quad \text{if } s_0 \text{ is the original shape}$$

$$\text{transpose}(\text{transpose}(x, p), p^{-1}) = x$$

These identities allow the compiler to collapse redundant layout operations, reducing memory traffic and improving cache behavior.

Graph-theoretically, algebraic simplification can be viewed as contracting nodes whose functions are algebraic identities or whose composition yields a simpler equivalent function. If a subgraph G_{sub} computes a function h that can be expressed more compactly, the compiler replaces G_{sub} with a single node v_h and rewires edges accordingly. This reduces both node and edge counts:

$$|V'| = |V| - |V_{sub}| + 1, \quad |E'| < |E|$$

while preserving $f_G = f_{G'}$.

The hardware implications of these algebraic passes are significant. Each removed identity node eliminates a kernel launch, a memory read, and a memory write. Simplifying reshape and transpose chains reduces data movement and improves cache locality. Collapsing multiple arithmetic operations into a single fused node allows better use of vector units and tensor cores, as the compiler can generate wider SIMD instructions or more efficient batched kernels. Shorter operator chains also reduce intermediate buffer lifetimes, enabling more aggressive buffer reuse and lowering peak SRAM usage.

Moreover, algebraic simplification prepares the graph for downstream compilation and auto-tuning. A graph with fewer, more meaningful nodes presents clearer optimization opportunities to IR dialects and polyhedral schedulers. It reduces the search space for auto-tuned pipelines, focusing their effort on genuinely impactful parameters rather than on noise introduced by redundant operations. In this way, algebraic passes act as a structural filter, ensuring that the compilation pipeline operates on a graph that is mathematically clean and hardware-friendly.

With algebraic simplification removing identity operations, collapsing redundant expression chains, and streamlining layout transforms, the graph is now structurally and mathematically cleaner. The next step is to exploit the fact that many tensors and parameters in AI models are static and known at compile time. By evaluating these constant subgraphs ahead of execution,

the compiler can fold their effects into fixed tensors, eliminate entire computation paths, and simplify quantized dataflows. This is the role of quantized-graph constant folding, which turns static structure into precomputed values and further reduces runtime cost.

iii. Quantized-Graph AI Constant Folding for Static Tensor and Parameter Evaluation

Quantized-graph AI constant folding focuses on exploiting the static structure of a model—its fixed weights, biases, scale factors, and quantization parameters—to precompute as much work as possible at compile time. In quantized networks, many subgraphs operate entirely on constants or on tensors whose values are known and never change. Evaluating these subgraphs ahead of execution and replacing them with constant tensors reduces runtime computation, simplifies dataflows, and stabilizes numerical behavior. This process is mathematically grounded in function evaluation, affine transformations, and range propagation.

Formally, consider a compute graph G = (V, E) with a subset of nodes $V_c \subseteq V$ whose inputs are all constants. Let C denote the set of constant input tensors to this subgraph, and let h be the function computed by $G_c = (V_c, E_c)$. If:

$$\forall x, \quad G_c(C) = h(C) = K,$$

for some constant tensor K, then the entire subgraph G_c can be evaluated once at compile time and replaced by a single constant node holding K. All intermediate nodes and edges in G_c are removed, and any consumers of G_c's output are rewired to read from the new constant node. This is the essence of constant folding: precompute h(C) and eliminate the dynamic computation.

In quantized graphs, values are represented by integer tensors with associated scale and zero-point parameters. A typical quantization mapping is:

$$x_{\text{real}} = s_x \cdot (x_{\text{int}} - z_x),$$

where s_x is the scale and z_x is the zero-point. Chains of quantize/dequantize operations can often be reduced to a single equivalent affine transform. For example, if a tensor is dequantized and then requantized with different parameters:

$$y_{\text{int}} = \text{round}\left(\frac{s_x}{s_y}(x_{\text{int}} - z_x) + z_y\right).$$

the composite mapping from x_{int} to y_{int} is:

$$y_{\text{int}} = \text{round}\left(\frac{s_x}{s_y}(x_{\text{int}} - z_x) + z_y\right).$$

If this mapping is applied to constant tensors (e.g., weights), it can be evaluated once and stored as pre-quantized weights, eliminating the runtime dequantize/requantize pair. Even when applied to activations, the compiler can sometimes fold chains of affine transforms into a single equivalent transform, reducing the number of quantization nodes.

Batch normalization folding is another classic example. In a quantized convolutional layer followed by batch normalization, the batch-norm parameters γ, β, μ, σ can be folded into the convolution weights and biases. In the real domain:

$$\text{BN}(y) = \gamma \cdot \frac{y - \mu}{\sigma} + \beta.$$

If $y = W_x + b$, then:

$$\text{BN}(Wx + b) = \gamma \cdot \frac{Wx + b - \mu}{\sigma} + \beta = \left(\frac{\gamma}{\sigma}W\right)x + \left(\frac{\gamma}{\sigma}(b - \mu) + \beta\right).$$

The folded weights and biases are:

$$W' = \frac{\gamma}{\sigma}W, \quad b' = \frac{\gamma}{\sigma}(b - \mu) + \beta.$$

In a quantized setting, these folded parameters are then quantized once and stored as constants. The batch-norm node is removed, and the convolution node is updated to use W’ and b’. This reduces runtime computation and simplifies the graph.

Constant folding also applies to activation thresholds, lookup tables, and precomputed masks. If a ReLU6 or clipping operation is applied to a constant tensor, its result can be computed once and stored. If a static attention mask is constructed from fixed patterns, the mask can be precomputed and the construction subgraph removed. In all cases, the mathematical principle is the same: evaluate any function whose inputs are constants and replace it with its result.

Range propagation is another important aspect in quantized graphs. Given integer ranges and scales, the compiler can infer the possible value ranges of intermediate tensors. This allows it to detect redundant saturation, clipping, or casting operations. For example, if a tensor is known to

lie within [0,255] and is cast to an 8-bit type, the cast may be redundant. If a clipping operation enforces a range that is already guaranteed by upstream quantization, it can be removed. These decisions are based on interval arithmetic:

$$x \in [a,b] \Rightarrow f(x) \in [f\min(a,b), f\max(a,b)],$$

where f_{min}, f_{max} are derived from the function's behavior over the interval.

The hardware implications of quantized-graph constant folding are substantial. Every folded subgraph eliminates one or more kernels, reduces memory traffic, and shrinks the live set of intermediate tensors. Pre-quantized weights reduce the need for runtime quantization, lowering latency and simplifying dataflows. Folding batch-norm and similar parameterized operations into upstream layers reduces the number of passes over activations, improving cache locality and bandwidth utilization. Simplifying quantize/dequantize chains reduces integer-to-float conversions and back, which are often expensive on specialized accelerators.

Moreover, constant folding stabilizes numerical behavior by removing dynamic recomputation of the same values. Fixed tensors are computed once with high precision and then reused, reducing the risk of accumulated rounding errors. This is particularly important in deeply quantized pipelines, where repeated conversions can introduce drift.

Constant folding also interacts positively with downstream compilation and auto-tuning. A graph with fewer dynamic operations and more precomputed constants presents a cleaner optimization surface. IR dialects see fewer nodes, polyhedral schedulers handle simpler iteration spaces, and auto-tuned pipelines focus on genuinely dynamic kernels rather than on trivial constant computations. In this way, quantized-graph constant folding acts as a bridge between mathematical simplification and hardware-aware optimization.

With constant subgraphs evaluated ahead of time and quantized parameters folded into upstream operators, the graph now carries fewer dynamic tensors and shorter computation chains. The remaining challenge is to manage the memory footprint of the tensors that must still be produced at runtime. This is where intermediate-buffer minimization becomes critical, analyzing buffer lifetimes across fused execution blocks, reusing or aliasing storage where possible, and aligning layouts with SRAM and cache characteristics. By treating memory as an optimization target in its own right, the next stage ensures that the simplified, folded graph can execute within tight on-chip budgets while sustaining high throughput.

iv. AI Intermediate-Buffer Minimization Across Fused Operator Execution Blocks

Intermediate-buffer minimization is the final stage of graph simplification, targeting the memory footprint of tensors produced during execution. After fusion, algebraic simplification, and constant folding have reduced the number of operators and eliminated redundant computation, the remaining challenge is to ensure that the dynamic tensors produced by fused execution blocks occupy as little memory as possible. This is essential for modern accelerators, where on-chip SRAM is limited and memory bandwidth is often the dominant bottleneck.

At its core, buffer minimization is a problem of **lifetime analysis**. Each tensor t_i produced during execution has a live interval $[b_i, e_i]$, where b_i is the point in the topological order when the tensor is created, and e_i is the last point at which it is consumed. Two tensors can share the same memory region if their intervals do not overlap:

$$[b_i, e_i] \cap [b_j, e_j] = \emptyset.$$

This is equivalent to the classical interval-graph coloring problem. Construct an interval graph H where each vertex corresponds to a tensor and edges connect tensors with overlapping lifetimes. Minimizing the number of memory regions is equivalent to finding the chromatic number $\chi(H)$. In practice, compilers use greedy coloring heuristics that are optimal for interval graphs, ensuring efficient reuse of memory.

Fusion dramatically reshapes these intervals. When multiple operators are fused into a single execution block, intermediate tensors that previously existed between operators may no longer need to be materialized. Instead, their values can remain in registers or SRAM tiles. Mathematically, if a fused operator h computes:

$$h(x) = g(f(x)),$$

then the intermediate tensor y=f(x) may not need a buffer at all. Its live interval collapses to zero length, and it is eliminated from the interval graph. This reduces the chromatic number and lowers peak memory usage.

Buffer aliasing is another powerful technique. If two tensors have non-overlapping lifetimes, they can be assigned to the same memory region:

$$t_i \leftrightarrow m_k, \quad t_j \leftrightarrow m_k \quad \text{if } [b_i, e_i] \cap [b_j, e_j] = \emptyset.$$

This reduces the total number of allocated buffers. Aliasing is especially effective in fused blocks, where many intermediate tensors have short lifetimes.

Layout-aware minimization ensures that buffers are sized and aligned to match the accelerator's memory architecture. For example, GPUs require alignment to avoid bank conflicts, while NPUs may require tile-aligned buffers to match systolic array dimensions. If a buffer t_i has shape S_i and alignment requirement A, the actual allocated size is:

$$\text{alloc}(t_i) = \left\lceil \frac{|S_i|}{A} \right\rceil A.$$

Minimization strategies attempt to pack buffers so that aligned sizes overlap efficiently, reducing fragmentation.

Another mathematical tool is **dominance analysis**. If a tensor is produced inside a fused block and consumed only within that block, its lifetime is strictly contained within the block's execution interval. This allows the compiler to allocate a single scratch buffer for the entire block and reuse it for all internal intermediates. Formally, if:

$$b_{\text{block}} \leq b_i < e_i \leq e_{\text{block}},$$

then:

$$t_i \subseteq \text{scratch}_{\text{block}}.$$

This reduces the number of distinct buffers and improves locality.

Hardware implications are profound. Minimizing intermediate buffers reduces peak SRAM usage, allowing larger tiles to fit on-chip. Larger tiles improve locality, reduce DRAM traffic, and increase arithmetic intensity. Buffer reuse reduces allocation overhead and fragmentation. Eliminating intermediate tensors reduces memory bandwidth pressure, which is often the limiting factor in AI workloads. On GPUs, fewer buffers mean fewer global memory accesses and better cache behavior. On NPUs and TPUs, tighter buffer packing allows more efficient systolic execution.

Intermediate-buffer minimization also interacts synergistically with auto-tuned pipelines. A graph with fewer buffers allows more aggressive tiling and vectorization. It reduces register pressure and improves occupancy. It simplifies schedule search by reducing the number of memory-related constraints. In this way, buffer minimization is not merely a memory

optimization—it is a structural enabler for downstream compilation.

Graph simplification transforms the compute graph from a raw, unfused, memory-heavy topology into a streamlined, mathematically optimized structure. Node-fusion strategies collapse compatible operators into SRAM-efficient execution blocks. Algebraic simplification removes identity operations, redundant reshapes, and structurally unnecessary nodes. Quantized-graph constant folding evaluates static tensors and parameters at compile time, eliminating entire computation paths. Intermediate-buffer minimization reduces memory footprints across fused blocks through lifetime analysis, aliasing, and layout-aware packing. Together, these transformations produce a graph that is smaller, faster, and more hardware-aligned, forming the foundation upon which IR dialects, polyhedral schedulers, auto-tuned pipelines, and machine-code ingestion layers operate. Graph simplification is therefore the structural precondition for efficient AI execution, ensuring that the compilation pipeline begins with a graph that is already lean, mathematically sound, and memory-efficient.

With the compute graph now simplified, fused, folded, and memory-optimized, the next frontier is to design neural architectures that are inherently aligned with hardware constraints rather than optimized only after the fact. Hardware-aware neural architecture search extends the principles of graph simplification into the model-design phase, incorporating latency, memory footprint, bandwidth limits, and accelerator-specific execution patterns directly into the search objective. By embedding hardware constraints and latency-driven loss functions into the architecture search process, the system can discover models whose structure is not only expressive and accurate but also intrinsically optimized for the underlying device.

c. Hardware-Aware AI Neural Architecture Search with Constraints and Latency-Driven Loss Functions

Hardware-aware neural architecture search (NAS) extends AI optimization beyond compilation and computational graph transformation by incorporating hardware characteristics directly into neural network design. Conventional model development often begins with an architecture selected primarily for predictive accuracy, after which developers attempt to reduce its computational cost through pruning, quantization, operator fusion, and hardware-specific compilation. Although these techniques can improve execution efficiency, the original architecture may still contain structural characteristics that are poorly matched to the target platform. Hardware-aware NAS addresses this limitation by searching for architectures that satisfy application requirements while accounting for the computational, memory, energy, and timing constraints of the intended deployment environment. **Rather than optimizing only how a model executes on hardware, hardware-aware NAS also optimizes the model's structure for the hardware on which it will execute.**

The search process explores alternative architectural configurations, including the number and arrangement of layers, operator types, channel dimensions, convolutional kernel sizes, attention-head configurations, expansion ratios, and other model-specific design parameters. Each candidate architecture is evaluated according to its predictive performance and its expected or measured deployment cost. Depending on the application, these costs may include inference latency, peak memory consumption, energy per inference, model size, memory bandwidth requirements, and computational throughput. Hardware-aware NAS therefore treats architecture selection as a constrained optimization problem in which model quality must be balanced against the practical limitations of the execution platform.

Hardware Constraints and Architecture Search Spaces

The effectiveness of hardware-aware NAS depends on how accurately the search space reflects the characteristics of the target hardware. Modern computing platforms differ substantially in their processing units, memory hierarchies, supported numerical formats, parallel execution models, and power-management behavior. A neural network architecture that performs efficiently on one accelerator may execute less efficiently on another, even when both devices provide similar theoretical computational throughput.

Consequently, the search process may incorporate constraints related to cache capacity, available on-chip memory, memory bandwidth, register pressure, vector widths, tensor-processing unit dimensions, and parallel execution-group sizes. These characteristics influence which operations can be executed efficiently and how intermediate data should be organized. For example, convolutional dimensions that align with an accelerator's preferred matrix-operation shapes may improve hardware utilization, whereas irregular dimensions may require padding, additional data movement, or less efficient computational kernels. Similarly, an attention configuration may offer favorable computational complexity but perform poorly if its intermediate tensors exceed available fast memory or create excessive data-transfer overhead.

The architecture search space can be designed to reflect these hardware characteristics. Instead of considering every theoretically possible neural network, the search algorithm may prioritize operator families and tensor dimensions supported efficiently by the target platform. It may also exclude candidates that violate hard constraints, such as a maximum memory footprint or a strict latency deadline. This approach reduces the search space and focuses the optimization process on architectures that are both functionally suitable and practically deployable.

However, hardware constraints should not be interpreted as universal rules. The most efficient channel dimensions, attention configurations, or operator combinations depend on the accelerator architecture, compiler implementation, numerical precision, and workload. An

operation that maps efficiently to one GPU may not be equally efficient on an NPU or CPU. Hardware-aware NAS must therefore evaluate architectural choices in the context of the intended software and hardware stack rather than assume that a single architectural pattern is optimal across all platforms.

Measured Latency, Surrogate Models, and Search Efficiency

Directly measuring every candidate architecture on physical hardware can be expensive. Neural architecture search may generate thousands of candidates, and each candidate may require compilation, warm-up, repeated inference measurements, and evaluation under representative operating conditions. To make the search computationally manageable, hardware-aware NAS commonly combines direct measurements with performance-estimation techniques.

A latency lookup table is one approach. The system measures supported operators or kernel configurations on the target hardware and records their execution costs. During architecture evaluation, these measurements can provide approximate latency estimates for candidate networks. Such estimates are useful when the architecture consists of operators whose costs can be characterized individually, although interactions among kernels, memory transfers, and runtime scheduling may make the total latency differ from the sum of isolated measurements.

A second approach uses a surrogate model to predict hardware performance. A surrogate may estimate latency, energy consumption, or memory usage from architectural features such as tensor dimensions, operator types, depth, and channel counts. The search algorithm uses these predictions to rank candidates and decide which architectures warrant more expensive evaluation. Surrogate models may be learned from previously measured configurations, generated using analytical performance models, or constructed through combinations of analytical and empirical methods.

Differentiable latency surrogates provide another option when the architecture-search method requires gradients. In such systems, a differentiable approximation of hardware cost allows the search algorithm to estimate how architectural changes affect the optimization objective. This can make it possible to optimize architecture parameters jointly with task-related objectives. However, a differentiable surrogate is an approximation rather than a guarantee of actual execution time. Its accuracy depends on the quality and coverage of the measurements used to construct it and on how closely the searched architectures resemble the configurations on which it was evaluated.

For this reason, a reliable hardware-aware search pipeline generally validates promising candidates through actual execution on the target platform. Final measurements should use representative input dimensions, batch sizes, numerical precision, software configurations, and

runtime conditions. Where relevant, evaluation should also account for warm-up effects, concurrent workloads, thermal behavior, and power-management policies. This combination of modeling and empirical validation helps prevent the search process from selecting architectures that appear efficient in theory but perform poorly in deployment.

Pareto-Optimal Architectures and Multi-Objective Trade-Offs

Predictive accuracy, latency, energy consumption, and memory usage often conflict with one another. Increasing model depth or width may improve accuracy but also increase computation and memory requirements. Reducing the number of operations may lower latency but remove representational capacity needed for a demanding task. Similarly, an architecture that minimizes energy per inference may not provide the highest throughput under heavy concurrent workloads.

Multi-objective NAS addresses these conflicts by identifying a collection of architectures that represent different trade-offs among the objectives. An architecture is Pareto-optimal when no alternative architecture improves at least one objective without worsening another, assuming the objectives and constraints have been defined consistently. The resulting Pareto frontier may include a highly accurate model with relatively high latency, a smaller model with lower energy consumption, and intermediate alternatives that balance these properties.

This collection is often more useful than a single nominally optimal architecture because deployment requirements vary. A cloud-based service may favor throughput and resource utilization, whereas a mobile device may prioritize energy efficiency and memory capacity. An autonomous system may require a balance of predictive accuracy, bounded latency, and reliable operation under changing environmental conditions. Pareto-based analysis allows system designers to select an architecture that matches the actual requirements instead of assuming that the model with the fewest parameters or the lowest average latency is always preferable.

Hardware-aware NAS can also reveal architectural patterns that are particularly effective on a given platform. Certain convolutional configurations may align well with vector or matrix-processing units, while particular attention dimensions may better match the supported matrix-operation shapes. Other architectures may reduce memory traffic by limiting intermediate activation sizes or by enabling more effective reuse of data. These patterns are hardware-dependent findings rather than universal design rules, and they should be confirmed through measurements on the intended execution platform.

Hardware-Aligned Topology Generation and Deployment Validation

The final objective of hardware-aware NAS is to identify model structures that can be

implemented efficiently by the complete deployment stack. Architecture selection must therefore account for the interaction among the neural network, compiler, runtime, and processor. A theoretically efficient architecture may not deliver its expected benefits if the compiler lacks an optimized implementation for one of its operators or if the runtime introduces substantial overhead between computational stages.

Hardware-aligned topology generation can address these interactions by favoring operators and

tensor dimensions that are supported effectively by the target accelerator. The search process may select layer dimensions that improve vector or matrix-unit utilization, reduce padding overhead, limit intermediate-memory requirements, or enable compatible operations to be fused. It may also account for the availability of low-precision arithmetic and the numerical constraints associated with its use.

Nevertheless, architecture search and compilation are complementary rather than interchangeable. NAS determines which model structures should be considered, while the compiler determines how a selected structure is transformed into executable operations. Graph simplification and operator fusion can further improve the resulting implementation. A model identified by NAS must therefore pass through the compilation and deployment pipeline before its actual performance can be established.

Deployment validation is especially important for systems subject to strict timing and energy constraints. Dynamic voltage and frequency scaling (DVFS), thermal throttling, competing workloads, and runtime scheduling can alter execution time and energy consumption. A candidate that satisfies its latency target under isolated benchmark conditions may behave differently under sustained or concurrent workloads. Where multiple hardware platforms are involved, each target may require its own measurements, performance models, or architecture configuration.

Cross-platform deployment introduces an additional consideration: generalization across hardware. An architecture optimized for one accelerator may perform poorly on another because of differences in memory bandwidth, supported operators, parallelism, and compiler maturity. If portability is a requirement, the search objective may incorporate measurements from multiple devices, impose constraints for each supported platform, or identify a family of architectures tailored to different hardware configurations. Such strategies make the deployment trade-offs explicit rather than assuming that one model will be equally efficient everywhere.

Ultimately, **hardware-aware neural architecture search integrates model design with the physical and operational constraints of the target computing platform**. Hardware-informed

search spaces guide architectural exploration, latency-driven objectives connect predictive quality with execution cost, and measured performance or surrogate models make the search process more practical. Multi-objective optimization identifies viable trade-offs among accuracy, latency, energy, and memory, while deployment validation determines whether the selected architecture satisfies its real-world requirements.

Within the broader cross-layer optimization framework, hardware-aware NAS complements

intermediate-representation optimization and computational graph simplification. Rather than relying exclusively on compiler transformations to compensate for an inefficient model structure, it seeks architectures that are better suited to the target hardware from the outset. Combined with efficient compilation, graph optimization, and runtime measurement, this approach helps produce AI systems that meet application-specific performance requirements while using computational and physical resources effectively.

Mathematical Frameworks for Hardware-Aware AI Neural Architecture Search with Constraints and Latency-Driven Loss Functions

1. Multi-Objective AI Genetic Search Incorporating Measured Hardware Latency Signals

Genetic NAS algorithms evolve architectures through mutation, crossover, and selection. In hardware-aware NAS, the fitness function incorporates **measured latency signals** from the target accelerator. If an architecture A has accuracy Acc(A) and measured latency L(A), the fitness function becomes:

$$F(A) = Acc(A) - \lambda L(A),$$

where λ controls the trade-off between accuracy and latency. More advanced formulations include multi-objective Pareto optimization:

$$\text{maximize } (Acc(A), -L(A), -Mem(A), -BW(A)),$$

where Mem(A) is memory footprint and BW(A) is bandwidth consumption.

Latency is measured by compiling candidate architectures into executable kernels and timing them on the target hardware. Measured latency captures microarchitectural effects such as warp divergence on GPUs, systolic array tile inefficiencies on TPUs, memory-bank conflicts on NPUs, cache thrashing on CPUs, and quantization overhead on mixed-precision accelerators. These effects cannot be predicted by FLOPs alone, making measured latency essential. This

produces **ground-truth latency**, capturing effects that FLOPs cannot: cache behavior, warp divergence, pipeline stalls, and quantization overhead.

Genetic search uses these signals to evolve architectures toward hardware-optimal forms—shallower but wider layers for GPUs, tile-friendly blocks for NPUs, and systolic-aligned structures for TPUs. Over generations, the population converges toward architectures that are not only accurate but also deeply aligned with the physical characteristics of the target device.

2. Hardware-Proxy AI Models with Differentiable Latency-Estimator Surrogates

Direct latency measurement is expensive. To accelerate NAS, hardware-aware systems train **differentiable latency-estimator surrogates** that predict latency from architectural features. If an architecture is represented by feature vector x_A, the surrogate model predicts:

$$\hat{L}(A) = f_\theta(x_A),$$

where f_θ is a learned function (MLP, GNN, or transformer). The surrogate is trained on a dataset of architectures and their measured latencies:

$$\theta = \arg\min_\theta \sum_A \left(L(A) - f_\theta(x_A)\right)^2.$$

Once trained, the surrogate becomes part of the NAS loss function:

$$L_{NAS}(A) = L_{task}(A) + \alpha \hat{L}(A),$$

allowing gradient-based NAS to optimize architectures for latency without requiring expensive hardware measurements at every step. This enables continuous search over architectural parameters such as convolution kernel sizes, attention head counts, hidden-layer widths, depth multipliers, and quantization bit-widths.

Surrogates capture device-specific behaviors such as tensor-core utilization patterns, register pressure, shared-memory tile alignment, pipeline stall probabilities, and quantization/dequantization overhead. This allows NAS to explore architectures that would be infeasible to evaluate exhaustively using real hardware measurements.

3. Energy-Per-Inference AI Penalty Functions Embedded in NAS Optimization Costs

Energy consumption is increasingly important for mobile, embedded, and large-scale inference. Hardware-aware NAS incorporates **energy-per-inference penalties** into the optimization

objective. If E(A) is the measured or predicted energy cost of architecture A, the NAS loss becomes:

$$L(A) = L_{task}(A) + \beta E(A),$$

where β controls the trade-off between accuracy and energy.

Energy models often use:

$$E(A) = \sum_{i \in \text{ops}(A)} P_i \cdot t_i,$$

where P_i is power consumption of operator i and t_i is its execution time. This formulation encourages architectures that minimize expensive operations such as large convolutions, wide attention blocks, deep matrix multiplications, and high-precision quantization paths.

Energy-aware NAS produces architectures that are suitable for battery-powered devices, edge accelerators, and large-scale inference clusters where energy cost dominates operational expense. Energy-aware NAS also discovers architectures that reduce battery drain on mobile devices, thermal load on embedded systems, and operational cost in large inference clusters. It also encourages quantization-friendly and fusion-friendly designs that reduce memory traffic—one of the largest contributors to energy consumption.

4. Cross-Silicon AI Architecture Generalization for Heterogeneous Accelerator Targets

Modern AI systems must run across heterogeneous hardware: GPUs, NPUs, TPUs, CPUs, and custom ASICs. Hardware-aware NAS incorporates **cross-silicon generalization constraints**, ensuring that architectures perform well across multiple devices.

If latency is measured on multiple accelerators d∈D, the NAS objective becomes:

$$L(A) = L_{task}(A) + \sum_{d \in D} \alpha_d L_d(A),$$

where $L_d(A)$ is latency on device d. This encourages architectures that are robust to hardware variation.

Cross-silicon NAS often discovers architectures with:

- modular blocks that map well to different execution units
- balanced compute/memory ratios

- quantization-friendly structures
- tile-aligned shapes that generalize across systolic and SIMD hardware
- fusion-friendly operator sequences
- memory-efficient tensor layouts

These architectures are portable, future-proof, and efficient across diverse deployment environments.

Cross-silicon NAS is essential for cloud providers, mobile ecosystems, and multi-accelerator inference pipelines, where a single model must run efficiently on many different devices.

5. Latency-Driven Loss Functions and Performance Modeling

A central feature of hardware-aware NAS is the integration of execution cost into the architecture evaluation objective. Traditional NAS methods may optimize predictive accuracy while using parameter count or floating-point operations (FLOPs) as proxies for computational efficiency. Although these metrics provide useful information about model complexity, they do not reliably predict real-world inference latency. Two networks with similar FLOP counts can exhibit substantially different execution times because of differences in memory access, operator support, parallelism, kernel-launch overhead, and hardware utilization.

Latency-driven objectives address this limitation by incorporating estimates or measurements of inference time directly into the search process. A general multi-objective formulation can be expressed as

$$\min_{\mathcal{A}} \left[\mathcal{L}_{\text{task}}(\mathcal{A}), T(\mathcal{A}), E(\mathcal{A}), M(\mathcal{A})\right]$$

subject to

$$T(\mathcal{A}) \leq T_{\max}$$

$$E(\mathcal{A}) \leq E_{\max}$$

$$M(\mathcal{A}) \leq M_{\max}$$

where:

- $\mathcal{A}$ denotes a candidate neural network architecture.

- $\mathcal{L}_{\text{task}}(\mathcal{A})$ represents the task-specific loss, such as classification error or a suitable training objective.
- $T(\mathcal{A})$ represents inference latency.
- $E(\mathcal{A})$ represents energy consumption per inference.
- $M(\mathcal{A})$represents memory requirements.
- $T_{\max}$, $E_{\max}$, and $M_{\max}$ are application-specific limits.

This formulation illustrates that architecture search may involve several competing objectives rather than a single universal measure of quality. The exact constraints depend on the deployment environment. For example, a battery-powered edge device may impose a strict energy budget, while a real-time perception system may require inference to complete within a defined deadline. Some applications may also impose maximum model-size or memory-capacity requirements.

Alternatively, the objectives can be combined into a single optimization function:

$$\begin{aligned}\mathcal{J}(\mathcal{A}) = \mathcal{L}_{\text{task}}(\mathcal{A}) \\ + \lambda_T \phi_T\big(T(\mathcal{A})\big) \\ + \lambda_E \phi_E\big(E(\mathcal{A})\big) \\ + \lambda_M \phi_M\big(M(\mathcal{A})\big)\end{aligned}$$

The objective is to minimize this function:

$$\min_{\mathcal{A}} \mathcal{J}(\mathcal{A})$$

An alternative approach combines the objectives into a scalar loss:

Where:

- $\mathcal{J}(\mathcal{A})$ = total optimization objective.
- $\mathcal{L}_{\text{task}}(\mathcal{A})$ = task-specific loss.
- ϕ_T, ϕ_E, and ϕ_M = penalty functions for latency, energy, and memory.
- λ_T, λ_E, and λ_M = weighting coefficients controlling the importance of each penalty.

The penalty functions can be designed to increase the cost of architectures that approach or exceed deployment limits. Hard constraints can also be enforced separately when exceeding a limit is unacceptable.

This distinction matters because minimizing average latency is not necessarily equivalent to satisfying a real-time deadline. A model may have a low average inference time yet occasionally exceed the maximum permitted response time. Applications with strict timing requirements may therefore need to consider high-percentile latency, worst-case execution-time estimates, or other deadline-oriented measures in addition to average performance. The appropriate measure depends on whether the system is designed for high-throughput processing, interactive response, or time-critical control.

Hardware-aware neural architecture search (NAS) extends conventional neural network design by incorporating hardware characteristics directly into the architecture optimization process. Rather than selecting architectures solely on the basis of predictive accuracy or theoretical computational complexity, hardware-aware NAS evaluates candidate models in relation to the resource constraints, execution characteristics, and energy requirements of their intended deployment platforms. This process requires optimization methods that address competing objectives, estimate hardware-specific performance, and balance computational efficiency against model quality. Because no single method fully captures these requirements, hardware-aware NAS combines complementary techniques to guide architecture selection toward deployment-ready solutions.

Table 8.4-F3 — Hardware-Aware NAS Optimization Dimensions presents five complementary approaches to architecture optimization: multi-objective genetic search, differentiable latency surrogates, energy-per-inference penalties, cross-silicon generalization, and latency-driven loss functions and performance modeling. Multi-objective genetic search explores alternative architectures while balancing competing objectives. Differentiable latency surrogates estimate execution time to accelerate candidate evaluation, while energy-per-inference penalties incorporate energy consumption into the optimization objective. Cross-silicon generalization addresses performance variation across hardware platforms, and latency-driven loss functions and performance models help align architecture selection with inference-time requirements. These approaches can be combined to evaluate neural architectures in terms of predictive quality, execution efficiency, resource constraints, and compatibility with their intended deployment environments.

Table 8.4-F3 — Hardware-Aware NAS Optimization Dimensions

NAS Dimension	Core Purpose	Key Mechanisms	Mathematical Foundations	Hardware Impact
Multi-Objective Genetic Search	Evolve architectures using real hardware signals	Mutation, crossover, Pareto selection	Multi-objective optimization, latency measurement	Produces architectures tuned to actual device behavior
Differentiable Latency Surrogates	Enable fast gradient-based NAS	Learned latency models, hardware proxies	Regression, differentiable prediction, feature embeddings	Captures device-specific execution patterns
Energy-Per-Inference Penalties	Reduce power consumption	Power-time models, energy-aware loss	Energy modeling, weighted optimization	Produces energy-efficient architectures
Cross-Silicon Generalization	Ensure portability across hardware	Multi-device latency constraints	Multi-domain optimization, robustness analysis	Architectures run efficiently on heterogeneous accelerators
Latency-Driven Loss Functions and Performance Modeling	Optimize neural architectures to meet inference-latency targets while preserving task performance	Latency-aware loss functions, hardware-specific latency predictors, surrogate models, constraint-based optimization, and empirical latency profiling	Multi-objective optimization, weighted loss functions, regression-based latency estimation, constrained optimization, and performance modeling	Produces architectures that balance predictive accuracy with measured or estimated inference latency, supporting deadline-aware deployment on target hardware

Table 8.4-F3 illustrates hardware-aware neural architecture search (NAS) that coordinates multiple optimization strategies to balance predictive accuracy, inference latency, energy consumption, memory requirements, and cross-platform compatibility. Effective architecture selection therefore requires evaluating how network structure interacts with optimization objectives, performance-prediction models, and the computational characteristics of the target hardware. By integrating these factors into the search process, NAS can identify architectures that meet application requirements while making efficient use of available hardware resources.

Multi-Objective Genetic Search. Multi-objective genetic search explores a population of candidate neural architectures and iteratively refines it using genetic operations such as mutation, crossover, and selection. Each candidate is evaluated against multiple objectives, which may include predictive accuracy, inference latency, energy consumption, and memory requirements. Mutation introduces changes to architectural parameters, while crossover combines characteristics of existing candidates to generate new designs. Selection then favors candidates that provide desirable trade-offs among the specified objectives. These trade-offs can be represented by a *Pareto frontier*, which consists of architectures for which no objective can be improved without worsening at least one other objective. For example, a deeper network may achieve higher predictive accuracy but require more computation and energy than a shallower network. By exploring these alternatives, multi-objective genetic search identifies architectures with different performance characteristics, enabling selection according to the accuracy, latency, energy, and resource constraints of the intended application and hardware platform.

Differentiable Latency Surrogates

Differentiable latency surrogates are predictive models that estimate the inference latency of candidate neural architectures from their structural characteristics and the properties of the target hardware. These characteristics may include operator types, tensor dimensions, layer configurations, memory-access patterns, and hardware execution capabilities. The surrogate is trained using latency measurements collected from previously evaluated architectures, allowing it to approximate the relationship between architectural design choices and execution time. When the surrogate is differentiable, its latency predictions can be incorporated into gradient-based optimization, enabling the search process to adjust architectural parameters in directions expected to reduce latency. For example, a surrogate may estimate how changing a convolutional layer's channel width or replacing an operator affects inference time on a particular accelerator. This estimation reduces the need to execute every candidate on physical hardware during the search process. The accuracy of the surrogate depends on the quality and

coverage of its training data, so selected architectures are subsequently profiled on the target platform to verify their actual performance.

Energy-Per-Inference Penalties

Energy-per-inference penalties incorporate the energy required to execute a neural network inference into the architecture optimization objective. Energy consumption depends on several interacting factors, including the number and type of computational operations, processor utilization, memory access, data movement, execution duration, and operating power. A candidate architecture may therefore achieve low latency without minimizing energy consumption. In energy-aware NAS, an energy estimate or measurement is incorporated into the optimization process as a penalty or objective, encouraging the search to identify architectures that satisfy task-performance requirements while reducing energy use. For example, a neural network with fewer operations and lower memory traffic may consume less energy than a larger model, provided that the hardware executes the smaller model efficiently. Energy-per-inference penalties are especially relevant to battery-powered devices, embedded AI systems, and platforms with limited power or thermal budgets. Their implementation requires a defined measurement boundary and representative operating conditions so that the energy attributed to each inference reflects the intended deployment environment.

Cross-Silicon Generalization

Cross-silicon generalization concerns the ability of a neural architecture to maintain acceptable performance across different hardware platforms. GPUs, neural processing units (NPUs), tensor processing units (TPUs), and other accelerators differ in their computational units, memory hierarchies, supported operators, parallel execution capabilities, and compiler implementations. These differences influence how efficiently a given architecture executes on each device. For example, an architecture that benefits from a GPU's parallel execution model may not achieve the same latency on an NPU whose optimized operators and memory organization favor a different computational pattern. Hardware-aware NAS can incorporate measurements or predictions from multiple devices into its optimization process, using device-specific latency constraints and performance objectives to identify architectures that meet deployment requirements across the selected platforms. The resulting architecture may offer a practical balance between performance on individual devices and portability across the target hardware range. Deployment still requires appropriate compilation, runtime configuration, and validation for each platform because cross-silicon generalization does not imply identical execution behavior or performance across devices.

Latency-Driven Loss Functions and Performance Modeling

Latency-driven loss functions incorporate inference latency into the objective used to evaluate and optimize candidate neural architectures. In conventional neural network training, the loss function primarily measures task-related error, such as classification error or prediction deviation. In hardware-aware NAS, the optimization objective can also account for the time required to execute an inference on the target platform. Performance modeling supports this process by estimating latency from architectural features, operator characteristics, hardware specifications, and software execution conditions. A latency-aware objective may combine task loss with a penalty for excessive inference time, while a constrained formulation may require every selected architecture to satisfy a specified latency limit. For example, a real-time perception system may require a neural network to produce an output within a defined time budget. The search process can use latency estimates to favor architectures that maintain the required predictive performance while meeting that budget. Because actual execution time depends on factors such as memory contention, compiler optimization, runtime scheduling, and thermal conditions, the final architecture must be evaluated under representative deployment conditions. For systems with strict real-time requirements, performance evaluation may also consider latency distributions, high-percentile response times, and worst-case execution time, where it can be established reliably.

Integrating the Optimization Dimensions

The five optimization dimensions—multi-objective genetic search, differentiable latency surrogates, energy-per-inference penalties, cross-silicon generalization, and latency-driven loss functions with performance modeling—address complementary aspects of hardware-aware NAS. Multi-objective genetic search explores alternative architectures and identifies trade-offs among competing goals. Differentiable latency surrogates estimate execution performance efficiently, reducing the need for repeated hardware measurements during the search. Energy-per-inference penalties incorporate power efficiency into architecture selection, while cross-silicon generalization extends the optimization process across heterogeneous hardware platforms. Latency-driven loss functions and performance models connect architectural decisions to explicit inference-time requirements. These techniques can be integrated within a single workflow. For example, a genetic search may use a differentiable surrogate to estimate candidate latency, include energy consumption as an additional optimization objective, and evaluate promising architectures against latency constraints across several accelerators. The selected architecture can then be compiled and profiled on the intended deployment platforms to verify predictive performance, latency, energy consumption, and resource utilization.

Table 8.4-F3 describes the principal optimization dimensions used in hardware-aware neural

architecture search (NAS), including multi-objective genetic search, latency prediction, energy optimization, and cross-device generalization. These dimensions can be combined to guide architecture selection according to the computational and operational requirements of a deployment platform. Figure 8.4-F3 illustrates how these optimization techniques are incorporated into a workflow that begins with candidate neural architectures and progressively refines their selection through performance estimation, energy-aware optimization, and evaluation across different hardware platforms.

Figure 8.4-F3 — Hardware-Aware NAS Optimization Flow illustrates the main stages of hardware-aware neural architecture search. The process begins by defining candidate architectures through design variables such as layer types, network widths and depths, and quantization modes. Multi-objective genetic search explores these candidates using criteria such as measured inference latency, Pareto optimization, and memory or bandwidth constraints. Differentiable latency surrogates estimate the execution performance of candidate architectures using learned predictors and hardware-specific features, reducing the need for repeated measurements on physical devices. Energy-per-inference penalties incorporate energy consumption into architecture evaluation, allowing the search to account for power efficiency alongside task performance. Cross-silicon generalization then evaluates architectural suitability across different hardware platforms by considering device-specific latency constraints and robustness objectives. These stages guide the selection of a hardware-optimized neural architecture designed to meet the application's requirements for latency, energy efficiency, and portability.

The optimization process can operate iteratively. Measured execution results can be used to update latency predictors, energy estimates can influence the ranking of candidate architectures, and evaluations across multiple devices can reveal the need for further architectural adjustments. Through these interactions, architecture search incorporates information about both neural network structure and hardware execution behavior, enabling the selection of models suited to their intended deployment environments.

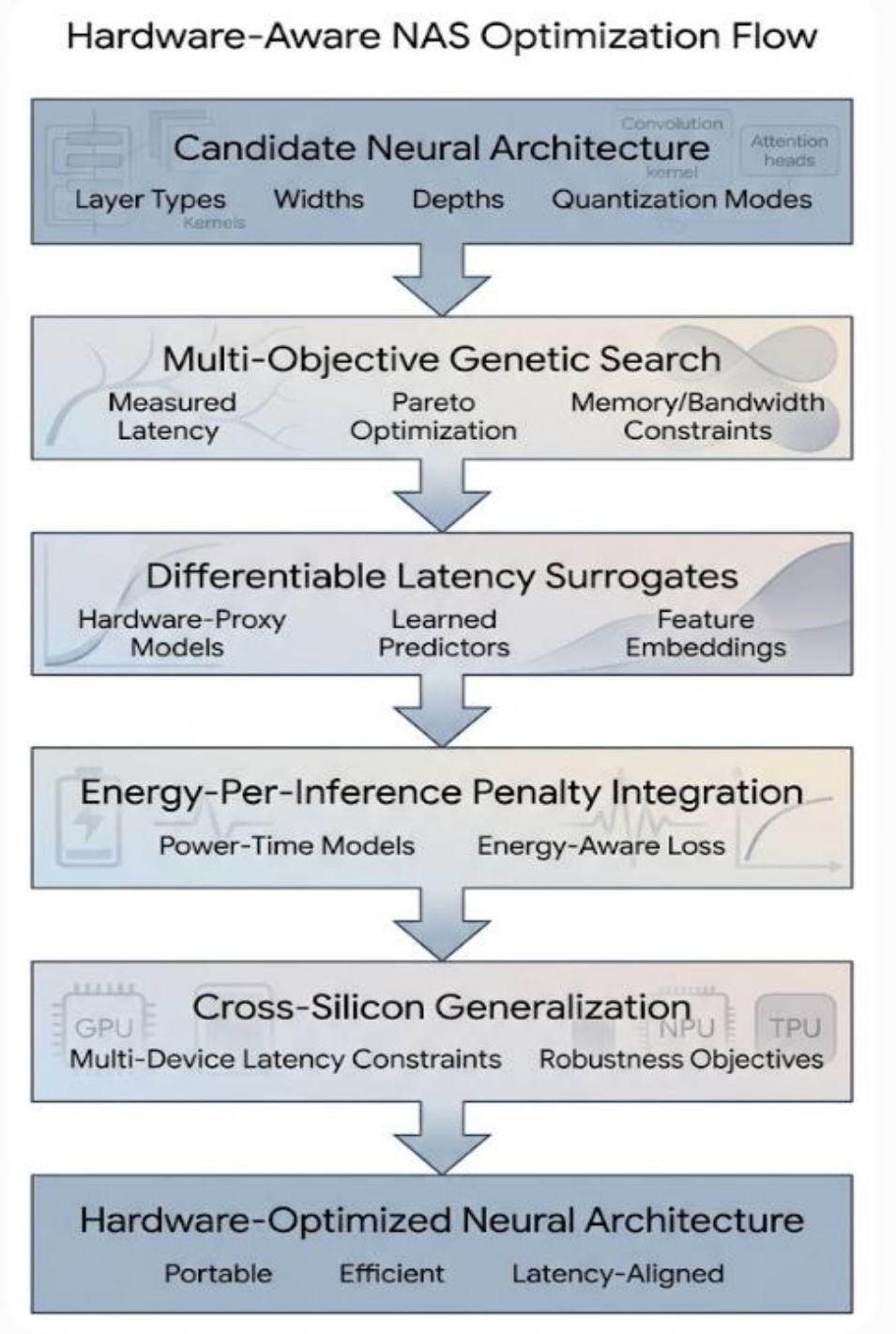


Figure 8.4-F3 — Hardware-Aware NAS Optimization Flow

Workflow illustrating how candidate neural architectures are evaluated and refined through multi-objective genetic search, differentiable latency estimation, energy-aware optimization, and cross-silicon evaluation to meet the performance, efficiency, and portability requirements of deployment hardware.

Legend:

The figure comprises six principal stages, connected by downward arrows to represent the progression from candidate architecture specification to hardware-optimized architecture.

- ***Candidate Neural Architecture:*** *Defines the architecture search space through design variables such as layer types, network widths and depths, and quantization modes.*
- ***Multi-Objective Genetic Search:*** *Explores candidate architectures using genetic operations such as mutation, crossover, and selection, with evaluation criteria that include inference latency, Pareto-based optimization, and memory or bandwidth constraints.*
- ***Differentiable Latency Surrogates:*** *Estimates device-specific inference latency using learned predictors, hardware-related features, and architectural representations, reducing the need to execute every candidate on physical hardware.*
- ***Energy-Per-Inference Penalty Integration:*** *Incorporates estimated or measured energy consumption into architecture evaluation through power–time models and energy-aware loss functions.*
- ***Cross-Silicon Generalization:*** *Evaluates candidate architectures across different hardware platforms, including graphics processing units (GPUs), neural processing units (NPUs), and tensor processing units (TPUs), using device-specific performance constraints and portability requirements.*
- ***Hardware-Optimized Neural Architecture:*** *Represents the selected architecture, with its suitability determined by task performance, inference latency, energy consumption, resource requirements, and compatibility with the intended deployment platforms.*

Figure 8.4-F3 presents hardware-aware neural architecture search (NAS) as a structured optimization pipeline that progressively refines candidate neural architectures according to the performance, energy, memory, and portability requirements of the intended deployment environment.

The search process incorporates architectural exploration, hardware-specific performance estimation, energy-aware optimization, and evaluation across different accelerator platforms. Each stage contributes information that helps determine which neural network configurations are suitable for deployment under practical hardware constraints.

Hardware-aware neural architecture search (NAS) begins by defining a candidate architecture and progressively refining its design according to the performance, energy, memory, and portability requirements of the intended deployment environment. The search process incorporates architectural exploration, hardware-specific performance estimation, energy-

aware optimization, and evaluation across different accelerator platforms. Each stage contributes information that helps determine which neural network configurations are suitable for deployment under practical hardware constraints.

Candidate Neural Architecture. The search begins with a representation of the neural network design space, including layer types, network widths and depths, and quantization modes. These parameters determine the model's computational structure, parameter count, activation-memory requirements, numerical precision, and potential for parallel execution. For example, increasing network width may improve predictive accuracy but also increase computation and memory traffic, while quantization can reduce storage and computational costs at the potential expense of model accuracy. Defining these architectural choices establishes the set of candidate configurations that NAS can explore.

Multi-Objective Genetic Search. Evolutionary search generates and evaluates alternative architectures through operations such as mutation, crossover, and selection. Each candidate is assessed against multiple objectives, including predictive quality, inference latency, memory consumption, and bandwidth requirements. Measured latency on the target hardware can provide empirical evidence of execution performance, while memory and bandwidth constraints help eliminate designs that exceed available resources. Pareto-based selection retains architectures that offer different trade-offs among competing objectives rather than assuming that one candidate is best in every dimension. This approach is particularly useful when improving one performance measure may degrade another.

Differentiable Latency Surrogates. Evaluating every candidate directly on physical hardware can be expensive, especially when the search space contains many architectural configurations. A latency surrogate addresses this problem by learning a relationship between architectural features and measured execution times. Inputs may include operator types, tensor dimensions, layer configurations, memory-access patterns, and hardware characteristics. Once trained, the model estimates the latency of new candidates without requiring a complete hardware benchmark for each one. When the surrogate is differentiable, its predictions can also provide gradients that support gradient-based architecture optimization. In practice, surrogate predictions should be calibrated against measurements from the intended hardware because estimation errors can lead the search toward architectures that perform poorly when executed.

Energy-Per-Inference Penalty Integration. Energy consumption introduces another constraint into architecture selection. An energy-aware objective incorporates estimated or measured inference energy into the search process, allowing the optimizer to account for the cost of executing a model as well as its predictive performance and latency.

For calculating energy consumed per inference:

Energy consumed = Average power × Inference duration

In mathematical notation:

$$\mathbf{E_{inf} = P_{avg} \times T_{inf}}$$

Where:

- E_{inf} is energy consumed per inference, measured in joules (J).
- P_{avg} is average power during inference, measured in watts (W).
- T_{inf} is inference duration, measured in seconds (s).

For example, if a neural network consumes an average of 50 watts for 0.2 seconds during inference:

$$E_{inf} = 50 \times 0.2 = 10 \text{ joules}$$

For integrating energy consumption into the NAS optimization objective

The optimization objective can be expressed as:

$$\mathbf{J(A) = L_{task}(A) + \lambda_E \times E_{inf}(A)}$$

Where:

- J(A) = combined optimization objective.
- A = candidate neural architecture.
- $L_{task}(A)$ = task-related loss for architecture A.
- $E_{inf}(A)$ = energy consumed per inference by architecture A.
- λ_E = weighting coefficient that controls the importance of energy efficiency.

The objective is minimized to balance predictive performance and energy consumption. A larger energy-weighting coefficient places greater emphasis on reducing energy use, although the task-loss and energy terms may need normalization to ensure that their relative contributions are meaningful.

3. Apply energy constraints

Alternatively, NAS can minimize task-related loss while requiring energy consumption to remain below a specified limit:

$$\textbf{Minimize: } L_{task}(A)$$

Subject to:

$$E_{inf}(A) \leq E_{max}$$

Where E_{max} is the maximum allowable energy consumption per inference.

This constrained formulation is useful when a device has a strict energy budget, such as a battery-powered embedded system.

Cross-Silicon Generalization. Neural architectures can behave differently across GPUs, neural processing units (NPUs), tensor processing units (TPUs), and other accelerators because these platforms differ in compute resources, memory hierarchies, supported numerical formats, compiler optimizations, and operator implementations. An architecture that performs well on one device may experience higher latency or greater energy consumption on another. Cross-silicon evaluation therefore compares candidate architectures across the hardware platforms relevant to deployment, using device-specific latency, energy, memory, and compatibility constraints. This evaluation can identify designs that perform consistently across multiple platforms or reveal when separate architecture configurations are needed for different devices. Portability must also account for software support, including compiler compatibility and the availability of optimized implementations for the operations used by the model.

Hardware-Optimized Neural Architecture. The search produces one or more candidate architectures that satisfy the application's requirements and offer favorable trade-offs among predictive performance, latency, energy consumption, memory usage, and platform compatibility. The final selection depends on the deployment objectives: a real-time control system may prioritize predictable latency, whereas a battery-powered device may place greater emphasis on energy per inference. A candidate selected through surrogate-based optimization should be benchmarked on the intended hardware, with measurements of latency, energy, memory usage, and task performance used to verify that it meets the required constraints. If validation reveals discrepancies between predicted and actual performance, the measurements can inform the performance models and guide further optimization.

The stages are interconnected rather than strictly isolated. Genetic search can use surrogate predictions to evaluate candidates efficiently; energy estimates can change which architectures remain attractive under a multi-objective criterion; and cross-silicon evaluation can expose trade-offs that are not apparent when optimizing for a single device. Updated hardware measurements can, in turn, improve the surrogates and influence subsequent search decisions. Although the workflow is presented as a sequence, practical NAS implementations may revisit

earlier stages as new candidates, performance estimates, or validation results become available.

The next discussion is to examine **multi-objective genetic search**, which initiates architectural exploration by generating alternative network configurations and evaluating their relative merits. By combining evolutionary operators with hardware-relevant fitness measures, this search can explore a diverse set of architectures while accounting for measured latency, predictive performance, and resource constraints. Its candidate evaluations also provide useful training data for latency surrogates, connecting empirical hardware measurements to the later stages of energy-aware optimization and cross-platform evaluation.

i. Multi-Objective AI Genetic Search Incorporating Measured Hardware Latency Signals

Multi-objective AI genetic search serves as the entry point to hardware-aware Neural Architecture Search (HW-NAS), establishing the evolutionary pressures that guide candidate architectures toward solutions that are simultaneously accurate, efficient, and hardware compatible. The AI-specific framing is particularly important because this process extends far beyond conventional heuristic optimization. Instead, it functions as a machine-guided exploration of an architectural design space in which each candidate network is represented as an evolving *architectural genome*. Within this framework, model structures act as digital organisms whose survival and reproduction are governed by a multi-dimensional fitness function encompassing not only predictive performance but also latency, energy consumption, memory footprint, bandwidth utilization, thermal behavior, and accelerator efficiency.

Through successive generations of selection, crossover, mutation, and evaluation, the search process progressively discovers architectures that balance algorithmic effectiveness with physical execution constraints. In this sense, evolution occurs simultaneously in both the computational and hardware domains. High-performing candidates are not merely those that achieve superior accuracy, but those that demonstrate favorable execution characteristics when mapped onto real accelerator fabrics, memory hierarchies, and communication infrastructures. As a result, multi-objective genetic search transforms architecture design from a purely model-centric exercise into a hardware–software co-design process in which neural-network topology and system-level performance evolve together toward deployment-ready solutions.

Architectural Genomes and Evolutionary Pressure

Each neural architecture A is encoded as a **genome vector** g_A, containing:

- layer types (conv, attention, MLP, depthwise, fused ops)
- structural hyperparameters (widths, depths, kernel sizes, head counts)
- quantization modes (bit-widths, per-channel vs per-tensor)

- fusion-friendly patterns (conv-BN-ReLU blocks, attention-softmax-scale chains)
- memory-access patterns (stride, dilation, tiling shape)

The genetic algorithm treats these genomes as mutable entities. Mutation operators perturb architectural parameters, crossover operators recombine structural motifs, and selection operators choose the fittest architectures for the next generation.

Mathematical Framing: Multi-Objective Fitness

The fitness function incorporates **measured hardware latency**, making the search explicitly grounded in real device behavior. If an architecture has accuracy Acc(A), measured latency L(A), memory footprint Mem(A), and bandwidth consumption BW(A), the fitness is:

$$F(A) = \omega_1 Acc(A) - \omega_2 L(A) - \omega_3 Mem(A) - \omega_4 BW(A).$$

This is a **multi-objective optimization problem**, where the search seeks architectures on the Pareto frontier:

$$\text{Pareto}(Acc, L, Mem, BW).$$

The AI system evaluates each architecture by compiling it into kernels, executing it on the target accelerator, and measuring latency under realistic conditions. This produces **ground-truth latency**, capturing effects that FLOPs cannot:

- tensor-core utilization efficiency
- warp divergence and thread-block imbalance
- systolic array tile alignment
- memory-bank conflicts
- cache thrashing
- quantization/dequantization overhead
- DRAM vs SRAM access ratios

These signals become part of the evolutionary pressure. Architectures that align naturally with hardware execution patterns survive; those that do not are eliminated.

AI-Driven Evolution: Learning Hardware-Aligned Patterns

Over successive generations, the AI system learns structural patterns that correlate directly with low latency:

- **Shallow-wide blocks** optimized for GPUs
- **Tile-aligned convolution shapes** tailored for NPUs
- **Matrix-multiplication-friendly layouts** structured for TPUs
- **Quantization-friendly operator sequences** that preserve precision
- **Fusion-friendly block structures** designed to minimize memory bandwidth overhead
- **Memory-efficient tensor layouts** maximizing cache locality

The genetic algorithm implicitly discovers these patterns through repeated evaluation and selection. This underscores a fundamental shift in the design paradigm: the system is not manually engineered to favor specific structural forms, but instead learns them organically through evolutionary feedback driven by empirical hardware measurements.

Hardware Implications

This stage ensures that the search begins with architectures that are already trending toward hardware-optimal forms. It reduces the burden on later stages (surrogates, energy penalties, cross-silicon constraints) by establishing a strong initial bias toward architectures that "fit" the hardware.

With genetic search establishing the evolutionary pressure that aligns architectures with real hardware behavior, the next challenge is scalability. Direct latency measurement is accurate but expensive, requiring compilation and execution for every candidate. To accelerate the search while preserving hardware fidelity, the pipeline introduces **hardware-proxy AI models**—differentiable latency-estimator surrogates trained to predict latency from architectural features. These surrogates allow gradient-based NAS to operate continuously over the architectural space, enabling rapid refinement without constant hardware evaluation. The next discussion explores how these AI models are constructed, trained, and integrated into the NAS loss function to provide fast, differentiable approximations of device-specific latency.

ii. Hardware-Proxy AI Models with Differentiable Latency-Estimator Surrogates

Hardware-proxy AI models serve as the second major pillar of hardware-aware NAS. They provide a fast, differentiable approximation of hardware latency, enabling gradient-based optimization over architectural parameters. This stage introduces an explicitly AI-driven

mechanism: a learned surrogate model that predicts latency from architectural features, allowing NAS to operate continuously rather than relying solely on discrete evolutionary evaluations.

Latency Surrogates as Learned Hardware Simulators

A hardware-proxy latency surrogate is an AI model trained to approximate the behavior of a physical accelerator. It acts as a **learned hardware simulator**, capturing device-specific execution characteristics without requiring full compilation and runtime measurement for every candidate architecture.

The surrogate model f_θ is trained on a dataset of architectures and their measured latencies:

$$\theta = \operatorname{argmin}_\theta \sum_A \left(L(A) - f_\theta(x_A)\right)^2,$$

where:

- x_A is the feature vector describing architecture A
- L(A) is the measured hardware latency
- $f_\theta(x_A)$ is the predicted latency

This transforms NAS into a **hybrid AI system**: part evolutionary search, part learned hardware modeling.

Feature Engineering: Encoding Architectural Structure for AI Prediction

The feature vector x_A encodes structural and hardware-relevant properties of the architecture, including:

- convolution kernel sizes, strides, dilations
- attention head counts, sequence lengths, projection dimensions
- tensor shapes and memory footprints
- quantization bit-widths and scaling modes
- operator fusion patterns
- tiling and layout characteristics
- estimated DRAM/SRAM access ratios

These features allow the surrogate to learn correlations between architectural structure and hardware latency.

Mathematical Framing: Differentiable Latency Prediction

The surrogate produces a differentiable latency estimate:

$$\hat{L}(A) = f_\theta(x_A),$$

which is incorporated directly into the NAS loss function:

$$L_{NAS}(A) = L_{task}(A) + \alpha \hat{L}(A).$$

Because $\hat{L}(A)$ is differentiable, gradient-based NAS can optimize architectural parameters such as:

- kernel sizes
- hidden-layer widths
- depth multipliers
- attention head counts
- quantization bit-widths

This enables **continuous optimization**, something impossible with raw hardware measurements.

AI-Driven Learning: Capturing Device-Specific Execution Patterns

The surrogate learns complex hardware behaviors that are difficult to model analytically:

- tensor-core utilization efficiency
- warp scheduling and divergence patterns
- systolic array tile alignment
- shared-memory bank conflicts
- cache reuse and eviction patterns
- quantization/dequantization overhead
- pipeline stall probabilities

These behaviors emerge naturally from the training data, allowing the surrogate to act as a **device-specific latency oracle**.

Acceleration of NAS: Reducing Hardware Evaluation Cost

Direct latency measurement requires:

- compiling the architecture
- generating kernels
- executing them on hardware
- collecting timing data

This is expensive and slow. Surrogates reduce evaluation cost by several orders of magnitude, enabling:

- rapid exploration of architectural variants
- continuous gradient-based refinement
- large-scale NAS experiments
- multi-objective optimization with latency as a differentiable term

The surrogate does not replace hardware measurement entirely; instead, it acts as a **fast inner loop**, while periodic hardware measurements recalibrate the surrogate.

Hardware Implications

By providing fast, differentiable latency estimates, surrogates allow NAS to explore architectures that would be infeasible to evaluate exhaustively. They enable fine-grained optimization of architectural parameters that directly influence hardware execution, producing models that are tightly aligned with device-specific performance characteristics.

With differentiable latency surrogates enabling rapid, continuous exploration of the architectural space, the next step is to incorporate energy consumption into the optimization objective. Latency alone does not capture the full cost of inference, especially for mobile, embedded, and large-scale deployments where power efficiency is critical. To address this, hardware-aware NAS introduces **energy-per-inference penalty functions**, allowing the AI system to optimize architectures not only for speed but also for energy efficiency. The following discussion examines how these energy models are constructed, how they interact with latency-aware optimization, and how they reshape the search landscape toward architectures that minimize power consumption while maintaining accuracy.

iii. Energy-Per-Inference AI Penalty Functions Embedded in NAS Optimization Costs

Energy-per-inference penalty functions introduce a critical dimension into hardware-aware NAS: **power efficiency as an explicit AI-optimized objective**. While latency determines responsiveness, energy determines feasibility—whether a model can run on battery-powered devices, embedded systems, or large-scale inference clusters without exceeding thermal or operational budgets. This stage reframes NAS as a **multi-constraint AI optimization problem**, where architectures must satisfy both algorithmic and physical constraints.

Energy as a Learned, Optimized Behavioral Constraint

In this stage, the AI system treats energy consumption as a **behavioral property** of the architecture—something that can be learned, predicted, and optimized. Just as accuracy reflects the model's cognitive performance, energy reflects its physical footprint. NAS becomes a dual-domain AI process: optimizing both the *intelligence* of the model and the *cost* of running that intelligence.

The NAS loss function incorporates energy explicitly:

$$L(A) = L_{task}(A) + \beta E(A),$$

where:

- $L_{task}(A)$ is the task-specific loss (e.g., cross-entropy)
- $E(A)$ is the energy-per-inference estimate
- β controls the trade-off between accuracy and energy

This transforms NAS into a **multi-objective AI optimization**, where architectures must satisfy both cognitive and physical constraints.

Mathematical Framing: Power-Time Energy Modeling

Energy consumption is modeled as:

$$E(A) = \sum_{i \in \text{ops}(A)} P_i \cdot t_i,$$

where:

- P_i is the instantaneous power draw of operator i
- t_i is the execution time of operator i

This formulation captures the fact that energy is not simply proportional to FLOPs. Instead, it depends on:

- memory access patterns
- quantization modes
- operator fusion opportunities
- tensor shapes and tiling
- hardware-specific power curves

The AI system learns these relationships through repeated evaluation, forming an implicit model of how architectural structure influences energy.

AI-Driven Learning: Discovering Energy-Efficient Architectural Motifs

Over time, the NAS pipeline learns structural motifs that reduce energy consumption:

- depthwise convolutions instead of full convolutions
- fused conv-BN-activation blocks
- low-precision quantization paths
- attention blocks with reduced head counts
- smaller projection dimensions
- memory-efficient tensor layouts
- operator sequences that minimize DRAM access

These motifs emerge naturally from the optimization process. The AI system does not need to be told which structures are energy-efficient—it **discovers** them through the penalty function.

Energy-Latency Interaction: Joint Optimization

Energy and latency are not independent. Many operations that reduce latency also reduce energy, but not always. For example:

- aggressive parallelization reduces latency but may increase power draw
- quantization reduces energy but may increase latency if dequantization is required
- fused operators reduce both latency and energy by minimizing memory traffic

The NAS pipeline learns these trade-offs automatically. The AI system explores architectures that balance both objectives, discovering Pareto-optimal designs that minimize energy without sacrificing responsiveness.

Hardware Implications

Energy-aware NAS produces architectures that:

- run longer on battery-powered devices
- reduce thermal load on embedded systems
- lower operational cost in large inference clusters
- minimize cooling requirements
- reduce peak power draw during bursts of computation

This stage ensures that the architectures discovered by NAS are not only fast but also sustainable and deployable across power-constrained environments.

With energy-per-inference penalties embedded into the NAS optimization cost, the search process now accounts for both latency and power efficiency. However, modern AI systems must operate across a diverse ecosystem of accelerators—GPUs, NPUs, TPUs, CPUs, and custom ASICs—each with unique execution characteristics. To ensure that discovered architectures remain efficient across this heterogeneous landscape, hardware-aware NAS introduces **cross-silicon generalization constraints**, enabling the AI system to optimize models for multiple devices simultaneously. The next discussion explores how NAS incorporates multi-device latency signals, robustness objectives, and cross-hardware performance modeling to produce architectures that generalize across silicon generations and accelerator families.

iv. Cross-Silicon AI Architecture Generalization for Heterogeneous Accelerator Targets

Cross-silicon generalization is the final and most outward-facing dimension of hardware-aware NAS. It ensures that the architectures discovered by the AI system are not narrowly optimized for a single accelerator but instead perform robustly across a heterogeneous ecosystem of devices—GPUs, NPUs, TPUs, CPUs, and custom ASICs. This stage introduces an explicitly AI-driven capability: **multi-device performance modeling**, where the NAS pipeline learns how architectural structures behave across different silicon topologies and incorporates that knowledge into the optimization objective.

Multi-Device Performance as a Learned Generalization Task

In this stage, the AI system treats hardware diversity as a **generalization challenge** analogous to

domain adaptation in machine learning. Each accelerator type represents a "domain" with its own execution characteristics:

- GPUs emphasize warp scheduling, tensor-core utilization, and memory coalescing.
- NPUs emphasize tile-aligned convolution shapes, fused operator blocks, and SRAM locality.
- TPUs emphasize systolic array alignment, matrix multiplication throughput, and static memory planning.
- CPUs emphasize cache hierarchy behavior, branch prediction, and vectorization.
- ASICs emphasize fixed-function pipelines, quantization paths, and deterministic dataflow.

The NAS pipeline learns how architectural motifs interact with these domains, enabling it to discover architectures that generalize across them.

Mathematical Framing: Multi-Device Latency Constraints

If latency is measured or predicted for multiple devices $d \in D$, the NAS objective becomes:

$$L(A) = L_{task}(A) + \sum_{d \in D} \alpha_d L_d(A),$$

where:

- $L_d(A)$ is latency on device d,
- α_d is the weighting factor for that device.

This formulation transforms NAS into a **multi-domain optimization problem**, where architectures must satisfy performance constraints across several hardware targets simultaneously.

AI-Driven Learning: Discovering Cross-Silicon Architectural Motifs

Through repeated evaluation and surrogate-based prediction, the AI system learns structural motifs that generalize well across silicon types:

- **Balanced compute-to-memory ratios** that avoid bottlenecks on both SIMD and systolic hardware.
- **Quantization-friendly operator sequences** that map efficiently to NPUs and ASICs.

- **Tile-aligned tensor shapes** that reduce fragmentation on NPUs and TPUs.
- **Fusion-friendly blocks** that minimize DRAM traffic across all accelerators.
- **Moderate depth-width tradeoffs** that avoid extreme specialization for any single device.
- **Operator layouts** that maintain stable performance across varying memory hierarchies.

These motifs emerge naturally from the optimization process. The AI system does not need explicit rules for each device; instead, it **learns** cross-silicon invariants through multi-device feedback.

Robustness Objectives: Avoiding Over-Specialization

A key risk in hardware-aware NAS is over-specialization—discovering architectures that perform exceptionally well on one device but poorly on others. Cross-silicon constraints prevent this by penalizing architectures that exhibit large performance variance across devices:

$$\mathrm{Var}_D(L_d(A)) = \frac{1}{|D|} \sum_{d \in D} (L_d(A) - L(A))^2,$$

where L(A) is mean latency across devices.

NAS minimizes this variance term, encouraging architectures that maintain stable performance across heterogeneous accelerators.

Hardware Implications

Cross-silicon generalization produces architectures that:

- run efficiently on cloud GPUs, mobile NPUs, and edge TPUs
- maintain predictable latency across hardware generations
- reduce the need for device-specific model variants
- simplify deployment pipelines
- increase portability and future-proofing
- reduce engineering overhead for multi-platform inference

This stage ensures that the architectures discovered by NAS are not only optimized for today's hardware but also resilient to tomorrow's.

Hardware-aware NAS transforms neural architecture search from a purely algorithmic

exploration into a multi-constraint AI optimization pipeline that integrates real device behavior, learned hardware proxies, energy modeling, and cross-silicon robustness. Multi-objective genetic search anchors the process in empirical latency signals, ensuring that architectures evolve toward hardware-aligned forms. Differentiable latency surrogates accelerate exploration by providing fast, AI-driven predictions of device-specific performance. Energy-per-inference penalties introduce power efficiency as a first-class optimization objective, enabling NAS to discover architectures suitable for mobile, embedded, and large-scale inference environments. Cross-silicon generalization ensures that these architectures remain efficient across heterogeneous accelerators, producing models that are portable, robust, and future-proof. Together, these mechanisms form a comprehensive hardware-aware NAS framework that designs neural architectures intrinsically optimized for the physical realities of modern AI hardware.

With hardware-aware NAS producing architectures that are structurally aligned with device constraints and capable of efficient execution across heterogeneous accelerators, the next challenge is ensuring that these architectures remain reliable under real-world operating conditions. Modern AI systems must operate under dynamic thermal loads, fluctuating memory availability, transient hardware faults, and runtime variability across silicon generations. To address these challenges, the next discussion introduces **silicon-to-software AI observability**, where runtime telemetry, execution-path monitoring, and physical fault-mitigation hooks provide continuous visibility into model behavior on actual hardware. This observability layer closes the loop between architecture design and deployment, enabling AI systems to detect anomalies, adapt to hardware conditions, and maintain correctness even under adverse physical environments.

d. Silicon-to-Software AI Observability with Runtime Telemetry and Physical Fault-Mitigation Hooks

Silicon-to-software AI observability connects the physical operating state of AI hardware with the software mechanisms responsible for executing, monitoring, and managing AI workloads. It enables the runtime to use information about processor utilization, temperature, power consumption, memory pressure, communication activity, and hardware errors when making execution decisions. Rather than treating an accelerator as a black-box inference engine, this approach establishes a feedback path through which hardware telemetry informs scheduling, resource allocation, performance optimization, and fault management. Its effectiveness depends on the availability, accuracy, and timeliness of telemetry, as well as the runtime's ability to translate observed conditions into appropriate responses.

High-Frequency AI Hardware-Counter Profiling and Coordinated Telemetry Orchestration Layers

High-frequency hardware-counter profiling provides AI systems with detailed, time-sensitive information about the physical execution characteristics of neural network workloads. Depending on the hardware platform, telemetry may be collected from GPU execution units and warp schedulers, NPU processing tiles, TPU systolic arrays, CPU vector units, memory controllers, thermal sensors, and power-management mechanisms. These sources provide complementary measurements of computational utilization, instruction execution, memory activity, temperature, power consumption, and operating frequency.

The value of hardware-counter profiling lies in its ability to correlate software execution with underlying hardware behavior. For example, low accelerator utilization combined with high memory-access latency may indicate a data-delivery bottleneck, while sustained high utilization and rising temperature may indicate thermal pressure. Sampling frequency and collection overhead must be carefully managed so that profiling provides sufficiently timely information without significantly disrupting the workload being monitored.

Telemetry as a Real-Time Feedback Signal

The AI runtime can treat hardware telemetry as a feedback signal for monitoring and optimizing execution. A coordinated telemetry-orchestration layer collects and correlates measurements, identifies deviations from expected operating conditions, and supplies relevant information to scheduling, resource-management, and fault-mitigation mechanisms. Depending on the system's requirements, these mechanisms may:

- Monitor execution behavior and identify performance bottlenecks.
- Detect anomalies in computational utilization, memory activity, temperature, power consumption, or hardware error reports.
- Adjust workload scheduling and resource allocation in response to changing operating conditions.
- Tune supported kernel parameters or select alternative execution configurations.
- Trigger fault-detection, recovery, or isolation procedures when hardware error signals or predefined thresholds indicate a problem.

AI-driven analytics can supplement conventional monitoring rules by identifying complex patterns across multiple telemetry sources or estimating emerging performance and reliability

problems. The runtime can then use these results to recommend or initiate appropriate adaptations, subject to predefined constraints and validation requirements.

This arrangement forms a closed-loop control process: hardware telemetry describes the current operating state, the orchestration layer evaluates that information, and the runtime applies an appropriate response. Subsequent measurements help determine whether the response improved performance or restored operation within the required limits. To support real-time applications, the complete feedback loop—including measurement, analysis, decision-making, and actuation—must operate within the application's timing budget. Deterministic safeguards and validated fault-handling policies remain necessary whenever unpredictable adaptation could compromise timing, correctness, or safety.

Runtime telemetry and hardware-state monitoring. Modern AI accelerators expose information through hardware performance counters, thermal sensors, voltage and current monitors, memory controllers, communication interfaces, and error-reporting mechanisms. Performance counters can reveal cache misses, memory-bandwidth utilization, processor occupancy, and accelerator-unit activity. On GPUs and other parallel processors, additional metrics may indicate execution divergence, tensor-unit utilization, or resource contention, depending on the hardware's monitoring capabilities. Thermal sensors track temperature changes that may lead to dynamic voltage and frequency scaling (DVFS) or thermal throttling. Power monitors characterize energy consumption and transient changes in electrical demand, while memory and interconnect telemetry can reveal congestion, contention, and communication bottlenecks.

These signals provide complementary views of system behavior. For example, high accelerator utilization does not necessarily indicate efficient execution: a workload may remain busy while waiting for data from memory. Similarly, elevated temperature may reflect sustained computational demand, inadequate cooling, or a combination of operating conditions. Interpreting telemetry therefore requires correlating measurements across compute, memory, power, and thermal subsystems rather than relying on a single metric.

Telemetry-driven runtime optimization. The runtime can use hardware-state information to adapt execution to changing workloads and operating conditions. When thermal limits approach, a runtime may reduce workload intensity, adjust scheduling, or move suitable tasks to another available processing unit. When memory-bandwidth contention becomes significant, it may reschedule operators, improve data locality, reuse intermediate tensors, or fuse operations to reduce data movement. When power consumption approaches a configured budget, the system may adjust execution frequency, batch size, or workload placement, provided that these changes remain compatible with application requirements.

Such adaptations must account for the relationship between resource utilization and end-to-end performance. Operator fusion, for example, can reduce memory traffic but may increase register pressure or limit parallelism. Moving a workload to another accelerator may alleviate thermal or computational pressure but introduce data-transfer overhead. Runtime optimization must therefore evaluate both the expected benefit of an intervention and its associated costs. Where predictable execution time is required, adaptation policies should also account for worst-case or high-percentile latency, not just average performance.

Physical fault detection and mitigation. Runtime observability also connects hardware error signals to software-level fault-management mechanisms. Error-correcting code (ECC) reports can identify and, on supported hardware, correct certain memory errors. Parity checks can detect inconsistencies in protected data or communication paths. Watchdog timers can identify tasks that exceed expected execution intervals, while link-health indicators can reveal communication failures or degradation. Depending on the platform, additional mechanisms may report processor faults, memory errors, or abnormal operating conditions.

These signals can initiate a sequence of fault-management actions. The system may record diagnostic information, retry an operation, restart an affected component, isolate an unavailable resource, or redirect execution to a healthy device. Redundant computation or replicated models may provide additional protection when supported by the system architecture and permitted by the application's latency and resource budgets. However, detection does not automatically establish the cause of a fault, and recovery is not always possible. A robust design must define fault thresholds, distinguish transient events from persistent failures where feasible, and specify the conditions under which continued execution is safe.

Cross-layer feedback and predictive maintenance. Silicon-to-software observability becomes more effective when telemetry is analyzed across multiple layers. Hardware counters describe execution behavior, operating-system and runtime metrics reveal scheduling and resource contention, and application-level measurements indicate whether the system is meeting its task and timing requirements. Correlating these observations can help distinguish hardware limitations from software inefficiencies and identify recurring performance degradation.

Long-term telemetry can also support predictive maintenance. Trends in corrected memory errors, thermal excursions, power behavior, or link-reliability indicators may reveal changes that warrant further investigation. Statistical models or machine-learning techniques can analyze these trends to estimate the likelihood of particular failure conditions, provided that sufficient representative data are available. Such estimates should be treated as evidence for diagnosis or preventive action rather than definitive proof that a component is about to fail. Appropriate

validation and uncertainty assessment are especially important when maintenance or recovery decisions affect safety-critical operation.

Real-time constraints and fault resilience. Observability is particularly important in systems that must operate under strict timing, reliability, or safety requirements. Telemetry collection and analysis consume processing resources and may introduce overhead, so monitoring frequency, data volume, and response latency must be considered during system design. The runtime must also distinguish between actions that can be performed dynamically and those that require a controlled transition or system restart. For a real-time AI application, a mitigation strategy is useful only if it can respond within the available timing budget or move the system into a defined safe state when that budget can no longer be met.

Observability alone does not guarantee deterministic execution, fault tolerance, or safety. These properties require explicit timing analysis, validated fault-handling policies, appropriate hardware protection mechanisms, and verification of the complete system. Telemetry provides the information needed to detect deviations and initiate responses; the design of the control and recovery mechanisms determines whether those responses preserve required behavior.

Integration with hardware-aware neural architecture search. Silicon-to-software observability complements hardware-aware neural architecture search (NAS) by connecting design-time optimization with actual deployment behavior. Hardware-aware NAS selects architectures using performance estimates, energy models, resource constraints, and measurements from target platforms. Runtime observability then reveals how the selected architecture behaves under real operating conditions, including changing workloads, thermal limits, memory contention, and hardware errors. These observations can identify discrepancies between predicted and measured performance and provide data for recalibrating latency or energy models, refining optimization constraints, and guiding subsequent architecture searches.

This feedback loop connects architecture design, hardware execution, and operational monitoring within a unified hardware–software co-design process. Hardware-aware NAS helps identify architectures suited to the intended platform, while runtime observability assesses whether those architectures continue to meet operational requirements after deployment. Together with validated fault-detection and mitigation mechanisms, these techniques support adaptive optimization, resource management, and resilience across changing operating conditions.

Mathematical Framing: Counter-Driven Performance Models

Let C(t) be the vector of hardware counters at time t. The AI system maintains a predictive model:

$$\hat{S}(t) = f_{\phi}(C(t)),$$

where $\hat{S}(t)$ is the predicted system state (latency, thermal load, memory pressure). Deviations between predicted and actual states indicate anomalies:

$$\Delta(t) = S_{\text{actual}}(t) - \hat{S}(t).$$

Large deviations trigger mitigation actions.

Operational Impact

This layer enables:

- real-time detection of thermal throttling
- early identification of memory-bank conflicts
- detection of warp divergence spikes
- monitoring of quantization overhead
- dynamic tuning of fused operator blocks

It is the foundation of silicon-to-software observability.

In-Flight AI Tensor Integrity Checks for Transient Bit-Flip Detection and Recovery

Transient bit-flips occur due to cosmic rays, voltage fluctuations, thermal stress, and silicon aging. In-flight tensor integrity checks detect and correct these errors before they propagate.

Integrity Checking as Cognitive Self-Monitoring

The AI runtime performs **self-monitoring**, analogous to biological error-correction mechanisms. It continuously verifies tensor integrity using:

- parity bits
- ECC (error-correcting codes)
- checksum validation
- hash-based tensor fingerprints
- statistical anomaly detection

Mathematical Framing: Tensor Consistency Verification

For a tensor T, the runtime computes a consistency signature:

$$\sigma(T) = h(T),$$

where h is a hash or checksum function. During execution:

$$\sigma(T_{\text{expected}}) \;\; \sigma(T_{\text{observed}}).$$

If mismatched, the AI system triggers:

- tensor reconstruction
- re-execution of the operator
- fallback to redundant computation paths
- isolation of faulty memory regions

Operational Impact

This layer prevents:

- silent data corruption
- cascading numerical errors
- incorrect model outputs
- instability in quantized pipelines

It is essential for mission-critical and safety-critical AI deployments.

Dynamic AI Faulty-Core Isolation with Automatic Model Re-Routing and Execution Failover

Accelerators contain many compute cores—SMs, tiles, MAC arrays, vector units. Some may degrade or fail during operation. Dynamic faulty-core isolation detects malfunctioning units and reroutes execution.

Fault Isolation as Adaptive Neural Routing

The AI runtime behaves like a biological neural system rerouting signals around damaged neurons. It identifies faulty cores using:

- abnormal latency spikes
- incorrect tensor signatures

- thermal anomalies
- repeated ECC corrections
- inconsistent hardware-counter patterns

Mathematical Framing: Core-Reliability Scoring

Each core k receives a reliability score:

$$R_k = g(C_k, E_k, T_k),$$

where:

- C_k = counter anomalies
- E_k = error-correction events
- T_k = thermal deviations

Cores with $R_k < \tau$ are isolated.

Execution is rerouted using a dynamic mapping function:

$$M: \text{ops} \rightarrow \text{healthy cores}.$$

Operational Impact

This layer enables:

- graceful degradation
- uninterrupted inference
- automatic failover
- extended hardware lifespan
- resilience against partial silicon failure

It is crucial for long-running AI services and edge devices.

Predictive AI Silicon-Wear Telemetry Integrated with Cloud-Scale Orchestration Feedback Loops

Silicon degrades over time due to electromigration, thermal cycling, and voltage stress. Predictive telemetry models this wear and integrates with cloud orchestration.

Wear Modeling as Long-Term Predictive Cognition

The AI system learns a **long-term predictive model** of silicon health:

$$\hat{W}(t) = f_{\psi}(C(t), T(t), E(t)),$$

where:

- C(t) = hardware counters
- T(t) = thermal history
- E(t) = error-correction events

The model predicts future degradation:

$$W_{\text{future}} = \hat{W}(t + \Delta).$$

Cloud-Scale Feedback Loops

Predicted wear feeds into orchestration systems that:

- migrate workloads
- rebalance clusters
- adjust cooling profiles
- schedule maintenance
- retire aging hardware gracefully

Operational Impact

This layer ensures:

- long-term reliability
- reduced downtime
- proactive fault mitigation
- optimized hardware lifecycle management

It closes the loop between silicon telemetry and cloud-scale AI operations.

The four observability mechanisms—high-frequency hardware-counter profiling, in-flight tensor

integrity checks, dynamic faulty-core isolation, and predictive silicon-wear telemetry—form a layered defense system that allows AI workloads to operate reliably across diverse and aging hardware. To consolidate these mechanisms into a clear structural overview, Table 8.4-F4 organizes the core dimensions of silicon-to-software observability, highlighting their operational purpose, AI-driven framing, and the specific mitigation capabilities they introduce. This table provides a concise architectural map of how runtime telemetry and fault-mitigation hooks collectively transform the AI execution environment into a resilient, self-monitoring, and self-correcting system.

Table 8.4-F4 presents the foundational dimensions that define silicon-to-software observability in modern AI systems. Each dimension corresponds to a distinct runtime capability: real-time hardware telemetry, tensor-level integrity verification, adaptive isolation of faulty compute units, and predictive modeling of long-term silicon wear. Together, these capabilities form a unified observability framework that spans from the lowest physical counters to the highest orchestration layers. The table clarifies how each dimension contributes to runtime reliability, how AI framing transforms telemetry into actionable intelligence, and how these mechanisms collectively ensure correctness and continuity under real-world operating conditions.

Table 8.4-F4 — Silicon-to-Software AI Observability Dimensions

Dimension	Core Purpose	Key Mechanisms	AI Framing	Operational Impact
High-Frequency Hardware-Counter Profiling	Real-time visibility	Warp counters, tile metrics, thermal sensors	Telemetry as feedback signals	Detects anomalies, tunes execution
In-Flight Tensor Integrity Checks	Prevent silent corruption	ECC, checksums, fingerprints	Self-monitoring	Ensures correctness under transient faults
Dynamic Faulty-Core Isolation	Maintain availability	Reliability scoring, rerouting	Adaptive neural routing	Enables failover and graceful degradation
Predictive Silicon-Wear Telemetry	Long-term reliability	Wear modeling, cloud feedback	Predictive cognition	Optimizes lifecycle and

Dimension	Core Purpose	Key Mechanisms	AI Framing	Operational Impact
				reduces downtime

The first dimension, high-frequency hardware-counter profiling, provides the AI runtime with continuous visibility into the physical execution characteristics of the model. Warp metrics, tile counters, thermal sensors, and memory-controller signals act as real-time feedback inputs. The AI system interprets these counters through predictive models, enabling anomaly detection and dynamic tuning of execution paths. This dimension establishes the sensory foundation of silicon-to-software observability.

The second dimension, in-flight tensor integrity checks, protects the AI system from transient bit-flips and silent data corruption. Using ECC, checksums, and tensor fingerprints, the runtime performs continuous self-verification. This AI framing treats integrity checking as cognitive self-monitoring, ensuring that numerical correctness is preserved even under thermal stress, voltage fluctuations, or cosmic-ray events. It prevents small physical faults from cascading into large-scale inference errors.

The third dimension, dynamic faulty-core isolation, introduces adaptive resilience. By scoring compute cores based on reliability signals—counter anomalies, ECC events, thermal deviations—the AI runtime identifies malfunctioning units and reroutes execution around them. This mechanism behaves like adaptive neural routing, preserving availability and enabling graceful degradation. It is essential for long-running inference services and edge deployments where hardware cannot be replaced immediately.

The fourth dimension, predictive silicon-wear telemetry, extends observability into long-term reliability. By modeling wear patterns using thermal history, counter trends, and error-correction events, the AI system predicts future degradation. These predictions feed into cloud-scale orchestration loops that rebalance workloads, schedule maintenance, and retire aging hardware gracefully. This dimension transforms observability from reactive fault handling into proactive lifecycle management.

Together, the dimensions in Table 8.4-F4 illustrate how silicon-to-software observability transforms AI execution into a self-aware, fault-tolerant, and future-proof system. Each dimension contributes a unique capability—real-time sensing, self-verification, adaptive routing, and predictive cognition—forming a comprehensive runtime framework that ensures correctness, availability, and resilience across heterogeneous and evolving hardware

environments.

The observability dimensions summarized in Table 8.4-F4 establish the conceptual scaffolding for runtime reliability in modern AI systems. They describe how hardware telemetry, tensor integrity verification, faulty-core isolation, and predictive wear modeling collectively form a multi-layered defense against physical faults and execution anomalies. Figure 8.4-F4 translates these dimensions into a visual flow, illustrating how signals originating at the silicon level propagate upward through increasingly sophisticated software-driven mitigation layers. This figure reinforces the idea that observability is not a single mechanism but a coordinated, hierarchical pipeline that transforms raw hardware counters into actionable intelligence and ultimately into fault-tolerant AI execution.

Figure 8.4-F4 depicts the full runtime observability pipeline that enables AI systems to maintain correctness and resilience under real-world hardware conditions. Beginning with high-frequency hardware-counter telemetry, the flow progresses through tensor integrity checks, faulty-core isolation, and predictive silicon-wear modeling before culminating in reliable, fault-tolerant AI execution. Each block represents a distinct observability layer, and the downward arrows emphasize the sequential transformation of raw physical signals into structured mitigation actions. The figure highlights how silicon-level data is continuously interpreted, validated, and acted upon by software-level intelligence to preserve system stability.

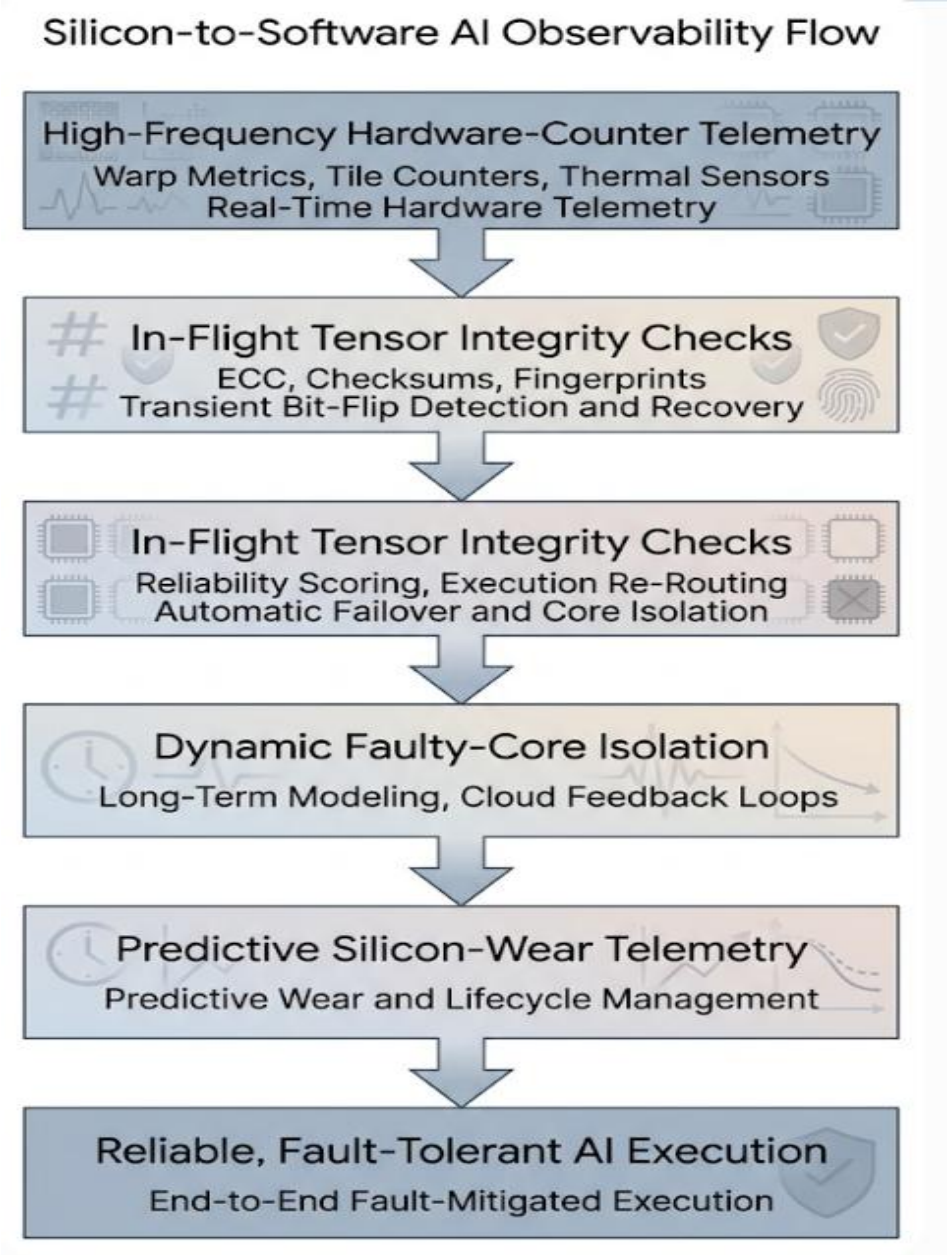


Figure 8.4-F4 — Silicon-to-Software AI Observability Flow
A layered runtime pipeline showing how hardware telemetry, tensor integrity verification, faulty-core isolation, and predictive silicon-wear modeling combine to produce reliable, fault-tolerant AI execution across heterogeneous and aging accelerators

Legend:

- ***High-Frequency Hardware-Counter Telemetry*** *— real-time signals from warp schedulers, tile engines, thermal sensors, and memory controllers.*

- ***In-Flight Tensor Integrity Checks*** *— ECC, checksums, and fingerprinting mechanisms that detect transient bit-flips and prevent silent corruption.*
- ***Dynamic Faulty-Core Isolation*** *— reliability scoring and execution re-routing that bypass malfunctioning compute units.*
- ***Predictive Silicon-Wear Telemetry*** *— long-term degradation modeling integrated with cloud-scale orchestration feedback loops.*
- ***Reliable, Fault-Tolerant AI Execution*** *— the final stabilized runtime environment resulting from coordinated observability layers.*

Figure 8.4-F4 begins with **high-frequency hardware-counter telemetry**, representing the raw sensory layer of the observability stack. Warp metrics, tile counters, and thermal readings provide continuous insight into the physical behavior of the accelerator. These signals act as the earliest indicators of anomalies such as throttling, memory contention, or unexpected execution stalls.

The flow then moves into **in-flight tensor integrity checks**, where ECC, checksums, and fingerprinting mechanisms verify the correctness of tensors as they move through the compute pipeline. This layer prevents transient bit-flips from silently corrupting model outputs, ensuring numerical stability even under thermal or voltage stress.

Next, the diagram transitions into **dynamic faulty-core isolation**, where the runtime identifies malfunctioning compute units through reliability scoring and reroutes execution around them. This adaptive behavior allows the system to maintain availability even when parts of the silicon degrade or fail, enabling graceful degradation rather than catastrophic failure.

The fourth layer, **predictive silicon-wear telemetry**, shifts the focus from immediate fault detection to long-term reliability. By modeling wear patterns using historical thermal data, counter trends, and error-correction events, the system forecasts future degradation. These predictions feed into cloud-scale orchestration systems that rebalance workloads, schedule maintenance, and retire aging hardware proactively.

Finally, the flow culminates in **reliable, fault-tolerant AI execution**, representing the stabilized runtime environment produced by the coordinated action of all preceding layers.
Figure 4.10-125 makes clear that observability is not a single mechanism but a multi-layered pipeline that transforms raw hardware signals into structured mitigation strategies, ensuring correctness, resilience, and continuity across heterogeneous and evolving silicon.

With the observability dimensions now clearly structured in Table 8.4-F4 and visually contextualized in Figure 8.4-F4, the next step is to examine how silicon-level signals initiate the

entire fault-tolerance pipeline. The observability stack begins at the physical substrate of the accelerator, where high-frequency hardware counters—warp metrics, tile-engine statistics, thermal readings, voltage fluctuations, and memory-controller signals—provide the raw sensory input that drives all higher-level mitigation behaviors. These counters form the earliest and most granular indicators of performance drift, thermal stress, or emerging silicon anomalies. Understanding how these signals are captured, orchestrated, and interpreted by AI-driven telemetry layers is essential, because this first stage determines the fidelity, responsiveness, and reliability of every subsequent integrity check, isolation mechanism, and predictive wear model. The following discussion explores how coordinated telemetry orchestration transforms raw hardware counters into actionable intelligence that anchors the entire silicon-to-software observability framework.

i. High-Frequency AI Hardware-Counter Profiling with Coordinated Telemetry Orchestration Layers

High-frequency hardware-counter profiling is the foundational sensory layer of silicon-to-software observability. It provides the AI runtime with continuous, fine-grained visibility into the physical state of the accelerator. Modern GPUs, NPUs, TPUs, CPUs, and ASICs expose hundreds of hardware counters—warp metrics, tile-engine statistics, systolic-array utilization, cache-miss rates, thermal readings, voltage fluctuations, and memory-controller signals. These counters form the raw telemetry stream that drives all higher-level fault-mitigation behaviors.

Telemetry as Real-Time Sensory Input

In this stage, the AI runtime behaves like a biological organism with a rich sensory system. Hardware counters act as **real-time sensory inputs**, continuously informing the AI about:

- how kernels are executing
- how memory is being accessed
- how thermal conditions are evolving
- how voltage and frequency are fluctuating
- how compute units are behaving under load

The AI system interprets these signals through learned models, transforming raw telemetry into actionable intelligence. This creates a **closed-loop AI control system**, where sensing, prediction, and adaptation occur continuously during execution.

Telemetry Orchestration Layers: Coordinated Signal Processing

Raw hardware counters are noisy, high-frequency, and device-specific. To make them useful, the AI runtime employs **telemetry orchestration layers** that:

- normalize counter streams across heterogeneous accelerators
- filter noise and transient spikes
- aggregate counters into meaningful composite metrics
- correlate signals across compute, memory, and thermal domains
- feed processed telemetry into predictive models and anomaly detectors

These orchestration layers behave like a multi-stage signal-processing pipeline, transforming low-level counters into structured, interpretable state representations.

Mathematical Framing: Predictive State Modeling

Let C(t) be the vector of hardware counters at time t. The AI system maintains a predictive model:

$$\hat{S}(t) = f_{\phi}(C(t)),$$

where:

f_{ϕ} is a learned function (MLP, transformer, or graph model)

$\hat{S}(t)$ is the predicted system state (latency, thermal load, memory pressure, execution stability)

The runtime compares predicted and actual states:

$$\Delta(t) = S_{\text{actual}}(t) - \hat{S}(t),$$

where large deviations indicate anomalies such as:

- warp divergence spikes
- tile-engine stalls
- cache thrashing
- thermal runaway

- voltage instability
- memory-bank conflicts

These anomalies trigger mitigation actions in higher layers.

AI-Driven Adaptation: Real-Time Execution Tuning

The AI runtime uses telemetry to adapt execution dynamically:

- adjusting kernel launch parameters
- modifying tile sizes
- tuning quantization paths
- rebalancing memory access patterns
- throttling or boosting compute units
- redistributing workloads across cores

This transforms the runtime into an **adaptive AI system**, capable of responding to physical conditions in real time.

Operational Impact

High-frequency hardware-counter profiling enables:

- early detection of performance drift
- prevention of thermal throttling
- identification of emerging silicon faults
- stabilization of quantized pipelines
- reduction of latency variance
- improved reliability under fluctuating workloads

It is the sensory foundation upon which all subsequent observability layers depend.

With high-frequency hardware-counter telemetry providing continuous visibility into the physical execution environment, the next challenge is ensuring that the numerical data flowing through the model remains correct. Even when hardware counters appear normal, transient bit-flips can corrupt tensors due to cosmic rays, voltage fluctuations, thermal stress, or aging silicon. These faults are silent, unpredictable, and potentially catastrophic if left unchecked. To

address this, the observability pipeline introduces **in-flight AI tensor integrity checks**, where ECC, checksums, and fingerprinting mechanisms verify tensor correctness during execution. The following discussion explores how these integrity checks operate, how they detect transient corruption, and how the AI runtime recovers from such faults without interrupting inference.

ii. In-Flight AI Tensor Integrity Checks for Transient Bit-Flip Detection and Recovery

In-flight tensor integrity checks form the second defensive layer of silicon-to-software observability. While hardware-counter telemetry reveals *behavioral anomalies* in the accelerator, tensor integrity checks protect the *numerical correctness* of the data flowing through the model. This layer is essential because transient bit-flips—caused by cosmic rays, voltage fluctuations, thermal stress, or silicon aging—can silently corrupt tensors without leaving any trace in hardware counters. These faults are rare but dangerous: a single flipped bit in an activation tensor can propagate through dozens of layers, producing incorrect outputs that appear superficially valid.

Tensor Integrity Checking as Cognitive Self-Verification

In this stage, the AI runtime behaves like a cognitive system performing **self-verification**. Just as biological organisms maintain internal consistency through error-checking mechanisms, the AI system continuously validates the correctness of tensors as they move through the compute pipeline.

The runtime uses multiple integrity-checking mechanisms:

- **ECC (Error-Correcting Codes)** for memory regions
- **checksums** for intermediate tensors
- **hash-based fingerprints** for critical tensors
- **statistical anomaly detectors** for activation distributions
- **redundant computation paths** for high-risk operations

These mechanisms operate *in flight*, meaning they run concurrently with model execution rather than as offline diagnostics.

Mathematical Framing: Tensor Consistency Signatures

For a tensor T, the runtime computes a consistency signature:

$$\sigma(T) = h(T),$$

where h is a checksum, hash, or fingerprint function. During execution, the runtime verifies:

$$\sigma(T_{\text{expected}}) \quad \sigma(T_{\text{observed}}).$$

If the signatures mismatch, the AI system concludes that a transient bit-flip or corruption event has occurred.

AI-Driven Detection: Statistical and Structural Anomaly Models

Beyond deterministic checksums, the AI runtime employs **statistical anomaly detection**:

- monitoring activation distributions
- detecting improbable tensor patterns
- identifying sudden spikes or collapses in values
- comparing tensors against learned distribution models

Let D(T) be the distribution descriptor of tensor T. The AI system maintains a learned model:

$$\hat{D}(T) = f_\theta(T),$$

and flags anomalies when:

$$\|D(T) - \hat{D}(T)\| > \epsilon.$$

This allows detection of subtle corruption events that deterministic checks may miss.

Recovery Mechanisms: Correcting Corrupted Tensors

When corruption is detected, the runtime triggers recovery actions:

- **tensor reconstruction** from redundant copies
- **re-execution** of the operator that produced the tensor
- **fallback** to a safe computation path
- **isolation** of the memory region involved
- **logging** of the event for predictive wear modeling

These actions occur without interrupting inference, preserving continuity and correctness.

Operational Impact

In-flight tensor integrity checks:

- prevent silent numerical corruption
- maintain correctness under thermal or voltage stress
- protect quantized pipelines from catastrophic errors
- reduce the risk of cascading faults
- provide early indicators of silicon degradation
- feed error-correction events into predictive wear models

This layer ensures that the AI system's internal data remains trustworthy even when the underlying hardware experiences transient faults.

With tensor integrity checks ensuring that numerical data remains correct during execution, the next challenge is maintaining availability when parts of the accelerator begin to malfunction. Even when tensors are intact, compute cores—SMs, tiles, MAC arrays, vector units—may degrade or fail due to thermal stress, voltage instability, or silicon wear. These failures manifest as abnormal latency spikes, repeated ECC corrections, or inconsistent hardware-counter patterns. To preserve uninterrupted inference, the observability pipeline introduces **dynamic faulty-core isolation**, where the AI runtime identifies malfunctioning compute units and reroutes execution around them. The following discussion explores how reliability scoring, execution remapping, and automatic failover combine to create a resilient, self-healing AI execution environment.

iii. Dynamic AI Faulty-Core Isolation with Automatic Model Re-Routing and Execution Failover

Dynamic faulty-core isolation is the third defensive layer in the silicon-to-software observability stack. While hardware-counter telemetry provides real-time visibility and tensor integrity checks ensure numerical correctness, faulty-core isolation preserves *availability* by ensuring that inference continues even when parts of the accelerator degrade or fail. Modern accelerators contain dozens to thousands of compute units—SMs, tiles, MAC arrays, vector units—and any subset of these may become unreliable due to thermal stress, voltage instability, manufacturing variation, or silicon aging. This layer enables the AI runtime to detect malfunctioning cores, isolate them, and reroute execution around them without interrupting inference.

Fault Isolation as Adaptive Neural Routing

In this stage, the AI runtime behaves like a biological neural system rerouting signals around

damaged neurons. Each compute core is treated as a functional node in a distributed execution graph. The AI system continuously evaluates the reliability of each node using:

- abnormal latency spikes
- repeated ECC corrections
- inconsistent hardware-counter patterns
- thermal anomalies
- tensor integrity mismatches
- execution stalls or partial kernel failures

These signals feed into a learned reliability model that assigns each core a dynamic health score.

Mathematical Framing: Core-Reliability Scoring

Let k be a compute core. The AI runtime maintains a reliability score:

$$R_k = g(C_k, E_k, T_k, I_k),$$

where:

- C_k = hardware-counter anomalies
- E_k = error-correction events
- T_k = thermal deviations
- I_k = tensor-integrity anomalies

The function g is a learned model (MLP, transformer, or graph-neural network) that predicts the likelihood that core k will produce correct results under load.

Cores with reliability below a threshold:

$$R_k < \tau$$

are marked as faulty and isolated from the execution graph.

AI-Driven Execution Re-Routing

Once a core is isolated, the AI runtime dynamically remaps operations using a routing function:

$$M: ops \rightarrow healthy\ cores.$$

This mapping is updated in real time, ensuring that:

- kernels avoid faulty cores
- tensor operations are reassigned to reliable units
- fused operator blocks are re-scheduled
- parallel workloads are redistributed
- quantized pipelines bypass unstable compute paths

The AI system performs this re-routing without interrupting inference, preserving continuity even under partial hardware failure.

Automatic Failover: Graceful Degradation Instead of Catastrophic Failure

Faulty-core isolation enables **graceful degradation**:

- If a few cores fail, workloads are redistributed.
- If many cores fail, the runtime reduces parallelism but maintains correctness.
- If failure becomes severe, the system triggers upstream orchestration to migrate workloads.

This prevents catastrophic failure modes such as:

- kernel crashes
- corrupted outputs
- deadlocks
- thermal runaway
- system-wide inference interruption

Operational Impact

Dynamic faulty-core isolation provides:

- uninterrupted inference under partial silicon failure
- resilience against aging hardware
- reduced downtime for edge devices

- improved reliability for long-running cloud workloads
- early indicators of deeper silicon degradation
- input signals for predictive wear modeling

It is the adaptive backbone of fault-tolerant AI execution.

With faulty-core isolation ensuring that inference continues even when parts of the accelerator fail, the next challenge is anticipating failures *before* they occur. Hardware degradation is not random—it follows long-term patterns shaped by thermal cycling, voltage stress, electromigration, and workload intensity. To capture these patterns, the observability pipeline introduces **predictive AI silicon-wear telemetry**, where long-term counter trends, thermal histories, and error-correction events feed into learned models that forecast future degradation. These predictions integrate with cloud-scale orchestration systems, enabling proactive workload migration, maintenance scheduling, and lifecycle optimization. The next discussion explores how predictive wear modeling closes the loop between silicon telemetry and large-scale AI operations.

iv. Predictive AI Silicon-Wear Telemetry Integrated with Cloud-Scale Orchestration Feedback Loops

Predictive silicon-wear telemetry is the fourth and final layer of the silicon-to-software observability stack. While the earlier layers detect anomalies, correct corrupted tensors, and isolate faulty cores, this layer focuses on **anticipating future failures before they occur**. Modern accelerators degrade over time due to electromigration, thermal cycling, voltage stress, and sustained high-intensity workloads. These degradation patterns are not random—they follow measurable trajectories that can be learned, modeled, and forecasted by AI systems.

Silicon-Wear Modeling as Long-Horizon Predictive Cognition

In this stage, the AI runtime behaves like a long-horizon predictive cognitive system. It continuously ingests telemetry signals—thermal histories, counter trends, ECC events, voltage fluctuations—and uses them to infer the underlying health of the silicon. The system builds a **temporal model** of wear progression, enabling it to forecast future degradation and proactively mitigate risk.

The AI system maintains a predictive wear model:

$$\hat{W}(t) = f_{\psi}(C(t), T(t), E(t), H(t)),$$

where:

- C(t) = hardware-counter trends
- T(t) = thermal history
- E(t) = error-correction events
- H(t) = historical reliability scores
- f_ψ = learned temporal model (LSTM, transformer, or temporal GNN)

The model predicts future degradation:

$$W_{\text{future}} = \hat{W}(t + \Delta),$$

allowing the system to anticipate failures before they manifest.

Telemetry Sources: Long-Term Physical Indicators

Predictive wear modeling draws from multiple long-term indicators:

- **thermal cycling amplitude** (ΔT across workloads)
- **frequency of ECC corrections**
- **voltage droop events**
- **persistent warp divergence anomalies**
- **tile-engine stall patterns**
- **cache-miss rate drift**
- **latency variance over time**

These signals collectively reveal the physical stress experienced by the accelerator.

AI-Driven Forecasting: Identifying Imminent Failure Zones

The AI system identifies:

- cores approaching reliability thresholds
- memory regions showing increasing ECC frequency
- tiles exhibiting rising thermal instability
- systolic array segments with declining throughput
- quantization pipelines with growing error variance

These predictions allow the runtime to take proactive action.

Cloud-Scale Orchestration Feedback Loops

Predictive wear telemetry integrates with cloud-scale orchestration systems that:

- **migrate workloads** away from degrading hardware
- **rebalance clusters** to reduce stress on vulnerable nodes
- **schedule maintenance** before catastrophic failure
- **adjust cooling profiles** to slow wear progression
- **retire aging hardware gracefully**
- **update deployment policies** based on wear forecasts

This creates a **closed-loop system** where silicon telemetry informs cloud-level decisions, and cloud-level decisions reduce silicon stress.

Operational Impact

Predictive silicon-wear telemetry provides:

- proactive fault mitigation
- reduced downtime
- extended hardware lifespan
- improved cluster reliability
- optimized workload distribution
- early warning signals for catastrophic failure modes

It transforms observability from reactive fault handling into **predictive lifecycle management**.

Silicon-to-software observability forms the runtime backbone of fault-tolerant AI execution. High-frequency hardware-counter telemetry provides real-time visibility into the physical behavior of the accelerator, enabling early detection of anomalies. In-flight tensor integrity checks ensure numerical correctness by detecting and recovering from transient bit-flips. Dynamic faulty-core isolation preserves availability by rerouting execution around malfunctioning compute units. Predictive silicon-wear telemetry extends observability into the future, forecasting degradation and integrating with cloud-scale orchestration systems to proactively mitigate risk. Together, these layers create a resilient, self-monitoring, and

self-healing AI execution environment capable of maintaining correctness, stability, and continuity across heterogeneous and aging hardware.

With silicon-to-software observability providing continuous visibility, fault detection, and predictive mitigation across the hardware stack, the next challenge is securing the execution environment itself. Modern AI workloads operate in increasingly adversarial contexts, where attackers may attempt to exploit shared hardware resources, infer model behavior through side-channels, or compromise sensitive data through physical or microarchitectural leakage. To address these threats, the next discussion introduces **full-stack AI secure enclaves**, where cryptographic hardware isolation, encrypted execution paths, and side-channel defense layers create a hardened environment for AI computation. This security layer complements observability by ensuring not only that the system runs reliably, but also that it runs securely—even under adversarial conditions.

e. Full-Stack AI Secure Enclaves with Cryptographic Hardware Isolation and Side-Channel Defense Layers

Full-stack AI secure enclaves provide protected execution environments for AI workloads that process sensitive data, proprietary model parameters, or security-critical information. As AI systems operate across cloud platforms, shared accelerators, edge devices, and embedded systems, security must extend beyond application software to the hardware and runtime components responsible for executing a model. An enclave establishes an isolated execution domain in which designated code and data receive protection through hardware-enforced access controls and, where supported, cryptographic mechanisms. Its security depends on the underlying processor architecture, memory-protection design, trusted computing base, and the threats the implementation is designed to address.

Cryptographic Hardware Isolation and Protected Memory. Secure enclaves use hardware-enforced boundaries to restrict access to designated memory and execution resources. Depending on the platform, these mechanisms may include protected memory regions, encrypted memory, authenticated memory access, secure boot, and cryptographic verification of software components. Model weights, input tensors, intermediate activations, and other sensitive state can be protected while stored or processed within the supported security boundary. However, encryption alone does not guarantee confidentiality and integrity during computation. The implementation must also control access to plaintext data, protect cryptographic keys, and prevent unauthorized modification of protected state.

AI accelerators introduce additional isolation challenges because workloads may move data between CPUs, GPUs, NPUs, memory controllers, and peripheral devices. Direct memory access

(DMA) enables efficient transfers without continuous CPU intervention, but device access must be constrained to authorized memory regions. Secure accelerator integration therefore requires appropriate device-access controls, memory isolation, protected communication paths where supported, and carefully managed transitions between trusted and untrusted components. These mechanisms reduce the risk that unauthorized processes or compromised devices could access sensitive data through shared memory or peripheral interfaces.

Side-Channel Defense and Microarchitectural Protection. Hardware isolation does not automatically eliminate side-channel leakage. Even when direct access to protected memory is blocked, an attacker may infer information from execution time, cache behavior, memory contention, power consumption, or electromagnetic emissions. Such observations can reveal information about model parameters, input data, or internal execution paths, depending on the implementation and the attacker's capabilities.

Side-channel defenses must therefore be selected according to the relevant threat model. Constant-time algorithms can reduce timing variations associated with secret-dependent operations. Cache partitioning, controlled resource sharing, and disciplined memory-access patterns can limit certain forms of microarchitectural leakage. Power-analysis resistance may require circuit-level countermeasures, masking, noise generation, or other techniques appropriate to the hardware. Randomized execution or memory-access patterns may provide additional protection in specific circumstances, but they can introduce performance overhead and do not guarantee that leakage is eliminated. Security evaluation must assess these measures against realistic attacks rather than assuming that enclave isolation alone provides complete side-channel resistance.

Fault Detection and Secure Recovery. Enclave implementations may also depend on error-correcting memory, parity checks, watchdog mechanisms, hardware error reporting, and runtime integrity checks to detect faults that could affect execution. These mechanisms serve purposes distinct from cryptographic isolation: they help identify errors, preserve data integrity, and support controlled recovery. When a fault is detected, the system may terminate an operation, invalidate affected state, restart a protected component, or transfer execution to a verified recovery path. The appropriate response depends on the platform's capabilities and the application's security requirements.

Fault handling must also account for attacks that deliberately induce errors through voltage manipulation, clock disturbance, thermal stress, or other physical techniques. Detection mechanisms may identify some such events, but not every physical fault is observable, and detection does not necessarily prevent exploitation. Security-sensitive applications may therefore require additional fault-injection testing, integrity verification, and policies that

prevent potentially compromised results from being accepted or released.

Security Across the AI Execution Stack. Full-stack enclave protection must account for the

interactions among model loading, compilation, memory management, accelerator execution, runtime scheduling, and result delivery. A protected model can still be exposed if its weights are transferred through an unprotected buffer, if a device is granted excessive memory access, or if sensitive information appears in logs or intermediate outputs. Similarly, a secure execution domain may not protect against vulnerabilities in untrusted interfaces or against information revealed through outputs that an authorized user can observe.

Consequently, enclave design requires coordinated protection of code, model parameters, input data, intermediate state, cryptographic keys, and communication interfaces. Developers must define which components are trusted, how data cross security boundaries, how identities and permissions are verified, and how errors or suspicious behavior are handled. The design must also account for performance costs, including encryption, integrity checking, protected data movement, and additional isolation boundaries. These costs should be measured under representative workloads to ensure that the security configuration meets the application's latency and resource requirements.

Cross-Layer Optimization for Secure AI Execution. Secure enclaves operate within a larger hardware–software system in which model architecture, compiler transformations, memory management, accelerator scheduling, and security enforcement interact. Cross-layer optimization coordinates these components to improve execution efficiency while preserving the confidentiality, integrity, and isolation requirements of the application. Rather than optimizing each layer independently, the design process evaluates how decisions at one layer affect performance, resource consumption, and security at other layers.

At the compiler level, intermediate representations (IRs) provide a foundation for translating high-level AI models into hardware-specific execution plans. Frameworks and compiler infrastructures such as MLIR and TVM support transformations including operator lowering, tensor and loop optimization, memory tiling, vectorization, scheduling, and accelerator-specific code generation. Graph-level techniques such as constant folding, dead-code elimination, algebraic simplification, and operator fusion can reduce unnecessary computation and memory traffic. However, these transformations must preserve the model's intended semantics and respect security boundaries. For example, an optimization that moves an operation outside a protected execution domain or exposes an intermediate tensor to an untrusted buffer may violate the security policy even if it improves performance.

Hardware-aware neural architecture search (NAS) extends cross-layer optimization to the design

of the neural network itself. Candidate architectures can be evaluated according to predictive performance, latency, energy consumption, memory requirements, and compatibility with the target accelerator. Hardware characteristics such as cache capacity, supported tensor operations, memory bandwidth, register availability, and numerical precision influence the efficiency of candidate architectures. When secure execution introduces additional costs, architecture evaluation should also account for the overhead associated with protected memory, cryptographic operations, integrity checks, and secure data transfers. This helps identify models that meet application requirements within the constraints of the actual protected execution environment.

Runtime observability provides another component of cross-layer optimization. Hardware counters, thermal sensors, power monitors, memory metrics, and error-reporting mechanisms supply information about execution behavior and physical operating conditions. The runtime can use this information to identify bottlenecks, adjust resource allocation, and invoke predefined mitigation procedures. However, telemetry and diagnostic mechanisms must themselves respect enclave boundaries: monitoring data should not expose protected model parameters, sensitive inputs, cryptographic keys, or other confidential state. Runtime adaptations must also account for their effects on latency, correctness, reproducibility, and security.

The interaction among these layers creates trade-offs that cannot always be resolved by optimizing a single metric. Operator fusion may reduce memory traffic but increase register pressure. Stronger isolation or more frequent integrity checks may improve protection but increase latency. Moving a workload to another accelerator may alleviate resource contention but introduce secure data-transfer overhead. Cross-layer optimization evaluates these interactions against the application's requirements rather than assuming that maximum computational throughput is always the appropriate objective.

Integration and Validation of the Full-Stack Design. Effective secure AI execution requires joint validation of architectural choices, compiler transformations, hardware isolation, runtime behavior, and fault-handling mechanisms. Testing should assess not only predictive accuracy and execution speed but also memory isolation, access-control enforcement, side-channel exposure, fault response, and the overhead introduced by security protections. For systems with strict timing requirements, validation must also establish whether the complete execution and mitigation paths meet the required latency bounds. Where these bounds cannot be maintained, the system needs a defined response appropriate to its safety and operational requirements.

Silicon-to-software observability and secure enclaves provide complementary capabilities within

this design. Observability helps identify changes in hardware behavior and execution performance, while enclaves establish protected execution boundaries and restrict unauthorized access to sensitive state. Cross-layer optimization coordinates these capabilities with model design, compilation, and resource management. Together, they support AI systems that are optimized not only for computational efficiency but also for confidentiality, integrity, reliability, and the constraints of their deployment environments.

The four mechanisms examined next—encrypted memory paging, hardware-bound multiparty cryptographic aggregation, power-analysis resistance, and deterministic compute padding—address distinct aspects of this broader security problem. Encrypted memory paging protects sensitive data as it moves between memory and storage; multiparty cryptographic aggregation helps combine information while limiting exposure of individual contributions; power-analysis resistance targets leakage through physical power measurements; and deterministic compute padding seeks to reduce information revealed by variations in execution time or workload activity. Each mechanism has specific assumptions and limitations, so its suitability must be assessed in relation to the hardware platform, adversary capabilities, performance budget, and overall security architecture.

Taken together, secure enclaves and cross-layer optimization complete the hardware–software co-design perspective developed in Section 8.4. Neural architecture design, compiler optimization, runtime observability, and cryptographic protection must be considered as interacting parts of one system. The goal is not simply to accelerate AI inference or isolate sensitive computation, but to deliver the required model performance while respecting the security, reliability, resource, and timing constraints of the intended deployment environment.

Encrypted AI Memory-Paging for Confidential GPU Core-Slice Execution

Encrypted AI memory-paging ensures that all data entering or leaving GPU core slices remains cryptographically protected. This mechanism prevents attackers from observing intermediate tensors, gradients, or model parameters through memory snooping, DMA attacks, or compromised hypervisors.

1. Confidential Execution as Cryptographic Cognitive Shielding

The AI runtime treats memory as a **confidential cognitive workspace**. Every tensor, activation, and intermediate result is encrypted before being paged into GPU memory. Decryption occurs only within isolated core slices, ensuring that sensitive data is never exposed in plaintext outside the enclave.

Mechanisms

- **AES-XTS or ChaCha20-Poly1305 encryption** for memory pages
- **per-core ephemeral keys** derived from hardware root-of-trust
- **encrypted scratchpad buffers** for fused operator blocks
- **secure DMA channels** for host-device transfers

Operational Impact

- prevents memory-snooping attacks
- protects model parameters and embeddings
- enables confidential multi-tenant GPU sharing
- ensures privacy for sensitive inference workloads

2. Hardware-Bound AI Multi-Party Cryptographic Aggregation Protocols

This mechanism enables secure aggregation of AI model updates or inference results across multiple parties without exposing raw data. It is essential for federated learning, multi-tenant inference, and distributed AI pipelines.

Secure Aggregation as Cryptographic Collective Cognition

The AI system behaves like a distributed cognitive network where each participant contributes encrypted updates. Hardware-bound keys ensure that only authorized enclaves can decrypt aggregated results.

Mechanisms

- **secure multi-party computation (MPC)** for gradient aggregation
- **homomorphic encryption** for encrypted inference
- **hardware-rooted attestation** to verify enclave authenticity
- **zero-knowledge proofs** for correctness without disclosure

Operational Impact

- prevents data leakage across tenants
- enables privacy-preserving federated learning

- ensures trust in distributed AI pipelines
- enforces cryptographic isolation across hardware boundaries

3. AI Power-Analysis Resistance via Dummy-Computation Masking Protocols

Power-analysis attacks attempt to infer model parameters or data by measuring power consumption patterns. Dummy-computation masking introduces controlled noise into power traces, preventing attackers from extracting meaningful information.

Masking as Cognitive Noise Injection

The AI runtime injects **synthetic computational noise**—dummy operations, randomized memory accesses, and controlled jitter—to obscure the true execution pattern. This is analogous to biological systems adding noise to neural signals to prevent adversarial inference.

Mechanisms

- **randomized fused-operator blocks**
- **dummy tensor multiplications**
- **masked memory-access patterns**
- **power-trace equalization loops**

Operational Impact

- neutralizes power-analysis attacks
- prevents extraction of model weights
- protects cryptographic operations within enclaves
- ensures confidentiality even under physical probing

4. Deterministic AI Compute-Padding Techniques for Timing-Side-Channel Neutralization

Timing-side-channels exploit variations in execution time to infer sensitive information. Deterministic compute-padding ensures that all operations—regardless of input—take identical time.

Deterministic Execution as Cognitive Timing Discipline

The AI runtime enforces **strict timing discipline**, ensuring that execution paths are indistinguishable. This prevents attackers from inferring model structure, branching behavior, or data-dependent execution patterns.

Mechanisms

- **constant-time operator execution**
- **deterministic kernel launch intervals**
- **fixed-latency memory accesses**
- **padding loops for variable-length operations**

Operational Impact

- eliminates timing-side-channel leakage
- protects conditional logic and branching
- ensures confidentiality for sensitive inference
- enables secure multi-tenant GPU scheduling

The four secure-enclave mechanisms—encrypted memory-paging, hardware-bound cryptographic aggregation, power-analysis resistance, and deterministic compute-padding—collectively define the defensive perimeter that protects AI workloads from physical, microarchitectural, and timing-based attacks. While the preceding discussions describe each mechanism in depth, Table 8.4-F5 consolidates these defenses into a unified structural overview. It highlights how each dimension contributes to confidentiality, integrity, and side-channel resistance, how AI framing transforms cryptographic isolation into cognitive protection, and how these mechanisms operate together to form a hardened execution environment. This table provides a concise architectural map of the full-stack enclave, clarifying the role each defense layer plays in securing AI computation under adversarial conditions.

Table 8.4-F5 presents the core dimensions of secure-enclave defense in modern AI systems. Each dimension corresponds to a distinct protection mechanism that operates at a different layer of the hardware-software stack: encrypted memory-paging protects data in motion and at rest; hardware-bound cryptographic aggregation secures multi-party collaboration; power-analysis resistance obscures physical execution traces; and deterministic compute-padding neutralizes timing-side-channels. Together, these mechanisms form a comprehensive security framework that ensures AI workloads remain confidential, tamper-resistant, and immune to microarchitectural leakage. The table clarifies how each mechanism works, how AI framing conceptualizes the defense, and how these layers combine to create a secure enclave capable of resisting sophisticated adversarial techniques.

Table 8.4-F5 — Full-Stack AI Secure Enclave Defense Dimensions

Dimension	Core Purpose	Key Mechanisms	AI Framing	Operational Impact
Encrypted AI Memory-Paging	Confidential execution	AES-XTS, ephemeral keys, secure DMA	Cognitive shielding	Prevents memory snooping and data leakage
Hardware-Bound Cryptographic Aggregation	Secure multi-party AI	MPC, homomorphic encryption, attestation	Collective cognition	Enables privacy-preserving distributed AI
Power-Analysis Resistance	Prevent physical inference	Dummy ops, masked access, noise injection	Cognitive noise	Neutralizes power-analysis attacks
Deterministic Compute-Padding	Prevent timing leakage	constant-time ops, padding loops	Timing discipline	Eliminates timing-side-channels

The first dimension, **encrypted AI memory-paging**, establishes the foundational confidentiality layer. By encrypting all memory pages entering or leaving GPU core slices, the enclave ensures that sensitive tensors, gradients, and model parameters never appear in plaintext outside the secure execution boundary. This mechanism acts as a cryptographic shield around the AI system's cognitive workspace, preventing memory-snooping attacks and enabling confidential multi-tenant GPU sharing.

The second dimension, **hardware-bound cryptographic aggregation**, extends security beyond a single device. It enables secure multi-party AI computation—federated learning, distributed inference, and collaborative model updates—without exposing raw data. Hardware-rooted attestation ensures that only trusted enclaves participate, while MPC and homomorphic encryption allow encrypted contributions to be aggregated without decryption. This mechanism transforms distributed AI into a form of cryptographic collective cognition, where collaboration occurs securely across hardware boundaries.

The third dimension, **AI power-analysis resistance**, protects against physical side-channel attacks that attempt to infer model parameters or data by analyzing power consumption patterns. Dummy-computation masking introduces controlled noise into power traces, obscuring the true execution pattern. This mechanism behaves like cognitive noise injection,

preventing adversaries from extracting meaningful information even under direct physical probing.

The fourth dimension, **deterministic compute-padding**, neutralizes timing-side-channels by enforcing constant-time execution. Regardless of input size, branching behavior, or conditional logic, the enclave ensures that all operations take identical time. This timing discipline prevents attackers from inferring sensitive information through execution-time variations, protecting both model structure and data-dependent behavior.

Together, the dimensions in Table 8.4-F5 illustrate how full-stack secure enclaves transform AI execution into a cryptographically isolated, side-channel-resistant environment. Each dimension contributes a unique defensive capability—confidential memory, secure collaboration, physical-trace obfuscation, and timing neutrality—forming a comprehensive security architecture that protects AI workloads from sophisticated adversarial threats.

The defense dimensions summarized in Table 8.4-F5 establish the structural foundation of secure AI enclaves, showing how cryptographic isolation, secure multi-party aggregation, power-trace masking, and deterministic timing discipline collectively harden the execution environment against adversarial extraction. Figure 8.4-F5 translates these dimensions into a visual flow, illustrating how each defense layer builds upon the previous one to form a vertically integrated security pipeline. This figure reinforces the idea that enclave security is not a single mechanism but a coordinated, multi-layered architecture in which cryptographic protection, physical-trace obfuscation, and timing neutrality converge to produce a fully isolated, side-channel-resistant AI runtime.

Figure 8.4-F5 depicts the complete hardening pipeline that transforms raw AI computation into a cryptographically isolated, side-channel-resistant execution environment. Beginning with encrypted memory-paging, the flow progresses through hardware-bound cryptographic aggregation, power-analysis resistance, and deterministic compute-padding before culminating in a fully isolated enclave. Each block represents a distinct security layer, and the downward arrows emphasize the sequential reinforcement of confidentiality, integrity, and microarchitectural neutrality. The figure highlights how secure enclaves integrate cryptographic primitives with physical-layer defenses to protect AI workloads from sophisticated adversarial techniques.

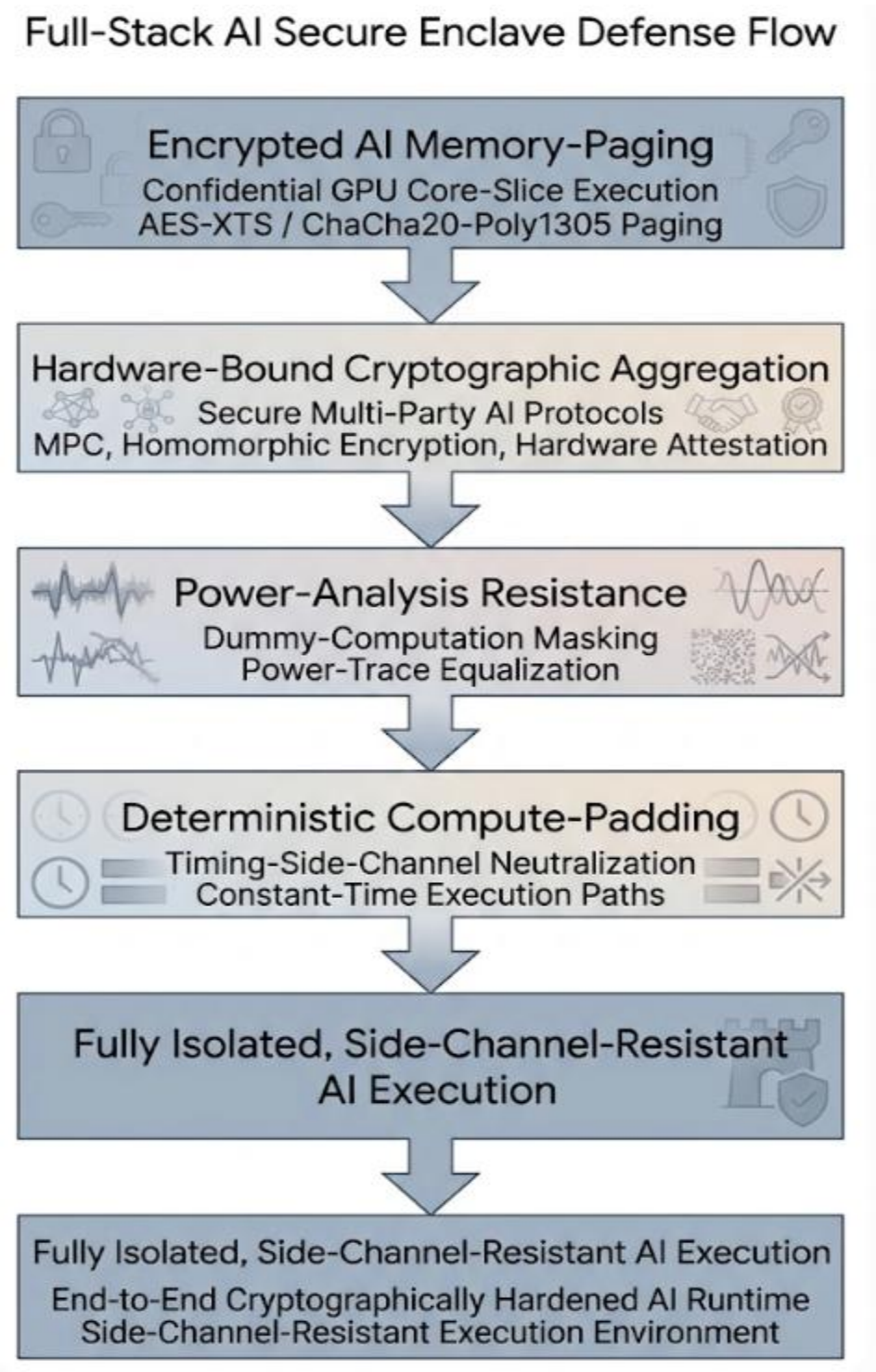


Figure 8.4-F5 — Full-Stack AI Secure Enclave Defense Flow

A vertically layered security pipeline illustrating how encrypted memory-paging, hardware-bound cryptographic aggregation, power-analysis masking, and deterministic compute-padding combine to produce a fully isolated, side-channel-resistant AI execution environment.

Legend:

- ***Encrypted AI Memory-Paging*** *— cryptographic protection of GPU core-slice memory using AES-XTS or ChaCha20-Poly1305.*
- ***Hardware-Bound Cryptographic Aggregation*** *— secure multi-party AI protocols using MPC, homomorphic encryption, and hardware attestation.*
- ***Power-Analysis Resistance*** *— dummy-computation masking and power-trace equalization to obscure physical execution patterns.*
- ***Deterministic Compute-Padding*** *— constant-time execution paths and timing-neutral padding loops to eliminate timing-side-channels.*
- ***Fully Isolated AI Execution*** *— the final hardened enclave providing end-to-end cryptographic and side-channel resistance.*

The figure begins with **encrypted AI memory-paging**, representing the cryptographic perimeter of the enclave. By encrypting all memory pages entering or leaving GPU core slices, this layer ensures that sensitive tensors and model parameters remain confidential even in multi-tenant or adversarial environments. It establishes the enclave's foundational isolation boundary.
The flow then moves into **hardware-bound cryptographic aggregation**, where secure multi-party protocols allow distributed AI workloads to collaborate without exposing raw data. MPC, homomorphic encryption, and hardware attestation ensure that only trusted enclaves participate and that aggregation occurs entirely over encrypted values. This layer extends enclave security across devices and participants.

Next, the diagram transitions into **power-analysis resistance**, which protects against physical side-channel attacks. Dummy-computation masking and power-trace equalization introduce controlled noise into the accelerator's power profile, preventing attackers from inferring model parameters or data through power-consumption patterns. This layer hardens the enclave against physical probing.

The fourth layer, **deterministic compute-padding**, neutralizes timing-side-channels by enforcing constant-time execution. Regardless of input size or branching behavior, the enclave ensures that all operations take identical time, preventing attackers from inferring sensitive information through timing variations. This layer provides microarchitectural neutrality.

Finally, the flow culminates in **fully isolated, side-channel-resistant AI execution**, representing the hardened runtime environment produced by the coordinated action of all preceding layers. The figure makes clear that secure enclaves are not a single mechanism but a multi-layered defense stack that integrates cryptographic isolation, secure collaboration, physical-trace obfuscation, and timing discipline into a unified security architecture.

With the defense dimensions in Table 8.4-F5 clarified and Figure 8.4-F5 illustrating how these layers interlock to form a vertically integrated enclave, the next step is to examine the foundational mechanism that initiates the entire security pipeline: encrypted AI memory-paging. This first layer establishes the cryptographic perimeter of the enclave, ensuring that every tensor, activation, and intermediate value entering or leaving GPU core slices remains protected under strong encryption. By treating memory as a confidential cognitive workspace, the enclave prevents adversaries from observing or extracting sensitive data through memory snooping, DMA interception, or hypervisor compromise. Understanding how encrypted paging is orchestrated, how keys are derived from hardware roots-of-trust, and how core-slice isolation is enforced is essential, because this mechanism anchors all subsequent defenses—secure aggregation, power-trace masking, and deterministic timing discipline. The following discussion explores how encrypted memory-paging transforms raw GPU execution into a cryptographically shielded environment suitable for confidential AI workloads.

i. Encrypted AI Memory-Paging for Confidential GPU Core-Slice Execution

Encrypted AI memory-paging is the foundational security layer of full-stack AI secure enclaves. It establishes the cryptographic perimeter that ensures all data entering or leaving GPU core slices remains confidential, integrity-protected, and inaccessible to adversaries—even those with privileged system access. This mechanism is essential for multi-tenant GPU environments, federated learning deployments, and any AI workload involving sensitive data or proprietary model parameters.

Cryptographic Memory as a Cognitive Isolation Boundary

In this stage, the AI runtime treats memory as a **protected cognitive workspace**, analogous to a secure mental buffer where internal thoughts and representations must remain hidden from external observers. Every tensor, activation, gradient, and intermediate representation is encrypted before being paged into GPU memory. Decryption occurs only within isolated core slices, ensuring that plaintext data never exists outside the enclave's cryptographically sealed execution boundary.

This framing positions encrypted paging as a form of **cognitive shielding**, where the AI system's internal state is protected from external inspection, tampering, or inference.

Core Mechanisms of Encrypted AI Memory-Paging

1. Per-Core Ephemeral Encryption Keys

Each GPU core slice derives ephemeral keys from a hardware root-of-trust (TPM, TEE, or secure element). These keys:

- are unique per core
- rotate frequently
- never leave the hardware boundary
- are inaccessible to the host OS or hypervisor

This ensures that even if the host is compromised, the attacker cannot decrypt enclave memory.

2. AES-XTS or ChaCha20-Poly1305 Page Encryption

Memory pages are encrypted using high-performance, low-latency cryptographic primitives:

- **AES-XTS** for deterministic block-aligned paging
- **ChaCha20-Poly1305** for high-throughput streaming tensors

These algorithms provide confidentiality and integrity without introducing unacceptable latency overhead.

3. Encrypted Scratchpad Buffers for Fused Operators

Fused operator blocks (e.g., GEMM + activation + quantization) use encrypted scratchpads to ensure intermediate values remain protected during multi-stage execution.

4. Secure DMA Channels

Host-to-device and device-to-host transfers occur through secure DMA channels that:

- encrypt data in transit
- authenticate endpoints
- prevent bus-snooping attacks
- enforce enclave boundary integrity

Threats Neutralized by Encrypted Memory-Paging

Encrypted paging protects against:

- **memory-snooping attacks** (malicious hypervisors, compromised drivers)
- **DMA interception**
- **cold-boot attacks**
- **GPU memory scraping**

- **multi-tenant inference leakage**
- **model-parameter theft**
- **tensor reconstruction attacks**

It ensures that even if an attacker gains physical or privileged access, they cannot observe or extract sensitive AI data.

Mathematical Framing: Encrypted Paging Pipeline

Let P be a memory page containing tensor T. The enclave encrypts:

$$E = \mathrm{Enc}_{K_{\mathrm{core}}}(P),$$

where K_{core} is the ephemeral per-core key.

During execution:

$$P_{\mathrm{decrypted}} = \mathrm{Dec}_{K_{\mathrm{core}}}(E),$$

and plaintext exists **only** inside the isolated core slice.

The enclave enforces:

$$\forall P: P_{\mathrm{plaintext}} \notin \text{global memory}.$$

This invariant is the foundation of confidential GPU execution.

Operational Impact

Encrypted AI memory-paging enables:

- confidential inference on shared GPUs
- secure training with sensitive datasets
- protection of proprietary model architectures
- isolation of multi-tenant workloads
- compliance with privacy regulations
- resistance to privileged attackers

It is the first and most essential layer of secure enclave hardening.

With encrypted memory-paging establishing a cryptographically sealed execution boundary around each GPU core slice, the next challenge is enabling secure collaboration across multiple enclaves. Modern AI workloads—federated learning, distributed inference, multi-tenant model serving—require multiple parties to contribute data or model updates without exposing raw information. To support these scenarios, the enclave stack introduces **hardware-bound multi-party cryptographic aggregation**, where secure multi-party computation, homomorphic encryption, and hardware attestation allow enclaves to collaborate while maintaining strict confidentiality. The following discussion explores how these protocols transform distributed AI into a cryptographically protected collective computation environment.

ii. Hardware-Bound AI Multi-Party Cryptographic Aggregation Protocols

Hardware-bound AI multi-party cryptographic aggregation is the second major defense layer in full-stack AI secure enclaves. While encrypted memory-paging protects data within a single GPU core slice, multi-party aggregation enables **secure collaboration across multiple enclaves**—whether distributed across devices, tenants, or geographic regions. This mechanism is essential for federated learning, confidential multi-tenant inference, secure model-update pipelines, and privacy-preserving analytics.

It ensures that multiple parties can contribute data, gradients, or inference results **without ever exposing raw information**, and that only authenticated, attested enclaves can participate in the aggregation process.

Secure Aggregation as Cryptographic Collective Cognition

In this stage, the AI system behaves like a **distributed cognitive network**, where each enclave contributes encrypted updates that collectively form a shared model or inference result. The enclaves do not trust each other individually; instead, they trust the **hardware-rooted cryptographic fabric** that binds them.

This framing positions multi-party aggregation as a form of **collective cognition under cryptographic protection**, where:

- each enclave thinks independently,
- contributions remain encrypted,
- aggregation occurs without decryption,
- and the final result is revealed only to authorized enclaves.

This allows AI systems to collaborate securely even in adversarial or multi-tenant environments.

Core Mechanisms of Hardware-Bound Cryptographic Aggregation

1. Secure Multi-Party Computation (MPC) for Gradient Aggregation

MPC enables multiple enclaves to compute a joint function (e.g., gradient sum) without revealing individual inputs.

- gradients remain encrypted
- aggregation occurs over ciphertext
- no party learns another party's data
- only the final aggregated result is decrypted

This is essential for federated learning and distributed training.

2. Homomorphic Encryption for Encrypted Inference

Homomorphic encryption allows enclaves to perform computation directly on encrypted tensors.

- inference occurs without decryption
- model parameters remain confidential
- input data remains private
- output is decrypted only by authorized enclaves

This enables secure cloud inference for sensitive workloads.

3. Hardware-Rooted Attestation

Each enclave proves its authenticity using hardware attestation:

- verifies enclave identity
- ensures correct enclave configuration
- prevents rogue or spoofed participants
- binds cryptographic keys to hardware roots-of-trust

Attestation ensures that only legitimate enclaves can join the aggregation group.

4. Zero-Knowledge Proofs for Correctness Without Disclosure

Zero-knowledge proofs allow enclaves to prove:

- correctness of computation
- validity of updates
- integrity of aggregation

without revealing underlying data.

This prevents malicious enclaves from injecting poisoned gradients or tampered results.

Threats Neutralized by Hardware-Bound Aggregation

This mechanism protects against:

- **data leakage across tenants**
- **model-update poisoning**
- **malicious participant impersonation**
- **gradient inversion attacks**
- **cross-device inference leakage**
- **compromised aggregator servers**

It ensures that distributed AI remains confidential, trustworthy, and tamper-resistant.

Mathematical Framing: Encrypted Aggregation Pipeline

Let xi be the contribution from enclave i. Each enclave encrypts:

$$c_i = \mathrm{Enc}_{K_i}(x_i),$$

where K_i is the hardware-bound key.

Aggregation occurs over ciphertext:

$$C = \sum_i c_i.$$

Only authorized enclaves possessing the joint decryption capability can compute:

$$X = \mathrm{Dec}(C),$$

yielding the aggregated result without exposing individual contributions.

This ensures:

$$\forall i: x_i \notin \text{plaintext outside enclave.}$$

Operational Impact

Hardware-bound cryptographic aggregation enables:

- privacy-preserving federated learning
- secure multi-tenant inference
- confidential distributed model updates
- tamper-resistant collaborative AI pipelines
- trustless collaboration across hardware boundaries

It transforms distributed AI into a cryptographically protected collective computation environment.

With hardware-bound cryptographic aggregation enabling secure collaboration across enclaves, the next challenge is protecting the enclave from **physical side-channel attacks**. Even when data is encrypted and aggregation is secure, attackers may attempt to infer sensitive information by measuring power consumption patterns during AI computation. These attacks can reveal model parameters, input data, or cryptographic keys. To counter this threat, the enclave stack introduces **AI power-analysis resistance**, where dummy-computation masking and power-trace equalization obscure physical execution signatures. The following discussion explores how controlled noise injection transforms the enclave into a physically opaque execution environment, preventing adversaries from extracting information through power-analysis techniques.

iii. AI Power-Analysis Resistance via Dummy-Computation Masking Protocols

AI power-analysis resistance targets a very specific class of attacks: adversaries who try to infer secrets—model weights, keys, or even input data—by watching how much power the hardware consumes over time. Even when everything is encrypted and enclaves are attested, the physical power trace can still betray patterns. Dummy-computation masking is about turning that trace into noise.

Noise as cognitive camouflage

In this layer, the enclave behaves like a cognitive system deliberately **camouflaging its internal activity**. Real computations are blended with synthetic ones so that, from the outside, the

power profile looks statistically uniform and uninformative. The AI runtime doesn't just "do extra work"—it **curates** dummy operations to shape the power signal.

Core mechanisms

- **Dummy fused-operator blocks:** The runtime injects extra matrix multiplies, convolutions, or activation chains that do not affect the model state but consume similar power as real operations.
- **Randomized tensor paths:** Non-critical tensors are routed through decoy compute paths to add variability to memory access and ALU usage.
- **Masked memory-access patterns:** Reads/writes are padded with extra accesses to unrelated regions so that an attacker cannot correlate specific addresses or access bursts with sensitive operations.
- **Power-trace equalization loops:** When the model would naturally be "quiet" (e.g., sparse inputs, pruned branches), the enclave adds synthetic load to keep the overall power envelope flat.

Mathematical framing: shaping the power envelope

Let $P_{real}(t)$ be the power consumption of genuine AI computation at time t, and $P_{dummy}(t)$ the power from masking operations. The enclave aims for a target envelope $P_{target}(t)$ such that:

$$P_{\text{real}}(t) + P_{\text{dummy}}(t) \approx P_{\text{target}}(t)$$

with $P_{target}(t)$ chosen to be:

- high-entropy (no obvious patterns)
- statistically similar across different inputs
- independent of secret-dependent branches

From the attacker's perspective, any attempt to infer secrets from P(t) collapses into noise.

Threats neutralized

Differential power analysis against cryptographic routines inside the enclave

- **Model-weight extraction** via repeated trace comparison
- **Input-classification leakage** based on characteristic power signatures

- **Key-recovery attacks** targeting hardware-bound keys

Operational trade-offs

- **Overhead:** extra computations cost energy and time, so masking must be tuned—strong enough to break attacks, light enough to keep SLAs.
- **Policy:** different workloads may use different masking profiles (e.g., stronger for key handling, lighter for generic inference).
- **Integration:** masking logic is tightly coupled with the scheduler so that dummy work never interferes with correctness or QoS.

This layer turns the enclave into a **physically opaque** execution environment: even with a probe on the power rails, the attacker sees only curated noise.

Once power-analysis resistance has blurred the physical energy footprint of AI computation, the next attack surface is **time itself**. Adversaries can still try to infer secrets by measuring how long operations take—whether certain branches run, whether particular inputs trigger faster or slower paths, or whether cryptographic routines leak timing differences. To close this gap, the enclave stack introduces **deterministic AI compute-padding**, where execution is deliberately shaped so that all relevant operations take the same amount of time, regardless of input or internal state. The next discussion explores how constant-time operators, fixed-latency memory access, and padded control flows neutralize timing-side-channels and complete the side-channel defense envelope.

iv. Deterministic AI Compute-Padding Techniques for Timing-Side-Channel Neutralization

Deterministic AI compute-padding is the final defensive layer in the secure-enclave stack. Even when memory is encrypted, multi-party aggregation is cryptographically protected, and power-analysis resistance obscures physical traces, attackers may still attempt to infer secrets by measuring **how long** operations take. Timing-side-channels are subtle but powerful: variations in execution time can reveal branching behavior, sparsity patterns, conditional logic, or even cryptographic key bits. Deterministic compute-padding eliminates these leaks by enforcing **constant-time execution**, transforming the enclave into a timing-neutral environment where no observable temporal signal correlates with sensitive data.

Timing Discipline as Cognitive Rhythm Control

In this layer, the AI runtime behaves like a cognitive system enforcing a **strict internal rhythm**. Regardless of input complexity, sparsity, or branching, the enclave maintains a uniform execution cadence. Sensitive operations—cryptographic routines, conditional branches, sparse

tensor paths—are padded with deterministic compute blocks so that their external timing footprint is indistinguishable.

This framing positions deterministic compute-padding as a form of **cognitive rhythm control**, where the enclave deliberately shapes its temporal behavior to prevent adversarial inference.

Core Mechanisms of Deterministic Compute-Padding

1. Constant-Time Operator Execution

Operators that normally vary in execution time (e.g., sparse GEMM, conditional activation functions) are padded with dummy operations to ensure uniform latency.

- Sparse operations are padded to match dense execution time.
- Conditional branches execute both paths, discarding the unused result.
- Quantized kernels add fixed-latency padding loops.

2. Fixed-Latency Memory Access

Memory operations are padded so that:

- cache hits and misses appear identical
- variable-length reads are normalized
- memory-access bursts are masked
- address-dependent timing differences are eliminated

This prevents attackers from inferring memory-access patterns.

3. Deterministic Kernel Launch Intervals

Kernel launches occur at fixed intervals, independent of workload characteristics.

- prevents timing inference across kernel boundaries
- eliminates latency signatures associated with specific inputs
- ensures predictable temporal behavior across the enclave

4. Padded Control-Flow Execution

Control-flow structures (loops, branches, conditionals) are padded so that:

- loop iterations always take the same time

- branching paths execute deterministically
- early exits are replaced with padded dummy work

This neutralizes timing differences caused by data-dependent control flow.

Threats Neutralized by Deterministic Compute-Padding

This mechanism protects against:

- **timing-side-channel attacks**
- **branch-prediction leakage**
- **sparsity-pattern inference**
- **conditional-logic leakage**
- **cryptographic key-bit timing attacks**
- **model-structure inference through latency analysis**

It ensures that no external observer can correlate execution time with sensitive internal behavior.

Mathematical Framing: Timing Neutralization Constraint

Let $T_{real}(x)$ be the execution time of an operation on input x. The enclave enforces:

$$T_{\text{real}}(x) + T_{\text{padding}}(x) = T_{\text{constant}}$$

for all valid inputs x, where:

- $T_{padding}(x)$ is the deterministic padding time
- $T_{constant}$ is the fixed target latency

This ensures:

$$\frac{\partial T}{\partial x} = 0,$$

meaning execution time is **independent** of input, internal state, or branching behavior.

Operational Impact

Deterministic compute-padding enables:

- timing-neutral cryptographic routines
- secure multi-tenant inference
- protection of conditional logic and sparse models
- elimination of timing-based leakage vectors
- predictable latency for real-time workloads
- full temporal isolation of enclave execution

It completes the side-channel defense envelope by neutralizing the last major observable signal: **time**.

Full-stack AI secure enclaves illustrate how cross-layer optimization can integrate security, computational efficiency, and operational reliability into a unified AI execution architecture. As AI workloads increasingly operate across shared accelerators, edge devices, distributed computing platforms, and cloud infrastructures, protecting model parameters, intermediate tensors, training data, and inference results requires more than a single security mechanism. Confidentiality and integrity depend on coordinated protections spanning the processor, memory hierarchy, interconnects, compiler toolchains, execution runtime, and application layer. Cross-layer optimization provides the architectural framework for coordinating these protections while accounting for their effects on latency, throughput, memory consumption, power efficiency, and system reliability.

At the foundation of this architecture, hardware-enforced isolation establishes protected execution boundaries for sensitive AI workloads. Trusted execution environments (TEEs), secure enclaves, access-control mechanisms, and hardware-supported memory protection can restrict unauthorized access to selected computational states and data structures. Within these boundaries, model parameters, input tensors, intermediate activations, cryptographic keys, and execution metadata can receive protection appropriate to their sensitivity. Encrypted memory and protected paging extend confidentiality mechanisms beyond the immediate processor context, helping safeguard sensitive information when it must be transferred between protected memory regions and external storage. These protections must be designed to account for memory reuse, page movement, context switching, device access, and the lifecycle of cryptographic keys. Encryption alone does not guarantee complete isolation: access patterns, metadata, implementation flaws, and compromised components may still expose information unless the surrounding architecture addresses those risks.

Cross-layer optimization further requires that cryptographic protection be integrated with the AI execution pipeline rather than added after performance-critical decisions have already been

made. Encryption, decryption, integrity verification, and secure memory management consume computational resources and can introduce additional data movement. Their overhead may become particularly significant for workloads involving large tensors, frequent memory transfers, distributed inference, or high-throughput model serving. Hardware cryptographic acceleration, efficient memory layouts, protected buffer reuse, and carefully scheduled data transfers can reduce some of these costs. Compiler and runtime systems can also minimize unnecessary movement of sensitive data, limit the lifetime of temporary tensors, and avoid copying protected information into untrusted memory without an explicit security justification. The objective is to preserve the required security properties while reducing avoidable overhead throughout the execution path.

Secure collaboration introduces an additional challenge when AI computation spans multiple devices, organizations, or administrative domains. Hardware-supported isolation can protect local computation, while cryptographic protocols such as secure multiparty computation and secure aggregation can allow participants to contribute to a joint computation without directly disclosing their raw inputs to one another. The appropriate combination depends on the application, trust assumptions, communication environment, and threat model. Secure aggregation, for example, can protect individual contributions under specified protocol assumptions, but it does not automatically guarantee that every intermediate result or final model output is free from information leakage. Effective distributed AI security must therefore coordinate enclave attestation, participant authentication, key management, message integrity, protocol validation, and controls over the information released by the computation. It must also consider collusion, participant compromise, communication failures, and the possibility that repeated outputs may reveal sensitive characteristics of the underlying data.

Physical and microarchitectural side channels demonstrate why cryptographic isolation alone is insufficient. An attacker may attempt to infer secret information from observable variations in power consumption, electromagnetic emissions, cache activity, memory-access patterns, processor contention, or execution time. Even when the contents of memory are encrypted, the manner in which a workload accesses that memory may reveal useful information. Countermeasures must therefore be selected according to the capabilities of the underlying hardware and the attacker's assumed access. Constant-time implementations can reduce secret-dependent timing variation; carefully designed memory-access patterns can limit some forms of access-pattern leakage; and power-analysis countermeasures can reduce correlations between secret-dependent computation and observable physical traces. Depending on the platform, these measures may incorporate masking, balanced implementations, noise generation, dummy operations, or specialized hardware support. However, such techniques are not interchangeable, and their effectiveness must be demonstrated against the relevant attack

model rather than assumed from their presence alone.

Timing protection requires particular care in AI systems because their workloads are often dynamic. Input-dependent computation, variable sequence lengths, conditional execution, memory allocation, accelerator scheduling, and communication delays can all produce timing variation. Deterministic compute-padding and constant-time execution strategies can reduce leakage when execution duration might otherwise depend on sensitive values. Yet padding does not automatically eliminate timing channels: contention, cache behavior, memory traffic, operating-system activity, and shared-device scheduling may still reveal information. Moreover, excessive padding can increase latency, power consumption, and resource occupancy, potentially undermining real-time requirements. A cross-layer design must therefore distinguish between timing predictability for operational purposes and timing independence for security purposes. Where both are required, the architecture should define appropriate execution bounds, isolate competing workloads where feasible, constrain secret-dependent behavior, and validate residual leakage through systematic testing.

These considerations make the security–performance trade-off a central concern in full-stack optimization. Stronger isolation may limit resource sharing; constant-time execution may increase computational work; cryptographic verification may introduce additional processing stages; and physical-trace obfuscation may consume extra energy. Conversely, overly aggressive optimization can weaken security if it removes integrity checks, exposes intermediate tensors, introduces data-dependent shortcuts, or permits uncontrolled sharing of hardware resources. Cross-layer optimization must therefore treat security requirements as architectural constraints rather than optional features to be considered after throughput tuning. Performance improvements are acceptable only when they preserve the required confidentiality, integrity, isolation, and leakage-resistance properties.

A practical secure-enclave architecture consequently combines several complementary layers: hardware-rooted trust and isolation; cryptographic protection for sensitive data and communication; memory-access and execution controls that limit information leakage; runtime monitoring and integrity verification; secure coordination among distributed participants; and recovery procedures for detected faults or policy violations. Attestation can help a remote party verify that an expected platform or software configuration is participating in a computation, provided that the attestation mechanism and its trust chain are themselves sound. Runtime monitoring can detect selected deviations from expected behavior, while fault-containment mechanisms can limit the impact of compromised or malfunctioning components. Secure update and key-revocation procedures are also necessary because an enclave's initial integrity does not guarantee that it will remain trustworthy throughout its operational lifetime.

The resulting architecture should be evaluated as a complete system rather than as a collection of independently certified components. Relevant measurements include inference latency, latency variation, throughput, energy per operation, memory overhead, cryptographic processing cost, and resource utilization. Security evaluation should additionally examine isolation boundaries, memory-protection behavior, attestation validity, resistance to relevant timing and physical side channels, fault response, and the consequences of compromised components. Testing should cover realistic workloads, concurrent execution, resource contention, device resets, interrupted communication, and attempts to access or manipulate protected data. Where formal verification or hardware security evaluation is appropriate, these methods should complement—not replace—deployment-representative testing and continuous assessment of implementation assumptions.

Ultimately, full-stack AI secure enclaves demonstrate the broader principle of cross-layer optimization: security, performance, reliability, and predictability must be engineered together because each depends on decisions made throughout the computational stack. Encrypted memory, cryptographic collaboration, physical side-channel defenses, deterministic execution strategies, and hardware-enforced isolation provide complementary forms of protection, but none independently establishes complete security. Their effectiveness emerges from the consistency of their integration, the validity of their threat assumptions, and the rigor of their verification.

Cross-layer optimization therefore transforms secure AI execution from a narrowly defined hardware feature into a system-wide engineering discipline. It coordinates model execution, memory protection, cryptographic operations, accelerator scheduling, runtime controls, and distributed communication to preserve the properties required by the application while managing the associated performance costs. The central objective is not simply to make an AI workload execute faster or to place it inside an isolated processor region. It is to ensure that computation remains efficient enough for its operational purpose, sufficiently predictable for its timing requirements, and adequately protected against the threats within its defined security model. In this sense, secure enclaves represent one important application of cross-layer optimization: they demonstrate how a vertically integrated AI architecture can coordinate computational capability with confidentiality, integrity, and resilience without treating any one of these requirements as independent of the others.

Assessments & Exercises: Set 1

Section 8.4: Hardware–Software Co-Design: AI Accelerators, Sensor Pipelines, and Cross-Layer Optimization

PART I — MULTIPLE CHOICE QUESTIONS (10 QUESTIONS)

Instructions: Select the single best answer for each question.

Question 1: What is the primary objective of hardware–software co-design in AI systems?

A. Increasing programming-language portability
B. Separating hardware and software development activities
C. Optimizing system performance through coordinated hardware and software decisions
D. Eliminating the need for specialized accelerators

Question 2: Within the roofline model, a workload is considered memory-bound when:

A. Computational throughput exceeds memory bandwidth requirements
B. Performance is limited primarily by data movement rather than arithmetic capability
C. Tensor cores are operating at peak utilization
D. Arithmetic intensity has reached its maximum value

Question 3: Which architectural technique is specifically designed to reduce unnecessary computation while preserving accelerator efficiency?

A. Dynamic voltage scaling
B. Structured sparsity
C. Cache invalidation
D. Pipeline flushing

Question 4: What is the primary benefit of SRAM tiling in attention-based AI architectures?

A. Increasing parameter count
B. Improving optical communication bandwidth
C. Reducing off-chip memory accesses and increasing data reuse
D. Eliminating the need for attention mechanisms

Question 5: Linear-attention and state-space architectures primarily address which challenge?

A. Operating-system compatibility
B. Long-context memory and bandwidth scaling limitations
C. Internet connectivity constraints
D. Compiler installation complexity

Question 6: In a mixture-of-experts (MoE) architecture, sparse expert routing is used to:

A. Activate all experts simultaneously
B. Reduce network latency through optical interconnects
C. Selectively activate only the most relevant computational pathways
D. Replace memory hierarchies with tensor cores

Question 7: What is the primary purpose of tile-optimized kernel compilation?

A. Increasing model parameter counts
B. Aligning computation with accelerator geometry and memory topology
C. Eliminating compiler optimizations
D. Replacing distributed training systems

Question 8: Processing-in-memory (PIM) architectures seek to improve efficiency primarily by:

A. Increasing clock frequency indefinitely
B. Reducing the distance between computation and stored data
C. Eliminating memory completely
D. Using only optical processors

Question 9: A coarse-grained reconfigurable array (CGRA) differs from a fixed-function accelerator because it:

A. Operates only with FP32 arithmetic
B. Uses no routing infrastructure
C. Dynamically adapts computational topology to changing workloads
D. Eliminates hardware scheduling mechanisms

Question 10: Which software paradigm is most directly responsible for coordinating trillion-parameter AI models across multiple accelerators?

A. Static memory allocation
B. Distributed orchestration using tensor, pipeline, and context parallelism
C. Single-thread execution control
D. Local cache eviction only

PART II — SCENARIO-BASED ANALYSIS (3 SCENARIOS)

Scenario 1: Autonomous Vehicle Perception Platform

An autonomous vehicle manufacturer is deploying a next-generation perception stack that combines:

- Multi-camera systems
- LiDAR
- Radar
- Transformer-based perception models
- Real-time planning systems

During testing, engineers observe:

- Excessive memory-bandwidth consumption
- High attention-computation latency
- Underutilized tensor cores
- Reduced frame rates during long-context processing
- Increased thermal load during peak traffic conditions

Questions

1. Identify the primary hardware and software bottlenecks affecting system performance.

2. Explain how memory-optimized attention mechanisms could reduce bandwidth pressure.

3. Analyze how arithmetic intensity influences accelerator utilization.

4. Discuss the role of structured sparsity in improving computational efficiency.

5. Recommend hardware–software co-design strategies that could improve real-time performance while maintaining perception accuracy.

Scenario 2: Large-Scale Distributed Language Model Deployment

A research organization is training a multi-hundred-billion-parameter language model across a cluster of accelerators.

Operational challenges include:

- Communication overhead between devices
- Uneven workload distribution

- Memory-capacity limitations
- Pipeline bubbles in model execution
- Growing KV-cache requirements

Engineers are considering tensor parallelism, activation partitioning, and distributed context management.

Questions

1. Explain the purpose of tensor parallelism in large-scale AI training.

2. Analyze the causes of pipeline bubbles within distributed execution environments.

3. Discuss how activation partitioning reduces memory pressure.

4. Evaluate the benefits and challenges of distributed context parallelism.

5. Recommend an orchestration strategy that balances scalability, throughput, and memory efficiency.

Scenario 3: Edge AI Industrial Inspection System

An industrial manufacturer is deploying an edge AI inspection platform on a resource-constrained device.

System characteristics include:

- Limited onboard memory
- Restricted power budget
- FPGA/CGRA-style accelerator fabric
- Conditional-computation inference pipeline
- Real-time defect detection requirements

Observed issues include:

- Variable latency between workloads
- Routing congestion inside the spatial fabric
- Memory-fragmentation effects
- Uneven expert utilization in the conditional-computation architecture

- Frequent model updates from centralized infrastructure

Questions

1. Explain how reconfigurable spatial architectures address diverse workload requirements.

2. Analyze the causes of routing congestion in CGRA-based systems.

3. Discuss how conditional computation can improve efficiency in edge AI deployments.

4. Evaluate the role of dynamic memory management in maintaining predictable inference performance.

5. Recommend a combined hardware–software optimization strategy that improves utilization, reduces latency, and supports scalable deployment at the edge.

PART III — EXTENDED SYSTEMS ENGINEERING EXERCISE

Designing a Next-Generation Edge AI Co-Designed Platform

An engineering team is tasked with developing an AI platform with the following requirements:

- Real-time decision making
- Multi-modal sensing
- Edge deployment constraints
- Long-context reasoning capability
- Distributed accelerator support
- Energy-efficient operation
- Future scalability to larger foundation models

Assignment

Develop a systems-engineering analysis addressing:

1. Hardware–software co-design principles.

2. Accelerator selection and architecture.

3. Memory hierarchy design.

4. Attention and long-context optimization strategies.

5. Structured sparsity implementation.

6. Conditional-computation mechanisms.

7. Distributed orchestration architecture.

8. Compiler and kernel-optimization strategies.

9. Reconfigurable spatial-computing opportunities.

10. Reliability, scalability, and deployment considerations.

Analysis Requirements

The analysis should explain how hardware architecture, software infrastructure, memory systems, compiler technologies, and AI model design can be integrated into a unified optimization framework capable of supporting efficient, scalable, and reliable edge AI deployment.

Solutions and Model Answers: Set 1

Section 8.4: Hardware–Software Co-Design: AI Accelerators, Sensor Pipelines, and Cross-Layer Optimization

PART I — MULTIPLE CHOICE QUESTIONS (ANSWER KEY)

1: What is the primary objective of hardware–software co-design in AI systems?

Correct Answer: C. Optimizing system performance through coordinated hardware and software decisions

Justification: Hardware–software co-design seeks to optimize overall system behavior by jointly considering accelerator architecture, memory systems, software frameworks, compiler strategies, and AI models rather than designing each component independently.

2: Within the roofline model, a workload is considered memory-bound when:

Correct Answer: B. Performance is limited primarily by data movement rather than arithmetic capability

Justification: In the roofline model, a workload is memory-bound when memory bandwidth constrains performance more than available computational throughput.

3: Which architectural technique is specifically designed to reduce unnecessary computation while preserving accelerator efficiency?

Correct Answer: B. Structured sparsity

Justification: Structured sparsity removes unnecessary computation while preserving hardware-friendly execution patterns that maintain tensor-core and vector-lane efficiency.

4: What is the primary benefit of SRAM tiling in attention-based AI architectures?

Correct Answer: C. Reducing off-chip memory accesses and increasing data reuse

Justification: SRAM tiling keeps active data resident in fast on-chip memory, minimizing expensive memory transfers and improving attention throughput.

5: Linear-attention and state-space architectures primarily address which challenge?

Correct Answer: B. Long-context memory and bandwidth scaling limitations

Justification: Linear-attention and state-space architectures were developed to address the growing memory and computational costs associated with long-sequence processing.

6: In a mixture-of-experts (MoE) architecture, sparse expert routing is used to:

Correct Answer: C. Selectively activate only the most relevant computational pathways

Justification: Sparse expert routing allows only a subset of experts to participate in processing a given input, reducing unnecessary computation while preserving model capacity.

7: What is the primary purpose of tile-optimized kernel compilation?

Correct Answer: B. Aligning computation with accelerator geometry and memory topology

Justification: Tile-optimized compilation maps neural operations onto hardware-specific execution resources such as tensor cores, vector lanes, and memory banks.

8: Processing-in-memory (PIM) architectures seek to improve efficiency primarily by:

Correct Answer: B. Reducing the distance between computation and stored data

Justification: Processing-in-memory architectures improve efficiency by bringing computation closer to memory, reducing energy-intensive data movement.

9: A coarse-grained reconfigurable array (CGRA) differs from a fixed-function accelerator because it:

Correct Answer: C. Dynamically adapts computational topology to changing workloads

Justification: CGRA architectures support runtime reconfiguration of compute and communication resources to match workload requirements.

10: Which software paradigm is most directly responsible for coordinating trillion-parameter AI models across multiple accelerators?

Correct Answer: B. Distributed orchestration using tensor, pipeline, and context parallelism

Justification: Distributed orchestration mechanisms enable large AI systems to scale across multiple accelerators while coordinating computation, memory, and communication.

PART II — SCENARIO-BASED ANALYSIS (MODEL ANSWERS)

Scenario 1: Autonomous Vehicle Perception Platform

1. Identify the primary hardware and software bottlenecks affecting system performance.

Model Answer:

The primary bottlenecks include:

- Memory-bandwidth limitations caused by attention operations.
- Excessive KV-cache growth during long-context processing.
- Underutilization of tensor-core resources.
- Thermal constraints resulting from sustained high workloads.
- Latency associated with transferring Q, K, and V tensors between memory hierarchies.

The system is therefore constrained by both memory movement and execution efficiency rather than raw arithmetic capability alone.

2. Explain how memory-optimized attention mechanisms could reduce bandwidth pressure.

Model Answer:

Memory-optimized attention techniques such as SRAM tiling, FlashAttention-style implementations, KV-cache partitioning, and attention-window restrictions reduce repeated memory transfers. By increasing data reuse and limiting movement between on-chip and off-chip memory, these methods lower bandwidth consumption and improve throughput.

3. Analyze how arithmetic intensity influences accelerator utilization.

Model Answer:

Arithmetic intensity measures the amount of computation performed for each unit of data movement. Higher arithmetic intensity allows hardware resources to remain active for longer periods after data are loaded into memory. As arithmetic intensity increases, workloads move closer to the compute-bound region of the roofline model and tensor-core utilization improves.

4. Discuss the role of structured sparsity in improving computational efficiency.

Model Answer:

Structured sparsity removes low-value computations while preserving accelerator-friendly execution patterns. Techniques such as 2:4 sparsity reduce arithmetic workload, memory traffic, and energy consumption while maintaining efficient tensor-core execution. The result is improved throughput and lower operational cost.

5. Recommend hardware–software co-design strategies that could improve real-time performance while maintaining perception accuracy.

Model Answer:

Recommended strategies include:

- Memory-optimized attention implementations.
- Structured sparsity and quantization.
- Hardware-aware kernel compilation.
- SRAM-aware tiling and cache optimization.
- Dynamic workload scheduling.
- Tensor-core-aware operator fusion.
- Mixed-precision execution.
- Thermal-aware workload management.

These integrated approaches improve throughput while preserving perception quality and real-time responsiveness.

Scenario 2: Large-Scale Distributed Language Model Deployment

1. Explain the purpose of tensor parallelism in large-scale AI training.

Model Answer:

Tensor parallelism divides large matrix computations across multiple accelerators. Rather than requiring a single device to execute all operations, computation is partitioned so that each accelerator processes a portion of the tensor workload. This enables support for models that exceed the memory and compute capacity of individual devices.

2. Analyze the causes of pipeline bubbles within distributed execution environments.

Model Answer:

Pipeline bubbles occur when some accelerator stages remain idle while waiting for data from preceding stages. Causes include:

- Load imbalance among stages.
- Uneven computation times.
- Communication delays.
- Inefficient micro-batch scheduling.
- Inconsistent workload partitioning.

These factors reduce overall utilization and lower throughput.

3. Discuss how activation partitioning reduces memory pressure.

Model Answer:

Activation partitioning distributes intermediate neural-network activations across multiple accelerators rather than storing them on a single device. This approach lowers per-device memory requirements and enables larger models and batch sizes while maintaining stable execution.

4. Evaluate the benefits and challenges of distributed context parallelism.

Model Answer:

Benefits:

Supports longer context windows.

- Reduces per-device memory consumption.
- Enables distributed KV-cache storage.
- Improves scalability for long-context reasoning.

Challenges:

Increased communication overhead.

- Synchronization complexity.
- Context-consistency requirements.
- Greater dependency on high-bandwidth interconnects.

5. Recommend an orchestration strategy that balances scalability, throughput, and memory efficiency.

Model Answer:

An effective strategy combines:

- Tensor parallelism for large matrix operations.
- Pipeline parallelism for model-layer distribution.
- Context parallelism for long-sequence processing.

- Activation partitioning for memory efficiency.
- Overlapped communication and computation to reduce idle time.
- Dynamic load balancing across accelerators.

This hybrid orchestration approach maximizes resource utilization while maintaining scalability.

Scenario 3: Edge AI Industrial Inspection System

1. Explain how reconfigurable spatial architectures address diverse workload requirements.

Model Answer:

Reconfigurable spatial architectures dynamically adjust compute resources, routing pathways, and execution topologies based on workload demands. This flexibility allows the accelerator to support varying execution patterns efficiently while maintaining high utilization.

2. Analyze the causes of routing congestion in CGRA-based systems.

Model Answer:

Routing congestion can result from:

- Excessive communication among tiles.
- Sparse expert-routing patterns.
- Imbalanced workload distribution.
- Limited routing resources.
- Simultaneous activation of multiple communication-intensive tasks.

These conditions increase latency and reduce overall throughput.

3. Discuss how conditional computation can improve efficiency in edge AI deployments.

Model Answer:

Conditional computation activates only the model components required for a specific input. This reduces:

- Energy consumption.
- Memory bandwidth usage.
- Computational workload.

- Thermal output.

At the same time, model capacity remains available when needed for more complex inputs.

4. Evaluate the role of dynamic memory management in maintaining predictable inference performance.

Model Answer:

Dynamic memory management prevents fragmentation, optimizes cache utilization, and improves locality. Techniques such as memory defragmentation, page migration, and adaptive retention policies help maintain deterministic latency and reduce performance degradation during extended operation.

5. Recommend a combined hardware–software optimization strategy that improves utilization, reduces latency, and supports scalable deployment at the edge.

Model Answer:

A comprehensive optimization strategy should include:

Hardware Measures

- CGRA routing optimization.
- Structured sparsity support.
- Low-precision arithmetic (INT4/FP4).
- Local memory tiling and caching.

Software Measures

- Hardware-aware kernel compilation.
- Dynamic load balancing.
- Conditional-computation routing.
- Memory-defragmentation policies.
- Latency-masking execution methods.

System-Level Measures

- Edge/cloud workload partitioning.
- Model quantization.

- Real-time scheduling controls.
- Runtime topology adaptation.

Together, these techniques improve overall efficiency, reduce latency, and support scalable resource-constrained deployment.

PART III — EXTENDED SYSTEMS ENGINEERING EXERCISE

Sample Solution Framework

A comprehensive response should address the following areas:

Hardware–Software Co-Design

- Joint optimization of models, accelerators, memory systems, and runtime frameworks.

Accelerator Architecture

- Tensor-core accelerators.
- Reconfigurable fabrics.
- Hybrid edge accelerators.

Memory Hierarchy Design

- SRAM tiling.
- Hierarchical cache structures.
- KV-cache optimization.
- Memory-locality strategies.

Attention Optimization

- FlashAttention-style kernels.
- State-space architectures.
- Linear-attention mechanisms.
- Context-partitioning approaches.

Structured Sparsity

- 2:4 sparsity.
- Block sparsity.
- Zero-skip execution scheduling.

Conditional Computation

- Sparse expert routing.
- Dynamic workload allocation.
- Adaptive execution pathways.

Distributed Orchestration

- Tensor parallelism.
- Pipeline parallelism.
- Context parallelism.
- Load-balancing strategies.

Compiler Optimization

- Tile-aware kernel generation.
- Vector-lane mapping.
- Shared-memory staging.
- Hardware-specific code generation.

Reconfigurable Computing

- Dynamic routing.
- CGRA topology adaptation.
- Runtime graph remapping.

Reliability and Scalability

- Thermal management.
- Fault tolerance.
- Communication efficiency.

- Predictable real-time execution.

Overall Conclusion

An effective hardware–software co-design strategy integrates model architecture, compiler technology, memory systems, accelerators, communication fabrics, and runtime orchestration into a unified optimization framework. Such integration enables edge AI platforms to achieve high performance, low latency, efficient resource utilization, and long-term scalability while operating within practical hardware constraints.

Assessments & Exercises: Set 2

Section 8.4: Hardware–Software Co-Design: AI Accelerators, Sensor Pipelines, and Cross-Layer Optimization

PART I — MULTIPLE CHOICE (10 QUESTIONS)

1. What is the primary objective of hardware–software co-design in AI systems?

A. To maximize processor clock frequency regardless of energy consumption
B. To optimize hardware and software together under system-level constraints
C. To eliminate the need for software compilers
D. To ensure that all AI models execute on identical hardware

2. Why must AI model architecture be considered during hardware selection for edge deployment?

A. Model architecture determines every characteristic of the operating system
B. All model architectures require the same computational resources
C. Model architecture influences computational workload, memory requirements, and execution patterns
D. Hardware selection has no effect on model performance

3. Which factor most directly explains why an AI accelerator with high theoretical computational throughput may deliver disappointing application performance?

A. The accelerator has too many arithmetic units in every possible workload
B. The application uses a neural network rather than a conventional algorithm
C. The model has been trained on more than one dataset
D. Memory transfers, data movement, synchronization, or unsupported operations create bottlenecks

4. What is a principal benefit of AI compiler optimization through operator fusion?

A. It can reduce intermediate data movement and the overhead associated with separate operator executions
B. It guarantees that every neural network will achieve higher accuracy
C. It eliminates the need for memory management
D. It automatically makes all execution deterministic

5. Why is timestamping important in a multimodal sensor pipeline?

A. It increases the physical resolution of every sensor
B. It eliminates calibration requirements
C. It helps establish the temporal relationship among measurements collected by different sensors
D. It guarantees that all sensors produce data at the same sampling frequency

6. Which statement best describes the role of sensor fusion in an AI system?

A. It replaces all physical sensors with a single virtual sensor
B. It combines information from multiple sources to support a more comprehensive representation of the environment
C. It ensures that noisy sensor measurements cannot affect model predictions
D. It eliminates the need to evaluate sensor reliability

7. What distinguishes real-time performance from simply achieving a high average inference throughput?

A. Real-time performance depends only on the number of processor cores
B. Real-time performance requires every operation to execute at the same clock frequency
C. High average throughput guarantees that every result arrives before its deadline
D. Real-time performance requires attention to timing constraints, deadline compliance, and execution variability

8. Which technique can help improve the temporal predictability of competing workloads on an embedded AI platform?

A. Scheduling policies that account for task priorities, deadlines, and resource contention
B. Allowing every workload to use all available resources without coordination
C. Increasing model size whenever inference latency rises
D. Removing synchronization between dependent processing stages

9. Why should model quantization be evaluated together with the target accelerator and application requirements?

A. Quantization always reduces accuracy to an unacceptable level
B. Quantization affects only the model file size, not execution
C. The benefits depend on supported numerical formats, hardware execution efficiency, and the resulting model accuracy
D. Quantization eliminates the need for compiler optimization

10. Which example best illustrates cross-layer optimization?

A. Selecting a processor solely because it has the highest advertised TOPS rating
B. Coordinating model precision, compiler transformations, accelerator capabilities, memory transfers, and scheduling to meet latency, energy, and accuracy requirements
C. Improving sensor resolution without evaluating its effect on bandwidth or processing time
D. Optimizing a neural network using accuracy as the only evaluation metric

PART II — SHORT-ANSWER QUESTIONS (6 QUESTIONS)

1. Explain the purpose of hardware–software co-design.
Describe two limitations of optimizing AI software and hardware independently.

2. Compare two AI hardware platforms.
Explain how computational throughput, memory bandwidth, energy consumption, programmability, and thermal limits can influence the choice of an accelerator for an edge AI application.

3. Analyze a sensor-pipeline bottleneck.
A robotic platform combines camera and inertial measurement unit data. Explain how timestamping, synchronization, buffering, and preprocessing can affect the quality and latency of the information delivered to the AI model.

4. Explain the difference between average latency and worst-case execution time.
Why can average inference latency alone be insufficient when an AI system must respond within a strict deadline?

5. Evaluate a model-compression strategy.
Explain how quantization and pruning can reduce resource requirements. Identify at least two potential trade-offs or limitations that engineers should evaluate before deployment.

6. Explain cross-layer optimization.
Describe how a change in model architecture can affect compiler behavior, accelerator utilization, memory traffic, energy consumption, and end-to-end latency.

PART III — APPLIED ENGINEERING EXERCISES (4 EXERCISES)

Exercise 1: Edge AI Accelerator Selection

An autonomous inspection robot must process camera images and produce a perception result every 40 milliseconds. The system operates from a limited battery supply and has a restricted thermal envelope.

Three candidate platforms are available:

Parameter	Platform A	Platform B	Platform C
Peak AI throughput	20 TOPS	35 TOPS	28 TOPS
Measured end-to-end inference latency	28 ms	34 ms	22 ms
Average power during the test workload	8 W	12 W	10 W
Peak memory usage	1.8 GB	2.4 GB	1.5 GB

Assume the measurements were obtained using the same model, input workload, and measurement boundary.

Tasks:

a. Identify which platforms satisfy the 40 ms latency target under the measured test conditions.

b. Calculate the inference-only energy per result for each platform using:

$$E = P \times t$$

where P is average power in watts and t is inference latency in seconds.

c. Rank the platforms according to measured latency, estimated inference energy per result, and memory usage.

d. Explain why these measurements are insufficient by themselves to establish that a platform will meet a hard real-time deadline under all operating conditions.

e. Recommend a platform for further evaluation and justify your recommendation using the application's latency, energy, and memory constraints.

Exercise 2: Sensor Synchronization and End-to-End Latency

A mobile robot combines camera and inertial measurement unit data before running a perception model. The processing stages have the following nominal latencies:

Processing Stage	Latency
Sensor acquisition and transfer	6 ms
Synchronization and preprocessing	4 ms
AI inference	18 ms
Postprocessing and decision generation	5 ms

Tasks:

a. Calculate the nominal end-to-end processing latency, assuming the stages execute sequentially and the listed values exclude overlapping work.

b. Determine whether the pipeline meets a 35 ms end-to-end latency target under these nominal conditions.

c. If inference latency increases by 8 ms during a high-load period, calculate the new nominal end-to-end latency and determine whether the target is met.

d. Explain how buffering, sensor timestamping, asynchronous transfers, or preprocessing acceleration might affect the pipeline.

e. Propose a measurement plan that captures both average latency and high-percentile or worst-case timing behavior.

Exercise 3: Hardware-Aware Model Optimization

An edge vision model currently uses 32-bit floating-point arithmetic. The deployment team is considering an 8-bit quantized version and structured pruning to reduce computational and memory requirements.

Tasks:

a. Explain how reducing numerical precision can affect model storage, memory traffic, and inference performance.

b. Describe the difference between structured and unstructured pruning, including why the distinction matters for hardware execution.

c. Identify accuracy and robustness tests that should be performed before deploying the optimized model.

d. Explain how the target accelerator's supported data types and sparsity capabilities influence

the effectiveness of these techniques.

e. Design an experiment that compares the original model, the quantized model, and the quantized-plus-pruned model using consistent evaluation conditions.

f. Define a set of acceptance criteria that includes accuracy, latency, energy consumption, and memory footprint.

Exercise 4: Cross-Layer Optimization Under Thermal Constraints

An embedded AI system initially meets its latency target. During sustained operation, however, the accelerator heats up and reduces its operating frequency. Inference latency increases, causing occasional missed deadlines.

Tasks:

a. Explain how thermal constraints can affect accelerator performance and system-level timing.

b. Identify information that should be collected from hardware telemetry, the AI runtime, and the real-time scheduler to diagnose the problem.

c. Propose at least three potential interventions. Consider model optimization, scheduling, memory traffic, workload placement, and thermal management.

d. Explain the possible trade-offs among latency, accuracy, energy consumption, and thermal stability.

e. Develop a validation plan to determine whether the proposed changes improve performance during sustained operation rather than only during short tests.

f. Explain why a successful cross-layer optimization should be evaluated at the complete-system level rather than through accelerator throughput alone.

PART IV — INTEGRATIVE DESIGN CHALLENGE

Design an Edge AI System Under Multiple Constraints

Design a conceptual hardware–software architecture for an autonomous industrial inspection platform that must:

- Process data from at least two different sensor types.
- Run an AI perception model on an embedded computing platform.

- Operate within a specified power and thermal budget.
- Meet a defined end-to-end response-time target.
- Handle sensor degradation or temporary data loss.
- Protect sensitive model parameters or input data where required.
- Maintain safe system behavior when computational or sensing resources become unavailable.

Required deliverables:

System architecture: Draw or describe the sensor, processing, memory, accelerator, runtime, and control components.

Model selection: Justify the model architecture and its computational requirements.

Hardware selection: Compare at least two plausible computing platforms.

Sensor pipeline: Describe acquisition, timestamping, synchronization, preprocessing, and data transfer.

Software and scheduling: Explain how the model is compiled, deployed, and scheduled alongside other tasks.

Performance budget: Establish a latency budget and an energy or power budget.

Failure handling: Describe how the system detects and responds to sensor faults, missed deadlines, or thermal throttling.

Security considerations: Identify relevant protections and explain their performance overhead.

Validation plan: Define tests for accuracy, latency, resource utilization, sustained thermal behavior, and fault recovery.

Design trade-off analysis: Explain which requirements are most difficult to satisfy simultaneously and how the proposed design balances them.

Students should clearly distinguish measured results, estimated values, design assumptions, and requirements that still require verification.

Solutions and Model Answers: Set 2

Section 8.4: Hardware–Software Co-Design: AI Accelerators, Sensor Pipelines, and Cross-Layer Optimization

PART I — MULTIPLE CHOICE (ANSWER KEY)

1. What is the primary objective of hardware–software co-design in AI systems?

B — To optimize hardware and software together under system-level constraints.
Co-design considers the interactions among model structure, hardware capabilities, software execution, memory, energy, and application requirements.

2. Why must AI model architecture be considered during hardware selection for edge deployment?

C — Model architecture influences computational workload, memory requirements, and execution patterns.
Model structure affects the operations performed, the intermediate data retained, and the memory and compute resources required during inference.

3. Which factor most directly explains why an AI accelerator with high theoretical computational throughput may deliver disappointing application performance?

D — Memory transfers, data movement, synchronization, or unsupported operations create bottlenecks.
Peak arithmetic throughput does not establish end-to-end application performance. Data movement and inefficient execution can limit the realized benefit of an accelerator.

4. What is a principal benefit of AI compiler optimization through operator fusion?

A — It can reduce intermediate data movement and the overhead associated with separate operator executions.
Operator fusion can combine compatible operations, potentially reducing memory traffic and kernel-launch overhead. The actual benefit depends on the graph, compiler, and hardware.

5. Why is timestamping important in a multimodal sensor pipeline?

C — It helps establish the temporal relationship among measurements collected by different sensors.
Timestamping supports alignment of measurements captured at different times. Accurate synchronization may also require clock coordination and compensation for sensor-specific delays.

6. Which statement best describes the role of sensor fusion in an AI system?

B — It combines information from multiple sources to support a more comprehensive representation of the environment.
Sensor fusion can improve state estimation, but its effectiveness depends on calibration, synchronization, sensor quality, and the fusion method.

7. What distinguishes real-time performance from simply achieving a high average inference throughput?

D — Real-time performance requires attention to timing constraints, deadline compliance, and execution variability.
Average throughput can conceal occasional long delays. A time-critical system must be evaluated against its actual timing requirements.

8. Which technique can help improve the temporal predictability of competing workloads on an embedded AI platform?

A — Scheduling policies that account for task priorities, deadlines, and resource contention.
Appropriate scheduling can improve predictability, although hard real-time guarantees also require analysis of execution times, shared-resource interference, and other sources of delay.

9. Why should model quantization be evaluated together with the target accelerator and application requirements?

C — The benefits depend on supported numerical formats, hardware execution efficiency, and the resulting model accuracy.
Quantization may reduce memory traffic and improve execution efficiency, but the result depends on hardware support and the model's sensitivity to reduced precision.

10. Which example best illustrates cross-layer optimization?

B — Coordinating model precision, compiler transformations, accelerator capabilities, memory transfers, and scheduling.
This approach considers the complete system and balances multiple requirements instead of optimizing one component in isolation.

PART II — SHORT-ANSWER MODEL RESPONSES

1. Explain the purpose of hardware–software co-design.

Hardware–software co-design coordinates hardware architecture and software implementation so that their combined behavior meets application requirements. Independent optimization can produce mismatches: a model may exceed available memory, an accelerator may lack efficient support for important operators, or a compiler may generate an execution schedule that causes excessive data movement or deadline violations.

2. Compare two AI hardware platforms

An accelerator should be evaluated using the intended workload rather than peak throughput alone. Relevant factors include measured end-to-end latency, memory capacity and bandwidth, supported numerical formats, energy consumption, programmability, software maturity, and sustained thermal performance. The best choice depends on the application's constraints and must be verified through representative testing.

3. Analyze a Sensor-pipeline bottlenecks

Timestamping records when measurements are acquired or observed by the system. Synchronization aligns measurements in time, while buffering accommodates differences in arrival rates. Preprocessing may reduce noise or transform raw measurements into model-ready representations. These stages can improve input quality but may also introduce delay, memory use, and additional computation. The design must balance temporal alignment, data quality, and response time.

4. Explain the difference between average latency and worst-case execution time

Average latency describes typical execution performance over a set of measurements. Worst-case execution time estimates or bounds the longest execution time under a defined set of conditions. A system with a low average latency may still miss deadlines if occasional execution delays exceed the allowed interval. Hard real-time claims require suitable timing analysis and validation under relevant operating conditions; average measurements alone are insufficient.

5. Evaluate q model-compression strategy

Quantization reduces the numerical precision used to represent model parameters or intermediate activations. Pruning removes selected parameters, connections, channels, or other model structures. These methods can reduce storage, memory traffic, or computation, but they may also reduce accuracy, affect robustness, or provide little speedup when the target hardware does not efficiently exploit the chosen representation or sparsity pattern. Validation should measure accuracy, latency, energy, memory use, and performance under representative and degraded input conditions.

6. Explain cross-layer optimization

A model architecture determines the workload presented to the compiler. Compiler transformations determine how that workload is mapped onto processor units and memory. Accelerator characteristics influence throughput and data movement, while runtime scheduling affects contention and latency. Consequently, a change that reduces arithmetic operations may still increase memory traffic or synchronization overhead. Cross-layer optimization evaluates these interactions using system-level measurements and application requirements.

PART III — APPLIED ENGINEERING EXERCISES: MODEL SOLUTIONS

Exercise 1: Edge AI Accelerator Selection

a. Latency target

All three platforms meet the 40 ms target under the stated test conditions:

- Platform A: 28 ms
- Platform B: 34 ms
- Platform C: 22 ms

These results demonstrate nominal compliance in the measured workload, not a guarantee of deadline compliance under every operating condition.

b. Inference-only energy per result

Using $E = P \times t$

- Platform A: $8 \times 0.028 = 0.224$ joules
- Platform B: $12 \times 0.034 = 0.408$ joules
- Platform C: $10 \times 0.022 = 0.220$ joules

These are estimates based on average power during the test and measured inference latency. They exclude energy consumed by other system components unless those components were included in the power measurement.

c. Rankings

Latency: C, A, B

Estimated inference energy: C, A, B

Memory usage: C, A, B

Platform C performs best on all three listed measures in this example. Its suitability still depends on other requirements, including software compatibility, sustained thermal performance, reliability, and actual workload behavior.

d. Limitations of the measurements

The table does not establish worst-case execution time, high-percentile latency under stress, performance during thermal throttling, or behavior during resource contention. Additional testing is required before making hard real-time claims.

e. Recommendation

Platform C is the strongest initial candidate based on the supplied data. It has the lowest measured latency, lowest estimated inference energy per result, and lowest memory usage. The recommendation should remain provisional until sustained-load, thermal, fault, and integration tests are completed.

Exercise 2: Sensor Synchronization and End-to-End Latency

a. Nominal latency

$T_{total} = 6 + 4 + 18 + 5 = 33$ ms

b. Target assessment

The nominal 33 ms latency meets the 35 ms target, leaving a 2 ms margin.

c. Increased inference latency

The new inference latency is 18 + 8 = 2618 + 8 = 26 ms.

$T_{total} = 6 + 4 + 26 + 5 = 41$ ms

The pipeline exceeds the 35 ms target by 6 ms.

d. Potential improvements

Timestamping and synchronization can improve temporal alignment but may add processing or waiting time. Asynchronous transfers and overlapping compatible operations may reduce end-to-end latency. Faster preprocessing or more efficient buffering may also help. Each change should be evaluated for effects on data integrity, resource contention, and timing predictability.

e. Measurement plan

Measure latency at each stage and across the complete pipeline. Record average, median, high-percentile, and maximum observed latency over representative workloads. Repeat tests under

high utilization, variable sensor arrival rates, sustained thermal load, and resource contention. Where hard real-time guarantees are required, complement empirical testing with appropriate timing analysis.

Exercise 3: Hardware-Aware Model Optimization

a. Quantization

Moving from 32-bit to 8-bit representations can reduce storage requirements for affected tensors to approximately one-quarter of their original size, assuming the same number of values and ignoring metadata, alignment, and auxiliary storage. It may also reduce memory traffic and enable faster arithmetic where the hardware efficiently supports 8-bit operations. Actual performance depends on the model and implementation.

b. Structured versus unstructured pruning

Unstructured pruning removes individual weights or connections, producing irregular sparsity. Structured pruning removes organized units such as channels, filters, or blocks. Structured pruning can be easier for hardware to exploit because it may produce smaller dense operations or more regular data layouts. Hardware with specialized sparse execution may also benefit from particular unstructured patterns.

c. Accuracy and robustness tests

Tests should include representative validation data, important edge cases, degraded sensor inputs, and conditions likely to occur in deployment. Evaluation should compare task-specific metrics and relevant failure modes before and after compression.

d. Accelerator support

The target accelerator must efficiently support the selected precision and sparsity pattern. If the compiler or hardware falls back to slower operations, conversion steps, or dense execution, the expected benefit may not materialize.

e. Experimental design

Evaluate the original model, the quantized model, and the quantized-plus-pruned model using

the same dataset, input dimensions, preprocessing, hardware, software versions, and measurement boundary. Measure accuracy, latency distribution, energy, memory usage, and sustained performance.

f. Acceptance criteria

Acceptance criteria should be defined before testing. They may include minimum accuracy, maximum end-to-end latency, maximum energy per inference, maximum memory footprint, and required behavior under degraded inputs. Numerical thresholds should be derived from the target application's requirements rather than assumed universally.

Exercise 4: Cross-Layer Optimization Under Thermal Constraints

a. Thermal effects

Sustained high temperature can trigger frequency reduction or other power-management behavior. Reduced compute performance may increase inference latency and contribute to missed deadlines.

b. Diagnostic information

Collect accelerator temperature, clock frequency, power consumption, utilization, memory bandwidth, inference timing, queue depth, scheduler delays, and deadline-miss records. Correlate these measurements over time to determine whether the latency increase aligns with thermal throttling, resource contention, or another bottleneck.

c. Potential interventions

Possible interventions include:

- Quantizing or restructuring the model to reduce computation.
- Reducing unnecessary memory transfers or improving operator fusion.
- Adjusting task scheduling and resource allocation.
- Distributing workloads across suitable processing units.
- Improving cooling or revising power-management settings within platform limits.

Each intervention should be tested because reducing computational load or changing scheduling can introduce other trade-offs.

d. Trade-offs

A smaller model may reduce latency and energy but affect accuracy. More aggressive scheduling can improve the response time of critical tasks while delaying lower-priority work. Additional cooling may improve sustained performance but increase system size, cost, or power use. The design must balance these effects against the application requirements.

e. Validation plan

Run sustained tests long enough to reach representative thermal conditions. Measure end-to-end latency, deadline compliance, accuracy, energy consumption, temperature, and clock frequency. Repeat tests across relevant ambient temperatures and workload patterns. Compare the optimized system against the baseline.

f. System-level evaluation

Accelerator throughput does not capture all sources of delay or energy use. Sensor acquisition, preprocessing, memory transfers, synchronization, scheduling, security, and postprocessing can dominate application behavior. System-level evaluation reveals whether the proposed optimization actually improves the complete application.

PART IV — INTEGRATIVE DESIGN CHALLENGE: EVALUATION RUBRIC

Because multiple architectures can be valid, this challenge should be assessed according to the quality of the engineering reasoning rather than a single prescribed solution.

Evaluation Dimension	**Suggested Weight**
System architecture and component integration	15%
Model and hardware selection	15%
Sensor pipeline and synchronization	10%
Software execution and scheduling	10%
Latency, energy, and resource budgets	15%
Fault handling and safe degradation	10%
Security and its performance implications	10%
Validation methodology and measurable acceptance criteria	10%
Trade-off analysis and technical justification	5%
Total	**100%**

A strong submission should identify its assumptions, distinguish estimates from measurements, justify the selected architecture, and demonstrate how the proposed system would be

validated. Students should not claim deterministic timing, fault tolerance, or security guarantees without explaining the mechanisms and evidence required to support those claims.

Conclusion

Volume IV: Edge AI Hardware, Silicon Accelerators & Systems Co-Design

Part III: Hardware–Software Co-Design and System Optimization

Part III — *Hardware–Software Co-Design and System Optimization in AI Systems* — has established that modern artificial intelligence systems cannot be adequately understood, designed, or evaluated through a software-centric perspective alone. Their performance, reliability, security, and operational efficiency emerge from the coordinated behavior of algorithms, compiler toolchains, execution runtimes, memory hierarchies, processing architectures, sensor interfaces, and physical devices. As AI systems move from controlled computing environments into embedded platforms, autonomous machines, industrial equipment, robotics, and distributed edge-to-cloud infrastructures, the relationship between computation and the physical substrate becomes an essential determinant of system behavior. Hardware–software co-design therefore represents more than a technique for improving computational efficiency: it is a foundational engineering principle for building AI systems that can operate predictably, adapt to changing conditions, and maintain trustworthy behavior under real-world constraints.

Section 8.4 examined this principle across the interconnected layers of AI computation, from model architecture and specialized accelerators to software execution paradigms, sensor pipelines, real-time frameworks, and cross-layer optimization. These layers cannot be optimized independently without risking inefficiencies or failures elsewhere in the system. A model architecture that is computationally efficient in isolation may generate irregular memory-access patterns that overwhelm an accelerator's bandwidth. A high-throughput processor may fail to deliver timely results if sensor acquisition, data movement, preprocessing, and synchronization introduce excessive latency. Similarly, an efficient inference pipeline may become unsuitable for safety-critical deployment if its execution time varies unpredictably, its thermal behavior is poorly controlled, or its failure modes cannot be detected and contained. The central lesson is that AI system performance must be evaluated end to end, with explicit attention to the interactions among computational demand, physical resources, timing requirements, and operational risk.

Memory organization and data movement illustrate the importance of this integrated perspective. On-chip SRAM and other local memories can provide substantially lower access latency and energy consumption than off-chip DRAM, although the actual advantage depends on the memory technology, access pattern, capacity, and implementation. Consequently, model structures, tensor layouts, operator schedules, and compiler transformations must account for

the physical organization of the target platform. Data reuse, memory locality, buffer allocation, operator fusion, and carefully managed intermediate representations can reduce unnecessary transfers and help keep frequently accessed data close to the processing elements that consume it. These optimizations are especially important for edge AI devices, where memory capacity, bandwidth, power consumption, and thermal dissipation constrain the amount of computation that can be sustained.

Compiler and accelerator co-design extends these principles from memory management to the execution of model operations. Effective compilation translates high-level AI graphs into hardware-aware execution plans that exploit the capabilities and limitations of the target architecture. GPU workloads benefit from suitable thread mapping, occupancy, and memory-access patterns; systolic neural processing units benefit from appropriately tiled matrix and convolution operations; and tensor-oriented accelerators benefit from layouts and schedules that make efficient use of their supported matrix operations. The precise mapping must reflect each platform's instruction set, data types, memory hierarchy, parallel execution model, and numerical requirements. Operator fusion, quantization-aware optimization, graph simplification, and hardware-in-the-loop evaluation can further reduce execution overhead and improve resource utilization. However, optimization must preserve the required model accuracy and numerical behavior. Maximum throughput alone is not a sufficient objective when an application also imposes strict limits on latency, energy consumption, memory use, or output error.

The same cross-layer reasoning applies to sensor pipelines and real-time execution. In physical AI systems, useful computation begins with the acquisition of data from cameras, microphones, inertial measurement units, radar, lidar, industrial sensors, and other sources. Those inputs must be transported, synchronized, decoded, filtered, transformed, and delivered to the appropriate inference stages. Delays or inconsistencies introduced at these boundaries can undermine the value of an otherwise fast model. Section 8.4 therefore highlighted the importance of designing sensor interfaces, preprocessing stages, buffering strategies, data-transfer mechanisms, and inference runtimes as parts of a coordinated pipeline. Zero-copy data paths, hardware-assisted preprocessing, event-driven processing, and carefully controlled synchronization can reduce overhead where the platform supports them. Real-time frameworks complement these mechanisms through scheduling policies, bounded-resource management, priority control, deadline monitoring, and explicit handling of overload conditions. Together, these capabilities help align computational execution with the temporal requirements of the physical environment.

Predictability, however, requires more than minimizing average latency. A real-time AI system

must also account for latency variation, resource contention, thermal throttling, communication delays, and changing workloads. A design that meets its deadline under nominal conditions may fail when several sensors become active simultaneously, memory bandwidth is saturated, or the processor enters a thermally constrained operating state. Deterministic engineering therefore requires measurable execution budgets, characterization under representative and adverse workloads, and explicit policies for degraded operation. Where hard real-time guarantees are required, those guarantees must be established through appropriate system analysis and verification rather than inferred from average benchmark performance. Where strict determinism is unattainable, the architecture should still quantify timing variation, monitor deadline risk, and define safe responses to missed deadlines or unavailable resources.

Section 8.4 also demonstrated that reliability must be addressed across the entire hardware–software stack. Physical devices are subject to thermal stress, voltage fluctuations, manufacturing variation, aging, transient errors, and component degradation. Software may encounter corrupted data, unexpected execution states, resource exhaustion, or failures in device communication. These risks interact: a hardware fault may corrupt a tensor, disrupt a sensor stream, or cause an execution deadline to be missed, while software may fail to recognize that the underlying hardware is no longer operating within its expected limits. A resilient architecture therefore combines hardware diagnostics, integrity checks, runtime monitoring, fault containment, recovery procedures, and appropriate redundancy. Telemetry concerning temperature, voltage, memory errors, performance counters, and device health can inform decisions about workload placement, operating frequency, resource allocation, and component isolation. Predictive models may help identify emerging degradation, but their outputs should be treated as estimates and validated against observed system behavior. The objective is not to assume that faults can always be prevented; it is to detect relevant abnormalities, limit their consequences, recover when possible, and preserve essential functions when full performance is no longer available.

Security adds another dimension to this integrated design. AI models, input data, intermediate tensors, compiled kernels, and runtime state can all become targets for unauthorized access, manipulation, or observation. Hardware-rooted trust mechanisms, secure boot, cryptographic attestation, protected memory, and trusted execution environments can help establish and maintain the integrity and confidentiality of selected components. Side-channel countermeasures, access controls, memory-protection mechanisms, and integrity verification can further reduce exposure to particular attack classes. Yet these protections are not automatic guarantees of security. Their effectiveness depends on the threat model, hardware implementation, software configuration, key management, and the surrounding system architecture. Security mechanisms can also introduce costs in latency, memory consumption,

power, and operational complexity. Their integration must therefore be evaluated alongside performance and reliability requirements, ensuring that protective measures do not silently undermine critical execution deadlines or create new failure paths.

Cross-layer optimization provides the framework for coordinating these competing requirements. Rather than treating model design, compilation, accelerator scheduling, memory management, sensor processing, real-time control, reliability, and security as separate engineering activities, it considers their dependencies throughout the system lifecycle. A change in model precision may alter accelerator utilization, memory traffic, numerical error, and execution time. A different buffering strategy may improve throughput while increasing data age or memory pressure. A more aggressive scheduling policy may reduce latency for one workload while creating contention for another. Likewise, a security mechanism may reduce exposure to an attack but require additional computation or data movement. These trade-offs cannot be resolved reliably through isolated optimization. They require shared performance models, hardware-aware profiling, representative workloads, system-level measurements, and iterative validation across the complete execution path.

This approach also changes how AI systems should be evaluated. Model accuracy remains important, but it must be considered alongside end-to-end latency, latency variation, throughput, energy per inference, memory footprint, thermal stability, reliability, recoverability, and security. For physical AI applications, evaluation should additionally consider sensor timing, data freshness, synchronization error, communication loss, and the system's response to unexpected environmental conditions. Testing should extend beyond nominal operating points to include stress conditions, resource contention, degraded components, workload transitions, and plausible fault scenarios. Hardware-in-the-loop testing and deployment-representative experiments can reveal interactions that software-only benchmarks overlook. The result is a more complete basis for determining whether an AI system is merely computationally capable or genuinely suitable for its intended operational environment.

The broader implication is that AI intelligence, as realized in deployed systems, is inseparable from the architecture that senses, transports, computes, stores, protects, and acts upon information. Model capabilities establish what a system may be able to infer, but the hardware–software substrate determines whether those inferences can be produced within the available time, energy, memory, and safety constraints. A system that generates highly accurate predictions but cannot deliver them before an operational deadline may be ineffective. A system that performs efficiently but cannot detect corrupted inputs or contain hardware failures may be unreliable. A system that delivers predictable performance while exposing sensitive models or intermediate data may be unsuitable for its security requirements. Effective AI

engineering must therefore optimize not simply the model, but the complete chain of computation and control through which model outputs acquire operational value.

In conclusion, Part III establishes hardware–software co-design and cross-layer optimization as essential foundations for the next generation of embedded, edge, hybrid, and cloud-assisted AI systems. Specialized accelerators provide computational capability; memory hierarchies and compiler toolchains determine how efficiently that capability is used; sensor pipelines connect computation to the physical world; real-time frameworks align execution with temporal constraints; and reliability and security mechanisms help preserve correct and trustworthy operation. Their value emerges most fully when these elements are designed and validated together rather than assembled as independent components. The resulting architecture must balance performance with predictability, efficiency with robustness, and adaptability with verifiable constraints.

With this foundation, Volume IV concludes by presenting AI hardware not as a passive platform on which software happens to run, but as an active part of the system's computational behavior, operational resilience, and security posture. The decisive engineering challenge is to ensure that every layer—from sensing and memory access to accelerator execution and system orchestration—contributes coherently to the behavior required by the application. This is the central principle of hardware–software co-design: **reliable and effective AI emerges not from optimizing individual components in isolation, but from engineering the complete system as an integrated, measurable, and resilient computational architecture.**

Summary

Volume IV: Edge AI Hardware, Silicon Accelerators & Systems Co-Design

Part III: Hardware–Software Co-Design and System Optimization

Artificial intelligence systems increasingly operate in environments where computational performance must be balanced against physical limitations, including power consumption, thermal dissipation, memory capacity, communication bandwidth, and response time. These constraints are particularly important in edge AI applications, where inference and decision-making take place on embedded processors, autonomous machines, robotic platforms, industrial equipment, and other resource-constrained systems. In such environments, a model's predictive accuracy alone does not establish its suitability for deployment. Its computational requirements, execution characteristics, energy consumption, and interaction with the surrounding hardware and software must also satisfy the needs of the application.

Part III, *Hardware–Software Co-Design and System Optimization*, examines the methods used to develop AI systems by coordinating decisions across model architectures, hardware accelerators, software execution environments, sensor pipelines, real-time frameworks, and system-level optimization mechanisms. Its central principle is that the performance of a deployed AI system emerges from the interaction of these components. Improving an individual component does not necessarily improve the complete system; effective engineering requires evaluating how computation, data movement, memory access, scheduling, sensing, and operational constraints influence one another.

A. Model Architectures in AI Systems establishes the relationship between neural network structure and deployment requirements. Model architecture influences computational complexity, memory footprint, parallelism, numerical precision, and inference latency. Convolutional networks, transformers, recurrent networks, state-space models, and other architectures impose different demands on processors and memory systems. Techniques such as quantization, pruning, knowledge distillation, structured sparsity, and neural architecture search can reduce resource requirements, but their benefits depend on the target hardware, workload, and acceptable changes in predictive quality. Model design must therefore consider both the learning task and the conditions under which inference will occur.

B. Hardware Accelerators in AI Systems examines the silicon architectures that execute AI workloads. CPUs, GPUs, neural processing units, tensor accelerators, digital signal processors, field-programmable gate arrays, and application-specific integrated circuits offer different combinations of programmability, parallelism, throughput, memory bandwidth, and energy efficiency. Their effectiveness depends on factors such as data reuse, arithmetic precision,

memory hierarchy, interconnect performance, and thermal limits. Accelerator selection and design must account for the actual computational patterns of the target model rather than relying solely on peak performance specifications.

C. Software Paradigms in AI Systems explains how AI models are translated into executable workloads and mapped onto heterogeneous computing platforms. Compilers, intermediate representations, computational graphs, operator libraries, runtime systems, and device-specific programming frameworks enable optimization across the software stack. Graph simplification, operator fusion, memory planning, loop tiling, vectorization, code generation, and scheduling can reduce unnecessary computation and data movement. However, these transformations must preserve required numerical behavior and remain compatible with the capabilities and limitations of the target hardware.

D. Sensor Pipelines in AI Systems addresses the movement of information from physical sensors to AI models and downstream decision-making components. Image sensors, cameras, microphones, radar, lidar, inertial measurement units, and industrial sensors produce data that may require calibration, filtering, synchronization, preprocessing, buffering, and format conversion. These operations affect latency, memory consumption, bandwidth, and the quality of the information available to inference. Sensor fusion introduces additional challenges because different sources may operate at different sampling rates and exhibit different timing characteristics or failure modes. Coordinating sensor interfaces, data movement, preprocessing, and model execution is therefore essential for preserving useful information while meeting system constraints.

E. Real-Time Frameworks in AI Systems examines the mechanisms used to coordinate computation under timing constraints. In real-time applications, producing a correct result after its deadline may be equivalent to producing an unusable result. Relevant concerns include end-to-end latency, execution-time variation, scheduling policies, interrupt handling, resource contention, communication delays, and workload isolation. Real-time operating systems, priority-based scheduling, bounded resource allocation, and deadline-aware runtime mechanisms can improve predictability. Nevertheless, predictable execution must be established through appropriate system design, analysis, and testing; neither an accelerator nor a real-time framework automatically guarantees that every AI workload will meet its deadline.

F. Cross-Layer Optimization in AI Systems integrates the preceding areas into a unified engineering methodology. Model topology affects processor utilization and memory traffic; compiler transformations influence instruction selection and data reuse; accelerator architecture determines which operations execute efficiently; sensor pipelines contribute preprocessing and communication costs; and runtime scheduling influences whether

application deadlines can be met. Security and reliability mechanisms introduce additional requirements that must be considered alongside performance and energy consumption.

Cross-layer optimization coordinates these interactions through hardware-aware neural architecture search, design-space exploration, compiler and graph optimization, hardware-aware model compression, runtime telemetry, resource allocation, and system-level performance evaluation. It also considers how protected memory, secure enclaves, cryptographic isolation, side-channel defenses, and fault-mitigation mechanisms influence the design and operation of AI systems. Such protections can improve security, but their effectiveness depends on the threat model and implementation, and their computational overhead must be included in system evaluation.

Across all six areas, a recurring distinction is the difference between component-level efficiency and end-to-end system performance. Peak accelerator throughput, model parameter count, memory bandwidth, and average inference latency each describe only part of the system. A meaningful evaluation must identify the measurement boundaries and account for relevant preprocessing, data transfers, synchronization, inference, postprocessing, runtime overhead, and security or monitoring operations. Energy measurements likewise require a defined system boundary and workload.

The design process must also balance competing objectives. Lower numerical precision may improve throughput and energy efficiency while affecting model accuracy. More specialized hardware may improve performance for a particular workload while reducing flexibility. Additional monitoring and security mechanisms may improve observability or protection while consuming memory, computation, or time. The appropriate configuration therefore depends on the application, target platform, operating environment, workload characteristics, and consequences of failure.

Ultimately, Part III presents hardware–software co-design as an integrated approach to AI system engineering. Model architectures establish computational requirements; accelerators provide execution capabilities; software paradigms map and optimize workloads; sensor pipelines deliver the information required for inference; real-time frameworks coordinate execution under timing constraints; and cross-layer optimization reconciles the requirements of the complete system. Together, these areas provide a foundation for developing edge AI systems that are efficient, responsive, reliable, secure, and appropriate for their intended deployment environments.

APPENDIX A: TECHNICAL SUPPORTING MATERIAL AND REFERENCE SPECIFICATIONS

Volume IV: Edge AI Hardware, Silicon Accelerators & Systems Co-Design

Part III: Hardware–Software Co-Design and System Optimization

A.1 Purpose of This Appendix

This appendix consolidates the technical supporting materials and reference specifications relevant to the hardware–software co-design methodologies, optimization techniques, and system architectures examined in Part III of Volume IV. Because effective hardware–software co-design spans multiple interconnected disciplines—including AI model architectures, semiconductor technologies, accelerator architectures, memory systems, compiler frameworks, communication interfaces, and runtime environments—a centralized technical reference provides a consistent foundation for understanding and applying the engineering concepts developed in this part.

The appendix is intended to serve as a practical technical resource for readers, researchers, system architects, and engineering professionals by providing:

- **Quick-reference technical specifications:** Consolidated hardware characteristics, architectural parameters, and relevant technology specifications supporting hardware–software integration.
- **Standardized terminology:** Consistent definitions and descriptions of technical concepts, components, optimization techniques, and methodologies used throughout Part III.
- **Key equations and performance metrics:** A structured reference to important mathematical relationships, computational models, and evaluation metrics relevant to accelerator performance and system optimization.
- **Architectural comparison criteria:** Common technical parameters for evaluating processors, AI accelerators, memory architectures, and hardware–software execution platforms.
- **Engineering calculations and design trade-off analysis:** Supporting information for assessing computational requirements, memory utilization, data movement, energy consumption, latency, and alternative architectural configurations.
- **Consistent measurement conventions:** Standardized units, definitions, and evaluation criteria for comparing accelerator throughput, computational efficiency, memory performance, power consumption, and energy efficiency.

By bringing these materials together, Appendix A reduces the need to repeatedly introduce foundational specifications, equations, and definitions within individual sections. It also establishes a common technical basis for interpreting performance data, conducting engineering calculations, comparing architectural alternatives, and evaluating cross-layer hardware–software optimization decisions.

Accordingly, this appendix serves as an integral technical reference supporting the analysis, implementation, and evaluation of hardware–software co-designed edge AI systems presented in Part III.

A.2 Common AI Hardware Performance Metrics

Evaluating AI hardware requires a consistent set of performance metrics that characterize computational capability, memory performance, execution speed, power consumption, and resource efficiency. These metrics help engineers compare processors and accelerators, identify system bottlenecks, and assess whether a hardware platform can satisfy the performance and operational requirements of an AI workload.

The following table summarizes commonly used AI hardware performance metrics, their symbols, typical units, and engineering significance.

Metric	Symbol	Typical Units	Description
Arithmetic Throughput	FLOP/s	GFLOP/s, TFLOP/s, PFLOP/s	Rate at which a processor or accelerator performs floating-point operations. Reported values may represent theoretical peak or measured sustained performance.
Arithmetic Intensity	AI	FLOPs/Byte	Ratio of floating-point operations performed to bytes of data transferred from a specified level of the memory hierarchy. Indicates the balance between computation and data movement.
Memory Bandwidth	BW	GB/s, TB/s	Rate at which data can be transferred between memory and processing units. Actual bandwidth depends on the memory subsystem, access patterns, and workload characteristics.
Latency	L	s, ms, µs, ns	Elapsed time required to complete an operation or produce a result. For AI inference, latency may refer

			to end-to-end request time or a specific processing stage.
Throughput	T	Tokens/s, Images/s, Samples/s, Inferences/s	Amount of useful work completed per unit of time. The appropriate unit depends on the AI workload and measurement boundary.
Power Consumption	P	W	Rate at which a processor or system consumes electrical energy during operation. Measurements should specify whether they cover the accelerator, processor, or complete system.
Energy Efficiency	η	FLOP/J, FLOP/s/W, Tokens/J, Inferences/J	Amount of computation or useful workload completed per unit of energy. The selected measure should reflect the workload and system boundary being evaluated.
Memory Capacity	M	MB, GB, TB	Amount of data that a memory device or subsystem can hold. Capacity may refer to registers, cache, SRAM, HBM, DRAM, or other storage resources.
Hardware Utilization	U	%	Percentage of available processing or hardware resources actively engaged in executing a workload over a defined measurement interval.
Occupancy	Occ	%, ratio	Proportion of an accelerator's execution capacity occupied by active workloads. On GPUs, for example, occupancy commonly refers to active resident warps relative to the maximum number of resident warps supported by a multiprocessor.

Engineering Perspective

These metrics should be interpreted together rather than evaluated independently. High arithmetic throughput does not necessarily produce high application-level performance if memory bandwidth, data movement, synchronization, or execution latency becomes the limiting factor. Similarly, high hardware utilization or occupancy does not automatically indicate

efficient execution; performance also depends on workload characteristics, resource contention, memory access patterns, and instruction-level efficiency.

For meaningful comparisons, measurements should identify the hardware configuration, numerical precision, workload, batch size, measurement interval, and relevant system boundaries. Distinguishing theoretical peak performance from sustained workload performance is particularly important when evaluating AI accelerators for edge deployments, where power, thermal capacity, memory availability, and latency requirements impose additional constraints.

A.3 Roofline Model Reference Equations

Peak Performance Limit

$$P_{max} = \min(P_{compute}, AI \times BW)$$

Where:

- P_{max} = achievable performance
- $P_{compute}$ = peak compute throughput
- AI = arithmetic intensity
- BW = memory bandwidth

Arithmetic Intensity

$$AI = \frac{\text{Total Operations}}{\text{Bytes Accessed}}$$

Higher arithmetic intensity generally indicates greater opportunity to achieve compute-bound execution.

Compute-Bound Threshold

$$AI_{threshold} = \frac{P_{peak}}{BW}$$

Used to determine the memory-bound to compute-bound transition.

A.4 AI Numerical Precision Reference

Numerical precision is a fundamental consideration in AI hardware design because it influences computational accuracy, model stability, memory requirements, data-transfer volume, power consumption, and inference or training performance. Modern AI accelerators support multiple numerical formats to balance computational efficiency with the precision requirements of different workloads.

The following table summarizes commonly used floating-point, integer, and microscaling formats, including their representation widths, relative dynamic ranges, and typical AI applications.

Format	Representation Width	Dynamic Range	Typical Use
FP64 (Double Precision)	64 bits	Very high	Scientific computing, numerical simulation, and applications requiring high numerical precision.
FP32 (Single Precision)	32 bits	High	General-purpose numerical computing, conventional AI training, and operations requiring a broad dynamic range.
TF32 (TensorFloat-32)	19-bit format	Comparable to FP32	Tensor-core matrix operations and accelerated AI training on supported hardware, typically with FP32 accumulation.
BF16 (Brain Floating Point)	16 bits	High; comparable to FP32	AI training and inference workloads that benefit from reduced memory usage while retaining a broad dynamic range.
FP16 (Half Precision)	16 bits	Moderate; narrower than BF16	Mixed-precision AI training and inference, particularly where hardware provides efficient FP16 execution.

FP8 (8-bit Floating Point)	8 bits	Format-dependent	Advanced AI training and inference on supported accelerators. Common variants include E4M3 and E5M2, which provide different trade-offs between precision and dynamic range.
INT8 (8-bit Integer)	8 bits	Scale- and quantization-dependent	Quantized AI inference, edge deployment, and hardware-accelerated neural network execution.
FP4 (4-bit Floating Point)	4 bits	Format-dependent and limited	Emerging low-precision AI training and inference on hardware that supports the corresponding format.
INT4 (4-bit Integer)	4 bits	Scale- and quantization-dependent	Low-bit model quantization and memory-efficient AI inference, including deployment on supported edge accelerators.
MX Formats (Microscaling Formats)	Variable; commonly 4, 6, or 8 bits per element	Depends on element format and shared block scaling	Low-precision AI training and inference using shared scaling factors to support efficient computation across blocks of values.

Engineering Considerations

Numerical formats differ not only in representation width but also in exponent range, significand precision, accumulation behavior, and quantization requirements. Consequently, formats with the same bit width may exhibit substantially different numerical characteristics.

Several distinctions are particularly important:

FP32 and FP64: These conventional floating-point formats provide broad dynamic ranges, with FP64 offering greater precision and a wider exponent range than FP32. Their computational cost and hardware support vary across accelerator architectures.

TF32: This format uses an 8-bit exponent and a 10-bit fraction, together with a sign bit, giving it a 19-bit representation. Its exponent range is comparable to FP32, while its significand precision

is reduced. On supported NVIDIA tensor-core hardware, TF32 operations commonly use FP32 accumulation.

BF16 and FP16: Both use 16-bit representations, but BF16 retains an exponent range comparable to FP32, whereas FP16 provides greater significand precision over a narrower dynamic range. This distinction influences numerical stability and mixed-precision training strategies.

FP8 and FP4: These low-bit floating-point formats have multiple variants with different allocations of bits to exponent and significand fields. Their numerical behavior therefore depends on the specific format and implementation.

INT8 and INT4: These integer formats generally rely on quantization parameters, such as scaling factors and, where applicable, zero points, to represent model values. Their effective numerical range and precision depend on the quantization scheme.

MX Formats: Microscaling formats use a shared scaling factor for a block of low-precision values. The element representation and block-scaling mechanism together determine the effective numerical range and precision.

Practical Selection Criteria

Selecting a numerical format requires evaluating model accuracy, numerical stability, hardware support, memory capacity, computational throughput, and energy efficiency. Lower-bit representations can reduce memory traffic and storage requirements, but they do not automatically improve execution speed or energy efficiency. The actual benefit depends on accelerator architecture, supported arithmetic operations, compiler optimization, kernel implementation, and runtime behavior.

For edge AI systems, numerical precision is especially important because it directly affects the balance among model accuracy, memory footprint, power consumption, and computational performance. Precision selection should therefore be validated using representative workloads on the intended deployment hardware rather than determined solely by nominal bit width.

A.5 AI Accelerator Taxonomy

AI accelerators can be classified into several architectural categories according to their degree of programmability, computational specialization, hardware configurability, and underlying processing mechanisms. Each category offers different trade-offs among computational performance, energy efficiency, flexibility, development complexity, and workload compatibility.

A.5.1 General-Purpose Accelerators

Representative Architectures

- Graphics Processing Units (GPUs)
- Many-core processors
- Vector processors

Key Characteristics

- **High programmability:** Support a broad range of computational workloads through flexible instruction sets and programming models.
- **Architectural flexibility:** Accommodate diverse AI operations, numerical formats, and parallel processing requirements.
- **Broad software ecosystems:** Benefit from established compiler frameworks, programming environments, libraries, and development tools.
- **Workload versatility:** Support AI inference and training alongside conventional scientific, graphics, and general-purpose computing tasks.
- **Resource-sharing capability:** Can execute multiple workloads, although resource contention may affect performance predictability.

General-purpose accelerators are particularly useful when workload diversity, software compatibility, and programming flexibility are important design considerations.

A.5.2 Domain-Specific Accelerators

Representative Architectures

- Tensor Processing Units (TPUs)
- Neural Processing Units (NPUs)
- Artificial Intelligence Application-Specific Integrated Circuits (AI ASICs)

Key Characteristics

- **High computational efficiency:** Optimize hardware resources for frequently executed AI operations, particularly matrix multiplication, tensor processing, and multiply–accumulate operations.
- **Workload specialization:** Provide execution structures tailored to neural-network operations and supported computational patterns.

- **Reduced energy per operation:** Can improve energy efficiency through specialized datapaths, optimized dataflows, and reduced instruction overhead.
- **Architectural specialization:** Often incorporate dedicated processing arrays, local memory, and optimized data-transfer mechanisms.
- **Reduced general-purpose flexibility:** May support a narrower range of operations, numerical formats, and execution patterns than general-purpose processors.

Domain-specific accelerators are particularly suitable for applications with well-characterized AI workloads and stringent performance or energy-efficiency requirements. Their effectiveness depends on operator support, compiler compatibility, memory organization, and the ability to map the target models efficiently to the available hardware.

A.5.3 Reconfigurable Accelerators

Representative Architectures

- Field-Programmable Gate Arrays (FPGAs)
- Coarse-Grained Reconfigurable Arrays (CGRAs)

Key Characteristics

- **Adaptable hardware organization:** Allow portions of the computational architecture or processing resources to be configured for different workloads.
- **Custom execution pipelines:** Support application-specific datapaths, parallel processing structures, and optimized dataflow arrangements.
- **Hardware-level optimization:** Enable designers to tailor computational resources and data movement to the requirements of particular AI operations.
- **Implementation flexibility:** Can accommodate changing workloads or evolving algorithms without requiring a complete redesign of the silicon.
- **Programming and development complexity:** Require specialized design tools and hardware-aware programming techniques, with complexity varying by architecture and abstraction level.

Reconfigurable accelerators provide a middle ground between general-purpose programmability and fixed-function specialization. They are useful when workload-specific optimization is important but the flexibility to modify hardware functionality remains a design requirement.

A.5.4 Emerging Accelerator Architectures

Representative Technologies

- Processing-in-Memory (PIM) systems
- Photonic accelerators
- Neuromorphic processors
- Memristive computing arrays

Key Characteristics

- **Alternative computational paradigms:** Explore approaches that differ from conventional processor-centric architectures and traditional digital computation.
- **Reduced data-movement overhead:** Processing-in-memory approaches seek to perform selected computations closer to or within memory structures, potentially reducing data transfers.
- **High-throughput parallelism:** Photonic architectures exploit optical signal processing to investigate high-bandwidth computation and communication.
- **Event-driven processing:** Neuromorphic processors use brain-inspired architectures that can support sparse, asynchronous, and event-based workloads.
- **In-memory analog computation:** Memristive arrays can exploit device conductance and physical properties to perform selected operations, including analog matrix-vector computations.
- **Technology and implementation challenges:** Practical deployment may be constrained by device variability, precision, conversion overhead, programming models, manufacturing maturity, and integration requirements.

Emerging accelerator architectures explore alternative ways to improve computational efficiency, data locality, parallelism, and energy consumption. Although promising, their practical advantages depend on workload suitability, device characteristics, system integration, software support, and demonstrated performance under realistic operating conditions.

A.5.5 Comparative Architectural Overview

The following table summarizes the principal distinctions among the four accelerator categories.

Accelerator Category	Primary Strength	Principal Trade-Off	Typical Application Context
General-purpose	Flexibility and broad programmability	May provide lower workload-specific efficiency	Diverse AI workloads and heterogeneous computing
Domain-specific	High efficiency for targeted AI operations	Reduced flexibility outside supported workloads	Neural-network inference and specialized AI processing
Reconfigurable	Adaptable hardware organization and custom datapaths	Greater development and programming complexity	Application-specific acceleration and evolving workloads
Emerging	Alternative computational and memory architectures	Technology maturity and integration challenges	Specialized research and next-generation AI systems

Engineering Perspective

Accelerator selection should not be based on architectural category alone. It requires evaluating the target model, computational workload, numerical precision, memory requirements, data-transfer patterns, power and thermal limits, software ecosystem, and execution-time requirements.

Furthermore, theoretical computational efficiency does not necessarily translate into superior application performance. Compiler support, memory bandwidth, data movement, workload utilization, and system integration can substantially influence realized results.

For hardware–software co-design, the most appropriate accelerator is therefore the architecture that provides the best overall balance among computational capability, energy efficiency, programmability, integration complexity, and the operational requirements of the intended edge AI application.

A.6 Memory Hierarchy Reference

The memory hierarchy defines how data is stored, accessed, and transferred across the computational components of an AI system. Each memory level provides a different balance of access latency, bandwidth, capacity, persistence, and energy consumption. In accelerator-based

AI systems, efficient memory hierarchy design is essential for minimizing data movement, maintaining computational utilization, and supporting predictable execution.

The following table summarizes the principal memory types used in AI computing systems and their typical characteristics.

Memory Type	Relative Access Latency	Relative Bandwidth	Typical Capacity	Primary Role in AI Systems
Registers	Lowest	Highest per access path	Bytes to KB per processing element or execution unit	Store operands, intermediate values, addresses, and frequently accessed data directly within processing units.
Static Random-Access Memory (SRAM)	Very Low	Very High	KB to MB, depending on implementation	Provides fast on-chip storage for caches, buffers, scratchpads, and intermediate tensor data.
High-Bandwidth Memory (HBM)	Low to Moderate	Extremely High	Several GB to hundreds of GB per accelerator configuration	Supplies high-bandwidth access to model weights, activations, and other large tensor data structures in high-performance AI accelerators.
Dynamic Random-Access Memory (DRAM)	Moderate	High	Tens to hundreds of GB, or more in larger systems	Provides system memory for model loading, data preprocessing, CPU operations, and workloads that exceed on-chip or accelerator-local memory capacity.
Solid-State Drive (SSD/NVMe)	High	Moderate to High	Hundreds of GB to multiple TB	Provides persistent, nonvolatile storage for model checkpoints,

Memory Type	Relative Access Latency	Relative Bandwidth	Typical Capacity	Primary Role in AI Systems
				datasets, application data, and model-loading operations.
Persistent Storage	Highest in the hierarchy	Generally Lower than semiconductor memory	TB to PB	Supports long-term storage of datasets, model archives, logs, checkpoints, and other information used by AI infrastructure.

Note: The latency and bandwidth classifications are qualitative and relative, not fixed performance specifications. Actual values depend on the memory technology, device architecture, interface, access pattern, transfer size, and system configuration. Capacity ranges are illustrative rather than architectural limits. SSD/NVMe is a storage-device and interface category, whereas persistent storage describes a broader storage role that can include SSDs and other nonvolatile technologies.

Engineering Perspective

AI workload performance depends not only on computational throughput but also on the ability to supply data to processing units at the required rate. When memory bandwidth or data-transfer latency becomes a limiting factor, additional computational capacity may not produce proportional improvements in overall performance.

The memory hierarchy therefore plays a central role in hardware–software co-design:

- **Data locality:** Keep frequently accessed weights, activations, and intermediate results close to the processing units whenever capacity permits.
- **Memory bandwidth:** Match data-transfer capacity to accelerator throughput to reduce memory-related stalls.
- **Capacity management:** Account for model parameters, intermediate activations, attention-related state, and runtime buffers when determining memory requirements.
- **Data movement:** Minimize unnecessary transfers among registers, SRAM, HBM, DRAM, and persistent storage.

- **Memory allocation:** Coordinate compiler decisions, runtime memory management, and hardware resources to improve utilization and reduce allocation overhead.
- **Execution predictability:** Evaluate memory contention, access patterns, transfer latency, and buffering behavior when designing systems with real-time requirements.

An effective memory architecture balances capacity, bandwidth, latency, energy consumption, and cost. For edge AI systems, these considerations are particularly important because limited memory capacity and power budgets can constrain model size, inference throughput, and sustained execution performance.

The computational and memory requirements of sequence-processing architectures vary significantly according to their attention mechanisms, internal representations, and execution strategies. Understanding these differences is important when selecting AI models for hardware-constrained environments, particularly edge platforms with limited memory capacity, bandwidth, and computational resources.

The following comparison summarizes the asymptotic computational and memory complexity of three major architectural approaches: full self-attention, linear attention, and state-space models (SSMs).

Notation: Let (n) denote the input sequence length. The complexity expressions below describe scaling with respect to (n), assuming fixed model dimensions, including hidden size and attention feature dimensions. Actual resource requirements also depend on implementation, batch size, numerical precision, and hardware architecture.

A.7.1 Full Self-Attention

Computational Complexity: $O(n^2)$

Memory Complexity: $O(n^2)$

Full self-attention computes pairwise relationships among sequence positions. For a sequence of length (n), the attention mechanism generates an (n \times n) attention-score matrix, resulting in quadratic computational complexity with respect to sequence length.

Conventional implementations also require quadratic memory to materialize and store the attention matrix or associated intermediate results. Consequently, memory consumption and computational cost increase substantially as sequence length grows.

Memory-efficient implementations, such as FlashAttention, reduce the need to materialize the complete attention matrix in high-bandwidth memory. These approaches can substantially

reduce memory overhead while retaining exact attention computation, although the underlying attention computation remains quadratic in sequence length.

A.7.2 Linear Attention

Computational Complexity: O(n)

Memory Complexity: O(1) to O(n)

Linear attention uses alternative formulations of the attention computation to reduce or avoid explicit construction of the full pairwise attention matrix. Under suitable formulations and fixed feature dimensions, computational complexity can scale linearly with sequence length.

Memory requirements depend on the implementation and execution mode. Recurrent inference implementations can maintain a fixed-size accumulated state, resulting in (O(1)) memory with respect to sequence length. Training implementations may require (O(n)) memory to retain intermediate activations or other sequence-dependent information.

Linear attention can therefore offer substantial computational and memory advantages for long-sequence processing, although its efficiency and model behavior depend on the specific formulation and approximation or kernelization strategy employed.

A.7.3 State-Space Models (SSMs)

Computational Complexity: O(n)

Memory Complexity: O(1) to O(n)

State-space models process sequential information through structured state-transition mechanisms rather than explicitly computing all pairwise token interactions. Their computational complexity can scale linearly with sequence length under suitable implementations and fixed state dimensions.

During recurrent inference, an SSM can update a fixed-size internal state as each new input arrives. This results in (O(1)) memory with respect to sequence length. During training, however, parallel sequence processing, intermediate activation storage, and implementation-specific algorithms may require memory that scales with sequence length.

Structured state-space architectures therefore provide an alternative approach to long-context modeling, with potential advantages in computational efficiency, memory usage, and streaming inference.

A.7.4 Comparative Complexity Summary

Architecture	Computational Complexity	Memory Complexity	Principal Characteristic
Full self-attention (conventional implementation)	$O(n^2)$	$O(n^2)$	Explicit pairwise attention across sequence positions
Linear attention	$O(n)$	$O(1) – O(n)$	Linear sequence scaling through alternative attention formulations
State-space models	$O(n)$	$O(1) – O(n)$	Sequential state updates and structured sequence processing

Note: Complexity expressions represent asymptotic scaling with sequence length, assuming fixed model dimensions. Memory complexity is implementation- and execution-dependent. In particular, recurrent inference may require constant-size state storage, whereas training may require sequence-dependent activation memory.

Engineering Implications for Edge AI

The choice of sequence-processing architecture directly affects the computational and memory resources required for deployment.

Full self-attention provides flexible pairwise interaction modeling but can become computationally and memory intensive for long sequences.

Linear attention reduces sequence-length scaling under suitable formulations, making it attractive for applications involving extended input sequences and constrained computational resources.

State-space models provide structured mechanisms for processing long sequences and can support memory-efficient streaming inference through fixed-size recurrent states.

For edge AI deployment, architectural selection should consider more than asymptotic

complexity. Actual performance depends on hidden dimensions, state size, numerical precision, memory bandwidth, hardware acceleration support, parallelization strategy, and compiler and runtime optimization.

Accordingly, the most suitable architecture is determined by the application's sequence-processing requirements and the computational, memory, power, and latency constraints of the target platform.

A.8 Structured Sparsity Reference

Structured sparsity reduces computational and memory requirements by organizing inactive weights, connections, or computational paths according to predefined patterns. Unlike unstructured sparsity, in which individual elements are removed without regard to their positions, structured approaches impose regular patterns that can be more readily mapped to accelerator architectures.

The following table summarizes common sparsity types, representative patterns, and their relative alignment with hardware acceleration.

Sparsity Type	Representative Pattern or Example	Accelerator Alignment	Engineering Considerations
Unstructured Sparsity	Individual weights are pruned at arbitrary positions, producing irregular patterns of active and inactive elements.	**Low**	Can reduce the number of model parameters and theoretical operations, but irregular memory access, indexing overhead, and load imbalance may limit practical acceleration. Specialized sparse kernels and hardware support are often required.
Block Sparsity	Groups of weights are removed in predefined blocks, such as 16 × 16 matrices or other hardware-compatible block dimensions.	**Moderate to High**	Regular block patterns improve memory organization and enable more efficient sparse computation. Performance depends on block dimensions, sparsity distribution, and accelerator support.

Sparsity Type	Representative Pattern or Example	Accelerator Alignment	Engineering Considerations
2:4 Structured Sparsity	In each group of four elements, two are retained and two are pruned.	**High on Supported Hardware**	Provides a regular sparsity pattern that can be efficiently accelerated by hardware designed to recognize and process 2:4 sparse representations. Benefits depend on supported data types, operators, software kernels, and model compatibility.
Expert Sparsity (Mixture of Experts)	Only a selected subset of experts is activated for each input token through routing decisions.	**Workload- and Architecture-Dependent**	Reduces the number of experts activated per token, but introduces routing, token-dispatch, load-balancing, and communication overhead. Efficient execution requires appropriate accelerator mapping and runtime support.
Dynamic Sparsity	Active computational elements or connections are selected or generated during execution according to runtime inputs or changing workload conditions.	**Variable**	Can adapt computation to input characteristics and resource conditions. However, dynamic indexing, control overhead, irregular execution, and changing memory-access patterns can reduce predictability and limit hardware utilization.

Engineering Perspective

The practical value of sparsity depends on whether reduced computation translates into measurable improvements in execution time, memory traffic, energy consumption, and resource utilization. A lower parameter count or theoretical operation count does not necessarily produce faster inference.

Hardware-friendly sparsity patterns, particularly block sparsity and supported 2:4 structured sparsity, can offer more predictable opportunities for accelerator optimization. By contrast, unstructured and dynamic sparsity may require specialized kernels, indexing mechanisms, and

runtime coordination to realize their potential benefits.

Expert sparsity introduces a different optimization dimension: conditional computation. Although only a subset of experts is activated for each token, the resulting performance depends on routing efficiency, expert placement, workload distribution, and inter-accelerator communication.

For hardware–software co-design, sparsity should therefore be evaluated across the model representation, compiler and kernel implementation, accelerator capabilities, memory hierarchy, and runtime execution strategy. The relevant objective is not simply to maximize sparsity, but to achieve **hardware-efficient sparsity** that reduces actual system resource consumption while preserving model accuracy and the required execution characteristics.

A.9 Distributed AI Parallelism Taxonomy

Distributed AI parallelism encompasses the architectural strategies used to divide model computation, data processing, and memory requirements across multiple processors, accelerators, or computing nodes. These strategies are particularly important when a single device cannot provide sufficient computational throughput, memory capacity, or processing bandwidth to execute a model efficiently.

Different parallelism techniques distribute workloads along different dimensions. They may be applied independently or combined within a hybrid execution architecture, depending on model size, hardware topology, communication bandwidth, memory capacity, and application requirements.

A.9.1 Data Parallelism

Definition: Replicates the model across multiple processors or accelerators, with each device processing a different subset of the input data.

Operational Characteristics:

- Each accelerator maintains a replica of the model parameters.
- Input batches are partitioned among participating devices.
- Each device independently computes gradients during distributed training.
- Gradients are synchronized or aggregated to update model parameters consistently.
- During inference, independent input requests or batches can be distributed across replicas.

Primary Advantages:

- Increases training throughput through concurrent processing of multiple data batches.
- Supports scalable processing of independent inference requests.
- Can be implemented using established distributed communication frameworks.

Principal Trade-Offs:

- Model parameters must generally fit in the memory of each participating device.
- Gradient synchronization introduces communication overhead during training.
- Scaling efficiency depends on batch size, interconnect bandwidth, and synchronization frequency.

A.9.2 Tensor Parallelism

Definition: Partitions individual tensor operations, particularly large matrix multiplications, across multiple processors or accelerators.

Operational Characteristics:

- Large weight matrices are divided along selected dimensions.
- Individual devices compute portions of the same mathematical operation.
- Intermediate results are exchanged or combined through collective communication operations.
- Multiple devices cooperate to execute layers that may exceed the computational or memory capacity of a single accelerator.

Primary Advantages:

- Distributes the computational and memory requirements of large model layers.
- Enables execution of models with parameter matrices too large for one device.
- Exploits parallel hardware resources within individual computational layers.

Principal Trade-Offs:

- Requires frequent communication and synchronization between participating devices.
- Performance depends strongly on interconnect bandwidth and communication latency.

- Partitioning and workload balancing can introduce implementation complexity.

A.9.3 Pipeline Parallelism

Definition: Divides a model into sequential groups of layers or computational stages, assigning different stages to separate processors or accelerators.

Operational Characteristics:

- Each device executes a designated portion of the model.
- Intermediate activations are transferred between successive pipeline stages.
- Multiple microbatches can be processed concurrently to improve pipeline utilization.
- Stage execution is coordinated to manage data dependencies and minimize idle time.

Primary Advantages:

- Distributes model layers across devices.
- Reduces the amount of model computation and parameter storage assigned to each device.
- Enables concurrent execution of different model stages.

Principal Trade-Offs:

- Pipeline bubbles can reduce accelerator utilization.
- Stage imbalance can create bottlenecks and increase end-to-end latency.
- Intermediate activation transfers introduce communication and memory overhead.

A.9.4 Context Parallelism

Definition: Partitions the input sequence or context across multiple processors or accelerators to distribute the computational and memory requirements associated with long-context processing.

Operational Characteristics:

- A long input sequence is divided into smaller segments assigned to different devices.
- Each device processes its assigned portion of the sequence.
- Attention or other sequence-dependent operations may require communication of information across partitions.

- Distributed context representations are coordinated to preserve the dependencies required by the model.

Primary Advantages:

- Supports processing of sequences that exceed the practical context-processing capacity of a single device.
- Distributes sequence-related memory and computational requirements.
- Can improve scalability for long-context Transformer and other sequence-processing architectures.

Principal Trade-Offs:

- Cross-partition communication can introduce substantial overhead.
- Attention mechanisms may require additional synchronization or exchange of key and value information.
- Performance depends on sequence length, partitioning strategy, communication topology, and model architecture.

A.9.5 Expert Parallelism

Definition: Distributes the expert networks of a Mixture-of-Experts (MoE) model across multiple processors or accelerators, allowing different experts to execute on different devices.

Operational Characteristics:

- Expert networks are assigned to different devices or groups of devices.
- A gating or routing mechanism selects the experts responsible for processing individual tokens.
- Tokens are dispatched to the appropriate expert locations.
- Expert outputs are combined to produce the resulting model representation.

Primary Advantages:

- Distributes the parameter storage requirements of large MoE models.
- Allows conditional computation by activating only selected experts for each token.
- Supports scaling model capacity without requiring every expert to execute for every input token.

Principal Trade-Offs:

- Token dispatch and result aggregation introduce communication overhead.
- Uneven expert selection can create workload imbalance.
- Routing decisions and inter-device communication can affect latency and throughput.
- Expert placement and capacity management require careful architectural planning.

A.9.6 Comparative Overview

Parallelism Strategy	Primary Partitioning Dimension	Main Objective	Principal Communication Requirement
Data Parallelism	Input data or batches	Increase data-processing throughput	Gradient synchronization during training
Tensor Parallelism	Tensor dimensions and matrix operations	Distribute computation within model layers	Collective operations and intermediate-result exchange
Pipeline Parallelism	Model layers or computational stages	Distribute model execution across devices	Activation transfer between stages
Context Parallelism	Input sequence or context	Distribute long-sequence processing	Cross-partition sequence and attention information exchange
Expert Parallelism	MoE expert networks	Distribute expert parameters and conditional computation	Token dispatch and expert-result aggregation

Engineering Considerations

Distributed parallelism is not inherently beneficial in every deployment environment. Its effectiveness depends on whether the computational advantages outweigh the communication, synchronization, memory, and scheduling overhead introduced by distributing the workload.

The appropriate strategy should be selected according to:

- Model parameter count and memory footprint.
- Input batch size and sequence length.

- Computational intensity and memory-bandwidth requirements.
- Accelerator memory capacity and interconnect topology.
- Communication latency and synchronization overhead.
- Workload balance and resource utilization.
- End-to-end inference latency and throughput requirements.
- Power consumption, thermal constraints, and deployment complexity.

In practice, large-scale AI systems frequently combine multiple parallelism strategies. For example, data parallelism may be combined with tensor and pipeline parallelism, while MoE architectures may additionally use expert parallelism. Context parallelism can be incorporated when long-sequence processing creates substantial memory or computational demands.

For edge AI systems, however, distributed execution must be evaluated particularly carefully. Communication overhead, network variability, power limitations, and real-time response requirements may outweigh the benefits of additional processing resources. The objective is therefore to select a parallel execution strategy that improves overall application performance while remaining consistent with the hardware, communication, and operational constraints of the target system.

A.10 Communication Fabric Reference

Communication fabrics provide the data-transfer infrastructure that connects processors, accelerators, memory subsystems, and distributed computing nodes. Their bandwidth, latency, topology, scalability, and communication overhead directly influence AI system performance, particularly in workloads involving large models, distributed inference, and multi-accelerator execution.

The following table summarizes major communication fabrics and their typical roles in AI hardware architectures.

Fabric	Typical Use	Primary Function and Engineering Considerations
PCI Express (PCIe)	Host-to-device communication	Provides a standardized high-speed interface between CPUs, GPUs, AI accelerators, storage devices, and other peripherals. Its performance depends on the PCIe generation, lane configuration, and system implementation.

Fabric	Typical Use	Primary Function and Engineering Considerations
NVLink	High-bandwidth GPU-to-GPU communication	Provides a dedicated high-speed interconnect for communication among supported NVIDIA GPUs and, in certain platforms, between CPUs and GPUs. It supports data exchange and collective operations in multi-GPU systems.
NVSwitch	Scalable multi-GPU interconnection	Provides switched connectivity among multiple NVLink-enabled GPUs, enabling high-bandwidth communication across larger accelerator configurations. System performance depends on switch topology, link capacity, and supported platform architecture.
InfiniBand	AI cluster and data-center interconnection	Provides high-performance networking for distributed AI training and inference. Features such as Remote Direct Memory Access (RDMA) can reduce CPU involvement and communication overhead when supported by the hardware and software stack.
Ethernet	General-purpose networking and AI cluster connectivity	Provides widely deployed network connectivity for communication among servers, storage systems, edge devices, and data-center infrastructure. Performance depends on link speed, network topology, congestion control, and protocol configuration.
Optical Fabrics	High-bandwidth, scalable interconnection in large AI systems	Use optical transmission technologies to support high-capacity communication across servers, racks, and data-center infrastructure. Silicon photonics and optical interconnect technologies are being developed to improve bandwidth density, power efficiency, and communication scalability, although adoption and maturity vary by implementation.

Engineering Perspective

Communication-fabric selection should account for more than nominal bandwidth. End-to-end performance also depends on transfer latency, topology, congestion, synchronization overhead, data-transfer size, software support, and the degree of communication required by the AI workload.

For example, PCIe commonly supports host-to-accelerator data movement, while NVLink and NVSwitch provide specialized connectivity within supported multi-GPU platforms. InfiniBand and Ethernet extend communication across computing nodes, supporting distributed workloads. Optical interconnect technologies offer additional approaches to scaling bandwidth and connectivity in large systems.

In distributed AI architectures, communication overhead can become a significant performance bottleneck. Consequently, fabric selection should be coordinated with model partitioning, parallelization strategy, memory placement, and runtime scheduling. The objective is to minimize unnecessary data movement while maintaining the bandwidth, latency, and scalability required by the target workload.

A.11 Thermal Design Reference

Junction Temperature

$$T_j = T_a + P \times R_\theta$$

Where:

- T_j = junction temperature
- T_a= ambient temperature
- P = power
- R_θ = thermal resistance

Power Density

$$PD = \frac{Power}{Area}$$

High power-density regions are candidates for thermal hotspots.

A.12 AI Memory Consumption Estimation

Estimating memory consumption is essential when selecting AI models and hardware platforms for training and inference. Memory requirements depend on model size, numerical precision, execution configuration, sequence length, batch size, and memory architecture.

A.12.1 Model Parameter Storage

The memory required to store model parameters is calculated by multiplying the total number of parameters by the number of bytes required to store each parameter.

Formula:

$$\textit{Parameter Memory (Bytes)} = \textit{Total Number of Parameters} \times \textit{Bytes per Parameter}$$

Example:

A model containing 7 billion parameters stored in FP16 requires:

$$\mathbf{7{,}000{,}000{,}000 \times 2 = 14{,}000{,}000{,}000\ Bytes = 14\ GB}$$

This estimate accounts for parameter storage alone. It excludes activations, KV cache allocation, runtime buffers, and framework overhead.

A.12.2 Key–Value (KV) Cache Estimation

Autoregressive Transformer models maintain a KV cache during inference to store previously computed attention keys and values. This avoids recomputing those representations for every generated token, but memory consumption increases as the cached sequence length and batch size grow.

Formula:

$$\textit{KV Cache Memory (Bytes)} = 2 \times \textit{Batch Size} \times \textit{Number of Layers} \times \textit{Sequence Length} \times \textit{Number of KV Heads} \times \textit{Head Dimension} \times \textit{Bytes per Element}$$

Where:

- **2** = accounts for both key and value tensors.
- **Batch Size** = number of sequences processed concurrently.
- **Number of Layers** = total Transformer layers.
- **Sequence Length** = number of cached tokens.
- **Number of KV Heads** = key–value heads per layer.
- **Head Dimension** = dimensionality of each attention head.
- **Bytes per Element** = storage size of each cache element.

For standard multi-head attention (MHA), the number of key–value heads typically equals the

number of attention heads. Grouped-query attention (GQA) and multi-query attention (MQA) use fewer key–value heads, reducing KV cache memory requirements.

A.12.3 Total Inference Memory Estimation

A practical inference memory estimate must account for model parameters, KV cache allocation, intermediate computations, and runtime overhead.

Formula:

$$\textit{Total Inference Memory} = \textit{Parameter Memory} + \textit{KV Cache Memory} + \textit{Activation Memory} + \textit{Runtime Memory}$$

Where:

- **Parameter Memory** = memory allocated for model parameters.
- **KV Cache Memory** = memory allocated for cached attention keys and values.
- **Activation Memory** = memory used by intermediate tensors and temporary execution data.
- **Runtime Memory** = memory allocated for runtime buffers, communication, workspace, and framework overhead.

Actual memory requirements depend on implementation details, memory allocation strategies, batching, context length, numerical precision, and hardware architecture. Memory fragmentation and reserved workspace can also increase physical memory requirements.

Engineering Perspective

Parameter storage provides a baseline estimate of model memory requirements, while KV cache allocation is a major variable in autoregressive inference. Longer context windows and larger batch sizes increase KV cache consumption. GQA and MQA can reduce this requirement by using fewer key–value heads.

These estimates help engineers assess accelerator memory capacity, determine feasible batch sizes and context lengths, and evaluate whether a model can operate within the memory constraints of an edge AI platform. They should be treated as planning estimates and validated against the actual model implementation, inference runtime, and target hardware.

A.13 Edge AI Design Constraints

Edge AI systems operate within physical, computational, and environmental constraints that

influence their architecture, performance, and deployment feasibility. Unlike centralized computing platforms, edge devices often have limited power availability, thermal dissipation capacity, memory resources, physical space, and network connectivity.

These constraints are interdependent. For example, increasing computational throughput may increase power consumption and heat generation, while reducing memory capacity may require model compression, workload partitioning, or more frequent data transfers. Similarly, strict latency requirements may limit the feasibility of cloud-based processing or computationally intensive model architectures.

The following table summarizes the principal design constraints and their typical engineering implications.

A.13.1 Principal Edge AI Design Constraints

Design Constraint	Typical Engineering Impact	Key Design Considerations
Power Budget	Limits available computational resources and sustained processing capability.	Accelerator selection, operating voltage, clock frequency, numerical precision, workload scheduling, and energy-efficient model execution.
Thermal Budget	Limits sustained throughput and may trigger thermal throttling under intensive workloads.	Heat dissipation, cooling architecture, thermal management, workload distribution, and sustained operating temperature.
Memory Capacity	Restricts model size, batch size, context length, and the storage of intermediate activations.	Model quantization, pruning, memory-efficient architectures, activation reuse, and memory allocation strategies.
Latency Budget	Constrains model complexity, data-transfer overhead, and the time available for inference and downstream processing.	Lightweight model architectures, optimized kernels, accelerator scheduling, communication latency, and end-to-end response-time analysis.
Network Connectivity	Limits dependence on remote computing resources and may	Local inference, edge–cloud partitioning, bandwidth availability, network

Design Constraint	Typical Engineering Impact	Key Design Considerations
	introduce communication delays or service interruptions.	reliability, and communication-aware workload placement.
Physical Size and Form Factor	Restricts component selection, board layout, enclosure dimensions, and available cooling solutions.	System integration, packaging density, thermal design, power delivery, sensor placement, and mechanical constraints.

A.13.2 Interdependencies Among Design Constraints

The constraints listed above should not be treated as independent design parameters. Changes made to improve one aspect of system performance may affect several others.

For example:

- **Power and thermal coupling:** Higher accelerator utilization can increase power consumption and heat generation, potentially reducing sustained performance through thermal throttling.
- **Memory and computational coupling:** Reducing available memory may require smaller models, lower batch sizes, or additional data transfers, affecting computational efficiency and latency.
- **Latency and network coupling:** Remote inference may provide access to greater computational resources but introduces network latency, bandwidth dependence, and connectivity risks.
- **Physical size and thermal coupling:** Compact enclosures restrict heat-dissipation options and may limit the sustained power available to processors and accelerators.
- **Model complexity and resource coupling:** Larger models may improve certain application capabilities while increasing computational demand, memory requirements, energy consumption, and execution time.

A.13.3 Engineering Implications

Effective edge AI design requires balancing these constraints against the functional and operational requirements of the target application. Architectural decisions should therefore consider the complete hardware–software execution path rather than optimizing individual components in isolation.

A practical design process should:

1. Establish explicit power, thermal, memory, latency, connectivity, and physical-size requirements.

2. Select model architectures and accelerator configurations appropriate to those constraints.

3. Evaluate memory utilization, data movement, and computational efficiency under representative workloads.

4. Assess sustained performance under realistic thermal and power conditions.

5. Determine which workloads must execute locally and which can tolerate remote processing.

6. Validate system performance under expected operating conditions, including resource contention and foreseeable environmental variations.

Engineering Perspective

The defining challenge of edge AI is not simply to maximize computational performance within a small device. It is to deliver the required intelligence within a finite physical and operational envelope.

Successful hardware–software co-design therefore requires coordinated optimization of model complexity, accelerator architecture, memory organization, data movement, power consumption, thermal behavior, and execution timing. The resulting system must be evaluated against its actual deployment requirements, with particular attention to sustained performance, resource utilization, and operational reliability.

A.14 AI Accelerator Evaluation Checklist

Selecting an AI accelerator requires evaluating more than its peak computational performance. The suitability of an accelerator depends on its ability to execute the target workload efficiently while meeting memory, communication, reliability, software, power, and operational requirements.

The following checklist provides a structured framework for assessing AI accelerators across five principal evaluation categories.

A.14.1 Computational Performance

Evaluation Criteria

- **Peak Floating-Point Operations per Second (FLOPs):** Maximum theoretical arithmetic throughput, typically specified separately for supported numerical precisions such as FP32, FP16, BF16, or FP8.
- **Tensor Processing Throughput:** Computational capacity for matrix multiplication, tensor operations, and other accelerated AI workloads.
- **Arithmetic Intensity:** Ratio of computational operations to data transferred from memory, commonly expressed as operations per byte.
- **Numerical Precision Support:** Availability of floating-point and integer formats, including FP32, FP16, BF16, FP8, and INT8, where supported.
- **Sustained Workload Performance:** Measured computational throughput under representative model architectures, batch sizes, and execution conditions.

Evaluation Objective: Determine whether the accelerator provides sufficient computational capacity and numerical-format support for the intended AI workloads, rather than relying exclusively on theoretical peak performance.

A.14.2 Memory Architecture and Data Movement

Evaluation Criteria

- **High-Bandwidth Memory (HBM) Bandwidth:** Available memory-transfer bandwidth and its ability to sustain the data requirements of compute-intensive workloads.
- **Memory Capacity:** Total available accelerator memory for model parameters, activations, intermediate tensors, and runtime data structures.
- **Cache Hierarchy:** Organization and capacity of registers, local memory, caches, and other on-chip storage resources.
- **Memory Utilization:** Effectiveness of available memory capacity and bandwidth during actual workload execution.
- Data-Reuse Efficiency: Ability to reuse weights, activations, and intermediate results while minimizing unnecessary transfers between memory levels.
- **Memory Access Latency:** Time required to access data from different levels of the memory hierarchy.

Evaluation Objective: Assess whether the memory subsystem can supply data efficiently to computational units without creating bandwidth bottlenecks, excessive data movement, or capacity limitations.

A.14.3 Communication and Execution Coordination

Evaluation Criteria

- **Interconnect Bandwidth:** Data-transfer capacity between accelerators, processors, memory devices, and other system components.
- **Interconnect Latency:** Communication delay associated with transferring data between connected processing resources.
- **Pipeline Efficiency:** Effectiveness of overlapping computation, memory transfers, and communication across execution stages.
- **Synchronization Overhead:** Time and computational resources consumed by coordination among processing units and distributed workloads.
- **Multi-Accelerator Scalability:** Ability to maintain useful performance as additional accelerators or processing nodes are introduced.
- **Communication Efficiency:** Proportion of execution resources devoted to useful computation rather than data exchange and coordination.

Evaluation Objective: Determine whether communication pathways and execution coordination mechanisms support efficient accelerator utilization and acceptable end-to-end application latency.

A.14.4 Reliability, Thermal Behavior, and Fault Tolerance

Evaluation Criteria

- **Error-Correcting Code (ECC) Support:** Availability of mechanisms for detecting and correcting supported memory errors.
- **Thermal Operating Margin:** Ability to sustain the required workload within specified operating-temperature limits without excessive thermal throttling.
- **Fault-Tolerance Mechanisms:** Support for detecting, containing, recovering from, or mitigating hardware and execution faults.
- **Operational Reliability:** Evidence of stable operation under representative workload

intensity and environmental conditions.

- **Power and Thermal Protection:** Availability of monitoring, power-management, and thermal-control mechanisms.
- **Diagnostic and Error Reporting:** Support for identifying hardware faults, memory errors, and abnormal execution conditions.

Evaluation Objective: Establish whether the accelerator can maintain stable operation within the intended power, thermal, and environmental envelope, with appropriate error-management and recovery capabilities.

A.14.5 Software Ecosystem and Development Support

Evaluation Criteria

- **Compiler Ecosystem:** Availability and maturity of compilers, optimization tools, intermediate representations, and hardware-specific code-generation capabilities.
- **AI Framework Support:** Compatibility with relevant machine-learning frameworks, model formats, operators, and computational libraries.
- **Runtime Environment:** Support for workload scheduling, memory management, device coordination, and accelerator execution.
- **Kernel and Operator Optimization:** Availability of optimized kernels, operator libraries, and mechanisms for custom implementation.
- **Profiling and Performance Analysis:** Tools for measuring computational utilization, memory behavior, communication overhead, and execution latency.
- **Deployment and Maintenance Support:** Availability of software updates, debugging tools, documentation, and long-term platform support.

Evaluation Objective: Determine whether the software environment enables efficient development, optimization, deployment, debugging, and maintenance of AI applications on the target accelerator.

A.14.6 Overall Evaluation and Selection Considerations

The five evaluation categories should be considered together rather than treated as independent measures. An accelerator with exceptional computational throughput may still perform poorly in practice if memory bandwidth is insufficient, communication overhead is excessive, or the

software ecosystem cannot efficiently utilize its hardware resources.

Before selecting an accelerator, engineering teams should also consider the following application-level requirements:

Evaluation Dimension	Key Selection Question
Computational performance	Can the accelerator execute the target AI workload at the required throughput and latency?
Memory architecture	Can model parameters, activations, and intermediate data fit within available memory resources?
Communication	Can data transfers and synchronization be completed without unacceptable overhead?
Reliability	Can the accelerator operate consistently within the intended environmental and thermal conditions?
Software ecosystem	Are the required compilers, frameworks, libraries, and runtime tools available and sufficiently mature?
Power efficiency	Can the workload execute within the platform's power and energy budgets?
Real-time behavior	Can critical operations satisfy their specified timing requirements under representative operating conditions?
Integration complexity	Can the accelerator be integrated with the existing processor, memory, sensor, and communication architecture?

Engineering Perspective

Accelerator evaluation should combine architectural specifications with measurements obtained from representative application workloads. Peak FLOPs, memory bandwidth, and theoretical efficiency provide useful initial indicators, but they do not independently establish actual application performance.

A comprehensive evaluation should include model-specific benchmarking, sustained throughput measurements, end-to-end latency, memory utilization, power consumption, thermal behavior, communication overhead, and software compatibility. Where real-time requirements apply, timing analysis and validation under defined operating assumptions are also necessary.

Ultimately, the most appropriate accelerator is not necessarily the device with the highest peak performance. It is the architecture that provides the best overall balance of computational capability, memory efficiency, communication performance, reliability, software support, and energy consumption while satisfying the functional and operational requirements of the intended edge AI application.

A.15 Common Symbols and Abbreviations Used Throughout Volume IV, Part III

This A.15 provides a consolidated reference to the principal symbols, abbreviations, and technical terms used throughout Part III of Volume IV. These conventions promote consistency when discussing AI accelerator architectures, memory systems, computational performance, distributed processing, and hardware–software optimization.

Symbol / Abbreviation	Meaning	Description / Context
FLOP	Floating-Point Operation	A single arithmetic operation performed using floating-point numbers.
FLOPs/s	Floating-Point Operations per Second	A measure of floating-point computational throughput, commonly used to describe accelerator performance.
BW	Bandwidth	Data-transfer capacity, typically expressed in bytes per second (B/s) or bits per second (bit/s), depending on context.
AI	Arithmetic Intensity	Ratio of computational operations to bytes transferred from memory, commonly expressed as FLOPs per byte.
KV	Key–Value	Refers to the key and value tensors used in attention mechanisms.
KV Cache	Key–Value Cache	Memory storage for previously computed key and value representations during autoregressive inference.
MoE	Mixture of Experts	A model architecture that uses a routing mechanism to activate selected expert networks for individual inputs or tokens.

Symbol / Abbreviation	Meaning	Description / Context
NPU	Neural Processing Unit	A specialized processor designed to accelerate neural-network and other AI workloads.
CGRA	Coarse-Grained Reconfigurable Array	A reconfigurable computing architecture composed of programmable processing elements and configurable interconnections.
PIM	Processing-in-Memory	An architectural approach that performs selected computations within or near memory structures to reduce data movement.
SRAM	Static Random-Access Memory	A semiconductor memory technology commonly used for registers, caches, and on-chip buffers.
HBM	High-Bandwidth Memory	A stacked-memory technology designed to provide high data-transfer bandwidth for processors and AI accelerators.
WDM	Wavelength-Division Multiplexing	An optical communication technique that transmits multiple data channels simultaneously using different wavelengths of light.
ADC	Analog-to-Digital Converter	A circuit that converts analog signals into digital representations.
DAC	Digital-to-Analog Converter	A circuit that converts digital values into corresponding analog signals.

Notation and Usage Conventions

For consistency throughout Part III, the following conventions apply:

- **FLOP** denotes an individual floating-point operation, whereas **FLOPs/s** denotes floating-point computational throughput.
- **BW** denotes bandwidth; the associated unit and context should be specified when necessary.
- **AI** denotes arithmetic intensity in computational-performance discussions, rather than

artificial intelligence, unless the surrounding context clearly indicates otherwise.

- **KV** refers to key–value representations in attention mechanisms, while **KV Cache** identifies the memory structure used to retain these representations during inference.
- **Memory bandwidth** is generally expressed in bytes per second, whereas network and interconnect data rates may be expressed in bits per second.

Complexity expressions and performance metrics should be interpreted according to the definitions, assumptions, and measurement conventions established in the relevant sections.

These conventions provide a consistent terminology framework for interpreting equations, architectural descriptions, performance comparisons, and engineering analyses throughout Part III.

A.16 Recommended Industry Reference Specifications

Hardware–software co-design for edge AI requires familiarity with established industry standards, technical specifications, software interfaces, and engineering frameworks. These references provide common architectural definitions, interoperability requirements, implementation guidelines, and evaluation practices across semiconductor technologies, high-performance interconnects, AI software platforms, and safety-critical systems.

The following references are recommended for readers, researchers, system architects, and engineering professionals working with AI accelerators and integrated edge computing platforms.

A.16.1 Semiconductor Technologies and Hardware Architectures

Recommended Standards and Technical Specifications

- **PCI Express (PCIe):** Industry-standard high-speed serial interconnect specifications governing communication between processors, accelerators, memory devices, and peripheral components.
- **Compute Express Link (CXL):** High-speed interconnect specifications supporting cache-coherent communication and memory sharing among processors, accelerators, and memory devices.
- **JEDEC High Bandwidth Memory (HBM) Standards:** Memory interface and device specifications defining high-bandwidth stacked-memory technologies used in advanced computing and AI accelerator platforms.

- **Universal Chiplet Interconnect Express (UCIe):** Chiplet interconnect specifications supporting standardized die-to-die communication, interoperability, and heterogeneous integration.
- **IEEE Semiconductor and Advanced Packaging Standards:** Relevant IEEE standards and technical publications addressing semiconductor packaging, electronic interconnections, materials, reliability, and advanced integration technologies.

Engineering Relevance: These specifications provide the foundation for designing interoperable accelerator platforms, high-bandwidth memory subsystems, heterogeneous computing architectures, and chiplet-based systems.

A.16.2 Networking and High-Performance Interconnects

Recommended Standards and Technical References

- **InfiniBand Architecture Specification:** Defines high-performance interconnect architecture, communication protocols, and mechanisms for low-latency, high-throughput data exchange in clustered and distributed computing environments.
- **Ethernet IEEE 802 Standards:** Establishes networking specifications covering physical-layer communication, data-link operation, switching, and related networking capabilities. Relevant specifications include IEEE 802.3 Ethernet and IEEE 802.1 bridging and network-management standards.
- **Silicon Photonics Industry References:** Technical publications and industry consortium resources addressing optical interconnect technologies, photonic integration, optical transceivers, and high-bandwidth communication for advanced computing systems.

Engineering Relevance: These references support the design and evaluation of communication fabrics connecting processors, accelerators, memory systems, and distributed AI computing resources. They are particularly relevant when communication bandwidth and latency influence overall system performance.

A.16.3 AI Software, Compilers, and Runtime Infrastructure

Recommended Specifications and Technical Documentation

- **PyTorch Framework and Compiler Documentation:** Reference materials covering AI model development, execution, graph compilation, operator optimization, and runtime integration.
- **Triton Language and Compiler Documentation:** Technical specifications and

programming references for developing optimized GPU kernels and specialized parallel computational operations.

- **Open Neural Network Exchange (ONNX):** An open model representation and interoperability ecosystem supporting the exchange and execution of machine-learning models across compatible frameworks and hardware platforms.
- **Multi-Level Intermediate Representation (MLIR):** Compiler infrastructure supporting extensible intermediate representations and transformation pipelines for heterogeneous hardware and domain-specific optimization.

Engineering Relevance: These software resources provide the foundations for model representation, hardware-aware compilation, kernel optimization, operator fusion, runtime execution, and deployment across heterogeneous accelerator architectures.

A.16.4 Functional Safety, Software Assurance, and AI Risk Management

Recommended Standards and Frameworks

- **ISO 26262 — Road Vehicles: Functional Safety:** Addresses functional safety requirements and lifecycle processes for electrical and electronic systems in road vehicles.
- **IEC 61508 — Functional Safety of Electrical/Electronic/Programmable Electronic Safety-Related Systems:** Establishes a general framework for functional safety throughout the lifecycle of safety-related electrical, electronic, and programmable electronic systems.
- **RTCA DO-178C — Software Considerations in Airborne Systems and Equipment Certification:** Provides software lifecycle objectives and assurance guidance for airborne systems and equipment subject to aviation certification.
- **NIST AI Risk Management Framework (AI RMF 1.0):** Provides a voluntary framework for identifying, assessing, managing, and monitoring risks associated with AI systems throughout their lifecycle.

Engineering Relevance: These standards and frameworks support the development and evaluation of safety-related systems, software assurance processes, and responsible AI risk-management practices. Their applicability depends on the intended application, regulatory environment, system classification, and certification requirements.

A.16.5 Reference Selection and Application Guidance

The references listed above serve different purposes and should be selected according to the technical requirements of the target system.

Technical Domain	Primary Reference Areas	Principal Engineering Application
Semiconductor hardware	PCIe, CXL, JEDEC HBM, UCIe, IEEE packaging references	Accelerator integration, memory architecture, and chiplet interoperability
Networking and interconnects	InfiniBand, IEEE 802 Ethernet, silicon photonics references	High-throughput communication and distributed computing
AI software infrastructure	PyTorch, Triton, ONNX, MLIR	Model compilation, execution optimization, and hardware portability
Functional safety and assurance	ISO 26262, IEC 61508, DO-178C	Safety engineering and software assurance
AI risk management	NIST AI RMF	AI risk identification, assessment, and management

Engineering Perspective

Industry standards and technical specifications provide a common foundation for developing interoperable and maintainable hardware–software architectures. However, compliance with an individual specification does not automatically establish overall system performance, functional safety, cybersecurity, or real-time determinism.

Engineering teams should therefore consult the applicable revisions of these documents, verify compatibility with the target hardware and software platforms, and evaluate their requirements within the context of the complete system architecture.

For safety-related and regulated applications, applicable standards must be incorporated into

the appropriate development, verification, validation, documentation, and certification processes. For AI accelerator development, software and hardware references should be evaluated together to ensure that the selected architecture can support the intended computational workloads and deployment requirements.

A.17 Open-Source AI Compiler Toolchain Architecture Map

Purpose

Modern AI accelerators depend on software toolchains that translate high-level neural-network

models into optimized computational representations and executable workloads tailored to specific hardware architectures. These toolchains connect model development, graph representation, compiler optimization, kernel generation, runtime execution, and hardware-specific interfaces.

Understanding the compiler stack is essential to hardware–software co-design because accelerator performance depends not only on the underlying silicon architecture but also on how effectively software maps computational workloads onto available hardware resources. Compiler decisions influence operator execution, memory allocation, data movement, parallelization, and the utilization of specialized processing units.

The following architecture map presents the principal layers of an AI compiler toolchain and representative frameworks used across contemporary AI systems.

Layered AI Compiler Toolchain Architecture

Layer	Representative Frameworks and Technologies	Primary Function	Typical Output or Responsibility
AI Framework and Model Development Layer	PyTorch, TensorFlow, JAX	Defines, trains, and prepares neural-network models using high-level programming interfaces and tensor operations.	Model definitions, computational operations, and model execution graphs.
Graph Representation and Intermediate Representation (IR) Layer	ONNX, Torch FX, MLIR	Represents computational graphs and model operations in forms suitable for transformation, analysis, and compiler processing.	Interchange formats, graph representations, and intermediate compiler representations.
Compiler Optimization Layer	Apache TVM, XLA, IREE, MLIR-based compiler pipelines	Performs graph-level and hardware-aware transformations, including operator fusion, layout optimization, and computation scheduling.	Optimized computational graphs, intermediate representations, and target-specific execution plans.

Layer	Representative Frameworks and Technologies	Primary Function	Typical Output or Responsibility
Kernel Programming and Generation Layer	Triton, CUTLASS, specialized compiler backends	Develops, generates, and optimizes low-level computational kernels for matrix operations, tensor processing, and other accelerator workloads.	Hardware-oriented kernels and optimized computational routines.
Runtime and Execution Management Layer	ONNX Runtime, IREE Runtime, OpenXLA runtime components	Manages model execution, resource allocation, graph execution, memory handling, and interaction with supported execution providers or hardware backends.	Runtime scheduling, operator dispatch, memory management, and execution coordination.
Hardware Backend and Programming Interface Layer	CUDA, ROCm, Intel oneAPI/SYCL, Vulkan	Provides programming interfaces, libraries, drivers, and execution mechanisms that connect software workloads to supported hardware platforms.	Device-specific execution commands, kernel launches, and hardware resource access.
Physical Hardware Layer	GPUs, TPUs, NPUs, FPGAs, CGRAs, and other AI accelerators	Executes computational workloads using specialized processing units, memory hierarchies, and interconnect architectures.	Physical computation, data storage, and hardware-level parallel execution.

Note: This table represents a conceptual toolchain architecture, not a mandatory sequence of independent software components. Frameworks, intermediate representations, compilers, runtimes, and hardware backends may overlap or interact directly. Actual deployment pipelines vary according to the selected framework, compiler, accelerator, and software ecosystem.

Common AI Compiler Frameworks and Technologies

The following frameworks illustrate major approaches to AI compilation, kernel development, and hardware-specific optimization.

Apache TVM

An open-source, tensor-oriented compiler framework designed to optimize machine-learning workloads across heterogeneous hardware platforms. TVM supports graph-level transformations, operator scheduling, and hardware-specific code generation, enabling deployment across different processor and accelerator architectures.

Triton

An open-source programming language and compiler ecosystem for developing efficient parallel kernels, particularly for GPU workloads. Its tile-based programming model allows developers to express tensor computations while the compiler handles aspects of memory access, parallel execution, and hardware-specific optimization.

MLIR (Multi-Level Intermediate Representation)

An open-source compiler infrastructure that provides extensible intermediate representations and transformation mechanisms for building domain-specific and hardware-specific compiler pipelines. MLIR supports multiple abstraction levels, facilitating optimization and lowering from high-level computational graphs to lower-level execution representations.

XLA (Accelerated Linear Algebra)

An optimizing compiler used in the TensorFlow and JAX ecosystems. XLA transforms

computational graphs and tensor operations into optimized executable programs for supported hardware targets. Its optimization capabilities include operation fusion, algebraic simplification, and device-oriented code generation.

IREE (Intermediate Representation Execution Environment)

An open-source compiler and runtime project designed to support deployment across heterogeneous hardware environments, including resource-constrained and edge-oriented platforms. IREE provides compilation, code-generation, and execution components that help translate high-level computational representations into deployable workloads.

ONNX Runtime

An open-source cross-platform inference and execution framework for models represented in

the Open Neural Network Exchange (ONNX) format. It provides graph optimization and execution-provider mechanisms that connect model inference workloads to supported hardware backends.

Terminology clarification: ONNX is an open model representation and interchange format, whereas ONNX Runtime is an execution framework. Similarly, MLIR is compiler infrastructure rather than a standalone AI model framework. These distinctions are important when describing the individual responsibilities of the toolchain.

Compiler Optimization Categories

AI compiler toolchains apply transformations at different levels of the computational pipeline. The following categories represent major optimization techniques relevant to accelerator performance.

Optimization Category	Primary Objective	Potential System-Level Benefit
Operator Fusion	Combine compatible graph operations into larger computational units.	Reduces intermediate tensor transfers and kernel-launch overhead.
Kernel Fusion	Combine multiple operations within a single accelerator kernel.	Improves data locality and reduces repeated memory access.
Memory Scheduling and Allocation	Coordinate buffer allocation, reuse, and data movement across the memory hierarchy.	Reduces memory overhead and improves resource utilization.
Tensor Layout Transformation	Rearrange tensor dimensions, memory formats, and data organization to match hardware execution requirements.	Improves memory access efficiency and accelerator compatibility.
Graph Partitioning	Divide computational graphs into executable subgraphs assigned to different processors or accelerators.	Enables heterogeneous execution and workload distribution.

Optimization Category	Primary Objective	Potential System-Level Benefit
Quantization	Reduce numerical precision while maintaining acceptable model accuracy.	Can reduce memory consumption and improve throughput on supported hardware.
Sparse Execution Optimization	Exploit structured or unstructured sparsity through specialized representations and kernels.	Reduces computational work and data movement when hardware and software support the selected sparsity pattern.
Parallelization and Distributed Execution	Partition workloads across processing units, accelerators, or computing nodes.	Increases available computational parallelism, subject to communication and synchronization overhead.

Hardware–Software Co-Design Significance

Compiler frameworks are a central component of modern accelerator engineering because they determine how model computations are represented, transformed, scheduled, and executed on physical hardware. Their decisions influence several important system characteristics:

- **Arithmetic intensity:** Compiler transformations affect the relationship between computational operations and data movement.
- **Accelerator utilization:** Kernel mapping, operation fusion, and execution scheduling influence the effective use of specialized processing units.
- **Memory efficiency:** Tensor layouts, buffer allocation, and memory scheduling affect bandwidth utilization and data locality.
- **Communication overhead:** Graph partitioning and distributed execution determine how frequently data must move between processing units and computing nodes.
- **Execution latency:** Kernel-launch overhead, synchronization, memory access, and scheduling decisions contribute to end-to-end execution time.
- **Portability:** Intermediate representations and hardware abstraction mechanisms can simplify deployment across different accelerator architectures, although hardware-specific optimization may still be necessary.

- **Execution predictability:** Static scheduling, controlled memory allocation, and bounded execution paths can support more predictable behavior, but timing guarantees require system-level analysis and validation.

Engineering Perspective

An effective AI compiler toolchain must coordinate model representation, graph optimization, kernel generation, runtime execution, and hardware-specific resource management. Optimizing an individual layer in isolation may not produce the best overall system performance. For example, operator fusion can reduce memory transfers but increase register pressure or intermediate storage requirements. Similarly, graph partitioning can improve accelerator utilization while introducing additional communication and synchronization overhead.

Hardware–software co-design therefore requires compiler optimization to be evaluated against the characteristics of the target accelerator, including its computational architecture, memory hierarchy, supported numerical formats, interconnects, and execution model.

The practical objective is to translate model-level computational requirements into efficient hardware execution while balancing throughput, memory utilization, power consumption, portability, and end-to-end latency. For edge AI and real-time applications, these optimizations must also be assessed under representative workloads and operating conditions to determine whether the resulting execution behavior meets the system's timing and resource constraints.

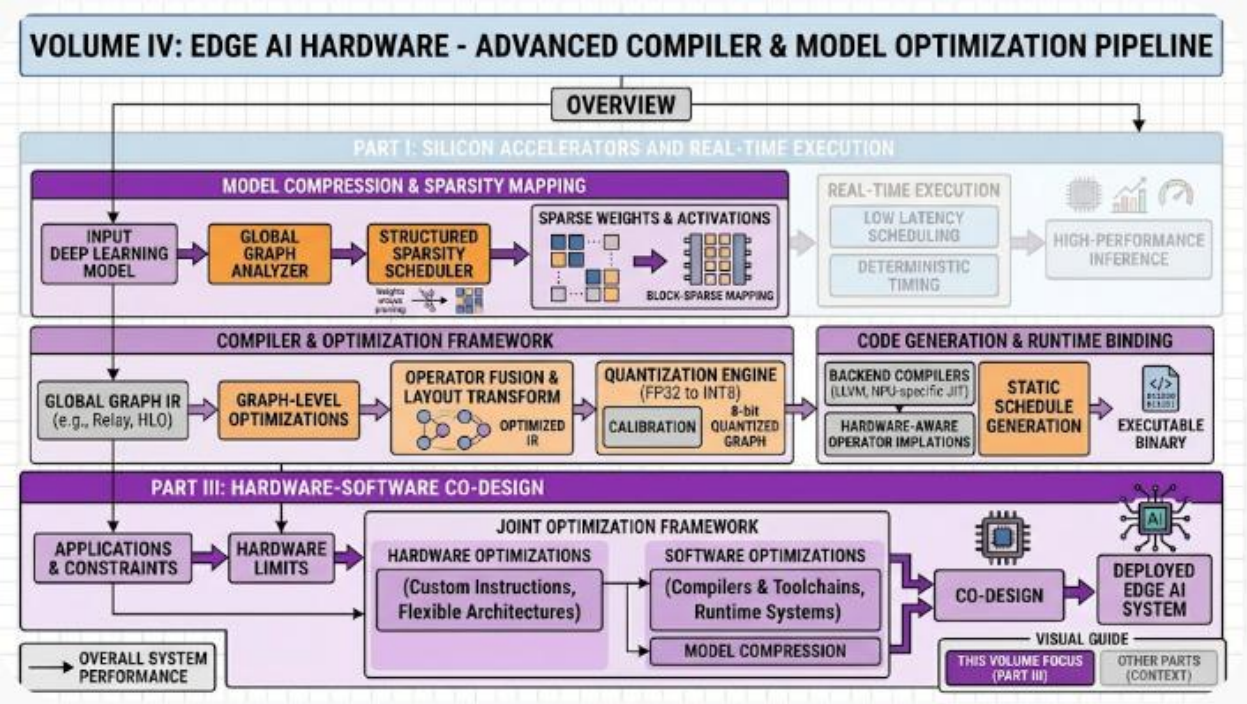


Figure A3— End-to-End Edge AI Model Optimization, Compression, and Compiler Deployment Pipeline.

The workflow illustrates the progression from neural-network design and hardware-aware neural architecture search (HW-NAS) through pruning, quantization, graph optimization, compiler lowering, kernel generation, runtime orchestration, and deployment on edge AI accelerators. The pipeline demonstrates how hardware–software co-design principles are applied throughout the AI development lifecycle to improve latency, energy efficiency, memory utilization, and deployment scalability.

Figure A3.1 integrates the concepts discussed throughout Appendix A by illustrating the complete optimization pathway used in modern AI deployment workflows. Beginning with model architecture selection, the process incorporates hardware-aware neural architecture search (HW-NAS) to align network structure with deployment constraints. Subsequent stages perform model compression, structured sparsity optimization, quantization, graph-level transformations, kernel generation, and accelerator-specific compilation. Runtime frameworks then schedule execution across target hardware platforms including GPUs, NPUs, TPUs, FPGAs, and edge accelerators. The figure demonstrates that AI performance is increasingly determined by the combined effect of algorithm design, compiler technology, runtime orchestration, and hardware architecture rather than by any individual component in isolation.

A.18 Model Compression & Quantization Reference Standards

Purpose

Model compression enables increasingly capable AI models to operate within the memory, computational, power, and bandwidth constraints of resource-limited hardware platforms. By reducing model size, numerical precision, or computational activity, compression techniques can improve deployment efficiency across edge devices, embedded systems, mobile platforms, and accelerator-based computing environments.

Model compression encompasses several complementary approaches, including pruning, structured sparsity, quantization, knowledge distillation, low-rank factorization, weight sharing, and conditional computation. These techniques can reduce storage requirements and computational demand, although their practical benefits depend on model architecture, hardware capabilities, compiler support, and runtime implementation.

The following reference summarizes major compression techniques and their primary objectives.

Compression Taxonomy

Technique	Primary Purpose	Typical Method	Potential Engineering Benefit
Pruning	Remove parameters or connections that contribute relatively little to model performance.	Eliminate selected weights, neurons, channels, or other model components.	Reduces parameter count and may reduce computation when supported by efficient sparse execution.
Structured Sparsity	Organize pruning according to hardware-compatible patterns.	Remove predefined groups, blocks, channels, or fixed patterns such as 2:4 sparsity.	Enables more efficient accelerator execution than arbitrary unstructured pruning on compatible hardware.
Quantization	Reduce the numerical precision used to represent model parameters and intermediate computations.	Convert higher-precision values into lower-bit integer or floating-point representations.	Reduces model storage and memory bandwidth requirements and may improve inference throughput.
Knowledge Distillation	Transfer learned behavior from a larger model to a smaller model.	Train a student model using outputs, probability distributions, intermediate representations, or other guidance from a teacher model.	Produces smaller models that can retain useful capabilities of larger models.
Low-Rank Factorization	Reduce the dimensionality and computational complexity of large parameter matrices.	Approximate a matrix using smaller factorized matrices or lower-rank representations.	Reduces parameter storage and matrix-operation requirements when the approximation is effective.

Technique	Primary Purpose	Typical Method	Potential Engineering Benefit
Weight Sharing	Reduce the number of independently stored model parameters.	Allow multiple connections or model components to use shared parameter values, including clustering-based representations.	Reduces storage requirements and can improve model compactness.
Dynamic Routing and Conditional Computation	Avoid activating all model components for every input.	Selectively activate experts, subnetworks, or computational paths according to input-dependent routing decisions.	Reduces active computation per input, although routing and communication overhead may offset some gains.

Common Quantization Formats

Quantization represents model values using reduced numerical precision. The choice of numerical format affects representable range, precision, memory consumption, arithmetic behavior, and hardware compatibility.

Format	Nominal Bit Width	Typical Use	Engineering Considerations
INT8	8-bit integer	Production inference across supported CPUs, GPUs, and NPUs.	Widely supported in inference environments. Quantization scales and zero points are used to map real-valued tensors into integer representations.
INT4	4-bit integer	Memory-efficient inference for large models and resource-constrained platforms.	Can substantially reduce weight storage, but requires compatible kernels and careful handling of quantization error and activation precision.
FP8	8-bit floating point	Training and inference on	Provides floating-point representations with reduced storage requirements. Different FP8

Format	Nominal Bit Width	Typical Use	Engineering Considerations
		supported advanced accelerators.	encodings offer different tradeoffs between numerical range and precision.
FP4	4-bit floating point	Emerging low-precision inference and specialized accelerator workloads.	Offers high storage efficiency but imposes significant numerical precision constraints. Practical use depends on scaling methods, model characteristics, and hardware support.
Microscaling (MX) Formats	Format-dependent, commonly low-bit data with shared block-level scaling	Emerging accelerator architectures and low-precision AI computation.	Uses shared scaling information across groups of values to support efficient low-precision representation. Specific formats define their own data types, scaling rules, and numerical behavior.

Note: INT8, INT4, FP8, and FP4 identify numerical representation families rather than complete quantization specifications. Actual implementation details, including scaling, rounding, saturation, accumulation precision, and supported operations, vary across hardware platforms and software frameworks. MX formats refer to a family of microscaling data formats rather than a single bit width.

Quantization Approaches

Quantization can be introduced at different stages of model development. Two widely used approaches are post-training quantization and quantization-aware training.

Post-Training Quantization (PTQ)

Post-training quantization applies reduced-precision representations to a previously trained model. Depending on the method, it may use a representative calibration dataset to estimate activation ranges and determine quantization parameters.

Advantages:

- Can be applied without retraining the original model.
- Simplifies deployment workflows and reduces additional training requirements.

- Supports conversion of existing models into hardware-compatible inference representations.
- Provides a practical approach for evaluating lower-precision deployment configurations.

Engineering Considerations:

- Quantization error can reduce model accuracy, particularly at very low bit widths.
- Calibration data should adequately represent the expected inference workload.
- Performance improvements depend on accelerator support and optimized execution kernels.

Quantization-Aware Training (QAT)

Quantization-aware training incorporates simulated quantization effects into the training process. The model is trained or fine-tuned while accounting for the numerical limitations expected during lower-precision inference.

Advantages:

- Can improve accuracy retention under reduced-precision inference.
- Helps models adapt to quantization effects during training.
- Can support more aggressive quantization when ordinary post-training methods produce unacceptable accuracy loss.

Engineering Considerations:

- Requires additional training or fine-tuning resources.
- Introduces complexity into the model development and deployment pipeline.
- Final accuracy and performance must be evaluated using the actual target quantization format and inference implementation.

Compression Efficiency Metrics

Compression techniques should be evaluated using measurable indicators that account for model size, memory requirements, computational demand, and retained model quality.

1. Compression Ratio

The compression ratio measures the relationship between the original model size and the compressed model size.

$$\text{Compression Ratio} = \frac{\text{Original Model Size}}{\text{Compressed Model Size}}$$

Where:

- Original Model Size = Storage size of the original model.
- Compressed Model Size = Storage size after compression.

A higher compression ratio indicates a greater reduction in stored model size.

2. Memory Reduction

Memory reduction expresses the proportional decrease in model storage requirements.

$$\text{Memory Reduction (\%)} = \left(1 - \frac{\text{Compressed Model Size}}{\text{Original Model Size}}\right) \times 100$$

This expression calculates the percentage reduction in model storage requirements.

3. Parameter Reduction

Parameter reduction measures the percentage decrease in the number of stored model parameters.

$$\text{Parameter Reduction (\%)} = \left(1 - \frac{\text{Compressed Parameter Count}}{\text{Original Parameter Count}}\right) \times 100$$

Where:

- Original Parameter Count = Number of parameters before compression.
- Compressed Parameter Count = Number of parameters after compression.

This metric measures the percentage decrease in the number of model parameters; it's particularly relevant to pruning, low-rank factorization, and knowledge-distillation workflows.

4. Accuracy Retention

Accuracy retention measures the extent to which a compressed model preserves the performance of its original counterpart.

$$\text{Accuracy Retention (\%)} = \frac{\text{Compressed Model Accuracy}}{\text{Original Model Accuracy}} \times 100$$

Where:

- Original Model Accuracy = Accuracy of the original model.
- Compressed Model Accuracy = Accuracy of the compressed model.

This metric indicates how much of the original model's accuracy is retained after compression.

Important distinction: Accuracy retention is a relative measure, not the same as the absolute accuracy change. For example, if the original model achieves 95% accuracy and the compressed model achieves 93%, accuracy retention is approximately 97.89%, while the absolute accuracy loss is 2 percentage points.

5. Inference Performance

Compression should also be evaluated using actual deployment performance, including:

- Inference latency and end-to-end response time.
- Throughput under representative batch sizes.
- Peak memory consumption during execution.
- Energy consumption per inference or processed input.
- Model-loading time and initialization overhead.

Engineering Consideration: A reduction in model size or theoretical operation count does not automatically produce proportional improvements in latency, throughput, or energy efficiency. Actual gains depend on hardware support, memory behavior, compiler optimization, and runtime execution.

Industry and Technical Reference Frameworks

The following open-source frameworks, software ecosystems, and technical specifications provide practical support for model quantization and compressed-model deployment.

Framework or Reference	Primary Role	Relevance to Model Compression and Quantization
ONNX and ONNX Runtime Quantization Tools	Model representation and inference execution	Support quantization workflows, model optimization, and deployment across supported execution providers.
NVIDIA TensorRT Quantization Tools	Hardware-specific inference optimization	Provide precision calibration, quantization, and optimized inference capabilities for supported NVIDIA hardware.
OpenVINO Model Optimization Toolkit	Model optimization and deployment	Supports model compression and quantization workflows for compatible Intel hardware platforms.
OpenXLA	Compiler infrastructure for machine-learning workloads	Provides compiler and execution infrastructure for optimizing computational graphs and mapping workloads to supported hardware.
TensorFlow Model Optimization Toolkit	Model compression and optimization	Provides techniques for pruning, quantization-aware training, and other model optimization workflows within supported TensorFlow environments.
OCP Microscaling (MX) Specifications	Low-precision numerical representation	Defines microscaling data formats and associated representation conventions for supported AI computing applications.

Note: These references serve different purposes. ONNX is a model interchange format; ONNX Runtime is an execution framework; TensorRT and OpenVINO provide vendor-associated optimization and deployment capabilities; OpenXLA is compiler infrastructure; and the OCP MX specifications define numerical formats. Their availability and capabilities depend on the relevant software version and hardware platform.

Engineering Perspective

Model compression and quantization are important mechanisms for aligning AI model requirements with the physical constraints of edge and accelerator-based systems. However, compression should not be treated as an isolated model-level operation. Its effectiveness

depends on the interaction among model architecture, numerical representation, memory hierarchy, accelerator instructions, compiler optimization, and runtime execution.

For hardware–software co-design, the compression strategy should be selected according to the target workload and deployment environment. For example, INT8 quantization may provide a practical balance between numerical accuracy and computational efficiency on supported hardware, while INT4 and FP4 formats may offer greater memory savings at the cost of more demanding accuracy and implementation considerations. Structured pruning can improve execution efficiency when the target accelerator supports the corresponding sparsity pattern. Knowledge distillation and low-rank factorization offer additional approaches when model architecture and accuracy requirements permit them.

The overall objective is to reduce the resource requirements of an AI model while preserving the accuracy, throughput, latency, and operational reliability required by the application. In real-time edge AI systems, compressed models must also be validated under representative workloads and operating conditions to establish whether their execution behavior satisfies the system's timing and resource constraints.

A.19 Hardware-Aware Neural Architecture Search (HW-NAS) Parameters

Purpose

Hardware-Aware Neural Architecture Search (HW-NAS) is an automated architecture optimization methodology that evaluates neural-network designs according to both predictive performance and hardware deployment characteristics. Unlike conventional Neural Architecture Search (NAS), which often emphasizes model accuracy or computational efficiency in isolation, HW-NAS incorporates target hardware constraints directly into the architecture search and evaluation process.

By jointly considering model architecture, computational requirements, memory behavior, inference latency, energy consumption, and hardware resource utilization, HW-NAS seeks to identify neural-network configurations that satisfy application requirements while operating

efficiently on specific hardware platforms.

Traditional NAS and Hardware-Aware NAS Objectives

Traditional NAS Objective

Traditional Neural Architecture Search primarily seeks to maximize predictive accuracy:

$$\mathcal{A}^* = \arg\max_{\mathcal{A} \subset \mathcal{S}} \ \mathrm{Accuracy}(\mathcal{A})$$

Where:

- A^* = Selected optimal neural-network architecture.
- A = Candidate neural-network architecture.
- S = Architecture search space.
- Accuracy(A) = Predictive accuracy of the candidate architecture.

Depending on the search methodology, traditional NAS may also incorporate model complexity, parameter count, or computational cost.

Interpretation: Traditional NAS searches for an architecture that achieves the highest predictive accuracy within the defined search space.

Hardware-Aware NAS Objective

Hardware-Aware NAS extends the optimization process to consider predictive accuracy and hardware deployment efficiency simultaneously.

$$\mathcal{A}^* = \arg\max_{\mathcal{A}\in\mathcal{S}} \left[\mathrm{Accuracy}(\mathcal{A}), -\mathrm{Latency}(\mathcal{A}), -\mathrm{Energy}(\mathcal{A}), -\mathrm{Memory}(\mathcal{A})\right]$$

Subject to hardware and application constraints, such as:

$$\begin{aligned}\mathrm{Latency}(\mathcal{A}) &\le L_{\max}\\ \mathrm{Energy}(\mathcal{A}) &\le E_{\max}\\ \mathrm{Memory}(\mathcal{A}) &\le M_{\max}\\ \mathrm{Area}(\mathcal{A}) &\le A_{\max}\end{aligned}$$

Where:

- L_{max} = Maximum permitted inference latency.
- E_{max} = Maximum permitted energy consumption.
- M_{max} = Available memory budget.
- A_{max} = Maximum permitted hardware area, where applicable.

Interpretation: HW-NAS seeks architectures that maximize predictive accuracy while minimizing latency, energy consumption, and memory requirements, subject to the available hardware resources.

Important mathematical distinction: The HW-NAS expression is a multi-objective optimization problem. It generally produces a set of Pareto-optimal architectures rather than one universally optimal solution. The final architecture is selected according to the application's performance priorities and deployment constraints.

The negative signs indicate that latency, energy consumption, and memory requirements are minimized while predictive accuracy is maximized.

In practice, HW-NAS is generally a multi-objective optimization problem. Its results may form a **Pareto frontier**, representing architectures for which no objective can be improved without compromising at least one other objective. The final architecture is selected according to application priorities and deployment constraints.

Key Optimization Parameters

The following parameters provide a reference for evaluating candidate architectures during hardware-aware search.

Parameter	Description	Optimization Objective
Accuracy	Measures predictive quality using application-appropriate evaluation metrics, such as classification accuracy, F1 score, or task-specific error.	Maximize predictive performance while maintaining required quality.
Inference Latency	Measures the time required to process an input or complete an inference operation.	Minimize execution time and satisfy application timing requirements.
Throughput	Measures the number of inputs, tokens, or inference operations processed per unit of time.	Maximize processing capacity under the target workload and resource limits.
Energy Consumption	Measures the energy required to execute an inference or process a defined workload.	Minimize energy per inference or per unit of useful computation.
Memory Footprint	Measures memory required for model parameters, activations, intermediate tensors, runtime buffers, and other execution state.	Minimize memory requirements while satisfying available capacity.

Parameter	Description	Optimization Objective
Compute Utilization	Measures the effective use of available processing resources, such as GPU execution units, tensor-processing units, or FPGA logic resources.	Improve resource utilization without creating additional bottlenecks.
Thermal Budget	Defines the permissible thermal operating range and associated power or cooling constraints.	Maintain acceptable operating temperatures and sustained performance.
Bandwidth Consumption	Measures data-transfer requirements across memory interfaces and communication links.	Reduce unnecessary data movement and avoid bandwidth-related bottlenecks.
Hardware Area	Measures the silicon or programmable logic resources required by an architecture when hardware implementation is part of the search.	Satisfy chip-area or programmable-resource constraints.

Implementation Note: *The operational classification of compute utilization, thermal behavior, and memory bandwidth depends on the target hardware platform and search methodology, as a single metric may function as an evaluation parameter, an explicit optimization objective, or a hard operational constraint. For instance, peak junction temperature or dynamic power may serve as an unconstrained evaluation metric during baseline benchmarking, an explicit minimization objective within an evolutionary cost function, or a non-negotiable operational ceiling that bounds the valid hardware design space. To prevent optimization instability and guarantee reproducible execution bounds, the system specification must explicitly define the architectural role of each metric prior to running platform-specific design space exploration loops.*

Search Space Components

HW-NAS explores combinations of architectural and execution-related parameters. The search space determines which candidate models can be generated and evaluated.

1. Network Topology

Network topology defines the overall structure and connectivity of the neural network.

Typical search parameters include:

- **Depth:** Number of layers or computational stages.
- **Width:** Number of channels, neurons, attention heads, or hidden dimensions.
- **Connectivity:** Arrangement of connections among layers and computational blocks.
- **Expansion Ratios:** Relative dimensions of intermediate processing layers.
- **Residual Structures:** Placement and configuration of skip connections.

2. Operator Selection

Operator selection determines which computational building blocks are used within the architecture.

Representative choices include:

- Standard, depthwise, and pointwise convolutions.
- Conventional and efficient attention mechanisms.
- State-space model modules.
- Feed-forward and gated neural-network blocks.
- Mixture-of-Experts (MoE) modules.
- Hardware-specific operator implementations.

The selection process should account for the computational characteristics and availability of optimized kernels on the target accelerator.

3. Numerical Precision Selection

Precision selection determines the numerical representation used for model parameters, activations, and intermediate computations.

Representative formats include:

- FP32 — 32-bit floating point.
- FP16 — 16-bit floating point.
- BF16 — 16-bit brain floating point.
- FP8 — 8-bit floating point.

- INT8 — 8-bit integer.
- INT4 — 4-bit integer.

Lower-precision formats can reduce memory consumption and improve computational efficiency on supported hardware. However, numerical accuracy, operator compatibility, and accumulation precision must be evaluated as part of the search.

4. Sparsity Selection

Sparsity selection determines whether and how inactive model parameters or computational paths are introduced.

Representative approaches include:

- **Unstructured Sparsity:** Individual weights are removed without a predefined structural pattern.
- **Structured Sparsity:** Weights or connections are removed according to regular patterns, such as blocks, channels, or hardware-supported 2:4 structures.
- **Dynamic Sparsity:** Active connections or computational paths vary according to input data or runtime conditions.

The practical value of each approach depends on accelerator support, compiler optimization, and the efficiency of the corresponding sparse execution kernels.

5. Memory and Dataflow Configuration

Some HW-NAS methodologies also explore memory and execution characteristics, including:

- Tensor layout and memory organization.
- Data reuse and buffering strategies.
- On-chip memory allocation.
- Operator scheduling and fusion.
- Dataflow and computation mapping.
- Communication requirements among processing elements.

These parameters are particularly relevant when the search process incorporates accelerator-specific execution models or hardware design variables.

Evaluation Platforms

HW-NAS can target a range of processor and accelerator architectures. The following platforms represent common evaluation environments.

Hardware Platform	Typical Evaluation Focus
Graphics Processing Units (GPUs)	Parallel throughput, tensor-processing utilization, memory bandwidth, and kernel execution efficiency.
Tensor Processing Units (TPUs)	Matrix-operation efficiency, supported numerical formats, dataflow organization, and accelerator utilization.
Neural Processing Units (NPUs)	Low-power inference, operator compatibility, on-chip memory utilization, and edge deployment efficiency.
Edge AI Accelerators	Inference latency, energy consumption, memory capacity, and sustained operation under constrained power budgets.
Field-Programmable Gate Arrays (FPGAs)	Logic utilization, pipeline organization, parallelism, memory interfaces, and hardware customization.
Coarse-Grained Reconfigurable Arrays (CGRAs)	Processing-element utilization, dataflow mapping, interconnection requirements, and reconfiguration overhead.

Evaluation Methodology

Reliable HW-NAS requires candidate architectures to be evaluated under conditions representative of their intended deployment environment.

A typical evaluation process includes:

1. Define application requirements: Establish accuracy targets, latency limits, throughput requirements, power budgets, and memory constraints.

2. Define the search space: Specify permissible network topologies, operators, numerical formats, sparsity patterns, and other architectural variables.

3. Identify the target hardware: Select the accelerator architecture, memory configuration, software stack, and runtime environment.

4. Evaluate candidate architectures: Measure predictive performance and estimate or

benchmark hardware execution characteristics.

5. Apply optimization constraints: Eliminate architectures that violate mandatory resource or performance requirements.

6. Identify Pareto-optimal candidates: Compare architectures across competing objectives without assuming that one configuration is optimal for every application.

7. Validate the selected architecture: Perform deployment-level measurements using the intended compiler, runtime, hardware configuration, and representative workloads.

Hardware measurements are important because analytical estimates and surrogate performance models may not fully capture compiler behavior, memory contention, communication overhead, or runtime effects.

Hardware–Software Co-Design Significance

HW-NAS represents an important application of hardware–software co-design because neural-network architecture selection is directly informed by the characteristics of the intended execution platform.

Rather than optimizing a model exclusively for predictive accuracy and adapting it to hardware afterward, HW-NAS incorporates deployment considerations into the architecture search process.

Its principal co-design dimensions include:

- **Computational constraints:** Align network operations and computational complexity with available processing resources.
- **Memory hierarchy:** Account for registers, SRAM, accelerator memory, DRAM, and associated data-transfer requirements.
- **Communication costs:** Consider data movement among processing units, accelerators, and distributed computing nodes.
- **Energy budgets:** Evaluate computational efficiency and energy consumption under application-specific power constraints.
- **Thermal constraints:** Account for sustained operating conditions and potential performance degradation caused by thermal limitations.
- **Numerical precision:** Match model precision requirements with supported accelerator

formats and optimized execution paths.

- **Execution behavior:** Evaluate inference latency, throughput, scheduling overhead, and runtime characteristics under representative workloads.

Engineering Perspective

Hardware-Aware Neural Architecture Search extends neural-network optimization beyond model-level predictive performance by incorporating the physical and operational characteristics of the target computing platform. It provides a systematic approach for exploring architectures that balance accuracy, computational efficiency, memory requirements, energy consumption, and deployment constraints.

However, HW-NAS does not automatically guarantee optimal hardware utilization or deterministic real-time execution. Search results depend on the quality of the search space, the accuracy of performance models, the fidelity of hardware measurements, and the representativeness of evaluation workloads. Final candidates must therefore be validated using the actual deployment toolchain and target hardware.

For edge AI and real-time applications, the central objective is to identify architectures that preserve required model quality while satisfying latency, memory, power, thermal, and computational constraints. This approach connects neural architecture design directly to accelerator capabilities and system-level engineering requirements.

APPENDIX B: GLOSSARY

Volume IV: Edge AI Hardware, Silicon Accelerators & Systems Co-Design

Part III: Hardware–Software Co-Design and System Optimization

A

Accelerator Utilization — The proportion of an AI accelerator's available computational resources that is actively performing useful work during a specified interval. Utilization depends on workload parallelism, data availability, memory bandwidth, scheduling, and execution efficiency.

Activation — The output produced by a neural network layer, typically after applying a mathematical transformation to its input. Activations may require substantial temporary memory during inference.

Activation Memory — Memory used to store intermediate outputs generated as a model executes. Activation memory requirements depend on tensor dimensions, execution order, batch size, and the number of intermediate values that must remain available.

Arithmetic Logic Unit (ALU) — Hardware component responsible for performing arithmetic and logical operations.

Analog-to-Digital Converter (ADC) — Electronic circuit that converts analog signals into digital representations for processing by digital hardware systems.

Application-Specific Integrated Circuit (ASIC) — An integrated circuit designed for a particular application or a restricted class of workloads or a semiconductor device designed for a specific application rather than general-purpose computation. An **AI ASIC** is a custom-designed integrated circuit optimized specifically for AI and machine-learning workloads; it can provide high efficiency for supported operations but generally offers less flexibility than a general-purpose processor.

Architecture Search — The systematic exploration of alternative neural network structures to identify architectures that meet specified objectives, such as predictive quality, latency, energy consumption, or memory capacity.

Arithmetic Intensity — The ratio of arithmetic operations performed to the amount of data transferred, usually measured in operations per byte. It helps characterize whether a workload is likely to be limited by computation or memory bandwidth.

B

Batch Size — The number of inputs processed together in a model execution batch. Largerbatches can improve hardware utilization but may increase memory requirements and the time an individual input waits for processing.

Bandwidth — The maximum rate at which data can be transferred between system components or the amount of data transferred per unit of time through a communication channel or memory interface. Effective bandwidth can constrain AI inference even when computational capacity is available.

Brain Floating Point 16 — A 16-bit floating-point numerical format widely used for AI training and inference due to its balance between dynamic range and computational efficiency.

Buffer — A memory region used to hold data temporarily while it moves between processing stages, devices, or components operating at different rates.

Buffering Latency — Delay introduced when data must wait in a buffer before the next processing stage can consume it. Buffering can improve throughput while increasing end-to-end latency.

C

Cache — A small, relatively fast memory that stores copies of data or instructions to reduce access time compared with retrieving them from a slower memory level.

Cache Locality — The extent to which a workload repeatedly accesses data or instructions already available in a cache. Good locality can reduce memory traffic and improve execution performance.

Calibration — The process of relating sensor measurements to known references or correcting systematic measurement errors. Calibration helps ensure that sensor outputs are suitable for downstream processing and fusion.

Central Processing Unit (CPU) — General-purpose processor responsible for executing software instructions and coordinating system operations.

Clock Domain Crossing (CDC) — Mechanisms used to safely transfer data between circuits operating on different clock signals.

Compute Unified Device Architecture (CUDA) — Parallel computing platform and programming model developed by NVIDIA for GPU computation.

Convolutional Neural Network (CNN) — A deep-learning architecture commonly used for image processing and computer vision applications.

Configurable Logic Block (CLB) — The fundamental programmable component within FPGA architectures.

Coarse-Grained Reconfigurable Arrays (CGRAs) — A programmable accelerator architectures composed of interconnected processing elements that can be dynamically configured to execute different computational graphs and dataflow patterns. CGRAs provide a middle ground between the flexibility of FPGAs and the efficiency of fixed-function accelerators.

Compiler — Software that transforms a program or model representation into a form executable by a target processor or accelerator. An AI compiler may perform graph transformations, operator lowering, scheduling, memory planning, and hardware-specific code generation.

Compiler Backend — The compiler component responsible for translating an intermediate representation into instructions, kernels, or executable code suitable for a target processor or accelerator.

Computational Graph — A directed graph representing mathematical operations and the dependencies between them in an AI model or computational workload.

Compute-Bound Workload — A workload whose performance is primarily limited by available computational throughput rather than by data transfer or another system resource.

Compute Express Link (CXL) — A high-speed interconnect standard designed to improve communication among processors, memory devices, and accelerators.

Concurrency — The overlapping execution or progress of multiple tasks. Concurrency can improve resource utilization but may introduce synchronization requirements and resource contention.

Cross-Layer Optimization — The coordinated optimization of interacting AI system layers, including model architecture, compilation, hardware, memory, sensing, runtime execution, and security mechanisms.

Cycle Time — The duration of one clock cycle in a synchronous digital circuit. A shorter cycle time permits a higher clock frequency, subject to physical and implementation constraints.

D

Data Acquisition — The process of obtaining measurements or data from sensors, instruments, or other input sources.

Data Locality — The practice or property of keeping data close to the processing units that use it, thereby reducing data-transfer cost, latency, and energy consumption.

Data Movement — The transfer of data between memory levels, processors, accelerators, sensors, or other system components. Data movement can consume substantial time and energy.

Dataflow Architecture — A hardware organization in which computation and data movement are arranged around the flow and reuse of data through processing elements.

Deadline — The latest permitted completion time for a task or operation. Missing a deadline may have different consequences depending on whether the task is hard real-time, firm real-time, or soft real-time.

Design-Space Exploration (DSE) — The systematic evaluation of alternative hardware, software, model, and configuration choices to identify designs that satisfy specified objectives and constraints.

Deterministic Execution — Execution whose relevant behavior, such as timing or output, is predictable under explicitly defined assumptions and conditions. Determinism is not automatically guaranteed by using specialized hardware.

Digital-to-Analog Converter (DAC) — Device that converts digital information into analog electrical signals.

Digital Signal Processor (DSP) — A processor designed to execute signal-processing operations efficiently, often including filtering, transforms, and arithmetic patterns used in sensor and AI pipelines, or a specialized processor optimized for high-speed mathematical operations on signal data.

Direct Memory Access (DMA) — A mechanism that allows a device or controller to transfer data to or from memory with reduced direct intervention from the CPU.

Dynamic Power — Electrical power associated with switching activity in digital circuits. It depends on factors including switching frequency, effective capacitance, and supply voltage.

Dynamic Random Access Memory (DRAM) — Volatile memory technology commonly used for system main memory.

E

Edge AI — Artificial intelligence deployed on or near the devices that generate or consume data, rather than relying exclusively on remote cloud processing.

End-to-End Latency — The total elapsed time between defined starting and ending points in a system workflow. In AI applications, the measurement may include acquisition, preprocessing, data transfer, inference, postprocessing, and communication.

Energy per Inference — The energy consumed to complete one inference under a specified workload and measurement boundary. Comparisons require consistent treatment of idle power, preprocessing, data movement, and other system overhead.

Error-Correcting Code (ECC) — Hardware mechanism that detects and corrects memory errors to improve system reliability.

Execution Graph — A representation of the operations and dependencies that a runtime system executes, potentially including device placement, synchronization, and data-transfer steps.

Execution Time — The time required for a specified task or operation to execute under a defined set of conditions.

F

Fault Detection — The process of identifying evidence that a hardware or software component is malfunctioning or behaving outside expected limits.

Fault Mitigation — Actions taken to reduce the effects of a detected or anticipated fault, such as isolating a faulty resource, retrying a computation, switching to a fallback model, or entering a safe state.

Fault Tolerance — The ability of a system to continue providing an acceptable level of service despite specified faults. Fault tolerance depends on the faults considered and the mechanisms implemented.

Feature Extraction — The transformation of raw data into representations intended to capture information useful for a downstream task.

Ferroelectric Random Access Memory (FeRAM) — A non-volatile memory technology that retains information without power.

Field-Programmable Gate Array (FPGA) — A reconfigurable integrated circuit whose logic and interconnections can be programmed after manufacturing, or a programmable semiconductor

device whose logic structures can be configured after manufacturing. FPGAs can implement specialized AI and signal-processing pipelines.

Floating-Point Operation (FLOP) — A single arithmetic calculation involving floating-point numbers.

- **4-Bit Floating Point (FP4)** — An ultra-low-precision numerical format designed for highly optimized inference workloads.
- **8-Bit Floating Point (FP8)** — A reduced-precision format used in advanced AI accelerators for training and inference.
- **16-Bit Floating Point (FP16)** — A reduced-precision floating-point format used extensively in AI training and inference.
- **32-Bit Floating Point (FP32)** — A standard floating-point format commonly used in scientific and machine-learning computation.
- **Floating-Point Operations per Second (FLOPS)** — A performance metric measuring computational throughput.

Floating-Point Precision (FLP) — The numerical format used to represent real-valued quantities approximately, such as FP32 or FP16. Precision affects numerical range, accuracy, memory use, and computational efficiency.

Firmware — Software stored in or closely associated with hardware that controls device initialization, low-level operation, and hardware-specific functions.

First-In, First-Out (FIFO) — A buffering mechanism in which data are processed in the same order in which they arrive.

G

Gaussian Error Linear Unit (GELU) — Non-linear activation function commonly used in transformer architectures such as BERT and GPT models.

General Matrix–Matrix Multiplication (GEMM) — The fundamental / foundational

linear-algebra operation used extensively in neural-network training and inference.

General-Purpose Processor — A processor designed to support a broad range of computational tasks rather than a single specialized workload.

Graph Optimization — Transformations applied to a computational graph to reduce

unnecessary operations, improve execution order, combine compatible operators, or improve resource use while preserving the required semantics.

Graceful Degradation — The ability of a system to maintain an acceptable reduced level of functionality when resources fail, environmental conditions worsen, or full performance cannot be sustained.

Graphics Processing Unit (GPU) — A highly parallel processor originally developed for graphics workloads and widely used for machine learning because it can execute large numbers of parallel operations, or massively parallel processor widely used for AI training, inference, graphics rendering, and scientific computing.

H

Hardware Accelerator — A processing component designed to execute a particular class of computations more efficiently than a general-purpose processor under supported conditions.

Hardware–Software Co-Design — A development methodology in which hardware architecture and software components are designed and optimized together to satisfy application requirements.

Hardware Counter — A hardware-provided measurement facility that records events such as instructions executed, cache misses, memory traffic, or processor cycles. Available events vary by platform.

Hardware-Aware Neural Architecture Search (HW-NAS) — Neural architecture search that evaluates model candidates using properties or measurements of the intended deployment hardware, such as latency, memory footprint, energy, or supported operators.

Heterogeneous Computing — A computing approach that uses different types of processing resources, such as CPUs, GPUs, DSPs, and NPUs, within one system.

High-Bandwidth Memory (HBM) — A three-dimensional stacked memory architecture providing extremely high memory bandwidth for AI and HPC systems.

High-Bandwidth Memory (HBM) Bandwidth — The maximum rate at which data can be transferred between High-Bandwidth Memory (HBM) devices and a processor, accelerator, GPU, TPU, or AI computing system. It represents one of the most important performance metrics in modern AI hardware because many large-scale AI workloads are limited by memory movement rather than arithmetic capability.

Host–Device Transfer — The movement of data between a host processor's memory and the

memory or accessible storage of an accelerator or other device.

High-Performance Computing (HPC) — Computing systems designed to solve computationally intensive scientific and engineering problems.

Hardware-Aware Neural Architecture Search (HW-NAS) — Neural architecture search methods that incorporate hardware constraints directly into model-design optimization.

I

4-Bit Integer Format (INT4) — Ultra-low-precision integer representation commonly used in compressed AI inference models.

8-Bit Integer Format (INT8) — A quantized numerical format widely adopted for AI inference acceleration.

Inference — The process of applying a trained model to input data to produce predictions, classifications, representations, or other outputs.

Inference Latency — The elapsed time required for an inference operation under a specified measurement boundary. It may refer to model execution alone or to a broader end-to-end pipeline.

Instruction Set Architecture (ISA) — The programmer-visible specification of a processor's instructions, registers, data types, and execution behavior.

Intermediate Representation (IR) — A structured program representation used between a high-level model or source program and lower-level executable instructions. IRs facilitate analysis, optimization, and code generation, or an internal compiler representation used during software and hardware optimization.

Intermediate Representation Execution Environment (IREE) — A compiler and runtime framework for deploying machine-learning workloads across heterogeneous hardware platforms.

Interrupt — A signal that requests processor attention and may cause execution to transfer to a handler. Interrupt behavior and handling overhead can affect real-time timing.

J

Just-in-Time (JIT) Compilation — Compilation performed during program execution rather than exclusively before deployment. JIT compilation can adapt code to runtime information but introduces compilation overhead that must be considered.

Just After Execution (JAX) — A high-performance machine-learning framework emphasizing automatic differentiation and accelerator optimization.

K

Kernel — A computational routine executed on a processor or accelerator. In AI systems, a kernel often implements an operation such as matrix multiplication, convolution, normalization, or an elementwise transformation.

Key-Value Cache (KV Cache) — Memory structure used in transformer architectures to store prior attention states and accelerate autoregressive inference.

Knowledge Distillation — A model-training technique in which a smaller or otherwise different student model learns from outputs or representations produced by a teacher model.

L

Large Language Model (LLM) — A large-scale neural-network model trained on massive text corpora to perform language-related tasks.

Latency — The elapsed time between a defined event and its corresponding result. The meaning of latency depends on the chosen start and end points.

Latency Budget — The amount of time allocated to a task or stage within an end-to-end timing requirement.

Loop Tiling — An optimization that divides loop iterations into smaller blocks to improve data reuse, cache behavior, or mapping onto hardware processing units.

M

Memory Bandwidth — The rate at which data can be transferred to or from a memory system.

Memory Footprint — The amount of memory required by a model or workload during a specified phase of operation, including relevant parameters, activations, temporary buffers, and runtime structures.

Memory Hierarchy — The organization of storage into levels with different capacities, access latencies, bandwidths, and energy costs, such as registers, caches, local accelerator memory, and main memory.

Memory Tiling — The organization of computation so that data is processed in blocks that fit efficiently within a chosen level of the memory hierarchy.

Microarchitecture — The internal organization and implementation of a processor, including execution units, pipelines, caches, scheduling, and interconnects.

Micro-Scaling Format (MX Format) — A block-scaled numerical representation designed to improve efficiency in low-precision AI computation.

Mixture of Experts (MoE) — A neural-network architecture that selectively activates specialized expert subnetworks for different inputs.

Model Compression — Techniques that reduce model storage or execution requirements,

including quantization, pruning, factorization, and knowledge distillation.

Model Quantization — The representation of model parameters or activations using reduced or otherwise selected numerical precision to lower storage or computational costs.

Multi-Level Intermediate Representation (MLIR) — A compiler infrastructure designed to support diverse hardware targets and AI workloads.

N

Neural Architecture Search (NAS) — An automated or semi-automated process for exploring candidate neural network architectures according to defined search criteria, or automated discovery of neural-network architectures.

Neural Processing Unit (NPU) — A processor or accelerator designed to execute neural-network operations efficiently, or a specialized accelerator designed to execute neural-network workloads efficiently, particularly in edge devices. Supported operations and performance vary by implementation.

Non-Volatile Memory (NVM) — Memory that retains stored information when power is removed.

Numerical Accuracy — The closeness of a numerical result to a reference or intended result. In AI deployment, numerical changes can affect both low-level calculations and model-level predictive quality.

O

Open Neural Network Exchange (ONNX) —An open standard for representing and exchanging machine-learning models among frameworks.

Operator — A mathematical or computational operation in an AI model, such as convolution, matrix multiplication, activation, normalization, or attention.

Operator Fusion — A compiler or runtime optimization that combines compatible operations into a single execution unit to reduce intermediate data movement or execution overhead.

Out-of-Order Execution — A processor technique that allows eligible instructions to execute in an order different from their original program order while preserving the required architectural behavior.

P

Parallelism — The ability to perform multiple operations or tasks concurrently. AI workloads may exploit data, instruction, thread, pipeline, or device-level parallelism.

Peak Floating-Point Operations per Second (Peak FLOPs) — The theoretical maximum computational throughput that a processor, accelerator, or computing system can achieve under ideal operating conditions. It represents the highest number of floating-point arithmetic operations that can be executed in one second when all computational units are fully utilized.

Peripheral Component Interconnect Express (PCIe) — A high-speed communication interface used to connect processors, accelerators, and peripheral devices.

Phase-Change Memory (PCM) — A non-volatile memory technology that stores information through changes in material phase states.

Phase-Locked Loop (PLL) — Electronic control circuit used to synchronize timing and clock frequencies.

Processing Element (PE) — An individual compute unit within a parallel accelerator architecture.

Processing-in-Memory (PIM) — A computing architecture that performs calculations directly within or near memory arrays.

Post-Training Quantization (PTQ) — Quantization applied to a trained model, generally without performing a full quantization-aware training procedure, or a quantization technique applied after neural-network training has been completed. Calibration or limited adjustment may be used depending on the method.

Power Budget — The maximum or target power consumption allocated to a component or system under specified operating conditions.

Pruning — The removal or suppression of model parameters, connections, channels, or other structures judged unnecessary for a target task. Actual hardware benefits depend on the resulting sparsity pattern and execution support.

Predictive Maintenance — The use of measurements, models, or historical data to estimate degradation or failure risk and support maintenance decisions before a fault occurs.

Q

Quantization-Aware Training (QAT) — A training or fine-tuning method that models quantization effects during training to help a model retain performance when deployed with reduced numerical precision, or a training methodology that incorporates quantization effects during optimization.

Queueing Delay — Time spent waiting for a resource or service before processing begins. Queueing delay can contribute significantly to end-to-end latency under contention.

R

Real-Time System — A system whose correctness depends partly on completing specified operations within defined timing constraints.

Real-Time Operating System (RTOS) — An operating system designed to support timing-sensitive workloads through mechanisms such as priority scheduling, predictable synchronization, and controlled interrupt handling.

Retrieval-Augmented Generation (RAG)
An AI architecture that supplements generation models with external knowledge retrieval.

Resistive Random Access Memory (RRAM)
A non-volatile memory technology used in emerging AI and in-memory computing architectures.

Runtime — The software environment and services involved in executing a program or model, including resource management, dispatch, synchronization, and memory handling.

Runtime Telemetry — Measurements collected during execution, potentially including latency, utilization, memory traffic, power, temperature, and hardware error indicators.

S

Scheduling — The assignment and ordering of tasks or operations on available processing resources.

Sensor Fusion — The combination of information from multiple sensors to produce a more complete or reliable estimate of the environment or system state.

Sensor Pipeline — The sequence of acquisition, preprocessing, synchronization, transfer, and

other operations that prepares sensor data for an AI model or downstream system.

Side-Channel Attack — An attack that attempts to infer sensitive information from indirect observations, such as execution timing, power consumption, electromagnetic emissions, or cache behavior.

Secure Enclave — A hardware-supported or otherwise isolated execution environment intended to protect specified code and data from certain software or system threats. Protection depends on the implementation and threat model.

Sigmoid Linear Unit (SiLU) — Activation function that multiplies an input by its sigmoid activation, commonly used in modern deep-learning models, or a non-linear activation function, also known as Swish, commonly used in modern deep-learning architectures.

Single Error Correction, Double Error Detection (SECDED)
A commonly used ECC method capable of correcting single-bit errors and detecting double-bit errors.

Single Instruction, Multiple Data (SIMD) — A parallel processing architecture in which a single instruction operates simultaneously on multiple data elements, or a parallel-computing model in which one instruction operates simultaneously on multiple data elements.

Single Instruction, Multiple Threads (SIMT) — A parallel-execution model widely used by GPUs, where multiple threads execute the same instruction stream concurrently.

Software Stack — The layered collection of software components used to build and execute an application, including libraries, compilers, runtimes, operating systems, and device drivers.

Sparsity — The proportion or pattern of zero-valued or inactive elements in a model or data structure. Sparsity improves performance only when the relevant hardware and software can exploit it efficiently.

Static Memory Allocation — The assignment of memory regions before or at a fixed stage of execution, rather than allocating all memory dynamically during runtime.

Static Random Access Memory (SRAM) — High-speed memory technology commonly used for caches, buffers, and accelerator-local storage.

Structured Sparsity — Sparsity constrained to defined patterns, such as groups of weights or channels, that can be exploited by supported hardware or software implementations.

Synchronization — The coordination of operations or data from multiple tasks or sources to

establish a required ordering or temporal relationship.

T

Tensor — A multidimensional array used to represent data, model parameters, activations, or intermediate computational results.

Tensor Core — A specialized execution unit found in some processors that accelerates supported matrix or tensor operations, often using particular numerical formats.

Tensor Float 32 (TF32) — A reduced-precision floating-point format optimized for tensor-core operations.

Tensor Processing Unit (TPU) — A specialized AI accelerator optimized for large-scale tensor operations, deep-learning training, and inference workloads, or a specialized accelerator optimized for tensor operations and machine-learning workloads. TPUs typically incorporate systolic-array architectures, high-bandwidth memory subsystems, and specialized matrix-processing engines to maximize throughput for neural-network computation.

Tensor Virtual Machine (TVM) — An open-source compiler framework for optimizing AI workloads across multiple hardware platforms.

Thermal Throttling — A reduction in processor frequency or performance in response to thermal or power constraints.

Thermal Design Power (TDP) — A platform- or manufacturer-defined thermal design metric used to guide cooling requirements. It should not automatically be interpreted as the exact maximum or instantaneous power consumption.

Throughput — The amount of work completed per unit of time, such as inferences per second or processed frames per second.

Timing Jitter — Variation in the timing of an event, task execution, or output relative to an expected or scheduled time.

Transformer — A neural network architecture that uses attention mechanisms and related operations to model relationships among elements of an input sequence or representation.

U

Unified Memory — A memory architecture or programming model that provides a common or

coordinated address space across processors or devices. Its performance depends on the implementation and actual data movement.

Universal Chiplet Interconnect Express (UCIe) — An industry-standard interconnect specification enabling communication among chiplets within a package.

V

Vectorization — The execution of an operation across multiple data elements using vector instructions or vector processing hardware.

Very Long Instruction Word (VLIW) — An instruction-set architecture that schedules multiple operations within a single instruction.

Volatile Memory — Memory that generally loses its stored contents when power is removed, such as conventional SRAM and DRAM.

W

Wavelength-Division Multiplexing (WDM) — An optical communication technique that transmits multiple signals simultaneously over a single waveguide or fiber.

Worst-Case Execution Time (WCET) — An upper bound on the execution time of a specified task under defined hardware, software, and environmental assumptions. Establishing a trustworthy bound can be difficult on complex platforms with shared resources and dynamic behavior.

X

Accelerated Linear Algebra (XLA)
A compiler framework developed for optimizing machine-learning workloads on modern accelerators.

Execution Context — The information required to resume or manage a task's execution, potentially including registers, memory mappings, scheduling state, and device-specific state.

Z

Zero-Copy Data Transfer — A data-transfer approach that avoids one or more explicit data-copy operations, often by sharing accessible memory or using direct device access. Whether it improves performance depends on memory architecture, synchronization, and access costs.

Key Terms Frequently Referenced Throughout Part III

Acronym	Full Name
GEMM	General Matrix–Matrix Multiplication
GELU	Gaussian Error Linear Unit
SiLU	Sigmoid Linear Unit
SIMD	Single Instruction, Multiple Data
SIMT	Single Instruction, Multiple Threads
KV Cache	Key-Value Cache
HBM	High-Bandwidth Memory
PIM	Processing-in-Memory
CGRA	Coarse-Grained Reconfigurable Array
FPGA	Field-Programmable Gate Array
TPU	Tensor Processing Unit
NPU	Neural Processing Unit
HW-NAS	Hardware-Aware Neural Architecture Search
MoE	Mixture of Experts
ECC	Error-Correcting Code

This glossary is tailored specifically to the technical concepts, architectures, compiler frameworks, memory systems, accelerator technologies, and co-design methodologies discussed throughout **Volume IV, Part III: Hardware–Software Co-Design and System Optimization**.

APPENDIX C — ACRONYMS

Volume IV: Edge AI Hardware, Silicon Accelerators & Systems Co-Design

Part III: Hardware–Software Co-Design and System Optimization

ADC — Analog-to-Digital Converter

AI — Artificial Intelligence

AI ASIC — Artificial Intelligence Application-Specific Integrated Circuit

ALU — Arithmetic Logic Unit

API — Application Programming Interface

ASIC — Application-Specific Integrated Circuit

ASIL — Automotive Safety Integrity Level

AXI — Advanced eXtensible Interface

BF16 — Brain Floating Point 16

BW — Bandwidth

CAN — Controller Area Network

CAN-FD — Controller Area Network Flexible Data-Rate

CDC — Clock Domain Crossing

CGRA — Coarse-Grained Reconfigurable Array

CLB — Configurable Logic Block

CNN — Convolutional Neural Network

CPU — Central Processing Unit

CSI-2 — Camera Serial Interface 2

CUDA - Compute Unified Device Architecture

CXL — Compute Express Link

DAC — Digital-to-Analog Converter

DMA — Direct Memory Access

DNN — Deep Neural Network

DRAM — Dynamic Random Access Memory

DSP — Digital Signal Processor

DSE — Design-Space Exploration

ECC — Error-Correcting Code

EDA — Electronic Design Automation

EDP — Energy–Delay Product

FeRAM — Ferroelectric Random Access Memory

FIFO — First-In, First-Out

FLOP — Floating-Point Operation

FLOPS — Floating-Point Operations per Second

FP4 — 4-Bit Floating-Point

FP8 — 8-Bit Floating-Point

FP16 — 16-Bit Floating-Point

FP32 — 32-Bit Floating-Point

FPGA — Field-Programmable Gate Array

GELU — Gaussian Error Linear Unit

GEMM — General Matrix–Matrix Multiplication

GPU — Graphics Processing Unit

HBM — High-Bandwidth Memory

HPC — High-Performance Computing

HW-NAS — Hardware-Aware Neural Architecture Search

I/O — Input/Output

IC — Integrated Circuit

IMU — Inertial Measurement Unit

INT4 — 4-Bit Integer Representation

INT8 — 8-Bit Integer Representation

IPC — Instructions Per Cycle

IR — Intermediate Representation

IREE — Intermediate Representation Execution Environment

ISA — Instruction Set Architecture

JAX — Just After Execution

JIT — Just-in-Time Compilation

KPI — Key Performance Indicator

KV— Cache Key-Value Cache

L1 — Level-1 Cache

L2 — Level-2 Cache

L3 — Level-3 Cache

LLM — Large Language Model

LiDAR — Light Detection and Ranging

MAC — Multiply–Accumulate

MCU — Microcontroller Unit

ML — Machine Learning

MLIR — Multi-Level Intermediate Representation

MMU — Memory Management Unit

MIPI — Mobile Industry Processor Interface (MIPI Alliance interface standards)

MoE — Mixture of Experts

MX Format — Micro-Scaling Format

NAS — Neural Architecture Search

NPU — Neural Processing Unit

NVM — Non-Volatile Memory

ONNX — Open Neural Network Exchange

OOD — Out-of-Distribution

OS — Operating System

PCIe — Peripheral Component Interconnect Express

PE — Processing Element

PIM — Processing-in-Memory

PL — Phase-Locked Loop

PMU — Performance Monitoring Unit

PTQ — Post-Training Quantization

PWM — Pulse-Width Modulation

QAT — Quantization-Aware Training

QoS — Quality of Service

RAG — Retrieval-Augmented Generation

RAM — Random-Access Memory

RISC — Reduced Instruction Set Computer

ROM — Read-Only Memory

RRAM — Resistive Random-Access Memory

RTOS — Real-Time Operating System

SECSED — Single Error Correction, Double Error Detection

SiLU — Sigmoid Linear Unit

SIMD — Single Instruction, Multiple Data

SIMT — Single Instruction, Multiple Threads

SRAM — Static Random-Access Memory

SoC — System on a Chip

SIMD — Single Instruction, Multiple Data

SNR — Signal-to-Noise Ratio

SPI — Serial Peripheral Interface

SSD — Solid-State Drive

TDP — Thermal Design Power

TF32 — Tensor Float 32

TOPS — Tera Operations Per Second

TOPS/W — Tera Operations Per Second per Watt

TPU — Tensor Processing Unit

TSN — Time-Sensitive Networking

TVM — Apache TVM**:** An open-source machine-learning compiler framework that optimizes and deploys machine-learning models across diverse hardware platforms, including CPUs, GPUs, and specialized AI accelerators.

UCIe — Universal Chiplet Interconnect Express

USB — Universal Serial Bus

VLIW — Very Long Instruction Word

WCET — Worst-Case Execution Time

WDM — Wavelength-Division Multiplexing

WNS — Worst Negative Slack

XLA — Accelerated Linear Algebra

XPU — Processing Unit**:** A general term for a specialized or heterogeneous processing unit designed to accelerate specific computing workloads. It may refer to GPUs, TPUs, NPUs, or other application-specific and domain-specific processors. Its precise meaning depends on the hardware architecture and the context in which the term is used.